Fall 12-21-2011

# Activation and Catalytic Bond Forming Reactions at Carbon-Hydrogen Bonds of $\eta^6$-Tricarbonylchromium-Coordinated Benzylic Arenes

Genette I. McGrew
*University of Pennsylvania*, gimcgrew@yahoo.com

# Activation and Catalytic Bond Forming Reactions at Carbon-Hydrogen Bonds of $\eta^6$-Tricarbonylchromium-Coordinated Benzylic Arenes

**Abstract**
Polyarylmethanes are an extremely valuable molecular scaffold used in fields ranging from materials chemistry to medicinal chemistry. They are found in dyes and semiconductor dopants and in drugs and drug precursors that address a variety of ailments ranging form depression and allergies to cancer and vascular disease. However, general, selective methods to synthesize polyarylmethanes are still limited. This dissertation describes some of the exploratory work done to outline the synthetic possibilities of deprotonated tricarbonylchromium-stabilized benzylic arenes in the context of selective bond-forming reactions to form polyarylmethanes. Various $\eta^6$-arene-tricarbonylchromium complexes are deprotonated with the mild silamide base $LiN(SiMe_3)_2$ and used directly in selective palladium-catalyzed syntheses of polyarylmethanes and other potentially valuable molecules from aryl bromides, aryl triflates, and vinyl triflates as coupling partners. In the first chapter, we illustrate the unique aspects of tricarbonylchromium activation, such as the ability to activate not just one C–H bond, but up to six in one flask, leading to highly substituted and sterically hindered products not accessible through traditional methods. Additionally, the sterically bulky nature of the tricarbonylchromium group is exploited to direct chemistry to the opposite face of polycyclic systems, leading to stereoselective reactions difficult to achieve selectively by other methods. Compatibility with α-heteroatom substitution and β-hydrogens is also demonstrated. Finally, an unusual mode of isomerization during the cross-coupling processes is explored. In the second chapter, the methodology for the synthesis of polyarylmethanes is expanded to asymmetric syntheses of di- and tri-arylmethane complexes. Low-barrier high-throughput experimentation (HTE) methodology is successfully implemented in the search for a highly selective ligand to achieve asymmetric cross-coupling. Medicinally valuable diarylmetheylamines are obtained from tricarbonylchromium-coordinated tertiary benzylamines in good to excellent enantiomeric excess. Finally, in the third chapter we use the products of the asymmetric cross-coupling with benzylamines to introduce novel methods to synthesize a new modular chiral P^N ligand scaffold using a unimetal super-base. These ligands may be effective in future cross-coupling reactions and asymmetric catalysis.

**Degree Type**
Dissertation

**Degree Name**
Doctor of Philosophy (PhD)

**Graduate Group**
Chemistry

**First Advisor**
Patrick J. Walsh

**Keywords**
tricarbonylchromium, palladium-catalyzed, cross-coupling, asymmetric, organolithium, polyarylmethanes

# ACTIVATION AND CATALYTIC BOND FORMING REACTIONS AT C—H BONDS OF $\eta^6$-TRICARBONYLCHROMIUM-COORDINATED BENZYLIC ARENES

Genette Itoko McGrew

A Dissertation in Chemistry

Presented to the Faculties of the University of Pennsylvania in Partial Fulfillment of the Requirements for the Degree of Doctor of Philosophy

2011

Supervisor of Dissertation

_____

Patrick J. Walsh, Professor of Chemistry

Graduate Group Chairperson

_____

Gary A. Molander, Professor of Chemistry

Dissertation Committee

Donald H. Berry, Professor of Chemistry

Larry G. Sneddon, Professor of Chemistry

Eric J. Schelter, Assistant Professor of Chemistry

ACTIVATION AND CATALYTIC BOND FORMING REACTIONS AT
C—H BONDS OF $\eta^6$-TRICARBONYLCHROMIUM-COORDINATED BENZYLIC ARENES



## Dedication

This is dedicated to people like Tim. The ones who (probably) know who they are already. The ones who know (and put up with how) “about half an hour” turns into “two hours.” The ones who know the answer to the question, “so, are you going back to lab after this?”

## Acknowledgements

### *Pat Walsh and the Walsh lab*

First and foremost I must acknowledge the man behind it all, the brains and money and chief person-to-butt-heads-with, Pat Walsh. Without him, this document and its contents would not even exist. When I just joined the lab, he had said he was looking to expand the research of the group into some completely new areas. I hope that I have at least partially made good on his hopes for bringing to life some new directions to the organometallic chemistry done in our lab.

On a (mostly) non-chemistry note, I would like to also thank him for allowing me to flex my art and design muscles by letting me design the cover for the textbook that he and Prof. Kozlowski have written together, as well as designing the group website and inventory and doing other "techie" stuff.

Thank you to the Walsh lab members, past and present, many of whom have been sources of encouragement and company at late hours of the night. While we may not have been working on related chemistry, it has always been good to bounce ideas around and troubleshoot with them. I am particularly in debt to Alice Chong for Schlenk techniques and so many other pieces of lab know-how (and showing me where to find late-night discount food), Mike Kerrigan for teaching advice (and nostalgia), Petr Valenta for timely moments of random chemistry insight (and for getting me to drink beer), and to Luca Salvi for his warmth and feeling like family. Of the current members I must in particular acknowledge Jiadi, who is taking over a lot of my group jobs *and* the torch of $\eta^6$-arene chemistry. I am happy to say that as of the writing of this thesis, his first paper in tricarbonylchromium chemistry has been accepted to JACS, so I'm excited to see the continuation of this new area of study for the Walsh Lab.

I'd also like to acknowledge the lab undergraduates. Thanks to them I have had the opportunity to not only teach science and safety but also regale them with nerdy tales of chemistry. Oh, the places you'll go!

### *The Committee*

While we did not meet up so very often, I must thank my committee members past and present: Don Berry, Gary Molander, Larry Sneddon, and Eric Schelter for the advice and criticism they have provided, constantly pushing me to be a better and more efficient chemist.

*Chemistry peeps*

To the graduate students, postdocs, undergraduates, faculty, and staff who I have had the chance to interact with over the course of five and a half years here, in the wise words taken from The Hitchhiker's Guide to the Galaxy, "so long and thanks for all the fish." Well, OK, maybe it wasn't fish. Maybe it was liquid nitrogen, a sample of naphthalene, or some constructive criticism on a practice talk or research statement. Or maybe it was a bottle of beer, some company, some encouragement, a ride home late at night, or a healthy dose of down-to-earth-ness (or wackiness). In particular, I thank the people who have stuck with me all these years. I have received so much for which I am grateful.

*High-throughput experimental collaborators*

Without the high-throughput experimental collaboration and developments spearheaded by Gary Molander, Spencer Dreher (Merck & Co.), Marisa Kozlowski, and Patrick Walsh and generously funded by a NSF GOALI grant (CHE-0848460), the HTE work contained here would not have been possible. Cornell Stanciu and Simon Berritt are acknowledged in particular for their experimental work, invaluable help and training, and helpful discussion.

*Instrumentation and spectroscopy*

Patrick Carroll is acknowledged for his awesome X-ray crystallography work, and the NSF for funding an X-ray diffractometer (CHE-0840438).

George Furst, Jun Gu, and Sangrama Sahoo are acknowledged for department NMR facilities, especially Sahoo for NMR training and help. Rakesh Kohli is thanked for running the high-resolution mass spectrometry on my compounds, especially the ones that kept fragmenting strangely, and the NIH for funding a Waters LCTOF-Xe Premier ESI mass spectrometer (1S10RR23444-1).

Bruce Dolliver, Rico Vargas, Dan Burke and co. all are acknowledged for keeping the building together and running behind the scenes, and for repairing the things when they aren't.

Finally, Elena Kreimer at the Berkeley Microanalytical Laboratory is acknowledged for elemental analysis of compounds.

*Funding*

Thank you to NSF for providing money for research and living expenses (CHE-0848467, CHE-0848460: GOALI Award to UPenn and Merck).

And thank you to UPenn for paying me to teach its undergraduates in 245, 246, and 241.

*People*

I was about to write “real people” in the heading here, but then I stopped, a little embarrassed that I was about to actually write that. It’s not that being in chemistry makes one *not* a real person (far from it, please don’t make a face!), but it *is* true that being in chemistry puts a person in a universe that is markedly different from the world experienced by many of the people walking and driving by. It seems like the general consensus is that the chemistry graduate student life makes very little sense to those outside that universe, but that’s OK.

So, I am grateful to my family and also to my non-chemistry friends. Whether they were supportive of my bizarre decision to continue my pursuits of science or (in some cases) completely against it, I do appreciate the sanity-checks that they provided. Most of the time.

Sue McGrew is gratefully acknowledged for always letting me know that at any time I was welcome to run away and become an artist with her (in the words of Pat Walsh, “It is good to have a backup plan.” And well, it is good – and comforting – to have a few backup plans, right?). I also thank her for her kind offers to deal with problems I run in to with the shovels and chainsaw that are the tools of her current trade (though I have so far declined her help due to the fact that even a chainsaw isn’t going to give my reactions higher yield or ee). It’s fun to have a veritable rock star (or at least, a TV-star and a world-renowned sand sculptor) on your side.

Finally, Tim Kowalczyk is acknowledged on multiple personal and professional levels as my best friend, teammate, and computational chemistry colleague. He has been the most important presence in my day-to-day life, and has put up with my incessant rants of the highs and lows of experimental chemistry. Also, for some reason he continues to put up with my jabs, including the assertion that he’s not a “real” chemist because he doesn’t mix chemicals together.

## Abstract

ACTIVATION AND CATALYTIC BOND FORMING REACTIONS AT
C—H BONDS OF $\eta^6$-TRICARBONYLCHROMIUM-COORDINATED BENZYLIC ARENES

Genette I McGrew

Patrick J. Walsh

Polyarylmethanes are an extremely valuable molecular scaffold used in fields ranging from materials chemistry to medicinal chemistry. They are found in dyes and semiconductor dopants and in drugs and drug precursors that address a variety of ailments ranging form depression and allergies to cancer and vascular disease. However, general, selective methods to synthesize polyarylmethanes are still limited. This dissertation describes some of the exploratory work done to outline the synthetic possibilities of deprotonated tricarbonylchromium-stabilized benzylic arenes in the context of selective bond-forming reactions to form polyarylmethanes. Various $\eta^6$-arene-tricarbonylchromium complexes are deprotonated with the mild silamide base $LiN(SiMe_3)_2$ and used directly in selective palladium-catalyzed syntheses of polyarylmethanes and other potentially valuable molecules from aryl bromides, aryl triflates, and vinyl triflates as coupling partners. In the first chapter, we illustrate the unique aspects of tricarbonylchromium activation, such as the ability to activate not just one C–H bond, but up to six in one flask, leading to highly substituted and sterically hindered products not accessible through traditional methods. Additionally, the sterically bulky nature of the tricarbonylchromium group is exploited to direct chemistry to the opposite face of polycyclic systems, leading to stereoselective reactions difficult to achieve selectively by other methods. Compatibility with α-heteroatom substitution and β-hydrogens is also demonstrated. Finally, an unusual mode of isomerization during the cross-coupling processes is explored. In the second chapter, the methodology for the synthesis of polyarylmethanes is expanded to asymmetric syntheses of di- and tri-arylmethane complexes. Low-barrier high-throughput experimentation (HTE) methodology is successfully implemented in the search for a highly selective ligand to achieve asymmetric cross-coupling. Medicinally valuable diarylmetheylamines are obtained from tricarbonylchromium-coordinated tertiary benzylamines in good to excellent enantiomeric excess. Finally, in the third chapter we use the products of the asymmetric cross-coupling with benzylamines to introduce novel methods to synthesize a new modular chiral P∧N ligand scaffold using a unimetal super-base. These ligands may be effective in future cross-coupling reactions and asymmetric catalysis.

## Table of Contents

## List of Tables

## List of Figures

## List of Schemes

# Introduction

## Catalysis and new catalytic reactions

> **Synthetic Chemistry:** the science dealing with the formation of more complex chemical compounds from simpler substances.
>
> *Mosby's Medical Dictionary*, 8th Ed.[1]

The development of bond forming reactions is by definition the central component of modern synthetic chemistry. In particular, the exploration of efficient catalytic bond-forming processes is a significant practical goal for many research groups and can be found in nearly every branch of chemistry today. The motivators for catalysis discovery are varied, but aside from basic science, one very practical reason for the continued advancement of catalytic reaction methodology is to make resource consumption and output more efficient. Reducing the time and energy spent on chemical synthesis, as well as reducing the hazards of the reactions themselves, are advantages reaped through development of efficient catalytic bond-forming processes, and they may often translate directly to reduced costs for the synthesis of valuable commodities, increased rate of output within the context of pharmaceutical drug discovery, and a reduced environmental impact.[2] The vast potential economic impact of advances in catalysis cannot be undersold here: catalysis has been estimated to account for about $3 billion a year of the United States chemical industry, and that each U.S. dollar spent on catalysis generates over $150 in products shipped by the U.S. chemical industry (data from 2005).[3]

Consider the exploration of efficient stereo- and enantioselective metal-catalyzed C–C bond-forming processes, which is not only seen in modern synthetic organic chemistry, but in nearly every other branch of chemistry, from medicine to materials science. There have been many recent advances in transition metal-catalyzed cross-couplings[4] such as the Suzuki-Miyaura,[5] Heck,[6] and direct arylation reactions.[7] Within the broad range of products accessed through these catalytic methods are valuable compounds and substructures that are difficult or impossible to access selectively with other methods.

Within the Walsh Group, research has been focused around stereo- and enantio-selective C–C, C–O, and more recently, C–N bond formation reactions and one-pot catalytic synthetic methods. As researchers in the field of methodological chemistry and catalysis, we strive to find and develop processes that can then be used in the field. Method scalability and inexpensive methods that utilize mild conditions are ideal. Within this area, both tricarbonylchromium activation and palladium cross-coupling to form C–C bonds are new topics of exploration for us, and it has been an honor to be the person starting work on this chemistry.

This dissertation describes some of the exploratory work done to outline the synthetic possibilities of lithiated tricarbonylchromium species in the context of catalytic bond-forming reactions. We take a chromium-stabilized organolithium species and directly use it in the palladium-catalyzed synthesis of polyarylmethanes and other valuable molecules such as chiral ligand scaffolds that may not be possible to synthesize selectively using other methods.

The polyarylmethane framework is found in compounds that have found application in a broad number of chemical fields, from semiconductors to anti-cancer drugs.[8,9] In fact, the diarylmethane substructure is considered a "privileged scaffold" in medicinal chemistry, that is, it is a skeleton that is frequently observed in pharmacophores.[10] Most methods to obtain polyarylmethanes still rely on Friedel-Crafts-type reactions and other electrophilc aromatic substitution (EAS) variants. However, these come with significant electronic and steric limitations. Thus, broadening access to polyarylmethanes through other methods such as transition-metal cross-coupling has become a hot topic in the last several years, but cross-coupling reactions with at least one $sp^3$-hybridized carbon are generally considered challenging.[11] Within current transition-metal mediated coupling of benzylic substrates to generate di- or triarylmethanes,[12] the benzylic synthon employed is typically the electrophile (more carbocationic in character). However, using our $\eta^6$-arene-tricarbonylchromium-based methodology, a stabilized nucleophilic (carbanionic) benzylic synthon is created from an $sp^3$-carbon center, resulting in a complementary approach to the previous chemistry.

Our method for benzylic cross-coupling using tricarbonylchromium as activator is efficient in that multiple benzylic C–H bonds can be activated with one metal tricarbonyl, and also stereoselective in that the tricarbonyl chromium can force reactivity on one side of the arene and even allow asymmetric reaction. Additionally, using the up-and-coming new technology of low-barrier high-throughput experimentation (HTE) methods in collaboration with Merck & Co., we were able to

identify a successful ligand on micromolar scale that helped us take our original non-enantioselective protocol and develop a highly enantiosemetric version which allowed us to synthesize chiral diarylmethylamines in good enantiomeric excess (ee). It is my hope that the fruits from the development of this methodology can become tools in the synthetic chemist's toolbox.

Finally, the planar chiral metal arene framework also has members in a family of "privileged" molecules, but in this case, it is the family of privileged chiral ligand scaffolds in asymmetric synthesis. Chiral tricarbonylchromium arene frameworks are present in a variety of highly successful ligands for metal-catalyzed reactions, in particular, asymmetric reactions such as hydrogenation and cross-coupling. The development of a new family of chiral diarylmethylamine-based chiral ligands is ongoing, but we hope that both the superbase developed for the selective synthesis of these catalysts, as well as the catalysts themselves, find specific applications in synthetic chemistry and catalysis.

References.


[1] *Mosby's Medical Dictionary*; Elsevier: **2008**; pp 2056.

[2] Sheldon, R. A.; Arends, I. W. C. E.; Hanefeld, U. In *Introduction: Green Chemistry and Catalysis;* Green Chemistry and Catalysis; Wiley-VCH Verlag GmbH & Co. KGaA: 2007; 2007; pp 1-47.

[3] Crabtree, S.; Ellis, P.; *Platinum Metals Rev*. **2010**, *54*, 162.

[4] Pablo Espinet, A. M. E. *Angew. Chem., Int. Ed*. **2004**, *43*, 4704-4734.

[5] (a) Masahiro, M. *Angew. Chem., Int. Ed*. **2004**, *43*, 2201–2203. (b) Molander, G. A.; Ellis, N. *Acc. Chem. Res*. **2007**, *40*, 275-286. (c) Martin, R.; Buchwald, S. L. *Acc. Chem. Res*. **2008**, *41*, 1461–1473.

[6] (a) Fu, G. C. *Acc. Chem. Res*. **2008**, *41*, 1555-1564. (b) Marion, N.; Nolan, S. P. *Acc. Chem. Res*. **2008**, *41*, 1440–1449. (c) Würtz, S.; Glorius, F. *Acc. Chem. Res*. **2008**, *41*, 1523-1533. (d) Vilar, R.; Christmann, U. *Angew. Chem. Int. Ed*. **2005**, *44*, 366–374. (e) Metal-Catalyzed Cross Coupling Reactions; 2 ed.; de Meijere, A.; Diederich, F., Eds.; Wiley-VCH: Weinheim, Germany, **2004**.

[7] (a) Alberico, D.; Scott, M. E.; Lautens, M. *Chem. Rev*. **2007**, *107*, 174-238. (b) Li, Y.; Li, B.; Lu, X.; Lin, S.; Shi, Z. *Angew. Chem. Int. Edit. Engl*. **2009**, *48*, 3817–3820.

[8] For examples of polyarylmethanes in materials science and dyes, see: (a) Duxbury, D. F. *Chem. Rev*. **1993**, *93*, 381-433. (b) Nair, V.; Thomas, S.; Mathew, S. C.; Abhilash, K. G. *Tetrahedron* **2006**, *62*, 6731-6747. (c) Müller, T. J. J.; Netz, A.; Ansorge, M.; Schmälzlin, E.; Bräuchle, C.; Meerholz, K. *Organometallics* **1999**, *18*, 5066-5074.

[9] For examples of polyarylmethanes in medicinal chemistry, see: (a) Parai, M. K.; Panda, G.; Chaturvedi, V.; Manju, Y. K.; Sinha, S. *Bioorg. Med. Chem. Lett.* **2008**, *1,* 289-292. (b) Indig, G. L.; Anderson, G. S.; Nichols, M. G.; Bartlett, J. A.; Mellon, W. S.; Sieber, F. *J. Pharm. Sci.* **2000**, *1,* 88-99. (c) Palchaudhuri, R.; Nesterenko, V.; Hergenrother, P. J. *J. Am. Chem. Soc*. **2008**, *130*, 10274-10281.

[10] Welsch, M. E.; Snyder, S. A.; Stockwell, B. R. *Curr. Opin. Chem. Biol.* **2010**, *14*, 347-361.

[11] (a) Netherton, M. R.; Fu, G. C. *Adv. Syn. & Catal*. **2004**, *346*, 1525-1532. (b) Frisch, A. C.; Beller, M. *Angew. Chem., Int. Ed*. **2005**, *44*, 674-688.

[12] For examples of benzylic cross-coupling, see: (a) Molander, G. A.; Elia, M. D. *J. Org. Chem*. **2006**, *71*, 9198-9202. (b) Kuwano, R.; Yokogi, M. *Org. Lett*. **2005**, *7,* 945-947. (c) McLaughlin, M. *Org.*

*Lett*. **2005**, *7*, 4875-4878. (d) Kofink, C. C.; Knochel, P. *Org. Lett*. **2006**, *8*, 4121-4124. (e) Imao, D.; Glasspoole, B. W.; Laberge, V. S.; Crudden, C. M. *J. Am. Chem. Soc*. **2009**, *131*, 5024-5025.

Chapter 1

Arene tricarbonylchromium benzylic anions in cross-coupling

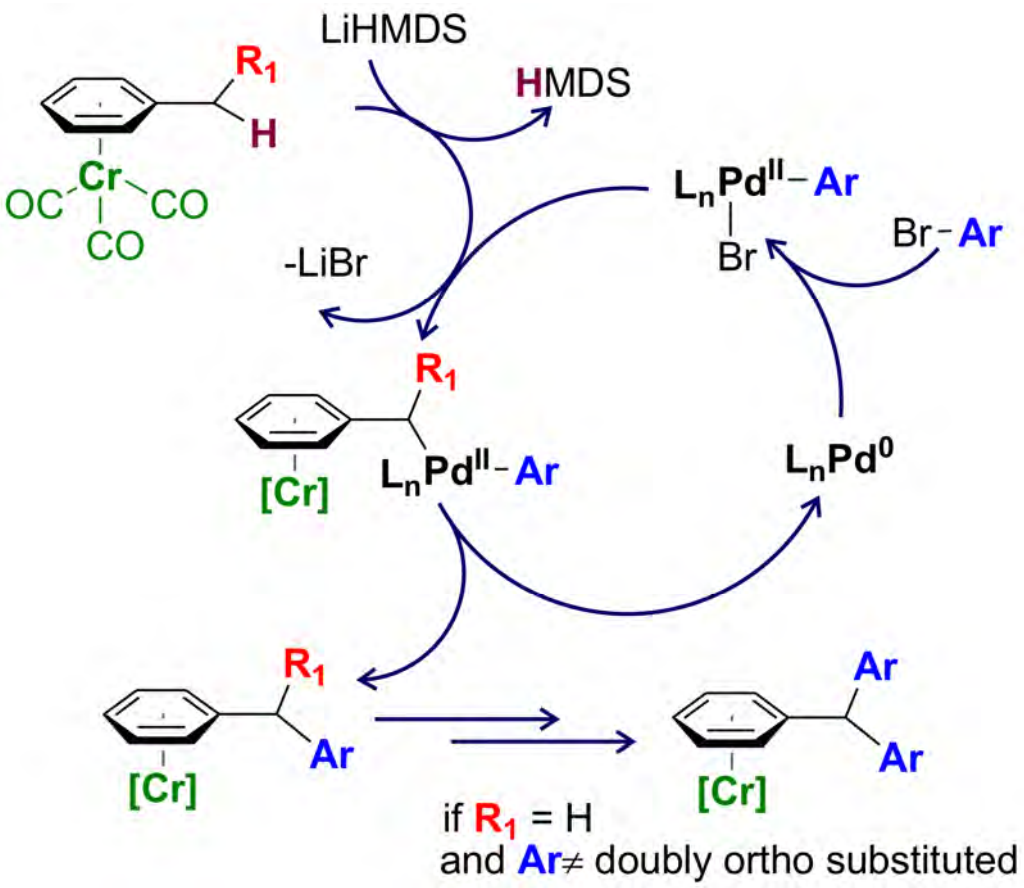

# Introduction

## *History and features of piano stool complexes*

The arene tricarbonylchromium complex, first reported in 1957,[1] was initially discovered upon attempts derivatize the bis-benzenechromium sandwich complex. Also called a "piano stool" complex, the tricarbonylchromium is a neutral chromium(0) complex with a pseudo-octahedral configuration. Other isoelectronic arene tricarbonyl complexes in groups 6 and 7 are also known. There are two main structural features of this and other arene tricarbonylmetal complexes. The first feature is a charge-neutral arene ring which is bound to the metal center in an $\eta^6$-fashion, like the cushion of a stool. The second is the presence of three electron-poor carbonyl ligands. The carbonyl ligands not only provide a large amount of steric bulk, but also accept electron density through back-bonding of *d*-electrons into the antibonding π* orbitals of the CO. Upon coordination to the $Cr(CO)_3$ metal fragment, the the arene ring is activated, and a drastic change in arene properties can be observed (Figure 1-1).[2]

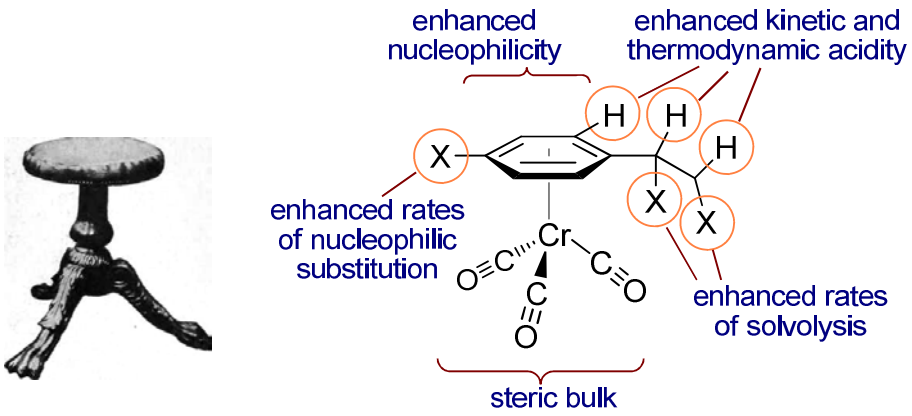


Figure 1-1: A photograph of a piano stool dated from the 1820s, compared to a generic tricarbonylchromium arene complex. Enhanced nucleophilicity, acidity of C–H bonds, and rates of solvolysis are characterisitic of these complexes. A sterically blocked face of the arene is also an important feature. All these properties are synthetically useful and conferred to an otherwise inert arene.

With these many activating properties of $\eta^6$-(Arene)tricarbonylchromium complexes, a number of research groups have taken advantage of these complexes for synthetic and catalytic use.[3,4,5] For

example, we can see enhanced nucleophilicity of the ring once it is coordinated to the $Cr(CO)_3$ group. This has recently been exploited in the activation of Ar-F bonds toward nucleophilic attack, as in the following example by Costa and coworkers (Scheme 1-1).[6] The steric bulk can also direct chemistry to a single side of the arene ring and enhance stereodifferentiation, allowing planar chirality and stereoselective syntheses, as in the total synthesis of (−)-steganone.[7] In the total synthesis of lasubine(I) by Kündig and coworkers, a Diels-Alder on the top face of the ring sets stereochemistry for the subsequent steps (Scheme 1-2).[8]

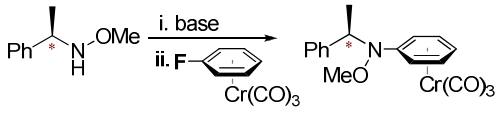


Scheme 1-1: Nucleophilic addition to the tricarbonylchromium-activated arene ring

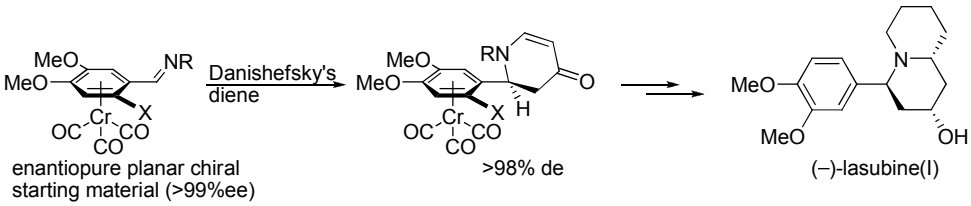


Scheme 1-2: Kündig's stereo- and diastereo- selective total synthesis of (−)-lasubine(I) uses the steric directing ability of the tricaronbylchromium for the highly selective (>98% de) Diels-Alder reaction

A third significant activating feature of the tricarbonylchromium group is the ability to stabilize charge on the coordinated arene, directly on the arene (anions), on the benzylic position (anions and cations),[9] and farther from the ring.[10] This enhanced thermodynamic — and kinetic[11] — acidity allows selective or directed deprotonation, often using comparatively mild conditions compared to conditions typically used for deprotonating unactivated C–H bonds. The combination of ease of arene lithiation and planar chiral geometry has led to the synthesis of various ligands utilizing the arene–$Cr(CO)_3$ scaffold, in particular structural analogues of ferrocenyl ligands and other asymmetric ligands with planar chiral and central chiral character (Figure 1-2).[12]

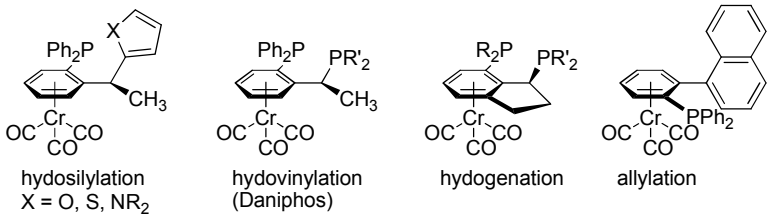


Figure 1-2: Chromium arene complexes as ligands for asymmetric catalysis

The enhanced acidity of the benzylic position has also expanded the use of the benzylic fragment from the familiar stabilized benzylic cations to stabilized benzylic anions as well. The chromium-stabilized benzylic species can thus exhibit reversed-polarity reactions, for example through deprotonation of the benzylic C–H with milder bases, followed by an electrophilic quench of the anionic carbon.[13] The synthetic utility of the tricarbonylchromium benzylic anion has been explored by several groups, including Kalinin and coworkers (Scheme 1-3).[14] Additionally, Kalinin et al have used transmetalation from lithium to zinc to generate a reagent for Negishi-style cross-coupling with aryl iodides, though yields were low (average <40% yield, Scheme 1-4).

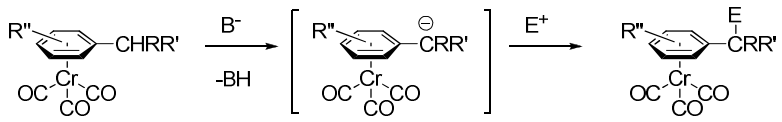

Scheme 1-3: Deprotonation and electrophilic quench of the benzylic position (Kalinin et al)[14]

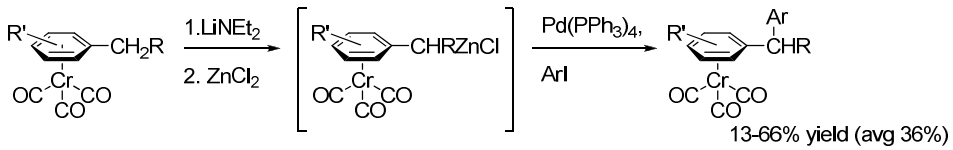


Scheme 1-4: Generation of a Negishi coupling reagent from a benzylic anion and use in palladium-catalyzed cross-coupling (Kalinin et al)[14]

Here we should emphasize the nature of the change in C–H bond acidity of a tricarbonylchromium benzylic complex versus the free arene. The benzylic position of a Cr-coordinated arene is considered about as acidic as nitrotoluene (using $pK_a$, a thermodynamic measure of acidity), but it is important to note that thermodynamic and kinetic acidities are not necessarily directly comparable.[15] This point in especially salient in arene-$Cr(CO)_3$ complexes. In

fact, coordination of an arene to the $Cr(CO)_3$ fragment increases the kinetic acidity of the benzylic C–H bond by a factor of ~$10^5$ in comparison to an uncoordinated benzylic arene.[11] These particular aspects of activation should be studied in greater depth. Considering the unusually stabilized tricarbonylchromium benzylic anion, we could imagine a highly stabilized organolithium species, for example, that could potentially be used in metal-catalyzed cross-coupling reactions. Specifically, we envisioned palladium-catalyzed cross-coupling reactions of an anionic benzylic species with easily-obtained aryl halides. Such a route could potentially be used for the synthesis of polyarylmethanes.

### *Polyarylmethanes and benzylic cross-coupling reactions*

Polyarylmethanes are a subset of useful chemical scaffold that have found application in a broad number of chemical fields, from dyes[16] and fluorophores in materials science[17,18] to medicinal chemistry, such as treatments for vascular disease[19] and cancer.[20] Of these, the diarylmethane substructure is considered a privileged structure — that is, the skeleton is a substructure frequently observed in biologically active natural products and pharmaceuticals. Triarylmethanes are currently being explored in several potential cancer drugs (Figure 1-3).[21] Developing methods to access polyarylmethanes has become an important topic in synthetic chemistry and catalysis over the last decade.[22]

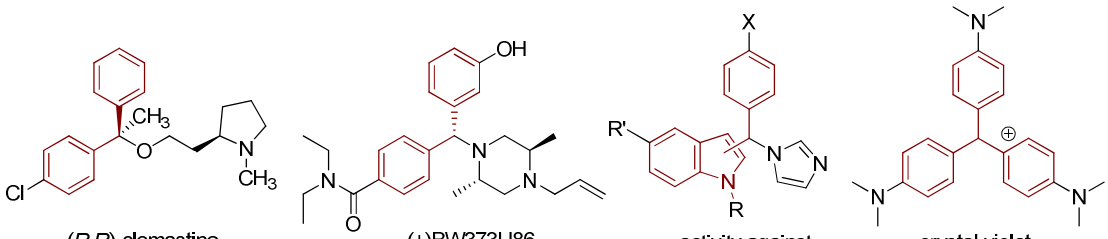


Figure 1-3: some biologically active polyarylmethanes

Most commercial methods to generate polyarylmethanes still rely on Friedel-Crafts-type electrophilic aromatic substitution (EAS) processes to generate them (Figure 1-4 A).[23] These reactions are typically are restricted in reactivity and selectivity. For example, the nucleophile

substrate must be electron-rich and unhindered for adequate reactivity. Additionally, the regioselectivity is highly dependent on sterics and the relative directing ability of the other arene substituents. Electron-poor- or *meta*- substitution of the arene tends to be problematic for these reasons. Other known alternatives that have been recently developed,[24,25] include metal-catalyzed cross-coupling at the $sp^3$ benzylic center.[26] However, cross-coupling reactions with at least one $sp^3$-hybridized carbon tend to be more difficult than reactions with $sp^2$– or *sp*-hybridized partners.[27] Therefore, current access to polyarylmethanes remains limited (Figure 1-4 B).[28]

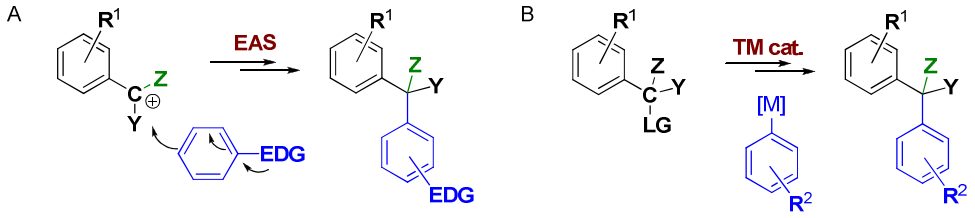


Figure 1-4: Typical syntheses of polyarylmethanes use carbocationic benzylic synthons, such as in [A] Friedel-Crafts reactions, or [B] transition-metal catalyzed cross-coupling with Bn-LG[a] species.

These existing methods for synthesis also typically make use of an electrophilic (carbocationic) benzylic synthon, with a leaving group such as a halide, carbonate, or ester in the benzlic position.[29] These reactions also often require heating and harsh conditions, or large excess of reagent for adequate reactivity.[30] While pharmaceutical products must increasingly be synthesized in enantiopure form, many processes still rely on chiral auxiliaries and chemical or chromatographic resolution of enantiomers. Finally, while there has been work on asymmetric synthesis of diarylmethanes and heteroaromatic triarylmethanes, there are still no existing methods to synthesize non-heteroaromatic triarylmethanes in a catalytic enantioselective manner.[31]

[a] LG = Leaving Group, e.g. halide, triflate, carbonate.

We wondered if it would be possible to create a complementary transition-metal mediated method for polyarylmethane synthesis that both circumvented some of these limitations and expanded access to this family of compounds by using the tricarbonylchromium-coordinated benzyllithium as the benzylic synthon (Scheme 1-5). Typically, carbanionic reagents for catalysis are based on metals such as boron, tin, or zinc to temper reactivity compared with alkali and alkali earth organometallics. They are also predominantly $sp^2$-hybridized at the C–M bond.[32] Direct use of an organolithium species in catalysis is considered by many to be impractical and difficult due to its high reactivity and low functional group tolerance. On the other hand, some limited examples of organolithium cross-coupling were explored in the 1970s.[33] The use of organolithium reagents as raw materials in catalysis has been touted as efficient and desirable because their use avoids stoichiometric transmetalation to milder but often more toxic metals. Many of carbanionic metal reagents are, in fact, derived from lithiated species, which are in turn often prepared from carbon–halogen bonds. We envisioned *in situ* deprotonation at the benzylic position with a mild base (Figure 1-5 B) would allow us to use the stabilized benzylic anion directly in a metal-catalyzed cross-coupling cycle (Figure 1-5 A, C,D, Scheme 1-5). Ideally, we could then install additional functionality by taking advantage of the remaining C–H bond(s) for further elaboration (Figure 1-5, E, Scheme 1-5).[34]

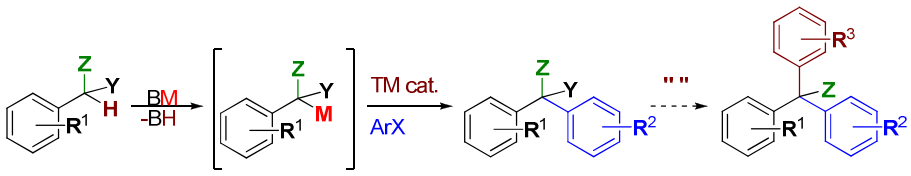


Scheme 1-5: Concept for the use of a stabilized benzylic anion synthon in a benzylic cross-coupling reaction. Ideally, one or more aromatic groups can be installed.

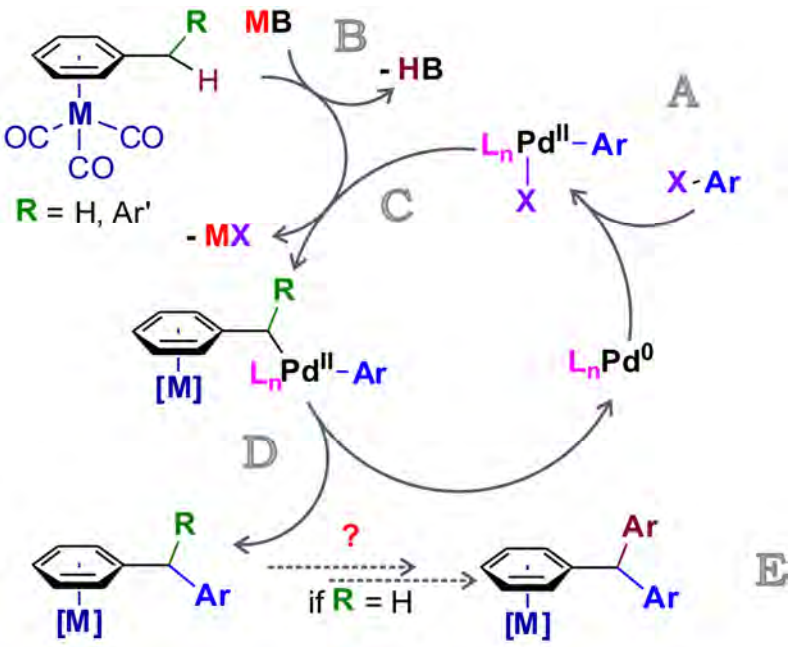


Figure 1-5: Envisioned palladium-catalyed cross-coupling cycle starting from [A] oxidative additon of an aryl halide to Pd(0), [B] in-situ deprotonation of the $sp^3$-benzylic C–H bond of a stabilized arene tricarbonylmetal complex, [C] transmetalation with the $L_nPd(II)ArX$ species, and then [D] reductive elimination to form the polyarylmethane and regenerate the Pd(0) species. [E] Further reaction, either sequentially or one-pot is considered.

## Initial Studies

### *Tricarbonylmolybdenum as activating metal fragment*

Initial studies were performed with molybdenum complexes of simple benzylic arenes, in part due to the lower stigma associated with using molybdenum as an activating metal relative to chromium. Chromium has received much negative attention due to its toxicity in higher-valent states.[35,36] Arene–molybdenum complexes also seemed to be an ideal solution to benzylic activation. The weaker arene–Mo bond was considered a favorable property for arene exchange, allowing the activating metal carbonyl to be catalytic. Arene exchange is known for the benzene molybdenumtricarbonyl complex at room temperature.[37] Thus, $\eta^6$-mesitylene molybdenumtricarbonyl (MoMes, **1**) and $\eta^6$-toluene molybdenumtricarbonyl (MoTol, **2**) were prepared in low yields consistent with literature procedures (Scheme 1-6).[38,39]

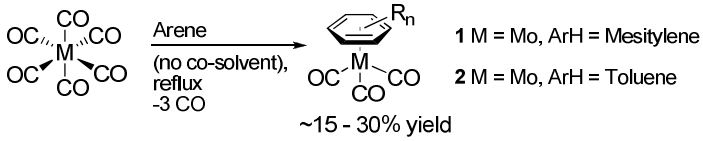


Scheme 1-6: General scheme for the synthesis of $\eta^6$-arene-tricarbonylmetal complexes from metal hexacarbonyl precursor.

Unfortunately, several disadvantages became clear during preliminary studies, mainly regarding practical concerns of stability and handling. The molybdenum complexes were extremely light and moisture sensitive and moderately unstable in solution. They were also easily oxidized by trace amounts of air and quickly displaced by strong donor ligands such as THF (Figure 1-6),[40] leading to decomposition products. Furthermore, after mild heating, metallic molybdenum is often deposited on reaction vessels. In fact, when a small amount of the more stable complex **1** was dissolved in THF, formation of undesired (and more air-sensitive) $(THF)_3Mo(CO)_3$ species[40] occurred within minutes. Because palladium-catalyzed coupling reactions with reactive organometallics tend to employ ethereal or coordinating solvents, this result ruled out a large fraction of initial reaction conditions. Additionally, common arene solvents exchange with the parent arene complex, likely limiting us to solvent compositions containing either aliphatic hydrocarbon or reagent arene as solvent. While molybdenum may be a metal to return to for the labile property of the arene, for initial cross-coupling reaction development, a more robust and easy-to-manage arene activator was desired.

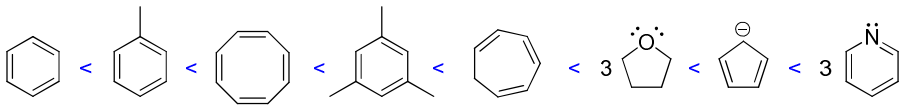


Figure 1-6: Order of stability of ligands in $L_3$-tricarbonylmolybdenum complexes. The range of energies here spans >30 kcal/mol relative to $\eta^6$-(benzene)tricarbonylmolybdenum.

### *Tricarbonylchromium as an alternative to molybdenum*

Tricarbonylchromium arene complexes were next explored as an alternative to molybdenum. Unlike molybdenum, in $\eta^6$-(arene)$Cr(CO)_3$ complexes the arene–Cr bond is not easily displaced by strongly donating ethereal solvents.[41] Moreover, the complexes are considerably more light- and

air- stable, and can even be purified via silica gel chromatography.[2] The complexes still have the ability to undergo arene exchange reactions, and can also be demetallated by simply adding iodine or exposing a solution of the complex to bright light and air.[42] Test complexes of tricarbonylchromium-coordinated toluene (CrTol, **3**) and diphenylmethane (CrDPM, **4a**) were synthesized in good yield from existing literature procedures.

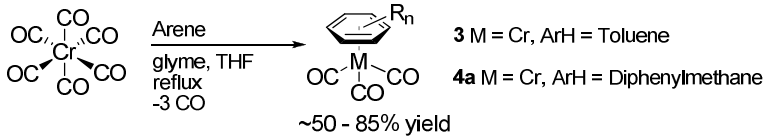


Figure 1-7: Synthesis of $\eta^6$-(arene)-tricaronylchromium complexes **3** and **4a**.

First, we examined conditions for deprotonation of the benzylic hydrogens of ($\eta^6$-arene)$Cr(CO)_3$ complexes. Selected thermodynamic acidities are noted below in Table 1-1.[43] It seemed that *tert*-butoxide and amide bases would be appropriate bases to start with due to a similar range of p$K_a$ values relative to the anticipated range of acidity in coordinated benzylic arenes. In particular, NaO*t*Bu and LiHMDS[a] have been successfully used for palladium-catalyzed α–arylation of ketones, another case where a highly labile and stabilized C–H bond undergoes deprotonation and cross-coupling.[44,45]

Table 1-1: Thermodynamic acidities of selected conjugate acids and free arenes.

| **Proton** | $^{i}Pr_2N$-**H** | HMDS-**H** | $^{t}$BuO-**H** | $PhCH_3$ | $Ph_2CH_2$ | $Ph_3C$-**H** | 4-$NO_2$-$C_6H_4$-$CH_3$ |
|---|---|---|---|---|---|---|---|
| **p$K_a$** | 36[a] | 30[b], 26[a] | 29.4[b] | 43[b] | 32.3[b] | 30.6[b] | 20.4[b] |

[a] p$K_a$ value in THF. [b] p$K_a$ value in DMSO.

CrTol **3** and CrDPM **4a** were reacted with base in NMR tubes to asses the extent of deprotonation in THF (Scheme 1-7). Addition of LiHMDS to CrDPM (**4a**) led to immediate change in color from

[a] LiHMDS = lithium hexamethylsilazane, $LiN(SiMe_3)_2$

yellow to a deep orange, and deprotonation was found to be approximately 50% overall.[a] In the case of CrTol (**3**), color change was not noticeable but this was not surprising: only about 10% of **3** was deprotonated with 1 equivalent of LiHMDS. Equilibrium for both LiHMDS deprotonation reactions was established quickly (within minutes), and decomposition of the anion did not seem to be a problem. Earlier work by Kalinin et al on benzylic ($\eta^6$-arene)$Cr(CO)_3$ complexes deprotonated using the much stronger lithium amide base $LiNEt_2$ indicated that the lithiated species were not thermally stable above 0 °C.[b,46] These favorable results paved the way for screening additional cross-coupling experiments.[c]

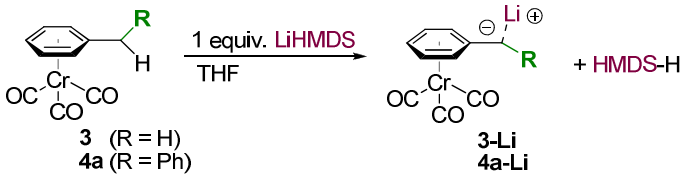


Scheme 1-7: Deprotonation experiments of **3** and **4a** using LiHMDS as base, observed by $^1H$ NMR. The monomeric organolithium is depicted for clarity.

[a] Extent of deprotonation was determined by integration of arene protons of **4a** vs **4a-Li** in protio-THF by $^1H$ NMR.

[b] Kalinin and coworkers claim that the practical barrier to using lithiated species of tricarbonylchromium for benzylic functionalization (generated using a strong lithium amide base $LiNEt_2$) is the insufficient thermal stability of the lithium derivatives, which are only "stable for a few minutes at 20 °C"

[c] Experiments with NaO*t*Bu as base were difficult to monitor *in situ* due to the low solubility of both the base and formation of orange insoluble precipitate.

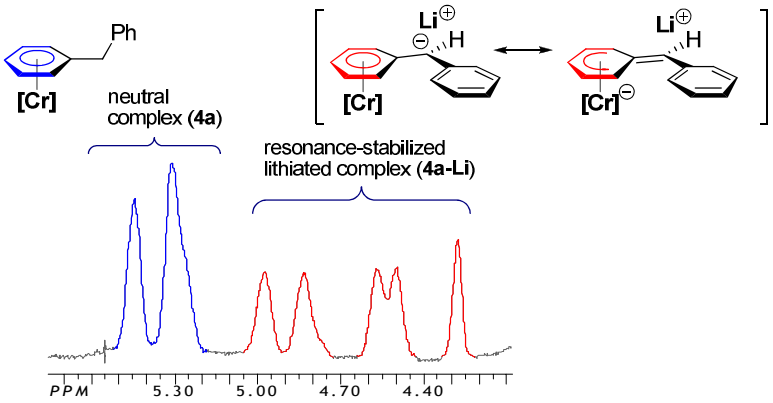


Figure 1-8: Inset of a protio-THF $^{1}$H NMR and diagram depicting the successful deprotonation (~50%) of **4a** (blue peaks), indicated by an upfield shift and diasterotopic arene hydrogens in **4a-Li** (red peaks) (Scheme 1-7). Monomeric anion is depicted for clarity.

*Coupling diarylmethanes with aryl bromides*[a]

The tricarbonylchromium complex of diphenylmethane CrDPM (**4a**) was used as a starting material for initial cross-coupling reactions due to the more stabilized nature of the chromium-coordinated diarylmethyl anion (Scheme 1-8). Thus, a THF solution of **4a**, 4-bromotoluene, a slight excess (1.5 equiv.) of base, and catalyst (3–10 mol%) was reacted at room temperature or 55–60 °C to yield the tricarbonylchromium-coordinated triarylmethane (**5a**) (Scheme 1-8, Table 1-2).

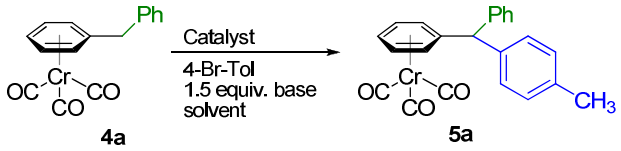


Scheme 1-8: Optimization of cross-coupling reaction with **4a** to form **5a**.

[a] Initial reaction optimization was done in collaboration with undergraduate researcher J. Temaismithi.

Table 1-2: Initial screen of conditions for the coupling reaction of **4a** with 4-bromotoluene.

| entry | catalyst | mol % | Base* | time (h) | yield (%) | rec. SM (%) |
|---|---|---|---|---|---|---|
| 1 | $PdBr_2(PPh_3)_2$ | 10 | $LiO^tBu$ | 24 | 0† | – |
| 2 | $PdBr_2(PPh_3)_2$ | 5 | $NaO^tBu$ | 24 | 0† | 67 |
| 3 | $PdCl_2(PPh_3)_2$ | 3 | LiHMDS | 20 | 70† | 5 |
| **4** | **$PdCl_2(PPh_3)_2$** | **3** | **LiHMDS** | **0.75** | **91** | **0** |
| 5 | $PdCl_2(PPh_3)_2$ | 3 | LDA | 12 | 50 | trace |
| 6 | $PdCl_2(PPh_3)_2$ | 5 | NaHMDS | 18 | 26 | 38 |
| 7 | $PdCl_2(PPh_3)_2$ | 5 | KHMDS | 20 | 9 | 48 |
| 8 | $NiCl_2(PPh_3)_2$ | 5 | LiHMDS | 20 | 0 | 29 |
| 9 | $Pd(PPh_3)_4$ | 5 | LiHMDS | 17 | 67 | <20 |
| 10 | $PdCl_2$(dppf) | 5 | LiHMDS | 19 | 78 | <20 |

* HMDS = hexamethyldisilazide, $N(SiMe_3)_2$; LDA = lithium diisopropylamide. †Conducted at room temperature.

Neither alkoxide bases $LiO^tBu$ or $NaO^tBu$ resulted in the formation of coupling product **5a** when run at room temperature in THF (entries 1 and 2). On the other hand, switching to LiHMDS[a] led to a bright red solution that showed clean and moderate conversion on TLC.[b] Unfortunately, attempts to isolate the product using a standard aqueous workup and extraction resulted in low isolated yields. A milder workup involving minimal use of water and direct column purification of the crude reaction mixture was found to be more suitable. Encouragingly, running the reaction for 20 h at room temperature, followed by the new purification procedure led to 70% isolated yield of the coupling product (entry 3). While organolithium reagents are typically sensitive to high temperatures, in our case raising the temperature to 55–60 °C led to clean and rapid formation of product after only 45 minutes. Thus, compound **5a** was obtained in 91% isolated yield using only 3 mol% of simple *bis*-triphenylphosphine palladium(II) precatalyst $PdCl_2(PPh_3)_2$ (entry 4). A stronger lithium base, such as LDA,[c] led to the formation of multiple products and decomposition (entry 5); adding any amount of butyllithium quickly led to decomposition of

[a] LiHMDS = Lithium hexamethyldisilazide, $LiN(SiMe_3)_2$
[b] TLC = Thin-Layer Chromatography, run on glass-backed silica.
[c] LDA = Lithium diisopropylamide, $iPr_2NLi$.

starting materials above 0 °C. Other bases such as NaHMDS (entry 6), and KHMDS (entry 7) were also explored, but the reactions became cloudy and were slower and less clean than with LiHMDS. A nickel precatalyst ($NiCl_2(PPh_3)_2$, entry 8) was ineffective, and decomposed the starting material over time (20 h). Other palladium-based precatalysts were also examined, but both $Pd(PPh_3)_4$ and $PdCl_2$(dppf)[a] were less active (entries 9 and 10). The optimal conditions listed in entry 4 of Table 1-2 were used as the base conditions for examining substrate scope of the coupling reaction.

## Diphenylmethane cross-coupling scope

CrDPM (**4a**) couples readily with a variety of aryl bromides to generate triarylmethane complexes **5a**–**5k** in good yield (81–94%) (Scheme 1-9, Table 1-3). 4-Bromotoluene (**5a**, entry 1, bromobenzene (**5b**, entry 2), and 2-bromonaphthalene (**5c**, entry 3) all provided ≥90% yield of desired coupling product. The presence of low to moderately electron-withdrawing groups on the aryl bromide also provided desired coupling products **5d** (4-Cl- substitution, entry 4) and **5e** (4-F substitution, entry 5), though yields in this case were slightly lower. The intact C–X (X = Cl, F) bonds have the potential to be further functionalized through lithium-halogen exchange or additional transition-metal mediated cross-coupling processes,[47] allowing additional structural complexity to be added. It should be noted that strongly electron-withdrawing aryl bromides showed little to no yield: desired product was not observed for *p*-$NO_2$-bromobenzene, and only 27% yield was obtained for *p*-$CF_3$ substituted product **5f** (entry 6). In the case of the very electron-rich *p*-$NMe_2$- and *p*-MeO- substituted products **5g** (entry 7) and **5h** (entry 8), yields were very high: 91% and 94%, respectively. This indicates that oxidative addition is not likely a bottleneck in the catalytic cycle.

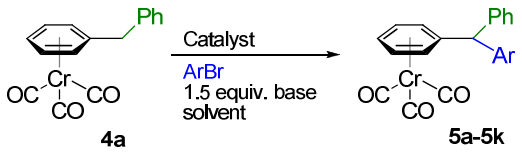


[a] dppf = bis-diphenylphosphinoferrocene

Scheme 1-9: Single coupling of **4a** with aryl bromides to form triarylmethane complexes: reaction scope (Table 1-3).

Table 1-3: Scope of the single-coupling reaction of **4a** with ArBr (Scheme 1-9).

| Entry* | | Ar = | yield† |
|---|---|---|---|
| 1 | **5a** | 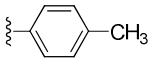 | 91‡ |
| 2 | **5b** |  | 92 |
| 3 | **5c** | 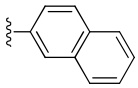 | 90 |
| 4 | **5d** | 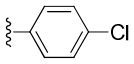 | 83 |
| 5 | **5e** | 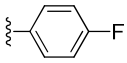 | 88 |
| 6 | **5f** | 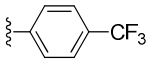 | 27 |
| 7 | **5g** | 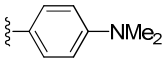 | 91 |
| 8 | **5h** | 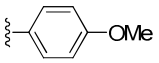 | 94 |
| 9 | **5i** | 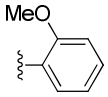 | 91 |
| 10 | **5j** | 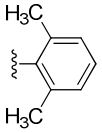 | 81◊ |
| 11 | **5k** | 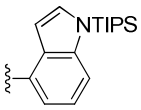 | 89 |

*Conducted at 55–60 °C using 1.5 equiv. LiHMDS, 1.5 equiv. ArBr, 3–5 mol % $PdCl_2(PPh_3)_2$, and THF as solvent. †Isolated yields. ‡Averaged over 3 runs. ◊A small amount (<10%) of unreacted starting material was also isolated.

Steric issues did not seem to be a concern for the substrates explored. Single *ortho*-substitution on the aromatic ring (2-MeO-, **5i**, Table 1-3, entry 9) gave an isolated yield comparable to arenes with *para*-substitution (91%); a single-crystal X-ray crystal structure was obtained, and is included below (Figure 1-9). Even the bulky 2,6-subsituted aryl bromide 2-bromo-1,3-dimethylbenzene was a successful reaction partner, though the reaction took longer and had a slightly lower yield of product **5j** (81%, entry 10). TIPS-protected 4-bromoindole showed good reactivity as well to provide **5k** in 89% yield (entry 11), illustrating the complementary synthetic utility of our method compared with EAS processes in producing medicinally relevant structures.[48] EAS methods to install the indole functionality would favour construction of the C–C bond at the 3-position (alternately, at the 2-position if the 3-position is blocked).[49]

In no instances was a second coupling event to form **6** observed, despite the fact that the benzylic C–H should be more acidic, and the anion should be more stabilized than the *mono*- or *di*- arylmethane complexes. This is likely due to sterics of the tertiary triarylbenzyllithium species, which should hamper transmetalation with the active catalyst center despite deprotonation of the triarylmethane.[a]

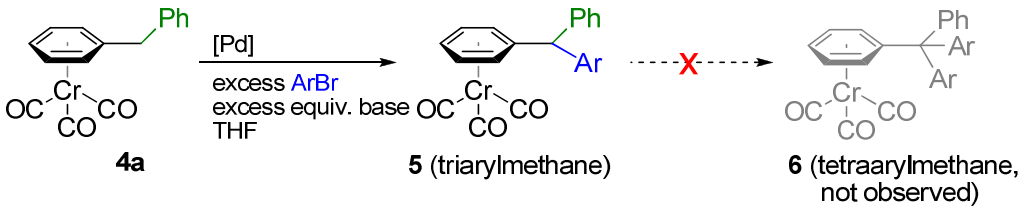


Scheme 1-10: No formation of tetraarylmethane product **6** was observed under these conditions.

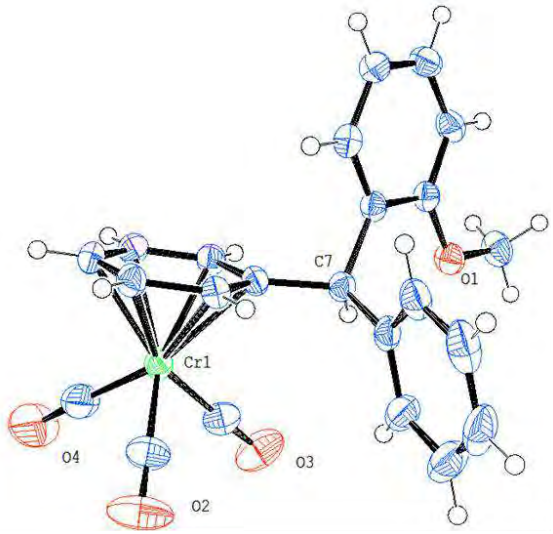


Figure 1-9: X-ray crystal structure of single-coupled product **5i**; thermal elipsoids are at 50% probability. Full details can be found on page 249.

[a] The topic of triarylmethane deprotonation is addressed in greater depth on p. 19 (Scheme 1-12).

## Examining cross-coupling at a less acidic toluene complex.

Following the success of coupling at the stabilized diphenylmethane complex, we considered the possibility of benzylic cross-coupling at the less acidic methyl of CrTol (**3**). Despite the low percentage of deprotonated species in solution noted in the NMR experiment discussed earlier (see Figure 1-8, p. 12), it was possible that the kinetically fast and reversible deprotonation would still allow cross-coupling to occur (similar to reactions with ketones, in which the active enolate species is a minor component of the solution). CrTol (**3**) was reacted with bromobenzene in THF with $PdBr_2(PPh_3)_2$ (Table 1-4). Disappointingly, coupling did not proceed at room temperature with 1 equivalent of base. However, upon adding larger excess of base to increase the fraction of deprotonated primary benzyllithium in solution, moderate amounts of product **5b** were observed (18% isolated yield) after 24h. Finally, upon heating the reaction and adding additional base, excellent conversion to coupling products was seen, resulting in up to 90% isolated yield of the triarylmethane complex (**5b**).

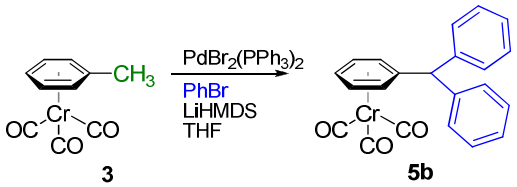


| Equiv. LiHMDS | Temp | Yield (%) |
|---|---|---|
| 2.2 | RT | 18 |
| 2.4 | 50 °C | 55 |
| 2.8 | 55 °C | 90 |

Table 1-4: Double-coupled triarylmethane **5b**, not the diarylmethane, was isolated after reaction of **3** with bromobenzene at elevated temperature and with excess base.

Interestingly, in all cases (even when only 1 equivalent of base was used), only the *tri*arylmethane complex **5b** was isolated as the main product. One might initially expect the more sterically-hindered secondary organolithium **4a-Li** to react slower with the palladium catalyst relatively to the primary organolithium **3-Li**. However, it seems that this effect is overridden by the greater acidity of the diphenylmethane intermediate **4a** relative to **3** (Scheme 1-11), leading to a predominance of **4-Li** in solution compared to **3-Li**. Thus, preferential reactivity of the

diarylmethane to form triarylmethane is observed, and little if any diarylmethane intermediate is intercepted.[a]

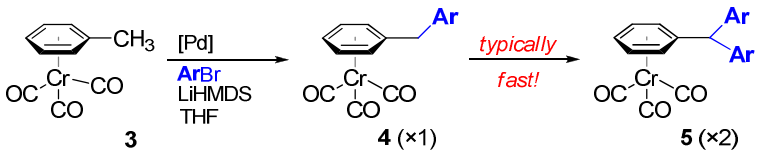


Scheme 1-11: Reaction of CrTol (**3**) with most aryl bromides yields *tri*-arylmethane due to the greater acidity of the diarylmethane **4** and higher proportion of **4-Li** in solution.

The scope of the double-coupling reaction was next explored. Triarylmethanes (Table 1-5, entries 1–8) were synthesized in good yields from CrTol (**3**) and aryl bromides using a moderate excess of LiHMDS (2.8 equiv.) and 4–8 mol % palladium catalyst loading (Scheme 1-11). As in the case of the single-coupling reaction with CrDPM **4a** (see p. 15), more electron-withdrawing aryl bromides (entries 2 and 3) performed slightly poorer with respect to the more electron-rich and electron-neutral aryl bromides (entries 1, 5–8) and required slightly higher catalyst to achieve similar yields. In the case of entries 4 and 6, some unexpected isomerization and side products were observed, which will be discussed in detail later in this chapter (see p. 40).

[a] Referring back to the $^1$H NMR deprotonation study (p. 25), the extent of deprotonation of Cr-diphenylmethane **4a** was several times higher than that of CrTol **3** (50% vs 10%) in THF.

Table 1-5: Single and double coupling reactions of **CrTol** (**3**) with aryl bromides to yield *di-* and *tri-*arylmethanes **4** and **5**.

| Entry# | | Ar = | Yield (%)* |
|---|---|---|---|
| 1 | **5b** |  | 90 |
| 2 | **5l** | 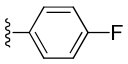 | 83 |
| 3 | **5m** | 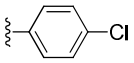 | 78 |
| 4 | **5n** | 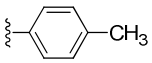 | 78+ |
| 5 | **5o** | 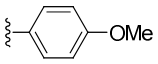 | 84 |
| 6 | **5p**,**5p'** | 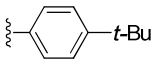 | 93† |
| 7 | **5q** | 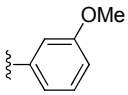 | 86‡ |
| 8 | **5r** | 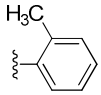 | 88 |
| 9 | **4b** | 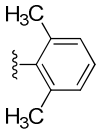 | 86+ |
| 10 | **4c** | 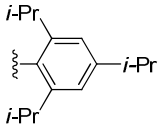 | 81‡ |

# Reactions were conducted at 45–60 °C using 2.8 equiv. LiHMDS, 3 equiv. ArBr, 4–8 mol% $PdCl_2(PPh_3)_2$, and THF as solvent. *Isolated yield. +Isolated yield of desired triarylmethane product; 6% walk/polymerization product isolated separately, see p.40. †Isolated in a mixture of isomers; running the same reaction with higher catalyst loading led to 82% yield of the major product **5p** after purification ‡Trace starting material **3** recovered.

While overall the isolated yields are slightly lower than the single-coupling case, it should be kept in mind that isolated yields are after two *consecutive* cross-coupling events, in which the single $Cr(CO)_3$ moiety activates two separate C–H bonds. This is a more efficient one-pot route compared to sequential installation of two aryl groups through generation and use of stoichiometric transmetalation reagents, which can only effect one coupling per equivalent. The crystal structure of the double-coupled triarylmethane **5n** was obtained and is included below (Figure 1-10).

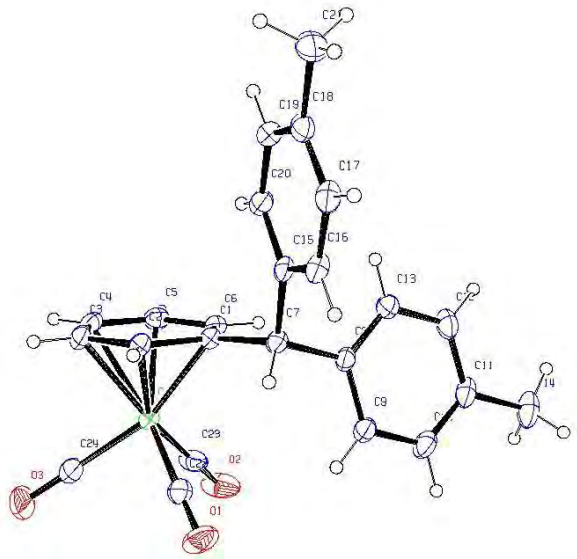

Figure 1-10: X-ray crystal structure of **5n**. Thermal ellipsoids are at 30% probability. Full details can be found on p. 257.

While a single *ortho* substituent on the aryl group did not seem to drastically affect the outcome of the double-coupling reaction to form sterically congested product **5r** (Table 1-5, entry 8), adding a second *ortho* substituent to the aryl bromide led to the exclusive isolation of diarylmethanes **4b** and **4c** in 81–86% yield (entries 9, 10). That is, the steric bulk was increased to such a level that the diarylmethane could not easily adopt a planar $sp^2$-hybridized benzylic position upon deprotonation (steric inhibition of conjugation, Figure 1-11 below), and the reaction stopped at a the single-coupling product. It should be noted that 1,3,5-triisopropylbromobenzene used in entry 10 is an extremely unusual coupling partner, as the massive sterics for this arene typically do not allow it to be a successful cross-coupling substrate.

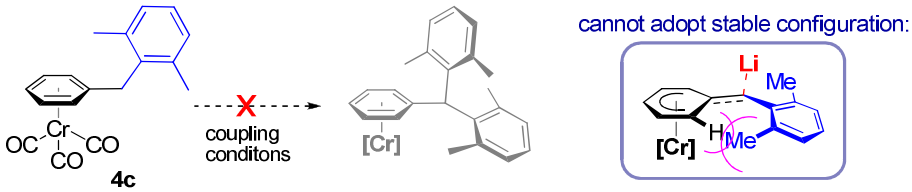


Figure 1-11: A deprotonated diarylmethane with two ortho substituents is not able to stabilize anionic charge on tricarbonylchromium thorugh conjugation due to steric limitations at the benzylic carbon, which cannot easily adopt an $sp^2$-configuration.

To verify that these bulky diarylmethanes do not deprotonate under our reaction conditions, a sample of **4c** was combined with LiHMDS (8 equiv.) and heated in THF for 15 h at 60 °C. Upon quenching with $D_2O$, no D incorporation was detected by $^1H$ NMR. The tricarbonylchromium complex did, however, partially decompose, likely due to the harsh conditions and lengthy reaction time.

As in the coupling reactions with CrDPM (**4a**), Tetraarylmethane products were not observed with these conditions (see Scheme 1-10, p. 16), despite the added stability of the tertiary benzylic anion. This led us to question whether the anion was forming in solution in the first place. Triarylmethane **5l** was deprotonated with 2 equivalents of LiHMDS at both room temperature and at 65 °C, then shaken with $D_2O$ to quench the anion (Scheme 1-12). While ~95% deuterium incorporation was observed for the heated reaction, no detectable deuterium incorporation was observed in the reaction at room temperature. This indicates that the triarylmethane has a higher thermodynamic acidity ($pK_a$), but that the kinetic barrier to deprotonation is higher than that of either the *di-* or *mono-* arylmethane.

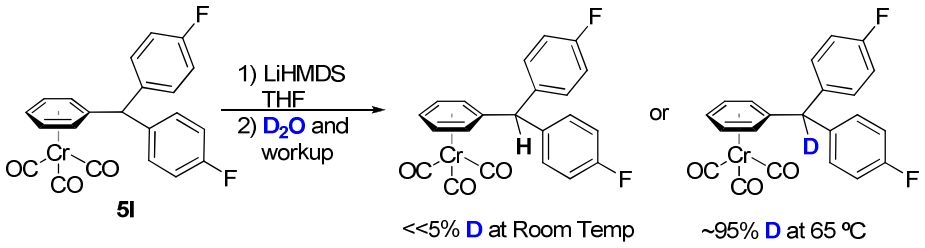


Scheme 1-12: Deprotonation experiments with triarylmethane **5l** indicates a higher acidity than a *di-* or *mono-* arylmethane, but the kinetic acidity is lower than expected: no noticeable D-incorporation was observed at room temperature (determined by $^1H$ NMR).

A large-scale reaction was run at 5 mmol to generate a triarylmethane that would not be able to be produced through traditional Friedel-Crafts processes (Scheme 1-13). The CrTol complex (**3**) was reacted with 3-bromoanisole to generate a solution of double-coupled product **5q**, which was directly decomplexed through exposure to sunlight and air. The decomplexed triarylmethane $PhCH(3\text{-}C_6H_4\text{-}OMe)_2$ **7** was isolated in 93% yield after chromatography.

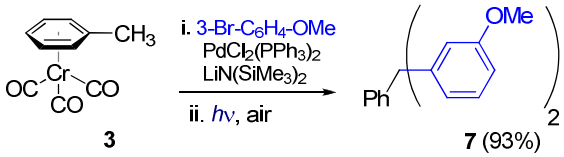


Scheme 1-13: Large-scale (5 mmol) coupling reaction and in-situ decomplexation gave triarylmethane **7** in 93% isolated yield after column chromatography.

## Activation of multiple benzylic positions on a single arene

If two coupling reactions could occur on a single methyl group of CrTol (**3**), then it seemed possible that multiple methyl groups such in tricarbonylchromium complexes of *p*-xylene **8** and mesitylene **9** could be activated as well. Referring back to Scheme 1-12, the triarylmethane complex's tertiary benzylic center is thermodynamically more acidic than the *di-* or *mono*-arylmethane center, so we were concerned that persistent deprotonation of the tertiary center and disfavored formation of a di-anion would hamper further reactivity of the other aryl methyl group (Scheme 1-14 below).

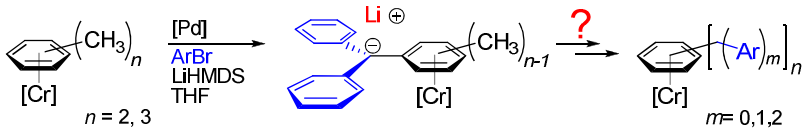


Scheme 1-14: Reaction at multiple benzylic positions on a single arene: Would the presence of a persistent triarylmethane anion prevent the less acidic tolyl proton from reacting?

The *p*-xylene complex **8** was reacted with the bulky (doubly *ortho*-substituted) aryl bromide 1,3,5-triisopropylbenzene, which was expected to only undergo coupling once per benzylic position, disfavoring further deprotonation and reaction. The reaction was sluggish due to the large size of the aryl bromide, but an encouraging mixture of single-coupled intermediate **10** and desired double-coupled product **11** was observed. Full conversion was obtained using more forcing conditions (≥5 equiv. base and >10 mol% catalyst loading with heating at 55 °C for 24 hours), and **11** was isolated in 73% yield (Scheme 1-14).

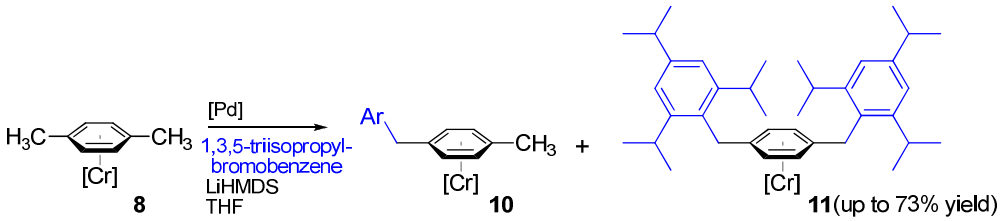


Scheme 1-15: Single coupling on each methyl of ($\eta^6$-*p*-xylene)Cr(CO)$_3$ (**8**) with the extremely bulky arene 1,3,5-triisopropylbromobenzene.

Moving on to a less sterically bulky aryl bromide in which deprotonatable triarylmethane centers could be generated and remain deprotonated in solution meant that an even larger excess of LiHMDS was expected to be necessary to form the tetraarylated product **12** (Scheme 1-16). In this case, nearly 10 equivalents of LiHMDS was required for full conversion (70% yield), also suggesting the possibility of polyanions such as **13-Li2** forming reversibly during the reaction.[50,a] The 70% isolated yield obtained here reflects a per-coupling yield of 91%.

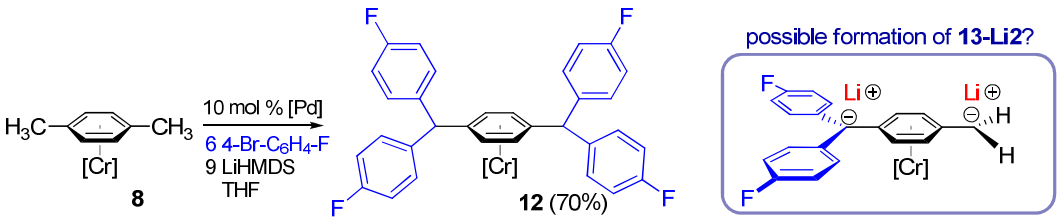


Scheme 1-16: *Tetra*-arylated complex **12** is formed in good yield from **8**, though large excess of base and 10 mol % catalyst loading is needed for full conversion.

We also examined arylation of the mesitylene complex **CrMes** (**9**) with both bulky 1,3,5-triisopropylbromobenzene and electron-rich 4-bromoanisole or slightly electron-poor 4-bromofluorobenzene. Coupling at 2 of the 3 methyl groups of the mesitylene did not pose much difficulty. Diarylation with 1,3,5-triisopropylbenzene led to product **14** in up to 55% yield, and tetraarylation with 4-bromofluorobenzenee provided **15** in up to 64% yield (Scheme 1-17).

[a] The tricarbonylchromium group has been known to stabilize *di-* and *tri*-anions directly on the arene ring, see work by S. Gibson and coworkers.

However, achieving full conversion to the $C_3$-symmetric products *tri*-arylated **16** from 1,3,5-triisopropylbenzene (up to 33% yield) or *hexa*-arylated **17** from 4-bromoanisole (43% yield, or >86% yield per coupling event) proved to be more difficult. This is not surprising, considering the massive crowding at the central arene due to the multiple aryl groups *and* the tricarbonylchromium group, which forces all benzylic aryl groups upward (see the x-ray crystal structure of **17**[a] below, Figure 1-12). In reactions of **CrMes** (**9**) with 1,3,5-triisopropylbenzene or 4-bromofluorobenzene, LDA was also examined as an alternative base to LiHMDS due to its greater basicity, in hopes that the *tri*- and *hexa*-arylated products could be isolated. However, the less substituted *di*- and *tetra*-coupled products **14** and **15**[b] were generated as the major product instead of the fully substituted $C_3$-symmetric products. Since equilibrium of deprotonation of the benzylic position is considered to lie far to the right for the much stronger LDA (p$K_a$ of $^i$Pr$_2$NH vs HMDS-H is 36 and 26, respectively, in THF solvent. See Table 1-1 on p. 10), this may support the idea that the $Cr(CO)_3$ group can stabilize more than one anion on the benzlic position (see Scheme 1-16 above). It is also possible that the lithiated species that is assumed to be oligomeric in solution does not transmetallate as readily with the diisopropylamine when there is excessive crowding.

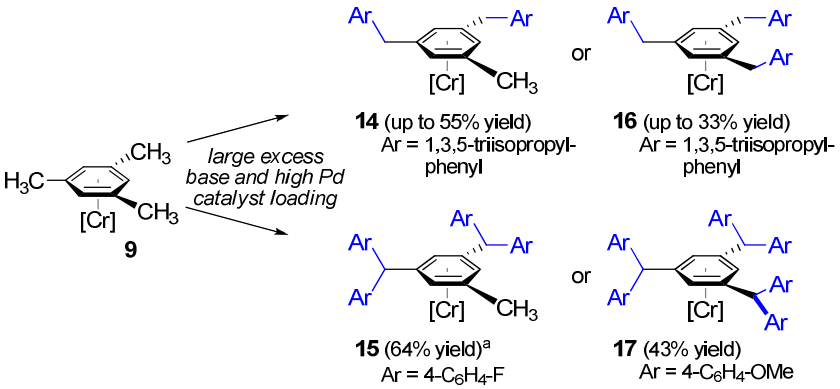


Scheme 1-17: Reactions using ($\eta^6$-mesitylene)$Cr(CO)_3$ **9** showed that coupling products **14** or **15** formed relatively easily at 2 of 3 methyl groups, though complete coupling to form the $C_3$-symmetric products **16** and **17**was difficult due to sterics. [a]LDA was used as base instead.

[a] The crystal structure for **17** can also be accessed through the Cambridge Crystallographic Data Centre (use the reference ID number: CCDC 775771).
[b] For **15**, LDA was used instead of LiHMDS

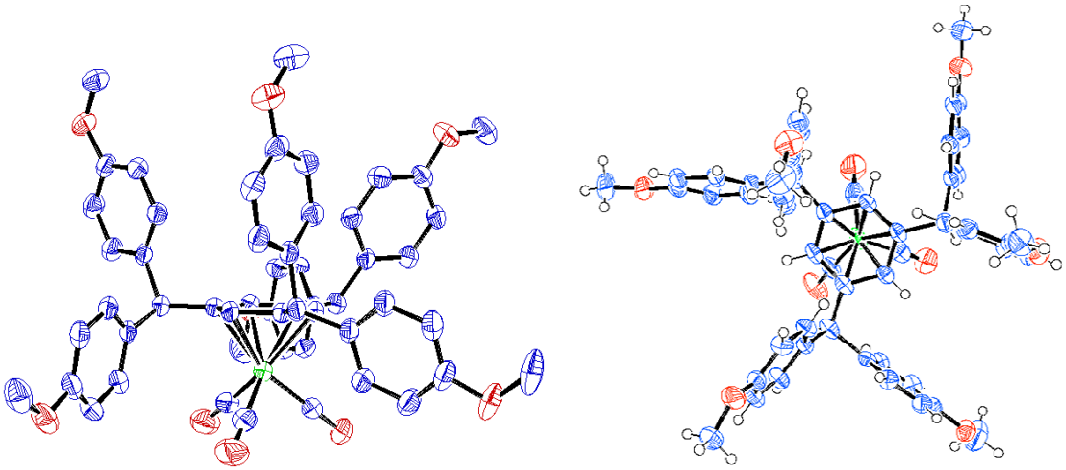

Figure 1-12: X-ray crystal structure (side and top views) of the pinwheel-like **17** illustrates the sterically crowded nature of the complex. Thermal ellipsoids are at 50% probability. CO ligands are unusually distorted, see full details on page 264.

Next we examined reaction with *ortho*-substituted xylene complex CroXyl (**18**, Scheme 1-18). Single arylation of each benzylic methyl could be achieved with a 2,6-*di*-substituted bromobenzene (this time using 2-bromo-1,3-dimethylbenzene) to give **19** in 85% yield. Using less the sterically demainding aryl bromide *N*,*N*-dimethy-4-bromoaniline and 3 equiv. of LiHMDS and running the reaction for 20 h provided the racemic planar chiral complex **20**, in which the two couplings happened at a single methyl, in 64% isolated yield; a symmetrical coupling product analogous to **19** was not observed. By simply increasing the amount of LiHMDS to 5 equiv. and increasing the run time of the reaction to 24 h, the *tri*-arylated product **21** was isolated as the major product (48% yield). Despite attempting reaction of CroXyl (**18**) with large amounts of excess base, formation of tetracoupled product **22** was not observed; as can ben seen in Scheme 1-19, both formation and transmetallation with **21-Li** would be extremely unfavorable due to sterics.

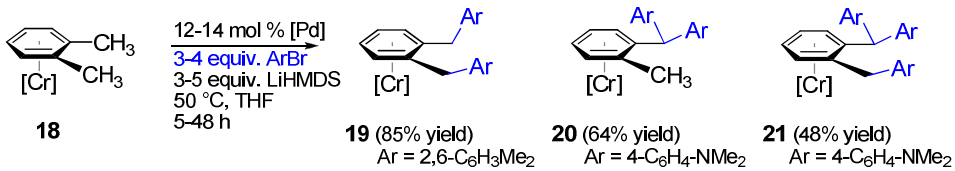


Scheme 1-18: Coupling of ($\eta^6$-*o*-xylene)Cr(CO)$_3$ **18** with various aryl bromides leads to symmetrical di-coupled **19**, planar chiral di-coupled **20**, and tri-coupled **21** products.

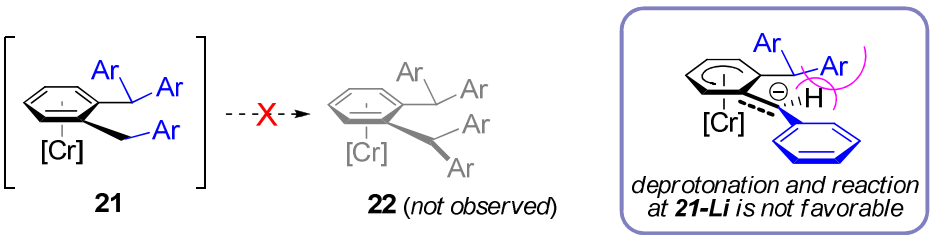


Scheme 1-19: In the coupling reaction of **18** with 4-$NMe_2$-$C_6H_4$-Br, the reaction stops at 3 coupling events due to sterics which prevent deprotonation and further reaction at the second benzylic site.

As seen in the activation and coupling at multiple C–H bonds of toluene, xylene, and mesitylene, the reactions presented here have a distinct advantage over other cross-coupling methods. Tricarbonylchromium allows us to perform up to 6 coupling reactions per equivalent of tricarbonylchromium to form highly symmetric complexes. We can also synthesize unusual planar-chiral complexes that lack central chirality centers. Further functionalization of Ar–F bonds[47] or deprotection and then functionalization of Ar–OMe bonds could potentially establish these polyarylated methanes as useful dendrimer cores.

## Compatibility with benzylic heteroatoms

### *Single coupling with aryl bromides α- to benzylic ethers*

So far, we have examined the reactions of carbon-substituted benzylic centers. We next considered the compatibility of the reaction with heteroatom substitution at the benzylic carbon. Polyarylated benzyl ethers are known to be particularly promising candidates in cancer drug development.[51] An alkyl benzyl ether complex ($\eta^{6\text{-}n}PrOC_6H_5)Cr(CO)_3$ (**23**) was synthesized to test for reactivity in the coupling reaction. It was expected to be a successful coupling partner due to a more stabilized benzyl anion influenced by the alkoxy subistution. Thus, **23** was reacted with bromobenzene in THF using the typical reaction conditions in the hopes of isolating **24a** as product (Scheme 1-20). However, the benzyl ether turned out to be a considerably more sensitive substrate under these conditions, and initially large amounts of highly polar dimerized products (**25**) lacking the propyl ether substitution were observed as baseline side products (Scheme 1-20). The proposed mechanism of elimination is given below (Scheme 1-21).

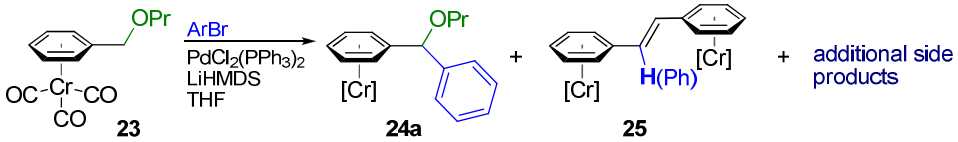


Scheme 1-20: Coupling reaction of tricarbonylchromium-coordinated benzyl ether **23** with PhBr under standard conditions led to multiple products, including the elimination dimer (**25**), a bis-tricarbonylchromium stilbene.

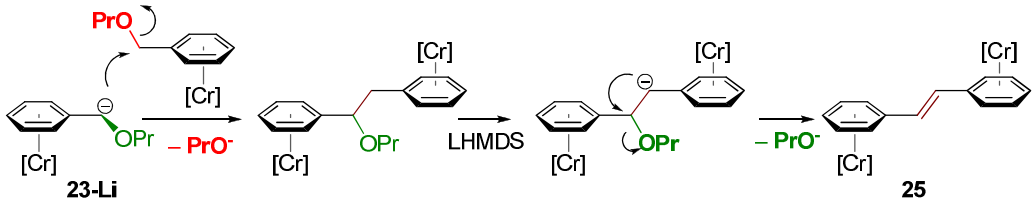


Scheme 1-21: Proposed mechanism for the formation of bis-tricarbonylchromium stilbene (**25**).

Luckily, the solution to the problem was relatively simple. Employing slow addition of a THF solution of LiHMDS added over several hours and high catalyst loadings avoided high concentrations of benzylic anion **23-Li** and circumvented excessive formation of **25**; **24a** was formed in good yield (Scheme 1-22 and entry 1, Table 1-6). Slightly electron-withdrawing *p*-bromofluorobenzene was a successful coupling partner (75% yield, Table 1-6, entry 2), as was electron-rich *p*-bromoanisole (80% yield, entry 3). Single and double *ortho*-substitution also were tolerated (entries 4 and 5), though in the case of 2-bromo-1,3-dimethylbenzene yields were lower (<60%). Note that the slow base addition protocol is slightly reminiscent of Murahashi's solution to a palladium-catalyzed coupling reaction of stabilized *ortho*-lithiated $sp^3$-carbon centers, in which a slow and precise rate of addition of their deprotonated $sp^2$-organolithium was required to minimize homocoupling product while preserving catalyst stability. [52]

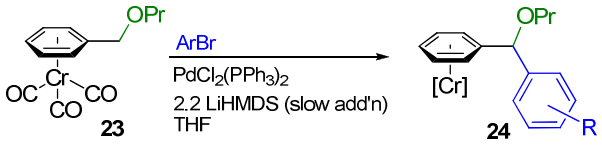


Scheme 1-22: Single coupling of $Cr(CO)_3$-benzylmethyl ether **23** with aryl bromides to yield diarylmethyl ether complexes **24a**–**24e** (Table 1-6). To minimize formation of stilbene dimers (**25**), slow addition of LiHMDS was required.

Table 1-6: Single coupling of ($\eta^6$-*n*PrO-$C_6H_5$)$Cr(CO)_3$ **23** with ArBr resulting in **24a**–**24e** (Scheme 1-22).

| Entry | | Ar = | Yield (%)* |
|---|---|---|---|
| 1 | **24a** |  | 81 |
| 2 | **24b** | 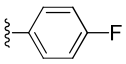 | 75 |
| 3 | **24c** | 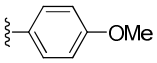 | 80 |
| 4 | **24d** | 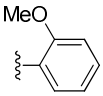 | 77 |
| 5 | **24e** | 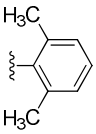 | 58 |

*isolated yields.

During a larger scale reaction of Cr-benzylpropylether **23** to form the diarylmethyl ether **24a**, a trace amount of a *less* polar side product was noticed on TLC. We originally hypothesized that this was a small fraction of the diarylmethane product that had eliminated propoxide. However, isolation of this material revealed the formation of a symmetrical product that still retained the propoxy group: the *tri*-aryl methyl ether **26a**, a fully-substituted benzylic center, was isolated in 3% yield (Scheme 1-23)!

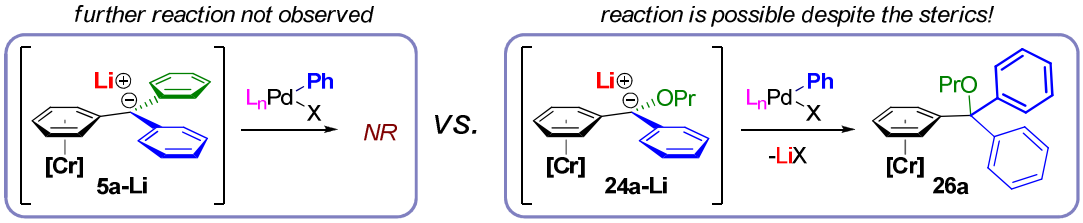


Scheme 1-23: Comparison of the deprotonated species **5b**, in which further arylation is not observed, and **24a**, in which further arylation to form the fully-substitued complex **26a** was observed.

*Double coupling to furnish fully-substituted triarylmethyl benzyl ethers.*

While the sterics of a lithiated chromium triarylmethane such as **5b-Li** (Scheme 1-23, above left) seem to be too great for transmetallation and further reaction to form tetraarylmethanes, the stabilized anion of tricarbonylchromium diarylmethyl benzyl ether **24a-Li** is surprisingly still able to undergo further reaction to form the fully substituted triarylmethane center. The difference in reactivity is likely due to the smaller size of the propoxy group vs aryl. We were interested to see whether larger amounts of triarylmethyl ether could be isolated by modifying these reaction conditions. By screening varying amounts of catalyst, base, and reaction time (Table 1-7), we saw that combining longer reaction times and higher amounts of LiHMDS with 10 mol % palladium catalyst loading could provide **26a** in good yields (up to 73% yield, Table 1-7, entry 5).

Table 1-7: Optimization of reaction conditions for one-pot synthesis of triphenylmethyl ether complex **26a** from simple tricarbonylchromium benzyl propyl ether **23**.

| entry | mol % [Pd]* | Time (h) | Equiv. LiHMDS† | Yield **24a** (%)# | Yield **26a** (%) |
|---|---|---|---|---|---|
| 1 | 7 | 1.5 | 2.0 | 73 | 1.5 |
| **2** | **10** | **1.3** | **2.2** | **77** | **–** |
| 3 | 8 | 48 | 2.2 | 44 | 20 |
| 4 | 10 | 48 | 2.3 | 18 | 43 |
| **5** | **10** | **16** | **4.0** | **9** | **73** |
| 6 | 5 | 48 | 4.0 | 57◊ | 14◊ |

Reactions are run in THF at 55 °C. *Unless otherwise stated, Pd catalyst = $PdCl_2(PPh_3)_2$. # Yields are after isolation. †Unless otherwise stated, LiHMDS was added to the reaction mixture slowly over 1.5–3 h. ◊Reaction was run with $PdCl_2$[norbornadiene] and racemic BINAP.

The optimized conditions above were used to form symmetrical and unsymmetrical tricarbonylchromium triarylmethyl ethers (Scheme 1-24). In Table 1-8, entries 1–3, yields of symmetrical **26a** and **26b**, and unsymmetrical **26c** are one-pot without isolation of the diarylmethylether intermediate **24a** or **24b**. In entries 4–7, the diarylmethyl ether intermediate was isolated separately (for yields, see entries in Table 1-6, p.28), and electron-rich (**26e**, Table 1-8, entries 4, 5, and 6) and sterically hindered (**26f**, entry 6) aryl bromides were good substrates. In the case of entries 4 and 5 it should be noted that the triarylmethyl propyl ether is chiral even after decomplexation from tricarbonylchromium. Unsymmetrical triarylmethanes mixing both

electron rich and electron poor groups are considered difficult compounds to make due to the electronic restrictions of typical Friedel-Crafts-type reactons.[53]

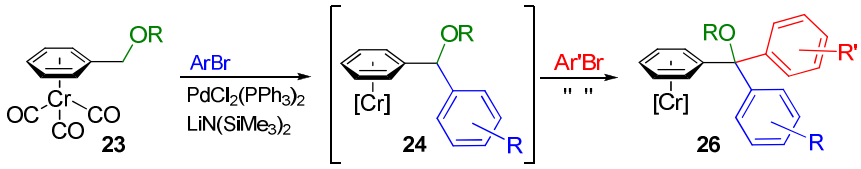


Scheme 1-24: One-pot and stepwise syntheses of symmetric and non-symmetric triarylmethanes.

Table 1-8: Synthesis of tricarbonylchromium-coordinated triarylmethyl benzyl ethers (Scheme 1-24).

One-pot reactions

| Entry | | Ar = | Ar' = | Yield (%) |
|---|---|---|---|---|
| 1 | **26a** |  |  | 81* |
| 2 | **26b** | 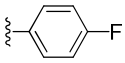 | 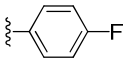 | 53* |
| 3 | **26c** |  | 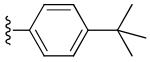 | 31*† |

Stepwise reactions

| Entry | | Ar = | Ar' = | Yield (%) |
|---|---|---|---|---|
| 4 | **26d** | 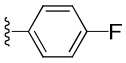 | 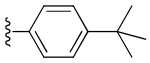 | 80# |
| 5 | **26e** | 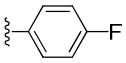 | 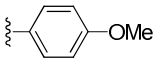 | 69# |
| 6 | **26f** |  |  | 59# |
| 7 | **26g** |  |  | 61# |

*Reactions in entries 1–3 start from benzyl propyl ether complex **23**; intermediate diarylmethyl ether complex was not isolated. #Isolated yields are starting from the diarylmethyl ether **24b** (entries 4 and 5) or from **24a** (entries 6 and 7). †1 equivalent of bromobenzene was added; 4-*tert*-butylbromobenzene was then added after full conversion to diarylmethyl ether intermediate **24a** was observed by TLC.

## *Coupling α- to benzylamines*

We next addressed cross-coupling α- to tertiary benzylic amines. It is known that, unlike other kinds of heteroaromatic substitution, α- amino substitution makes deprotonation at $sp^3$ carbon centers surprisingly difficult.[54,55] We initially synthesized a complex of *N*,*N*-dimethylbenzylamine

($\eta^6$-$Me_2NCH_2C_6H_5$)$Cr(CO)_3$ (**27**) to test our reaction strategy on tertiary amines. Subjecting **27** to palladium cross-coupling conditions similar to other standard (non-ether) chromium complexes yielded diphenylmethyl *N*,*N*-dimethylbenzylamine (**28a**), though the reaction was markedly slower than the aryl ether substrates. Larger amounts of LiHMDS were required to push the less reactive benzylamine to completion, but diarylmethylbenzylamines **28a**–**28d** were isolated in moderate to good yields (62–82%). Electron rich and poor aryl bromides and singly *ortho*-substituted 2-bromoanisole all served as good coupling partners (Scheme 1-25, Table 1-9, entries 1–4). The crystal structure of **28c** was obtained and is shown in Figure 1-13. Unfortunately, doubly ortho-substituted aryl bromide (in our case, 2-bromo-1,3-dimethylbenzene) was not effective, and no product **28e** was detected, indicating that this system is more sterically hindered and less reactive.

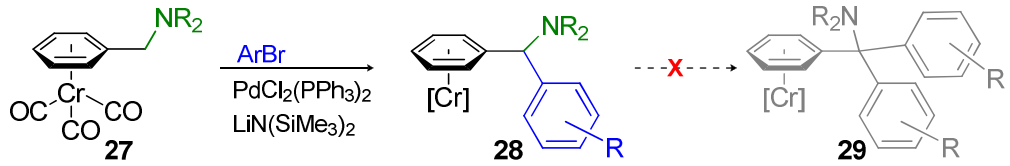


Scheme 1-25: Cross-coupling of N,N-dimethylbenzylamine tricarbonylchromium complex **27** with aryl bromides to yield diarylmethylamines in 62–82% yield (Table 1-9).

Table 1-9: Synthesis of diarylmethylamines **28a**–**28d** from **27**.

| Entry | | Ar = | Yield (%)* |
|---|---|---|---|
| 1 | **28a** |  | 82 |
| 2 | **28b** | 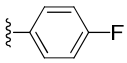 | 62 |
| 3 | **28c** | 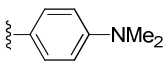 | 77 |
| 4 | **28d** | 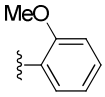 | 72 |
| 5 | **28e** | 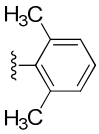 | – # |

*Isolated yields. # No coupling product was observed for this reaction.

Unlike the benzyl ether substrates, we were unable to observe any amount of di-coupling triarylmethylamine product **29**. Additionally, attempts to push the formation of these species by running the reaction with high catalyst loadings and large amounts of base failed to yield to triarylmethylamine products. It is likely that an entirely different set of deprotonation conditions and catalyst would be necessary. The diarylmethylamines we were able to synthesize are a very important class of molecules. The substructure is present in numerous medicines and drug candidates,[56] including the "non-drowsy" antihistamine cetirizine hydrochloride, marketed under the brand name Zyrtec.

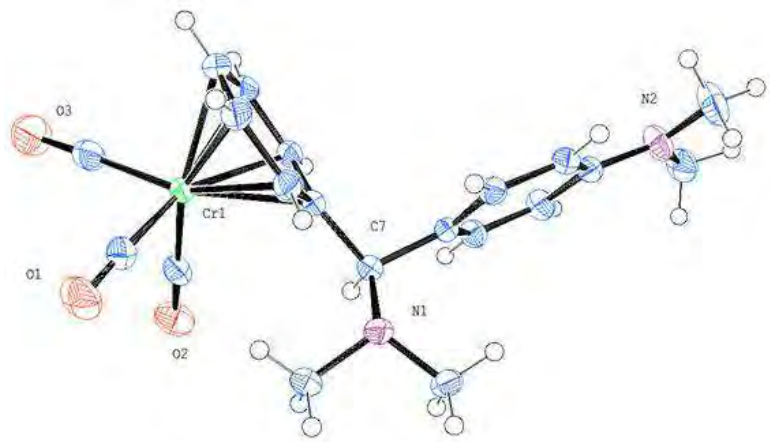


Figure 1-13: X-ray crystal structure of **28c**. Thermal ellipsoids are at 50% probability. Full details can be found on p. 276.

## Compatibility with β-hydrogens

### *β-hydrogens not constrained to ring systems.*

All the substrates explored thus far have a certain aspect of complexity removed from them which tends to be a significant issue that must be addressed in typical $sp^2$–$sp^3$- and $sp^3$–$sp^3$-cross-coupling reactions: that is, the presence of β-hydrogens. The simple tricarbonylchromium ethylbenzene substrate **30** was synthesized in excellent yield and subjected to the standard coupling conditions with $PdCl_2(PPh_3)_2$, excess LiHMDS, and 4-bromofluorobenzene (Scheme 1-26).

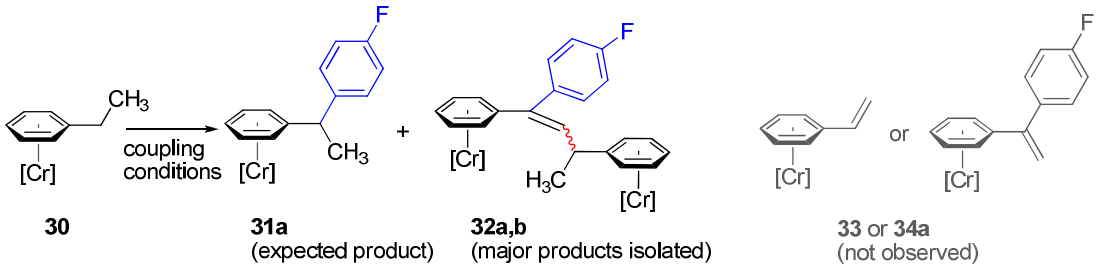


Scheme 1-26: Attempted cross-coupling of ($\eta^6$-ethylbenzene)$Cr(CO)_3$ **30** with 4-bromofluorobenzene using standard conditions leads to a large amounts of oligomeric side products.

To our disappointment, we did not see the desired 1,1-diarylethane **31a** as our main product. Instead, we observed a complex reaction mixture that included large amounts of polar oligomeric products such as diastereomers **32a** and **b**. Fluorobenzene was also observed in the $^{19}F$ NMR spectrum of the reaction mixture (Scheme 1-26 above). These products arise from β-hydride elimination to form $\eta^6$-styrene tricarbonylchromium **33** (and possibly **34**), followed by fast and irreversible nucleophilic attack by the benzylic anions in solution, such as **30-Li** (Scheme 1-27).

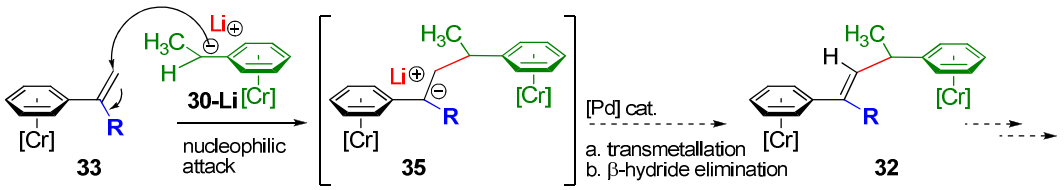


Scheme 1-27: Formation of undesired oligomers **32a,b** by nucleophilic attack by stabilized benzylic anions such as Li-ethylbenzene tricarbonylchromium **30-Li** on β-hydride elimination products such as **33**.

Because the rate of β-hydrogen elimination is influenced by several factors, such as competing rates of reductive elimination (Scheme 1-28) and the presence of open coordination sites on the metal center, we wondered if it would be possible to disfavor the formation of styrene-type products through changing the substrate. An electron-poor aryl undergoes reductive elimination from the metal center slower than an electron-rich aryl group,[57] so we decided to try 4-bromoanisole as a substrate in the same coupling reaction. Indeed, the more electron-rich aryl bromide showed different reactivity, with a reduction in oligomer formation that had been seen in the earlier test with 4-bromofluorobenzene. However, yields of desired **31b** were still relatively low (<60%). As in the case of reactions with the benzyl ethers (see p. 26), a slow addition of

LiHMDS helped, and clean formation of **31b** was observed in 70% yield (Scheme 1-29). Surprisingly, approximately 6% of side product **35**, the fully substituted quaternary carbon center, was observed, confirming the reactivity of the tertiary benzylic center of diarylethane **31b** towards further deprotonation and cross-coupling. Up to 18% yield of **35** was isolated in a later run, but higher yields were not obtained. Sterically congested 2-bromo-1,3-dimethylbenzene was also an acceptable partner. In this case, the sterics in the system would seem to preclude deprotonation of the single-coupled diarylethane product (see Figure 1-11, p.20). As expected, further-coupled products and β-hydrogen elimination products were not observed.

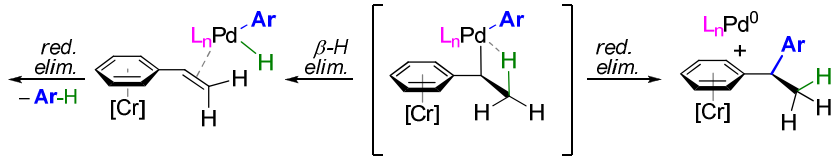


Scheme 1-28: Competing β-hydride elimination and reductive elimination processes from the palladium center.

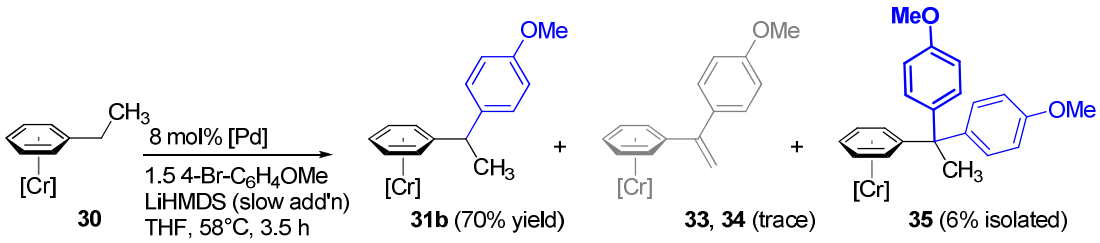


Scheme 1-29: Cross-coupling of ($\eta^6$-ethylbenzene)$Cr(CO)_3$ **30** with 4-bromoanisole using slow addition of LiHMDS minimized amouts of oligomeric side products.

Examining the effect of additional sterics on the the β-position of the ethylbenzene led us to react the substituted ethylbenzene ($\eta^6$-phenethylmorpholine)$Cr(CO)_3$ **36** with the aryl bromide 4-*tert*-butylbromobenzene using standard conditions (Scheme 1-30). We successfully obtained the expected coupling product **37** in 78% yield after isolation. However, when we tested the reactivity of a differently substituted but approximately electronically equivalent 2-bromotoluene as a reactant, no coupling product was observed, and the reaction conversion stalled without going to completion. Approximately 50% of the β-hydride eliminated styrene **38** was isolated instead (Scheme 1-30).

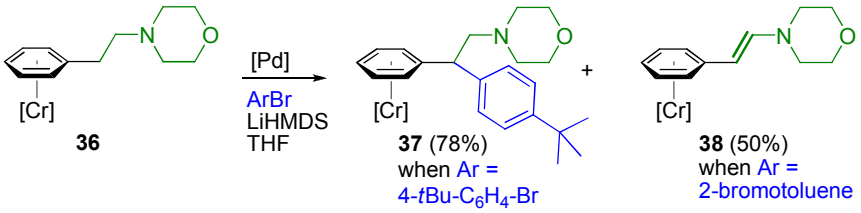


Scheme 1-30: Reaction with a substituted ethyl benzene ($\eta^6$-phenethylmorpholine)$Cr(CO)_3$ **36** showed formation of both standard coupling product **37**, or **38**, depending on the substitution of the aryl bromide used in the reaction.

The interesting steric and electronic effects at play in the palladium-catalyzed cross-coupling reaction of tricarbonylchromium complexed ethylbenzene derivatives with aryl bromides is still not very well-understood. Coupling reactions to form fully-substituted all-carbon $sp^3$-centers is very unusual, and further exploration of these substrates is ongoing. Additionally, coupling a different aryl bromide with isolated teryiary diarylmethyl products could lead to chiral all-carbon quaternary products, of which even racemic or achiral varieties are a "significant synthetic challenge."[58]

### *Reactivity of β-hydridogen-containing complexes in polycyclic systems*

It is well known that the $Cr(CO)_3$ group can effectively shield one face of coordinated arenes.[59] To take advantage of this property for stereoselective coupling reactions, we synthesized tricarbonylchromium complexes of indane **39** and tetrahydronaphthalene **40** to use in cross-coupling.[a] Employing excess LiHMDS in THF and unhindered aryl bromides, exclusively *cis*-substituted diarylated complexes **41a** and **41b** (Scheme 1-31) and **42a**, **42b**, and **42c** (Scheme 1-32) were obtained from indane and tetrahydronaphthalene starting materials **39** and **40**, respectively, in moderate yields. β-hydrogen elimination products and stereoisomers which could arise from palladium-mediated isomerization through β-hydride elimination and reinsertion were

[a] A tricarbonylchromium-coordinated complex of 9,10-dihydroanthracene was also synthesized. However, we were disappointed to find that under the cross-coupling reaction conditions, large amounts of free anthracene were isolated as the major product instead.

not observed. On the other hand, when 2-bromo-1,3-dimethylbenzene was used as coupling partner with indane complex **39**, the *mono*-arylated product was isolated **43a** and was the only product. No desired products (single coupled **44a** or double coupled **42**) were observed for this same aryl bromide when the tetrahydronaphthalene complex **40** was used as starting material. $^1$H NMR spectra of the *cis* complexes revealed that no *trans*-product was formed. An X-ray crystal structre was obtained for **41b**,[a] which confirms the *cis*-configuration of the two aryl groups (Figure 1-14). Isomers of 1,3-diarylindane are difficult to obtain as a single diastereomer by conventional methods, as their syntheses typically provides cis/trans mixtures, which are difficult to separate.[60] However, the stereoselective synthesis of these compounds are of interest in medicinal chemistry,[61] as the *cis*-1,3-diarylindane moiety is present in some potent nonpeptide endothelin receptor antagonists.[60]

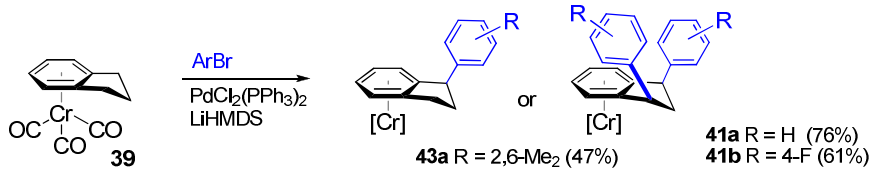


Scheme 1-31: Coupling reactions with excess ArBr and LiHMDS led to the isolation of double-coupled products **41a–b** from ($\eta^6$-indane)Cr(CO)$_3$ (**39**). Sterically hindered 2-bromo-1,3-dimethylbenzene led to exclusive isolation of the mono-arylated product **43a**.

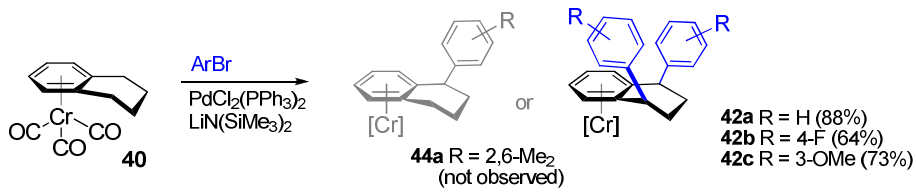


Scheme 1-32: Coupling reactions with excess ArBr and LiHMDS led to the isolation of double coupled products **42a–c** from the tricarbonylchromium tetrahydronaphthalene complex **40**. Reaction to form even monoarylated **44a** was not observed when 2-bromo-1,3-dimethylbenzene was used as ArBr.

[a] Determined by $^1$H NMR and X-ray diffraction of **41b**, Figure 1-14 (see p. 205 for the full report). The crystal structure can also be accessed through the Cambridge Crystallographic Data Centre (use the reference ID number: CCDC 765716).

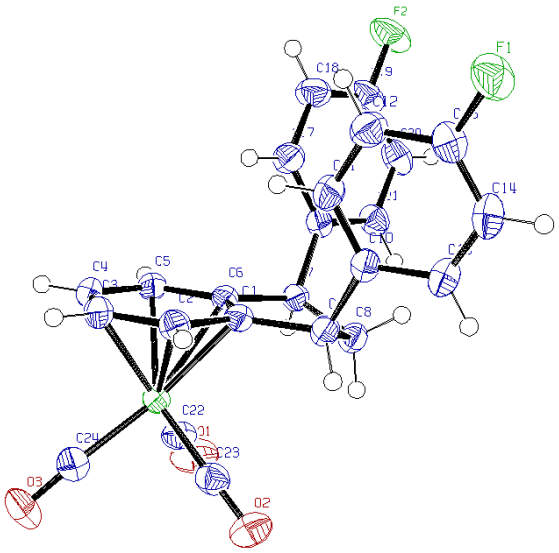


Figure 1-14: X-ray crystal structure of **41b**, showing the *cis*-stereochemistry of the aryl rings and the downward pucker of the cyclopentene ring. Thermal ellipsoids are at 50% probability. Further details can be found on p. 276.

By adjusting the conditions by running the reaction with fewer equivalents of base, the mono-arylated products **43b** and **43c** could be formed from **39**, though yields are lower than in the case of the doube-coupled products due to partial conversion to diarylated products (Scheme 1-33). For mono-arylation reactions of **40** to form **44b** and **44c**, adding less base to favor monoarylation led to formation of inseparable mixtures of what seemed to be the expected product (aryl group pointing *up*), combined with smaller amounts (<20%) of a similar isomer (likely the complex with aryl group pointing *down*, determined by $^{1}$H NMR analysis of coupling constants). While changing the catalyst loading, temperature, or identity of the aryl bromide coupling partner did not seem to impact the formation of this isomer, we found that changing the solvent mix to 40:60 toluene:THF prevented the formation of this isomer, and gratifyingly, **44b** and **44c** were isolated in moderate yields as well without isomeric impurities. It is not clear why the mono-coupling reactions (but not the double-coupling reactions to form **42a**–**c**) had problems, though it is possible that the conditions for monocoupling of tetrahyronaphthalene complex (**40**) in THF solvent favored a small amount of β-hydride elimination and isomerization. Finally, monoarylated indane complex **43c** could be isolated and re-subjected to coupling conditions to produce differently substituted diarylindane **41c** (Scheme 1-34).

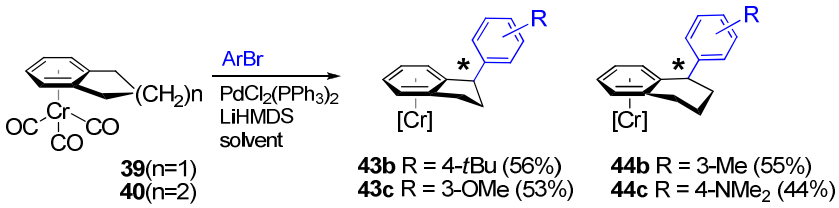


Scheme 1-33: Formation of racemic planar- and central- chiral mono-arylated indanes and tetrahydronaphthalenes **43** and **44**. In the case of tetrahydronaphthalene (**40**) reactions, a 40:60 mixture of Toluene:THF as solvent was necessary to avoid formation of isomerized products.

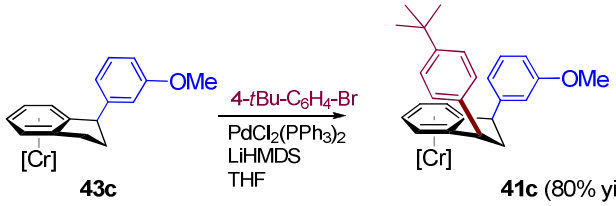


Scheme 1-34: unsymmetrical cis-substituted diarylindane could be obtained by subjecting **43c** to coupling conditions to provide racemic **41c** in 80% isolated yield.

Finally, to demonstrate the practical advantages to our method, double coupling of indane tricarbonylchromium (**39**) with bromobenzene, followed by exposure to light and air and purification by column chromatography provided 79% isolated yield of *cis*-1,3-diphenylindane (**45**, Scheme 1-35).

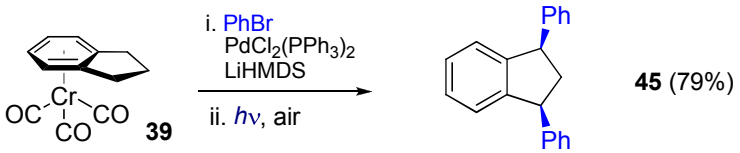


Scheme 1-35: The one-pot coupling of ($\eta^6$-indane)$Cr(CO)_3$ complex **39** and direct decomplexation of product provides *cis*-substituted 1,3-diphenylindane (**45**) in 79% yield after isolation.

## Polycyclic system with β-heteroatom substitution.

Tricarbonylchormium phthalan **46** was also explored as a substrate in cross-coupling. Initially, the substrate was of interest to Merck & Co. for stereoselective synthesis of a monoarylated phthalan.[a] While the project itself was ultimately abandoned, the synthesis of some phthalan derivatives are still presented here. As in the case of benzylic ethers, standard reaction conditions were low-yielding (initial test reaction exhibited 15 and 4% yield of the *mono*- and *di*-coupled products **47** and **48**, respectively) (Scheme 1-36). The stabilized benzylic anion could lead to ring opening to the aldehyde, which could either close back up, or be attacked by the strongly nucleophilic carbanions in solution (Scheme 1-37). In support of this hypothesis, aldehyde peaks were observed in the $^1$H NMR of the crude reaction mixture; additionally, small amounts of the other (*endo*-) stereoisomer of the mono-arylated phthalan were isolated as a side-product of the reaction. By either adding base slowly or using toluene as a co-solvent (40:60 toluene:THF), both mono- or di- coupled products could be observed, but this reaction was not fully optimized (Scheme 1-36). Cylohexenyl triflate was also examined as a coupling partner, and mono-coupled product **49** was isolated in 62% yield.

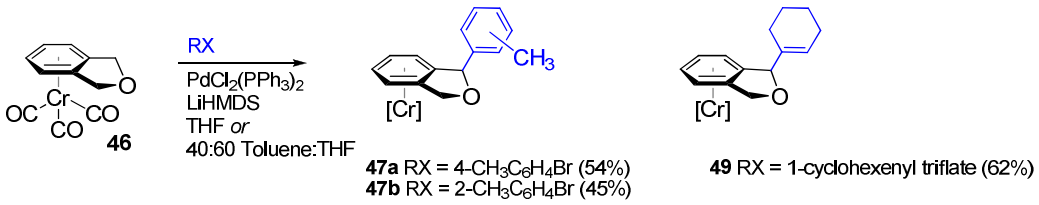


Scheme 1-36: Tricarbonylchromium pthlalan **46** as reactant gives mono- coupled products **47a** and **47b**. Using 1-cyclohexenyl trifluoromthanesulfonate provided **49** in 62% yield.

[a] The racemic complexes of phthalan derivatives were used as chiral chromatrography references for the asymmetric synthesis of monosubstituted phthalan, though no more than approximately 30% ee was obtained.

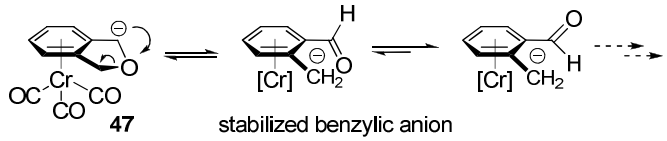


Scheme 1-37: Possible routes for decomposition arise from opening of the phthalan ring.

## Walking the tricarbonylchromium group

Here it should be noted that some odd behavior was observed with some of the cross-coupling reactions earlier in this chapter. Attempts to run the CrTol (**3**) coupling reaction with 4-bromotoluene at lower catalyst loadings (using higher temperatures to make up for the expected slower coupling at lower catalyst loadings) led to an extremely messy reaction in which an inseparable mixture of tricarbonylchromium-complexed arene products were isolated. Returning to running the reaction at higher catalyst loadings (8–10 mol% $PdCl_2(PPh_3)_2$ and 45–50 °C) provided the expected triarylmethane **5n** in 78% yield, which was lower than expected (see Table 1-5, entry 4, on p.19). Additionally, approximately 6% of an unexpected polyarylated side product **50** was isolated.

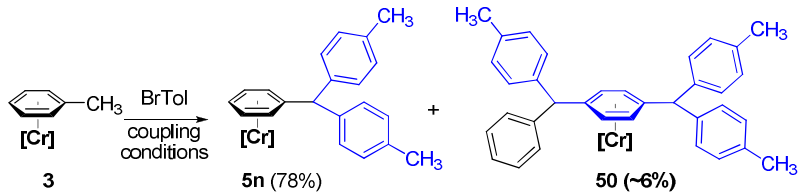


Scheme 1-38: Anomalous complex **50** is observed as a side product in the reaction of **3** with 4-bromotoluene.

Repeating the low catalyst-loading cross-coupling reaction with **3** and 4-*tert*-butylbromobenzene and quenching the reaction before completion led to a mixture of products. After isolation, two diarylmethane complexes and two triarylmethane complexes were obtained: the expected diarylmethane complex **4d**, its chromium-coordinated regioisomer **4d′**, the desired double-coupled triarylmethane complex **5p**, and the chromium-coordinated regioisomer **5p′** (Scheme 1-39). Indeed, the $Cr(CO)_3$ fragment was migrating to other aryl rings during reaction.

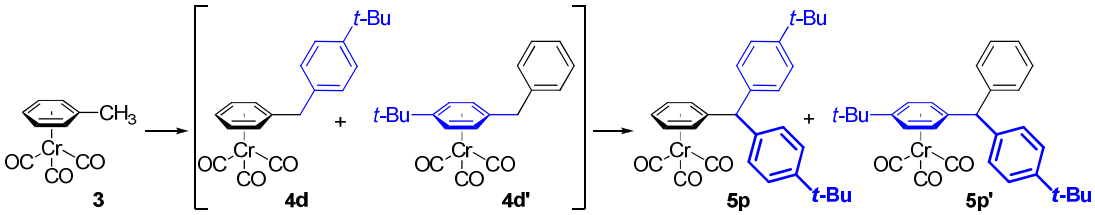


Scheme 1-39: The reaction of **3** with 4-*t*Bu-$C_6H_4Br$ at low catalyst loading also showed an unusual mixture of isomers, indicating migration of the tricarbonylchromium group.

Since arene exchange is generally not observed for arene tricaronbylchromium complexes except at higher temperatures or by replacing one of the carbonyl groups with a phosphine ligand containing a pendant donor group,[a,62] it is unlikely that the observed arene exchange is an intermolecular process. Rather, intramolecular arene exchange was more plausible. In work by Traylor and coworkers, the tricarbonylchromium group was seen to reversibly migrate across certain conjugated silbene molecular frameworks in which the $Cr(CO)_3$ was able to easily adopt bridging intermediates with $sp^2$-hybridized benzylic carbon(s) (Figure 1-15).[63] Additionally, the $Cr(CO)_3$ group is known to quickly migrate to the Cp-like[b] anionic side of deprotonated indene (isomerization is irreversible and complete when warmed above −20 °C).[64] It has also been reported to migrate under light or thermal excitation in substituted naphthalenes.[65]

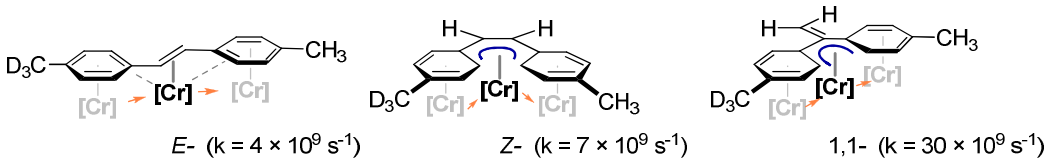


Figure 1-15: Internal tricarbonylchromium migration in di-*p*-tolylethylene isomers examined by Traylor et al. In the case of the *E*-isomer, the [Cr] group must temporarily adopt an $\eta^2$-bonding mode, leading to slowest exchange (approx. an order of magnitude less than the 1,1-isomer, in which the $Cr(CO)_3$ group crosses the conjugated system in an $\eta^5$-configuration).

[a] Work on arene exchange of (arene)dicarbonylchromium phosphine complexes has been explored by Semmelhack and coworkers.
[b] Cp = cyclopentadienyl anion, $C_5H_5^-$

In light of these known cases of tricaronbylchromium migration, we considered the possibility that in our case, the tricarbonylchromium group was taking advantage of the $sp^2$-hybridized benzylic carbanion in the intermediate **4d-Li** to migrate to the other arene, temporarily adopting an $\eta^5$-coordinated state before reaching the other aromatic group in **4d′-Li** (Scheme 1-40). Since in the 4-*t*Bu-$C_6H_4$- fragment, the alkyl-subistitution of the aromatic ring makes it slightly more electron-rich than simple phenyl, migration to the other aryl group is considered a slightly thermodynamically favorable process. However, is likely that the steps of the walking process happen reversibly, with the location of the $Cr(CO)_3$ becoming locked only after the second transmetallation and coupling process installs the final arene, giving a mixture of **5p** and **5p**′.

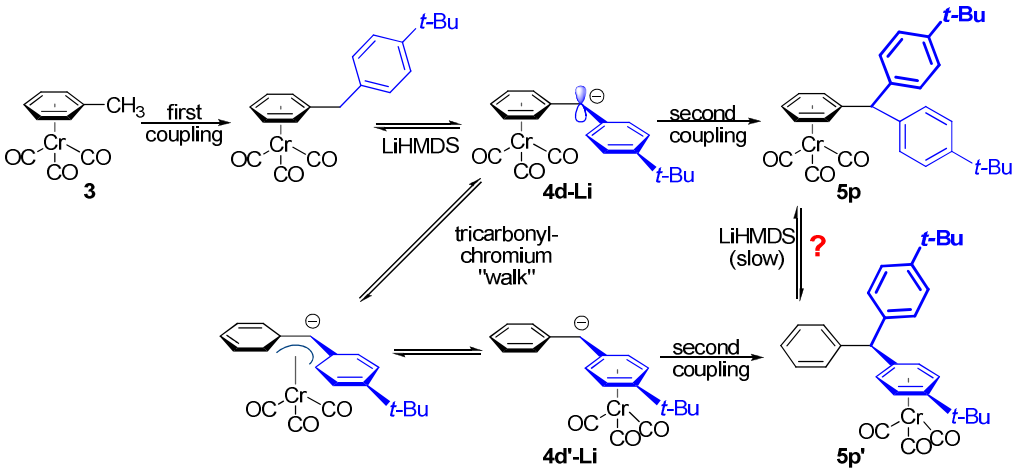


Scheme 1-40: Proposed mechanism for “walking” of the tricarbonylchromium group.

It was also considered possible for migration to occur in the triarylmethane if it were to become deprotonated. However, as noted in Scheme 1-12 (see p. 21), the kinetic barrier to deprotonation of that remaining acidic C–H bond is relatively high, leading us to expect lower proportions of deprotonated **5p** and **5p**′ in solution and a lower probability of walking after triarylmethane formation. Indeed, while monitoring the reaction by $^1$H NMR using low catalyst loadings of $Pd(PPh_3)_4$, the relative proportion of **4d**:**4d′** and **5p**:**5p**′ were found to be similar, supporting the claim that walking of the triarylmethane is not a significant factor in compared to walking in the diarylmethane. Running the coupling reaction of CrTol (**3**) with 4-*tert*-butylbromobenzene at various catalyst loadings (Table 1-10 and Figure 1-16) led to the conclusion that the rate of walking in the diarylmethane species seems to be approximately of

the same order of magnitude as the rate of palladium-catalyzed cross-coupling. Theoretically, by modulating the identity of the transmetalating ligand and maintaining a large excess of LiHMDS base, it should be possible to out-compete coupling processes and favor "walking" processes, leading to a stepwise walking/coupling reaction.

Table 1-10: amount of "walking" product observed at varying catalyst loadings (Scheme 1-40 and Figure 1-16).

| entry | [Pd] (mol%) | temp. (℃) | rxn time (h) | yield (%)[a] | ratio[b] **5p:5p′** |
|---|---|---|---|---|---|
| 1 | 10 | 60 | 3 | 70 | **>99 : 1** |
| 2 | 5 | 60 | 3 | 92 | **82 : 18** |
| 3 | 2 | 60 | 25 | 93 | **42 : 58** |
| 4 | 1.4 | 60 | 67 | 84 | **33 : 67** |

[a]Yield is the combined yield of regioisomers. [b]Ratio of **5p:5p′** was determined by $^1$H NMR integration of the benzylic CH.

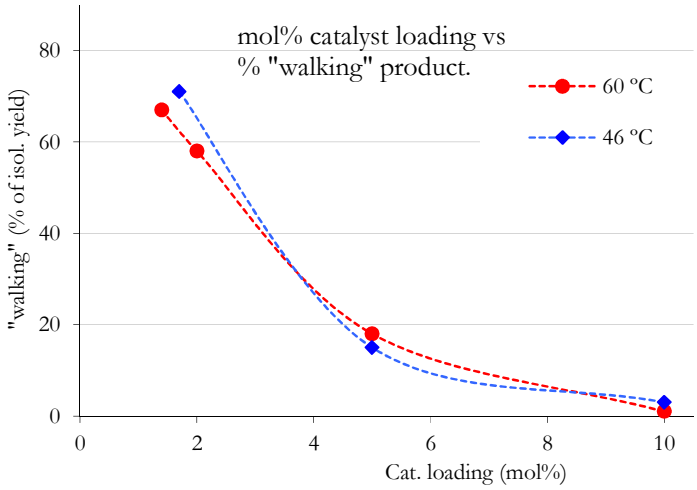


Figure 1-16: The influence of catalyst loading (and speed of reaction with deprotonated species) on the total amount of "walking" product (as % of total isolated yield).

Indeed, "outrunning" the second coupling seems to be critical to the success of an envisioned walking and polymerization, as the triarylmethane "walks" very slowly under reaction conditions with excess LiHMDS. To verify this, we started from a complex that contained one methyl on a free aryl group (**5a**, see p.12). The product of a walk and *then* further reaction at the new

benzylic carbon was observed (**51**), but formation of the walked product was slow (subsequent cross-coupling at the newly-activated tolyl position was, however, fast).

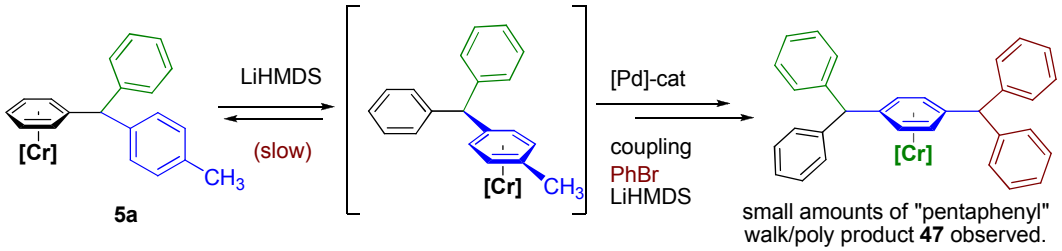


Scheme 1-41: Starting from **5a**, reaction with a large excess of LiHMDS and PhBr led to the isolation of small amounts of the first generation walk/polymerization product **51**.

These results seem to indicate that there is a possibility for developing reactions that exploit "walking" followed by cross-coupling. For example, by "walking" to an adjactent aryl group and then coupling with aryl bromides containing benzylic protons (illustrated in Scheme 1-38 and Scheme 1-41), a method for the synthesis of polymeric branched polyarylmethanes could be developed. Further work on "walking" and possible polymerization reactions is ongoing.

## Summary and conclusions

In summary, we have introduced an efficient method for benzylic cross-coupling reactions. Activation of the benzylic C–H's is accomplished by an ($\eta^6$-arene)Cr(CO)$_3$ complex and an organolithium which is formed reversibly using a base of moderate strength (LiHMDS).[66] The in-situ generated organolithium is directly employed in transmetallation to palladium in the cross-coupling cycle, and the activated arene can undergo multiple arylations to give polyarylated arene complexes that are easily demetallated and are potentially useful in medicinal and materials chemistry. Furthermore, this method enables the synthesis of organic compounds that would be very difficult to access through conventional cross-coupling reactions. In particular, we are able to access fully-substituted and quaternary *sp*$^3$-carbon centers and *cis*-disubstituted aryl indanes. The highly symmetric and potentially dendrimeric complexes, such as the bulky C$_3$-symmetric hexa-coupled arene **17** may be of interest in materials science.

Our method is complementary to existing approaches utilizing electrophilic aromatic substitution (Friedel-Crafts chemistry), and enables the selective synthesis of polyarylmethanes that are not

accessible through electrophilic aromatic substitution reactions alone. Currently, efforts are underway to broaden the application of our method to the generation of quaternary polyarylmethanes and their enantioselective syntheses, as well as to explore the migratory and potentially catalytic aspects of the activating tricarbonylchromium group itself.

## Experimental Section

### General Methods.

All reactions were performed under nitrogen using oven-dried glassware. Air- and moisture- sensitive solutions were handled under nitrogen and transferred via syringe. THF was freshly distilled from Na/benzophenone ketyl. Glyme and toluene were drawn from a Grubbs column. Unless otherwise stated, reagents were commercially available and used as purchased without further purification. Chemicals were obtained from Sigma-Aldrich or Acros, and solvents were purchased from Fisher Scientific. Reactions were monitored by thin-layer chromatography using Whatman Partisil® K6F 250 μm precoated 60 Å silica gel plates and visualized by short-wave ultra-violet light as well as by treatment with ceric ammonium molybdate (CAM) stain. NMR spectra were recorded in $CDCl_3$ on a Bruker 300 MHz Fourier-transform spectrometer. Chemical shifts are reported in ppm referenced to tetramethylsilane (TMS) or the $CHCl_3$ solvent residual peak at 7.26 ppm for $^1H$ and 77.23 ppm for $^{13}C\{^1H\}$; $^{19}F$ peaks were referenced to an external standard of trifluoroacetic acid in $CDCl_3$ at −76.55 ppm. Infrared spectra were obtained on NaCl using a Perkin-Elmer Spectrum 100 Series FTIR spectrometer. Chromium-complexed masses were recorded with Electrospray + (ES+) HRMS methods, and $[M]^+$ or $[M - (CO)_3]^+$ was confirmed by the presence of the characteristic chromium isotope pattern. Decomplexed masses were recorded with Chemical Ionization + (CI+) HRMS methods, and $[M]^+$ or $[MH]^+$ were observed.

Molybdenum complexes **1** and **2**,[67] and tricarbonylchromium complexes **3**, **4a**, **8**, **9**, **18**, **23**, **27**, **30**, **36**, **39**, **40**, and **46**[67,68,69,70,71] were prepared according to general literature procedure for the synthesis of arene tricarbonylmetal complexes from $M(CO)_6$ and parent arene (where M = Mo, Cr), and were crystallized from dichloromethane and hexanes or purified by column chromatography eluting in diethyl ether in either pentane or hexanes to afford pale yellow solids (**1** and **2**), bright yellow crystalline solids (**3**, **4a**, **8**, **9**, **18**, **27**, **30**, **36**, **39**, **40**, and **46**), or a viscous orange oil (**23**).

**Caution:** Care should be taken to avoid direct light exposure of reactions, as arene tricarbonylchromium complexes can decompose in solution under light. Compound **23** and **27** are best stored at or below 0 °C.

## Procedure for monitoring deprotonation of arene tricarbonylchromium complexes.

The following is representative of the procedure used to monitor deprotonation of tricarbonylchromium complexes in protio solution by $^1$H NMR using the characteristic arene shifts as handles.

A 5 mm NMR tube was charged with **4a** (24 mg, 0.08 mmol, 1 equiv), sealed with a septum, and purged with dry nitrogen. A 0.40 M solution of LiHMDS in dry THF (0.20 mL, 0.08 mmol, 1.0 equiv, freshly generated in a nitrogen atmosphere glovebox) was added to the NMR tube via syringe at room temperature, and an immediate color change to bright orange is observed. The homogeneous solution was diluted with ~0.3 ml of THF, taking care to match the solvent height of a sealed $d_8$-THF standard NMR tube, then shaken vigorously. The $^1$H NMR was recorded (without lock or sweep) on a 300 MHz spectrometer which was pre-shimmed using the sealed $d_8$-THF solvent standard as reference.

## General procedures and characterizations for benzylic coupling reactions.

The following procedures are representative of arene tricarbonylchromium coupling reactions with aryl bromides. Unless otherwise specified, chromatography was run in 2 – 50 % by volume diethyl ether in pentane or hexane.

### General procedure 1-A for benzylic cross-coupling of arene tricarbonylchromium complexes with aryl bromides:

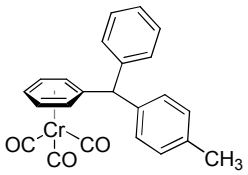


**5a – (4-$C_6H_4$-$CH_3$)PhCH($\eta^6$-$C_6H_5$)Cr(CO)$_3$**: An oven-dried glass reaction tube was charged with a small magnetic stirbar and CrDPM (PhCH$_2$($\eta^6$-$C_6H_5$)Cr(CO)$_3$, **4a**) (44.5 mg, 0.146 mmol, 1.0 equiv), sealed with a septum, and purged with nitrogen. $PdCl_2(PPh_3)_2$ (3.2 mg, 0.0045 mmol, 3 mol %) and LiHMDS (38 mg, 0.23 mmol, 1.6 equiv) were dissolved in 1.0 mL of dry THF under a nitrogen atmosphere, forming an orange solution, to which neat 4-bromotoluene (28 µL, 0.23 mmol, 1.6 equiv) was added. The catalyst, base, and aryl bromide solution was taken up by syringe and added to **4a**, which turned intensely red-orange. The reaction mixture was heated with stirring for 45 min at 57 °C, then allowed to cool. The orange solution was quenched with two drops of aqueous 2N HCl and allowed to stir for 5 min. The golden solution was opened to air and diluted with 3 mL diethyl ether, then filtered over a pad of $MgSO_4$ and silica. The pad was rinsed with an additional 1 mL diethyl ether and the solution was concentrated *in vacuo*, loaded directly onto a silica gel column, and

eluted with 20% diethyl ether in pentane. The title compound **5a** (52.6 mg, 0.133 mmol, 91% yield ) was obtained as a highly crystalline yellow solid. **$^1$H NMR** (300 MHz, $CDCl_3$) δ: 7.34 – 7.25 (m, 3H), 7.19 – 7.12 (m, 4H), 7.06 (d, *J* = 6.3 Hz, 2H), 5.38 – 5.33 (m, 1H), 5.24 – 5.20 (m, 3H), 5.13 – 5.09 (m, 2H), 2.33 (s, 3H) ppm; **$^{13}$C{$^1$H} NMR** (75 MHz) δ: 233.1, 141.8, 138.6, 137.0, 129.6, 129.5, 128.8, 127.3, 115.3, 95.55, 95.50, 93.2, 91.3, 54.6, 21.2 ppm; tricarbonylchromium-coordinated protons and carbons exhibit diastereotopic signals; *meta*- and *meta'*- proton signals overlap with the benzylic proton; *meta- and meta'*- carbon signals overlap; **IR:** 3027, 2923, 1963, 1877, 1512, 1494, 1453, 701, 661, 630 $cm^{-1}$. **HRMS** (ES+) calc'd for $C_{20}H_{18}Cr$ 310.0814, observed 310.0806 [M - $(CO)_3]^+$.

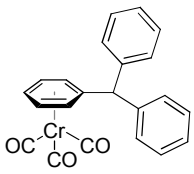


**5b – $Ph_2CH(\eta^6\text{-}C_6H_5)Cr(CO)_3$**: Using General procedure 1-A, **4a** (30.1 mg, 0.099 mmol, 1.0 equiv) was reacted with LiHMDS (27 mg, 0.16 mmol, 1.6 equiv) and $PdCl_2(PPh_3)_2$ (2.5 mg, 0.0036 mmol, 3.6 mol %) in 0.8 mL THF and bromobenzene (17 µL, 0.16 mmol, 1.6 equiv) for 50 min at 56 °C, yielding **5b** (34.6 mg, 0.091 mmol, 92% yield) as a bright yellow crystalline solid after silica gel chromatography eluting with 20% diethyl ether in pentane. **$^1$H NMR** (300 MHz, $CDCl_3$) δ: 7.36 – 7.26 (m, 6H), 7.18 (m, 4H), 5.36 (t, *J* = 6.3 Hz, 1H), 5.24-5.20 (m, 3H), 5.11 (d, *J* = 6.3 Hz, 2H) ppm; **$^{13}$C{$^1$H} NMR** (75 MHz) δ: 233.1, 141.6, 129.6, 128.8, 127.4, 114.9, 95.6, 93.3, 91.2, 54.9 ppm; tricarbonylchromium-coordinated arene *meta*- protons overlap with the benzylic proton; **IR** 3085, 3053, 3028, 1963 and 1878 (strong CO stretch), 1626, 1568, 1495, 1452, 1415, 1301, 1268, 1213, 1184, 1081, 923, 826, 758, 741, 702, 662, 630, 619, 534 $cm^{-1}$; **HRMS (ES+)** calc'd for $C_{19}H_{16}Cr$ 296.0657, observed 296.0650 [M -$(CO)_3]^+$. *Existing literature characterization corresponds with the characterization data for this compound.*[72]

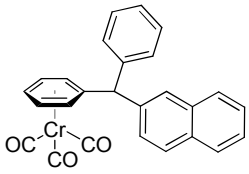


**5c – (2-naphthyl)PhCH($\eta^6$-$C_6H_5$)$Cr(CO)_3$**: Using General procedure 1-A, **4a** (15.2 mg, 0.050 mmol, 1.0 equiv) was reacted with LiHMDS (12 mg, 0.070 mmol, 1.4 equiv) and $PdCl_2(PPh_3)_2$ (1.7 mg, 0.0025 mmol, 5 mol %) in 0.6 mL THF and 2-bromonaphthalene (12.3 mg, 0.060 mmol, 1.2 equiv) for 1 h at 57 °C, yielding **5c** (19.5 mg, 0.045 mmol, 90% yield) as a pale yellow solid after silica gel chromatography eluting with 6% diethyl ether in pentane. **$^1$H NMR** (300 MHz, $CDCl_3$) δ: 7.84 - 7.80 (m, 2H), 7.78 - 7.75 (m, 1H), 7.56 (br s, 1H), 7.50 - 7.45 (m, 2H), 7.37 - 7.28 (m, 4H), 7.26 - 7.23 (m, 2H), 5.41 - 5.36 (m, 2H), 5.28 - 5.20 (m, 2H), 5.17 - 5.11 (m, 2H) ppm; **$^{13}$C{$^1$H} NMR** (75 MHz) δ: 233.1, 141.3, 139.4, 133.4, 132.6, 129.8, 128.8, 128.5, 128.3, 128.1, 127.9, 127.8, 127.5, 126.6, 126.4, 114.7, 95.8, 95.5, 93.4, 91.2, 55.0 ppm. Tricarbonylchromium-coordinated protons and carbons exhibit diastereotopic signals; *meta- and*

*meta'*- carbon signals overlap; **IR** 3059, 3028, 1963 and 1877 (strong CO stretches), 1600, 1494, 1453, 1414, 816, 748, 702, 630, 660 $cm^{-1}$.

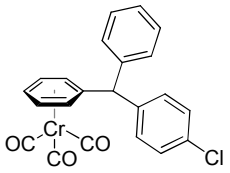

**5d – (4-$C_6H_4$-Cl)PhCH($\eta^6$-$C_6H_5$)Cr(CO)$_3$:** Using General procedure 1-A, **4a** (45.8 mg, 0.151 mmol, 1.0 equiv) was reacted with LiHMDS (40 mg, 0.24 mmol, 1.6 equiv) and $PdCl_2(PPh_3)_2$ (5.7 mg, 0.008 mmol, 5 mol %) in 2 mL THF and 1M 4-bromochlorobenzene THF solution (0.225 mL, 0.225 mmol, 1.5 equiv) for 6 h at 57 °C, yielding **5d** (51.8 mg, 0.125 mmol, 83% yield), as a highly crystalline yellow solid after purification by silica gel chromatography eluting with 20% diethyl ether in pentane. **$^1$H NMR** (300 MHz, $CDCl_3$) δ: 7.33 – 7.27 (m, 5H), 7.17 – 7.11 (m, 4H), 5.38 (t, *J* = 6.2 Hz, 1H), 5.23(m, 3H), 5.10 (d, *J* = 6.3 Hz, 1H), 5.05 (d, *J* = 6.3 Hz, 1H) ppm; $^{13}C\{^1H\}$ NMR (75 MHz) δ: 232.9, 141.24, 140.0, 133.4, 130.9, 129.5, 129.0, 128.9, 127.6, 114.2, 95.4, 95.2, 93.3, 91.2, 91.1, 54.3 ppm; tricarbonylchromium-coordinated protons and carbons exhibit diastereotopic signals; *meta*- and *meta'*-proton signals overlap with the benzylic proton; **IR** 3080, 3027, 1964 and 1879 (strong CO stretch), 1625, 1568, 1491, 1454, 1184, 1091, 1015, 923, 813, 755, 661, 629, 619 $cm^{-1}$; **HRMS** (ES+) calc'd for $C_{19}H_{15}ClCr$ 330.0267, 330.0258 $[M-(CO)_3]^+$.

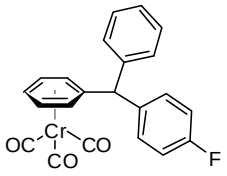

**5e – (4-$C_6H_4$-F)PhCH($\eta^6$-$C_6H_5$)Cr(CO)$_3$:** Using General procedure 1-A, **4a** (60.5 mg, 0.199 mmol, 1.0 equiv) was reacted with LiHMDS (60.5 mg, 0.36 mmol, 1.8 equiv) and $PdCl_2(PPh_3)_2$ (7.6 mg, 0.01 mmol, 5 mol %) in 3 mL THF and 4-bromofluorobenzene (35 µL, 0.3 mmol, 1.5 equiv) for 6 h at 60 °C, yielding **5e** (69.7 mg, 0.175 mmol, 88% yield) as a bright yellow crystalline solid after purification by silica gel chromatography. **$^1$H NMR** (300 MHz, $CDCl_3$) δ: 7.37 – 7.24 (m, 3H), 7.17 – 7.13 (m, 4H), 7.02 (t, *J* = Hz, 2H), 5.37 (t, *J* = 6.2 Hz, 1H), 5.25 – 5.20 (m, 3H), 5.12 (d, *J* = 6.8 Hz, 1H), 5.05 (d, *J* = 6.6 Hz, 1H) ppm**; $^{13}C\{^1H\}$ NMR** (75 MHz) δ:232.9, 162.1 (d, *J* = 347 Hz), 141.6, 131.13 (d, *J* = 8 Hz), 129.5, 128.9, 127.5, 115.7 (d, *J* = 21 Hz), 114.6, 95.5, 95.3, 93.4, 91.2, 91.1, 54.2 ppm; **$^{19}$F NMR** (282 MHz) δ: −115.4 (m) ppm; tricarbonylchromium-coordinated arene carbons and protons exhibit diastereotopic signals; *meta*- and *meta'*- proton signals overlap with the benzylic proton; **IR** 3079, 3027, 2895, 2746, 1964 and 1877 (strong CO stretch), 1624, 1507, 1495, 1454, 1303, 1224, 1183, 1098, 922, 819, 741, 702, 661, 629, 619 $cm^{-1}$; **HRMS** (ES+) calc'd for $C_{19}H_{15}CrF$ 314.0563, observed 314.0549 $[M-(CO)_3]^+$ .

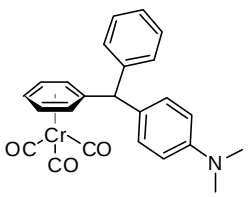

**5g – [4-$C_6H_4$-N($CH_3$)$_2$]PhCH($\eta^6$-$C_6H_5$)Cr(CO)$_3$:** Using General procedure 1-A, **4a** (30.2 mg, 0.099 mmol, 1.0 equiv) was reacted with LiHMDS (27 mg, 0.16 mmol, 1.6 equiv) and $PdCl_2(PPh_3)_2$ (3.1 mg, 0.004 mmol, 4 mol %) in 1 mL THF and 4-bromo-*N*,*N*-dimethylaniline (29.9 mg, 0.15 mmol, 1.5 equiv)

for 1 h at 52 °C, yielding **5g** (38.2 mg, 0.090 mmol, 91% yield) as a shiny pale yellow flakes after silica gel chromatography eluting with 6% diethyl ether in pentane. **$^1$H NMR** (300 MHz, $CDCl_3$) δ: 7.34 – 7.01 (m, 5H), 7.03 (d, *J* = 8.7 Hz, 2H), 6.68 (d, *J* = 8.8 Hz, 2H), 5.33 (t, *J* = 6.1 Hz, 1H), 5.25 – 5.20 (m, 2H), 5.16 – 5.08 (m, 3H), 2.94 (s, 6H) ppm; **$^{13}$C{$^1$H} NMR** (75 MHz) δ: 233.3, 149.7, 142.4, 130.2, 129.5, 129.2, 128.7, 127.1, 116.3, 112.6, 95.7, 95.4, 93.1, 91.4, 54.0, 40.7 ppm; tricarbonylchromium-coordinated protons and carbons exhibit diastereotopic signals; the *ortho'*-proton signal overlaps with the benzylic proton; *meta- and meta'*- carbon signals overlap; **IR** 3030, 2921, 2852, 2804, 1963 and 1878 (strong CO stretch), 611, 1520, 1452, 1352, 947, 702, 662, 630 $cm^{-1}$.

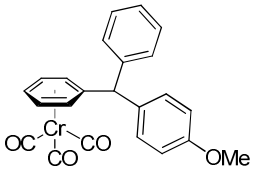


**5h – (4-$C_6H_4$-$OCH_3$)PhCH($\eta^6$-$C_6H_5$)$Cr(CO)_3$**: Using General procedure 1-A, **4a** (44.8 mg, 0.147 mmol, 1.0 equiv) was reacted with LiHMDS (39 mg, 0.23 mmol, 1.6 equiv) and $PdCl_2(PPh_3)_2$ (4.2 mg, 0.006 mmol, 4 mol %) in 1 mL THF and 4-bromoanisole (32 µL, 0.25 mmol, 1.7 equiv) for 45 min at 56 °C, yielding **5h** (56.7 mg, 0.138 mmol, 94% yield) as a yellow solid after silica gel chromatography eluting with 20% diethyl ether in pentane. **$^1$H NMR** (300 MHz, $CDCl_3$) δ: 7.35 – 7.26 (m, 3H), 7.17 (d, *J* = 6.9 Hz, 2H), 7.09 (d, *J* = 8.7 Hz, 2H), 6.86 (d, *J* = 8.7Hz, 2H), 5.35 (t, *J* = 6.6 Hz, 1H), 5.25 – 5.19 (m, 3H), 5.12 – 5.09 (m, 2H), 3.80 (s, 3H) ppm; **$^{13}$C{$^1$H} NMR** (75 MHz) δ: 233.1, 158.9, 142.1, 133.6, 130.6, 129.5, 128.8, 127.3, 115.5, 114.2, 95.51, 95.48, 93.2, 91.3, 55.5, 54.1 ppm; tricarbonylchromium-coordinated protons and carbons exhibit diastereotopic signals; *meta*- and *meta'*- proton signals overlap with the benzylic proton; *meta- and meta'*- carbon signals overlap; **IR** 3085, 3064, 3030, 3003, 2956, 2934, 2907, 2838, 1962 and 1875 (strong CO stretch), 1609, 1510, 1496, 1454, 1302, 1255, 1180, 1112, 1077, 1033, 922, 818, 741, 703, 662, 629, 619 $cm^{-1}$; **HRMS** (ES+) calc'd for $C_{20}H_{18}CrO$ 326.0763, observed 326.0933 $[M-(CO)_3]^+$.

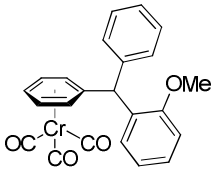


**5i – (2-$C_6H_4$-$OCH_3$)PhCH($\eta^6$-$C_6H_5$)$Cr(CO)_3$**: Using General procedure 1-A, **4a** (44.0 mg, 0.145 mmol, 1.0 equiv) was reacted with LiHMDS (38 mg, 0.23 mmol, 1.6 equiv) and $PdCl_2(PPh_3)_2$ (4 mg, 0.006 mmol, 4 mol %) in 1 mL THF and 2-bromoanisole (31 µL, 0.25 mmol, 1.7 equiv) for 1 h at 54 °C, yielding **5i** (54.0 mg, 0.132 mmol, 91% yield) as a highly crystalline yellow solid after silica gel chromatography eluting with 6% diethyl ether in pentane. **$^1$H NMR** (300 MHz, $CDCl_3$) δ: 7.30 – 7.19 (m, 6H), 6.94 – 6.86 (m, 3H), 5.63 (s, 1H), 5.37 (t, *J* = 6.1 Hz, 1H), 5.28 (d, *J* = 7.0 Hz), 5.16 (t, *J* = 6.5 Hz, 2H), 5.08 (d, *J* = 6.5 Hz), 3.77 (s, 3H) ppm; **$^{13}$C{$^1$H} NMR** (75 MHz) δ: 233.2, 141.2, 130.8, 130.2, 129.6, 128.6, 128.5, 127.1, 120.4, 114.4, 111.1, 96.2, 96.1, 93.8, 90.42, 90.39, 55.6, 47.9 ppm; tricarbonylchromium-coordinated protons and carbons exhibit diastereotopic signals; **IR** 3064,

3028, 2936 and 2838 (strong CO stretch), 1962, 1878, 1598, 1491, 1454, 1248, 1029, 755, 702, 662, 630 $cm^{-1}$.

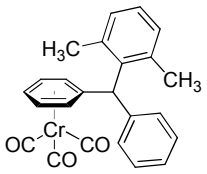

**5j – [2,6-$C_6H_3$-$(CH_3)_2$]PhCH($\eta^6$-$C_6H_5$)Cr(CO)$_3$:** Using General procedure 1-A, **4a** (60.5 mg, 0.199 mmol, 1.0 equiv) was reacted with LiHMDS (50.3 mg, 0.30 mmol, 1.5 equiv) and $PdCl_2(PPh_3)_2$ (6.8 mg, 0.01 mmol, 5 mol %) in 3.5 mL THF with 1-bromo-2,6-dimethylbenzene (55 µL, 0.4 mmol, 2 equiv) for 24 h at 58 °C, yielding **5j** (65.3 mg, 0.16 mmol, 81% yield) as a yellow solid after silica gel chromatography eluting with 10% diethyl ether in pentane (5.7 mg, 10% of starting material **4a** also isolated). **$^1$H NMR** (300 MHz, $CDCl_3$) δ: 7.36 – 7.25 (m, 3H), 7.14 (t, *J* = 7.4 Hz, 1H), 7.05 (broad d, *J* = 7.2 Hz, 2H), 5.84 (s, 1H), 5.30 – 5.25 (m, 4H), 5.09 (d, *J* = 6.3 Hz, 1H), 2.16 (very broad s, 6H) ppm; **$^{13}$C{$^1$H} NMR** (75 MHz) δ: 133.4, 138.5, 137.2, 129.6, 128.9, 127.7, 127.5, 116.6, 95.16, 92.7, 92.2, 91.6, 49.5 ppm; tricarbonylchromium-coordinated protons and carbons exhibit diastereotopic signals; *meta- and meta'-* carbon signals overlap; signals from the non-axial carbons of the xylyl group were not observed in the $^{13}C\{^1H\}$ NMR due to the hindered rotation. **IR** 3064, 3022, 2962, 2914, 2743, 1961 and 1873 (strong CO stretch), 1625, 1495, 1467, 1455, 1301, 1214, 1183, 1097, 1078, 924, 821, 772, 738, 662, 629, 619 $cm^{-1}$; **HRMS** (ES+) calc'd for $C_{21}H_{20}Cr$ 324.097, observed 324.0985 $[M-(CO)_3]^+$.

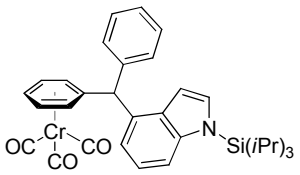

**5k – [1-(triisopropylsilyl)-1*H*-indol-4-yl]PhCH($\eta^6$-$C_6H_5$)Cr(CO)$_3$:** Using General procedure 1-A, **4a** (30.4 mg, 0.100 mmol, 1.0 equiv) was reacted with LiHMDS (25 mg, 0.15 mmol, 1.5 equiv) and $PdCl_2(PPh_3)_2$ (5 mg, 0.005 mmol, 7 mol %) in 1 mL THF and 4-bromo-1-TIPS-indole (45 mg, 0.13 mmol, 1.3 equiv) for 40 min at 58 °C, yielding **5k** (51.4 mg, 0.089 mmol, 89% yield) as a shiny pale yellow solid after silica gel chromatography eluting with 6% diethyl ether in pentane. **$^1$H NMR** (300 MHz, $CDCl_3$) δ: 7.42 (d, *J* = 8.3 Hz, 1H), 7.31 - 7.24 (m, 5H), 7.17 (d, *J* = 3.3 Hz, 1H), 7.08 (t, *J* = 7.8 Hz, 1H), 6.72 (d, *J* = 7.3 Hz, 1H), 6.51 (d, *J* = 2.6 Hz, 1H), 5.62 (s, 1H), 5.45 (d, *J* = 6.9 Hz, 1H), 5.38 (t, *J* = 6.2 Hz, 1H), 5.23 - 5.18 (m, 2H), 5.01 (d, *J* = 6.6 Hz, 1H), 1.67 (septet, *J* = 7.5 Hz, 3H), 1.12 (d, *J* = 7.5 Hz, 18H) ppm; **$^{13}$C{$^1$H} NMR** (75 MHz) δ: 233.3, 141.2, 140.6, 134.9, 131.5, 131.2, 129.7, 128.6, 127.3, 121.1, 120.1, 115.3, 113.1, 103.5, 96.9, 95.7, 93.7, 91.0, 90.8, 52.8, 18.4, 13.1 ppm; tricarbonylchromium-coordinated protons and carbons exhibit diastereotopic signals; **IR** 3062, 3027, 2949, 2869, 1966 and 1883 (strong CO stretch), 1600, 1426, 1283, 1148, 1016, 883, 751, 631, 661 $cm^{-1}$.

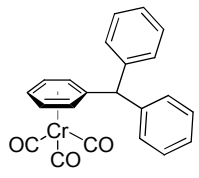

**5b** from **CrTol** (**3**): Using General procedure 1-A, ($\eta^6$-toluene)Cr(CO)$_3$ (**3**) (45.8 mg, 0.201 mmol, 1.0 equiv) was reacted with LiHMDS (93.5 mg, 0.57 mmol,

2.8 equiv) and 5.4 mg of $PdCl_2(PPh_3)$ in 2 mL THF with 64 µL of bromobenzene (0.6 mmol, 3 equiv) for 5 h at 57 °C, yielding 68.9 mg (0.181 mmol, 90% yield) of **5b**. All appearances and characterization data are consistent with that of **5b** obtained from cross-coupling of **4a** with bromobenzene (p. 48).

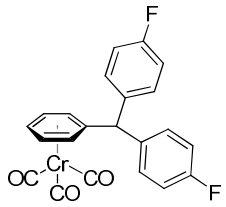

**5l – (4-$C_6H_4$-F)$_2$CH($\eta^6$-$C_6H_5$)Cr(CO)$_3$**: Using General procedure 1-A, **3** (45.5 mg, 0.199 mmol, 1.0 equiv) was reacted with LiHMDS (97 mg, 0.58 mmol, 2.9 equiv) and $PdCl_2(PPh_3)_2$ (5.1 mg, 0.007 mmol, 4 mol %) of in 2.5mL THF with 4-bromofluorobenzene (66 µL, 0.6 mmol, 3 equiv) for 5.5 h to yield **5l** (68.7 mg, 0.165 mmol, 83% yield) as a deep yellow solid after silica gel chromatography eluting with 13% diethyl ether in pentane. **$^1$H NMR** (300 MHz, $CDCl_3$) δ: 7.15 – 7.11 (m, 4H), 7.06 – 7.00 (t, *J* = 8.5 Hz, 4H), 5.39 (t, *J* = 6.1 Hz, 1H), 5.25 – 5.20 (m, 3H), 5.06 (d, *J* = 6.2 Hz, 2H) ppm; **$^{13}$C{$^1$H} NMR** (75 MHz) δ: 232.8, 62.1 (d, *J* = 246.5 Hz), 137.2, 131.0 (d, *J* = 8.0 Hz), 115.8 (d, *J* = 21.4 Hz), 114.2, 95.2, 93.4, 91.1, 53.4 ppm; **$^{19}$F NMR** (282 MHz) δ: −118.1 (m) ppm; tricarbonylchromium-coordinated arene *meta*- proton signals overlap with the benzylic proton; **IR** 3074, 3044, 1966 and 1880 (strong CO stretch), 1631, 1605, 1506, 1457, 1321, 1302, 1268, 1225, 1185, 1159, 1100, 924, 824, 661, 629 cm$^{-1}$; **HRMS** (ES+) calc'd for $C_{19}H_{14}CrF_2$ 332.0469, observed 332.0460 $[M-(CO)_3]^+$.

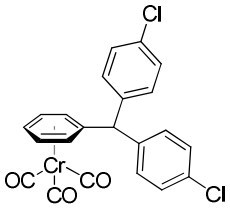

**5m – (4-$C_6H_4$-Cl)$_2$CH($\eta^6$-$C_6H_5$)Cr(CO)$_3$**: Using General procedure 1-A, **3** (11.4 mg, 0.050 mmol, 1.0 equiv) was reacted with LiHMDS (34 mg, 0.20 mmol, 4 equiv) and $PdCl_2(PPh_3)_2$ (3.9 mg, 0.005 mmol, 10 mol %) in 0.6 mL THF and 1M 4-bromochlorobenzene THF solution (0.125 mL, 0.125 mmol, 2.5 equiv) for 2 h at 53 °C to yield **5m** (17.5 mg, 0.039 mmol, 78%) as a highly crystalline yellow solid after silica gel chromatography eluting with 20% diethyl ether in pentane. **$^1$H NMR** (300 MHz, $CDCl_3$) δ: 7.31 (d, *J* = 8.4 Hz, 4H), 7.09 (d, *J* = 8.4 Hz, 4H), 5.38 (t, *J* = 6.2 Hz, 1H), 5.23 (t, *J* = 6.3Hz, 2H), 5.18 (s, 1H), 5.04 (d, *J* = 6.3 Hz, 2H) ppm; **$^{13}$C{$^1$H} NMR** (75 MHz) δ: 232.7, 139.6, 133.6, 130.8, 129.1, 113.5, 95.0, 93.3, 91.1, 53.6 ppm; **IR** 3090, 3027, 1965 and 1881 (strong CO stretch), 1490, 1405, 1092, 1014, 810, 659, 629 cm$^{-1}$.

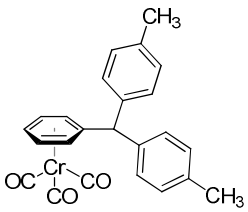

**5n – (4-$C_6H_4$-$CH_3$)$_2$CH($\eta^6$-$C_6H_5$)Cr(CO)$_3$**: Using General procedure 1-A, **3** (34 mg, 0.149 mmol, 1.0 equiv) was reacted with $LiN(SiMe_3)_2$ (64 mg 0.38 mmol, 2.6 equiv) and $PdCl_2(PPh_3)_2$ (8 mg, 0.01 mmol, 8 mol%) in 2 mL THF with 4-bromotoluene (50 µL, 0.4 mmol, 2.7 equiv) for 2 h at 62 °C to yield **5n** (47.6 mg, 0.117 mmol, 78% yield) as a fluffy bright yellow solid after silica gel chromatography. **$^1$H NMR** (300 MHz, $CDCl_3$) δ: 7.12 (d, *J* = 8.1 Hz, 4H), 7.05 (d, *J* = 8.1 Hz, 4H), 5.34 (t, *J* = 6.2 Hz, 1H), 5.22 (t, *J* = 6.3 Hz, 2H), 5.17 (s, 1H), 5.10 (d, *J* = 6.3 Hz, 2H), 2.33 (s, 6H); $^{13}$C{$^1$H}

NMR (75 MHz) δ: 233.3, 138.8, 136.9, 129.43, 129.42, 115.7, 95.5, 93.1, 91.4, 54.2, 21.3 ppm; **IR** 3022, 2921, 1963, 1878, 1626, 1567, 1510, 1456, 1300, 1214, 1188, 1113, 923, 810, 768, 736, 661, 631, 619, 534 $cm^{-1}$; **HRMS** (ES+) calc'd for $C_{21}H_{20}Cr$ 324.0970, found 324.0972 $[M-(CO)_3]^+$. *X-ray crystal structure was determined for this compound; see p.257.*

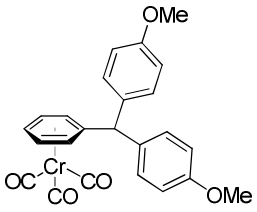


**5o – (4-$C_6H_4$-$OCH_3$)$_2$CH(η$^6$-$C_6H_5$)Cr(CO)$_3$**: UsingGeneral procedure 1-A, **3** (22.1 mg, 0.097 mmol, 1.0 equiv) was reacted with $LiN(SiMe_3)_2$ (62 mg, 0.37 mmol, 3.8 equiv) and $PdCl_2(PPh_3)_2$ (5.4 mg, 0.008 mmol, 8 mol%) in 1.3 mL THF and 4-bromoanisole (38 µL, 0.3 mmol, 3 equiv) for 2 h at 56 ºC to yield **5o** (35.8 mg, 0.081 mmol, 84% yield) as a bright yellow solid after column chromatography. **$^1$H NMR** (300 MHz, $CDCl_3$) δ: 7.08 (d, *J* = 8.6 Hz, 4H), 6.85 (d, *J* = 8.8 Hz, 4H), 5.34 (t, *J* = 6.2 Hz, 1H), 5.23 (t, *J* = 6.3 Hz, 2H), 5.15 (s, 1H), 5.09 (d, *J* = 6.3 Hz, 2H), 3.79 (s, 6H); **$^{13}$C{$^1$H} NMR** (75 MHz) δ: 233.2, 158.8, 134.1, 130.5, 116.0, 114.1, 95.4, 93.1, 91.4, 55.5, 53.3 ppm; **IR** 3077, 3038, 3000, 2934, 2904, 2837, 1961, 1875, 1766, 1616, 1567, 1509, 1464, 1301, 1245, 1180, 1112, 1034, 924, 820, 735, 678, 663, 630, 619, 535 $cm^{-1}$; **HRMS** (ES+) calc'd for $C_{21}H_{20}CrO_2$ 356.0868, observed 356.0862 $[M-(CO)_3]^+$.

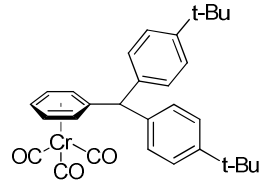


**5p – [4-$C_6H_4$-*t*Bu]$_2$CH(η$^6$-$C_6H_5$)Cr(CO)$_3$**: Using General procedure 1-A, **3** (34 mg, 0.149 mmol, 1.0 equiv) of was reacted with LiHMDS (70 mg , 0.42 mmol, 2.8 equiv) and $PdCl_2(PPh_3)_2$ (10.9 mg, 0.015 mmol, 10 mol %) in 4 mL THF with 4-*tert*-butyl-bromobenzene (65 µL, 0.45 mmol, 3 equiv) for 5 h at 46 ºC to yield **5d** (60.0 mg, 0.122 mmol, 82% yield) as a pale yellow solid after silica gel chromatography eluting with 3% diethyl ether in pentane. **$^1$H NMR** (300 MHz, $CDCl_3$) δ: 7.33 (d, *J* = 8.4 Hz, 4H), 7.10 (d, *J* = 8.4 Hz, 4H), 5.34 (t, *J* = 6.2 Hz, 1H), 5.22 (t, *J* = 6.3 Hz, 2H), 5.16 – 5.13 (m, 3H), 1.30 (S, 18H) ppm; **$^{13}$C{$^1$H} NMR** (75 MHz) δ: 233.3, 150.1, 138.7, 129.2, 125.6, 115.9, 95.6, 93.1, 91.3, 54.1, 34.7, 31.6 ppm; tricarbonylchromium-coordinated arene *ortho*- proton signals overlap with the benzylic proton; **IR** 3028, 2965, 2905, 2870, 1960 and 1880 (strong CO stretch), 1476, 1461, 1365, 1265, 704, 667, 623 $cm^{-1}$. **HRMS** (ES+) calc'd for $C_{27}H_{32}Cr$ 408.1909, found 408.1901 $[M-(CO)_3]^+$.

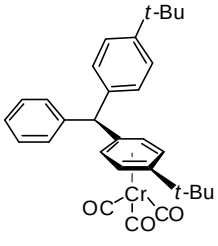


**5p′ – (4-$C_6H_4$-*t*Bu)CHPh(η$^6$-4-$C_6H_4$-*t*Bu)Cr(CO)$_3$**: The "walking" isomer is the more thermodynamically stable isomer due to the slightly more electron-rich coordinating arene. It can be synthesized from **5p** by heating with base in THF and then quenching with 2 drops water, diluting with ether, and filtering over a small plug of $MgSO_4$ and silica gel. **$^1$H NMR** (300 MHz, $CDCl_3$) δ: 7.32 (m, 4H), 7.26 (m, 1H), 7.20 (m, 2H), 7.11 (d, J = 8.2 Hz, 2H), 5.40 (m, 2H), 5.23 (s, 1H),

5.06 (m, 1H), 5.01 (m, 1H), 1.30 (s, 9H), 1.29 (s, 9H) ppm; **$^{13}C\{^1H\}$ NMR** (75 MHz) δ: 233.9, 150.2, 142.0, 138.7, 129.6, 128.7, 127.3, 125.7, 123.2, 115.7, 94.2, 94.0, 91.1, 54.1, 34.7, 34.1, 31.6, 31.3 ppm; **HRMS** (ES+): 408.1917 $[M-(CO)_3]^+$

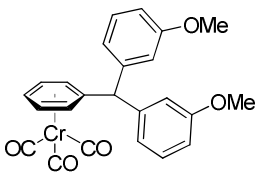


**5q – $(3\text{-}C_6H_4\text{-}OCH_3)_2CH(\eta^6\text{-}C_6H_5)Cr(CO)_3$**: Using General procedure 1-A, **3** (34.8 mg, 0.153 mmol, 1.0 equiv) was reacted with LiHMDS (96 mg, 0.57 mmol, 3.7 equiv) and $PdCl_2(PPh_3)_2$ (8.3 mg, 0.012 mmol, 8 mol %) in 3 mL THF and 3-bromoanisole (57 µL, 0.45 mmol, 3 equiv) for 1.5 h at 57 °C to yield **5q** (57.7mg, 0.131 mmol, 86% yield) as a yellow solid after silica gel chromatography eluting with 15% diethyl ether in pentane. **$^1H$ NMR** (300 MHz, $CDCl_3$) δ: 7.24 (t, *J* = 7.5 Hz, 2H), 6.82 – 6.73 (m, 6H), 5.36 (t, *J* = 6.1 Hz, 1H), 5.23 (t, *J* = 6.4 Hz, 2H), 5.17 – 5.13 (m, 3H), 3.79 (s, 6H) ppm; **$^{13}C\{^1H\}$ NMR** (75 MHz) δ: 233.1, 159.9, 143.0, 129.7, 122.0, 115.6, 114.9, 112.7, 95.5, 93.3, 91.3, 55.4, 54.9 ppm; tricarbonylchromium-coordinated arene *ortho*- proton signals overlap with the benzylic proton; **IR** 3079, 3005, 2940, 2837, 1961 and 1874 (strong CO stretch), 1598, 1584, 1488, 1455, 1266, 1049, 759, 662, 631 $cm^{-1}$; **HRMS** (ES+) calc'd for $C_{21}H_{20}CrO_2$ 356.0868, observed 356.0866 $[M-(CO)_3]^+$.

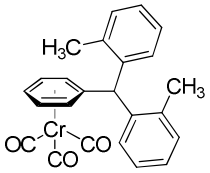


**5f – $(2\text{-}C_6H_4\text{-}CH_3)_2CH(\eta^6\text{-}C_6H_5)Cr(CO)_3$**: Using General procedure 1-A, **3** (45 mg, 0.197 mmol, 1.0 equiv) was reacted with LiHMDS (94 mg, 0.56 mmol, 2.8 equiv) and $PdCl_2(PPh_3)_2$ (13 mg, 0.018 mmol, 9 mol %) in 4.2 mL THF and 2-bromotoluene (75 µL, 0.6 mmol, 3 equiv) for 12 h at 58 °C to yield 70.7 mg (0.173 mmol, 88% yield) of **5r** as a yellow solid after silica gel chromatography eluting with 10% diethyl ether in pentane. **$^1H$ NMR** (300 MHz, $CDCl_3$) δ: 7.21 – 7.09 (m, 6H), 6.93 (d, *J* = 7.4 Hz, 2H), 5.52 (t, *J* = 6.1 Hz, 1H), 5.45 (s, 1H), 5.29 (d, *J* = 6.3 Hz, 2H), 5.11 (t, *J* = 6.3 Hz, 2H), 2.41 (s, 6H) ppm; **$^{13}C\{^1H\}$ NMR** (75 MHz) ppm 233.0, 140.0, 137.2, 131.2, 129.4, 127.2, 126.1, 111.9, 97.5, 95.8, 88.8, 47.5, 19.9 ppm; **IR** 3073, 3020, 2945, 2913, 1963 and 1877 (strong CO stretch), 1628, 1492, 1461, 1297, 1213, 1183, 1101, 1056, 923, 823, 742, 729, 663, 629 $cm^{-1}$.

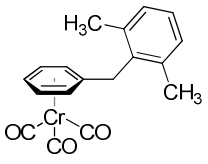


**4b – $[2,6\text{-}C_6H_3\text{-}(CH_3)_2]CH(\eta^6\text{-}C_6H_5)Cr(CO)_3$**: Using general procedure A, **3** (91.4 mg, 0.401 mmol, 1.0 equiv) was reacted with LiHMDS (98.5 mg, 0.59 mmol, 1.5 equiv) and $PdCl_2(PPh_3)_2$ (15.5 mg, 0.022 mmol, 5 mol %) in 4 mL THF and 1-bromo-2,6-dimethybenzene (0.11 mL, 0.8 mmol, 2 equiv) for 8 h at 63 °C to yield **4b** (114 mg. 0.343 mmol, 86% yield) as a fluffy yellow solid after silica gel chromatography eluting with 20% diethyl ether in pentane . **$^1H$ NMR** (300 MHz, $CDCl_3$) δ: 7.07 (m, 3H), 5.32 (t, *J* = 6.3 Hz, 2H), 5.21 (m, 3H), 3.91 (s, 2H), 2.33 (s, 6H) ppm; **$^{13}C\{^1H\}$ NMR** (75 MHz) δ: 233.4,

137.3, 134.6, 128.8, 127.4, 111.4, 93.9, 92.8, 91.8, 33.7, 20.7 ppm; tricarbonylchromium-coordinated arene *ortho*- and *para*- proton signals overlap; **IR** 3074, 3041, 2944, 1971 and 1858 (strong CO stretch), 1625, 1502, 1462, 1300, 1213, 1184, 1097, 923, 820, 775, 736, 672, 632, 616 $cm^{-1}$; **HRMS** (ES+) calc'd for $C_{15}H_{16}Cr$ 248.0657, observed 248.0653 $[M-(CO)_3]^+$.

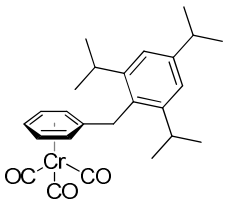

**4c – (2,4,6-$C_6H_2$-$^J$Pr$_3$)CH($\eta^6$-$C_6H_5$)Cr(CO)$_3$**: Using General procedure 1-A, **3** (45.5 mg 0.199 mmol, 1.0 equiv) was reacted with LiHMDS (50 mg, 0.30 mmol, 1.5 equiv) and $PdCl_2(PPh_3)_2$ (8.5 mg, 0.012 mmol, 6 mol %) in 1.5 mL THF and 2,4,6-triisopropylbromobenzene (74 µL, 0.4 mmol, 2 equiv) for 12 h at 63 ºC to yield **4c** (69.4 mg, 0.162 mmol, 87% yield) as a fluffy pale yellow solid after column chromatography eluting with 6% diethyl ether in pentane. **$^1$H NMR** (300 MHz, $CDCl_3$) δ: 7.02 (s, 2H), 5.33 (t, *J* = 6.4 Hz, 2H), 5.19 (m, 3H), 3.95 (s, 2H), 3.09 (m, *J* = 6.8 Hz, 2H), 2.89 (m, *J* = 6.9 Hz, 1H), 1.26 (d, *J* = 6.9 Hz, 6H), 1.20 (d, *J* = 6.8 Hz, 12H) ppm; **$^{13}$C{$^1$H} NMR** (75 MHz) δ: 233.4, 148.2, 147.7, 128.5, 121.6, 113.7, 94.1, 92.8, 91.7, 34.4, 31.5, 30.2, 24.5, 24.2 ppm; tricarbonylchromium-coordinated arene *ortho*- and *para*- proton signals overlap; **IR** ($CH_2Cl_2$ film) 2962, 2928, 2869, 1965 and 1882 (strong CO stretch), 1607, 1574, 1526, 1457, 1384, 1363, 1153, 879, 664, 630 $cm^{-1}$; H**R**MS (ES+) calc'd for $C_{22}H_{30}Cr$ 346.1753, observed 346.1765 $[M-(CO)_3]^+$.

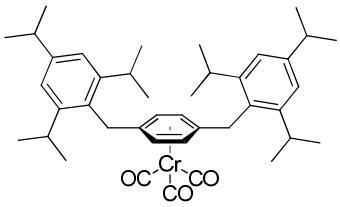

**11 – 1,4-[2,4,6-$C_6H_2$-$^J$Pr$_3$CH$_2$]$_2$($\eta^6$-$C_6H_4$)Cr(CO)$_3$**: Using General procedure 1-A, ($\eta^6$-*p*-xylene)$Cr(CO)_3$ (**8**) (23.9 mg, 0.099 mmol, 1.0 equiv) was reacted with LiHMDS (82 mg, 0.49 mmol, 4.9 equiv) and $PdCl_2(PPh_3)_2$ (8.4 mg, 0.012 mmol, 12 mol %) in 2.4 mL THF and 2,4,6-triisopropylbromobenzene (56 µL, 0.3 mmol, 3 equiv) for 24 h at 55 ºC to yield **11** (46.4 mg, 0.072 mmol, 73% yield) as a fluffy pale yellow solid after silica gel chromatography eluting with 3% diethyl ether in pentane. **$^1$H NMR** (300 MHz, $CDCl_3$) δ: 6.97 (s, 4H), 5.20 (s, 4H), 3.88 (s, 4H), 3.04 (m, *J* = 6.8Hz, 4H), 2.87 – 2.82 (m, *J* = 6.9Hz, 2H), 1.23 (d, *J* = 6.8 Hz, 12H), 1.15 (d, *J* = 6.9 Hz, 24 H) ppm; **$^{13}$C{$^1$H} NMR** (75 MHz) δ: 233.8, 148.1, 147.6, 128.6, 121.5, 112.2, 94.0, 34.4, 31.0, 30.1, 24.2, 24.2 ppm; **IR** 3058, 2962, 2928, 2869, 1962 and 1882 (strong CO stretch), 1608, 1462, 1384, 1363, 1101, 878, 667, 625 $cm^{-1}$; **HRMS** (ES+) calc'd for $C_{38}H_{54}Cr$ 562.3631, found 562.3657 $[M-(CO)_3]^+$.

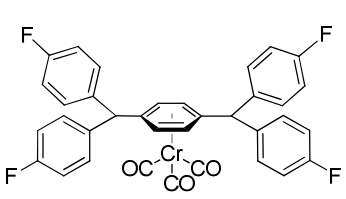

**12 – 1,4-[(4-$C_6H_4$-F)$_2$CH]$_2$($\eta^6$-$C_6H_4$)Cr(CO)$_3$**: Using General procedure 1-A, **8** (12.1 mg, 0.050 mmol, 1.0 equiv) was reacted with LiHMDS (75.6 mg, 0.45 mmol, 9.0 equiv) and $PdCl_2(PPh_3)_2$ (3.6 mg, 0.005 mmol, 10 mol %) in 1.0 mL THF and 4-bromofluorobenzene (33 µL, 0.3 mmol, 6 equiv) for 20 h at 58 –

60 ºC to yield **12** (21.5 mg, 0.035 mmol, 70% yield) as a highly crystalline pale yellow solid after silica gel chromatography eluting with 20% diethyl ether in pentane. **$^1$H NMR** (300 MHz, $CDCl_3$) δ: 7.12 (m, 4H), 7.02 (t, *J* = Hz, 4H), 1.32 (s, 9H) ppm; **$^{13}$C{$^1$H} NMR** (75 MHz) δ: 232.8, 162.1 (d, *J* = 247 Hz), 137.1, 130.9 (d, *J* = 8 Hz), 115.9 (d, *J* = 22 Hz), 114.6, 93.7, 35.0 ppm; **$^{19}$F NMR** (282 MHz) δ: −117.9 (m) ppm; **IR** 3112, 3077, 3044, 2884, 2747, 1963 and 1876 (strong CO stretch), 1766, 1630, 1567, 1505, 1468, 1300, 1223, 1183, 1159, 1100, 924, 826, 737, 665, 622 cm$^{-1}$. **HRMS (ES+)** calc'd for $C_{32}H_{22}CrF_4$ 618.0910, found 618.0919 $[M]^+$.

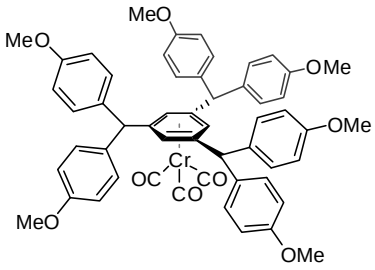


**17 – 1,3,5-[(4-$C_6H_4$-$OCH_3$)$_2$CH]$_3$($\eta^6$-$C_6H_3$)Cr(CO)$_3$:** Using General procedure 1-A, **($\eta^6$-mesitylene)Cr(CO)$_3$** (**9**) (25.5 mg (0.099 mmol, 1.0 equiv) was reacted with LiHMDS (188 mg, 1.1 mmol, 11 equiv) and $PdCl_2(PPh_3)_2$ (14.1 mg, 0.02 mmol, 20 mol %) in 2.6 mL of THF and 4-bromoanisole (0.125 mL, 1.0 mmol, 10 equiv) for 5 h at 55 ºC to yield **17** (38.6 mg, 0.043 mmol, 43% yield) as a yellow crystalline solid after silica gel chromatography eluting with 40% diethyl ether in pentane. **$^1$H NMR** (300 MHz, $CDCl_3$) δ: 6.96 (d, *J* = 8.6 Hz, 12H), 6.81 (d, *J* = 8.6 Hz, 2H), 4.94 (s, 3H), 4.93 (s, 3H), 3.81 (s, 18H) ppm; **$^{13}$C{$^1$H} NMR** (75 MHz) δ: 233.4, 158.6, 134.4, 130.3, 113.9, 113.6, 97.6, 55.5, 53.0 ppm; the tricarbonylchromium-coordinated arene proton signal overlaps with the benzylic proton sigmal; **IR** 3071, 3000, 2953, 2932, 2903, 2835, 1956 and 1874 (strong CO stretch), 1766, 1611, 1509, 1464, 1302, 1250, 1179, 1112, 1035, 925, 830, 736, 667, 625 cm$^{-1}$; **HRMS** (ES+) calc'd for $C_{54}H_{48}CrO_9$ 892.2703, found 892.2746 $[M]^+$. *X-ray crystal structure was determined for this compound;* *see p. 264.*

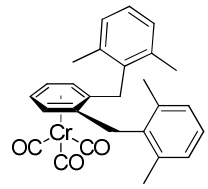


**19** – 1,2-[(2,6-$C_6H_3$-$Me_2$)$CH_2$]$_2$($\eta^6$-$C_6H_4$)Cr(CO)$_3$: Using General procedure 1-A, ($\eta^6$-*o*-xylene)Cr(CO)$_3$ (**18**) (12.2 mg, .0504 mmol, 1.0 equiv) was reacted with LiHMDS (50 mg, 0.30 mmol, 6 equiv) and $PdCl_2(PPh_3)_2$ (4.9 mg, 7 µmol, 14 mol %) in 0.75 mL THF and 2-bromo-1,3-dimethylbenzene (20 µL, 0.15 mmol, 3 equiv) for 5 h at 62 ºC to yield **19** (19.3 mg, 0.0428 mmol, 85% yield) as a pale yellow solid after silica gel chromatography eluting with 6% diethyl ether in pentane. **$^1$H NMR** (300 MHz, $CDCl_3$) δ: 7.13 (m, 6H), 5.10 (dd, *J* = 4.7, 2.9 Hz, 2H), 4.87 (dd, *J* = 4.6, 3.0 Hz, 2H), 4.11 (s, 1H), 2.37 (s, 12H) ppm; **$^{13}$C{$^1$H} NMR (**75 MHz) δ: 233.7, 137.6, 133.9, 128.8, 127.5, 109.9, 92.9, 92.1, 31.1, 20.3 ppm; **IR** 2923, 2853, 1952 and 1869 (strong CO stretch), 1470, 1434, 1381, 1027, 769, 666 cm$^{-1}$; **HRMS** (ES+) calc'd for 450.1287 $C_{27}H_{26}CrO_3$, found 450.1274 $[M]^+$.

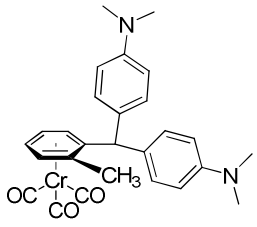

**20** – **1-[(4-C$_6$H$_4$-NMe$_2$)$_2$CH]-2-Me-(η$^6$-C$_6$H$_4$)Cr(CO)$_3$:** Using General procedure 1-A, (η$^6$-*o*-xylene)Cr(CO)$_3$ (**18**) (12.1 mg, 0.050 mmol, 1 equiv) was reacted with LiHMDS (26 mg, 0.15 mmol, 3 equiv) and $PdCl_2(PPh_3)_2$ (4.2 mg, 6 µmol, 12 mol %) in 0.7 mL THF and 4-bromo-*N*,*N*-dimethylaniline (30 mg, 0.15 mmol, 3 equiv) for 10 h at 48 ºC to yield **20** (15.4 mg, 0.032 mmol, 64% yield) as a yellow solid after silica gel chromatography eluting with 40% diethyl ether in pentane. **$^1$H NMR** (300 MHz, $CDCl_3$) δ: 7.06 (d, J = 8.8 Hz, 2H), 6.93 (d, *J* = 8.6 Hz, 2H), 6.67 (m, 4H), 5.39 (dt, *J* = 1.1, 6.3 Hz, 1H), 5.19 (s, 1H), 5.11 - 5.06 (m, 2H), 4.92 (dd, *J* = 0.7, 6.2 Hz, 1H), 2.93 (s, 6 H), 2.92 (s, 6H), 2.01 (s, 3H) ppm; **$^{13}$C{$^1$H} NMR** (75 MHz) δ: 233.9, 149.7, 149.4, 130.7, 130.4, 129.7, 128.7, 116.4, 112.7, 112.5, 110.3, 96.2, 94.6, 93.1, 89.8, 50.8, 40.8, 19.5 ppm; diastereotopic carbon signals on dimethylamino group overlap (40.8 ppm); **IR** 3074, 2922, 2854, 2804, 1958 and 1873 (strong CO stretche), 1611, 1520, 1352, 1227, 1203, 1166, 947, 816, 667, 630 cm$^{-1}$; **HRMS (ES+)** calc'd for $C_{24}H_{29}N_2$ 345.2331, found 345.2324 [MH - Cr(CO)$_3$]$^+$.

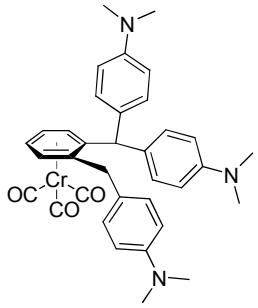

**21** –**1-[(4-C$_6$H$_4$-NMe$_2$)$_2$CH]-2-[(4-C$_6$H$_4$-NMe$_2$)CH$_2$](η$^6$-C$_6$H$_4$)Cr(CO)$_3$**: Using General procedure 1-A, (η$^6$-*o*-xylene)Cr(CO)$_3$ (**18**) (12.3 mg, 0.0508 mmol, 1 equiv) was reacted with LiHMDS (39 mg, 0.25 mmol, 5 equiv) and $PdCl_2(PPh_3)_2$ (5 mg, 7 µmol, 14 mol %) in 0.75 mL THF and 4-bromo-*N*,*N*-dimethylaniline (42 mg, 0.2 mmol, 4 equiv) for 24 h at 48 ºC to yield **21** (14.6 mg, 0.024 mmol, 48% yield) as a pale yellow solid after silica gel chromatography eluting with 40% diethyl ether in pentane. **$^1$H NMR** (300 MHz, $CDCl_3$) δ: 7.12 (d, *J* = 8.7 Hz, 2H), 6.97 (d, *J* = 8.7 Hz, 2H), 6.93 (d, *J* = 8.7 Hz, 2H), 6.71 - 6.63 (m, 6H), 5.38 (s, 1H), 5.27 (dt, *J* = 1.1, 6.3 Hz, 1H), 5.11 (dt, *J* = 1.1, 6.3 Hz, 1H), 4.90 (dd, *J* = 0.9, 6.4 Hz, 1H), 4.66 (dd, *J* = 1.0, 6.2 Hz, 1H), 3.88 (d, *J* = 16.6, Hz, 1H), 3.42 (d, *J* = 16.7 Hz, 1H), 2.94 (s, 6H), 2.93 (s, 6H), 2.92 (s, 6H) ppm; **$^{13}$C{$^1$H} NMR** (75 MHz) δ: 234.0, 149.73, 149.69, 149.5, 130.9, 130.8, 130.3, 129.8, 129.0, 124.3, 116.5, 115.1, 112.9, 112.5, 95.6, 94.0, 92.8, 90.6, 50.4, 50.83, 40.79, 35.9 ppm; diastereotopic carbons on dimethylamino groups overlap (112.9, 40.8 ppm); **IR** 2917, 2850, 2800, 1957 and 1870 (strong CO stretches), 1613, 1520, 1444, 1351, 1202, 1164, 947, 811, 667, 630 cm$^{-1}$; **HRMS** (ES+) calc'd for $C_{32}H_{38}N_3$ 464.3066, found 464.3051 [MH - Cr(CO)$_3$]$^+$.

General Procedure 1-B (for sensitive liquid substrates):

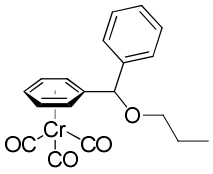

**24a – $^{n}$PrOPhCH(η$^{6}$-C$_6$H$_5$)Cr(CO)$_3$:** An oven-dried reaction tube was charged with a small magnetic stirbar, $PdCl_2(PPh_3)_2$ (8.5 mg, 0.012 mmol, 6 mol %) and LiHMDS (13 mg, 0.08 mmol, 0.4 equiv) under nitrogen and sealed with a septum. 1.4 mL of dry THF was added via syringe with stirring, forming a red-orange solution to which neat bromobenzene (27 µL, 0.26 mmol, 1.3 equiv) was added. The catalyst, base, and aryl bromide solution was allowed to stir for 5 min, and neat $^{n}$PrOCH$_2$(η$^{6}$-C$_6$H$_5$)Cr(CO) (**23**) (44 µL, 0.20 mmol, 1.0 equiv) was added. The reaction mixture was heated with stirring at 57 °C. A separate portion of LiHMDS (54 mg, 0.32 mmol, 1.6 equiv) was dissolved in 0.35 mL dry THF and added via syringe over 1.5 h. The reaction mixture was heated for an additional 30 min before cooling to room temperature and quenching with 2 drops $H_2O$. The orange solution was then opened to air, diluted with 3 mL diethyl ether, and filtered over a pad of $MgSO_4$ and silica. The pad was rinsed with additional diethyl ether and the resulting solution was concentrated *in vacuo,* loaded onto a silica gel column and eluted with 6% diethyl ether in pentane. The result was **24a** (58.9 mg, 0.162 mmol, 81% yield) as an orange oil. Upon storage at 0 °C, product crystallized as a pale yellow solid. **$^{1}$H NMR** (300 MHz, $CDCl_3$) δ: 7.39-7.32 (m, 5H), 5.70 (broad d, *J* = 6.3 Hz, 1H), 5.34 (dt, *J* = 1.4 Hz, 6.2 Hz, 1H), 5.26 - 5.17 (m, 2H), 5.12 - 5.09 (m, 1H), 5.00 (s, 1H), 3.49 - 3.36 (m, 2H), 1.65 (sextet, *J* = 7.0 Hz, 2H), 0.96 (t, *J* = 7.3 Hz, 3H) ppm; **$^{13}$C{$^{1}$H} NMR** (75 MHz) δ: 233.2, 140.5, 129.0, 128.7, 127.4, 113.9, 92.3, 92.2, 91.9, 91.7, 91.6, 81.5, 71.6, 55.6, 23.2, 10.9 ppm; tricarbonylchromium-coordinated protons and carbons exhibit diastereotopic signals; **IR** 3031, 2965, 2936, 2876, 1965 and 1881 (strong CO stretches), 1455, 1100, 1075, 753, 703, 661, 630 cm$^{-1}$; **HRMS** (ES+) calc'd for $C_{16}H_{18}CrO$ 278.0763, found 278.0753 [M -(CO)$_3$]$^{+}$.

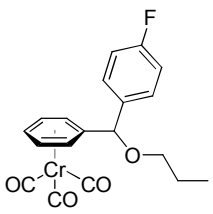

**24b – $^{n}$PrO(4-C$_6$H$_4$-F)CH(η$^{6}$-C$_6$H$_5$)Cr(CO)$_3$:** Using General Procedure 1-B, **23** (88 µl, 0.40 mmol, 1.0 equiv) was combined with LiHMDS (28 mg, 0.16 mmol, 0.25 equiv) and $PdCl_2(PPh_3)_2$ (16 mg, 0.022 mmol, 5.5 mol %) in 2.5 mL THF and 4-bromofluorobenzene (70 µL, 0.64 mmol, 1.6 equiv) and heated at 57 °C. More LiHMDS (108 mg, 0.64 mmol, 1.6 equiv) dissolved in 0.7 mL THF was added over 1h. The reaction was allowed to proceed for an additional 1.8 h, and yielded **24bb** (115 mg, 0.30 mmol, 75% yield) as a viscous orange oil after silica gel chromatography eluting with 6% diethyl ether in pentane. Upon storage at 0 °C, **24b** became a crystalline yellow-orange solid. **$^{1}$H NMR** (300 MHz, $CDCl_3$) δ: 7.37 - 7.33 (m, 2H), 7.07 (apparent t, *J* = 8.4 Hz, 2H), 5.65 (d, *J* = 6.2 Hz, 1H), 5.33 (t, *J* = 5.9 Hz, 1H), 5.27 - 5.18 (m, 2H), 5.09 (d, *J* = 6.2 Hz, 1H), 5.00 (s, 1H), 33.48 - 3.34 (m, 2H), 1.65 (sextet, *J* = 6.9 Hz, 2H), 0.95 (t, *J* = 7.3 Hz, 3H) ppm; **$^{13}$C{$^{1}$H} NMR** (75 MHz) δ: 233.0, 162.9 (d, *J* = 247 Hz), 136.2 (d, *J* = 3 Hz), 129.1 (d, *J* = 8.3 Hz),

115.9 (d, *J* = 21.9), 113.5, 92.4, 92.0, 91.9, 91.8, 91.7, 80.8, 71.7, 23.2, 10.9 ppm; $^{19}$F NMR (282 MHz) δ: −113.3 (m) ppm; tricarbonylchromium-coordinated protons and carbons exhibit diastereotopic signals; **IR** 3088, 2966, 2937, 2877, 1967 and 1885 (strong CO stretch), 1604, 1508, 1456, 1224, 1157, 1090, 823, 810, 660, 630 cm$^{-1}$.

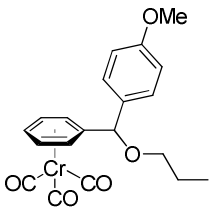


**24c – $^{n}$PrO(4-C$_6$H$_4$-OMe)CH(η$^6$-C$_6$H$_5$)Cr(CO)$_3$:** Using General Procedure 1-B, **23** (22 µl, 0.10 mmol, 1.0 equiv) was combined with LiHMDS (8 mg, 0.05 mmol, 0.5 equiv) and $PdCl_2(PPh_3)_2$ (3.5 mg, 0.005 mmol, 5 mol %) in 0.7 mL THF and 4-bromoanisole (18 µL, 0.15 mmol, 1.5 equiv) and heated at 58 °C. More LiHMDS (24 mg, 0.15 mmol, 1.5 equiv) dissolved in 0.3 mL THF was added over 30 min. The reaction was allowed to proceed for an additional 1 h, and yielded **24c** (31.4 mg, 0.080 mmol, 80% yield) as an orange oil after silica gel chromatography eluting with 20% diethyl ether in pentane. Upon storage at 0 °C, **24c** became a yellow-orange solid. **$^1$H NMR** (300 MHz, $CDCl_3$) δ: 7.28 (d, *J* = 8.6 Hz, 2H), 6.91 (d, *J* = 8.6 Hz, 2H), 5.69 (d, *J* = 6.5 Hz, 1H), 5.36 - 5.32 (m, 1H), 5.23 - 5.20 (m, 2H), 5.09 (br d, *J* = 5.7 Hz, 1H), 4.97 (s, 1H), 3.81 (s, 3H), 3.43 - 3.38 (m, 2H), 1.64 (sextet, *J* = 7.0 Hz, 2H), 0.95 (t, *J* = 7.4 Hz, 3H) ppm; **$^{13}$C{$^1$H} NMR** (75 MHz) δ: 233.2, 159.9, 132.5, 128.7, 114.4, 114.3, 92.3, 92.2, 92.1, 91.1, 91.7, 81.0, 71.4, 55.5, 23.2, 10.9 ppm; tricarbonylchromium-coordinated protons and carbons exhibit diastereotopic signals; **IR** 3087, 2964, 2936, 2876, 1965 and 1882 (strong CO stretches), 1610, 1510, 1457, 1248, 1172, 1095, 1033, 661, 631 cm$^{-1}$.

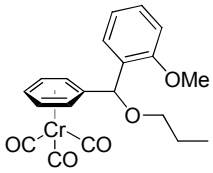


**24d – $^{n}$PrO(2-C$_6$H$_4$-OMe)CH(η$^6$-C$_6$H$_5$)Cr(CO)$_3$:** Using General Procedure 1-B, **23** (22 µl, 0.10 mmol, 1.0 equiv) was combined with LiHMDS (7 mg, 0.042 mmol, 0.4 equiv) and $PdCl_2(PPh_3)_2$ (4.9 mg, 0.007 mmol, 7 mol %) in 0.8 mL THF and 2-bromoanisole (20 µL, 0.16 mmol, 1.6 equiv) and heated at 58 °C. More LiHMDS (24 mg, 0.15 mmol, 1.5 equiv) dissolved in 0.2 mL THF was added over ~50 min. The reaction was allowed to proceed for an additional 1.7 h, and yielded **24d** (30.3 mg, 0.077 mmol, 77% yield) as an orange oil after silica gel chromatography eluting with 20% diethyl ether in pentane. **$^1$H NMR** (300 MHz, $CDCl_3$) δ: 7.40 (dd, *J* = 1.7, 7.6 Hz, 1H), 7.30 - 7.27 (m, 1H), 6.98 (t, *J* = 7.5 Hz, 1H), 6.91 (d, *J* = 8.3 Hz, 1H), 5.70 (d, *J* = 6.4 Hz, 1H), 5.52 (s, 1H), 5.41 (d, *J* = 6.3 Hz, 1H), 5.29 (dt, *J* = 1.4, 6.3 Hz, 1H), 5.24 - 5.15 (m, 2H), 3.88 (s, 3H), 3.47 - 3.38 (m, 2H), 1.65 (sextet, *J* = 7.0 Hz, 2H), 0.96 (t, *J* = 7.4 Hz, 3H) ppm; **$^{13}$C{$^1$H} NMR** (75 MHz) δ: 233.4, 157.1, 129.43, 129.36, 127.2, 121.2, 114.5, 110.8, 92.5, 92.2, 91.9, 91.8, 91.6, 74.1, 71.6, 55.6, 23.2, 10.9 ppm; tricarbonylchromium-coordinated protons and carbons exhibit diastereotopic signals; **IR** 3080, 2964, 2937, 2877, 1964 and 1882 (strong CO stretch), 1600, 1489, 1463, 1242, 1112, 1090, 1027, 757, 662, 631 cm$^{-1}$.

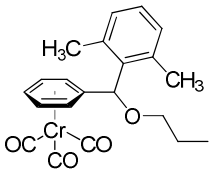

**24e – $^{n}$PrO(2,6-$C_6H_3Me_2$)CH($\eta^6$-$C_6H_5$)Cr(CO)$_3$:** Using General Procedure 1-B, **23** (22 µl, 0.10 mmol, 1.0 equiv) was combined with LiHMDS (8 mg, 0.05 mmol, 0.5 equiv) and $PdCl_2(PPh_3)_2$ (5.6 mg, 0.008 mmol, 8 mol %) in 1.0 mL THF and 2-bromo-1,3-dimethylbenzene (20 µL, 0.15 mmol, 1.5 equiv) and heated at 58 °C. More LiHMDS (26 mg, 0.15 mmol, 1.5 equiv) dissolved in 0.2 mL THF was added over ~40 min. The reaction was allowed to proceed for an additional 4.8 h, and yielded **24e** (22.5 mg, 0.058 mmol, 58% yield) as a yellow solid after silica gel chromatography eluting with 6% diethyl ether in pentane. **$^1$H NMR** (300 MHz, $CDCl_3$) δ: 7.13 (t, *J* = 7.5 Hz, 1H), 7.02 (br. d, *J* = 7.3 Hz, 2H), 6.12 (d, *J* = 6.3 Hz, 1H), 5.82 (s, 1H), 5.49 - 5.44 (m, 1H), 5.24 - 5.20 (m, 2H), 4.87 (broad d, *J* = 5.7 Hz, 1H), 3.44 - 3.38 (m, 1H), 3.36 - 3.30 (m, 1H), 2.6 - 2.1 (very br. s, 6H), 1.64 (sextet, 7.3 Hz, 2H), 0.96 (t, *J* = 7.4 Hz, 3H) ppm; **$^{13}$C{$^1$H} NMR** (75 MHz) ppm 233.4, 137.9, 136.1, 130.4, 128.6, 113.9, 92.8, 92.5, 92.4, 92.1, 91.1, 76.6, 71.0, 23.3, 20.9, 11.0 ppm; tricarbonylchromium-coordinated protons and carbons exhibit diastereotopic signals; non-axial carbons on the xylyl group exhibit diminished signals due to the hindered rotation; **IR** 3071, 2965, 2934, 2877, 1965 and 1881 (strong CO stretches), 1471, 1456, 1104, 1088, 774, 663, 629 cm$^{-1}$.

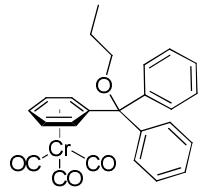

**26a – $^{n}$PrOPh$_2$C($\eta^6$-$C_6H_5$)Cr(CO)$_3$:** Using General Procedure 1-B, **23** (19 µl, 0.085 mmol, 1.0 equiv) was combined with LiHMDS (58 mg, 0.35 mmol, 4.1 equiv) and $PdCl_2(PPh_3)_2$ (6 mg, 0.009 mmol, 10 mol %) in 0.8 mL THF and bromobenzene (32 µL, 0.30 mmol, 3.5 equiv) and heated at 55 °C for 16 h, and yielded **26a** (27.1 mg, 0.062 mmol, 73% yield) as a pale yellow solid after silica gel chromatography eluting with 6% diethyl ether in pentane. **$^1$H NMR** (300 MHz, $CDCl_3$) δ: 7.43 - 7.35 (m, 10H), 5.71 (d, *J* = 6.0 Hz, 2H), 5.46 (t, *J* = 6.2 Hz, 1H), 5.04 (t, *J* = 6.5 Hz, 2H), 3.09 (t, *J* = 6.7 Hz, 2H), 1.69 (sextet, *J* = 7.0 Hz, 2H), 0.95 (t, *J* = 7.4 Hz, 3H) ppm; **$^{13}$C{$^1$H} NMR** (75 MHz) ppm 232.9, 141.2, 129.8, 128.2, 128.0, 118.7, 95.8, 95.4, 87.9, 84.4, 66.3, 23.2, 11.0 ppm; **IR** 3060, 3028, 2964, 2935, 2875, 1965 and 1887 (strong CO stretches), 1492, 1447, 1074, 1029, 753, 706, 660, 651, 633 cm$^{-1}$. **HRMS** (ES+) calc'd for $C_{25}H_{22}CrO$ 438.0923 found 438.091 $[M]^+$.

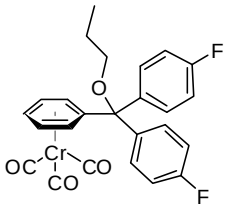

**26b – $^{n}$PrO(4-$C_6H_4$-F)$_2$C($\eta^6$-$C_6H_5$)Cr(CO)$_3$:** Using General Procedure 1-B, **23** (22 µl, 0.10 mmol, 1.0 equiv) was combined with LiHMDS (7 mg, 0.04 mmol, 0.4 equiv) and $PdCl_2(PPh_3)_2$ (7 mg, 0.01 mmol, 10 mol %) in 0.6 mL THF and 4-bromofluorobenzene (43 µL, 0.04 mmol, 4 equiv) and heated at 56 °C. More LiHMDS (70 mg, 0.42 mmol, 44.2 equiv) dissolved in 0.2 mL THF was added over 30 min. The reaction was allowed to proceed for an additional for 40 h, and yielded **26b** (27.4 mg, 0.058 mmol, 58% yield) as a pale yellow solid after silica gel chromatography eluting with

4% diethyl ether in pentane. **$^1$H NMR** (300 MHz, $CDCl_3$) δ 7.38 (m, 4H), 7.06 (t, *J* = 8.6 Hz, 4H), 5.65 (d, *J* = 6.4 Hz, 2H), 5.49 (t, *J* = 6.1 Hz, 1H), 5.04 (t, *J* = 6.4 Hz, 2H), 3.04 (t, *J* = 6.6 Hz, 2H), 1.68 (sextet, *J* = 7.0 Hz, 2H), 0.95 (t, *J* = 7.4 Hz, 3H); **$^{13}$C{$^1$H} NMR** (75 MHz) ppm 232.6, 162.6 (d, *J* = 248.3 Hz), 137.02 (d, *J* = 3 Hz), 131.82 (d, *J* = 8.3 Hz), 118.07, 115.03 (d, *J* = 21.1 Hz), 95.53, 95.49, 87.8, 83.7, 66.3, 23.2, 11.0; **$^{19}$F NMR** (282 MHz) ppm −113.8 (m); **IR** 3070, 2965, 2936, 2876, 1968 and 1889 (strong CO stretches), 1604, 1507, 1228, 1159, 1078, 831, 816, 657, 628 $cm^{-1}$.

General Procedure 1-C (for sensitive solid substrates):

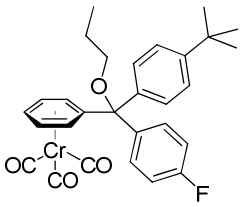


**26d – $^n$PrO(4-$C_6H_4$-F)(4-$C_6H_4$-$^t$Bu)C(η$^6$-$C_6H_5$)Cr(CO)$_3$:** An oven-dried reaction tube was charged with small magnetic stirbar and **$^n$PrO(4-$C_6H_4$-F)CH(η$^6$-$C_6H_5$)Cr(CO)$_3$** (**24b**) (19 mg, 0.050 mmol, 1.0 equiv), sealed with a septum, and purged with nitrogen. $PdCl_2(PPh_3)_2$ (3.2 mg, 0.0046 mmol, 9 mol %) and LiHMDS (8 mg, 0.04 mmol, 0.8 equiv) was dissolved in 0.6 mL of dry THF in a nitrogen atmosphere, forming an orange solution, to which neat 4-*tert*-butylbromobenzene (20 µL, 0.15 mmol, 3 equiv) was added. The catalyst, base, and aryl bromide solution was taken up by syringe and added to **24b**, which turned deep red. The reaction mixture was heated with stirring at 58 °C. A separate portion of LiHMDS (43 mg, 0.26 mmol, 5.2 equiv) was dissolved in 0.2 mL dry THF and added to the reaction mixture via syringe over 20 min, and then allowed to stir for an additional 24 before cooling to room temperature and quenching with 2 drops $H_2O$. The golden solution was then opened to air, diluted with 3 mL diethyl ether, and filtered over a pad of $MgSO_4$ and silica. The pad was rinsed with additional diethyl ether and the solution was concentrated *in vacuo,* loaded directly onto a silica gel column, and eluted with 3% diethyl ether in pentane. The result was **26d** (20.5 mg, 0.040 mmol, 80% yield) as a pale yellow solid. $^1$H NMR (300 MHz, $CDCl_3$) δ 7.45 - 7.41 (m, 2H), 7.36 (d, *J* = 8.6 Hz, 2H), 7.27 (d overlapping with solvent pk, *J* = 7.3 Hz, 2H), 7.06 (apparent t, *J* = 8.7 Hz, 2H), 5.79 (d, *J* = 6.8 Hz, 1H), 5.60 (d, *J* = 6.7 Hz, 1H), 5.47 (t, *J* = 6.2 Hz, 1H), 5.06 - 5.01 (m, 2H), 3.06 (apparent dt, *J* = 2.4, 6.6 Hz, 2H), 1.68 (sextet, *J* = 7.1 Hz, 2H), 0.96 (t, *J* = 7.4 Hz, 3H); $^{13}$C{$^1$H} NMR (75 MHz) ppm 232.9, 162.5 (d, *J* = 247 Hz), 151.3, 138.0, 137.4 (d, *J* = 3.8 Hz), 131.6 (d, *J* = 8.3 Hz), 129.5, 125.0, 118.8, 114.8 (d, *J* = 21 Hz), 95.9, 95.8, 95.5, 87.8, 87.7, 83.8, 66.2, 34.8, 31.5, 23.2, 11.1 ; $^{19}$F NMR (282 MHz) ppm −114.3 (m); tricarbonylchromium-coordinated protons and carbons exhibit diastereotopic signals; IR 3089, 2964, 2873, 1969 and 1893 (strong CO stretch), 1604, 1507, 1229, 1159, 1079, 830, 657, 626 $cm^{-1}$; HRMS (ES+) calc'd for $C_{29}H_{29}CrOF$ d512.1455, found 512.1478 $[M]^+$.

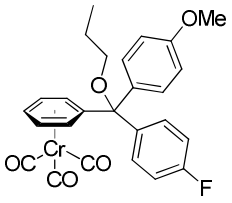


**26e – $^{n}$PrO(4-C$_6$H$_4$-F)(4-C$_6$H$_4$-OMe)C(η$^6$-C$_6$H$_5$)Cr(CO)$_3$:** Using General Procedure 1-C, **24b** (19 mg, 0.050 mmol, 1.0 equiv) was combined with LiHMDS (13 mg, 0.08 mmol, 1.6 equiv) and $PdCl_2(PPh_3)_2$ (3.5 mg, 0.005 mmol, 10 mol %) in 0.55 mL THF and 4-bromoanisole (19 µL, 0.15 mmol, 3.0 equiv) and heated at 55 ºC. More LiHMDS (20 mg, 0.12 mmol, 2.4 equiv) dissolved in 0.15 mL THF was added over 40 min. The reaction was allowed to proceed for an additional 16 h, and yielded **26e** (16.7 mg, 0.0343 mmol, 69 % yield) as a pale yellow solid after silica gel chromatography eluting with 6% diethyl ether in pentane. **$^1$H NMR** (300 MHz, $CDCl_3$) δ 7.41 (dd, *J* = 5.5, 8.5 Hz, 2H), 7.28 (d, *J* = 8.8 Hz, 2H), 7.06 (apparent t, *J* = 8.6 Hz, 2H), 6.88 (d, *J* = 8.7 Hz, 2H), 5.77 (d, *J* = 6.6 Hz, 1H), 5.55 (d, *J* = 6.6 Hz, 1H), 5.48 (t, *J* = 6.1 Hz, 1H), 5.08 - 5.00 (m, 2H), 3.82 (s, 3H), 3.11 - 2.99 (m, 2H), 1.67 (sextet, *J* = 7.0 Hz, 2H), 0.95 (t, *J* = 7.3 Hz, 3H); **$^{13}$C{$^1$H} NMR** (75 MHz) ppm .9, 162.4 (d, *J* = 248.0 Hz), 159.5, 137.6 (d, *J* = 3.4 Hz), 132.9, 131.4 (d, *J* = 8.1 Hz), 131.2, 118.9, 114.9 (d, *J* = 21.3 Hz), 113.4, 95.7, 95.6, 95.4, 88.0, 87.8, 83.7, 66.2, 55.6, 23.2, 11.1; **$^{19}$F NMR** (282 MHz) ppm −114.3 (m); tricarbonylchromium-coordinated protons and carbons exhibit diastereotopic signals; **IR** 2963, 2934, 2875, 1967 and 1889 (strong CO stretches), 1605, 1508, 1254, 1227, 1184, 1160, 1077, 1033, 830, 658, 628 cm$^{-1}$.

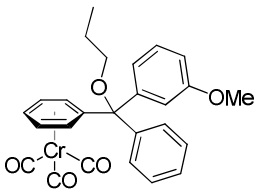


**26g – $^{n}$PrOPh(3-C$_6$H$_4$-OMe)C(η$^6$-C$_6$H$_5$)Cr(CO)$_3$:** Using General Procedure 1-C, **24a** (18 mg, 0.050 mmol, 1.0 equiv) was combined with LiHMDS (40 mg, 0.25 mmol, 5.0 equiv) and $PdCl_2(PPh_3)_2$ (3.5 mg, 0.005 mmol, 10 mol %) in 0.65 mL THF and 3-bromoanisole (18 µL, 0.15 mmol, 3.0 equiv) and heated at 58 ºC for 24 h, and yielded **26g** (14.4 mg, 0.0307 mmol, 61% yield) as a pale yellow solid after silica gel chromatography eluting with 10% diethyl ether in pentane. **$^1$H NMR** (300 MHz, $CDCl_3$) δ 7.40 - 7.33 (m, 5H), 7.27 (t, *J* = 8.0 Hz, 1H), 7.09 (br s, 1H), 6.94 - 6.88 (m, 2H), 5.79 (d, *J* = 6.8 Hz, 1H), 5.66 (d, *J* = 6.7 Hz, 1H), 5.46 (t, *J* = 6.2 Hz, 1H), 5.08 - 5.01 (m, 2H), 3.82 (s, 3H), 3.18 - 3.02 (m, 2H), 1.69 (sextet, *J* = 7.0 Hz, 2H), 0.96 (t, *J* = 7.4 Hz, 3H); **$^{13}$C{$^1$H} NMR** (75 MHz) ppm 232.9, 159.5, 142.9, 141.0, 129.9, 128.7, 128.2, 127.9, 122.5, 118.7, 115.5, 113.7, 95.8, 95.7, 95.4, 88.0, 87.9, 84.4, 66.4, 55.5, 23.2, 11.1; tricarbonylchromium-coordinated protons and carbons exhibit diastereotopic signals; **IR** 2963, 2926, 2873, 1964 and 1883 (strong CO stretches), 1598, 1488, 1448, 1254, 1075, 1029, 706, 657, 632 cm$^{-1}$.

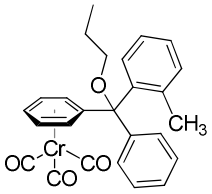


**26f – $^{n}$PrOPh(2-C$_6$H$_4$-Me)C(η$^6$-C$_6$H$_5$)Cr(CO)$_3$:** Using General Procedure 1-C, **24a** (18 mg, 0.050 mmol, 1.0 equiv) was combined with LiHMDS (17 mg, 0.10 mmol, 2.0 equiv) and $PdCl_2(PPh_3)_2$ (3.5 mg, 0.005 mmol, 10 mol %) in 0.6 mL THF and 2-bromotoluene (18 µL, 0.15 mmol, 3.0 equiv) and heated

at 58 ºC. More LiHMDS (33 mg, 0.20 mmol, 4.0 equiv) dissolved in 0.2 mL THF was added over 2h. The reaction was allowed to proceed for an additional 40 h, and yielded **26f** (13.3 mg, 0.0293 mmol, 59% yield) as a pale yellow solid after silica gel chromatography eluting with 6% diethyl ether in pentane. **$^1$H NMR** (300 MHz, $CDCl_3$) δ 7.46 - 7.39 (m, 3H), 7.36 - 7.18 (m, 5H), 7.15 - 7.12 (m, 1H), 5.78 (d, *J* = 6.4 Hz, 1H), 5.63 (d, *J* = 6.4 Hz, 1H), 5.47 (t, *J* = 6.2 Hz, 1H), 5.08 - 5.03 (m, 2H), 3.26 (dt, *J* = 8.9, 6.5 Hz, 1H), 2.90 (dt, *J* = 8.9, 7.0 Hz, 1H), 1.80 (s, 3H), 1.79 - 1.72 (m, 2H), 0.98 (t, *J* = 7.4 Hz, 3H); **$^{13}$C{$^1$H} NMR** (75 MHz) ppm, 144.3, 140.2, 138.5, 132.7, 129.8, 128.5, 128.02, 128.03, 127.8, 125.6, 118.2, 97.5, 95.7, 95.6, 87.4, 87.3, 84.7, 67.6, 23.3, 22.5, 11.0; tricarbonylchromium-coordinated protons and carbons exhibit diastereotopic signals; propoxy methylene protons exhibit diastereotopic signals in the $^1$H NMR; **IR** 3022, 2963, 2930, 2873, 1966 and 1887 (strong CO stretches), 1448, 1074, 750, 706, 659, 632 $cm^{-1}$.

General Procedure 1-D (for liquid substrates):

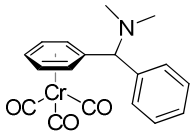


**28a – $Me_2NPhCH(\eta^6\text{-}C_6H_5)Cr(CO)_3$**: An oven-dried reaction tube was charged with small magnetic stirbar, $PdCl_2(PPh_3)_2$ (4.2 mg, 0.006 mmol, 6 mol %) and LiHMDS (38 mg, 0.23 mmol, 2.3 equiv) under nitrogen and sealed with a septum. 0.7 mL of dry THF was added via syringe with stirring, forming a red solution to which neat bromobenzene (17 µL, 0.16 mmol, 1.6 equiv) was added. The catalyst, base, and aryl bromide solution was allowed to stir for 5 min, and neat **$Me_2NCH_2(\eta^6\text{-}C_6H_5)Cr(CO)$** (**27**) (21 µL, 0.10 mmol, 1.0 equiv) was added dropwise and then heated at 56 ºC with stirring for 6 h. The dark reaction mixture was cooled to room temperature and quenched with 2 drops $H_2O$. The brownish orange solution was then opened to air and diluted with 3 mL diethyl ether, then filtered over a pad of $MgSO_4$ and silica. The pad was rinsed with additional diethyl ether and the solution was concentrated *in vacuo,* loaded directly onto a silica gel column and eluted with 50% diethyl ether in pentane. The result was **28a** (28.6 mg, 0.082 mmol, 82% yield) as an orange oil which solidified on standing. $^1$H NMR (300 MHz, $CDCl_3$) δ 7.39-7.28 (m, 5H), 5.91 - 5.88 (m, 1H), 5.33 - 5.26 (m, 3H), 5.17 - 5.12 (m, 1H), 4.14 (s, 1H), 2.24 (s, 6H) ; $^{13}$C{$^1$H} NMR (75 MHz) ppm 233.0, 140.0, 129.0, 128.6, 128.1, 114.0, 95.1, 94.5, 93.6, 91.0, 90.5, 73.4, 44.3; tricarbonylchromium-coordinated protons and carbons exhibit diastereotopic signals; IR 2946, 2864, 2823, 2781, 1962 and 1876 (strong CO stretches), 1611, 1521, 1454, 1353, 1016, 812, 663, 632 $cm^{-1}$; HRMS (ES+) calc'd for $C_{15}H_{17}Cr$ 263.0766, found 263.0757 $[M\text{-}(CO)_3]^+$.

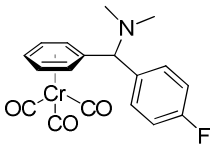

**28b – $Me_2N(4\text{-}C_6H_4\text{-}F)CH(\eta^6\text{-}C_6H_5)Cr(CO)_3$**: Using General Procedure 1-D, **27** (21 µl, 0.10 mmol, 1.0 equiv) was combined with LiHMDS (37 mg, 0.23 mmol, 2.3 equiv) and $PdCl_2(PPh_3)_2$ (4.9 mg, 0.007 mmol, 5 mol %) in 0.85 mL THF and 4-bromofluorobenzene (18 µL, 0.16 mmol, 1.6 equiv) and heated at 58 ºC for 5 h, yielding **28b** (22.7 mg, 0.062 mmol, 62% yield) as a yellow solid after silica gel chromatography eluting with 40% diethyl ether in pentane. $^1$H NMR (300 MHz, $CDCl_3$) δ 7.31 - 7.27 (m, 2H), 7.08 - 7.02 (m, 2H), 5.85 (d, *J* = 6.4 Hz, 1H), 5.34 (tt, *J* = 6.1, 1.1 Hz, 1H), 5.30 - 5.24 (m, 2H), 5.17 - 5.12 (m, 1H), 4.10 (s, 1H), 2.22 (s, 6H); $^{13}$C{$^1$H} NMR (75 MHz) ppm 232.8, 162.5 (d, *J* = 246.8 Hz), 136.0 (d, *J* = 3.0 Hz), 130.5 (d, *J* = 7.5 Hz), 115.6 (d, *J* = 24.2 Hz), 113.6, 95.5, 94.4, 93.9, 90.7, 90.2, 72.9, 44.3; $^{19}$F{$^1$H} NMR (282 MHz) ppm −114.2 (s); tricarbonylchromium-coordinated protons and carbons exhibit diastereotopic signals; ; IR 2925, 2851, 2825, 2780, 1965, 1881, 1605, 1506, 1455, 1223, 1157, 1014, 820, 660, 631 cm$^{-1}$.

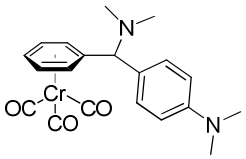

**28c – $Me_2N(4\text{-}C_6H_4\text{-}NMe_2)CH(\eta^6\text{-}C_6H_5)Cr(CO)_3$**: Using General Procedure 1-D, **27** (21 µl, 0.10 mmol, 1.0 equiv) was combined with LiHMDS (38 mg, 0.23 mmol, 2.3 equiv) and $PdCl_2(PPh_3)_2$ (3.5 mg, 0.005 mmol, 5 mol %) in 0.7 mL THF and 4-bromo-N,N-dimethylaniline (28 mg, 0.16 mmol, 1.6 equiv) and heated at 55 ºC for 4 h, yielding **28c** (30.1 mg, 0.077 mmol, 77% yield) as a yellow solid after silica gel chromatography eluting with 40% diethyl ether in pentane. **$^1$H NMR** (300 MHz, $CDCl_3$) δ 7.08 (d, *J* = 8.8 Hz, 2H), 6.68 (d, *J* = 8.8 Hz, 2H), 5.92 (br. d, *J* = 6.5 Hz, 1H), 5.36 (dt, *J* = 1.1, 6.4 Hz, 1H) 5.28 - 5.17 (m, 3H), 4.15 (s, 1H), 2.95 (s, 6H), 2.23 (s, 6H); **$^{13}$C{$^1$H} NMR** (75 MHz) ppm 233.3, 150.3, 130.1, 127.4, 115.6, 112.3, 94.26, 9.24, 92.9, 91.8, 91.5, 72.4, 44.1, 40.7; **IR** cm$^{-1}$; tricarbonylchromium-coordinated protons and carbons exhibit diastereotopic signals; IR 2950, 2867, 2824, 2780, 1963 and 1875 (strong CO stretches), 1454, 1015, 755, 705, 661, 630 cm$^{-1}$.

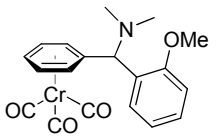

**28d – $Me_2NCH(2\text{-}C_6H_4\text{-}OMe)(\eta^6\text{-}C_6H_5)Cr(CO)_3$**: Using General Procedure 1-D, **27** (21 µl, 0.10 mmol, 1.0 equiv) was combined with LiHMDS (34 mg, 0.20 mmol, 2 equiv) and $PdCl_2(PPh_3)_2$ (4.2 mg, 0.006 mmol, 6 mol %) in 0.7 mL THF and 2-bromoaniline (22 µL, 0.17 mmol, 1.7 equiv) and heated at 58 ºC for 5 h, yielding **28d** (27.2 mg, 0.072 mmol, 72% yield) as a yellow solid after silica gel chromatography eluting with 30 – 40% diethyl ether in pentane. **$^1$H NMR** (300 MHz, $CDCl_3$) δ: 7.27 - 7.22 (m, 2H), 6.96 - 6.91 (m, 2H), 5.91 (d, *J* = 6.7 Hz, 1H), 5.39 (d, *J* = 6.6 Hz, 1H), 5.32 (tt *J* = 1.1, 6.2 Hz, 1H), 5.25 (dt, *J* = 1.4, 6.3 Hz, 1H), 5.11 (dt, *J* = 1.4, 6.3 Hz, 1H), 4.68 (s, 1H), 3.85 (s, 3H), 2.23 (s, 6H); **$^{13}$C{$^1$H} NMR** (75 MHz) δ: 33.0, 157.4, 129.3, 129.0, 128.9, 120.5, 114.9, 111.1, 95.9, 94.7, 93.9, 90.6, 89.9, 64.9, 55.6, 44.5; tricarbonylchromium-coordinated protons and carbons

exhibit diastereotopic signals; **IR** 2924, 2822, 2771, 1962 and 1881 (strong CO stretch), 1489, 1456, 1243, 1027, 755, 700, 662 $cm^{-1}$.

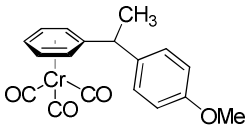


**31b – $CH_3CH(4\text{-}C_6H_4\text{-}OCH_3)(\eta^6\text{-}C_6H_5)Cr(CO)_3$:** Using General Procedure 1-C, **$CH_3CH_2(\eta^6\text{-}C_6H_5)Cr(CO)_3$ (30)** (24.4 mg, 0.10 mmol, 1.0 equiv) was combined with LiHMDS (13 mg, 0.08 mmol, 0.8 equiv) and $PdCl_2(PPh_3)_2$ (5.8 mg, 0.008 mmol, 8 mol %) in 0.85 mL of dry THF and 4-bromoanisole (19 µL, 0.15 mmol, 1.5 equiv) and heated at 58 °C. More LiHMDS (20 mg, 0.12 mmol, 1.2 equiv) dissolved in 0.15 mL THF was added over 30 min. The reaction was allowed to proceed for an additional 3.5 h and yielded **31b** (24.5 mg, 0.070 mmol, 70% yield) as a yellow-orange oil after silica gel chromatography eluting with 6% diethyl ether in pentane. **$^1$H NMR** (300 MHz, $CDCl_3$) δ 7.15 (d, *J* = 8.6 Hz, 2H), 6.86 (d, *J* = 8.6 Hz, 2H), 5.43 (d, *J* = 6.3 Hz, 1H), 5.38 - 5.34 (m, 1H), 5.29 - 5.21 (m, 2H), 5.10 (d, *J* = 6.1 Hz, 1H), 3.86 - 3.77 (m, 4H), 1.56 (d, *J* = 7.2 Hz, 3H); **$^{13}$C{$^1$H} NMR** (75 MHz) δ: 233.4, 158.8, 136.6, 128.6, 117.9, 114.3, 94.4, 92.8, 92.5, 92.1, 91.4, 55.5, 43.1, 21.3; tricarbonylchromium-coordinated protons and carbons exhibit diastereotopic signals; methoxy signal overlaps with the benzylic proton signal; **IR** 3089, 2971, 2936, 2838, 1962 and 1877 (strong CO stretch), 1611, 1511, 1457, 1247, 1180,1031, 835, 662, 630 $cm^{-1}$. **HRMS** (ES+) calc'd for $C_{15}H_{16}CrO$ 264.0606, found 264.0608 $[M\text{-}(CO)_3]^+$.

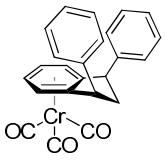


**41a – 1,3-*cis*-$Ph_2(\eta^6$-indane)$Cr(CO)_3$:** Using General procedure 1-A, **39**(25.5 mg, 0.100 mmol, 1.0 equiv) was reacted with LiHMDS (83 mg, 0.50 mmol, 5 equiv) and $PdCl_2(PPh_3)_2$ (4.3 mg, 0.006 mmol, 6 mol %) in 1 mL THF and bromobenzene (52 µL, 0.5 mmol, 5 equiv) for 5 h at 52 °C to yield **41a** (30.8 mg, 0.076 mmol, or 76%) as a yellow solid after silica gel chromatography eluting with 20% diethyl ether in pentane. **$^1$H NMR** (300 MHz, $CDCl_3$) δ 7.35 (m, 6H), 7.25 (m, 4H), 5.39 (dd, *J* = 4.5, 2.7 Hz, 2H), 5.22 (dd, *J* = 4.6, 3.0 Hz, 2H), 4.48 (t, *J* = 8.4 Hz, 2H), 3.11 (dt, *J* = 13.5, 8.4 Hz, 1H), 2.20 (dt, *J* = 13.5, 8.4 Hz, 1H); **$^{13}$C{$^1$H} NMR** (75 MHz) ppm 233.8, 143.5, 129.3, 128.4, 127.6, 119.0, 92.2, 91.8, 50.1, 45.8. **IR**: 3081, 3027, 2970, 2935, 2856, 1956 and 1877 and 1867 (strong CO stretch), 1602, 1494, 1450, 1427, 1263, 1152, 1078, 803, 760, 747, 696, 667, 632 $cm^{-1}$. **HRMS** (ES+) calc'd for $C_{21}H_{18}Cr$ 322.0814, found 322.0819 $[M\text{-}(CO)_3]^+$.

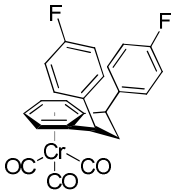


**41b – 1,3-*cis*-$(4\text{-}C_6H_4\text{-}F)_2(\eta^6$-Indane)$Cr(CO)_3$:** Using General procedure 1-A, **39** (12.6 mg, 0.049 mmol, 1.0 equiv) was reacted with LiHMDS (43 mg, 0.26 mmol, 5.1 equiv) and $PdCl_2(PPh_3)_2$ (3.6 mg, 0.005 mmol, 10 mol %) in 1.2 mL of THF and 4-bromofluorobenzene (27.5 µL, 0.25 mmol, 5 equiv) for 16 h at 53 °C to yield **41b** (12.1 mg, 0.030 mmol, or 61% yield) as a yellow solid after silica gel

chromatography eluting with 20% diethyl ether in pentane. **$^1$H NMR** (300 MHz, $CDCl_3$) δ 7.16 (m, 4H), 7.03 (t, *J* = 8.7 Hz, 4H), 5.36 (dd, *J* = 4.7, 2.7 Hz, 2H), 5.23 (dd, *J* = 4.8, 3.0 Hz, 2H), 4.45 (t, *J* = 8.3 Hz, 2H), 3.09 (dt, *J* = 13.5, 8.3 Hz, 1H), 2.10 (dt, 13.5, 8.3 Hz) ;**$^{13}$C{$^1$H} NMR** (75 MHz) ppm 233.3, 162.1 (d, *J* = 246 Hz), 138.9 (d, *J* = 2.9 Hz), 129.6 (d, *J* = 8.0 Hz), 118.0, 116.0 (d, *J* = 21.4 Hz), 91.9, 91.3, 49.0, 45.8; $^{19}$F NMR (282 MHz) ppm −118.3 (m); **IR** 3079, 3041, 2934, 1962 and 1875 (strong CO stretch), 1605, 1509, 1225, 1159, 1098, 834, 667, 630 $cm^{-1}$; **HRMS** (ES+) calc'd for $C_{21}H_{16}CrF_2$ 358.0625, found 358.0617 $[M-(CO)_3]^+$. *X-ray crystal structure was determined for this compound;* *see p. 283.*

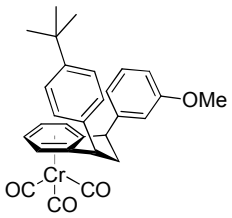


**41c – 1,3-*cis*-Ph(3-$C_6H_4$-OMe)($\eta^6$-indane)Cr(CO)$_3$**: Using General procedure 1-A, **43c** (35.9 mg, 0.0996 mmol, 1.0 equiv) was reacted with LiHMDS (33 mg, 0.20 mmol, 2.0 equiv) and $PdCl_2(PPh_3)_2$ (7 mg, 0.01 mmol, 10 mol %) in 1.0 mL THF and 4-bromo-*tert*-butylbenzene (22 µL, 0.15 mmol, 1.5 equiv) for 5 h at 57 °C to yield **41c** (40.1 mg, 0.0815 mmol, or 82%) as a yellow solid after silica gel chromatography eluting with 10% diethyl ether in pentane. **$^1$H NMR** (300 MHz, $CDCl_3$) δ 7.36 (d, *J* = 8.3 Hz, 2H), 7.26 (t, 7.9 Hz, 1H), 7.16 (d, *J* = 8.3 Hz, 2H), 6.84 - 6.79 (m, 2H), 6.72 - 6.71 (m, 1H), 5.44 - 5.40 (m, 2H), 5.24 - 5.21 (m, 2H), 4.49 - 4.41 (m, 2H), 3.75 (s, 3H), 3.09 (dt 13.5, 8.5 Hz, 1H), 2.20 (dt, 13.5, 8.2 Hz, 1H), 1.32 (s, 9H); **$^{13}$C{$^1$H} NMR** (75 MHz) ppm 233.6, 160.2, 150.3, 145.1, 140.3, 130.1, 127.8, 125.0, 120.5, 118.71, 118.66, 114.0, 112.5, 92.0, 91.9, 91.7, 91.5, 55.4, 49.9, 49.3, 45.1, 34.7, 31.5; **IR** 3027, 2963, 1962 and 1878 (strong CO stretch), 1600, 1455, 1268, 1050, 667, 630 $cm^{-1}$; **HRMS** (ES+) calc'd for $C_{26}H_{28}CrO$ 408.1545, found 408.1526 $[M-(CO)_3]^+$.

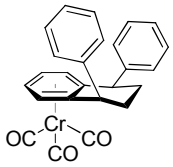


**42a** – 1,4-*cis*-$Ph_2$($\eta^6$-tetrahydronaphthalene)Cr(CO)$_3$: Using General procedure 1-A, ($\eta^6$-tetrahydronaphthalene)Cr(CO)$_3$ (**40**) (13.3 mg, 0.050 mmol, 1.0 equiv) was reacted with LiHMDS (42 mg, 0.25 mmol, 5 equiv) and $PdCl_2(PPh_3)_2$ (3.5 mg, 0.005 mmol, 10 mol %) of in 1 mL THF and bromobenzene (26 µL, 0.25 mmol, 5 equiv) for 12 h at 52 °C to yield **42a** (18.4 mg, 0.044 mmol, 88% yield) as a yellow solid after silica gel chromatography eluting with 20% diethyl ether in pentane. **$^1$H NMR** (300 MHz, $CDCl_3$) δ 7.36 (m, 4H), 7.28 (m, 2H), 7.21 (m, 4H), 5.23 (m, 2H), 5.17 (m, 2H), 4.10 (t, *J* = 6.3 Hz, 2H), 2.11 (m, 2H), 1.86 (m, 2H); **$^{13}$C{$^1$H} NMR** (75 MHz) ppm 233.6, 145.3, 128.9, 128.7, 127.1, 112.3, 94.8, 92.2, 44.5, 28.9.; **IR** 3085, 3029, 2937, 2855, 1951 and 1875 and 1856 (strong CO stretch), 1600, 1492, 1416, 1443, 1077, 1054, 1029, 831, 755, 700, 667, 635 $cm^{-1}$; **HRMS** (ES+) calc'd for $C_{22}H_{20}Cr$ 336.0970, found 336.0968 $[M-(CO)_3]^+$.

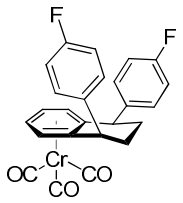

**42b – 1,4-*cis*-(4-$C_6H_4$-F)$_2$($\eta^6$-tetrahydronaphthalene)Cr(CO)$_3$**: Using General procedure 1-A, **40** (13.4 mg, 0.050 mmol, 1.0 equiv) was reacted with LiHMDS (42 mg, 0.25 mmol, 5 equiv) and $PdCl_2(PPh_3)_2$ (2.6 mg, 0.0037 mmol, 7 mol %) in 1 mL THF and 4-bromofluorobenzene (28 µL, 0.25 mmol, 5 equiv) for 5 h at 55 – 57 ºC to yield **42b** (14.6 mg, 0.033 mmol, 64% yield) as a yellow solid after silica gel chromatography eluting with 20% diethyl ether in pentane. **$^1$H NMR** (300 MHz, $CDCl_3$) δ 7.14 (m, 4H), 7.05 (t, *J* = 8.7 Hz, 4H), 5.25 (dd, *J* = 4.9, 2.9 Hz, 2H), 5.12 (dd, *J* = 4.8, 2.9 Hz, 2H), 4.08 (t, *J* = 6.2 Hz, 2H), 2.10 (m, 2H), 1.80 (m, 2H); **$^{13}$C{$^1$H} NMR** (75 MHz) ppm 233.3, 161.9 (d, *J* = 246 Hz), 140.9, 130.0 (d, *J* = 8.0 Hz), 115.9 (d, *J* = 21.3 Hz), 111.8, 94.6, 92.3, 43.7, 28.9; $^{19}$F NMR (282 MHz) ppm −118.7 (m); **IR** 3077, 3041, 2940, 2863, 1960 and 1871 (strong CO stretch), 1626, 1567, 1508, 1457, 1301, 1224, 1184, 1159, 1097, 924, 828, 736, 667, 628 cm$^{-1}$; **HRMS** (ES+) calc'd for $C_{22}H_{18}Cr$ 372.0782, found 372.0773 $[M-(CO)_3]^+$.

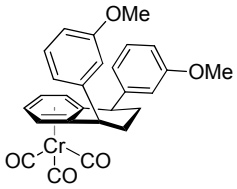

**42c – 1,4-*cis*-(3-$C_6H_4$-$OCH_3$)$_2$($\eta^6$-tetrahydronaphthalene)Cr(CO)$_3$**: Using General procedure 1-A, **40** (13.6 mg, 0.051 mmol, 1.0 equiv) was reacted with LiHMDS (42 mg, 0.25 mmol, 4.9 equiv) and $PdCl_2(PPh_3)_2$ (2.7 mg, 0.0037 mmol, 7 mol %) in 1 mL THF and 3-bromoanisole (32 µL, 0.25 mmol, 5 equiv) for 5 h at 55 ºC to yield **42c** (17.6 mg, 0.037 mmol, 73% yield) as a yellow solid after silica gel chromatography eluting with 20% diethyl ether in pentane. **$^1$H NMR** (300 MHz, $CDCl_3$) δ 7.27 (t, *J* = 8.0 Hz, 2H), 6.78 (m, 6H), 5.24 (m, 2H), 5.18 (m, 2H), 4.06 (t, *J* = 6.2 Hz), 3.80 (s, 6H), 2.09 (m, 2H), 1.87 (m, 2H); **$^{13}$C{$^1$H} NMR** (75 MHz) ppm 233.5, 160.0, 146.9, 129.9, 121.1, 114.8, 112.2, 112.1, 94.8, 92.3, 55.4, 44.4, 28.8; **IR** 3000, 2939, 2835, 1959 and 1874 (strong CO stretch), 1599, 1584, 1487, 1455, 1266, 1149, 1046m 783, 700, 667, 630 cm$^{-1}$; **HRMS** (ES+) calc'd for $C_{24}H_{24}CrO_2$ 396.1181, found 396.1149 $[M-(CO)_3]^+$.

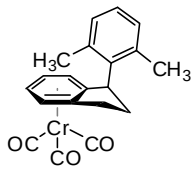

**43a – 1-(2,6-$C_6H_3Me_2$)($\eta^6$-indane)Cr(CO)$_3$**: Using General procedure 1-A, **39** (25.3 mg, 0.099 mmol, 1.0 equiv) was reacted with LiHMDS (67 mg, 0.40 mmol, 4.2 equiv) and $PdCl_2(PPh_3)_2$ (4.8 mg, 0.007 mmol, 7 mol %) in 1 mL THF and 1-bromo-2,6-dimethylbenzene (41 µL, 0.3 mmol, 3 equiv) for 10 h at 55 ºC to yield **43a** (0.047 mmol, 17 mg, or 47% yield) as a yellow solid after silica gel chromatography eluting with 3% diethyl ether in pentane. **$^1$H NMR** (300 MHz, $CDCl_3$) δ 7.07 (d, *J* = 4.5 Hz, 2H), 6.98 – 6.96 (m, 1H), 5.61 (d, *J* = 6.1 Hz, 1H), 5.24 (m, 3H), 5.04 (t, *J* = 9.0 Hz, 1H), 3.15 (t, *J* = 7.9 Hz, 2H), 2.66 (m, 1H), 2.48 (s, 3H), 2.16 (m, 1H), 1.96 (s, 3H); **$^{13}$C{$^1$H} NMR** (75 MHz) ppm 233.9, 139.5, 137.5, 136.0, 130.7, 128.7, 127.2, 119.4, 115.7, 92.2, 91.7, 91.2, 90.4, 45.6, 31.8, 30.1, 21.6, 21.5; methyl carbons and protons on the xylyl moiety exhibit diastereotopic signals; **IR** 2962, 1957 and 1867 (strong CO stretch), 1469, 1449, 1084, 773, 667, 631 cm$^{-1}$.

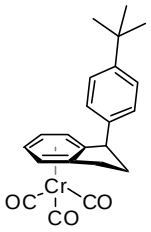

**43b – 1-(4-$C_6H_4$-$^t$Bu)($\eta^6$-indane)Cr(CO)$_3$**: Using General Procedure 1-C, **39** (22.5 mg, 0.0885 mmol, 1.0 equiv) was reacted with LiHMDS (13 mg, .078 mmol, 0.88 equiv) and $PdCl_2(PPh_3)_2$ (4.8 mg, 0.0068 mmol, 7.6 mol %) in 0.8 mL THF and 4-bromo-*tert*-butylbenzene (16 µL, 0.12 mmol, 1.3 equiv) and heated at 58 °C. More LiHMDS (21 mg, 0.13 mmol, 1.5 equiv) dissolved in 0.2 mL THF was added over 3 h. The reaction was allowed to proceed for an additional 2 h, and yielded **43b** (0.0497 mmol, 19.2 mg, or 56% yield) as a fluffy yellow solid after silica gel chromatography eluting with 3% diethyl ether in pentane. **$^1$H NMR** (300 MHz, $CDCl_3$) δ: 7.31 (d, *J* = 8.4 Hz, 2H), 7.01 (d, *J* = 8.3 Hz, 2H), 5.53 (d, *J* = 6.4 Hz, 1H), 5.39 (d, *J* = 6.4 Hz, 1H), 5.31 (dt, *J* = 6.2, 1.0 Hz, 1H), 5.21 (dt, *J* = 6.2, 1.0 Hz, 1H), 4.18 (dd, *J* = 8.5, 1.6 Hz, 1H), 3.08 - 3.00 (m, 1H), 2.79 - 2.70 (m, 1H), 2.66 - 2.54 (m, 1H) 2.10 - 2.02 (m, 1H), 1.30 (s, 9H); **$^{13}$C{$^1$H} NMR** (75 MHz) δ: 233.6, 150.0, 141.4, 126.8, 125.9, 116.6, 114.9, 92.5, 91.9, 91.5, 90.3, 49.3, 34.7, 33.3, 31.6, 30.8 ppm; **IR** 3087, 3028, 2964, 2868, 1963 and 1877 (strong CO stretches), 1510, 1452, 1434, 1365, 1270, 1017, 830, 670, 631 cm$^{-1}$. **HRMS** (ES+) calc'd for $C_{22}H_{22}CrO_3$ 386.0974, found 386.0981 $[M]^+$.

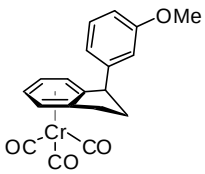

**43c – 1-(3-$C_6H_3$OMe)($\eta^6$-indane)Cr(CO)$_3$**: Using General Procedure 1-C, **39** (61.3 mg, 0.241 mmol, 1.0 equiv) was reacted with LiHMDS (25 mg, .15 mmol, 0.62 equiv) and $PdCl_2(PPh_3)_2$ (17.5 mg, 0.025 mmol, 10 mol %) in 2 mL THF and 3-bromoanisole (48 µL, 0.38 mmol, 1.6 equiv) and heated at 55 °C. More LiHMDS (50 mg, 0.30 mmol, 1.2 equiv) dissolved in 0.5 mL THF was added over 3h. The reaction was allowed to proceed for an additional 1 h, and yielded **43c** (0.128 mmol, 46.0 mg, or 53% yield) as a fluffy yellow solid after silica gel chromatography eluting with 6% diethyl ether in pentane. **$^1$H NMR** (300 MHz, $CDCl_3$) δ: 7.22 (t, *J* = 7.9 Hz, 1H), 6.77 (ddd, *J* = 8.3, 2.5, 1.8 Hz, 1H), 6.68 (d, *J* = 7.7 Hz, 1H), 6.62 (t, *J* = 1.9 Hz, 1H), 5.52 (d, *J* = 6.3 Hz, 1H), 5.39 (d, *J* = 6.3 Hz, 1H), 5.31 (dt, *J* = 0.9, 6.2 Hz, 1H), 5.22 (dt, *J* = 0.9, 6.2 Hz, 1H), 4.18 (dd, *J* = 8.6, 1.5 Hz, 1H), 3.75 (s, 3H), 3.09 - 2.97 (m, 1H), 2.80 - 2.69 (m, 1H), 2.66 - 2.56 (m, 1H), 2.09 - 2.02 (m, 1H); **$^{13}$C{$^1$H} NMR** (75 MHz) δ: 233.6, 160.1, 146.1, 130.1, 119.6, 116.2, 114.9, 113.6, 111.8, 92.5, 91.9, 91.4, 90.3, 55.4, 49.8, 33.2, 30.8 ppm; **IR** 3081, 2924, 2851, 1958 and 1866 (strong CO stretches), 1599, 1488, 1451, 1265, 1050, 777, 701, 670, 629 cm$^{-1}$.

General Procedure 1-E:

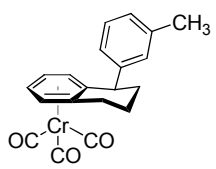

**44b** – 1-(3-$C_6H_4$-Me)($\eta^6$-tetrahydronaphthalene)Cr(CO)$_3$: An oven-dried glass reaction tube was charged with a small magnetic stirbar and ($\eta^6$-

tetrahydronaphthalene)$Cr(CO)_3$ (**40**) (19.9 mg, 0.0742 mmol, 1.0 equiv), sealed with a septum, purged with nitrogen, and dissolved in 0.3 ml toluene. $PdCl_2(PPh_3)_2$ (3.6 mg, 5 μ mmol, 7 mol %) and LiHMDS (38 mg, 0.23 mmol, 3 equiv) were dissolved in 0.45 mL of dry THF under a nitrogen atmosphere, forming an orange solution, to which 3-bromotoluene (15 μL, 0.12 mmol, 1.6 equiv) was added. The catalyst, base, and aryl bromide THF solution was taken up by syringe and added to the toluene solution of 24, which turned red-orange. The reaction mixture was heated with stirring for 4.5 h at 58 ºC, then allowed to cool and quenched with one drop of aqueous 2N HCl and allowed to stir for 5 min. The pale orange solution was opened to air and diluted with 2 mL diethyl ether and filtered over a pad of $MgSO_4$ and silica which was rinsed with an additional 1 mL diethyl ether. After concentration *in vacuo* and purification by silica gel flash chromatography eluting with 6% diethyl ether in pentane, **44b** (14.7 mg, 0.041 mmol, 55% yield) was obtained as an orange oil. **$^1$H NMR** (300 MHz, $CDCl_3$) δ 7.20 (t, *J* = 7.6 Hz, 1H), 7.06 (d, *J* = 7.9 Hz, 1H), 6.94 - 6.89 (m, 2H), 5.31 - 5.27 (m, 2H), 5.18 - 5.14 (ddd, *J* = 2.1, 5.3, 6.6 Hz, 1H), 5.06 (d, *J* = 6.7 Hz, 1H), 3.95 (dd, *J* = 5.8, 8.1 Hz, 1H), 2.82 - 2.67 (m, 2H), 2.33 (s, 3H), 2.20 - 2.12 (m, 1H), 1.87 - 1.69 (m, 3H); **$^{13}$C{$^1$H} NMR** (75 MHz) ppm 233.8, 145.5, 138.6, 129.4, 128.8, 127.8, 125.7, 112.1, 110.5, 95.3, 93.4, 92.6, 91.6, 44.5, 32.5, 29.1, 21.7, 20.5; **IR** 3019, 2939, 2862, 1957 and 1868 (strong CO stretch), 1606, 1456, 788, 704, 667, 632, 536 $cm^{-1}$; **HRMS** (ES+) calc'd for $C_{20}H_{18}CrO_3$ 358.0661, found 358.0660 $[M]^+$.

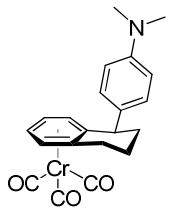


**44c** – 1-(4-$C_6H_4$-$NMe_2$)(η$^6$-tetrahydronaphthalene)$Cr(CO)_3$: Using General Procedure 1-E, a solution of (η$^6$-tetrahydronaphthalene)$Cr(CO)_3$ (**40**) (20.1 mg, 0.075 mmol, 1 equiv) in 0.3 ml Toluene was reacted with LiHMDS (32 mg, 0.19 mmol, 2.5 equiv) and $PdCl_2(PPh_3)_2$ (3.2 mg, 4.5 μmol, 6 mol %) of in 0.45 mL THF and 4-bromo-*N*,*N*-dimethylaniline (25 mg, 0.12 mmol, 1.6 equiv) for 6 h at 60 ºC to yield **44c** (12.9 mg, 0.033 mmol, 44% yield) as a yellow-orange oil after silica gel chromatography eluting with 20% diethyl ether in pentane. **$^1$H NMR** (300 MHz, $CDCl_3$) δ 6.99 (d, *J* = 8.7 Hz, 2H), 6.68 (d, *J* = 8.8 Hz, 2H), 5.30 - 5.24 (m, 2H), 5.17 - 5.13 (m, 1H), 5.11 (d, *J* = 6.3 Hz, 1H), 3.89 (dd, *J* = 5.7, 8.0 Hz, 1H), 2.94 (s, 6H), 2.81 - 2.67 (m, 2H), 2.17 - 2.08 (m, 1H), 1.88 - 1.65 (m, 3H); **$^{13}$C{$^1$H} NMR** (75 MHz) ppm 233.9, 149.7, 133.3, 129.3, 113.0, 112.9, 110.5, 95.5, 93.5, 92.6, 91.6, 43.5, 40.8, 32.4, 29.1, 20.5; **IR** 2921, 2850, 1954 and 1865 (strong CO stretch), 1610, 1520, 1446, 1348, 814, 666, 631, 534 $cm^{-1}$; **HRMS** (ES+) calc'd for $C_{18}H_{22}N$ 252.1752, found 252.1736 $[MH - Cr(CO)_3]^+$.

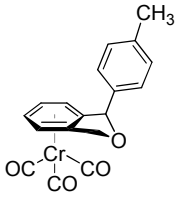


**47a** Using General Procedure 1-C, **46** (51 mg, 0.20 mmol, 1.0 equiv) was combined with LiHMDS (13 mg, 0.08 mmol, 0.4 equiv) and $PdCl_2(PPh_3)_2$ (14 mg, 0.02 mmol, 10 mol %) in 1.4 mL THF and 4-bromotoluene (44 μL, 0.36 mmol, 1.8 equiv) and heated at 57 ºC. More LiHMDS (56 mg, 0.32 mmol, 1.6 equiv)

dissolved in 0.4 mL THF was added over 4h. The reaction was allowed to proceed for an additional 20 h, and yielded **47a** (37.3 mg, 0.11 mmol, 54% yield) as a yellow solid after silica gel chromatography eluting with 20% diethyl ether in pentane. **$^1$H NMR** (300 MHz, $CDCl_3$) δ: 7.18 (apparent s, 4H), 5.96 (d, *J* = 1.8 Hz, 1H), 5.56 (d, *J* = 6.2 Hz, 1H), 5.39 (d, *J* = 6.2 Hz, 1H), 5.29 (dt, *J* = 0.8, 6.2 Hz, 1H), 5.22 - 5.15 (m, 2H), 5.01 (d, *J* = 12.3 Hz, 1H), 2.35 (s, 3H) ppm; **$^{13}$C{$^1$H} NMR** (75 MHz) δ: 232.5, 138.9, 138.1, 112.3, 109.6, 91.4, 91.1, 87.2, 85.9, 84.9, 72.0, 21.4 ppm; **IR** 3087, 2923, 2863, 1964, 1881, 1514, 1043, 1019, 805, 663, 629 $cm^{-1}$.

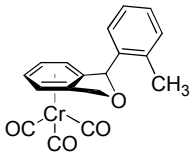


**47b** Using General Procedure 1-C, **46** (38 mg, 0.15 mmol, 1.0 equiv) was combined with LiHMDS (10 mg, 0.07 mmol, 0.5 equiv) and $PdCl_2(PPh_3)_2$ (9.5 mg, 0.013 mmol, 9 mol %) in 1 mL THF and 2-bromotoluene (25 µL, 0.21 mmol, 1.6 equiv) and heated at 57 ºC. More LiHMDS (41 mg, 0.24 mmol, 1.6 equiv) dissolved in 0.4 mL THF was added over 2h. The reaction was allowed to proceed for an additional 6 h, and yielded **47b** (23.6 mg, 0.068 mmol, 45% yield) as a yellow solid after silica gel chromatography eluting with 10% diethyl ether in pentane. **$^1$H NMR** (300 MHz, $CDCl_3$) δ: 7.25 - 7.23 (m, 2H), 7.22-7.13 (m, 1H), 7.06 (d, J = 7.6 Hz, 1H), 6.28 (br s, 1H), 5.58 (d, J = 6.2 Hz, 1H), 5.37 (d, J = 6.2 Hz, 1H), 5.32 (dt, J = 6.2, 0.9 Hz, 1H), 5.21 (dt, J = 6.2, 0.8 Hz, 1H), 5.11 (dd, J = 12.3, 2.0 Hz, 1H), 5.01 (d, J = 12.2 Hz, 1H), 2.48 (s, 3H) ppm; **$^{13}$C{$^1$H}** NMR (75 MHz) δ: 232.5, 138.4, 136.6, 131.3, 129.0, 126.9 126.5, 111.7, 110.5, 91.6, 90.9, 87.6, 85., 82.5, 71.7, 19.6 ppm; **IR** 2919, 2854, 1961 and 1873 (strong CO stretches), 1027, 754, 662, 626 $cm^{-1}$.

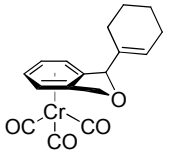


**49** – 1-(1-cyclohexenyl)($\eta^6$-phthalan)$Cr(CO)_3$: Using General Procedure 1-E, a solution of ($\eta^6$-phthalan)$Cr(CO)_3$ (**46**) (19.3 mg, 0.075 mmol, 1 equiv) in 0.6 ml Toluene was reacted with LiHMDS (20 mg, 0.12 mmol, 1.6 equiv) and $PdCl_2(PPh_3)_2$ (2.2 mg, 3 µmol, 4 mol %) of in 0.4 mL THF and 1-cyclohexenyl trifluoromethanesulfonate (16 µL, 0.085 mmol, 1.2 equiv) for 8 h at 50 ºC to yield **49** (15.8 mg, 0.047 mmol, 62% yield) as a yellow-orange oil after silica gel chromatography eluting with 20% diethyl ether in pentane. **$^1$H NMR** (300 MHz, CDCl3) δ: 5.83 - 5.80 (br s, 1H), 5.49 (d, *J* = 6.1 Hz, 1H), 5.42 (d, *J* = 6.0 Hz, 1H), 5.33 (br s, 1H), 5.37 (dt, *J* = 1.1, 6.1 Hz, 1H), 5.22 (dt, *J* = 1.1, 6.1 Hz, 1H), 5.00 (dd, *J* = 2.0, 12.2 Hz, 1H), 4.90 (d, *J* = 12.2 Hz, 1H), 2.07 - 1.96 (m, 3H), 1.76 - 1.51 (m, 5H) ppm; **$^{13}$C NMR** (75 MHz) δ: 232.6, 137.4, 127.3, 111.1, 110.2, 91.5, 91.0, 88.1, 87.0, 85.8, 72.2, 25.3, 23.5, 22.5, 22.4 ppm.

Procedure and characterization for decomplexation:

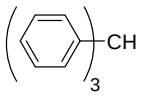

**Triphenylmethane**: **$Ph_2CH(\eta^6\text{-}C_6H_5)Cr(CO)_3$** (64.5 mg, 0.170 mmol) was dissolved in 1.5 mL $CHCl_3$ and 10 mL diethyl ether and placed in bright sunlight for 3 h, until the clear yellow solution became a muddy purple-brown color. This suspension was filtered and concentrated under reduced pressure. The dark residue was diluted with 1:10 $CHCl_3$ in hexanes and filtered again over a pad of $MgSO_4$ and silica gel, and solvent was evaporated from the colorless solution *in vacuo*, yielding **triphenylmethane** (40.5 mg, 0.166 mmol, 98% yield) as a white crystalline solid, with no further purification necessary. All characterization data is consistent with triphenylmethane, a well-known compound.

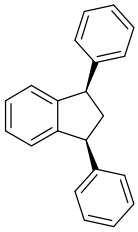

**45 – *cis*-1,3-diphenylindane**: Using General procedure 1-A, ($\eta^6$-indane)$Cr(CO)_3$ (**3**) (0.127 g, 0.499 mmol, 1.0 equiv) was reacted with LiHMDS (0.42 g, 2.51 mmol, 5.0 equiv) and $PdCl_2(PPh_3)_2$ (24 mg, 0.034 mmol, 7 mol %) of in 5 mL THF and bromobenzene (0.26 mL, 2.50 mmol, 5.0 equiv) for 5 h at 53 °C resulted in a deep red solution, which was quenched with 7 drops of aqueous 2N HCl solution, diluted with 6 mL diethyl ether and 1 mL $CHCl_3$ then filtered over a pad of $MgSO_4$ and silica gel. The red solution was placed in sun light for 5 h, and monitored for complete decomplexation by TLC. The cloudy solution was filtered, concentrated *in vacuo,* and chromatographed on silica gel with 6% diethyl ether in pentane to yield ***cis*-1,3-diphenylindane** (0.106 g, 0.392 mmol, 79% yield) as a highly crystalline white solid. **$^1$H NMR** (300 MHz, $CDCl_3$) δ: 7.38 – 7.23 (m, 10H), 7.16 (dd, *J* = 5.6, 3.2 Hz, 2H), 6.95 (ddd, *J* = 5.0, 3.1, 0.5 Hz, 2H), 4.35 (dd, *J* = 11.1, 7.2 Hz, 2H), 2.96 (dt, *J* = 12.5, 7.2 Hz, 1H), 2.14 (dt, *J* = 12.5, 11.1 Hz, 1H) ppm; **$^{13}C\{^1H\}$** NMR (75 MHz) δ: 147.4, 144.6, 128.8, 128.7, 127.0, 126.8, 124.9, 51.0, 48.2 ppm. **IR** 3082, 3061, 3022, 2934, 2865, 1599, 1492, 1454, 1476, 1344, 1073, 1029, 906, 768, 749, 735, 701 $cm^{-1}$. **HRMS** (CI+) calc'd for $C_{21}H_{18}$ 270.1409, found 270.1409 $[M]^+$. Characterization data of this product is consistent with existing literature data.[73]

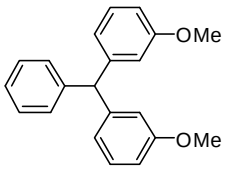

**7 – 3,3'-(phenylmethylene)bis(methoxybenzene)**: For the large-scale reaction, a 50 mL Shlenk flask was charged with a stirbar and LiHMDS (2.51 g, 15 mmol, 3 equiv) and $PdCl_2(PPh_3)_2$ (139 mg, 0.20 mmol, 4 mol %) under nitrogen. Base and catalyst were dissolved in 28 mL of dry THF, and 3-bromoanisole (1.9 mL, 15 mmol, 3 equiv) was added. ($\eta^6$-toluene)$Cr(CO)_3$ (**3**) (1.14 g, 5.0 mmol, 1.0 equiv) was added to the stirring brownish-orange solution in one portion, then heated at 55 °C for 5 h. The reaction was quenched with 0.2 mL of 2N HCl added dropwise, and solids formed in the stirred solution. The flask was opened to air and diluted with 20 mL $Et_2O$ and 3 mL $CHCl_3$, filtered over a pad of $MgSO_4$ and silica gel, rinsed with diethyl ether, and the yellowish-

orange clear solution was exposed to 12 h of sunlight. Precipitating solids were filtered from the brownish green suspension twice during the decomplexation process, and progress was monitored by TLC. The suspension was again filtered, concentrated in vacuo, and loaded onto a short silica gel column and eluted with hexanes, slowly increasing polarity to 3.5% diethyl ether in hexanes to yield **3,3'-(phenylmethylene)bis(methoxybenzene)** (1.42 g, 4.66 mmol, 93%) as a colorless solid. **$^{1}$H NMR** (300 MHz, $CDCl_3$) δ: 7.33 – 7.15 (m, 7H), 6.80 – 6.71 (m, 6H), 5.51 (s, 1H), 3.76 (s, 6H); **$^{13}$C{$^{1}$H}** NMR (75 MHz) δ: 159.8, 145.6, 143.8, 129.6, 129.4, 128.5, 126.6, 122.2, 115.8, 111.6, 57.0, 55.3. **IR** 3058, 3025, 3000, 2955, 2937, 2834, 1597, 1583, 1486, 1464, 1452, 1434, 1314, 1263, 1151, 1050, 878, 776, 758, 732, 697 $cm^{-1}$. **HRMS** (CI+) calc'd for $C_{21}H_{21}O_2$ 305.1542, found 305.1546 $[MH]^+$.

## Computational analysis of the deprotonated lithium species.

Computational analysis of the lithiated diphenylmethane tricarbonylchromium (**4a-Li**) is in agreement with similar computational studies (gas-phase model) presented by Merlic and co-workers, and confirms the *sp*$^2$-hybridized geometry of the benzylic center.[74,75] Tim Kowalczyk is gratefully acknowledged for his work on the quantum calculations presented here.

The geometry of complex **4a-Li** was optimized at the level of density functional theory with the B3LYP[76] functional and the SV(P)[77] basis set. The effect of the THF environment was modeled under the conductor-like screening model (COSMO)[78] with dielectric constant ε = 7.58 and with cavitation surface defined by Bondii atomic radii. The stability of the optimized geometry was confirmed via frequency calculations which presented no negative eigenvalues of the Hessian. All quantum chemistry calculations used the Turbomole[79] program package.

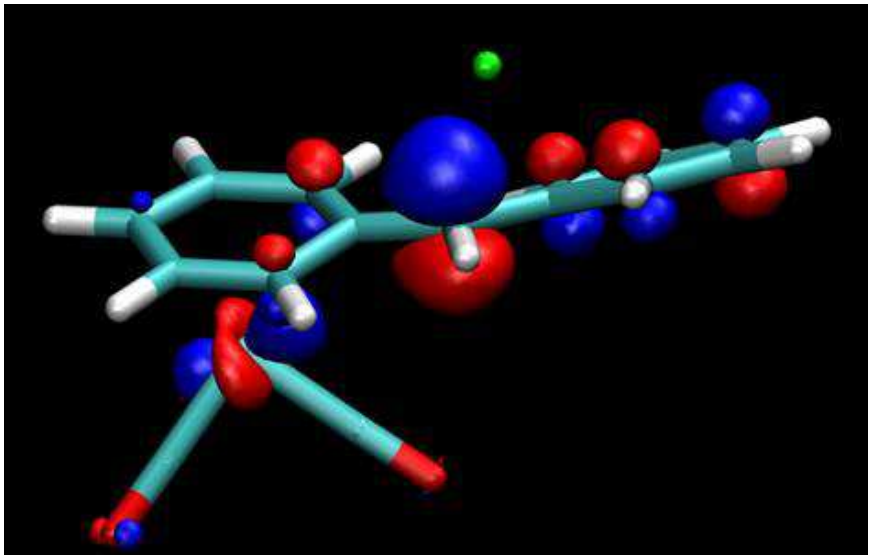

Figure 1-17: Optimized geometry of **4a-Li** with HOMO is pictured. The THF solvent environment was modeled using COSMO. Note that most of the charge is localized on benzylic carbon, with some charge density spread on the other phenyl rings and on the $Cr(CO)_3$ center.

## References


[1] Fischer, E. O.; Öfele, K. *Chem. Ber.* **1957**, *90*, 2532-2535.

[2] Herndon, J. W.; Laurent, S. E. in *Encyclopedia of Reagents for Organic Synthesis*, John Wiley & Sons, Chichester, **2008**.

[3] (a) Berger, A.; Djukic, J.; Michon, C. *Coord. Chem. Rev.*, **2002**, *225*, 215-238. (b) Ratni, H.; Kundig, E. P. *Org. Lett.* **1999**, *1*, 1997-1999. (c) Rosillo, M.; Dominguez, G.; Perez-Castells, J. *Chem. Soc. Rev.* 2007, **36**, 1589-16604.

[4] For examples of the activating qualities of $M(CO)_3$–coordination to arenes, see (a) Uemura, M., in *Org. React., Vol. 67,* John Wiley, NJ: 2006, pp. 217. (b) Merlic, C. A.; Walsh, J. C.; Tantillo, D. J.; Houk, K. N.; *J. Am. Chem. Soc.* **1999**, *121*, 3596. (c) Pfletschinger, A.; Dargel, T. K.; Bats, J. W.; Schmalz, H.-G.; Koch, W.; *Chem. Eur. J.* **1999**, *5*, 537. (d) Kündig, E. P. In *Topics in Organometallic Chemistry Vol. 7*, Berline; New York: 2004.

[5] Hegedus, L. S. Transition Metals in the Synthesis of Complex Organic Molecules; 2 ed.; University Science Books: Sausalito, **1999**.

[6] Costa, M. R.; Curto, M. J.; Davies, S. G.; Sanders, J.; Teixeira, F. C. *J. Chem. Soc., Perkin Trans 1* **2001**, 2850-2855.

[7] Tricarbonylchromium-coordination was used as a tool in two examples of the total synthesis of (−)-steganone: (a) Monovich, L. G.; Le Huérou, Y.; Rönn, M.; Molander, G. A. *J. Am. Chem. Soc.* **2000**, *122*, 52-57. (b) Uemura, M.; Daimon, A.; Hayashi, Y. *J. Chem. Soc. , Chem. Commun*. **1995**, 1943-1944.

[8] Ratni, H.; Kundig, E. P. *Org. Lett.* **1999**, *1*, 1997-1999.

[9] Merlic, C. A.; Walsh, J. C.; Tantillo, D. J.; Houk, K. N. *J. Am. Chem. Soc.* **1999**, *121*, 3596-3606.

[10] Ashraf, M.; Jackson, W. R. *J.Chem.Soc., Perkin Trans.2* **1972**, 103-106.

[11] Antonova, M. V.; Moiseev, S. K.; Kalinin, V. N.; Shapiro, I. O. *Russ. Chem. Bull*. **1989**, *38*, 2256-2259.

[12] Rosillo, M.; Dominguez, G.; Perez-Castells, J. *Chem. Soc. Rev.* **2007**, *36*, 1589-1604.

[13] Collman, J. P.; Hegedus, L. S.; Norton, J. R.; Finke, R. G. In *Synthetic Applications of Arene Transition-Metal Complexes; Principles and Applications of Organotransition Metal Chemistry*; University Science Books: Mill Valley, CA 94941, 1987; pp 921-19.

[14] Kalinin, V. N.; Cherepanov, I. A.; Moiseev, S. K., *J. Organomet. Chem.* **1997**, *536-537*, 437-455.

[15] Bordwell, F. G.; Matthews, W. S.; Vanier, N. R. *J. Am. Chem. Soc.* **1975**, *97*, 442-443.

[16] (a) Muthyala, R.; Katritzky, A. R.; Lan, X. *Dyes and Pigments* **1994**, *25*, 303. (b) Katritzky, A. R.; Gupta, V.;Garot, C.; Stevens, C. V.; Gordeev, M. F. *Heterocycles* **1994**, *38*, 345.

[17] For more examples of polyarylmethanes in materials science and dyes, see: (a) Nair, V.; Thomas, S.; Mathew, S. C.; Abhilash, K. G. *Tetrahedron* **2006**, *62*, 6731-6747. (b) Müller, T. J. J.; Netz, A.; Ansorge, M.; Schmälzlin, E.; Bräuchle, C.; Meerholz, K. *Organometallics* **1999**, *18*, 5066-5074.

[18] (a) Duxbury, D. F. *Chem. Rev.* **1993**, 381-433. (b) Shchepinov, M. S.; Korshun, V. A. *Chem. Soc. Rev*. **2003**, *32*, 170.

[19] Elliott, J. D.; Lago, M. A.; Cousins, R. D.; Gao, A.; Leber, J. D.; Erhard, K. D.;Nambi, P.; Elshourbagy, N. A.; Kumar, C. *J. Med. Chem.* **1994**, *37*, 1553.

[20] For examples of polyarylmethanes in medicinal chemistry, see: (a) Parai, M. K.; Panda, G.; Chaturvedi, V.; Manju, Y. K.; Sinha, S. *Bioorg. Med. Chem. Lett.* **2008***, 1,* 289-292. (b) Indig, G. L.; Anderson, G. S.; Nichols, M. G.; Bartlett, J. A.; Mellon, W. S.; Sieber, F. *J. Pharm. Sci.* **2000***, 1,* 88-99. (c) Palchaudhuri, R.; Nesterenko, V.; Hergenrother, P. J. *J. Am. Chem. Soc*. **2008**, *130*, 10274-10281.

[21] Abdelrahim, M.; Newman, K.; Vanderlaag, K.; Samudio, I.; Safe, S. *Carcinogenesis* **2006**, *27*, 717-728.

[22] Yu, J. -.; Kuwano, R. *Org. Lett.* **2008**, *10*, 973-976.

[23] See: (a) Nair, V.; Thomas, S.; Mathew, S. C.; Abhilash, K. G. *Tetrahedron* **2006**, *62*, 6731. (b) Nair, V.; Abhilash, K. G.; Vidya, N.; *Org. Lett.* **2005**, *7*, 5857. (c) Lin, S.; Lu, X. *J. Org. Chem*. **2007**, *72*, 9757. (d) Das, S. K.; Shagufta; Panda, G. *Tetrahedron Lett*. **2005**, *46*, 3097. (e) Yadav, J. S.; Reddy, B. V. S; Sunitha, S. *Adv. Syn. & Catal.* **2003**, *345*, 349. (f) Ramesh, C.; Barerjee, J.; Pal, R.; Das, B.; *Adv. Syn. & Catal*. **2003**, *345*, 557. (g) Schäfer, G.; Bode, J. W. *Angew. Chem. Int. Ed.* **2011**, *asap*.

[24] For a complementary procedure involving vicarious nucleophilic substitution of nitroarenes see: Katritzky, A. R.; Toader, D. *J. Org. Chem*. **1997**, *62*, 4137.

[25] Katritzky, A. R.; Lan, X.; Lam, J. N. *Chem. Ber.* **1991**, *124*, 1809.

[26] For a review on the transition-metal catalyzed arylation of $sp^3$ C–H bonds, see: Baudoin, O. *Chem. Soc. Rev*. **2011**, *40*, 4902-4911.

[27] (a) Netherton, M. R.; Fu, G. C. *Adv. Syn. & Catal*. **2004**, *346*, 1525-1532. (a) Frisch, A. C.; Beller, M. *Angew. Chem., Int. Ed*. **2005**, *44*, 674-688.

[28] (a) Molander, G. A.; Elia, M. D. *J. Org. Chem*. **2006**, *71*, 9198-9202. (b) Kuwano, R.; Yokogi, M. *Org. Lett*. **2005**, *7,* 945-947. (c) McLaughlin, M. *Org. Lett*. **2005**, *7*, 4875-4878. (d) Kofink, C.

C.; Knochel, P. *Org. Lett*. **2006**, *8*, 4121-4124. (e) Imao, D.; Glasspoole, B. W.; Laberge, V. S.; Crudden, C. M. *J. Am. Chem. Soc*. **2009**, *131*, 5024-5025.

[29] (a) Yu, J. -.; Kuwano, R. *Org. Lett.* **2008**, *10*, 973-976. (b) Schäfer, G.; Bode, J. W. *Angew. Chem. Int. Ed.* **2011**, *asap*.

[30] Li, Y.; Li, B.; Lu, X.; Lin, S.; Shi, Z. *Angew. Chem. Int. Edit. Engl*. **2009**, *48*, 3817-3820.

[31] For methods to synthesize asymmetric heteroaromatic di- and tri-arylmethanes, see: (a) Shi, B.; Maugel, N.; Zhang, Y.; Yu, J. *Angewandte Chemie International Edition* **2008***, 47*, 4882-4886. (b) Sun, F.; Zheng, X.; Gu, Q.; He, Q.; You, S. *European Journal of Organic Chemistry* **2010***, 2010*, 47-50. (c) Esquivias, J.; Arrayás, R. G.; Carretero, J. C. *Angewandte Chemie International Edition* **2006***, 45*, 629-633.

[32] See: (a) Molander, G. A.; Ellis, N.; *Acc. Chem. Res.* **2007**, *40*, 275. (b) Liégault, B.; Renaud, J.-L.; Bruneau, C.; *Chem. Soc. Rev.* **2008**, *37*, 290. (c) Imao, D.; Glasspoole, B. W.; Laberge, V. S.; Crudden, C. M.; *J. Am. Chem. Soc.* **2009**, *131*, 5024.

[33] (a) Murahashi, S. *J. Organomet. Chem.* **2002**, *653*, 27-33. (b) Murahashi, S.-I. et al, *Organic Syntheses,* **1990,** Coll. Vol. 7, 172; **1984,** Vol. 62, 39.

[34] Brewer, A. R. E.; Drake, A. F.; Gibson, S. E.; Rendell, J. T. *Org. Lett.* **2007**, *9*, 3487-3490.

[35] Cohen, M. D.; Kargacin, B.; Klein, C. B.; Costa, M. *Crit. Rev. Toxicol*. **1993**, *23*, 255-281.

[36] Barceloux, D. G.; Barceloux, D. *Clin. Toxicol.* **1999**, *37*, 173-194.

[37] Kündig, E. P.; Fabritius, C.; Grossheimann, G.; Romanens, P.; Butenschön, H.; Wey, H. G. *Organometallics* **2004**, *23*, 3741-3744.

[38] Woolins, J. D., Ed.; In *Inorganic Experiments*; VCH: Weinheim, **1994**; 194-195.

[39] Antonini, S.; Calderazzo, F.; Englert, U.; Grigiotti, E.; Pampaloni, G.; Zanello, P. *J. Organomet. Chem.* **2004**, *689*, 2158-2168.

[40] Hoff, C. D., *J. Organomet. Chem.* **1985**, *282*, 201-214.

[41] For more information on the relative stability of arene ligands, see Semmelhack, M. F.; Chlenov, A.; Ho, D. M. *J. Am. Chem. Soc.* **2005**, *127*, 7759-7773.

[42] Semmelhack, M. F.; Hall, H. T. *J. Am. Chem. Soc.* **1974**, *96*, 7092-7094.

[43] Acidities were referenced from the Ripin and Evans compilation table and data from Bordwell *et al*: (a) Bordwell, F. G.; Algrim, D.; Vanier, N. R. *J. Org. Chem.* **1977**, *42*, 1817-1819. (b) Bordwell, F. G. *Acc. Chem. Res.* **1988**, *21*, 456-463. (c) Bordwell, F. G.; Matthews, W. S.; Vanier, N. R. *J. Am. Chem. Soc.* **1975**, *97*, 442-443.

[44] Palucki, M.; Buchwald, S. L. *J. Am. Chem. Soc.* **1997**, *119*, 11108-11109.

[45] Hamann, B. C.; Hartwig, J. F. *J. Am. Chem. Soc.* **1997**, 11l9, 12382-12383.

[46] Kalinin, V. N.; Cherepanov, I. A.; Moiseev, S. K. *J. Organomet. Chem.* **1997**, *536-537*, 437-455.

[47] Ackermann, L.; Born, R.; Spatz, J. H.; Meyer, D. *Angew. Chem. , Int. Ed.* **2005**, *44*, 7216-7219.

[48] Polyarylmethane derivatives bearing privileged indoles have attracted interest due to their widespread occurrence in biologically active compounds. For more information, see: Sundberg, R. J. In *Indoles*; Academic Press: 1996.

[49] (a) Katritzky, A. R.; Gupta, V.; Garot, C.; Stevens, C. V.; Gordeev, M. F.; *Heterocycles* **1994**, *38*, 345. (b) Yadav, J. S.; Reddy, B. V. S.; Sunitha, S.; *Adv. Syn. & Catal.* **2003**, *345*, 349. (c) Ramesh, C.; Barerjee, J.; Pal, R.;Das, B.; *Adv. Syn. & Catal.* **2003**, *345*, 557. (d) Nair, V.; Abhilash, K. G.; Vidya, N.; *Org. Lett.* **2005**, *7*, 5857. (e) Esquivias, J.; Arrayás, R. G.; Carretero. J. C.; *Angew. Chem., Int. Ed.* **2006**, *45*, 629.

[50] Gibson, S. E.; Saladin, S. A.; Sur, S. *Chem. Commun.* **2000**, 2011-2012.

[51] (a)Dothager, R. S.; Putt, K. S.; Allen, B. J.; Leslie, B. J.; Nesterenko, V.; Hergenrother, P. J. *J. Am. Chem. Soc.* **2005**, *127*, 8686-8696. (b) Palchaudhuri, R.; Nesterenko, V.; Hergenrother, P. J. *J. Am. Chem. Soc.* **2008**, *130*, 10274-10281.

[52] Murahashi, S. *J. Organomet. Chem.* **2002**, *653*, 27-33.

[53] (a) Esquivias, J.; Arrayás, R. G.; Carretero. J. C.; *Angew. Chem., Int. Ed.* **2006**, *45*, 629. (b) Schäfer, G.; Bode, J. W. *Angew. Chem. Int. Ed.* **2011**, *asap*.

[54] Katritzky, A. R.; Qi, M. *Tetrahedron* **1998**, *54*, 2647-2668.

[55] Katritzky, A. R.; Gupta, V.; Garot, C.; Stevens, C. V.; Gordeev, M. F.; *Heterocycles* **1994**, *38*, 345.

[56] Yamada, K.; Tomioka, K. *Chem. Rev*. **2008**, *108*, 2874-2886.

[57] Hartwig, J. In *Organotransition Metal Chemistry: From Bonding to Catalysis*; University Science Books: 2010.

[58] (a) Bogle, K. M.; Hirst, D. J.; Dixon, D. J. *Org. Lett.* **2007**, *9*, 4901-4904. (b) Malcolm, S. C.; Ribe, S.; Wang, F.; Hewitt, M. C.; Bhongle, N.; Bakale, R. P.; Shao, L. *Tetrahedron Lett.* **2005**, *46*, 6871-6873.

[59] Uemura, M. In Org. React.; Overman, L. E., Ed.; John Wiley: NJ, **2006**; Vol. 67, p 217-659.

[60] Lantaño, B.; Aguirre, J. M.; Finkielsztein, L.; Alesso, E. N.; Brunet, E.; Moltrasio, G. Y.. *Synth. Commum.* **2004**, *34*, 625-641.

[61] Albicker, M. R.; Cramer, N. *Angew. Chem. Int. Edit.* **2009**, *48*, 1939-1942.

[62] Semmelhack, M. F.; Chlenov, A.; Ho, D. M. *J. Am. Chem. Soc.* **2005**, *127*, 7759-7773.

[63] Traylor, T. G.; Stewart, K. J. *J. Am. Chem. Soc.* **1986**, *108*, 6977-6985.

[64] Ceccon, A.; Gambaro, A.; Santi, S.; Valle, G.; Venzo, A. *J. Chem. Soc. , Chem. Commun.* **1989**, 51-53.

[65] Jahra, H. C.; Niegerb, M.; Dötz, K. H. *Chem. Commun.* **2003**, 2866-2867.

[66] For cross-coupling reactions with organolithium reagents see: Murahashi, S. *J. Organomet. Chem.* **2002**, *653*, 27-33.

[67] Woolins, J. D., Ed.; In *Inorganic Experiments*; VCH: Weinheim, **1994**; 194-195.

[68] Cram, D. J.; Wilkinson, D. I. *J. Am. Chem. Soc.* **1960**, *82*, 5721-5723.

[69] Mahaffy, C. A. L.; Pauson, P. L. *Inorg. Synth.* **1990**, *28*, 136-140.

[70] Ohlsson and Bengt et al*, J. Organomet. Chem*. **1989**, *365*, 243-267.

[71] Cambie, Richard C. et al, *J. Organomet. Chem*. **1988**, *342*, 315-337.

[72] Kaganovich, V. S.; Rybinskaya, M. I. *Russ. Chem. Bull*. **1993**, *42*, 1734-1737.

[73] Farnia, G.; Sandona, G.; Marcuzzi, F.; Melloni, G. *J. Chem. Soc. , Perkin Trans. 2*, **1988**, 247-254.

[74] Merlic, C. A.; Walsh, J. C.; Tantillo, D. J.; Houk, K. N. *J. Am. Chem. Soc.* **1999**, 121, 3596-3606.

[75] Pfletschinger, A.; Dargel, T. K.; Bats, J. W.; Schmalz, H.; Koch, W. *Chem. -Eur. J.* **1999**, 5, 537-545.

[76] Becke, A.D. Density-functional thermochemistry. 3. *J. Chem. Phys*. **1993**, *98*, 5648-5652.

[77] Weigend, F.; Ahlrichs, R. *Phys. Chem. Chem. Phys.* **2005**, *7*, 3297-3305.

[78] Klamt, A.; Schüürmann, G. *J. Chem. Soc., Perkin Trans. 2* **1993**, *5*, 799-805.

[79] Ahlrichs, R.; Bar, M.; Haser, M.; Horn, H.; Kolmel, C. *Chem. Phys. Lett.* **1989**, *162*, 165-169.

## Chapter 2

## Asymmetric benzyllithium cross-couplings

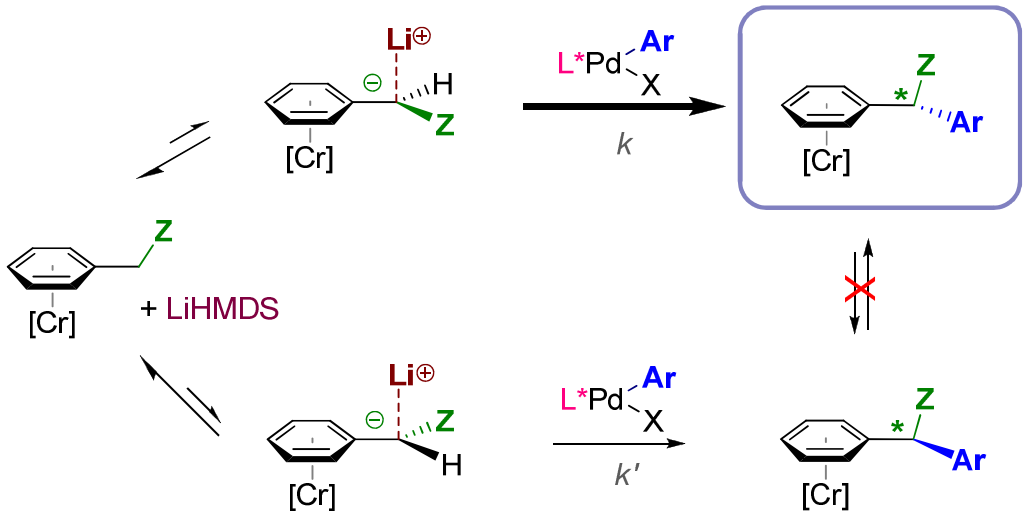

## Introduction

The development of enantio- and diastereo- selective metal-catalyzed carbon-carbon bond forming reactions has enabled efficient access to valuable chemical scaffolds often difficult or impossible to access through conventional methods. As noted in Chapter 1, the privileged diaryl- and triarylmethane frameworks are found in a large number of pharmacological compounds. Examples of biologically active chiral polyarylmethanes are given below (Figure 2-1).

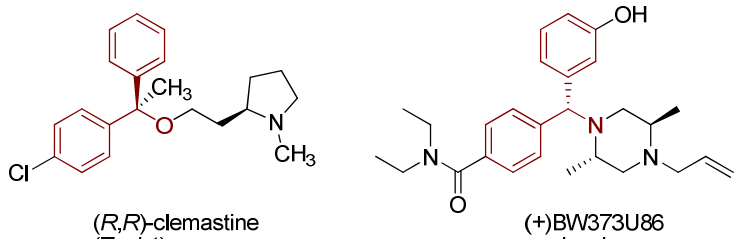


(*R*,*R*)-clemastine
(Tavist)
sedative antihistamine

(+)BW373U86
analgesic,
antidepressant

Figure 2-1: Some biologically active chiral polyarylmethanes.

Considering the importance of the privileged diaryl and triarylmethane frameworks, it is no surprise that medicinally relevant chiral diarylmethane derivatives have been heavily pursued.[1,2] On the other hand, the selective syntheses of unsymmetrical triarylmethanes is still considered very challenging, particularly when one or more of the aryl groups to be installed is electron-poor or sterically hindered.[3] For example, to the best of my knowledge, there have been only two published examples of nonracemic chiral triarylmethane syntheses (Scheme 2-1). The strategies employed were: a palladium-catalyzed directed desymmetrization of a tri(hetero/aryl)methane at the *ortho* position by Yu and coworkers,[4] and a chiral phosphoric acid-catalyzed Friedel-Crafts synthesis of substituted indolyl triarylmethanes by You and coworkers (most %*ee* were in the 50 – 60 range).[5] To date, there does not seem to be existing asymmetric syntheses of chiral non-heteroaromatic triarylmethanes. The asymmetric synthesis of polyarylmethanes is clearly an important area of exploration.

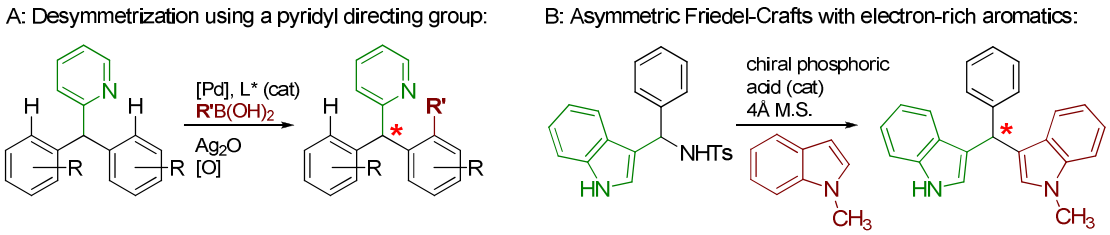


Scheme 2-1: Previous strategies for nonracemic tri-hetero/arylmethane syntheses. Yu uses desymmetrization of a 2-pyridyl substituted triarylmethane. You uses a chiral phosphoric acid to catalyze an asymmetric Friedel-Crafts alkylation of an electron-rich indole.

## Asymmetric cross-coupling at the benzylic position of tertiary benzylamines to form enantioenriched diarylmethyl benzylamines

Optically active benzyl amines possessing chirality α to the nitrogen are found in a variety of pharmaceuticals marketed today,[6] from Amoxicillin to Zyrtec. Their functions range from anaesthetics and antihistamines, to antibiotics and potential cancer drugs or cancer drug precursors (Figure 2-2).[7]

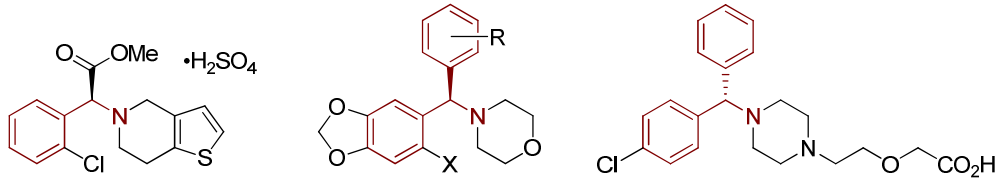

Clopidogrel
(Plavix):
prevent blood clotting

NSC368269,
NSC364724
anti-cancer

(*S*)-cetrizine hydrochloride
(Zyrtec)
non-drowsy antihistamine

Figure 2-2: Some examples of biologically active tertiary benzylamines that posess chirality in the α-position.

Despite the diarylmethyl amine family's prominence in medicinal chemistry, most syntheses of α-alkyl or α-aryl benzylamines are typically accomplished through Mannich-tpe reactions and generate racemic products.[8] To access enantioenriched diarylmethylamines, racemic mixtures are typically resolved through chromatography,[9] or chemical methods, such as crystallization with tartaric acid.[10] In the case of the popular antihistamine drug Zyrtec, the current industrial synthetic method involves diastereoselective synthesis using a chiral auxiliary.[11] Recently, asymmetric reduction of benzophenone imines has been reported, but *ortho*-substitution of

substrates is required for high enantioselectivity.[12,13] Catalytic asymmetric methods to prepare highly enantioenriched diarylmethyl amines has remained challenging.

Currently, asymmetric methods to prepare enantioenriched diarylmethanes involve asymmetric additions[14] to activated imine[15] or iminium species using metalated arene nucleophiles, such as tetraarylborates,[16] organostannanes[17], phenylzinc[18], or aryl rhodium (catalytic) reagents.[14,19] However, asymmetric cross-coupling of electrophiles to an $sp^3$ C–H bond α- to a tertiary amine has not yet been realized. Part of the reason for this lies in the fact that α–amino-substituted secondary organometallic partners for cross-coupling are difficult to access. A popular method for preparing some varieties of organometallic cross-coupling reagents (such as zinc and tin derivatives) is metathesis with an organolithium precursor, but lithiation α- to an unactivated amine is considered difficult, making this method for preparing cross-coupling reagents ineffective.[20]

As described in Chapter 1, we initially developed a non-enantioselective palladium-catalyzed cross-coupling reaction between tricarbonylchromium-coordinated benzylic arenes and aryl bromides using LiHMDS as a base (Scheme 2-2). We wondered if an enantioselective variant of this reaction would be feasible, made possible by some unique aspects of the activating metal fragment, the tricarbonylchromium group.

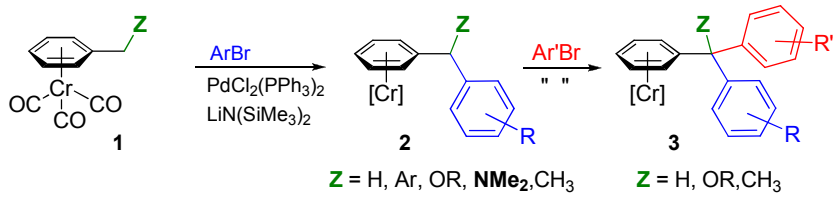


Scheme 2-2: Tricarbonylchromium-assisted synthesis of achiral and racemic polyarylmethanes using our methods (see Chapter 1).

We first considered whether we could synthesize enantioenriched relevant diarylmethylamines (Scheme 2-3). We decided to pursue the family of diarylmethylamines due to the medicinal relevance of their structures. Additionally, the system contained fewer complicating variables that could hamper enantioselectivity in the reaction. For example, diarylmethylamine products formed from achiral catalysts failed to undergo further arylation to form substituted triarylmethanes (Chapter 1, Scheme 1-25, p.31), minimizing competing coupling reactions which

may consume one (or both) enantiomers of product. Also, tricarbonylchromium "walking" (Chapter 1, p. 40) was not observed in the reaction with amines; this minimizes a potential source of product isomerization to side-products which could be difficult to separate from the desired product regioisomer.

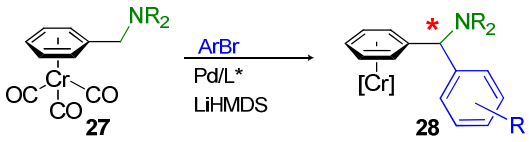


Scheme 2-3: Envisioned eantioselective synthesis of diarylmethylamine derivatives from benzylamine and aryl bromides. L* denotes a chiral ligand.

Due to the tricarbonylcrhomium group's ability to delocalize charge,[21] the lithiated intermediates **1-Li** and **1-Li'** were expected to be planar chiral and configurationally stable due to a partial double bond character[a] between *ipso* and benzylic carbons (Scheme 2-4).[22] However, we also hypothesized that due to the rapid and reversible nature deprotonation of **1** by LiHMDS, both enantiomers **1-Li** and **1-Li'** would be readily available for reaction. Providing that the diasteromeric transmetallation of **1-Li** to an enantioenriched L*Pd(II) center was faster than with **1-Li'** *and* irreversible, dynamic kinetic resolution (DKR) conditions would be achieved.[23] We anticipated that the aryl-alkyl Pd(II) intermediate **4** does not have a method for interconverting to **4'**, and that there is a lack of racemization pathways between product enantiomers.

[a] The bond is intermediate in length and strength between a single and double bond, determined by gas-phase calculations by Merlic and coworkers.

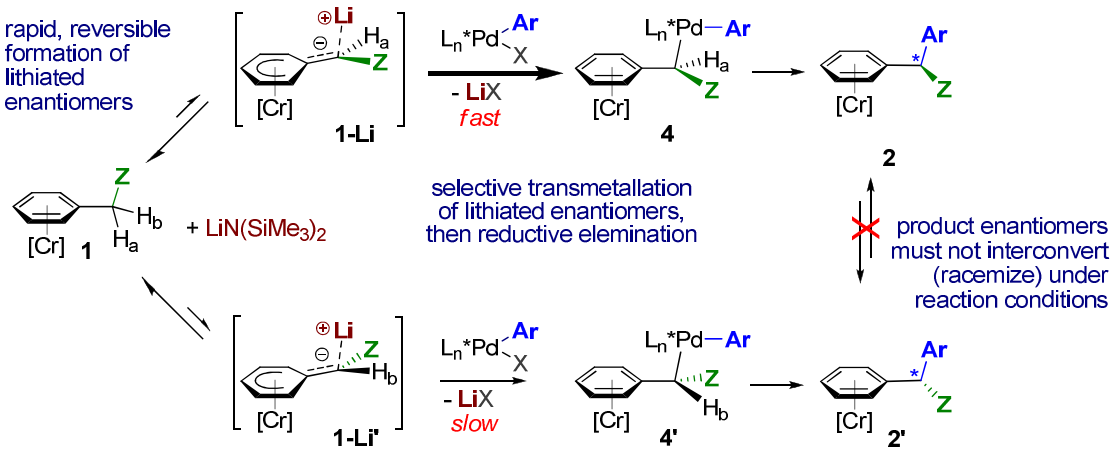


Scheme 2-4: Proposed asymmetric arylation of tricarbonylchromium-stabilized benzyllithium.

Considering the many chiral mono- and bi-dentate ligands available for reaction and the unusal nature of our proposed asymmetric organolithium cross-coupling, it was possible that an extremely specific ligand would be required for highly enantioselective reactions. However, many chiral ligands are expensive, and some can be rather difficult to obtain. We needed a rapid and cost-efficient method to identify promising chiral ligands, which would circumvent the conventional time-consuming and expensive screening of ligands at laboratory scale. Thankfully, an industrial collaboration with Merck & Co. under the GOALI[a] grant provided an opportunity to investigate a large range of chiral ligands using low-barrier high-throughput experimentation (HTE) procedures.

[a] GOALI (Grant Opportunities for Academic Liason with Industry) is an NSF-funded program to foster collaborative efforts and cross-pollination of techniques and ideas between industry and academia. See http://www.nsf.gov/pubs/2010/nsf10580/nsf10580.htm for more information. The PI in this program is G. Molander (UPenn) with Co-PIs: S. Dreher (Merck), M. Kozlowski (UPenn), and P. Walsh (UPenn).

*Initial High-throughput Screen of Ligands*[a]

## Considerations in HTE design.

Low-barrier high-throughput experimentation (HTE) is a new set of technologies in chemistry and catalysis which enables the rapid identification and optimization of reaction conditions (ligands, reagents, additives, etc) and even reaction discovery.[24] It is allows microscale experimentation of dozens to hundreds of reactions in parallel, saving time and reagent, which can (in the case of multi-hundred-dollar custom chiral ligands, for example), be extremely expensive if run on typicaly synthetic-lab scale. Through the GOALI grant, HTE reactions have been conducted both at Merck & Co. in Rahway, NJ, and at the new high-throughput screening center at the University of Pennsylvania. Opened in the fall of 2010, it is currently only one of three such academic facilities in the country.

Generally, reactions are run in multiples of 24- or 96- well plates (4×6 and 8×12 wells, respectively). The plates are loaded with glass vials in either 1 mL or 250 µL capacity, and numbering is as in a typical grid (i.e. A1, A2, B1, B2, etc. See Figure 2-3 B). Glass vials may be pre-dosed with reagent solutions, such as ligand, low-solubility reagents such as palladium precatalyst, or additives. Unnecessary solvent is removed by either a GeneVac, which is a vacuum centrifuge that can accommodate HTE reaction plates, or a blow-down tool, which runs a constant stream of nitrogen into each vial in order to evaporate solvent quickly. Reagents are then added via pipette or multi-channel pipette from standardized solutions.[b] Total reaction volume is approximately 10% of the vessel size with 25 µL or 100 µL volume reactions typically conducted (Figure 2-3 A). In practical terms, this translates to using the material of two 0.1 mmol-scale reactions to furnish one entire 96-well plate run in 250 µL vials. Finally, the reaction is sealed with screws by a metal plate lined with rubber mats and a PTFE liner film. This allows the reaction to maintain inert atmosphere outside of the glovebox and effectively contains vapors from reactions that are need to be heated (Figure 2-3, A).

---

[a] Initial ligand screens were run in collaboration with Dr. C. Stanciu at Merck & Co (Rahway).

[b] Homogeneous solutions are preferred in HTE screens. While non-homogeneous suspensions and slurries can also be added, they are more difficult to handle and require pipetting while the mixture is stirring vigorously, as well as a cut pipet tip to prevent clogging.

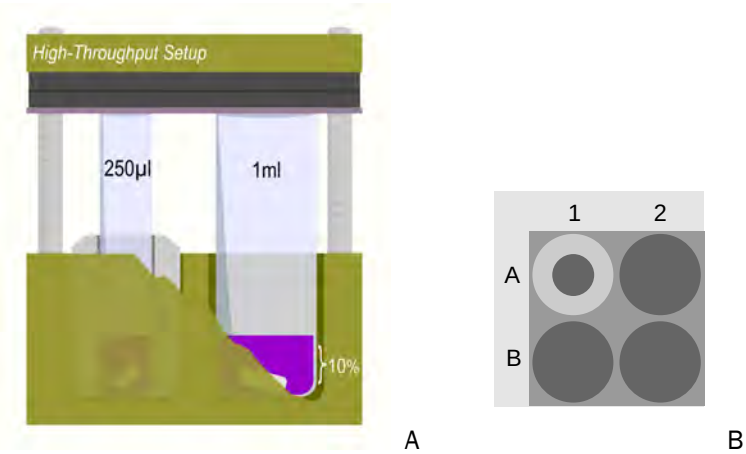


Figure 2-3: Schematic view of the high-throughput setup of a theoretical 2×2 plate. In the cut-away side view (A, Left), the reaction vial filling, seals, and screw fastening of the top are illustrated. In the unsealed top-view (B, Right), arrangement of reactions in a grid are shown. Both 1 mL and 250 µL reaction vessels are pictured, but typically only one size of vial is used at a time.

Once the reactions have been run for the specified time, they are quenched simultaneously, worked up in solubilizing organic solvents such as DMSO and acetonitrile with water. Analysis of the reactions is accomplished using HPLC (with internal standard, such as biphenyl, for conversion data) and SFC (for enantioselectivity). Provided that chromatographic methods are developed that successfully separate reaction components — such as starting materials, side-products, and product enantiomers — the large amount of intercomparable data that results from the screening can then be analyzed at once. All steps from reaction design, execution, and instrumental analysis can be accomplished within a few days. Thus, HTE ideally allows meaningful conclusions to be obtained in a fraction of the time of conventional lab-scale experimentation.[24]

## Reaction screening

Initially, we decided to focus on the α-arylation of dimethylbenzylamine (Chapter 1, p.31) because of the medicinal importance of chiral diarylbenzylamines. The *N,N'*-dimethylbenzyl amine complex ($\eta^6$-$Me_2NCH_2Ph$)$Cr(CO)_3$ (compound **27**)[25] was employed in a low-barrier high-throughput experimentation (HTE) screen with a large library of enantioenriched mono- and bidentate

phosphine ligands, palladium precursor $PdCl_2$[COD], 4-bromotoluene, and 1.3 equivalents of LiHMDS (Scheme 2-5) in hopes of forming enantioenriched tertiary diarylmethylamine **28f** (Scheme 2-5). The parallel reactions were run on extremely small (2 µmol, or ~0.5 mg **27**) scale to allow efficient use of our valuable (and expensive) catalysts and starting materials.[24] All in all, less than 0.5 mmol of tricarbonylchomium reagent was used in the screen of 192 reactions![a] Reactions were then analyzed for conversion to product (determined by HPLC relative to an internal standard), and those that showed product formation were then analyzed on chiral SFC.

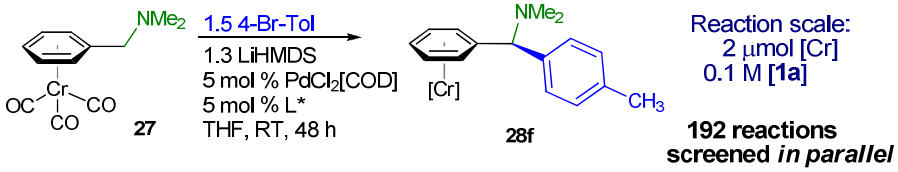


Scheme 2-5: Initial High-Throughput screen of ligands is conducted on microscale for the asymmetric cross-coupling of benzylamine **27** with 4-bromotoluene (2 µmol ~ 0.5 mg substrate) to form **28f**.

Table 2-1: Promising hits in the HTE screen of ligands (Scheme 2-5). Ligands given below showed conversion to product via HPLC, and were analyzed on chiral stationary-phase SFC for enantiomeric ratio (er).

| *Most promising hits (%ee only):* | | |
|---|---|---|
| Taniaphos | Mandyphos | Walphos |
| 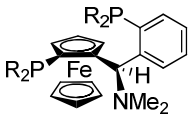 | 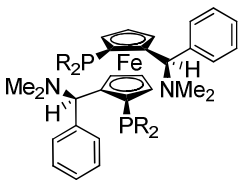 | 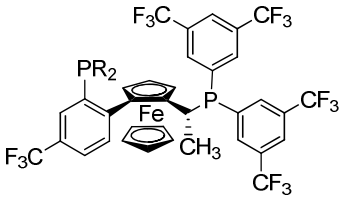 |
| R = Cy (SL-T002)<br>>9:1 *e.r.* | R = Cy (SL-M002)<br>>>9:1 *e.r.* | |
| R = Ph (SL-T001)<br>3:1 *e.r.* | R = Ph (SL-M001)<br>2:1 *e.r.* | R = Ph (SL-W018)<br>4:1 *e.r.* |

[a] For a full list of ligands screened, see Appendix V, Table V-1 and Table V-2 (p.330).

Although several of the ligands screened showed high conversion by HPLC, only a small handful of ligands exhibited enantioselectivity under these conditions (>2:1 er, Table 1-1). Dicyclohexyl phosphine derivatives of the Taniaphos[26] and Mandyphos[a,27] ligand family showed the greatest selectivity (>9:1 er for both ligands), although conversion to product in the case of Mandyphos was low relative to other ligands screened. Taniaphos and Mandyphos are modular "privileged scaffold"[b,28] ferrocene-amine phosphine ligands that have been known for producing extremely high selectivity in reactions, but their main popularity has been in rhodium-catalyzed asymmetric hydrogenation reactions and ring-opening reactions, not in cross-coupling.[29] It is possible that the tertiary amine functionality present in both ligands is one contributing factor in the success of Mandyphos and Taniaphos ligands by coordinating to **27-Li**. In fact, a similar hypothesis was made by Kumada *et al* in the case of an asymmetric cross-coupling reaction of secondary alkyl Grignards with aryl bromide. In their case, however, the organometallic magnesium species was hypothesized to be configurationally labile, rapidly undergoing inversion during their reaction.[30] In contrast, our system is expected to be configurationally stable as an organolithium, racemizing only upon protonation and subsequent deprotonation of the other benzylic C–H.

### *Further examination of "hits"*

The most promising ligands, cylcohexyl Mandyphos and cyclohexyl Taniaphos, were used in test reactions on laboratory scale to verify the ligands as "hits." Indeed, upon running the reactions using the same conditions but at larger scale, we found that the performance of both ligands was comparable to the results obtained by microscale HTE. Taniaphos had a higher conversion and a lower ee than Mandyphos, which exhibited very high enantioselectivity (>9:1 er) but very low conversion. Cyclohexl Mandyphos was chosen as the ligand with which to optimize the reaction.

---

[a] Ferriphos is the original moniker for Mandyphos (Phenyl) before it was expanded into the Mandyphos family of ligands.

[b] "Privileged" ligand substructures are "certain classes of synthetic catalysts [which] are enantioselective over a wide range of different reactions." For an overview of these successful ligands, see: Yoon, T. P.; Jacobsen, *Science* **2003**, *299*, 1691-1693.

Unfortunately, attempts to increase conversion on laboratory scale reactions while maintaining enantioselectivity encountered numerous setbacks. Increasing reaction concentration or equivalents of base led to higher rates of product decomposition over time (Figure 2-4 A), while lowering the temperature to increase the enantioselectivity resulted in very low conversions. A more troublesome trend was observed upon monitoring the reaction by chiral stationary phase SFC: the product ee *decreased as the reaction progressed* (Figure 2-4 B).

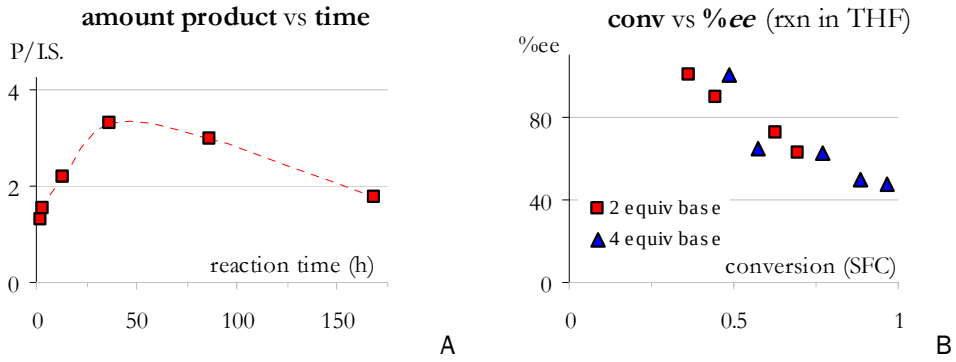


Figure 2-4: Erosion of product (**28f**) yield vs. internal standard (I.S.) over the course of reaction of **27** with 4-bromotoluene [A]. Erosion of enantiomeric excess of product **28f** over the course of reaction [B]. Reactions were run at 25 °C in pure THF with 10 mol% catalyst loading.

There were several possible reasons for the erosion in ee. It was unlikely, but possible, that slow racemization of chiral lithium intermediate (**27-Li**) through deprotonation and reprotonation was leading to the buildup of the slow-reacting enantiomer of **27-Li**, thus favoring reaction with the wrong enantiomer of organolithium. In such a scenario, the cross-coupling reaction would start to resemble a kinetic resolution in which further conversion would lead to successively lower product ee in the reaction mixture.[23] Another possibility for the loss of ee during the course of reaction was that the catalyst was becoming less selective over time. For example, salt or amine byproducts in the reaction could be changing the nature of either the transmetalating species or the catalyst, thereby lowering the selectivity for the desired enantiomer of **27-Li**.[31] Finally, there was also the possibility that the enantiomerically enriched product was somehow racemizing through an unanticipated pathway. Since any of these possibilities, or a combination thereof, could be leading to the drop in ee, we decided to turn our attention to a different substrate that might be more resistant to the erosion of ee during the course of reaction.

*Asymmetric cross-coupling of a benzylmorpholine complex.*

We examined several other benzylamine derivatives as potential alternatives for optimizing the cross-coupling reaction. First we switched to a phthalamide-protected benzylamine complex, but this substrate underwent partial decomposition under our cross-coupling. Going back to the simpler and more stable alkyl-substituted benzylic amines, we also attempted to use tricarbonylchromium-coordinated benzylpyrrolidine **52**, benzylpiperidine **53**, and benzylmorpholine **54** as substrates for cross-coupling. The complex of the five-membered ring amine benzylpyrrolidine (**52**) was inert to coupling conditions. However, both six-membered ring amine complexes **53** and **54** were successful substrates. Test reactions with Mandyphos were undertaken which monitored %ee of product over time.

We ultimately decided upon tricarbonylchromium benzylmorpholine **54**, which was not only a viable substrate for the enantioselective coupling, but seemed to exhibit far less erosion of ee during the course of the reaction. Additionally, the highly crystalline product **55a** could be easily recrystallized to higher enantiomeric purity. To determine whether racemization of the diarylmethylamine **55a** was possible under basic conditions, a sample of **55a** recrystallized to 94.6% ee was heated at 40 °C in THF with 4 equivalents of LiHMDS for 16 h. The reaction was then quenched with $D_2O$ (Scheme 2-6). No detectable deuterium incorporation (by $^1H$ NMR) and negligible (<1%) erosion of ee were observed. This result prompted us to begin an in-depth examination of the effect of various solvents and additives on the enantioselective cross-coupling reaction (Scheme 2-7).

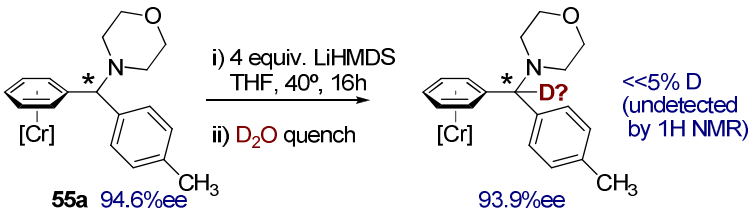


Scheme 2-6: Resistance of tricarbonylchromium diarylmethyl morpholine **55a** to deprotonation and racemization.

*Optimization of Reaction Conditions*

While it seemed that THF as a solvent was a key component of maintaining high reactivity during the course of the cross-coupling reaction, the addition of co-solvents had a noticeable impact on the ee of product **55a** (Table 2-2, entries 1–4). Several co-solvents such as dioxane and cyclopentylmethylether displayed an effect on the rate of reaction and enantioselectivity (Table 2-2, entries 2–4), but the reaction was cleanest and the enantioselectivity increase was most pronounced in the case of toluene co-solvent. Specifically, by varying the fraction of toluene relative to THF, a smooth increase in enantioselectivity (up to 81% ee) was observed at 35–40% by volume (Figure 2-5 A). The decomposition of product over time was also noticeably reduced, although yields remained low (<50% after isolation). Further increasing the percentage toluene negatively affected both enantioselectivity and conversion (Figure 2-5 A). When pure toluene was used as the reaction solvent, no conversion to product was observed. Similar results were observed with other reaction solvents without THF, such as pure glyme or dioxane.

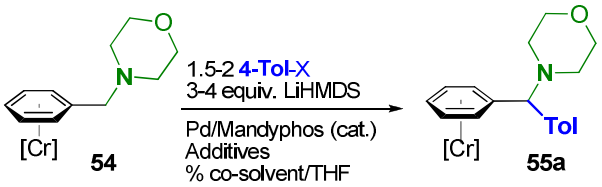


Scheme 2-7: Optimization of reaction conditions for the asymmetric cross-coupling of ($\eta^6$-benzylmorpholine)$Cr(CO)_3$

Table 2-2: Effect of solvent composition and amine in the asymmetric coupling reaction of 4-bromotoluene with $\eta^6$-tricarbonylchromium benzylmorpholine (**54**).

| Entry | X = | Additives (equiv.)* | % co-solvent# | temp (°C) | time (h) | % conv† | % ee |
|---|---|---|---|---|---|---|---|
| 1 | -Br | (none) | 0 | 50 | 9 | 95 | 55 |
| 2 | -Br | (none) | 40 (Diox) | 40 | 9 | 66 | 74 |
| 3 | -Br | (none) | 40 (CPME) | 40 | 9 | 66 | 80 |
| 4 | -Br | (none) | 40 (Tol) | 40 | 9 | 62 | 81 |
| 5 | -Br | H-B (2) | 40 (Tol) | 40 | 9 | 56 | 82 |
| 6 | -Br | TMEDA (1) | 40 (Tol) | 18 | 40 | 38 | 86 |

* H-B = Hüenig's Base (diisopropylethylamine), TMEDA = *N*,*N*,*N*′,*N*′-tetra-methylethylenediamine. # Unless otherwise stated, reactions are run at 0.08–0.1 M [**54**]; co-solvent abbreviations: Tol = Toluene, Diox = 1,4-Dioxane, CPME = cyclopentylmethylether. † % conversion to product determined by chiral HPLC or SFC.

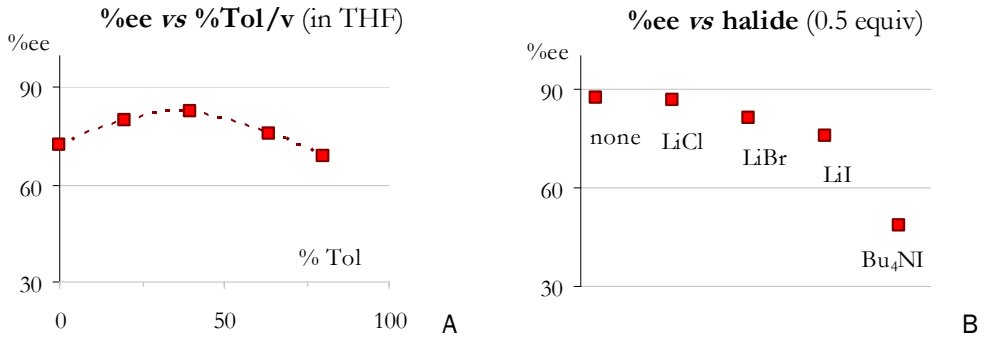


Figure 2-5: Enantiomeric excess dependence on solvent [A], and ee dependence on halide additives [B]. %ee were measured after reactions had reached 30–50% conversion.

Tertiary amines are known to decrease aggregation of organolithiums and enhance reactivity, leading us to examine amine additives in the cross-coupling reaction. Tertiary amines such as Hüenig's Base (*i*Pr$_2$NEt) were hoped to accelerate the reaction, perhaps due to reduced aggregation and/or stabilization of the benzyllithium (Table 2-2, entry 5). The popular bidentate tertiary amine TMEDA (*N*,*N*,*N*′,*N*′-tetramethylethylenediamine) significantly accelerated the reaction (Table 2-2, entry 6), allowing the reaction to be run at lower temperatures, providing an encouraging 86 %ee. Lithium halide additives additives were also examined, as they are known to affect reactions with organolithium species.[32] Unfortunately, as can be seen in Figure 2-5 B (above), addition of halide had a detrimental effect on the enantioselectivity (Cl < Br < I). Other metal salts and palladium precatalysts were also examined, but aside from some notable exceptions[a] the reaction was surprisingly robust to the presence of other salts in the reaction mixture, and improvements in ee were not observed.

At this point, we considered it prudent to re-screen chiral ligands, as well as screen additional members of the Mandyphos and Taniaphos ligand family. Since we had changed the coupling

[a] Tetrabutylammonium iodide ($Bu_4NI$), 15-Crown-5, silver(I) tetrafluoroborate, silver(I) trifluoromethanesulfonate, and Zinc(II) chloride were salt additives with a significant negative (>20% ee) impact on the enantioselectivity of the reaction. $Pd(ACN)_2Cl_2$, $PdCl_2$, and $PdSO_4$ were not viable precatalysts for the reaction.

partner from dimethyl-substituted benzylamine (**27**) to morpholino-substituted benzylamine (**54**), and the two systems did exhibit slightly different behavior (in particular, the apparent lower extent of racemization), we wanted to confirm that there was not a more effective ligand to use. Thus, a smaller-scale HTE screening was employed for the cross-coupling reaction, using **54** and 4-bromotoluene as reaction partners. Again, cyclohexyl Mandyphos was determined to be the most effective ligand in both conversion and selectivity (Figure 2-6, below).

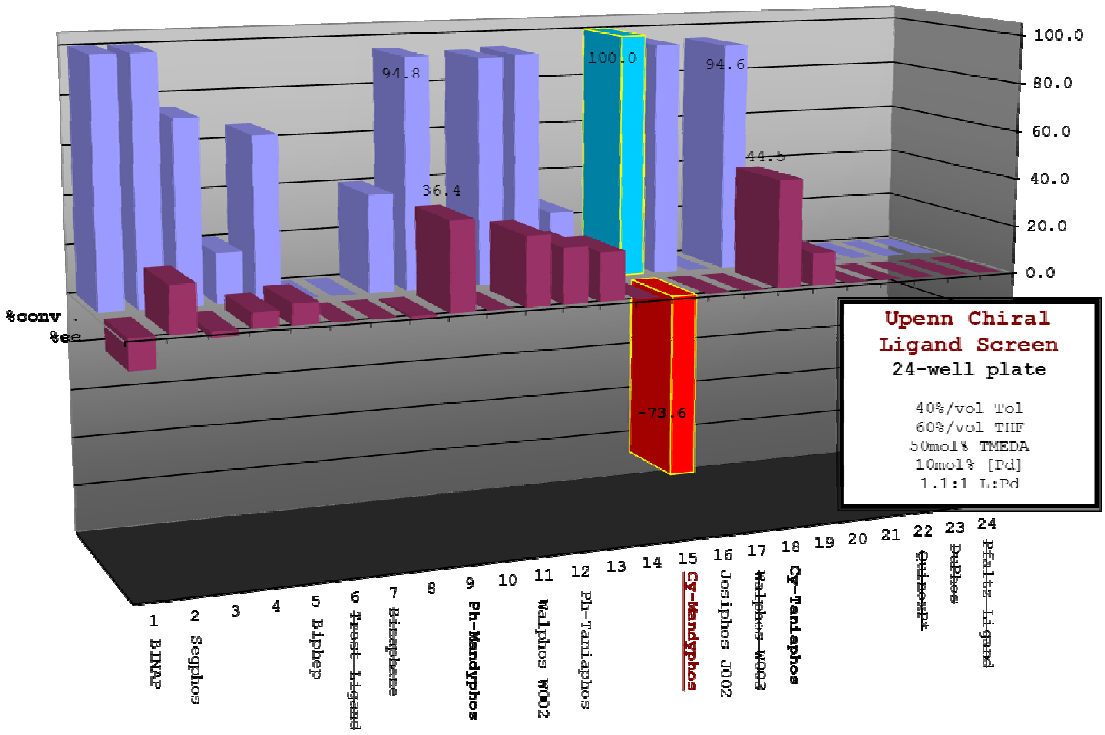


Figure 2-6: HTE of the benzylmorpholine reaction verifies that cyclohexyl-Mandyphos is still the most effective chiral ligand for the cross-coupling process under our conditions.

Additionally, a selection of six different Mandyphos ligands and six different Taniaphos ligands were examined (Figure 2-7). We noted that while the Mandyphos ligands all exhibited high conversion under these conditions, the cyclohexyl Mandyphos ligand (Figure 2-7, entry 2) was the most enantioselective. It seems that electronics (and to a lesser extent, sterics) at the phosphine centers plays a significant role in the high enantioselectivity of the catalyst. Cyclohexyl Mandyphos, while sterically bulky, is considered a more electron-rich and donating phosphorus center than aryl-substituted phosphines (entries 1, 3–6), and performs the best in this coupling

reaction. On the other hand, the electron-donating Mandyphos with methyl and methoxy aryl substitution (entry 4), as well as the electron-neutral phenyl substitutution (entry 1) showed moderate ee (25 and 38%, respectively). Electron-withdrawing Mandyphos with trifluoromethyl substitution (entry 3) performed poorly (<20% ee), as did the more sterically hindered aryl Mandyphos variants with xylyl and *o*-tolyl substitution (entries 5 and 6).

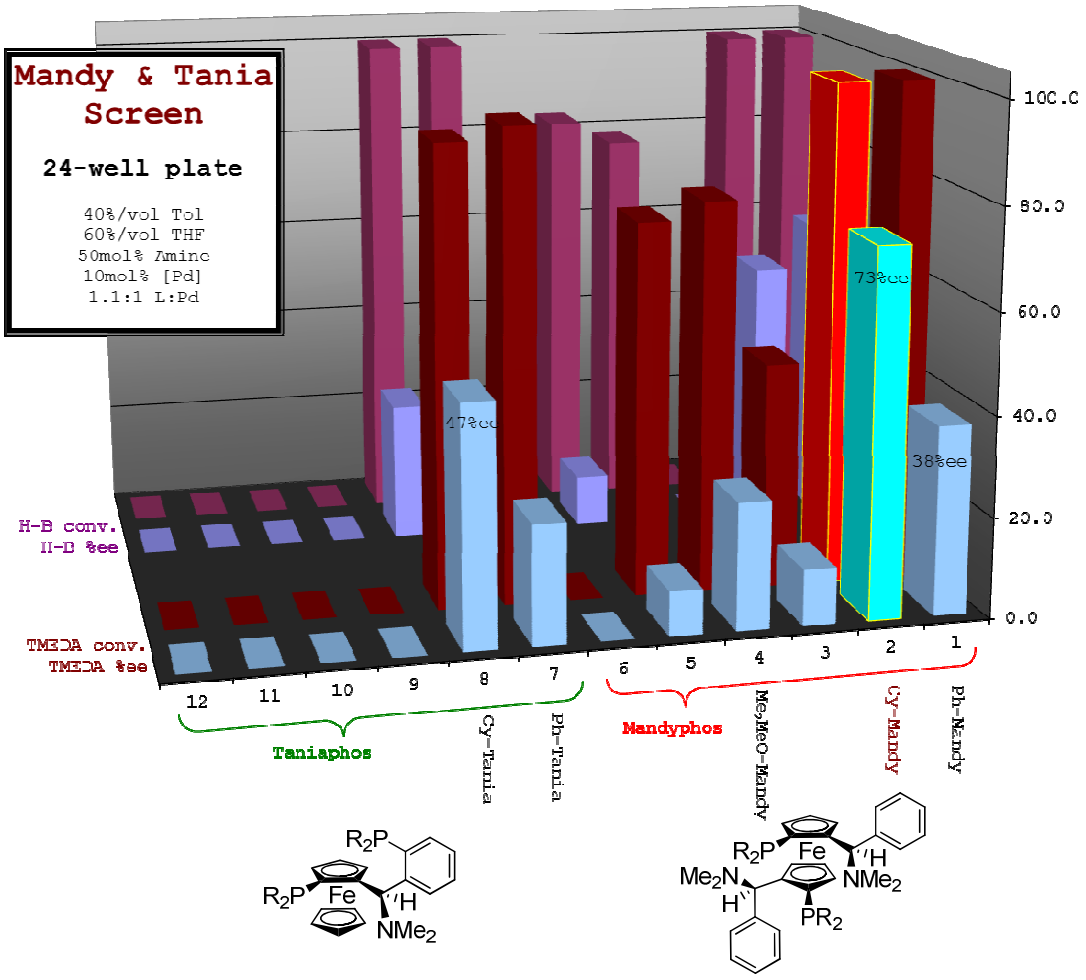


Figure 2-7: HTE screen of additional Mandyphos and Taniaphos ligands. Cyclohexyl Mandyphos and chelating tertiary amine are the most effective combination.

At this point we returned to the optimization of the system. Considering that the lithium halide additves specifically led to decreasing ee, we wondered if the stoichiometric equivalent of LiBr byproduct formed over the course of the cross-coupling reaction was at least partially responsible for the decreasing enantioselectivity observed with increasing conversion in the absence of amine. This may be due to the formation of *n*LiX•**54-Li** intermediates that are less diastereoselective in our proposed enantiodetermining transmetallation (Scheme 2-4, p.84). We have previously demonstrated that the negative impacts of LiCl on enantioselective reactions can be counteracted by sequestering the salt with polydentate amines.[33] Thus, amine additives were re-examined for the additional potential role of LiBr binding (Table 2-3).

Table 2-3: Effect of chelating amine additives and solvent composition in the asymmetric coupling reaction of 4-bromotoluene with $\eta^6$-tricarbonylchromium benzylmorpholine (**54**).

| Entry | X = | Additives (equiv.)# | % co-solvent† | temp (°C) | time (h) | % conv‡ | % ee |
|---|---|---|---|---|---|---|---|
| 1* | -Br | TMEDA (1) | 40 (Tol) | 18 | 40 | 38 | 86 |
| 2 | -Br | TMEDA (2) | 40 (Tol) | 18 | 40 | 41 | 91 |
| 3 | -Br | TEEDA (2) | 40 (Tol) | 18 | 12 | 58 | 75 |
| 4 | -Br | PMDTA (1) | 40 (Tol) | 18 | 48 | 60 | 77 |
| 5 | -Br | PMDTA (2) | 40 (Tol) | 18 | 42 | 35◊ | 90 |

* Entry 1 is re-listed from Table 2-3, entry 5. # TEEDA = *N*,*N*,*N*′,*N*′-tetraethylethylenediamine, TMEDA = *N*,*N*,*N*′,*N*′-tetra-methylethylenediamine, PMDTA = *N*,*N*,*N*′,*N*″,*N*″-pentamethyl-diethylenetriamine. † Unless otherwise stated, reactions are run at 0.08–0.1 M [**54**]. ‡ % conversion to product determined by chiral HPLC or SFC. ◊ isolated yields (%).

By varying equivalents of TMEDA, we found that decreasing the amount of amine or using large excess did not improve our reaction. However, using two equivalents of TMEDA further increased the ee of the reaction to 91% (Table 2-3, entry 2). We also examined an amine used previously in our group to sequester LiCl, *N*,*N*,*N*′,*N*′-tetraethylenediamine (TEEDA, entry 3). While the reaction was much faster (reaching >50% conversion in only 12 hours at room temperature), the ee was lower. Finally, we examined a tridentate ligand that is known for successfully binding LiBr: *N*,*N*,*N*′,*N*″,*N*″-pentamethyldiethylenetriamine (PMDTA, entries 4 and 5). In this case we were disappointed to see the low enantioselectivity using one equivalent of additive (entry 4). However, by increasing the amount of chelating ligand, we found that the optimal amount of this additive (2 equivalents, entry 5) led to 90% ee, though after isolation of the product we observed only 35% yield of **55a**.

*Introduction of aryl triflates in the asymmetric coupling of benzylamines*

In an effort to circumvent the detrimental formation of LiBr altogether, other aryl halide electrophiles were next examined as alternatives to bromotoluene (Table 2-4, entries 1–3). Chloride and tosylate leaving groups (entries 1 and 2) were unsuccessful even after heating. However, we found that the triflate leaving group provided clean reactivity and extremely high conversion at room temperature, with only slightly lower ee than many reactions with aryl bromide. Thus, we were pleased to obtain **55a** (entry 3) in 80% yield and 81% ee after isolation, using 2 equivalents of the triamine PMDTA as additive.

In order to further improve the enantioselectivity of this reaction, the temperature was lowered to 0 °C, but while the ee increased to 87%, the reaction was significantly slower (50% conversion after 24 h, Table 2-4 entry 4). On the other hand, since there was no longer any LiBr formation in this reaction, the amount of PMDTA was decreased to 1 equivalent (entry 5), and we were happy to see a restored reactivity (80% isolated yield), and slightly higher enantioselectivities as well (87% ee, entry 5). Most importantly, the enantioselectivity remained nearly constant over the course of the reaction. Finally, we verified that the amine additive was a necessary component of the reaction, as the extremely low conversions were observed in its absence (entries 7 and 8).

In the final phase of optimization, we found that addition of a small amount (2% by volume) of chlorobenzene resulted in a slight increase of the product ee to 92% (76% isolated yield, entry 9). The optimized conditions for the aryl triflate do not lead to the same improvements in aryl bromide, unfortunately: using the conditions from entry 9 (including chlorobenzene additive) with 4-bromotoluene did not show any significant effect in either yield or enantioselectivity (entry 10). The role of the chlorobenzene is not clear, but the impact of the addition of chlorbenzene or other aryl halide additives to the aryl triflate reaction is currently under investigation.

Table 2-4: Effect of electrophile leaving group in the asymmetric coupling reaction of Tol-X with **54** to yield **55a**.

| Entry | X = | Additives (equiv.)* | % co-solvent# | temp (°C) | time (h) | % conv† | % ee |
|---|---|---|---|---|---|---|---|
| 1 | -Cl | TMEDA (2) | 40 (Tol) | 35 | 24 | (trace) | - |
| 2 | -OTs | PMDTA (1) | 40 (Tol) | 50 | 24 | 0 | - |
| 3 | -OTf | PMDTA (2) | 40 (Tol) | 18 | 7 | 80‡ | 81 |
| 4 | -OTf | PMDTA (2) | 40 (Tol) | 0 | 24 | 50 | 87 |
| 5 | -OTf | PMDTA (1) | 40 (Tol) | 18 | 12 | 80‡ | 87 |
| 6 | -OTf | PMDTA (1) | 40 (Tol) | 5-10 | 48 | 73‡ | 89 |
| 7 | -OTf | (none) | 40 (Tol) | 18 | 12 | 18 | 79 |
| 8 | -OTF | (none) | 0 | 18 | 12 | 23 | 63 |
| 9 | -OTf | PMDTA (1) | 40 (Tol), 2 (PhCl) | 18 | 8 | 76‡ | 92 |
| 10 | -Br | PMDTA (1) | 40 (Tol), 2 (PhCl) | 18 | 48 | 32‡ | 88 |

* TMEDA = *N*,*N*,*N*′,*N*′-tetra-methylethylenediamine, PMDTA = *N*,*N*,*N*′,*N*″,*N*″-pentamethyl-diethylenetriamine. # Unless otherwise stated, reactions are run at 0.08–0.1 M [**1b**]; co-solvent abbreviations: Tol = Toluene, PhCl = chlorobenzene. † % conversion to product determined by chiral HPLC or SFC. ‡ isolated yields (%).

### *Substrate Scope*

Using conditions similar to the optimized conditions described above (Table 2-4, entry 9 for aryl triflates, and Table 2-3, entry 5 for aryl bromides), the scope of the cross-coupling was examined. Electron rich aromatics were good substrates (Table 2-5, entries 1–6), although increased steric congestion at the 2-position (entry 7) was less compatible with these conditions.[a] The cross-coupling was relatively insensitive to the nature of the benzylic amino group: benzylpiperazine complex **56**, benzyl piperazine complex **53**, and even the *N*,*N*-dimethybenzylamine complex **27** (Table 2-5, entries 8–10) which had proved to be problematic during the initial optimization studies underwent cross-coupling with similar enantioselectivities to the morpholino derivative

[a] 2-tolyl triflate did not furnish any coupling product.

**55c**. Vinyl triflate (entry 11) exhibited very high reactivity, but low enantioselectivity (53%). Lowering the temperature did not improve the ee by a significant amount (57% maxiumum ee obtained). This result indicates that the catalyst would need to be reoptimized for vinyl triflate cross-coupling.

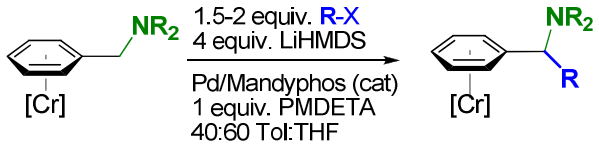


Scheme 2-8: Scope of the asymmetric cross-coupling of tertiary benzylamines to form enantioenriched α- substituted tertiary benzylamines.

Table 2-5: Scope of asymmetric cross-coupling of tertiary benzylamines with aryl triflates, aryl bromides, and vinyl triflate (Scheme 2-8).

| Entry* | –$NR_2$ | Ar–X | product | Temp (°C) | Time (h) | Yield (%) | ee (%) |
|---|---|---|---|---|---|---|---|
| 1 | 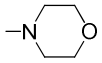 | 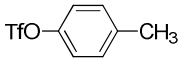 | **55a** | 18 | 8 | 76 | 92 |
| 2# | 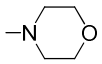 | 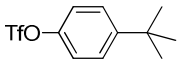 | **55b** | 0→18 | 24 | 74 | 90 |
| 3# | 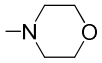 | 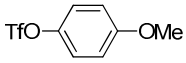 | **55c** | 0→18 | 18 | 72 | 87 |
| 4# | 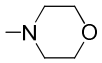 | 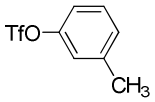 | **55d** | 0→18 | 20 | 72 | 90 |
| 5 | 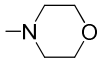 | 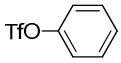 | **55e** | 0→19 | 16 | 80 | 89 |
| 6† | 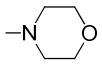 | 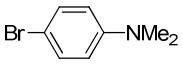 | **55f** | 19 | 60 | 59 | 84 |
| 7† | 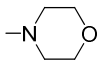 | 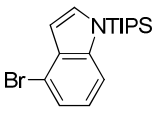 | **55g** | 18 | 48 | 36 | 62 |

| | | | | | | | |
|---|---|---|---|---|---|---|---|
| 8 | –$NMe_2$ | TfO– | **28a** | 0→19 | 24 | 66 | 87 |
| 9† | –N | TfO– | **57** | 8-10 | 60 | 72 | 85 |
| 10 | –N NMe | TfO– | **58** | 0→19 | 24 | 69 | 88 |
| 11 | –N O | TfO– | **59** | 0→18 | 18 | 88 | 53 |

* Reaction conditions: 1 equiv. [Cr] SM (0.08 M [Cr]), 4 equiv. LiHMDS, 1.5–2 equiv. R-X, 4–5 mol % $Pd_2Cl_2(allyl)_2$, 12 mol % cyclohexyl Mandyphos, 40:60 toluene:THF, 2%/vol PhCl, 1 equiv. PMDTA. # isolated yields and %*ee* were averaged over two runs. † PhCl was not used.

Certain aryl triflates, such as 3-pyridyl triflate and electron-poor triflates such as 3-trifluoromethylphenyl triflate were not compatible with these conditions. In fact, in the case of some electron-poor aryl triflates, we were baffled by the lack of even trace amounts of coupling product and the multiple side. Considering that the synthesis of racemic reference samples used electron-deficient aryl bromides in poor but isolable yield (generally 10–30%), and that the aryl triflates were expected to be significantly more reactive than the aryl bromides in this coupling reaction, we considered the possibility of alternative side reactions. Indeed, the stability of the aryl triflate itself proved to be the problem due to the formation of highly reactive aryne. Reacting a THF solution of 3-trifluoromethylphenyl triflate with the benzyne trap tetraphenyl cyclopentadienone at room temperature led to the isolation of the naphthalene product **60** (Scheme 2-9).

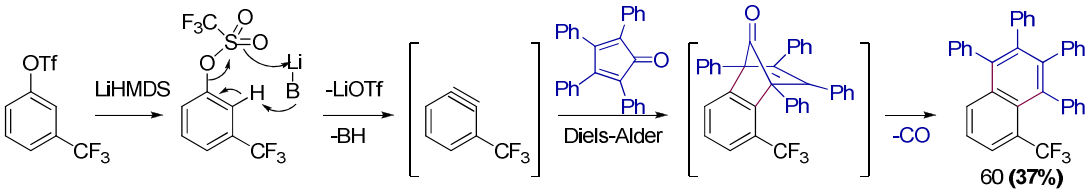


Scheme 2-9: Incompatibility of some electron-withdrawing aryl triflates was attributed to the formation of aryne in solution. This was verified by trapping the aryne with a cyclopentadienone to yield substituted naphthalene.

As an illustration of the synthetic utility of our method for the synthesis of enantioenriched diarylmethylamines, the purified enantioenriched chromium-coordinated diarylmethylamines was decomplexed without loss of ee by exposing a solution of the complex to light and air and filtering the suspension. Alternately, the crude reaction product (Scheme 2-10, **55c**) could also be demetallated by exposure to light and air and then purified by chromatography to give **61** in 63% yield and 85% ee (Scheme 2-10).

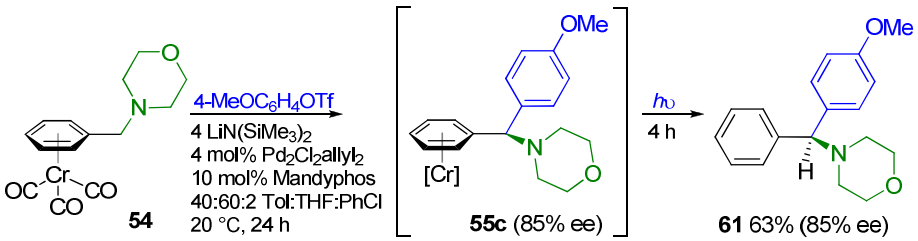


Scheme 2-10: Direct decomplexation of the reaction mixture in sunlight access to enantioenriched diarylmethylamines without loss of ee.

Finally, the absolute configuration of (−)-**55a** using the (+)-enantiomer of cyclohexyl Mandyphos (solution was recrystallized to >96% ee before crystallization for structural determination) was obtained via single-crystal X-ray crystallography, and determined to be (*R*) (Figure 2-8).

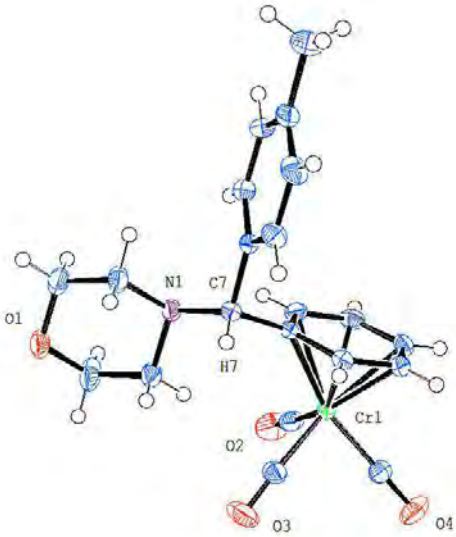


Figure 2-8: X-ray crystal structure of (*R*)-(−)-**55a**. Thermal ellipsoid are at 50% probability. Full details can be found on p. 290.

## *Summary and Conclusions*

In conclusion, we have developed a strategy for enantioselective functionalization of benzylic $sp^3$ carbons α– to tertiary amines to access core structures present in numerous biologically important diarylmethyl amines. Low-barrier high-throughput experimentation on a 2 μmol scale facilitated rapid identification of the ferrocene amine phosphine ligand cyclohexyl Mandyphos as the most effective ligand. Diastereoelective transmetallation of one enantiomer of a rapidly equilibrating tricarbonylchromium-coordinated benzyllithium species is the key step in this asymmetric cross-coupling with various $sp^2$–hybridized organic triflates and bromides. It is likely that the tertiary amine in the active Mandyphos catalyst is crucial in the enantiodetermining transmetallation reactions by coordination to the main group organometallic reagent. Further work is being aimed at expanding this unique asymmetric cross-coupling reaction to other benzylic arene systems, such as for chiral triarylmethane synthesis.

Additionally, work is being done to take the highly enantioenrichced chromium-coordinated products from these reactions and employing them as precursors to a family of modular diarylmethylamine P∧N ligands employing both planar and central chirality. This work is addressed in Chapter 3.[34]

## Experimental Section

### General Methods

Reactions were performed under nitrogen using oven-dried glassware. Air- and moisture- sensitive solutions were handled under nitrogen and transferred via syringe. Dry THF was freshly distilled from Na/benzophenone ketyl. Toluene was drawn from a Grubbs column. 1,4-Dioxane was commercially available anhydrous stabilized Acro Seal quality. Unless otherwise stated, reagents were commercially available and used as purchased without further purification. Chemicals were obtained from Sigma-Aldrich, Acros, or Strem, and used as received; solvents were purchased from Fisher Scientific. Reactions were monitored by thin-layer chromatography using Whatman Partisil® K6F 250 μm precoated 60 Å silica gel plates and visualized by short-wave ultra-violet light as well as by treatment with potassium permanganate ($KMnO_4$) or ceric ammonium molybdate (CAM) stain. NMR spectra were recorded in $CDCl_3$ on either a Bruker 300 MHz or 500 MHz Fourier-transform spectrometer. Chemical shifts are reported in ppm referenced to tetramethylsilane (TMS) or the $CHCl_3$ solvent residual peak at 7.26 ppm for $^1H$ and 77.23 ppm for $^{13}C\{^1H\}$; $^{19}F$ peaks were referenced to an external standard of trifluoroacetic acid in $CDCl_3$ at −76.55 ppm. Infrared spectra were obtained on NaCl plates using a Perkin-Elmer Spectrum 100 Series FTIR spectrometer. Optical rotations were recorded in HPLC-grade $CHCl_3$ using a JASCO DIP-370 digital polarimeter and values were averaged over a minimum of 3 runs. Chromium-complexed masses were recorded with Electrospray + (ES+) HRMS methods to within 5 ppm, and $[M]^+$, $[MH]^+$, $[M - (CO)_3]^+$, or $[M - C_4H_8NO]^+$ was confirmed by the presence of the characteristic chromium isotope pattern. Non-chromium-complexed mass was recorded with Chemical Ionization + (CI+) HRMS methods to within 5 ppm, and $[M]^+$ was observed. Where necessary, microanalysis for C, H, N composition was obtained and accurate to within 0.5%.

Compounds **27**, **53**, **54**, and **56** were prepared according to general literature procedure for the synthesis of arene tricarbonylchromium complexes from $Cr(CO)_6$ and parent arene.[35,36] Aryl trifluromethanesulfonates were prepared in good to excellent yield from the corresponding phenol according to the general literature procedure.[37,38]

**Caution:** Care should be taken to avoid direct light exposure of reactions, as arene tricarbonylchromium complexes can decompose in solution under bright light and air. In crystalline solid form, complexes are reasonably stable to light and can be stored at room temperature in air.

General procedure 2-A for the synthesis of benzylamine tricarbonylchromium complexes

Complexes were prepared according to general literature procedure for the synthesis of arene tricarbonylchromium complexes from $Cr(CO)_6$ and parent arene[35,36] and were crystallized from dichloromethane and hexanes at -20 ºC or purified by flash column chromatography eluting in methylene chloride or diethyl ether in hexanes to afford yellow crystalline solids. The following procedure is representative.

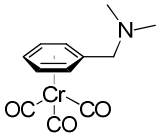

**27 – $Me_2NCH_2(\eta^6\text{-}C_6H_5)Cr(CO)_3$**: An oven-dried 50 mL round-bottom flask was charged with $Cr(CO)_6$ (1.54 g, 0.70 mmol, 1.0 equiv), fitted with a straight reflux condenser, and flushed with dry nitrogen for 30 minutes. *N,N*-Dimethylbenzylamine (2.1 mL, 14 mmol, 2.0 equiv), dry THF (1 mL), and dry 1,4-dioxane (2.5 mL) were added by syringe through the reflux condenser, and the mixture was refluxed in a 115 – 120 ºC oil bath for 2 days. The yellow-orange solution was allowed to cool, and completion of the reaction was verified by the absence of solid $Cr(CO)_6$ on the sides of the flask (from sublimation) after refluxing subsided. The reaction was opened to air, diluted with methylene chloride (5 mL) and filtered over a pad of Celite and $MgSO_4$. The clear yellow solution was concentrated under vacuo, layered with hexanes, and crystallized at -20º. After filtration, rinsing with cold hexanes and collecting a second crop of crystals, **27** (1.57 g, 5.8 mmol, 83% yield) was obtained as a bright yellow crystalline solid. *Spectral data is consistent with existing characterization*.[39]

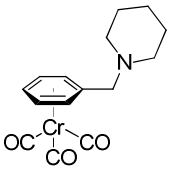

**1c**

**53 – $N\text{-}(C_5H_{10}N)CH_2(\eta^6\text{-}C_6H_5)Cr(CO)_3$**: Using General procedure 2-A, $Cr(CO)_6$ (0.44 g, 2.0 mmol, 1.0 equiv) was reacted with *N*-benzyl piperidine (0.52g, 3.0 mmol, 1.5 equiv) in 2.3 mL dioxane and 0.7 mL THF at 100-110 ºC for 5 days. Crystallization at -20 ºC yielded **53** (0.46 g, 1.5 mmol, 74% yield) as a bright yellow solid. **$^1$H NMR** (300 MHz, CDCl3) δ: 5.42 - 5.29 (m, 4H), 5.25 - 5.21 (m, 1H), 3.18 (s, 2H), 2.45 - 2.42 (m, 4H), 1.64 - 1.51 (m, 4H), 1.49 - 1.39 (m, 2H) ppm; **$^{13}C\{^1H\}$ NMR** ($CDCl_3$) δ: 233.2, 109.0, 94.2, 93.3, 91.5, 62.7, 54.7, 26.1, 24.3 ppm; **IR**: 3087, 2937, 2853, 2800, 2686, 1966 and 1878 (strong CO stretches), 1455, 1343, 1153, 1110, 995, 861, 662, 630, 533 $cm^{-1}$. **HRMS** (ES+) calc'd for $C_{15}H_{18}CrNO_3$ 312.0692, found 312.0687 $[MH]^+$.

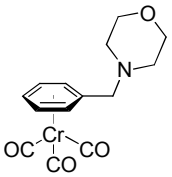

**54 – $N\text{-}(C_4H_8NO)CH_2(\eta^6\text{-}C_6H_5)Cr(CO)_3$**: Using General procedure 2-A, $Cr(CO)_6$ (0.44 g, 2.0 mmol, 1.0 equiv) was reacted with *N*-benzyl morpholine (0.5 mL, 3 mmol, 1.5 equiv) in 1.5 mL dioxane and 0.8 mL THF at 120 ºC for 2 days. Crystallization at -20 ºC yielded **54** (0.59 g, 1.9 mmol, 94 % yield after 2nd

crop) as a bright yellow crystalline solid. **$^1$H NMR** (300 MHz, $CDCl_3$) δ: 5.41 - 5.34 (m, 4H), 5.27 - 5.23 (m, 1H), 3.72 - 3.69 (m, 4H), 3.24 (s, 2H), 2.53 - 2.50 (m, 4H) ppm; **$^{13}$C{$^1$H} NMR** (75 MHz, $CDCl_3$) δ: 233.0, 107.7, 94.0, 93.2, 91.6, 67.1, 62.2, 53.7 ppm; **IR** 3066, 2971, 2867, 2817, 1961 and 1877 (strong CO stretches), 1458, 1285, 1115, 1007, 865, 662, 630, 531 $cm^{-1}$. **HRMS** (ES+) calc'd for $C_{14}H_{16}CrNO_4$ 314.0484, found 314.0497 $[MH]^+$.

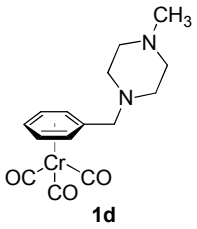

**1d**

**56 – *N*-($C_5H_{10}N$)$CH_2$($\eta^6$-$C_6H_5$)$Cr(CO)_3$**: Using General procedure 2-A, $Cr(CO)_6$ (0.44 g, 2.1 mmol, 1.0 equiv) was reacted with *N,N*-benzyl methylpiperazine (0.59 mL, 3.0 mmol, 1.5 equiv) in 1.5 mL dioxane and 0.5 mL THF at 105-115 ºC for 4 days. Crystallization at -18 ºC yielded **1d** (0.64 g, 1.9 mmol, 93% yield) as a yellow powdery solid. **$^1$H NMR** (300 MHz, CDCl3) δ: 5.39 - 5.33 (m, 4H), 5.26 - 5.21 (m, 1H), 3.24 (s, 2H), 2.6 - 2.4 (br m, 8H), 2.28 (s, 3H) ppm; **$^{13}$C{$^1$H} NMR** (75 MHz, $CDCl_3$) δ: 233.0, 108.1, 94.1, 93.3, 91.6, 61.8, 55.1, 53.1, 46.2 ppm; **IR**: (strong CO stretches), $cm^{-1}$. **HRMS** (ES+) calc'd for $C_{15}H_{19}CrN_2O_3$ 327.0795, found 327.0799 $[MH]^+$.

## General procedure 2-B for racemate synthesis

The following procedure is representative of the synthesis of racemic product standards used for HPLC and SFC analysis of asymmetric reactions and reaction screens:

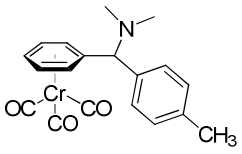

**28f – $Me_2NCH$(4-$C_6H_4$-$CH_3$)($\eta^6$-$C_6H_5$)$Cr(CO)_3$:** Racemic **28f** was prepared as a chromatography reference following the literature procedure for related compounds:[40] An oven-dried glass reaction tube was charged with a small magnetic stirbar and **27** (52 mg, 0.19 mmol, 1.0 equiv), sealed with a septum, and purged with nitrogen. $PdCl_2(PPh_3)_2$ (7 mg, 0.01 mmol, 5 mol %) and LiHMDS (68 mg, 0.4 mmol, 2 equiv) were dissolved in dry THF (1.5 mL) under a nitrogen atmosphere, forming an orange solution, to which neat 4-bromotoluene (38 µl, 0.3 mmol, 1.5 equiv) was added. The catalyst, base, and aryl bromide solution was taken up by syringe and added to **27**, which turned red-orange. The reaction mixture was heated with stirring for 20 h at 43 ºC, then allowed to cool. The orange solution was quenched with two drops of aqueous 2N HCl and allowed to stir for 5 min. The solution was opened to air and diluted with 4 mL diethyl ether, then filtered over a pad of $MgSO_4$ and silica. The pad was rinsed with an additional 1 mL diethyl ether and the solution was concentrated *in vacuo*, loaded directly onto a short silica gel column, and eluted with 50% diethyl ether in hexane. Racemic **28f** (53.8 mg, 0.15 mmol, 78% yield) was obtained as a yellow-orange solid. **$^1$H NMR** (300 MHz, $CDCl_3$) δ: 7.15 (appar. s, 4H), 5.91 (dt, J = 6.2, 1.0 Hz, 1H), 5.35 - 5.26 (m, 2H) 5.24 (d, J = 6.7 Hz,

2H), 5.16 (dd, J = 5.7, 1.3 Hz, 1H), 4.17 (s, 1H), 2.34 (s, 3H), 2.23 (s, 6H) ppm; **$^{13}C\{^1H\}$ NMR** (125 MHz, $CDCl_3$) δ: 233.1, 137.8, 136.8, 129.3, 129.1, 114.5, 94.7, 94.3, 93.3, 91.3, 91.0, 72.9, 44.2, 21.3 ppm. **IR:** 2924, 2867 2825, 2780, 1963 and 1876 (strong CO stretches), 1610, 1454, 1412, 1150, 116, 802, 662, 631, 531 $cm^{-1}$.

## *General considerations for low-barrier high-throughput experimentation (HTE) procedures*

Experimental design was aided by Symyx Library Studio software. Reactions were set up in a dry nitrogen atmosphere glovebox under constant purge of $N_2$. Microscale reactions were run in glass vials placed in a 96-well aluminum block and sealed using a Teflon lining and silicone rubber gaskets compressed by an aluminum top attached by screws. Liquids and solutions were dosed using microlitre Eppendorf pipettes and multi-channel pipettors. When evaporation of solvent was necessary, a Genevac vacuum centrifuge within the glovebox was used. Anhydrous solvents were used as purchased from Aldrich (sure-seal quality).[41]

### General procedure 2-C for screening conditions using HTE methods

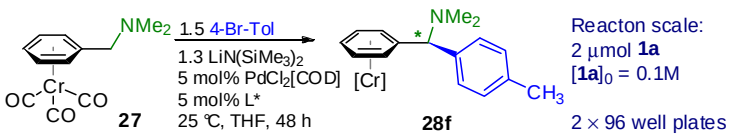


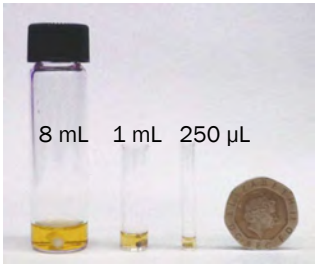


Scheme 2-11: General scheme for HTE screening to identify promising ligands for the asymmetric cross-coupling of **27** with 4-bromotoluene to yield enantioenriched diarylmethylamine **28f**. 2 µmol-scale (0.5 mg) reactions were run in parallel in 250 µL reaction vials, shown next to 1 mL and 8 mL vials for comparison.

**28f – (4-$C_6H_4$-$CH_3$)-*N*-($N(CH_3)_2$)CH($\eta^6$-$C_6H_5$)$Cr(CO)_3$:** Two 96-well aluminum blocks containing 96- 250 µL glass vials predosed with enantioenriched mono- and bidentate ligands[a] (either 0.2 µmol for monodentate or 0.1 µmol for bidentate ligands) were dosed with 38 µL of dichloro(1,5-cyclooctadiene)palladium(II) precatalyst [$PdCl_2$(COD)] in THF (0.003 M, 0.1 µmol, 5 mol%) and evaporated to dryness using a Genevac vacuum centrifuge. Small perylene magnetic stirbars were added to the reaction vials, and then 20 µL of a THF solution of *N*,*N*-dimethylbenzylamine tricarbonylchromium (**27**) (0.1 M, 2 µmol, 1.0 equiv), LiHMDS (0.13 M, 26 µmol, 1.3 equiv), and 4-bromotoluene (0.15 M, 3 µmol, 1.5 equiv) was added to each vial *via* multi-channel pipette. The 96-well plates were sealed and agitated at ~960 rpm for 48 h at room temperature.

**Work-up:** At 48 h the plates were opened to air and immediately quenched with 100 µL of a 0.5 M $H_3PO_4$ solution added via multi-channel pipet (to neutralize the excess LiHMDS), followed by 300 µL acetonitrile (containing 1 µmol 4,4'-di-*tert*-butylbiphenyl internal standard) and 100 µL DMSO (to ensure complete solubilization of the reaction mixture). The plates were then covered and stirred for 15–20 minutes for complete extraction of the product as well as to ensure good homogenization. 20 µL portions of the reaction mixture were then transferred by multi-channel pipet into 96-well HPLC blocks pre-filled with 750 µL acetonitrile. The blocks were then mounted directly on HPLC instruments for analysis using Agilent 1200 Series HPLC instruments with reverse phase C-18 columns and acetonitrile/water (buffered with 0.1% $H_3PO_4$) as mobile phase. Data processing was done on Agilent ChemStation software using the biphenyl as internal standard. Reactions that showed conversion of starting material to product (**28f**) were then run on an Agilent SFC instrument in 4% methanol (containing 25 mM isobutylamine additive) in $CO_2$ at 3 mL/min using a Chiralpak OJ-H column for %*ee* determination.

Five ferrocenyl ligands provided conversion to desired product **28f** as well as enantioselectivity. Cyclohexyl Taniaphos showed the highest reactivity and moderate enantioselectivity. Cyclohexyl Mandyphos (SL-M002) showed the greatest selectivity, though conversion to product was low.

[a] For a complete list of chiral ligands screened with these methods, see p. 331

## *Procedure for detailed study of asymmetric reaction using HTE methods*

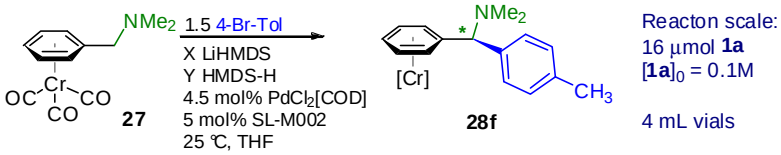


Scheme 2-12: General scheme for the detailed analysis of asymmetric reaction over time. Internal standard biphenyl was added during the work-up step.

Reactions were scaled to 16 µmol (8 × microscale size) in 4 mL glass screw-capped vials predosed with Mandyphos ligand and palladium precatalyst: THF solutions of chiral ligand Cyclohexyl Mandyphos (SL-M002) and $PdCl_2$[COD] were sequentially added to vials and evaporated by Genevac. Small PTFE-coated stirbars were then added to the vials. A solution of **28f** (1 equiv.), 4-bromotoluene (1.5 equiv.), and varying amounts of LiHMDS and HMDS-H at 0.1 or 0.5 M [Cr] was added, and vials were sealed and stirred at room temperature within the glovebox. 20 µL aliquots were periodically removed from the vials (at 2, 3.5, 13, 37, 86, and 168 hour intervals), and work-up and chromatographic analysis for these aliquots proceeded according to the work-up specified in General procedure 2-C.

## *General procedures and characterizations for benzylic coupling reactions*

The following procedures are representative. Unless otherwise specified, chromatography was run in a mixture of diethyl ether in hexanes, or a combination of hexanes, methylene chloride, and diethyl ether.

### General procedure 2-D for optimization of reaction conditions

Procedure for asymmetric cross-coupling of tricarbonylchromium benzylmorpholine (**54**) with *p*-tolyl halides to generate enantioenriched tertiary diarylmethylamine (**55a**).

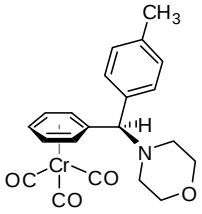


**55a** – **(*R*)-(−)-(4-$C_6H_4$-$CH_3$)-*N*-($C_4H_8NO$)CH($\eta^6$-$C_6H_5$)Cr(CO)$_3$:** An oven-dried reaction tube was charged with a small magnetic stirbar and $\eta^6$-benzylmorpholine tricarbonylchromium (**54**) (0.02 – 0.1 mmol scale, 1.0 equiv), and solid additives (0.5 – 2 equiv) sealed with a septum, and purged

with dry nitrogen. Dry toluene and liquid additives were added via syringe. A separate oven-dried vial was charged with palladium precatalyst (5 – 10 mol% Pd), cyclohexyl Mandyphos (1.5:1 L*:Pd ratio), and LiHMDS (3 – 4 equiv) under nitrogen and sealed with a septum cap. The precatalyst, ligand, and base were dissolved in dry THF. Then, 4-bromotoluene, 4-tolyl triflate, 4-chlorotoluene, or 4-tolyl tosylate (1.5 - 2 equiv) and liquid additives were added via syringe. The catalyst, base, and aryl halide solution was taken up with a syringe and added to the stirring solution of **54** and additives in toluene. The reaction was stirred at the specified temperature (between 0 °C and 55 °C) for 7 – 48 h. The solution was then quenched with 2 drops $H_2O$, opened to air, diluted with 3 mL diethyl ether, and filtered over a pad of $MgSO_4$ and silica gel. The pad was rinsed with additional diethyl ether, and the solution was analyzed via SFC (10% MeOH/$CO_2$, 4 mL/min, IA column) for conversion and enantiomeric excess. Where isolated yields were obtained, the filtrate was concentrated *in vacuo*, loaded directly onto a silica gel column, and eluted with 20 - 30% diethyl ether in pentane. The result was **55a** as a yellow solid. **$^1$H NMR** (300 MHz, $CDCl_3$) δ: 7.15 (apparent s, 4H), 5.92 - 5.90 (m, 1H), 5.35 - 5.29 (m, 2H), 5.26 (d, *J* = 6.6 Hz, 1H), 5.16 - 5.12 (m, 1H), 4.21 (s, 1H), 3.71 - 3.68 (m, 4H), 2.57 - 2.40 (m, 4H), 2.34 (s, 3H) ppm; **$^{13}$C{$^1$H} NMR** (75 MHz, $CDCl_3$) δ: 232.9, 138.1, 136.5, 129.4, 129.1, 113.1, 94.7, 94.5, 93.7, 91.1, 90.5, 72.5, 67.4, 52.5, 21.3 ppm, **IR**: 2958, 2924, 2853, 2817, 1964 and 1877 (strong CO stretch), 1455, 1116, 1006, 875, 662, 633 $cm^{-1}$. **$[\alpha]_D^{26}$** = −26.1° (c = 0.38, $CHCl_3$) for an 89 %*ee* sample. **Analysis** calc'd for $C_{21}H_{21}CrNO_4$: C 62.53 H 5.25 N 3.47, found C 62.25 H 5.38 N 3.37. *X-ray crystal structure was determined for this compound, see p. 290.*

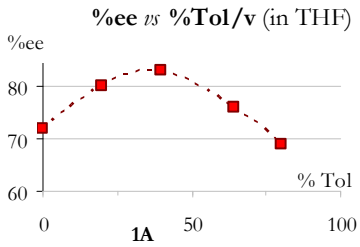


Figure 2-9: Enantiomeric excess variation on solvent composition.

Reactions were run with the benzylmorpholine complex **54**, 1.5 equiv. 4-bromotoluene and 3 equiv. LiHMDS at approx. 0.1 M [Cr], varying toluene composition from 0–80% by volume. Maximum enantioselectivity is observed at approximately 35–40%. When the fraction of toluene is increased past 40%, a steady decrease in enantioselectivity and conversion is observed. Conversion to product was not observed for pure toluene in the absence of THF.

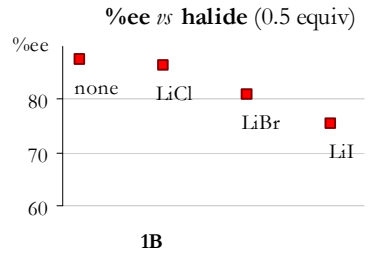


Figure 2-10: Effect of halide salts on enantiomeric excess.

Reactions were run with the benzylmorpholine complex **54**, 1.5 equiv. 4-bromotoluene, 3 equiv. LiHMDS, and 0.5 equiv. anhydrous halide source at approx. 0.1 M [**54**]. %ee were measured after reactions had reached 30–50% conversion (approx. 10h).

### General procedure 2-E for asymmetric reaction of benzylamine complexes with aryl triflates

Procedure for cross-coupling of tricarbonylchromium benzylamines (**27**, **53**, **54**, **56**) with aryl triflates to generate enantioenriched tertiary diarylmethylamines or α-vinyl benzylamine.

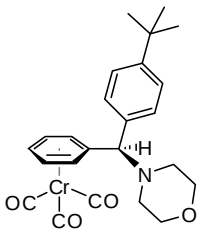


**55b – (−)-(4-$C_6H_4$-*t*-Bu)-*N*-($C_4H_8NO$)CH($\eta^6$-$C_6H_5$)Cr(CO)$_3$:** An oven-dried reaction tube was charged with a small magnetic stirbar and $\eta^6$-tricarbonylchromium benzylmorpholine (**54**) (25 mg, 0.080 mmol, 1.0 equiv), sealed with a septum, and purged with dry nitrogen. Dry toluene (0.4 mL) and PMDTA (17 µl, 0.080 mmol, 1.0 equiv) were added via syringe. A separate oven-dried vial was charged with $[(allyl)PdCl]_2$ (1.2 mg, 0.0032 mmol, 8 mol% Pd), cyclohexyl Mandyphos (8 mg, 0.009 mmol, 12 mol%), and LiHMDS (54 mg, 0.32 mmol, 4.0 equiv) under nitrogen and sealed with a septum cap. The precatalyst, ligand, and base were dissolved in dry THF (0.6 mL), and 4-*tert*-butylphenyl triflate (27 µl, 0.12 mmol, 1.5 equiv) and chlorobenzene (~20 µl, 2%/vol) were added next via syringe. The catalyst, base, and aryl halide solution was taken up with a syringe and added to the stirring mixture of **54**, triamine, and toluene. The reaction was immediately moved to an ice bath and allowed to warm to room temperature (18 °C) with stirring for 16 hours. The brownish orange solution was quenched with 2 drops $H_2O$, opened to air, diluted with 3 mL diethyl ether, and filtered over a pad of $MgSO_4$ and silica gel. The pad was rinsed with additional diethyl ether and the solution was concentrated *in vacuo*. The crude mixture was then loaded directly onto a silica gel column and eluted with 20 - 25% diethyl ether in pentane. The result was **55b** (31.2 mg, 0.070 mmol, 88 % yield, 91 %*ee*) as a yellow solid. **$^1$H NMR** (500 MHz, $CDCl_3$) δ: 7.35 (d, *J* = 8.4 Hz, 2H), 7.19 (d, *J* = 8.3 Hz, 2H), 5.90 (d, *J* = 6.4 Hz, 1H), 5.35 - 5.31 (m,

2H), 5.28 (dt, *J* = 1.1, 6.3 Hz, 1H), 5.13 (ddd, *J* = 1.2, 6.0, 6.8 Hz, 1H), 4.18 (s, 1H), 3.73 - 3.66 (m, 4H), 2.46 - 2.42 (br s), 2.53 - 2.49 (m, 2H), 1.30 (s, 9H) ppm; **$^{13}C\{^1H\}$ NMR** (125 MHz, $CDCl_3$) δ: 232.9, 151.3, 136.5, 128.7, 125.6, 113.1, 95.2, 94.8, 93.9, 90.8, 90.1, 72.5, 67.4, 52.5, 34.8, 31.5 ppm; **IR:** 2958, 2924, 2853, 2817, 1964 and 1877 (strong CO stretch), 1455, 1116, 1006, 875, 662, 633 $cm^{-1}$; **$[\alpha]_D^{23}$** = −13.6° (c = 0.50, $CHCl_3$).

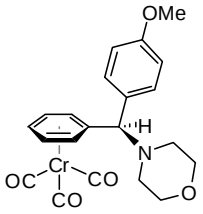


**55c – (−)-(4-$C_6H_4$-OMe)-*N*-($C_4H_8NO$)CH(*η*$^6$-$C_6H_5$)Cr(CO)$_3$:** Using General procedure 2-E, **54** (25 mg, 0.080 mmol, 1.0 equiv) and PMDTA (17 µl, 0.08 mmol, 1 equiv) in 0.4 mL toluene was combined with a solution of LiHMDS (54 mg, 0.32 mmol, 4 equiv), 4-methoxyphenyl triflate (22 µl, 0.12 mmol, 1.5 equiv), $[(allyl)PdCl]_2$ (1.2 mg, 0.0032 mmol, 8 mol% Pd), and cyclohexyl Mandyphos (7 mg, 0.009 mmol, 10 mol%) in 0.6 mL THF with 20 µl chlorobenzene additive. The reaction was stirred for 10 h at room temperature (18 °C). Compound **55c** (25.2 mg, 0.060 mmol, 75% yield, 86 %*ee*) was obtained as a yellow crystalline solid after silica gel chromatography eluting with 1:1 methylene chloride:hexanes and then 33% - 50% diethyl ether in hexanes. **$^1H$ NMR** (300 MHz, $CDCl_3$) δ: 7.19 (d, *J* = 8.7 Hz, 2H), 6.88 (d, *J* = 8.7 Hz, 2H), 5.89 (d, *J* = 5.8 Hz, 1H), 5.35 - 5.25 (m, 3H), 5.17 - 5.12 (m, 1H), 4.19 (s, 1H), 3.80 (s, 3H), 3.71 - 3.68 (m, 4H), 2.54 - 2.49 (m, 2H), 2.46 - 2.39 (m, 2H) ppm; **$^{13}C\{^1H\}$ NMR** (75 MHz, $CDCl_3$) δ: 232.9, 159.6, 131.7, 130.2, 114.1, 113.3, 94.8, 94.6, 93.7, 91.0, 90.7, 72.2, 67.4, 55.5, 52.5 ppm; **IR:** 2957, 2918, 2852, 2815, 1962 and 1876 (strong CO stretch), 1609, 1510, 1454, 1252, 1176, 1116, 1032, 875, 662, 632 $cm^{-1}$; **Analysis** calc'd for $C_{21}H_{21}CrNO_5$: C 60.14 H 5.05 N 3.34, found C 59.90 H 5.13 N 3.24; **$[\alpha]_D^{23}$** = −45.2° (c = 0.70, $CHCl_3$).

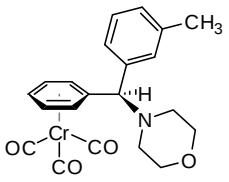


**55d – (−)-(3-$C_6H_4$-$CH_3$)-*N*-($C_4H_8NO$)CH(*η*$^6$-$C_6H_5$)Cr(CO)$_3$:** Using General procedure 2-E, **54** (25 mg, 0.080 mmol, 1.0 equiv) and PMDTA (17 µl, 0.08 mmol, 1 equiv) in 0.4 mL toluene was combined with a solution of LiHMDS (50 mg, 0.30 mmol, 4 equiv), 3-tolyl triflate (30 µl, 0.16 mmol, 2 equiv), $[(allyl)PdCl]_2$ (1.2 mg, 0.0032 mmol, 8 mol% Pd), and cyclohexyl Mandyphos (7 mg, 0.008 mmol, 10 mol%) in 0.6 mL THF with 20 µl chlorobenzene additive. The reaction was stirred for 20 h warming from a 0 °C ice bath to room temperature (19 °C). Compound **55d** (20 mg, 0.050 mmol, 62% yield, 91 %*ee*) was obtained as an orange oil after silica gel chromatography eluting with 1:1:5 methylene chloride:diethyl ether:hexanes, then 1:3 diethyl ether:hexanes. **$^1H$ NMR** (500 MHz, $CDCl_3$) δ: 7.40 (t, *J* = 8.4 Hz, 1H), 7.09 - 7.05 (m, 3H), 5.87 (d, *J* = 6.3 Hz, 1H), 5.32 (t, *J* = 6.1 Hz, 1H), 5.29 - 5.26 (m, 2H), 5.11 (t, *J* = 6.2 Hz, 1H), 4.14 (s, 1H), 3.69 - 3.65 (m, 4H), 2.52 - 2.48 (br s, 2H), 2.45 - 2.42 (m, 2H), 2.32 (s, 3H) ppm; **$^{13}C\{^1H\}$ NMR** (125 MHz, $CDCl_3$) δ: 232.8, 139.6, 138.5, 129.9, 129.0, 128.6, 126.0, 112.9, 95.1, 94.8, 94.0, 90.8, 90.2,

67.3, 52.6, 21.7 ppm; **IR:** 2968, 2918, 2854, 2814, 1964 and 1880 (strong CO stretch), 1453, 1116, 1007, 872, 661, 629 $cm^{-1}$; $[\alpha]_D^{26}$ = −13.5° (c = 1.0, $CHCl_3$).

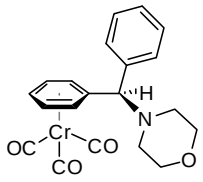

**55e – (−)-($C_6H_5$)-*N*-($C_4H_8NO$)CH($\eta^6$-$C_6H_5$)Cr(CO)$_3$:** Using General procedure 2-E, **54** (25 mg, 0.080 mmol, 1.0 equiv) and PMDTA (17 µl, 0.08 mmol, 1 equiv) in 0.4 mL toluene was combined with a solution of LiHMDS (54 mg, 0.32 mmol, 4 equiv), phenyl triflate (26 µl, 0.16 mmol, 2 equiv), $[(allyl)PdCl]_2$ (1.2 mg, 0.0032 mmol, 8 mol% Pd), and cyclohexyl Mandyphos (7 mg, 0.008 mmol, 10 mol%) in 0.6 mL THF with 20 µl chlorobenzene additive. The reaction was stirred for 16 h warming from a 0 °C ice bath to room temperature (18 °C). Compound **55e** (25 mg, 0.064 mmol, 80% yield, 89 %*ee*) was obtained as a yellow solid after silica gel chromatography eluting with 1:1:5 methylene chloride:diethyl ether:hexanes, then 1:1 diethyl ether:hexanes. **$^1$H NMR** (500 MHz, $CDCl_3$) δ: 7.37 - 7.26 (m, 5H), 5.90 (d, *J* = 5.9 Hz, 1H), 5.25 (t, *J* = 5.8 Hz, 1H), 5.30 - 5.28 (m, 2H), 5.14 (t *J* = 6.0 Hz, 1H), 4.20 (s, 1H), 3.73 - 3.66 (m, 4H), 2.54 - 2.50 (m, 2H), 2.46 - 2.42 (m, 2H) ppm; **$^{13}$C{$^1$H} NMR** (125 MHz) δ: 232.8, 139.6, 129.1, 128.8, 128.3, 112.6, 95.1, 94.7, 94.0, 90.8, 73.0, 67.3, 52.6 ppm; **IR:** 3084, 3030, 2957, 2918, 2853, 2814, 1963 and 1878 (strong CO stretches), 1452, 1278, 116, 1006, 874, 751 706 661, 630 $cm^{-1}$. $[\alpha]_D^{26}$ = −21.2° (c = 1.0, $CHCl_3$).

## General procedure 2-F for asymmetric reaction of benzylamine complexes with aryl bromides

Asymmetric cross-coupling of tricarbonylchromium benzylmorpholine (**54**) with aryl bromides to generate enantioenriched tertiary diarylmethylamines (**55f**, **55g**).

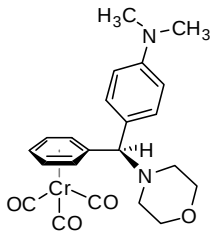

**55f – (−)-(4-$C_6H_4$-N($CH_3$)$_2$)-*N*-($C_4H_8NO$)CH($\eta^6$-$C_6H_5$)Cr(CO)$_3$:** An oven-dried reaction tube was charged with a small magnetic stirbar and $\eta^6$-tricarbonylchromium benzylmorpholine (**54**) (31.5 mg, 0.10 mmol, 1.0 equiv), sealed with a septum, and purged with dry nitrogen. Dry toluene (0.4 mL) and PMDTA (21 µl, 0.10 mmol, 1.0 equiv) were added via syringe. A separate oven-dried vial was charged with $[(allyl)PdCl]_2$ (1.8 mg, 0.005 mmol, 10 mol% Pd), cyclohexyl Mandyphos (10 mg, 0.012 mmol, 12 mol%), and LiHMDS (67 mg, 0.40 mmol, 4.0 equiv) under nitrogen and sealed with a septum cap. A solution of 4-bromo-*N,N*-dimethylaniline (26 mg, 0.13 mmol, 1.3 equiv) in 0.6 mL dry THF was then added to the precatalyst, ligand, and base, and

the solution was taken up by syringe and added to the stirring mixture of **54**, triamine, and toluene. The reaction was stirred at room temperature (18 °C) for 60 hours. The brown solution was quenched with 2 drops $H_2O$, then opened to air and diluted with 3 mL diethyl ether, then filtered over a pad of $MgSO_4$ and silica gel. The pad was rinsed with additional diethyl ether, and the filtrate was concentrated *in vacuo*, loaded directly onto a silica gel column, and eluted with 20 – 40% diethyl ether in hexanes. The result was **55f** (25.5 mg, 0.059 mmol, 59 % yield, 84 %*ee*) as a yellow solid. **$^1$H NMR** (300 MHz, $CDCl_3$) δ: 7.07 (d, *J* = 8.8 Hz, 2H), 6.68 (d, *J* = 8.8 Hz, 2H), 5.94 (d, *J* = 6.3 Hz, 1H), 5.38 - 5.28 (m, 2H), 5.25 (d, *J* = 6.7 Hz, 1H), 5.18 - 5.14 (m, 1H), 4.19 (s, 1H), 3.71 - 3.68 (m, 4H), 2.94 (s, 6H), 2.59 - 2.54 (m, 2H), 2.46 - 2.39 (m, 2H) ppm; **$^{13}$C{$^1$H} NMR** (75 MHz) δ: 233.2, 150.4, 130.1, 127.0, 114.2, 112.3, 94.5, 94.1, 93.3, 91.5, 91.1, 71.9, 67.4, 52.5, 40.6 ppm; **IR:** 3081, 2958, 2922, 2854, 1962 and 1877 (strong CO stretches), 1612, 1520, 1455, 116, 874, 802, 664, 632 cm$^{-1}$; **HRMS** (ES+) calc'd for $C_{22}H_{25}CrN_2O_4$ 433.1219 found 433.1205 $[MH]^+$; **$[\alpha]_D^{26}$** = −25.6° (c = 0.55, $CHCl_3$).

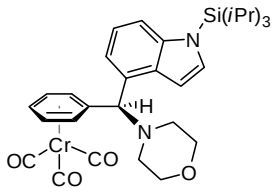


**55g** – (−)-[1-(triisopropylsilyl)-1H-indol-4-yl]-*N*-($C_4H_8NO$)CH($\eta^6$-$C_6H_5$)Cr(CO)$_3$: Using General procedure 2-F, **54** (31.3 mg, 0.10 mmol, 1.0 equiv) and PMDTA (21 µl, 0.10 mmol, 1.0 equiv) in 0.4 mL toluene was combined with a solution of LiHMDS (65 mg, 0.4 mmol, 4 equiv), $[(allyl)PdCl]_2$ (1.8 mg, 0.005 mmol, 10 mol% Pd), and cyclohexyl Mandyphos (10 mg, 0.012 mmol, 12 mol%), and 5-bromo-*N*-triisopropylsilylindole (42 mg, 0.12 mmol, 1.2 equiv) in 0.6 mL THF. The reaction was stirred for 48 h at room temperature (19 °C). Compound **55g** (21 mg, 0.036 mmol, 36% yield, 62 %ee) was obtained as an orange oil after silica gel chromatography eluting with 20 – 30% diethyl ether in hexanes. **$^1$H NMR** (300 MHz, CDCl3) δ: 7.44 (d, J = 8.3 Hz, 1H), 7.26 (d, J = 2.7 Hz, 1H), 7.09 (dd, J = 7.4, 8.2 Hz, 1H), 6.95 (d, J = 7.1 Hz, 1H), 6.78 (d, J = 2.8 Hz, 1H), 6.05 (d, J = 5.9 Hz, 1H), 5.42 (d, J = 6.7 Hz, 1H), 5.36 - 5.38 (m, 2H), 5.12 - 5.07 (m, 1H), 4.65 (s, 1H), 3.76 - 3.66 (m, 4H), 2.65 - 2.59 (m, 2H), 2.54 - 2.48 (m, 1H), 1.69 (7-tet, J = 7.5 Hz, 3H), 1.14 (d, J = 7.5 Hz, 18H) ppm; **$^{13}$C{$^1$H} NMR** (125 MHz) δ: 233.1, 141.5, 131.7, 131.6, 131.1, 121.2, 120.5, 113.81, 113.79, 103.8, 94.8 94.7, 93.6, 91.1, 90.5, 70.9, 67.6, 52.7, 18.4, 13.1 ppm; **IR**: 2951, 2923, 2868, 1964 and 1882 (strong CO stretches), 1454, 1427, 1280, 1149, 1118, 882, 755, 661, 630 cm-1; **HRMS** (ES+) calc'd for $C_{27}H_{32}CrNO_3Si$ 498.1557, found 498.1545 $[M - C_4H_8NO]^+$; **$[\alpha]_D^{25}$** = −11.3° (c = 1.0, $CHCl_3$).

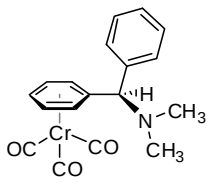


**2i**

**28a – (−)-$Me_2NCH(C_6H_5)(\eta^6$-$C_6H_5)Cr(CO)_3$**: Using General procedure 2-E, **27** (21.4 mg, 0.079 mmol, 1.0 equiv) and PMDTA (17 µl, 0.08 mmol, 1.0 equiv) in 0.4 mL toluene was combined with a solution of LiHMDS (54 mg, 0.32 mmol,

4 equiv), 4-phenyl triflate (26 µl, 0.16 mmol, 2 equiv), $[(allyl)PdCl]_2$ (1.1 mg, 0.003 mmol, 7 mol% Pd), and cyclohexyl Mandyphos (6.5 mg, 0.008 mmol, 10 mol%) in 0.6 mL THF with 20 µl chlorobenzene additive. The reaction was stirred for 10 h warming from a 0 °C ice bath to room temperature (19 °C). Compound **28a** (18.2 mg, 0.052 mmol, 66% yield, 87 %*ee*) was obtained as a yellow solid after silica gel chromatography eluting in 2:1–7:1 methylene chloride : hexanes to 3:1 methylene chloride : diethyl ether. **$^1$H NMR** (300 MHz, $CDCl_3$) δ: 7.39-7.27 (m, 5H), 5.91 - 5.88 (m, 1H), 5.34 - 5.26 (m, 3H), 5.17 - 5.12 (m, 1H), 4.15 (s, 1H), 2.24 (s, 6H) ppm; **$^{13}$C{$^1$H} NMR** (75 MHz) δ: 233.0, 140.0, 129.1, 128.6, 128.1, 114.1, 95.2, 94.5, 93.6, 91.0, 90.6, 73.5, 44.3 ppm; **IR:** 2946, 2864, 2823, 2781, 1962 and 1876 (strong CO stretches), 1611, 1521, 1454, 1353, 1016, 812, 663, 632 $cm^{-1}$. **HRMS** (ES+) calc'd for $C_{15}H_{17}Cr$ 263.0766, found 263.0757 $[M-(CO)_3]^+$. *Existing literature characterization for the racemate is consistent with the characterization data for this compound.*[40] **$[\alpha]_D^{25}$** = −21.5° (c = 1.0, $CHCl_3$).

Figure 2-11: Yellow homochiral crystals of **28a** formed after evaporation of a solution of purified **28a** in methylene chloride and hexanes; the image shows crystals after mother liquor was decanted. The photograph was taken on a Canon PowerShot SX100 digital camera (manual focus, ISO 100, 1/8 second exposure).

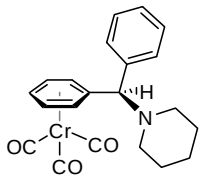


**57 – (−)-($C_6H_5$)-*N*-($C_5H_{10}N$)CH($\eta^6$-$C_6H_5$)Cr(CO)$_3$:** Using General procedure 2-E, **53** (31.3 mg, 0.10 mmol, 1.0 equiv) and PMDTA (21 µl, 0.10 mmol, 1.0 equiv) in 0.4 mL toluene was combined with a solution of LiHMDS (67 mg, 0.4 mmol, 4 equiv), 4-phenyl triflate (19 µl, 0.12 mmol, 1.2 equiv), $[(allyl)PdCl]_2$ (1.5 mg, 0.004 mmol, 8 mol% Pd), and cyclohexyl (8 mg, 0.009 mmol, 9mol%) in 0.6 mL THF. The reaction was stirred for 10 h at 8 – 10 °C. Compound **57** (27.9 mg, 0.072 mmol, 72% yield, 85 %*ee*) was obtained as a yellow crystalline solid after silica gel chromatography eluting 10 – 15% diethyl ether in hexanes. **$^1$H NMR** (500 MHz, $CDCl_3$) δ: 7.35 (t, *J* = 7.3 Hz, 2H), 7.31 - 7.28 (m, 1H), 7.24 (d, *J* = 6.9 Hz, 2H), 5.95 (d, *J* = 6.5 Hz, 1H), 5.35

(dt, *J* = 6.4, 1.0 Hz, 1H), 5.29 (t, *J* = 6.1 Hz, 1H), 5.21 (d, *J* = 6.7 Hz, 1H), 5.19 - 5.16 (m, 1H), 4.37 (s, 1H), 2.40 - 2.36 (m, 4H), 1.59 - 1.55 (m, 4H), 1.42 - 1.38 (m, 2H) ppm; **$^{13}C\{^1H\}$ NMR** (125 MHz) δ: 33.2, 139.3, 129.4, 128.5, 127.9, 114.4, 94.9, 94.6, 93.3, 91.4, 91.1, 72.7, 52.8, 26.6 24.6 ppm; **IR:** 3084, 3062, 3028, 2934, 2852, 2805, 2753, 1964 and 1880 (strong CO stretches), 1452, 752, 704, 662 631 $cm^{-1}$; **HRMS (**ES+) calc'd for $C_{21}H_{22}CrNO_3$ 388.1005, found 388.1017 $[MH]^+$; **$[\alpha]_D^{25}$** = −28.3° (c = 0.45, $CHCl_3$).

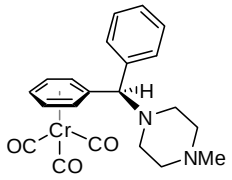


**58 – (−)-($C_6H_5$)-*N*-($MeNC_4H_8N$)CH(*η*$^6$-$C_6H_5$)Cr(CO)$_3$:** Using General procedure 2-E, **56** (26 mg, 0.080 mmol, 1.0 equiv) and PMDTA (17 µl, 0.080 mmol, 1.0 equiv) in 0.4 mL toluene was combined with a solution of LiHMDS (55 mg, 0.32 mmol, 4 equiv), 4-phenyl triflate (19 µl, 0.12 mmol, 1.5 equiv), $[(allyl)PdCl]_2$ (1.5 mg, 0.004 mmol, 10 mol% Pd), and cyclohexyl Mandyphos (10 mg, 0.012 mmol, 12 mol%) in 0.6 mL THF with 30 µl chlorobenzene additive. The reaction was stirred for 24 h warming from a 0 °C ice bath to room temperature (19 °C). Compound **58** (22 mg, 0.055 mmol, 69% yield, 88 %*ee*) was obtained as a yellow solid after silica gel chromatography eluting 5% methanol in methylene chloride. **$^1H$ NMR** (500 MHz, $CDCl_3$) δ: 7.37 - 7.26 (m, 5H), 5.90 (d, *J* = 6.0 Hz, 1H), 5.35 - 5.27 (m, 3H), 5.16 - 5.12 (m, 1H), 4.28 (s, 1H), 2.55 - 2.45 (m, 8H), 2.27 (s, 3H) ppm; **$^{13}C\{^1H\}$ NMR** (125 MHz) δ 232.6, 139.3, 128.9, 128.4, 127.9, 113.0, 94.9, 94.4, 93.5, 90.6, 90.1, 72.1, 53.5, 51.3, 45.8 ppm; **IR:** 3030, 2933, 2797, 1962 and 1878 (strong CO stretches), 1454, 1290, 1143, 1008, 751, 706, 663, 630, 534 $cm^{-1}$; **HRMS (**ES+) calc'd for $C_{21}H_{23}CrN_2O_3$ 403.1114, found 403.1129 $[MH]^+$; **$[\alpha]_D^{26}$** = −14.4° (c = 0.60, $CHCl_3$).

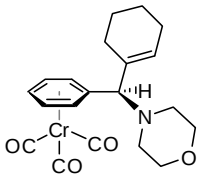


**59 – (−)-($C_6H_9$)-*N*-($C_5H_8NO$)CH(*η*$^6$-$C_6H_5$)Cr(CO)$_3$:** Using General procedure 2-E, **54** (31.3 mg, 0.10 mmol, 1.0 equiv) and PMDTA (21 µl, 0.10 mmol, 1.0 equiv) in 0.4 mL toluene was combined with a solution of LiHMDS (67 mg, 0.4 mmol, 4 equiv), 4-phenyl triflate (19 µl, 0.12 mmol, 1.2 equiv), $[(allyl)PdCl]_2$ (1.5 mg, 0.004 mmol, 8 mol% Pd), and cyclohexyl Mandyphos (8 mg, 0.009 mmol, 9mol%) in 0.6 mL THF with 20 µl chlorobenzene additive. The reaction was stirred for 18 h at 8 – 10 °C. Compound **59** (27.2 mg, 0.088 mmol, 88% yield, 53 %*ee*) was obtained as a pale yellow solid after silica gel chromatography eluting with 10 – 15% diethyl ether in hexanes. **$^1H$ NMR** (500 MHz, $CDCl_3$) δ: 7.35 (t, *J* = 7.3 Hz, 2H), 7.31 - 7.28 (m, 1H), 7.24 (d, *J* = 6.9 Hz, 2H), 5.95 (d, *J* = 6.5 Hz, 1H), 5.35 (dt, *J* = 6.4, 1.0 Hz, 1H), 5.29 (t, *J* = 6.1 Hz, 1H), 5.21 (d, *J* = 6.7 Hz, 1H), 5.19 - 5.16 (m, 1H), 4.37 (s, 1H), 2.40 - 2.36 (m, 4H), 1.59 - 1.55 (m, 4H), 1.42 - 1.38 (m, 2H) ppm; **$^{13}C\{^1H\}$** NMR (125 MHz) δ: 33.2, 139.3, 129.4, 128.5, 127.9, 114.4, 94.9, 94.6, 93.3, 91.4, 91.1, 72.7, 52.8, 26.6 24.6 ppm; **IR:** 3084, 3062, 3028, 2934, 2852, 2805, 2753, 1964 and

1880 (strong CO stretches), 1452, 752, 704, 662 631 $cm^{-1}$; **HRMS** (ES+) calc'd for $C_{16}H_{15}CrO_3$ 307.0426, found 307.0426 $[M - C_4H_8NO]^+$; $[\alpha]_D^{26} = -17.6°$ (c = 0.80, $CHCl_3$).

## *Procedures for directly obtaining decomplexed diarylmethylbenzylamines*

### General procedure 2-G: One-pot coupling and decomplexation in light and air.

Free diarylmethyl benzylamines can be obtained by exposure of a dilute solution of the crude asymmetric coupling reaction mixture to air and bright light, then filtration and column chromatography to obtain pure diarylmethyl benzylamine:[40]

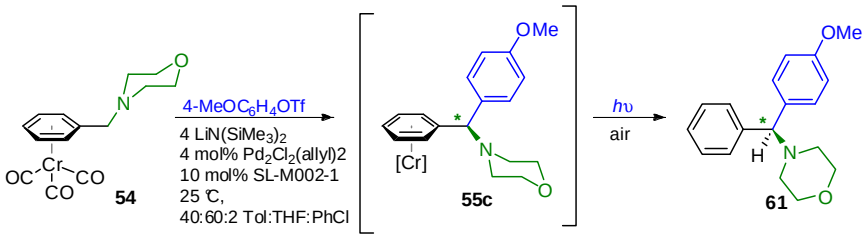


Scheme 2-13: General scheme for the one-pot coupling reaction and subsequent decomplexation to yield the free diarylmethylbenzylamine.

**61 – (−)-(4-$C_6H_4$-OMe)PhCH-*N*-($C_4H_8NO$):** An oven-dried reaction tube was charged with a small magnetic stirbar and $\eta^6$-tricarbonylchromium benzylmorpholine (**54**) (36.3 mg, 0.116 mmol, 1.0 equiv), sealed with a septum, and purged with dry nitrogen. Dry toluene (0.6ml) and PMDTA (25 µl, 0.12 mmol, 1.0 equiv) were added via syringe. A separate vial was charged with $[(allyl)PdCl]_2$ (2.2 mg, 0.006 mmol, 12 mol% Pd), cyclohexyl Mandyphos (13 mg, 0.015 mmol, 12 mol%), and LiHMDS (80 mg, 0.48 mmol, 4 equiv) under a nitrogen atmosphere, sealed with a septum cap, and dissolved in 0.9 mL dry THF. 4-anisole triflate (32 µl, 0.18 mmol, 1.5 equiv) and chlorobenzene (~30 µl, 2%/vol) were added next via syringe. This THF solution was taken up with a syringe and added to the stirring mixture of **54**, triamine, and toluene. The reaction was allowed to stir at to room temperature (20 °C) with stirring for 12 hours. The brownish orange solution was quenched with 2 drops $H_2O$, then opened to air, diluted with 3 mL diethyl ether, and then filtered over a pad of $MgSO_4$ and silica gel. The pad was rinsed with an additional 3 mL diethyl ether, and the yellow solution was diluted with hexane (~10 mL) and placed in sunlight for 4 hours. The cloudy solution was filtered over another pad of $MgSO_4$ and silica gel, concentrated *in vacuo*, loaded directly onto a silica gel column, and eluted with 0 - 20%

ethyl acetate in pentane. The result was **61** (20.3 mg, .072 mmol, 62 % yield, 85 %*ee*) as a colorless solid. **$^1$H NMR** (500 MHz, $CDCl_3$) δ: 7.41 (d, J = 7.4 Hz, 2H), 7.32 (d, J = 8.7 Hz, 2H), 7.27 (t, J = 7.5 Hz, 2H), 7.17 (t, J = 7.3 Hz, 1H), 6.81 (d, J = 8.7 Hz, 2H), 4.15 (s, 1H), 3.75 (s, 3H), 3.71 - 3.69 (m, 4H), 2.38 - 2.37 (m, 4H) ppm; **$^{13}$C{$^1$H} NMR** (125 MHz, $CDCl_3$) δ: 158.8, 143.0, 134.7, 129.2, 128.7, 128.0, 127.1, 114.1, 76.2, 67.5, 55.4, 52.9 ppm; **HRMS** (CI+): calc'dfor $C_{18}H_{21}NO_2$ 283.1572, obs 283.1574 $[M]^+$; $[\alpha]_D^{26}$ = −25.4° (c = 0.70 $CHCl_3$). *Spectral data is consistent with existing characterization*.[42,43]

### General procedure 2-H: Decomplexation from purified complex using light and air.

Alternately, the free complex can be obtained directly from the purified parent tricarbonylchromium complex by exposing a solution of the purified complex to air and bright direct light, then filtration and evaporation of solvent to obtain pure diarylmethyl benzylamine:[40]

A sample of **55c** (8.5 mg, 0.020 mmol, 83% ee) was dissolved in 0.4 mL methylene chloride, diluted with 1.6 mL hexanes, and placed in bright sunlight for 4 hours. During this time, the yellow color faded and a grayish green precipitate formed. The solution was filtered thorugh a plug of cotton and anhydrous $MgSO_4$, then solvent was evaporated under reduced pressure to yield **61** (4.2 mg, 0.015 mmol, 75% yield, 83% ee). Spectral data is consistent with that obtained for **61** using General procedure 2-G, above.

## References


[1] (a) P. D. O'Shea et al. *J. Org. Chem.* **2005**, *70*, 3021-3030. (b) Prat, L.; Dupas, G.; Duflos, J.; Quéguiner, G.; Bourguignon, J.; Levacher, V. *Tetrahedron Lett.* **2001**, *42*, 4515-4518. (c) Fang, F. G. 5426196, 1995.

[2] (a) Andersson, P. G.; Schink, H. E.; Osterlund, K. *J. Org. Chem.* **1998**, *63*, 8067-8070. (b) Welch, W. M.; Kraska, A. R.; Sarges, R.; Koe, B. K. *J. Med. Chem.* **1984**, *27*, 1508-1515.

[3] (a) Esquivias, J.; Arrayás, R. G.; Carretero, J. C. *Angew. Chem.Int. Ed.* **2006**, *45*, 629-633. (b) Schäfer, G.; Bode, J. W. *Angew. Chem. Int. Ed.* **2011**, *asap*.

[4] Shi, B.; Maugel, N.; Zhang, Y.; Yu, J. *Angew. Chem. Int. Ed.* **2008**, *47*, 4882-4886.

[5] Sun, F.; Zheng, X.; Gu, Q.; He, Q.; You, S. *Eur. J. Org. Chem.* **2010**, *2010*, 47-50

[6] Li, J. J. In *Contemporary Drug Synthesis*; Wiley-Interscience: 2004; pp 221.

[7] (a) Calderon, S. N.; Rice, K. C.; Rothman, R. B.; Porreca, F.; Flippen-Anderson, J.; Xu, H.; Becketts, K.; Smith, L. E.; Bilsky, E. J.; Davis, P.; Horvath, R. *J. Med. Chem*. **1997**, *40*, 695-704. (b) Broom, D. C.; Jutkiewicz, E. M.; Rice, K. C.; Traynor, J. R.; Woods, J. H. *The Japanese Journal of Pharmacology* **2002**, *90*, 1-6 (c) Jurd, L. *J. Heterocycl. Chem*. **1996**, *33*, 1227-1232. (d) Lézé, M.; Palusczak, A.; Hartmann, R. W.; Le Borgne, M. *Bioorg. Med. Chem. L*ett.**2008**, *18*, 4713-4715. (e) Le Borgne, M.; Marchand, P.; Delevoye-Seiller, B.; Robert, J.; Le Baut, G.; Hartmann, R. W.; Palzer, M. *Bioorg. Med. Chem. Lett*. **1999**, *9*, 333-336. (f) Childers, S. R.; Fleming, L. M.; Selley, D. E.; McNutt, R. W.; Chang, K. J. *Molecular Pharmacology* **1993**, *44*, 827-834. (g) Torregrossa, M. M.; Isgor, C.; Folk, J. E.; Rice, K. C.; Watson, S. J.; Woods, J. H. *Neuropsychopharmacology* **2003**, *29*, 649-659.

[8] Le Gall, E.; Haurena, C.; Sengmany, S.; Martens, T.; Troupel, M. *J. Org. Chem.* **2009**, *74*, 7970-7973.

[9] Pflum, D. A.; Wilkinson, H. S.; Tanoury, G. J.; Kessler, D. W.; Kraus, H. B.; Senanayake, C. H.; Wald, S. A. *Organic Process Research & Development* **2001**, *5*, 110-115

[10] Opalka, C. J.; D'Ambra, T. E.; Faccone, J.; Bodson, G. J.; Cossement, E. *ChemInform* **1995**, *26*

[11] (a) Bishop, M. J.; McNutt, R. W. *Bioorg. Med. Chem. Lett.* **1995**, *5*, 1311-1314. (b) Furness, M. S.; Zhang, X.; Coop, A.; Jacobson, A. E.; Rothman, R. B.; Dersch, C. M.; Xu, H.; Porreca, F.; Rice, K. C. *J. Med. Chem.* **2000**, *43*, 3193-3196. (c) Pflum, D. A.; Krishnamurthy, D.; Han, Z.; Wald, S. A.; Senanayake, C. H. *Tetrahedron Lett.* **2002**, *43*, 923-926.

[12] Hou, G.; Tao, R.; Sun, Y.; Zhang, X.; Gosselin, F. *J. Am. Chem. Soc*. **2010**, 132, 2124-2125

[13] Nguyen, T. B.; Wang, Q.; Guéritte, F. *Chem –Eur. J.* **2011**, *asap*.

[14] Kauffman, M. C.; Walsh, P. J. In *Stereoselective Synthesis 2*; Molander, G. A., Ed.; Thieme: Stuttgart, **2011**; Vol. 2; pp 449-495.

[15] Shintani, R.; Soh, Y.; Hayashi, T. *Org. Lett.* **2010**, 12, 4106-4109.

[16] Shintani, R.; Takeda, M.; Tsuji, T.; Hayashi, T. *J. Am. Chem. Soc.* **2010**, 132, 13168-13169.

[17] Hayashi, T.; Ishigedani, M. *J. Am. Chem. Soc.* **2000**, *122*, 976-977.

[18] Hermanns, N.; Dahmen, S.; Bolm, C.; Bräse, S. *Angew. Chem. Int. Ed.* **2002**, 41, 3692-3694.

[19] Tsai, A. S.; Tauchert, M. E.; Bergman, R. G.; Ellman, J. A. *J. Am. Chem. Soc.* **2011**, *133*, 1248-1250.

[20] Katritzky, A. R.; Yao, J.; Bao, W.; Qi, M.; Steel, P. J. *J. Org. Chem.* **1999**, *64*, 346-350

[21] Jaouen, G.; Top, S.; McGlinchey, M. J. *J Organomet. Chem.* **1980**, 195, C9-C12.

[22] (a) Merlic, C. A.; Walsh, J. C.; Tantillo, D. J.; Houk, K. N. *J. Am. Chem. Soc.* **1999**, 121, 3596-3606. (b) Pfletschinger, A.; Dargel, T. K.; Bats, J. W.; Schmalz, H.; Koch, W. *Chem. -Eur. J.* **1999**, 5, 537-545.

[23] Walsh, P. J.; Kozlowski, M. C. In *Fundamentals of Asymmetric Catalysis*; University Science Books: **2008**.

[24] For more information on high-throughput experimental procedures, see Dreher, S. D.; Dormer, P. G.; Sandrock, D. L.; Molander, G. A. *J. Am. Chem. Soc*. **2008**, 130, 9257-9259.

[25] Djukic, J.; Maisse, A.; Pfeffer, M.; de Cian, A.; Fischer, J. *Organometallics* **1997**, 16, 657-667.

[26] Ireland, T.; Tappe, K.; Grossheimann, G.; Knochel, P. *Chem. -Eur. J.* **2002**, *8*, 843-852.

[27] Lotz, M.; Ireland, T.; Almena Perea, J. J.; Knochel, P. *Tetrahedron: Asymmetry* **1999**, *10*, 1839-1842.

[28] Yoon, T. P.; Jacobsen, E. N. *Science* **2003**, *299*, 1691-1693.

[29] Spindler, F.; Malan, C.; Lotz, M.; Kesselgruber, M.; Pittelkow, U.; Rivas-Nass, A.; Briel, O.; Blaser, H. *Tetrahedron: Asymmetry* **2004**, *15*, 2299-2306.

[30] Hayashi, T.; Fukushima, M.; Konishi, M.; Kumada, M. *Tetrahedron Lett.* **1980**, 21, 79-82.

[31] The transmetallation process in a catalytic cycle is considered the least understood piece of the palladium-catalyzed cross-coupling cycle. See: Clarke, M. L.; Heydt, M. *Organometallics* **2005**, *24*, 6475-6478.

[32] (a) Hevia, E.; Mulvey, R. E. *Angew. Chem. Int. Ed*. **2011**, 50, 6448-6450. (b) Ma, Y.; Hoepker, A. C.; Gupta, L.; Faggin, M. F.; Collum, D. B. *J. Am. Chem. Soc.* **2010**, 132, 15610-15623. (c) Krasovskiy, A.; Krasovskaya, V.; Knochel, P. *Angew. Chem. Int. Ed.* **2006**, 45, 2958-2961.

[33] (a) Salvi, L.; Kim, J. G.; Walsh, P. J. *J. Am. Chem. Soc.* **2009**, 131, 12483-12493. (b) Kim, J. G.; Walsh, P. J. *Angew. Chem. Int. Ed.* **2006**, 45, 4175-4178 (c) Salvi, L.; Jeon, S.; Fisher, E. L.; Carroll, P. J.; Walsh, P. J. *J. Am. Chem. Soc.* **2007**, 129, 16119-16125

[34] Enantioenriced monoaryl dimethylbenzylamine phosphine complexes of tricarbonylchromium have been used successfully in asymmetric cross-coupling and alkylations. For examples, see (a) Uemura, M.; Miyake, R.; Nishimura, H.; Matsumoto, Y.; Hayashi, T. *Tetrahedron: Asymmetry* **1992**, *3*, 213-216. (b) Hayashi, Y.; Sakai, H.; Kaneta, N.; Uemura, M. *Journal of Organometallic Chemistry* **1995**, *503*, 143-148. (c) Kamikawa, K.; Sugimoto, S.; Uemura, M. *J. Org. Chem*. **1998**, *63*, 8407-8410.

[35] Woolins, J. D., Ed.; In *Inorganic Experiments*; VCH: Weinheim, **1994**, 194-195.

[36] Mahaffy, C. A. L.; Pauson, P. L. *Inorg. Synth*. **1990**, *28*, 136-140.

[37] Ritter, K. *Synthesis* **2002**, *1993*, 735-762.

[38] Kazmierski, I.; Gosmini, C.; Paris, J.; Périchon, J. *Synlett* **2006**, *2006*, 881-884.

[39] Djukic, J.; Maisse, A.; Pfeffer, M.; de Cian, A.; Fischer, J. *Organometallics* **1997**, *16*, 657-667.

[40] McGrew, G. I.; Temaismithi, J.; Carroll, P. J.; Walsh, P. J. *Angew. Chem. Int. Ed.* **2010**, *49*, 5541-5544.

[41] For more information on high-throughput experimental procedures, see Dreher, S. D.; Dormer, P. G.; Sandrock, D. L.; Molander, G. A. *J. Am. Chem. Soc.* **2008**, *130*, 9257-9259.

[42] Schiemann, K.; Showalter, H. D. H. *J. Org. Chem.* **1999**, *64*, 4972-4975.

[43] Murai, T.; Asai, F. *J. Am. Chem. Soc.* **2007**, *129*, 780-781.

## Chapter 3

## A new family of PΛN arene tricarbonylchromium ligands

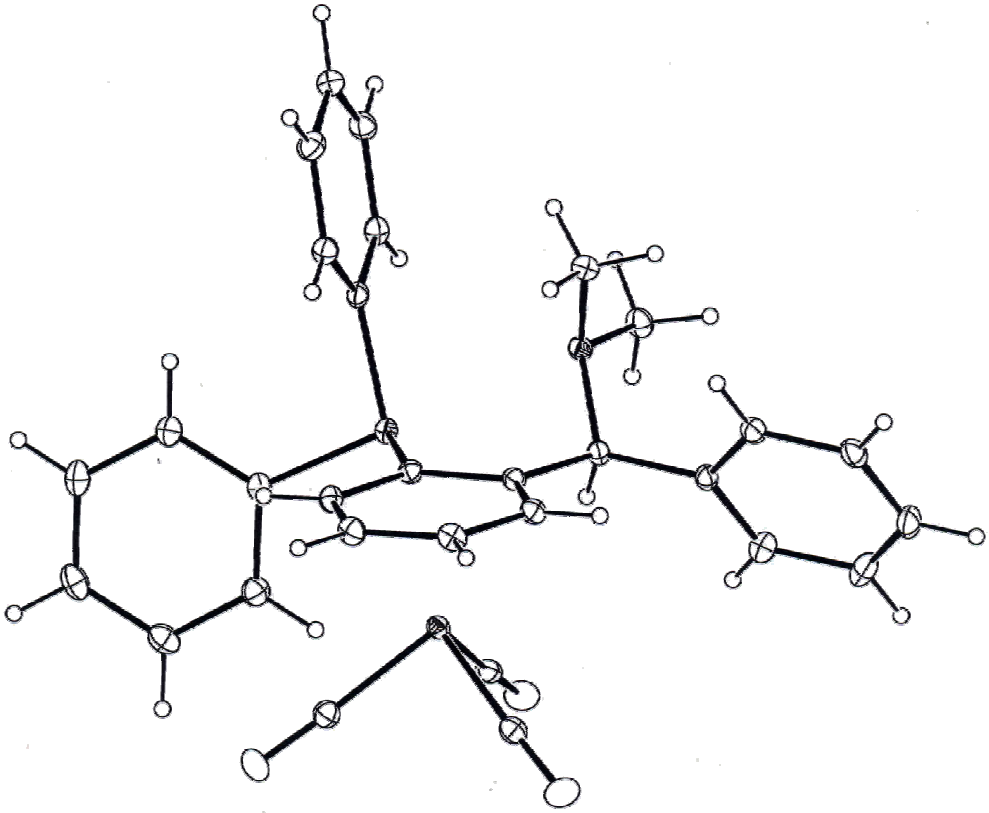

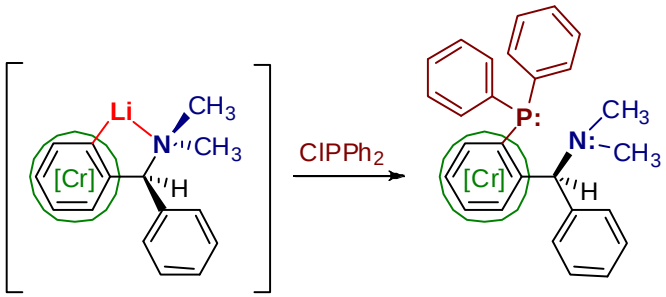

> "...the identification of new privileged ligands and catalysts remains enormously difficult and often requires a degree of serendipity."
>
> Yoon and Jacobsen, *Science* **2003**, *299*, 1693.

Widespread use of asymmetric catalysis would not be possible without easy and efficient access to enantioenriched ligands and catalysts. These ligands may incorporate central chirality, axial chirality (also known as helicity), or planar chirality (Figure 3-1). While in organic chemistry, the focus of asymmetry is often on central chirality about a carbon center, the most popular ligand scaffolds in asymmetric catalysis that are used to generate these stereogenic centers tend to incorporate other modes of chirality. For example, many ligands contain axial or planar chirality, or a combination of chirality modes.[1,2] Historically, $C_2$ symmetric ligands with axial chirality have dominated the field of asymmetric catalysis, but non-symmetric (especially polydentate) ligands have been known to increase asymmetric induction and in some cases have even provided higher ee than the most effective $C_2$-symmetric ligands.[3] Thus, the development of new enantioenriched $C_1$-symmetric ligands is an important area to pursue.

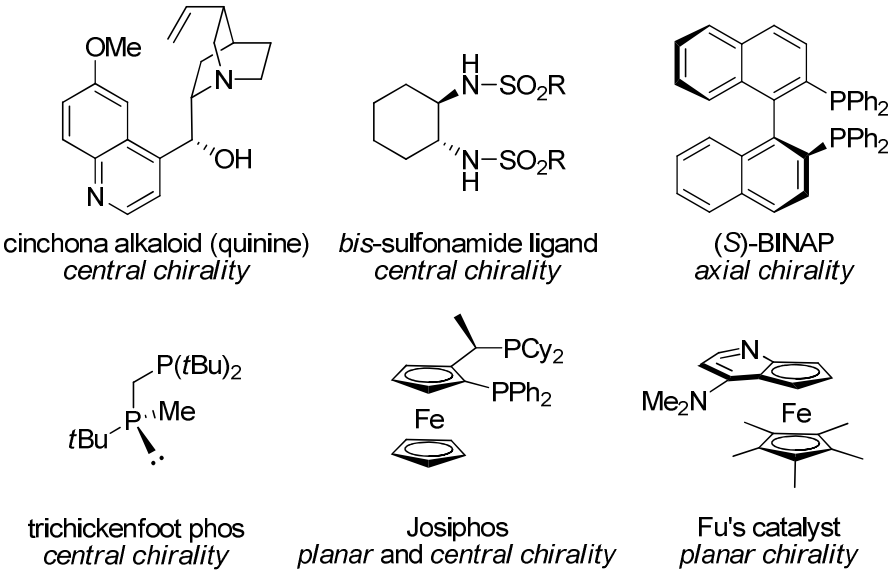


Figure 3-1: The three kinds of molecular chirality, illustrated in some common catalysts and ligands.

In order for the synthesis of chiral ligands to be practical, they should be made stereoselectively or the stereoisomers need to be separable.[4] A small number catalysts (such as MIB[a]) are known to exhibit positive nonlinear effects that partially offset the lower selectivity of a non-enantiomerically pure ligand.[5] Oftentimes, however, even a small reduction in the catalyst ee is detrimental to the performance of enantioselective catalysts. Additionally, even minor catalyst impurities can lead to compromised ee and lower yields, which may be amplified on industrial scale.[6]

Planar chiral ferrocenyl complexes, first synthesized stereoselectively 60 years ago, have found widespread use as ligand scaffolds in asymmetric catalysis, including large-scale industrial processes.[7] As noted in Chapter 2, the chiral ferrocenyl phosphine amines possessing both planar and central chirality (cyclohexyl Mandyphos[b]) proved to be the key to enabling the asymmetric cross-coupling of tricaronbylchromium-coordinated benzylic organolithiums. While in theory many chiral ferrocenyl scaffolds are possible, the majority of chiral ferrocene-based phosphine ligands are based on diastereoselective lithiations and other functionalizations of a single optically pure parent ferrocenylamine complex called Ugi's Amine (Figure 3-2).[8] This was due to Ugi's straightforward preparation of the amine in four steps and in high enantiomeric purity achieved by tartaric acid resolution, followed by recrystallization.[9,10] And, unlike some other ferrocenyl complexes, the amine complex could be diastereoselectivey metalated using the amino group as directing group (DOM, directed *ortho* metalation) and quenched with electrophiles with very high diastereoselectivity.[9]

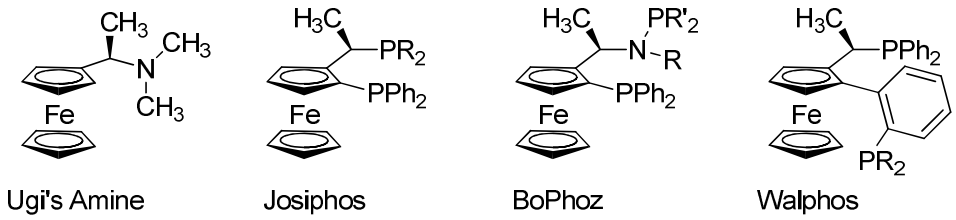


Figure 3-2: Ugi's Amine and related chiral ferrocene-based ligands Josiphos, Bophoz, and Walphos.

[a] MIB = (2*S*)-(−)-3-*exo*-(morpholino)isoborneol
[b] Ligands in the Mandyphos family are known for asymmetric hydrogenations, and due to demand, some of these ligands are now produced in multi-kilogram scale (Aldrich).

Tricarobonylchromium complexes can also exhibit planar chirality, and looking to the ferrocene ligands as an example, a structurally analogous and highly enantioenriched arene-chromium ligand scaffold precursor similar in to Ugi's Amine has been prepared (**A**, Figure 3-3). Unlike Ugi's Amine, however, the complex's parent arene is commercially available as enantiopure α-methyl benzylamine. The commercial availability of enantiopure starting material relieved the synthetic chemist of the need to resolve the enantiomers of the parent complex. Diastereoselective DOM and electrophilic phosphine quench on the tricarbonylchromium-complexed α-methylbenzylamine was demonstrated by Uemura and Hayashi 20 years ago.[11,12,13] The resulting phosphine-quenched tricarbonylchromium PΛN ligands, as well as bis-phosphine ligands such as Daniphos developed by Togni and coworkers[14] are shown in Figure 3-3. These chromium-complexed ligands are significantly easier to synthesize. They typically also perform better in catalysis than the *non*-coordinated arene ligands,[15,a] and thus these newer planar- and central- chiral ligands have found applications in a variety of catalytic reactions.[16]

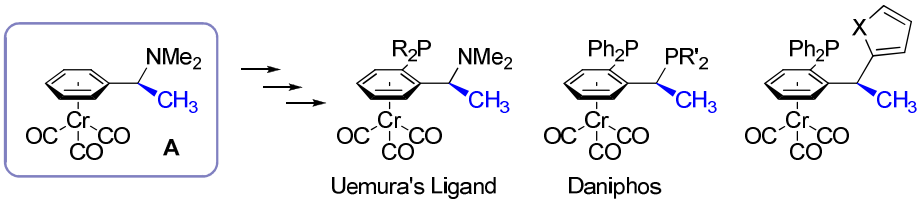


Figure 3-3: Variations on α-methylbenzylamine tricarbonylchromium ligand derivatives focus on changing the donating groups on the arene's benzylic position and *ortho* position, but preserves the α–methyl.

Interestingly, while other substitutions on the α-methylbenzylamine-coordinated tricarbonylchromium complex have been used as modular elements that could be varied in order to tune reactivity and selectivity (Figure 3-3), the chiral α-methyl substitution — an original part of the commercially available starting material — has not been used as a variable in tuning reactivity. A family of ligands with α– aryl substitution would likely have markedly different chiral environment compared with the known ligands with α– methyl substitution. Additionally, the

[a] Various chiral α-methyl benzylamine PΛN ligands without chromium have been synthesized by other groups, but tend to show low selectivity and low yields in synthesis due to difficulties in the DOM step.[15]

potential to easily install a number of different aryl groups at the α–position would add a desirable element of ligand modularity and tenability (Figure 3-4).[17]

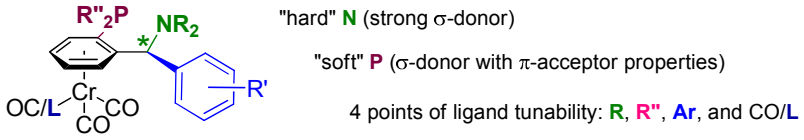


Figure 3-4: Notable aspects of the proposed family of PΛN ligands.

We expected our synthesis to proceed similar to the synthesis of Uemura's ligand, using diastereoselective *ortho*-lithiation of our diarylbenzylamine and then electrophilic quench with a chlorophosphine to yield the α-arylated PΛN ligand (Scheme 3-1).

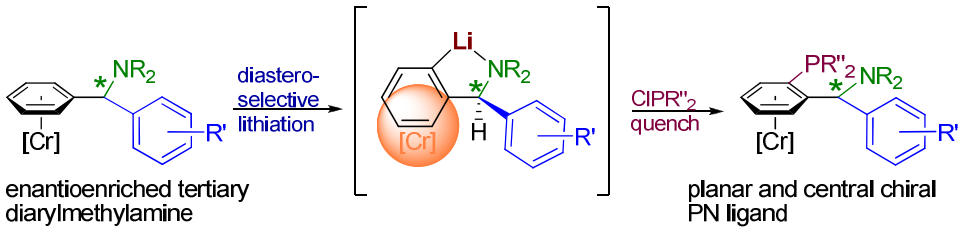


Scheme 3-1: Overview of the proposed PΛN ligand synthesis.

## *Ortho lithiation of the arene ring*[a]

Using the methods developed in Chapter 2, an enantioenriched diarylmethyl tricarbonylchromium complex **28a** was synthesized from **27** and phenyl triflate and then exposed to standard DOM conditions for α-methyl benzylamine chromium complexes. However, we were shocked to find that even when using excess *s*-butyllithium, exclusively unreacted starting material was recovered (Scheme 3-2). It was possible that either the steric bulk of the more bulky diarylmethylamine

[a] Deprotonation work was done in collaboration with C. Stanciu.

complex was preventing the lithiated species from quenching with the chlorodiphenylphosphine, or that the lithiation itself was not proceeding due to sterics or other unknown factors.

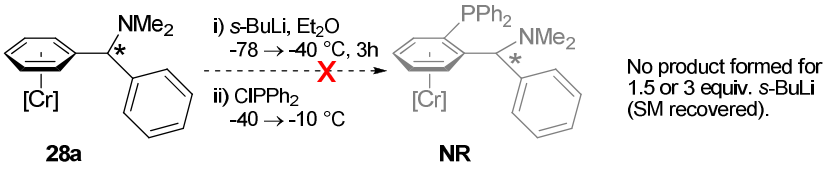


Scheme 3-2: Initial attempts at lithiation and quench of **28a** using standard literature procedure for a similar complex with α-methyl, not α-aryl, substitution, failed to provide product.

To test whether lithiation was occurring, several lithiation procedures were screened, starting with ones that have typically been successful on arene tricarbonylchromium complexes (Table 3-1, entries 1–5). However, no more than 25% deuterium incorporation could be achieved even with TMEDA[a] additive (entries 1 – 4), harsher conditions and large excess of base, or extended reaction times that would lead to degradation of even ethereal solvents. LDA did effect some deprotonation, but was not selective (entries 6 and 7). Schlosser's superbase[18] ("LiCKOR"), a 1:1 mixture of *n*-butyllithium and *t*BuOK, did succeed in deprotonating the complex, but the metalation was not regioselective, and moreover averaged more than 1 deuterium per ring (entries 9 and 10). Compound **28a** was even combined with 8 equivalents of *s*-butyllithium in ether and hexanes and heated at 45 °C for 48h, but no activity was observed for this complex, and the reaction remained yellow and homogeneous (entry 11). It seemed that the typical deprotonation reagents were not useful in the deprotonation of this complex. The diarylmethyl benzylmorpholine complex **55e** was also tested for deprotonation, but it did not react.

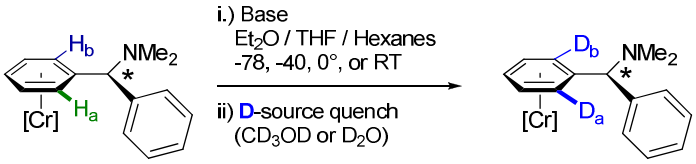


Scheme 3-3: Monitoring extent of deprotonation was done through deuterium quench studies.

[a] TMEDA = *N*,*N*,*N*′,*N*′-tetramethylethylenediamine

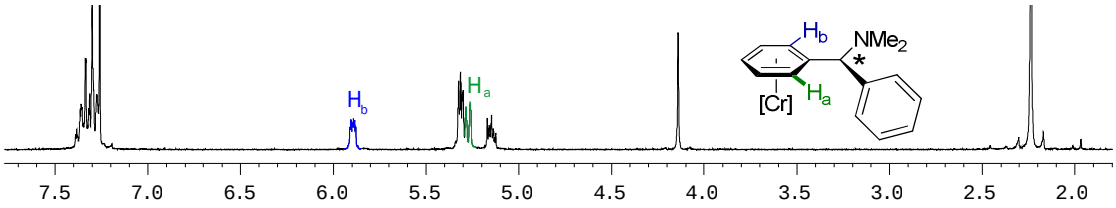


Figure 3-5: Protons $H_a$ (green) and $H_b$ (blue) are monitored for deuterium incorporation.

Table 3-1: Optimization of *ortho*-lithiation conditions (Scheme 3-3).

| Entry | Conditions* | Base | Equiv | T (°C) | Time (h) | %$D_a$ | %$D_b$ | Notes |
|---|---|---|---|---|---|---|---|---|
| 1 | Hex, TMEDA | *s*-BuLi | 3 | −78 → RT | 5 | < 5 | – | $CD_3OD$ quench. |
| 2 | THF, TMEDA | *s*-BuLi | 3 | −78 → RT | 5 | >10 | – | " " |
| 3 | THF, TMEDA | *n*-BuLi | 3 | RT | 5 h | <20 | < 5 | " " |
| 4 | THF, TMEDA | *n*-BuLi | 13 | RT | 24 | **~25** | – | " " |
| 5 | $Et_2O$ | *t*-BuLi | 3 | −78 → RT | 6 h | – | ~25 | >30% dec.# |
| 6 | THF | LDA | 4 | 0 → RT | **24** | **~30** | <10 | $D_2O$ quench. |
| 7 | $Et_2O$ | LDA | 8 | 0 → RT | 24 | – | – | Some dec. |
| 8 | Hex | *s*-BuLi | 3 | −78 → RT | | ~15 | < 5 | $CD_3OD$ quench. |
| 9 | "LiCKOR"† | *n*-BuLi<br>*t*-BuOK | 1.7<br>1.7 | −78 → 0 | | see note | | ~30% dec., unselective (~1.3 D per arene). |
| 10 | "LiCKOR" | *n*-BuLi<br>*t*-BuOK | 5<br>5 | −78 → −35 | | see note | | No dec., but unselective (>1.5 D per arene). |
| 11 | Hex/$Et_2O$ | *s*-BuLi | 8 | RT → 45 | 48 | – | ~5 | 48h heating, **no rxn**. |
| 12 | Hex/$Et_2O$ | *s*-BuLi<br>*n*-BuLi | 8<br>6 | RT | <30 min | N/A | | *Complete dec. upon addition of n-BuLi* |
| **13** | 6:1 Hex:$Et_2O$ | *s*-BuLi<br>*n*-BuLi | 8<br>6 | −78 → 0 | 1 | – | **~20** | ***Clean & selective!***<br>no dec. |
| 14 | "s&n"‡ | *s*-BuLi<br>n-BuLi | 3<br>3 | −78 → 5° | 2 | – | **~60** | Clean incorporation. |
| 15◊ | "s&n" | *s*-BuLi<br>n-BuLi | 3<br>3 | −78 → 5° | 2 | N/A | | >80% conversion to desired phosphine ligand. |

* Abbreviations: Hex = Hexanes; TMEDA = *N*,*N*,*N*′,*N*′-tetramethylethylenediamine. # dec. = decomposition. † "LiCKOR" = Schlosser's base, a superbasic 1:1 mixuture of *n*-butyllithium and *t*-BuOK, believed to generate an organopotassium species after deprotonation. ‡ "s&n" = a 1:1 mixture of *s*-butyllithium and *n*-butyllithium. ◊ reaction was quenched with excess chlorodiphenylphosphine to generate **62**.

Finally, to a stirring mixture of **28a** and s-butyllithium, some *n*-butyllithium was added (Table 3-1, entry 12). Immediately the yellow solution turned orange and then to brown; after quenching and work-up the starting complex was found to have completely decomposed (>5 products in observed by $^1$H NMR). Repeating these conditions, but this time starting carefully at -78 °C and warming to 0° and immediate quenching with methanol-D showed clean and selective incorporation of deuterium (20% D) on a different *ortho* proton ($H_b$) than observed with the previous conditions (Table 3-1, entry 13). Improved deuterium incorporation (60% D) could be obtained by running the lithiation for a longer period of time (~2h), while still reducing the amount of the two bases that were added (entry 14). Finally, the lithiation was conducted using the conditions described in entry 14, but this time quenching with $ClPPh_2$ to generate phosphine amine complex **62**. $^1$H NMR analysis of the crude reaction mixture showed >80% conversion to phosphine (entry 14) in a single regioisomer. Through-space coupling of the benzylic proton to the phosphorus (*I*=1/2, doublet observed in $^1$H NMR) indicated that the substitution was at the side that would allow stabilization of the organolithium by tertiary amine yet minimize steric interaction from the uncoordinated phenyl ring (Scheme 3-4). X-ray quality crystals from this reaction were obtained by crystallization at low temperature using chloroform and hexanes (see full report on p. 297).

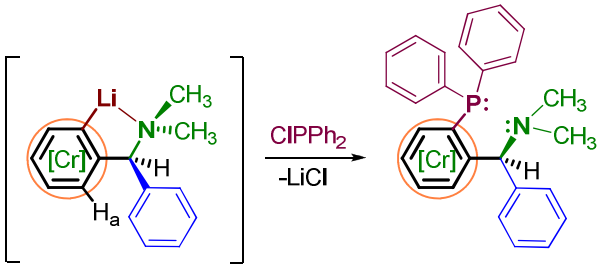


Scheme 3-4: The expected geometry for diastereoselective directed ortho lithiation. [Cr] is below the plane of the paper. The lithiated species is shown as monomeric for clarity.

Interestingly, when these same lithiation conditions (1:1 s-butyllithium:*n*-butyllithium in hexanes and diethyl ether) were attempted on the unsubstituted tertiary benzylamine complex **27**, deuterium incorporation was not observed, indicating that the custom base developed for the diastereoselective lithiation is a system extremely selective for the α–arylated benzylamine **28a**.

## A New Superbase: "s&n"

Our 1:1 mixture of *s*-butyllithium and *n*-butyllithium — which exhibits uniquely enhanced reactivity on our diarylmethylamine complex (**28a**) versus either of these bases separately — is a new variety of unimetallic superbase, according to Caubere's definition.[19] Our novel superbase, which we will refer to as the **"s&n" base**, has unique advantages aside from its diastereoselective *ortho*-lithiation of **28a**. Because both *n*- and *s*- butyllithium are reasonably priced and commercially available in solutions as well as reasonably stable under inert atmosphere, the generation and use of this superbase is remarkably inexpensive and convenient. It does not need to be generated in a glovebox or use multiple stages and reagent additions at variable temperature,[20] nor does it require low-temperature transfer of slurries, such as in the case of Schlosser's base (LiCKOR).[18] Additionally, the two alkyllithium reagents can be added sequentially without premixing, thus circumventing potentially long reaction times for generation of the active species, such as in the case of some LiCl TMP[a] metal amide bases,[21] or for the premixing of highly reactive and expensive reagents. For example, in one case of monometallic superbase use, premixing a 1:1 solution of *tert*-butyllithium and expensive isopropyllithium[b] was required in order to achieve optimum reactivity an order of magnitude higher than *tert*-butyllithium on its own).[19,22] It is hoped that the unimetallic superbase that we have developed here will find adoption as a useful tool in the selective lithiation of difficult or sterically congested substrates, though further exploration of the scope of lithiation substrates is still necessary. Our "s&n" base may also be considered a safer alternative to *tert*-butyllithium, which has recently received negative publicity after a 2009 lab accident involving transfer of a large quantity of *tert*-butyllithium solution led to the death of a student.

## Crystal structure and discussion of lithiation stereochemistry

The crystal structure for the phosphine-quenched product (**62**) from Table 3-1 (entry 14) was determined (Figure 3-6), and the regioselectivity of the reaction was confirmed. The high level of

[a] TMP = 1,1,6,6-tetramethylpiperidine
[b] isopropyllithium solution costs more than $200/100 mL : September 2011 data, Sigma-Aldrich.

diastereoselectivity in lithiation is attributed to the tertiary amine, which indeed serves as directing group (Scheme 3-4). Directed metalation of $H_a$ (Figure 3-5) was not observed in $^1H$ NMR of the crude reaction mixtures. Additionally, nearly enantiopure ligand (>>98% ee) can be obtained by using recrystallized starting material **28a** (a single crystallization can take material at 75–85% ee and enantioenrich it to 95–98% ee) and isolating crystals of ligand product (**62**) through crystallization in hexanes and DCM at −16 °C.

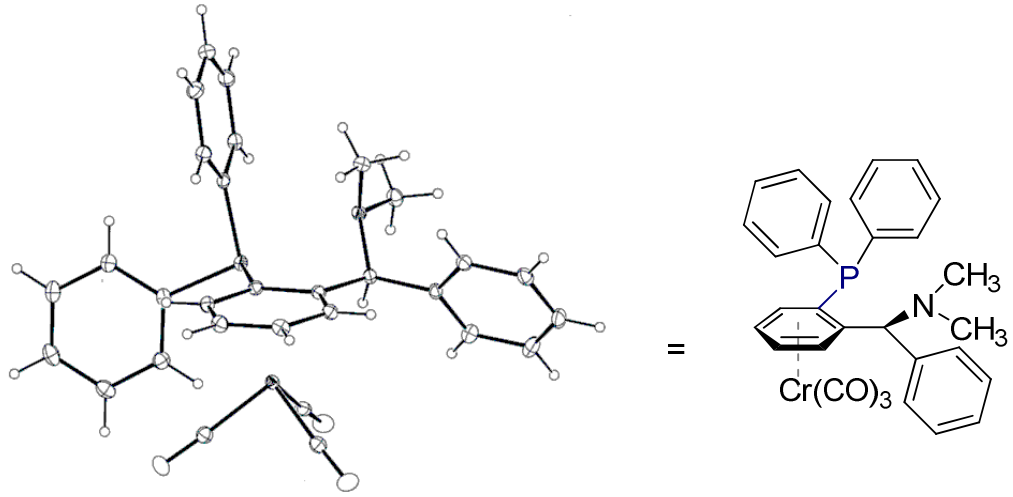


Figure 3-6: X-ray crystal structure of the racemic PN ligand. Thermal ellipsoids are at 30% probability.

### *Towards the synthesis of other Ligands in the family*

Encouraged by the successful synthesis of ligand **62**, we hoped to expand our single ligand into an entire ligand family. Thus, other variations of the PN ligand were attempted using a procedure similar to that used to synthesize **62** in the final entry of Table 3-1. First, different phosphine chlorides were used to quench the lithiated complex. Chlorodicyclohexylphosphine was also a suitable electrophile, though it took slightly longer to quench completely. Thus, the alkylphosphine-quenched product **63** was isolated after 2–3 hours of stirring for full consumption of the lithiated starting material. The crystal structure of **63** was obtained, and is shown in Figure 3-7.

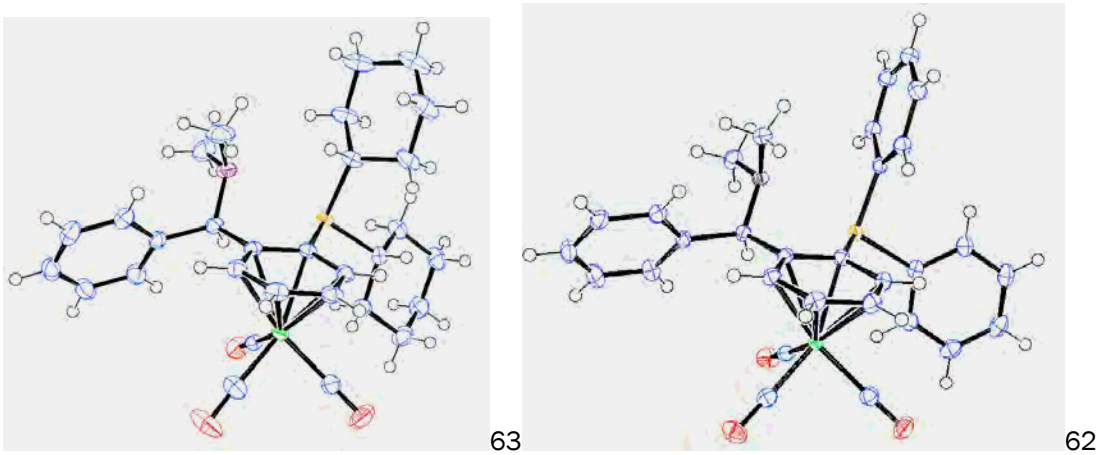

63 62

Figure 3-7: X-ray crystal structure of **63** (left), compared against the structure of **62** (right). Thermal ellipsoids are at 50% probability.

We next turned to a more electron-rich and bulky phosphine. However, quenching with di-*tert*-butylchlorophosphine led to exclusive isolation of the starting material, even after allowing the phosphine quenching step to proceed for 24h at room temperature. It seems that the two *tert*-butyl groups make the chlorophosphine simply too bulky to react with the organolithium intermediate. A slightly smaller ligand, the non-symmetrical racemic *tert*-butylchlorophenylphosphine, was used, in hopes that a diastereoselective quench of the lithiated species would result. However, this electrophile was also unsuccessful. In order to expand this ligand family using the phosphine center, it is likely that a smaller chlorophosphine electrophile will be necessary. Alternately, using diarylchlorophosphines with more electron-rich or electron-poor substitution on the two aryl groups would lead to ligands with tunable electronics and sterics. Further exploration on the synthesis of ligands with phosphine variants is ongoing.

The variation of this ligand class by changing the identity of the tertiary amine also unfortunately met with difficulties. In the case of morpholino- or piperidino- substituted chiral diarylmethylamines **55e** and **57**, using "s&n" base conditions and quenching with either chlorodicylohexylphosphine or chlorodiphenylphosphine led to isolation of starting material only. As in the earlier case of the dimethylbenzylamine derivative, we asked ourselves whether the complex was deprotonating and failing to quench due to steric reasons, or if the complex was not deprotonating in the first place. Unfortunately, deutherum quenches with either of these substrates showed no detectable incorporation of D in the molecule (determined by integration of $^{1}$H NMR). Apparently even the "s&n" superbase, which had been highly successful in the

dimethyl-substituted tertiary amine, was not effective here. In the case of the morpholino complex, using higher equivalents or allowing the temperature to raise above 0 °C merely led to slow conversion of the starting material to decomposition products, likely due to the base attacking the more acidic protons next to the morpholno oxygen. A different base or superbase may be required to open access to ligands with different amine substitution.

### *Synthesis of palladium-bound precatalysts from P∧N ligands*

Planar-chiral metal-coordinated P∧N ligands with ferrocene- and (arene)tricarbonylchromium-scaffolds are known to bind to catalytically active metals, such as palladium(II) and rhodium(I), and a limited number of crystal structures have been determined. In most cases, these ligands bind to the metal center in a bidentate fashion, through both the P and N donor atoms. We expected that a convenient palladium-bound precatalyst could be synthesized by combining our diarylmethylamine phosphine ligand with a simple palladium precatalyst.

Initially, the palladium(II) complex with norbornadiene [$PdCl_2$(norb)] was chosen, due to the low boiling point of norbornadiene, which would allow easy removal of the displaced neutral ligand. Thus, a 1:1 mixture of bright yellow ligand **62** was combined with $PdCl_2$[norb] in THF at room temperature to yield a deep orange solution, which upon evaporation of solvent provided the red-orange palladium-complexed **64**. However, THF proved to be difficult to remove completely, and subsequent syntheses of palladium bound complex **64** relied upon DCM as the solvent. The ligand-displacement reaction in DCM went rapidly (<1 h), and traces of solvent were easily removed under reduced pressure to yield desired 1:1 complex in quantitative (95%) yield. The dicyclohexylphosphine-substituted ligand **63** was also complexed to palladium using the same procedure as above to yield **65**.

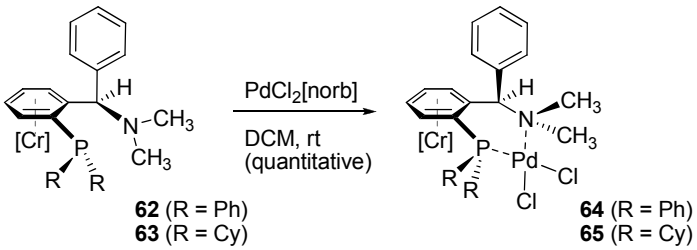


Scheme 3-5: Coordination of (arene)tricarbonylchromium PN ligands **62** and **63** with a palladium (II) source to yield pallaldium-bound complexes **64** and **65** in good (93–95%) yield.

In both complexes **64** and **65**, The coordination of the nitrogen to the palladium center was supported by the presence of diasterotopic amine methyl resonances observed in $^{1}$H NMR. We worked to verify this observation with a crystal structure. However, while the ligand **62** (like many tricarbonylchromium complexes) is a highly crystalline solid, the amorphous orange powder **64** proved extremely difficult to crystallize. X-ray diffraction-quality crystals were finally obtained using slow evaporation from a DCM solution at 0°C, and the binding of the ligand at both P and N donor sites was confirmed (Figure 3-8, see full report on pg. 318).

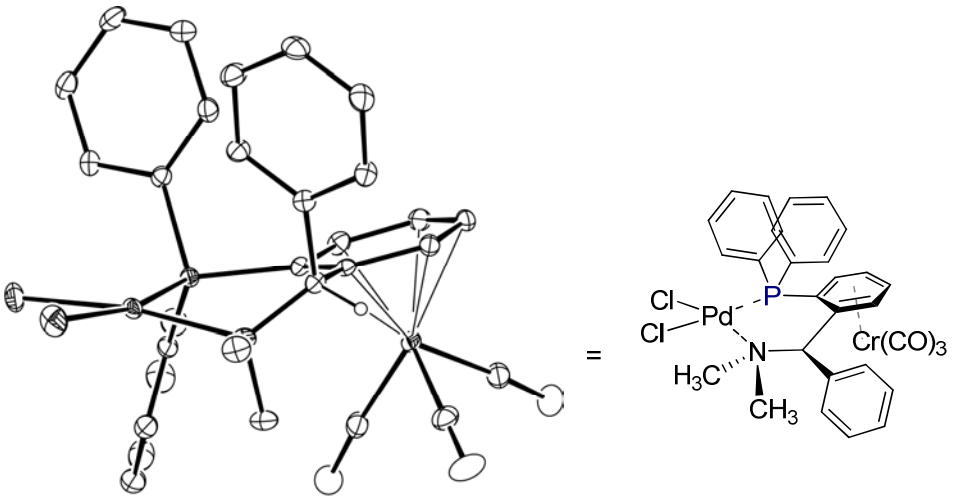


Figure 3-8: X-ray crystal structure of **64**. Thermal ellipsoids are at 50% probability.

*Comparison with existing complexes*

First, the structure of our new phosphine-amine ligand **62** is compared against the crystal structure of an α-methyl substituted diphosphine tricarbonylchromium ligand (Daniphos), Figure 3-9, below. The left-hand side of the chromium complexes show very different geometries.

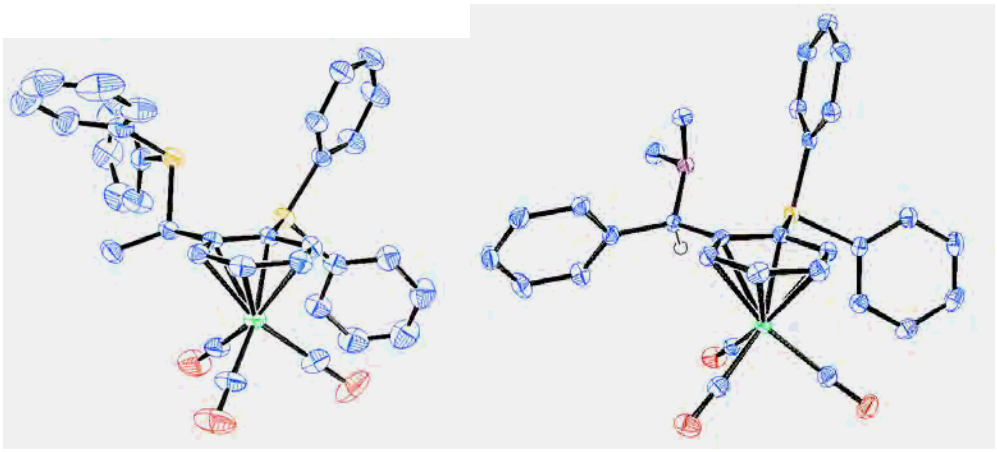

Figure 3-9: Comparision of two (arene)tricarbonylchromium ligands. Daniphos, a bis phosphine ligand derived from ligand precursor **A** (Figure 3-3), left, is compared against the new α-phenyl substituted PN ligand **62**, right. Non-benzylic hydrogens are omitted for clarity.

Next, the ligands are compared against each other upon coordination to a square-planar metal center. The α-methyl substituted diphosphine ligand Daniphos complexed to a pseudo-square planar rhodium[23] center is compared against the palladium-complexed precatalyst **64**. The geometry of the 6-membered ring comprising the substituted benzylic (arene)tricarbonylchromium ring carbons, benzylic carbon, two donor ligands, and metal center is extremely different between the two complexes. The comparisons are illustrated in Figure 3-10 (side view) and Figure 3-11 (front view) below. This difference in geometry around the metal center is likely due to the very large difference in steric demands at the benzylic center between a methyl and phenyl group interacting with the tricarbonylchromium group, which is a major influence in the geometry of the bound ligand. Considering this difference in configuration, it is likely that this new family of ligands will perform markedly different from each other in similar catalytic reactions.

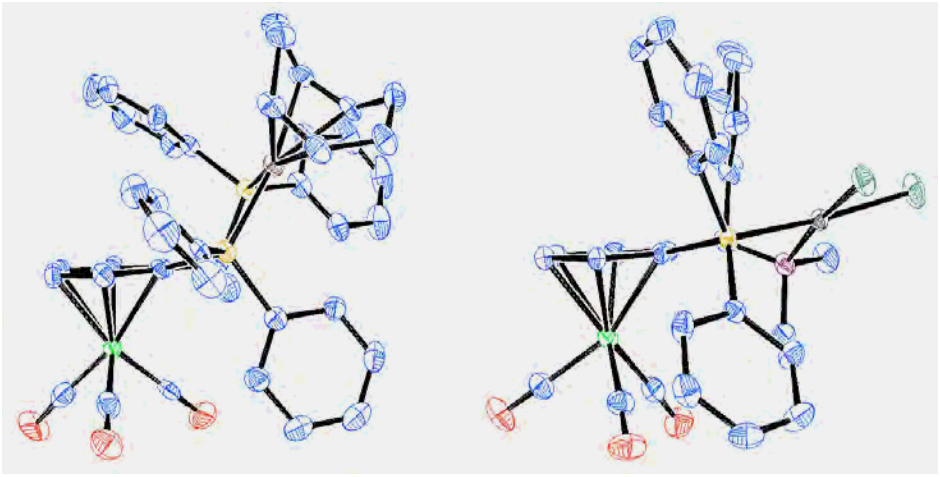

Figure 3-10: Comparision of side views of the structures of diphosphine Rh[COD]-bound ligand with α-methyl substitution on the benzylic position (left), versus the $PdCl_2$-bound PN ligand **64** with α-phenyl substitution on the benzylic position (right). Extremely different geometries are observed, despite both catalyst metal centers having pseudo-square planar configuration. Hydrogens are omitted for clarity.

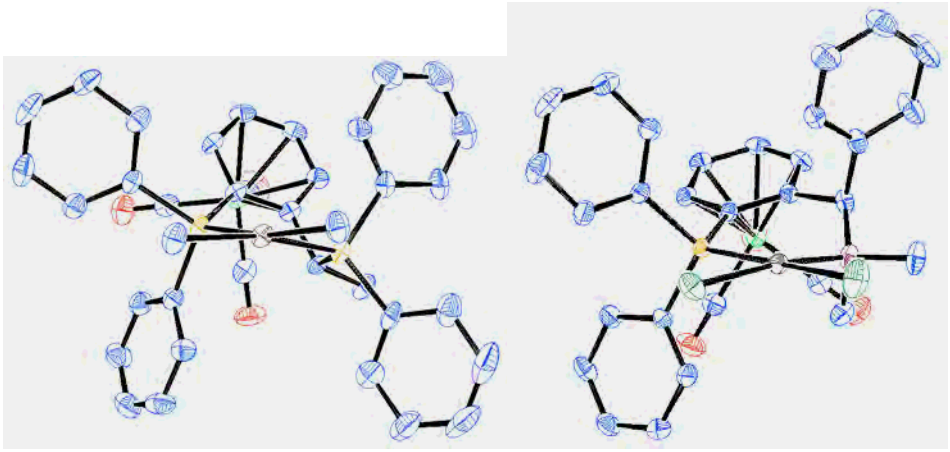

Figure 3-11: Comparison of front views of the structures of diphosphine Rh[COD]-bound ligand with α-methyl substitution on the benzylic position (Daniphos, left), versus PN ligand bound $PdCl_2$ complex with α–phenyl substitution **64** (right). Hydrogens and COD on rhodium are omitted for clarity.

The structure of the palladium-bound PΛN ligand developed by Uemura and coworkers (the ligand is shown in Figure 3-3, p.123) is also desired for comparison with our palladium-bound complex (**64**), but its X-ray crystal structure had not previously been determined. It is currently being synthesized based on existing literature procedure[12] in order to obtain crystallographic data that could provide a more direct structural comparision.

## Application of PΛN Ligands in Asymmetric Reaction[a]

As noted earlier, the existing enantioenriched α-methyl substituted ferrocenyl and tricarbonylchromium analogues of ligands **62** and **63** have been successfully used in a variety of reactions, ranging from hydrogenation and asymmetric addition reactions to allylic alkylation and cross-coupling processes with high enantioselectivity. The palladium-bound precatalysts **64** and **65** were employed in a test reaction to determine if catalytic activity and (ideally) some level of enantioselectivity could be obtained from reactions utilizing these new catalysts.

### *Palladium-catalyzed allylic alkylation reaction*

A well-used test reaction, the enantioselective allylic allylic alkylation reaction, was used to examine the catalytic activity of the new asymmetric ligand. The α-methyl substituted analogue (Uemura's ligand) has been known to be a successful catalyst for these reactions.[13] Thus, 1,3-diphenyl-1-acetoxypropene (compound **66**) was reacted with sodium dimethyl malonate (**67-Na**) using ligand **62** bound to palladium (catalyst **64**). The catalyst showed good activity at room temperature, and the allylation product (*E*)-dimethyl 2-(1,3-diphenylallyl)malonate **68** was successfully obtained in 82% yield. The ee for this reaction was only 15%, a very different value of selectivity compared with Uemura's α–methyl substituted analogue. However, more data is necessary before further conclusions can be made.

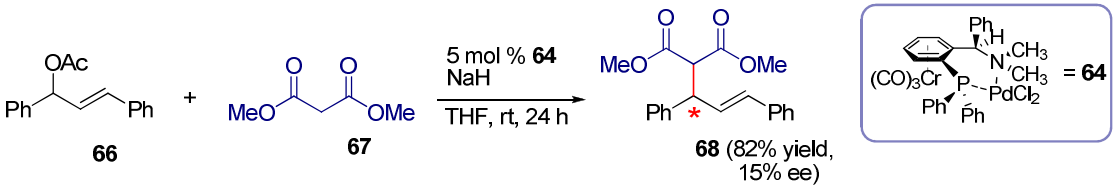


[a] Palladium-catalyzed reactions using **64** and **65** were done in collaboration with graduate researcher J. Zhang.

Scheme 3-6: Attempted asymmetric allylation reaction using **66** and **67-Na** to give **68**.

### *Asymmetric Kumada or Negishi coupling reactions*

It seems that choosing catalytic asymmetric reactions in which Uemura's ligands were not optimal would be a better illustrator of the different activity of our new catalyst. The asymmetric Kumada and Negishi couplings of secondary benzylic Grignard reagents with vinyl bromides had been attempted by Uemura and coworkers.[11] In this case, the enantioselectivities of their palladium-bound PΛN catalyst was 13-61%, depending on the main group metal (Mg or Zn) used in the coupling partner and on the identity of the vinyl. Work is underway to compare this reaction, as well as several others.[24]

### *Summary and Conclusions*

In summary, we have successfully demonstrated the synthesis of the first members of a new family of PΛN ligands incorporating both planar chirality and at least one central chiral center. While the starting diarylmethylamine complex was inert to most typical deprotonation protocols, a novel mixed butyllithium superbase nicknamed "s&n" was developed. This new superbase effects clean and diastereoselective deprotonation of the parent complex, allowing a subsequent quench with chlorophosphine electrophiles to generate a bidentate asymmetric PΛN ligand. These ligands could be easily combined with a simple palladium(II) source to form a 1:1 Pd:L complex bound through both P and N donor atoms. Work is currently bing carried out to expand the members of the ligand family, as well as test these ligands in various metal-catalyzed reactions to gauge their utility in asymmetric catalysis.

"Work to develop the next GenPhos are ongoing" –J.Z.

## Experimental Section

### General methods.

Reactions were performed under nitrogen or argon using oven-dried glassware and oven-dried vials fitted with PTFE-lined septum caps. Air- and moisture- sensitive solutions were handled under nitrogen or argon and transferred via syringe. Dry THF and diethyl ether were freshly distilled from Na/benzophenone ketyl. Dry toluene and hexanes were drawn from a Grubbs column. Unless otherwise stated, reagents were commercially available and used as purchased without further purification. Chemicals were obtained from Sigma-Aldrich, Acros, or Strem, and used as received; solvents were purchased from Fisher Scientific. Reactions were monitored by thin-layer chromatography using Whatman Partisil® K6F 250 μm precoated 60 Å silica gel plates and visualized by short-wave ultra-violet light as well as by treatment with potassium permanganate ($KMnO_4$) or ceric ammonium molybdate (CAM) stain. NMR spectra were recorded in $CDCl_3$ on either a Bruker 300 MHz or 500 MHz Fourier-transform spectrometer. Chemical shifts are reported in ppm referenced to tetramethylsilane (TMS) or the $CHCl_3$ solvent residual peak at 7.26 ppm for $^1H$ and 77.23 ppm for $^{13}C\{^1H\}$; $^{19}F$ peaks were referenced to an external standard of trifluoroacetic acid in $CDCl_3$ at −76.55 ppm. Infrared spectra were obtained on NaCl plates using a Perkin-Elmer Spectrum 100 Series FTIR spectrometer. Optical rotations were recorded in HPLC-grade $CHCl_3$ using a JASCO DIP-370 digital polarimeter and values were averaged over a minimum of 3 runs. Chromium-complexed masses were recorded with Electrospray + (ES+) HRMS methods to within 5 ppm, and $[M]^+$, $[MH]^+$, or $[M - Cl]^+$ was confirmed by the presence of the characteristic isotope patterns. Non-chromium-complexed mass was recorded with Chemical Ionization + (CI+) HRMS methods to within 5 ppm, and $[M]^+$ was observed.

Compound **27**, **53**, and **54** were prepared according to general literature procedure for the synthesis of arene tricarbonylchromium complexes from $Cr(CO)_6$ and parent arene (See Chapter 2, p 103).[25,26] Compound **28a**, **55e**, and **57** were prepared using our method for the asymmetric synthesis of diarylmethylamines (see Chapter 2). Racemic 1,3-diphenyl-1-acetoxypropene (**66**) was prepared according to the general literature procedure.[27]

**Caution:** Care should be taken to avoid direct light exposure of reactions, as arene tricarbonylchromium complexes can decompose in solution under bright light and air. In crystalline solid form, complexes are reasonably stable to light and can be stored at room temperature in air.

General procedure 3-A: Small-scale synthesis of PʌN ligands by directed *ortho*-lithiation and phosphine quench.

*Ligand syntheses*: due to the precious nature of the chiral starting materials, the reactions were generally run on 20 mg scale (about 60 µmol). Argon was used as an inert gas on the Schlenk line and both the diethyl ether and the hexane used as solvents were dried on a Grubb's type solvent system (SDS). Hexanes were degassed by 3 freeze/thaw cycles and stored under argon. The reaction was kept away from light by using aluminum foil to avoid decomposition of the chromium complex.

A typical procedure is described below:

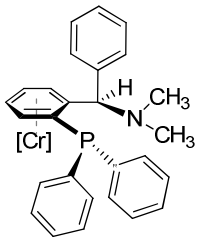


**62**: In a 4 mL vial provided with stir bar and PTFE-lined septum cap, 20 mg (58 µmol, 1 equiv) of the chromium phenyl dimethylamino compound were added and the vial was closed. An inert argon atmosphere was established with 3 vacuum/back-fill cycles through a needle inserted into the septum cap. Dry diethyl ether (300 µL) and dry hexanes (300 µL) were then added by syringe (in this order, to ensure solubility of the starting material) and the reaction mixture was cooled to -78˚C in a dry ice/acetone bath. At this temperature, 1.4 M s-buthyllithium in heptane (130 µL, 180 µmol, 3 equiv) and 2.5 M *n*-buthyllithium in hexanes (72 µL, ca. 180 µmol, 3 equiv) were added by syringe and the reaction was allowed to warm to 5–10˚C. No change in color was observed until the reaction temperature was -10˚C when the solution started to turn from bright yellow to orange to amber at the final temperature, which was indicative of the *ortho*-lithiation occurring. The vial was kept at 5–10˚C for an additional 2 h. Chlorodiphenylphosphine (108 µL, 600 µmol, 4 equiv. excess) was added neat, and the reaction was allowed to warm to room temperature for 4 h under argon. The mixture was quenched with 1 mL DI water and extracted with five 2 mL-portions of diethyl ether. The organic layers were combined, dried over $MgSO_4$, filtered through filter paper, and then evaporated and purified on a short alumina column using diethyl ether as eluent. The solvent was removed and the solids were dissolved in a 10:1 hexane:dichloromethane mixture and placed in a -30˚C freezer. X-ray quality single crystals grew over 3-4 days (see full report for **62** on p. 297). Yields are around 45%. **$^1$H NMR** (300 MHz, $CDCl_3$) δ: 7.50 - 7.45 (m, 2H), 7.42 - 7.32 (m, 13H), 5.36 (t, J = 6.4 Hz, 1H), 5.32 (d, J = 5.2 Hz, 1H), 5.14 - 5.10 (m, 2H), 4.98 (dt, J = 1.2, 6.4 Hz, 1H), 1.72 (s, 6H) ppm. **$^{13}$C{$^1$H} NMR** (125 MHz, $CDCl_3$) δ: 232.5, 137.1 (d, $J_{CP}$ = 4.6 Hz), 136.8 (d, $J_{CP}$ = 16.0 Hz), 135.5, 134.8 (d, $J_{CP}$ = 19.5 Hz), 132.9 (d, $J_{CP}$ = 21.7 Hz), 130.2, 129.1, 128.7, 128.58, 128.57 (d, $J_{CP}$ = 5.4 Hz), 128.44 (d, $J_{CP}$ = 8.3 Hz, 128.2, 120.0 (d, $J_{CP}$ = 18.6 Hz), 106.0 (d, $J_{CP}$ = 25.2 Hz), 99.5 (d, $J_{CP}$ = 3.8 Hz), 93.1, 91.6 (d, $J_{CP}$ = 3.8 Hz), 90.9 (d, $J_{CP}$ = 2.2 Hz), 69.6 (d, $J_{CP}$ = 13.2 Hz), 40.0 ppm. {CHECK} **$^{31}$P{$^1$H} NMR** (121 MHz,

$CDCl_3$) δ ⁻13.0 ppm; **IR** 3054, 2961, 2926, 2855, 2827, 2784, 1964 and 1885 (strong CO stretches), 1434, 1092, 1027, 877, 745, 698, 661, 621 $cm^{-1}$. **HRMS** (ES+) calc'd for $C_{30}H_{26}CrNO_3P$ 531.1055, found 532.1144 $[MH]^+$.

### General procedure 3-B: larger-scale modification of ligand synthesis.

A 4 dram screw-capped vial was charged with PTFE stirbar and **28a** (104 mg, 0.3 mmol, 1 equiv) and purged with Nitrogen. Diethyl ether (2 ml) and hexanes (2 mL) were added in succession, resulting in a clear, deep yellow solution. The reaction was cooled to −78 °C and sec-butyllithium (0.43 mL, 1.4 M, 0.60 mmol, 2 equiv) and then n-butyllithium (0.24 ml, 2.5 M, 0.60 mmol, 2 equiv) were added and slowly warmed to −20 °C over 1.2 h. The reaction was cooled to −40 °C, and chlorodiphenylphosphine (0.3 mL, 1.6 mmol, 5.3 equiv) was added to the reaction and allowed to stir for an additional 2 hours warming to 5 °C. The cloudy deep red/brown mixture was quenched with 1.5 mL of saturated aqueous $NaHCO_3$ and diluted with 2 mL diethyl ether. The layers were separated, and the aqueous layer was extracted three times with 3 mL diethyl ether, then the combined organic layers were dried over anhydrous $Na_2SO_4$ and filtered over a plug of silica. The resulting solution was concentrated under vacuo and then purified over silica gel using 20% diethyl ether in hexanes to yield **62** (73.5 mg, 0.138 mmol, 46% yield) after recrystallization. Characterization data is in agreement with spectra obtained using General procedure 3-A.

### General procedure 3-C for enantioenrichment of Cr-coordinated diarylmethylamine starting material.

After chromatography, complex **(*R*)-(−)-28a** (74–88% ee) was enantioenriched by crystallization. The complex was dissolved in a minimum (~0.2–0.4 mL per 50 mg) of dichloromethane, and then hexanes are added slowly (1.6–3.0 mL per 50 mg). Upon crystallization overnight in a −16 °C freezer, long yellow prisms of the homochiral material **(*R*)-(−)-28a** were obtained in high purity after the mother liquor is decanted (typically ≥97% ee is obtained, verified by re-dissolution of the entire crystalline sample and analysis by SFC, typically 30 – 50% isolated yield). **28a** obtained from the decanted mother liquor exhibits low ee as expected (10–45%); this material was used for test reactions with various chlorophosphines.

When highly enantioenriched diarylmethylamine (≥97% ee) is used for PΛN ligand starting material, crystallized ligand appears to be a single enantiomer by SFC analysis.

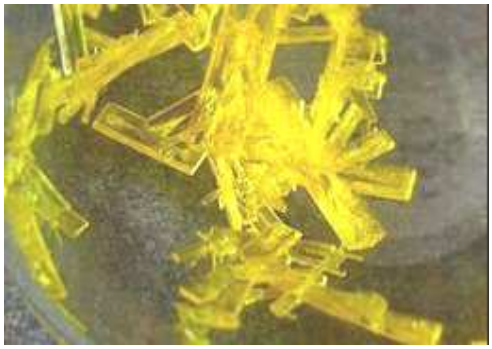

Figure 3-12: Nearly enantiopure diarylmethylamine (*R*)-(−)-**28a** (≥97% ee after dissolution of crystals and analysis on chiral SFC) can be isolated through a single recrystallization.

General procedure 3-D: Synthesis of palladium-bound PʌN ligand complexes.

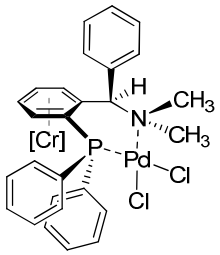


**64** (Using THF): In a nitrogen-filled glovebox, a sample of the diphenylphosphine-derivative of the PʌN ligand (**62**, 27 mg, 0.050 mmol, 1.0 equiv) was combined with $PdCl_2$[norbornadiene] (13 mg, 0.05 mmol, 1.0 equiv). To the solids, dry THF (3 mL) was added with stirring, and the suspension quickly became orange as the palladium source dissolves (the reaction is exothermic, which likely helps with the dissolution of palladium source). The reaction was stirred for 1 h and then the solvent was removed from the reddish solution *in vacuo*. A higher than expected mass (36 mg, 35 mg theor.) and $^1$H NMR indicated persistent presence of THF in the product. Rinsing the complex with dry diethyl ether and stripping solvent under vacuum led to **64** as a powdery orange solid in approximately quantitative yield. **$^1$H NMR** (500 MHz, $CDCl_3$) δ: 8.69 (ddd, *J* = 1.5, 7.9, 13.0 Hz, 2H), 7.78 – 7.73 (m, 3H), 7.60 (dd, *J* = 7.6, 12.7 Hz, 2H), 7.56 – 7.53 (m, 1H), 7.45 – 7.35 (m, 6H), 5.63 (t, *J* = 6.4 Hz, 1H), 5.41 (dd, *J* = 2.7, 6.4 Hz, 1H), 5.15 (t, *J* = 6.2 Hz, 1H), 5.05 (t, *J* = 6.3 Hz, 1H), 4.64 (d, *J* = 1.9 Hz, 1H), 3.16 (s, 3H), 3.11 (s, 3H) ppm; **$^{13}$C{$^1$H} NMR** (125 MHz, $CDCl_3$) δ: 229.6, 136.4 (d, $J_{CP}$ = 1.0 Hz), 134.9 (d, $J_{CP}$ = 10.0 Hz) 133.6 (d, $J_{CP}$ = 2 Hz), 132.3, 132.1 (d, $J_{CP}$ = 2.4 Hz), 130.3, 129.7, 129.6, 129.5, 128.8 (d, $J_{CP}$ = 8.1 Hz), 127.1 (d, $J_{CP}$ = 68 Hz), 126.1 (d, $J_{CP}$ = 55 Hz), 112.4 (d, $J_{CP}$ = 14.0 Hz), 97.1, 94.8, 93.6 (d, $J_{CP}$ = 35.3 Hz), 89.4 (d, $J_{CP}$ = 6.3 Hz), 87.9, 76.5 (d, $J_{CP}$ = 9.5 Hz), 53.6, 47.7 ppm; **$^{31}$P{$^1$H} NMR** (MHz, $CDCl_3$) δ: 24.9 (s) ppm; **HRMS** (CI+) calc'd. for $C_{30}H_{26}NO_3ClCrPdP$ 671.9779, found 671.9785 $[M - Cl]^+$. $[\alpha]_D^{26}$ = −18.0° (c = 0.50, $CHCl_3$) for a ≥98 %*ee* sample. *X-ray crystal structure was determined for the racemic compound, see p. 318.*

**64** (Alternately, using DCM): In a nitrogen-filled glovebox, a sample of the diphenylphosphine-derivative of the PʌN ligand (**62**, 24 mg, 0.045 mmol, 1.0 equiv) was combined with $PdCl_2$[norbornadiene] (12 mg, 0.045 mmol, 1.0 equiv) and dissolved in methylene chloride (3.0 mL). The resulting bright red-orange solution was stirred for 1.5 h under a nitrogen atmosphere. Hexanes (3 mL) were added to the solution while stirring, and a suspension formed. The solvent was then evaporated with a stream of dry nitrogen. Compound **64** was obtained as a powedery orange solid (30 mg, 0.042 mmol, 93% yield). Characterization data is consistent with the spectra obtained from **64** synthesized using THF as solvent.

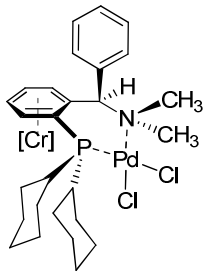


**65**: In a nitrogen-filled glovebox, a sample of the dicyclohexylphosphine-derivative of the PʌN ligand (**63**, 21 mg, 0.039 mmol, 1.0 equiv.) was combined with $PdCl_2$[norbornadiene] (10 mg, 0.039 mmol, 1.0 equiv) in 3 mL THF and stirred for 1.5 h under a nitrogen atmosphere. Compound **65** was obtained as a pale orange powdery solid in 95% yield (27 mg, 0.037 mmol) after redissolving the sticky solid in 1 mL methylene chloride, and re-evaporation of the solvent over a stream of dry nitrogen. **HRMS** (CI+) calc'd. for $C_{30}H_{36}NO_3ClCrPdP$ 684.0718, found 684.0726 $[M-Cl]^+$.

General procedure 3-E: Procedure for attempted asymmetric allylation reaction using complex.

Asymmetric alkylation of the allyl acetate below followed the literature procedure.[13]

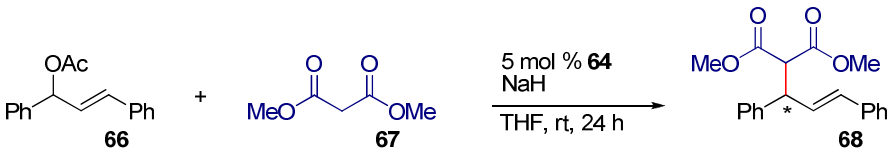


Scheme 3-7: General scheme for the asymmetric alkylation of allyl acetate **66** with malonate nucelophile to yield **68**.

**68**: To a mixture of racemic 1,3-diphenyl-1-acetoxypropene (**66**) (25.2 mg, 0.10 mmol, 1.0 equiv.) and Palldium catalyst (**64**, 3.6 mg, 5 mol %) in dry THF (0.3 mL) was added a solution of sodium dimethyl malonate (prepared in situ by adding equimolar amounts of NaH (3.0 mg, 0.12 mmol) and dimethyl malonate (**67**) (14 µL, 0.12 mmol) in dry THF (0.25 mL)) at room temperature under a nitrogen atmosphere. The reaction mixture was stirred at rt for 24 h. The reaction mixture was then quenched

with 2 drops of $H_2O$, diluted with 3 mL of ethyl acetate, and filtered over a pad of $MgSO_4$ and silica gel. The pad was rinsed with additional ethyl acetate and the solution was concentrated in vacuo. The crude material was loaded onto a silica gel column and purified by flash chromatography (eluted with 5–20% ethyl acetate in hexanes) to give the product (24.5 mg, 82% yield, 15% ee) as a yellow solid. NMR spectra is consistent with the spectra of the known compound in literature the previously published data.[27]

## References


[1] (a) Dai, L.; Tu, T.; You, S.; Deng, W.; Hou, X. *Acc. Chem. Res*. **2003**, *36*, 659-667. (b) Yoon, T. P.; Jacobsen, E. N. *Science* **2003**, *299*, 1691-1693.

[2] Interestingly, if only the planar chirality of the highly successful planar- and central- chiral ligand Josiphos is reversed from ($R$,$S_P$) while preserving the central chiral center to give ($R$,$R_P$), high enantioselecitivies of reaction have not yet been observed in any reactions, see: Štěpnička, P. In *Ferrocenes: ligands, materials and biomolecules*; J.Wiley: 2008

[3] Pfaltz, A.; Drury, W. J. *Proc. Natl. Acad. Sci. U.S.A.* **2004**, *101*, 5723-5726.

[4] Börner, A. In *Phosphorus Ligands in Asymmetric Catalysis: Synthesis and Applications*; John Wiley & Sons: 2008; .

[5] Walsh, P. J.; Kozlowski, M. C. In *Fundamentals of asymmetric catalysis*; University Science Books: 2008.

[6] Blaser, H. U.; Federsel, H.; Federsel, H. J. In *Asymmetric Catalysis on Industrial Scale: Challenges, Approaches and Solutions*; John Wiley & Sons: 2010; pp 580.

[7] Togni, A. *Angew. Chem. Int. Ed.* **1996**, *35*, 1475-1477.

[8] Dai, L. X.; Hou, X. L. In *Chiral Ferrocenes in Asymmetric Catalysis: Synthesis and Applications*; Wiley-VCH: 2009.

[9] Marquarding, D.; Klusacek, H.; Gokel, G.; Hoffmann, P.; Ugi, I. *J. Am. Chem. Soc.* **1970**, *92*, 5389-5393.

[10] Boaz, N. W. *Tetrahedron Lett.* **1989**, *30*, 2061-2064.

[11] Kamikawa, K.; Sugimoto, S.; Uemura, M. *J. Org. Chem.* **1998**, *63*, 8407-8410.

[12] Uemura, M.; Miyake, R.; Nishimura, H.; Matsumoto, Y.; Hayashi, T. *Tetrahedron: Asymmetry* **1992**, *3*, 213-216.

[13] Hayashi, Y.; Sakai, H.; Kaneta, N.; Uemura, M. *J. Organomet. Chem.* **1995**, *503*, 143-148.

[14] Vasen, D.; Salzer, A.; Gerhards, F.; Gais, H.; Sturmer, R.; Bieler, N. H.; Togni, A. *Organometallics* **2000**, *19*, 539-546.

[15] Dunina, V.; Golovan, E.; Gulyukina, N.; Grishin, Y.; Beletskaya, I. *Russ. Chem. Bull.* **1997**, *46*, 1331-1334.

[16] Rosillo, M.; Dominguez, G.; Perez-Castells, J. *Chem. Soc. Rev.* **2007**, *36*, 1589-1604.

[17] For a review on the use of tricarbonylchromium arene complexes as ligands in asymmetric catalysis, see: Bolm, C.; Muniz, K. *Chem. Soc. Rev.* **1999**, *28*, 51-59.

[18] Schlosser, M. Superbases for organic synthesis. *Pure Appl. Chem*. **1988**, *60*, 1627-1634

[19] For a review on known unimetallic superbases, see: Caubere, P. *Chem. Rev.* **1993** *93*, 2317-2334.

[20] Haag, B.; Mosrin, M.; Ila, H.; Malakhov, V.; Knochel, P. Angew. Chem. Int. Ed. **2011**, *asap*.

[21] Truong, T.; Alvarado, J.; Tran, L. D.; Daugulis, O. *Org. Lett.* **2010**, *12*, 1200-1203.

[22] Peascoe, W.; Applequist, D. E. *J. Org. Chem.* **1973**, *38*, 1510-1512.

[23] Braun, W.; Calmuschi, B.; Drexler, H.; Englert, U.; Heller, D.; Salzer, A., *Acta Crystallogr. , Sect. C: Cryst. Struct. Commun.* **2004,** *60*, m532-m536.

[24] The asymmetric Heck reaction of dihydrofurans with aryl triflates is considered another reaction in which our PN ligand may be successful, see: Hou, X.; Dong, D. X.; Yuan, K. *Tetrahedron: Asymmetry* **2004**, *15*, 2189-2191.

[25] Woolins, J. D., Ed.; In *Inorganic Experiments*; VCH: Weinheim, **1994**, 194-195.

[26] Mahaffy, C. A. L.; Pauson, P. L. *Inorg. Synth*. **1990**, *28*, 136-140.

[27] Watson, I. D. G.; Yudin, A. K. *J. Am. Chem. Soc.* **2005**, *127*, 17516.

# Appendix I

## NMR Spectra

*Triarylmethanes from CrDPM (**4a**)*

Figure I-1: $^{1}H$, $^{13}C\{^{1}H\}$ NMR spectra of **5a**.

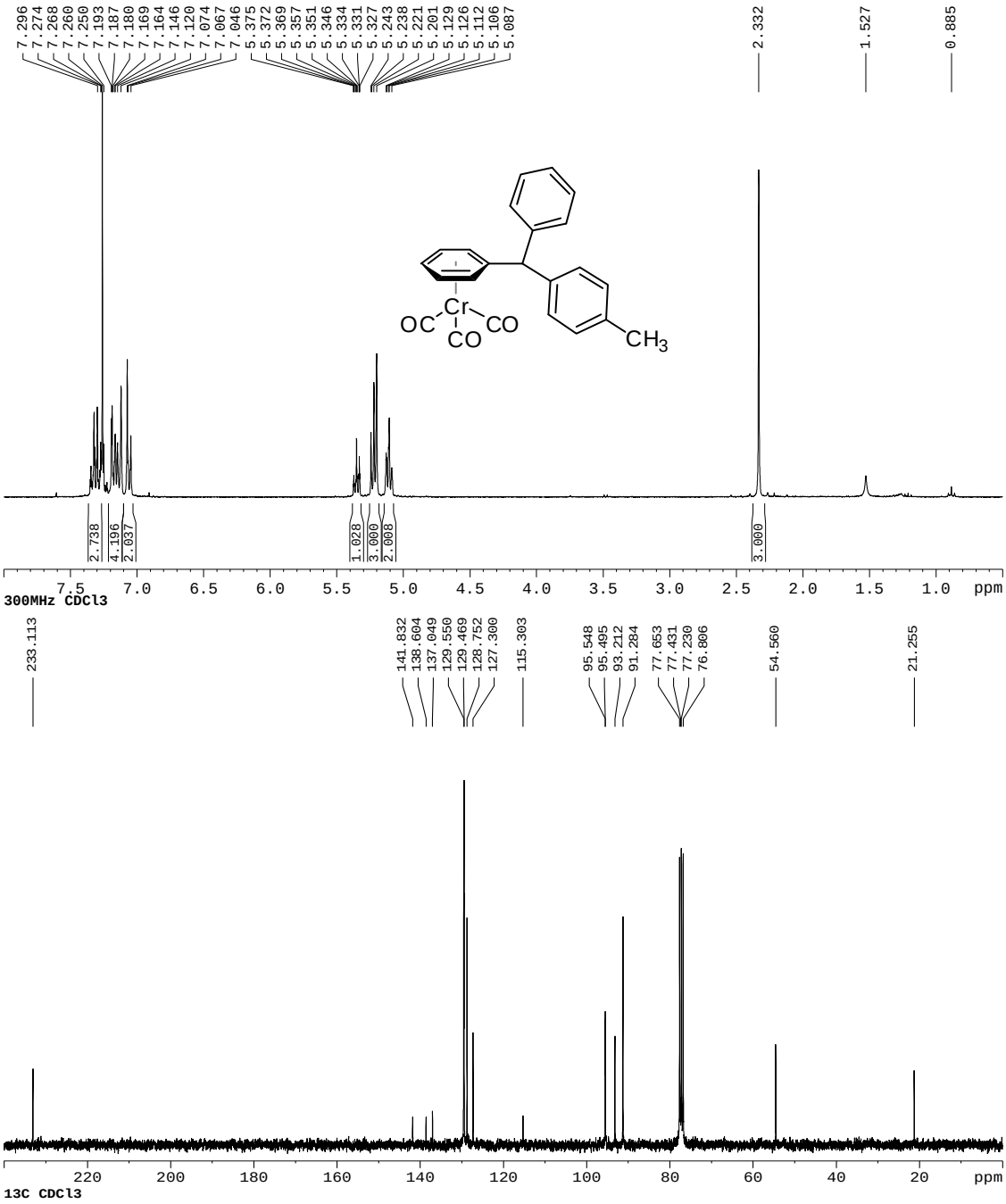

Figure I-2: $^{1}H$, $^{13}C\{^{1}H\}$ NMR spectra of **5b**.

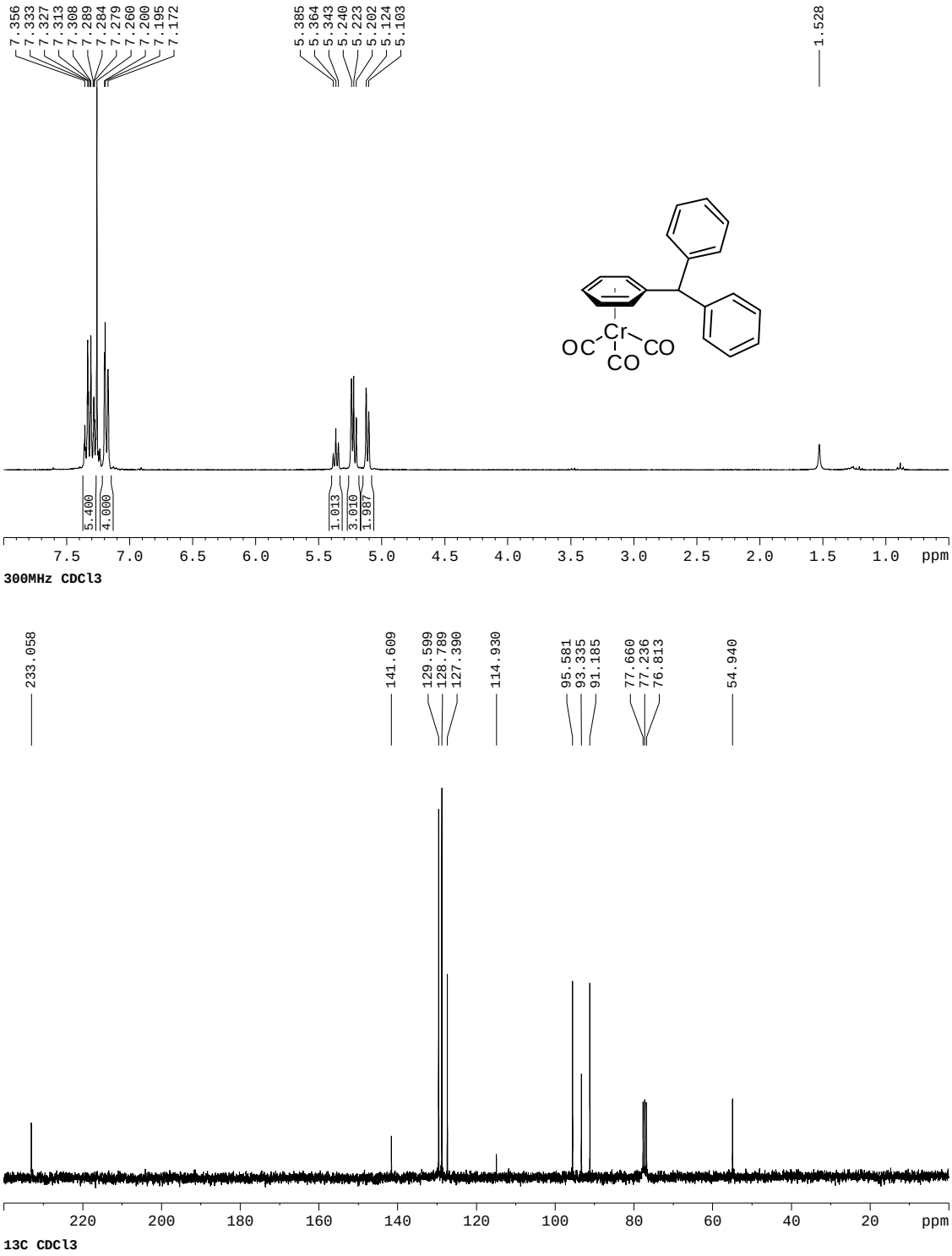

Figure I-3: $^{1}H$, $^{13}C\{^{1}H\}$NMR spectra of **5c**.

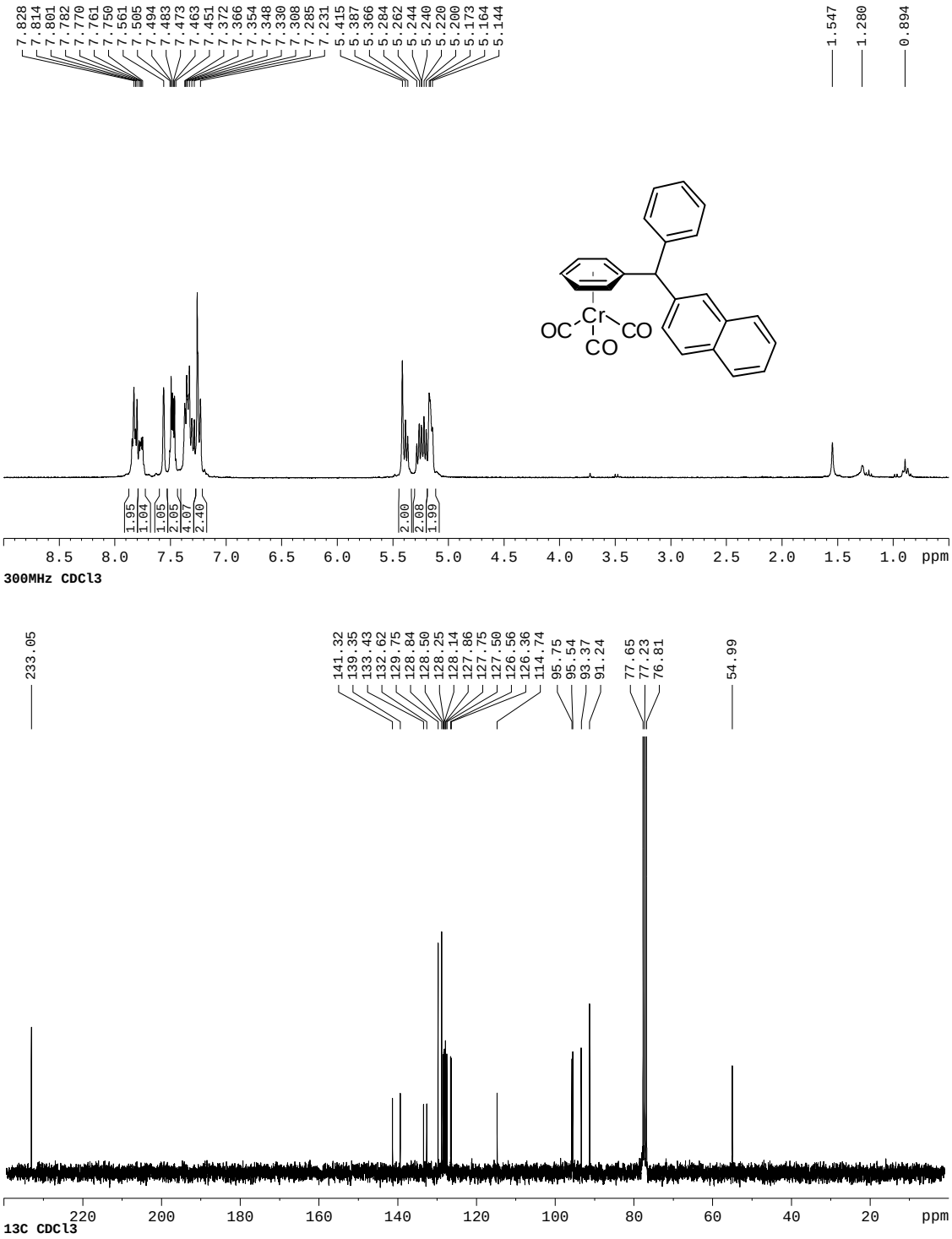

Figure I-4: $^{1}H$, $^{13}C\{^{1}H\}$ NMR spectra of **5d**.

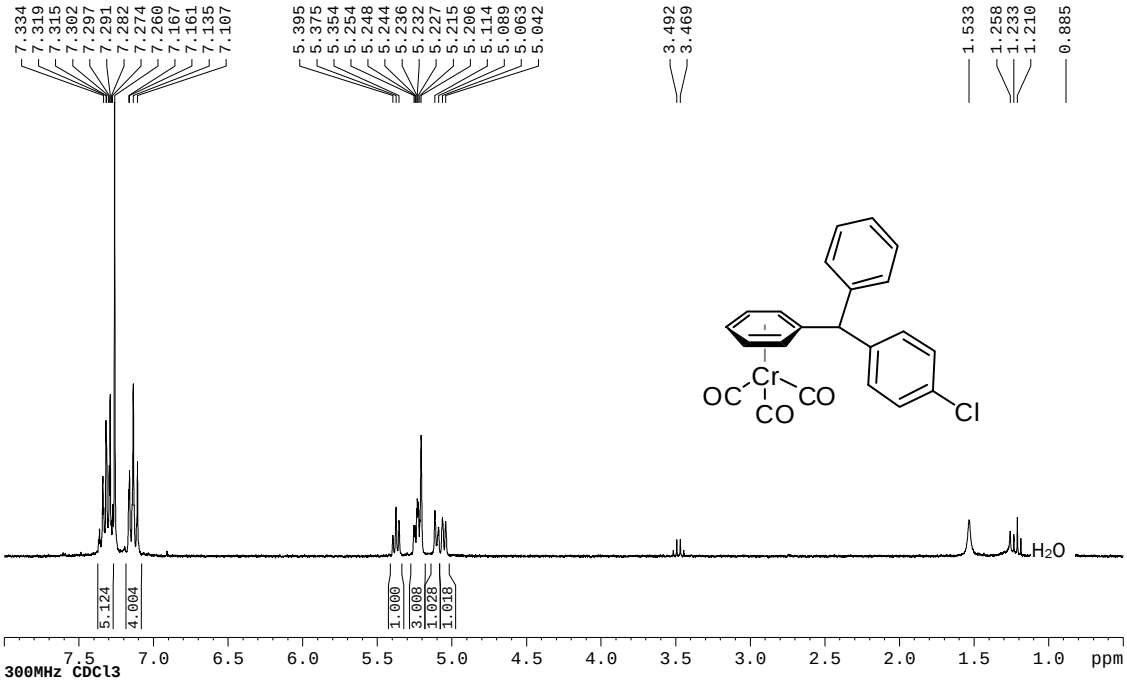


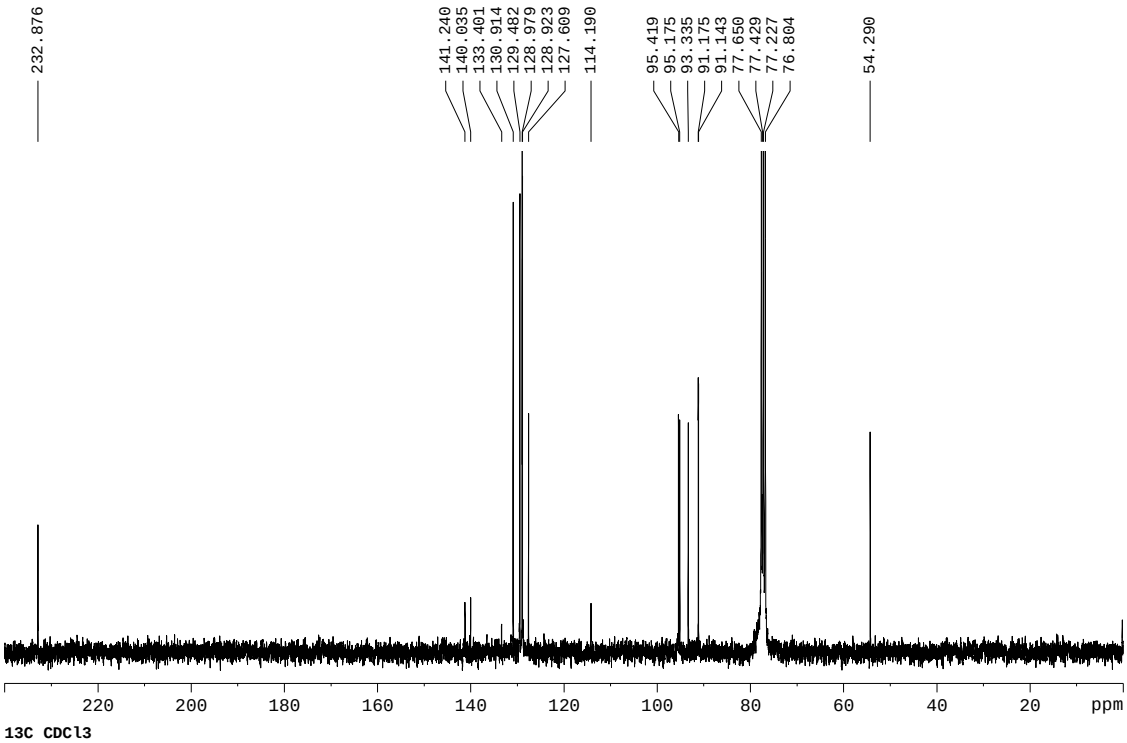

Figure I-5: $^{1}H$, $^{13}C\{^{1}H\}$, $\{^{1}H\}^{19}F$ NMR spectra of **5e**.

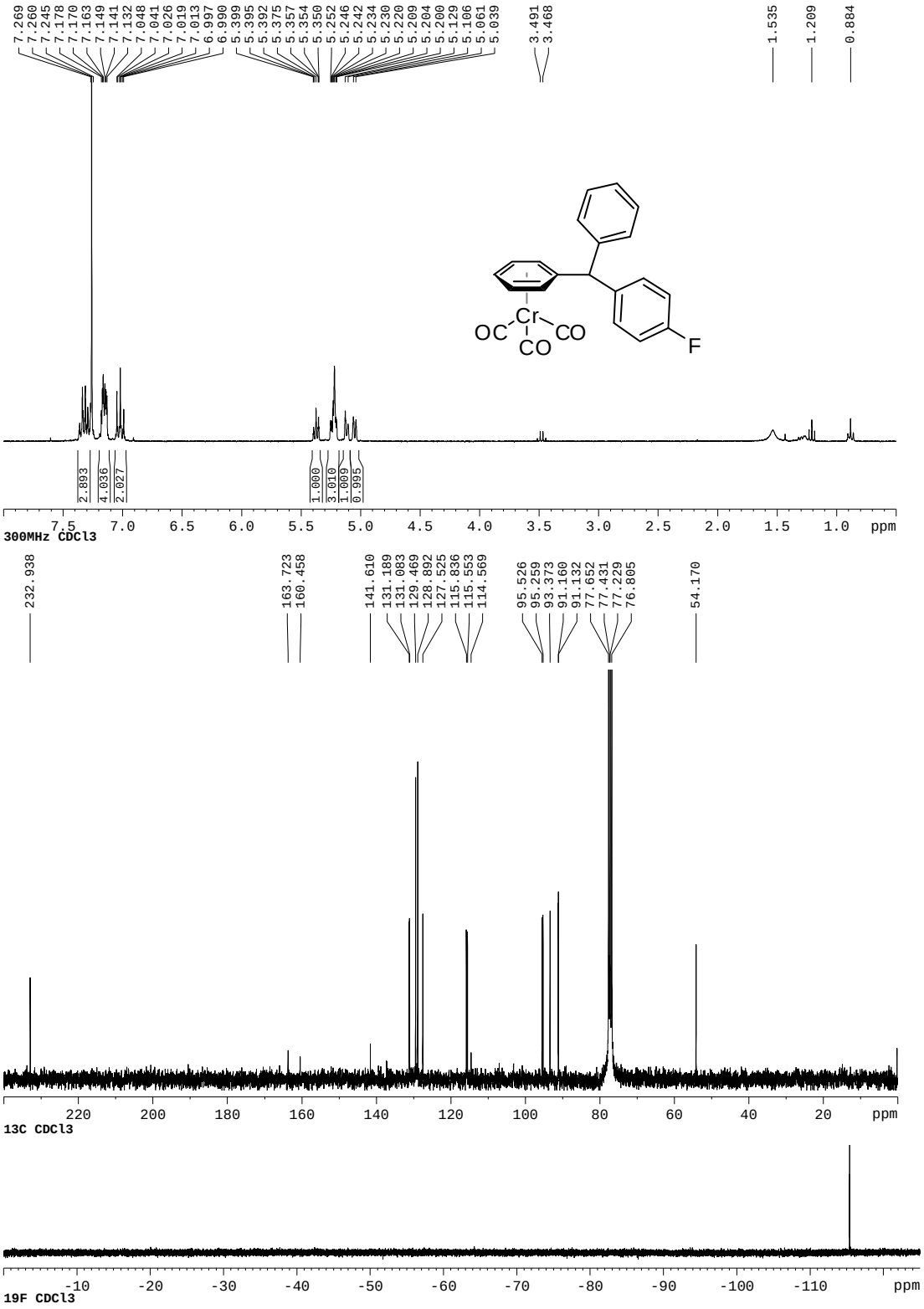

Figure I-6: $^{1}H$, $\{^{1}H\}^{19}F$ NMR spectra of **5f**.

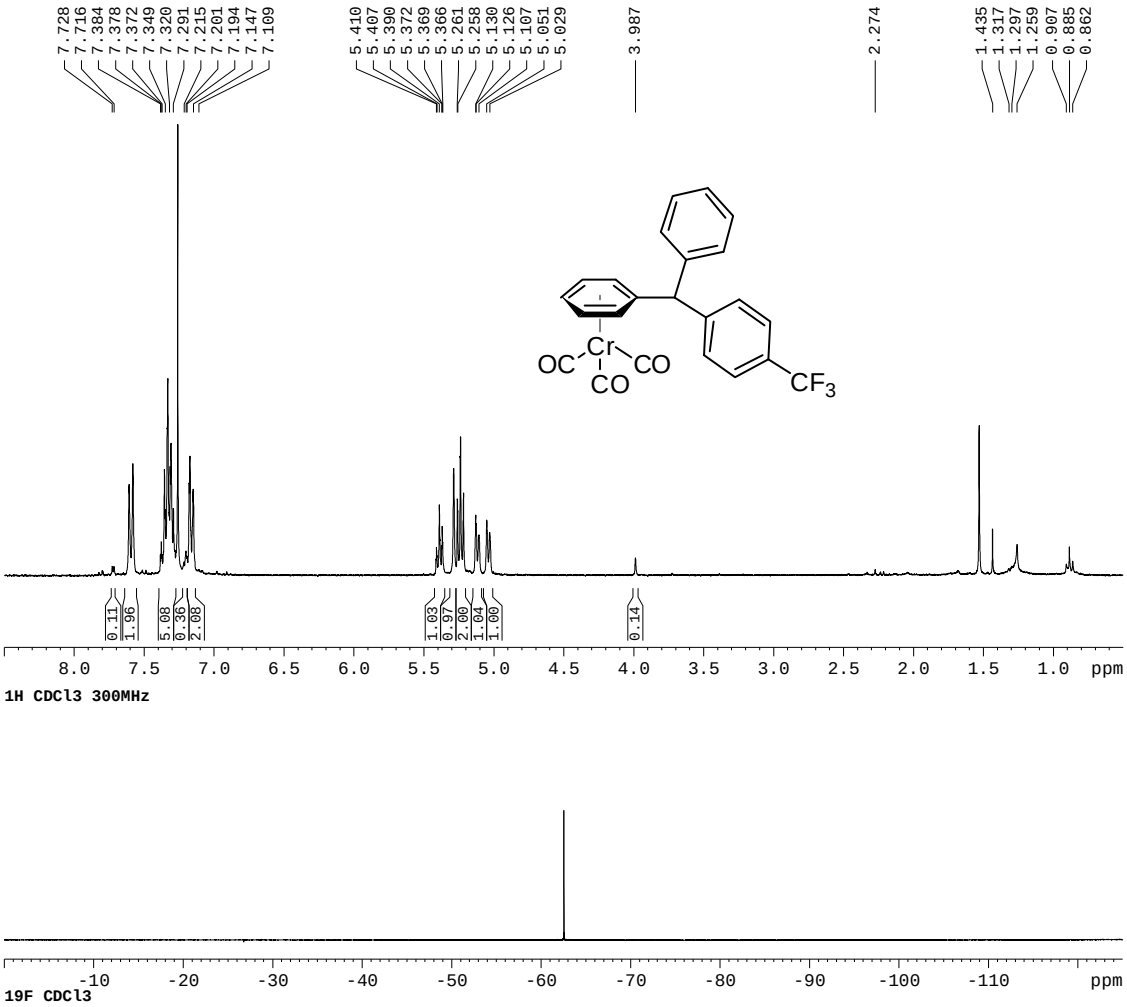

Figure I-7: $^{1}H$, $^{13}C\{^{1}H\}$ NMR spectra of **5g**.

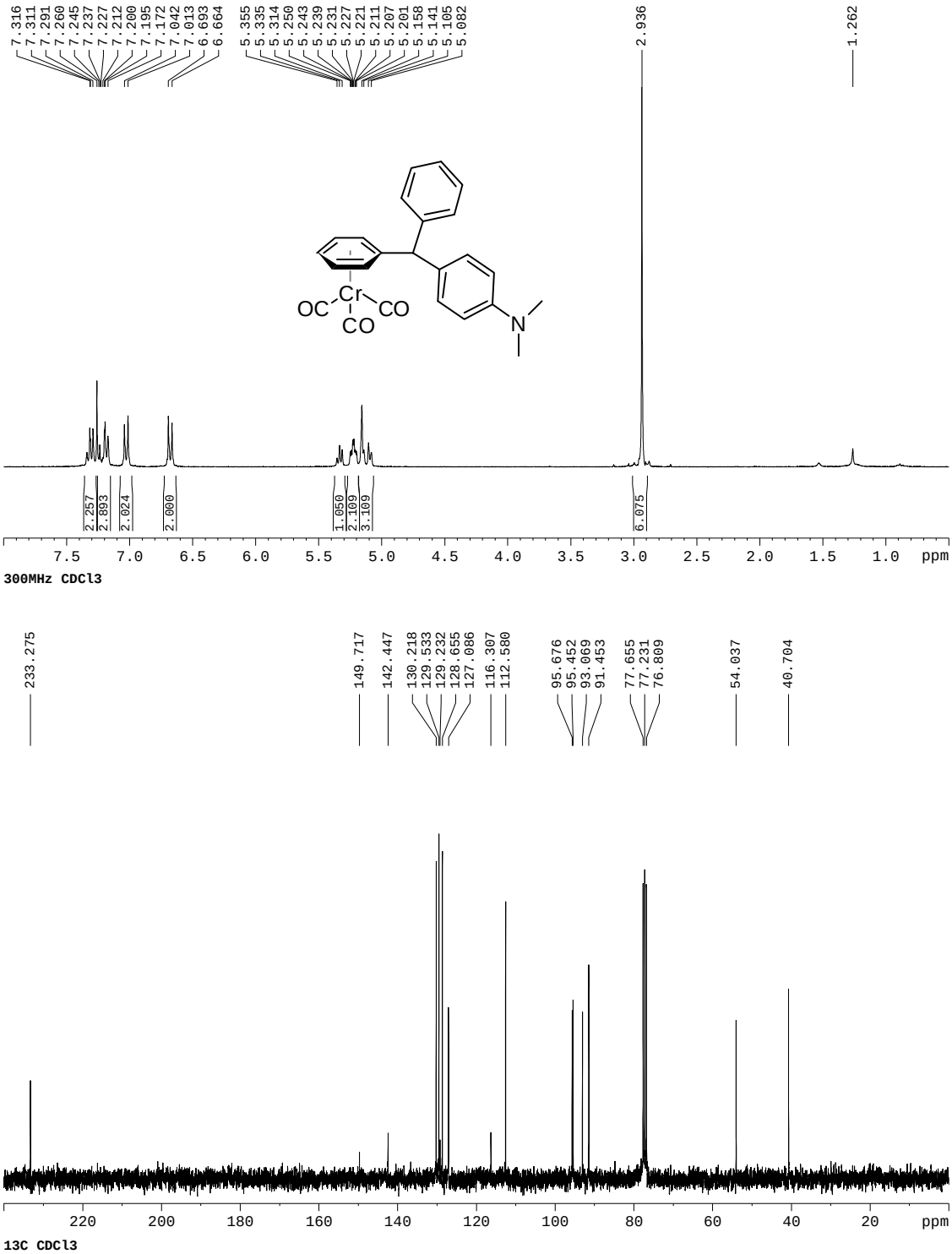

Figure I-8: $^{1}H$, $^{13}C\{^{1}H\}$ NMR spectra of **5h**.

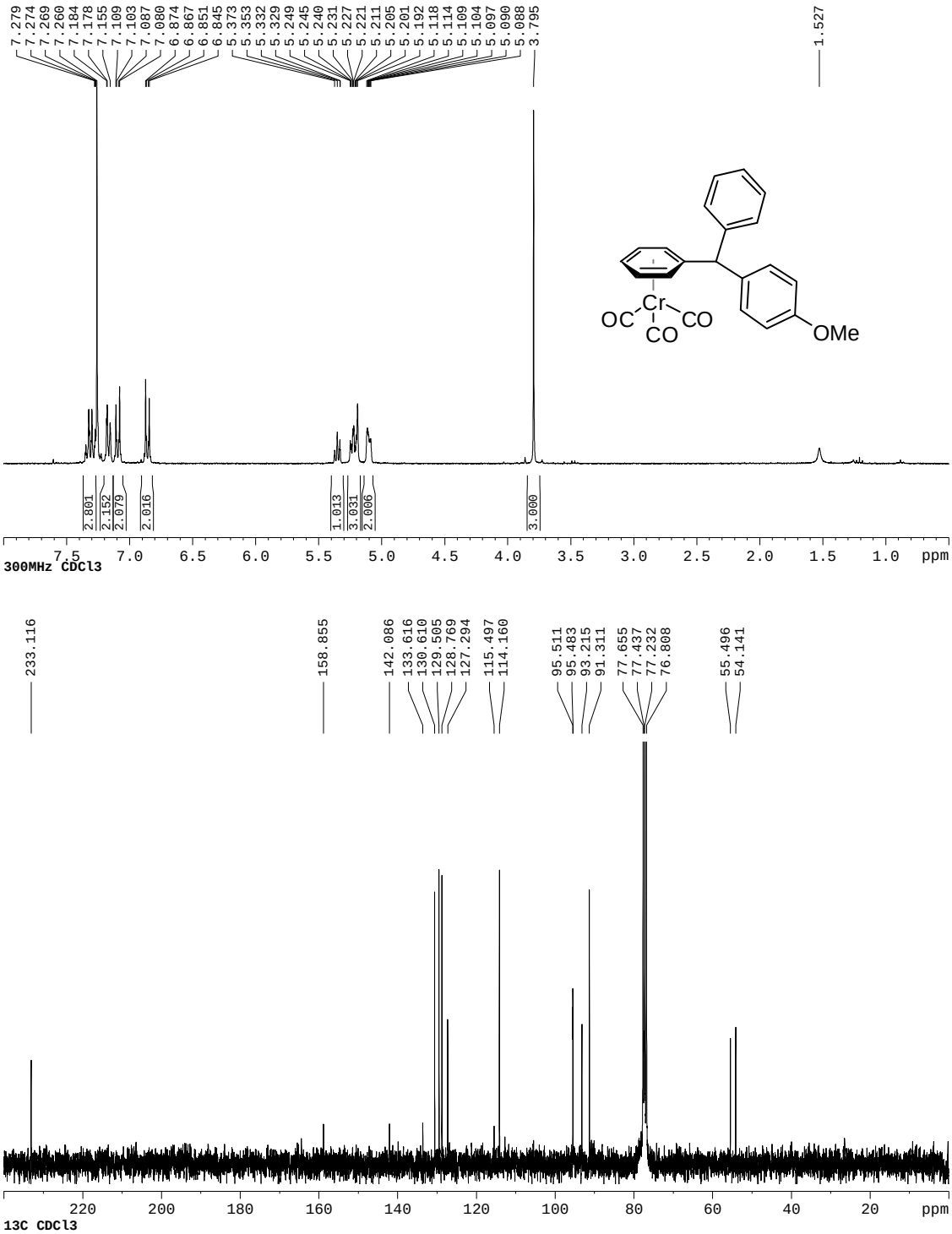

Figure I-9: $^{1}H$, $^{13}C\{^{1}H\}$ NMR spectra of **5i**.

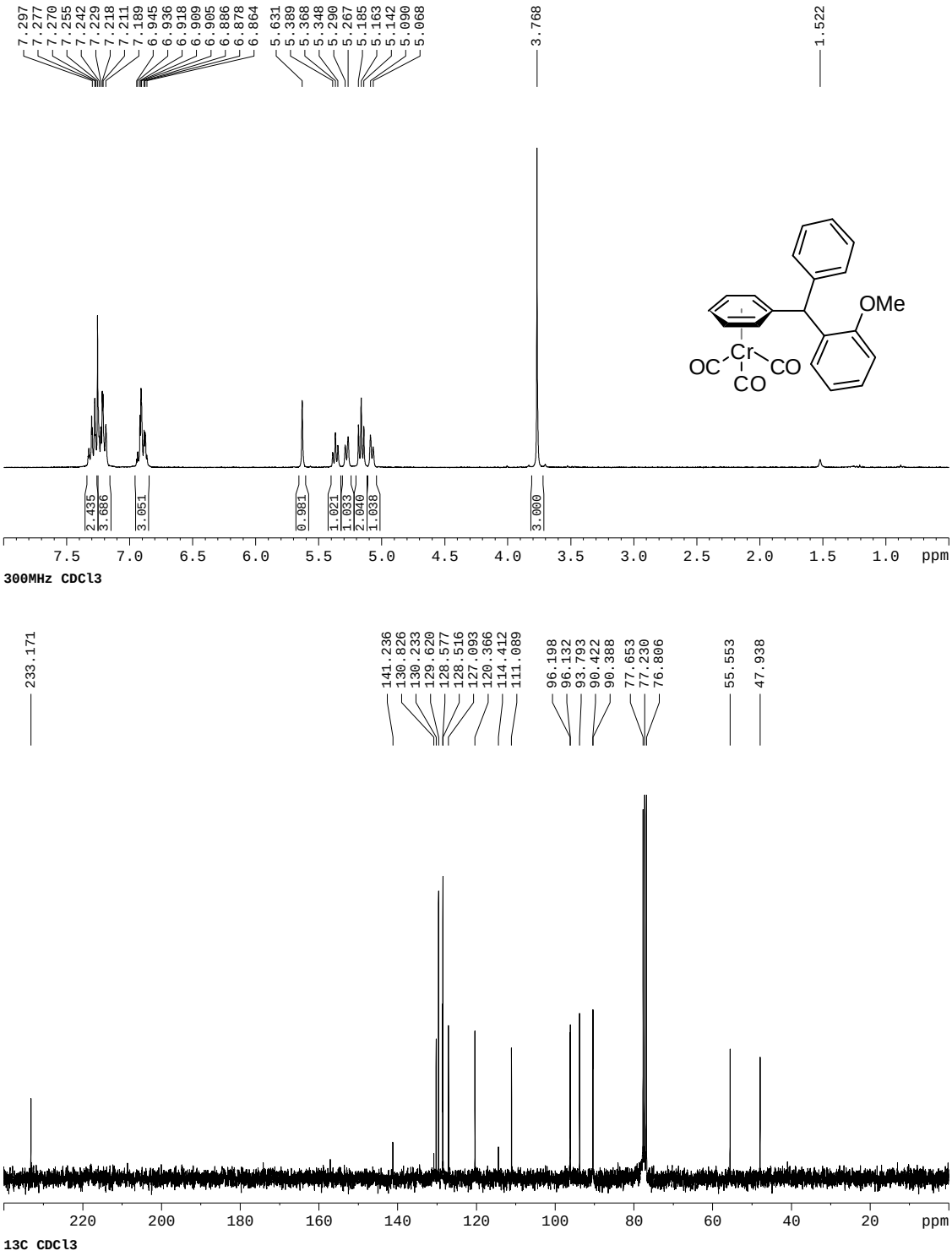

Figure I-10: $^{1}H$, $^{13}C\{^{1}H\}$ NMR spectra of **5j**.

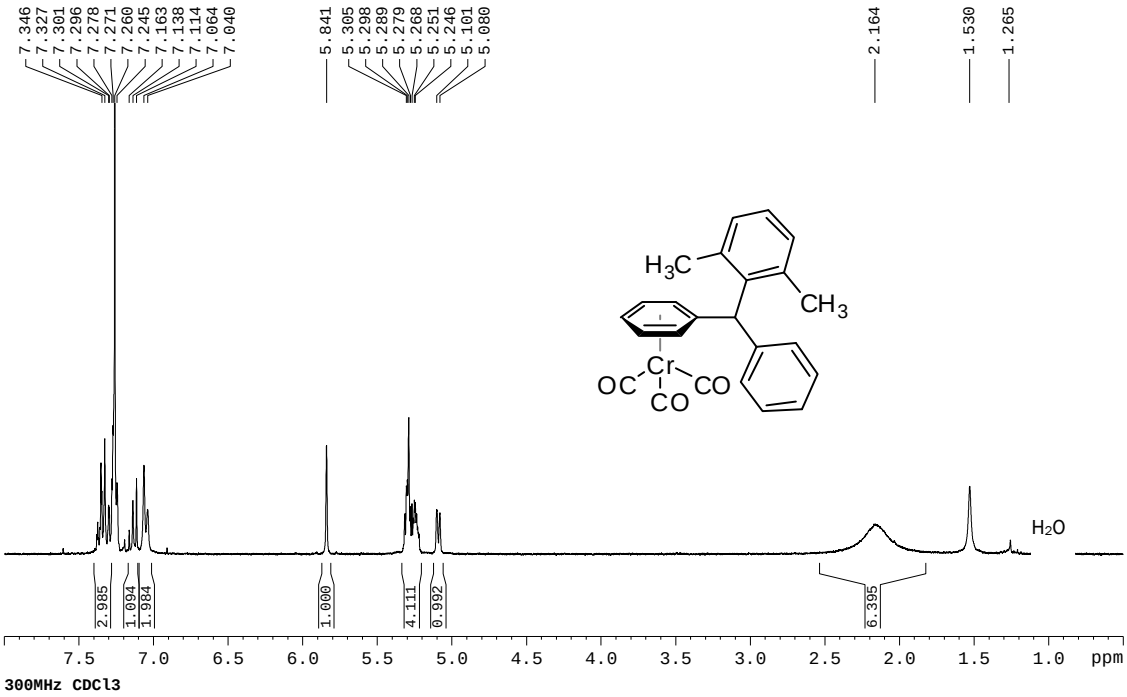


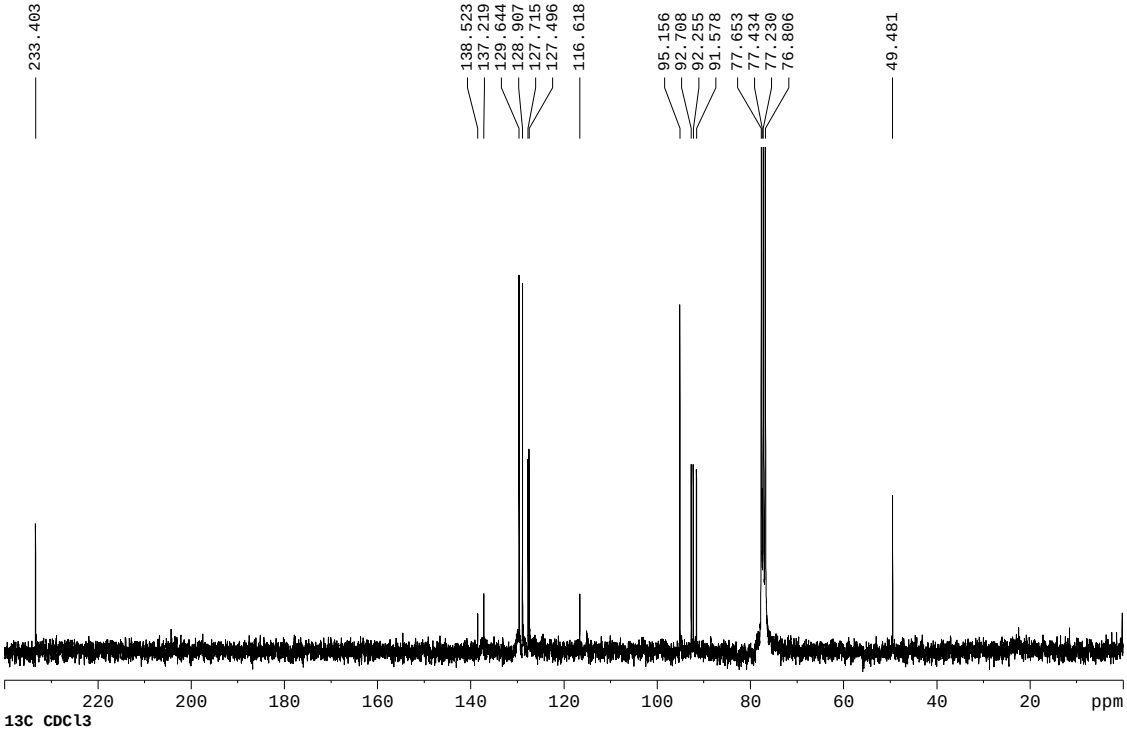

Figure I-11: $^{1}H$, $^{13}C\{^{1}H\}$ NMR spectra of **5k**.

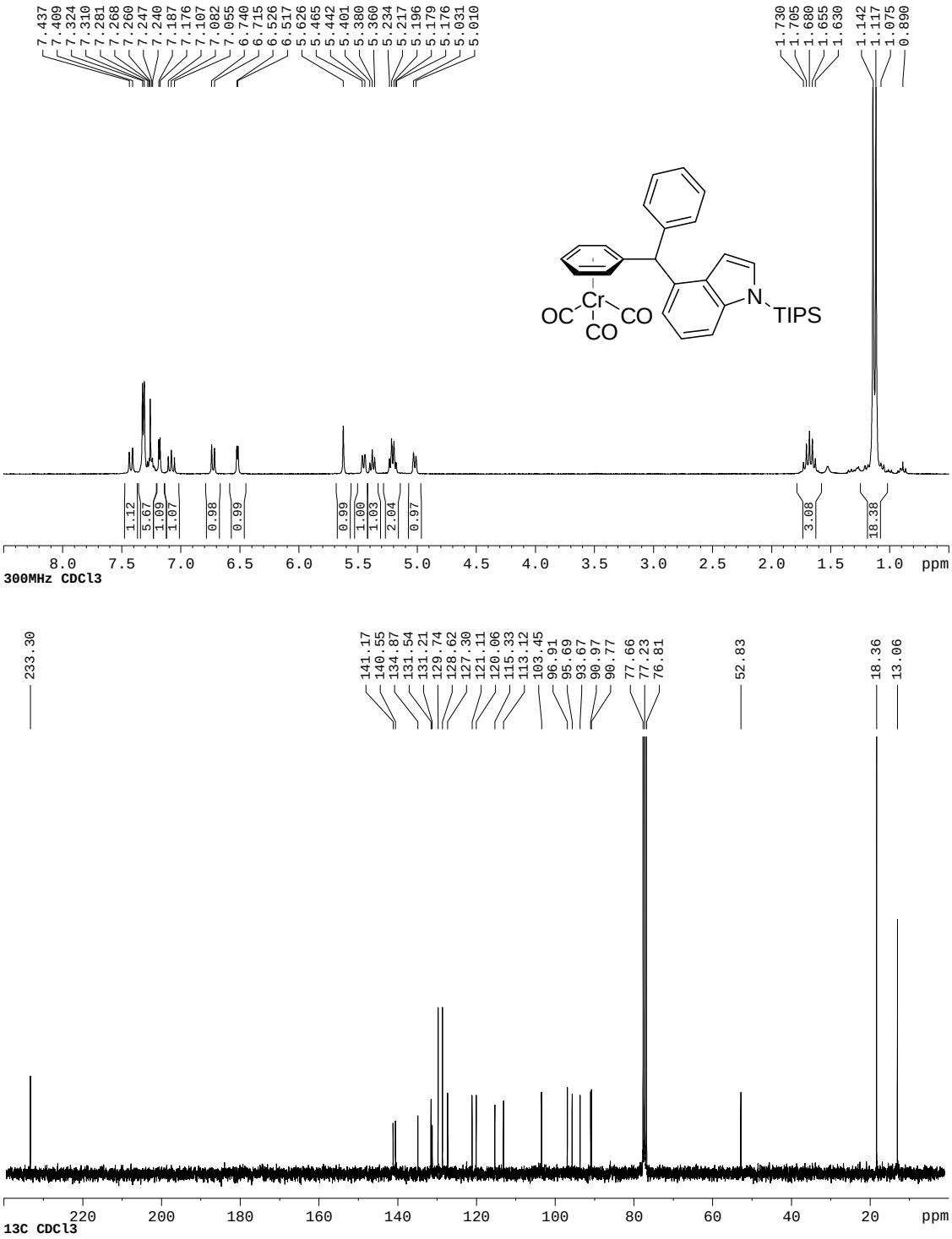

Figure I-12: $^{1}H$, $^{13}C\{^{1}H\}$, $^{19}F$ NMR spectra of **5l**.

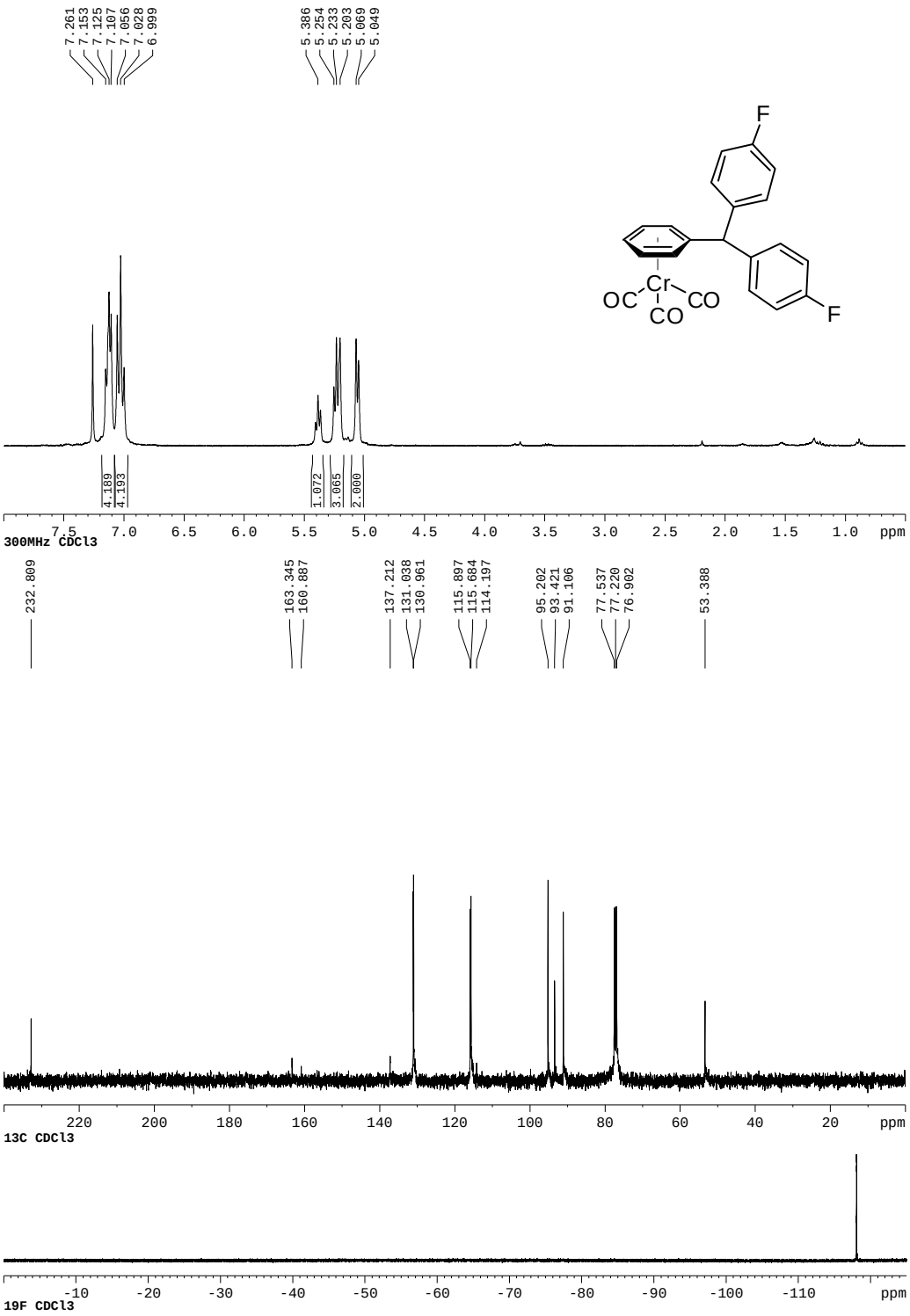

Figure I-13: $^{1}H$, $^{13}C\{^{1}H\}$ NMR spectra of **5m**.

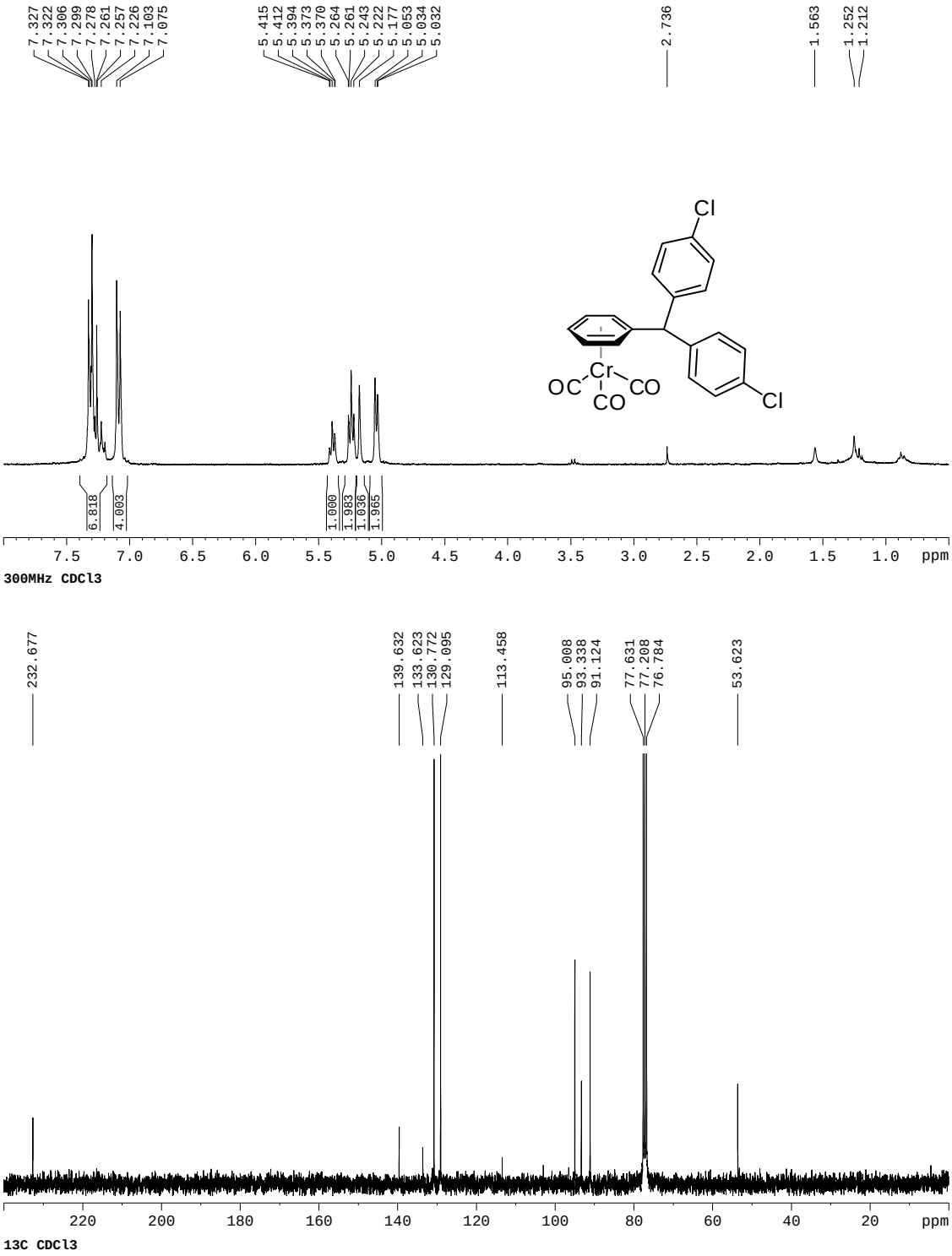

Figure I-14: $^{1}H$, $^{13}C\{^{1}H\}$ NMR spectra of **5n**.

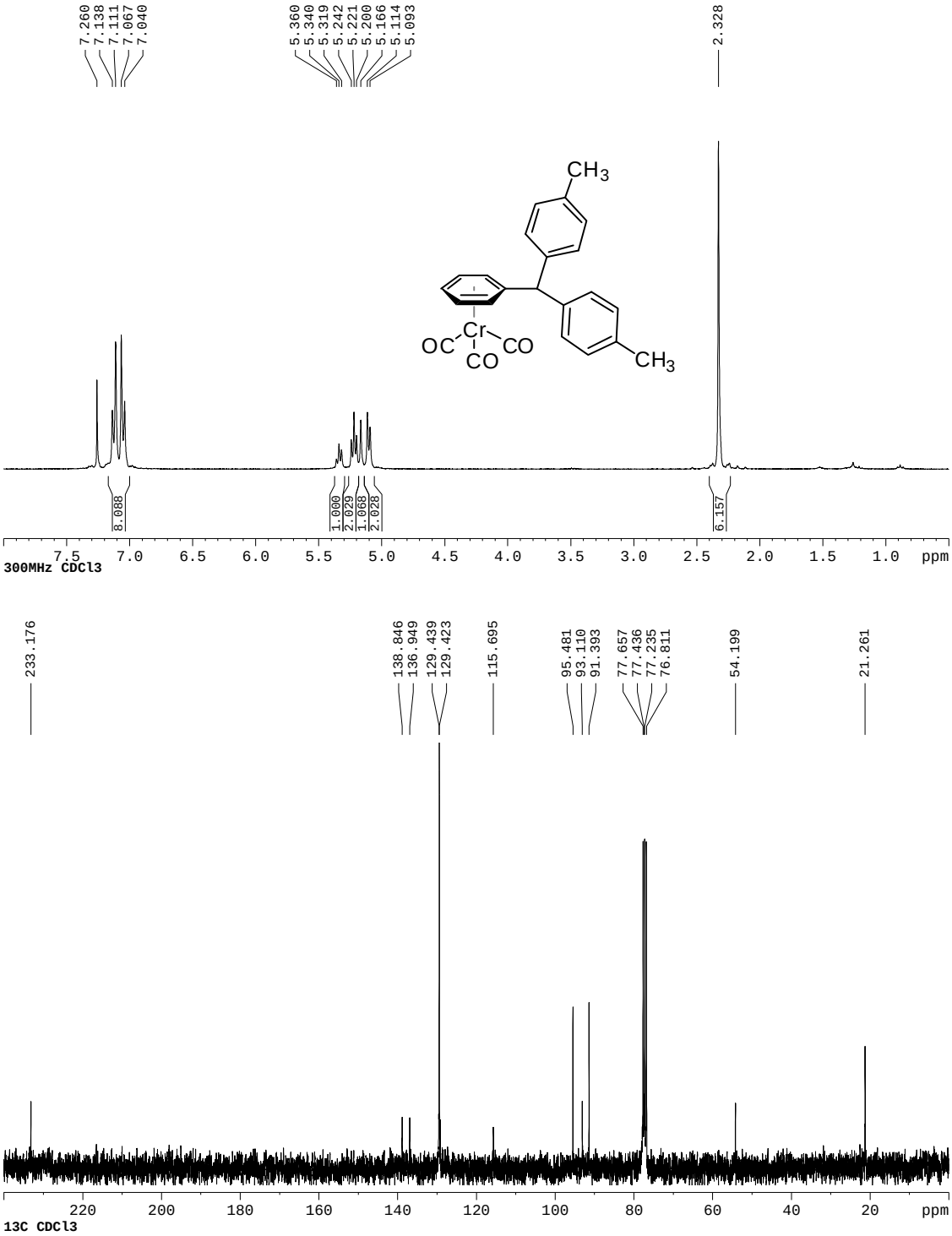

Figure I-15: $^{1}H$, $^{13}C\{^{1}H\}$ NMR spectra of **5o**.

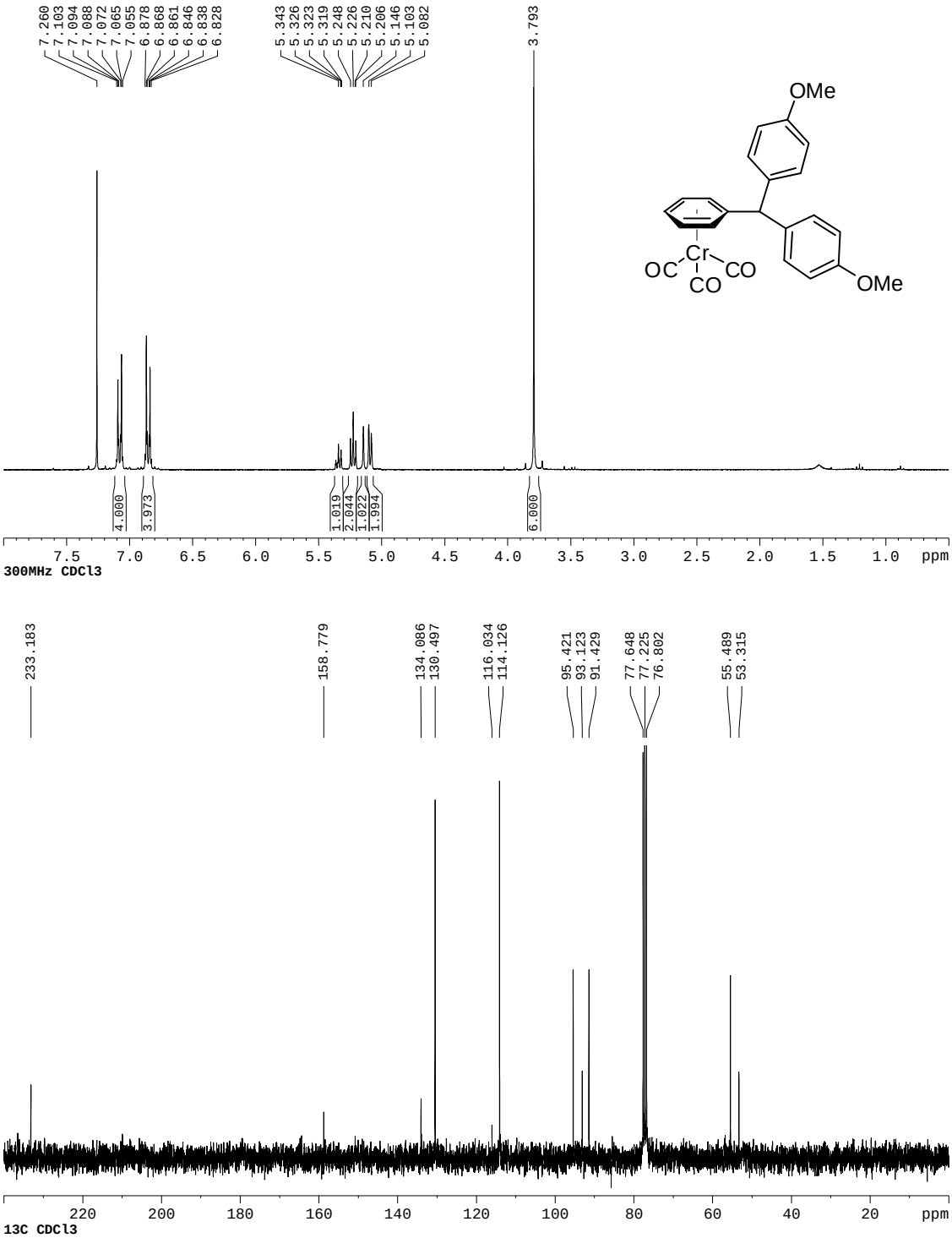

Figure I-16: $^{1}H$, $^{13}C\{^{1}H\}$ NMR spectra of **5p**.

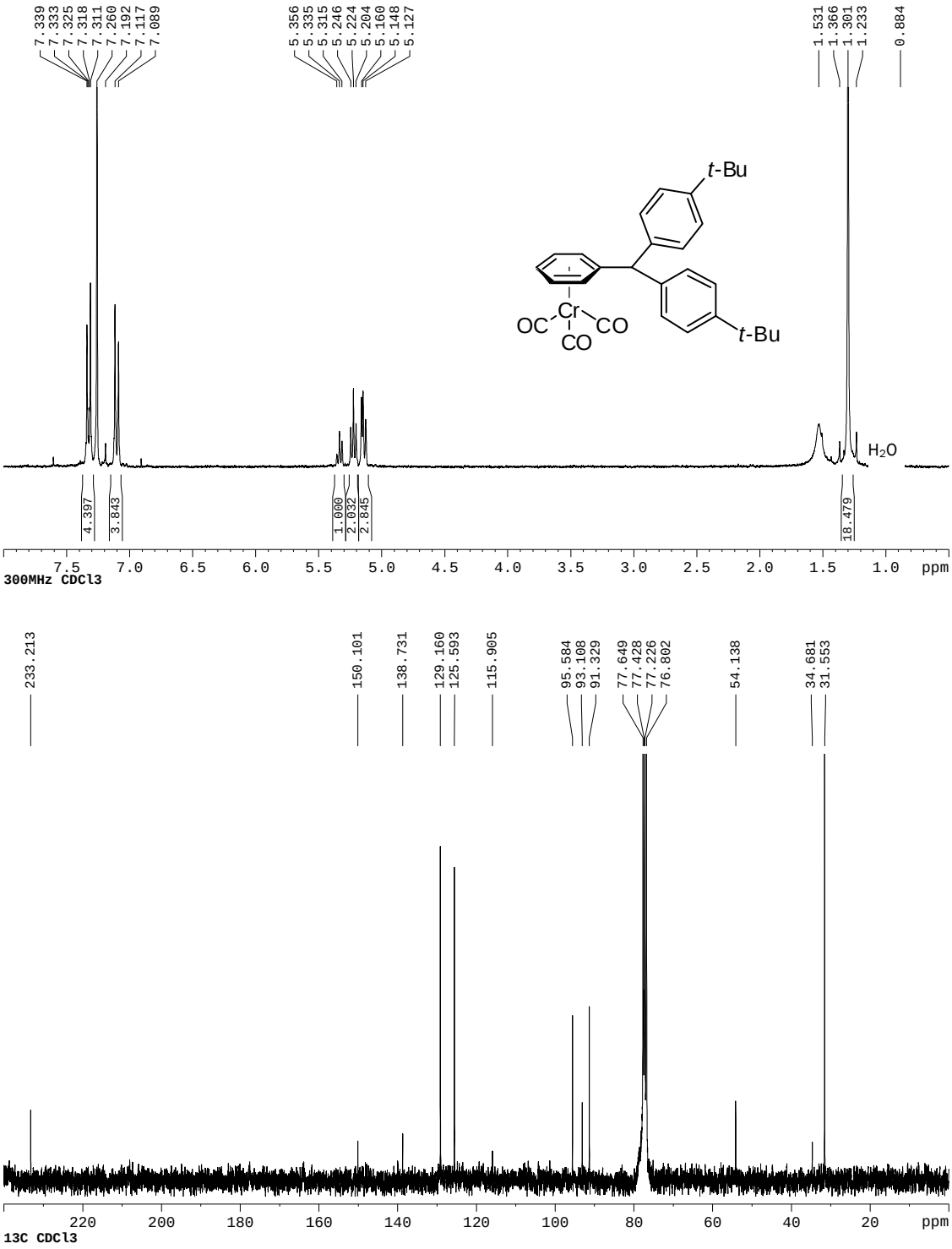

Figure I-17: $^{1}H$, $^{13}C\{^{1}H\}$NMR spectra of **5p'**

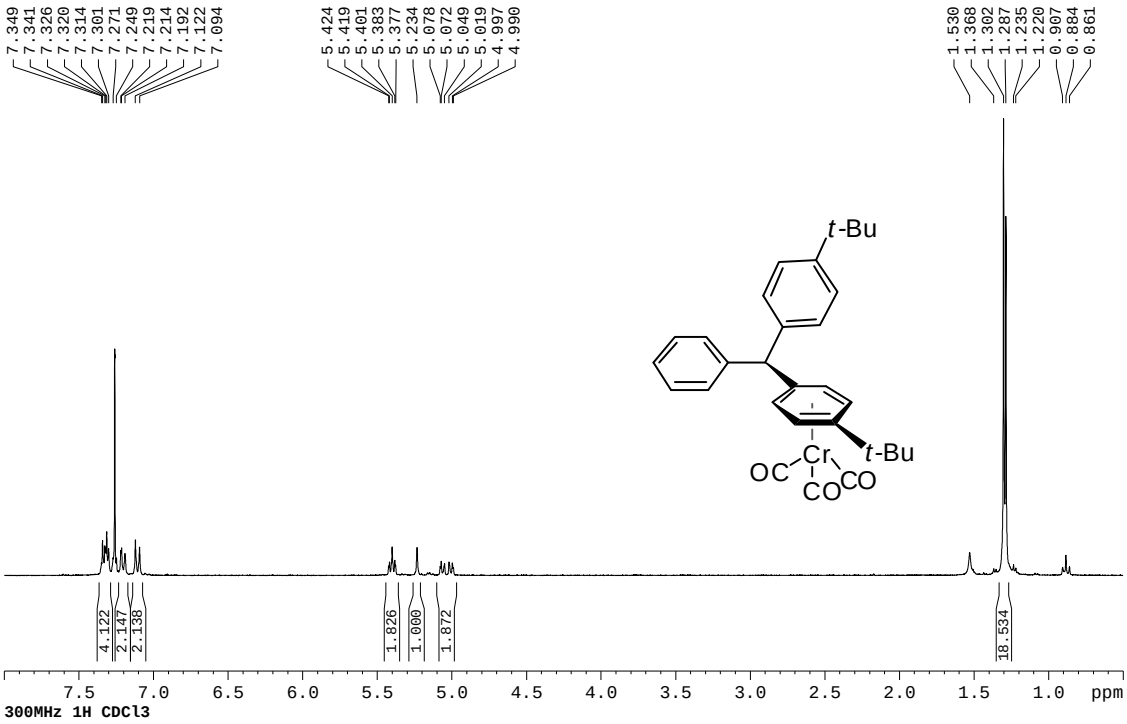


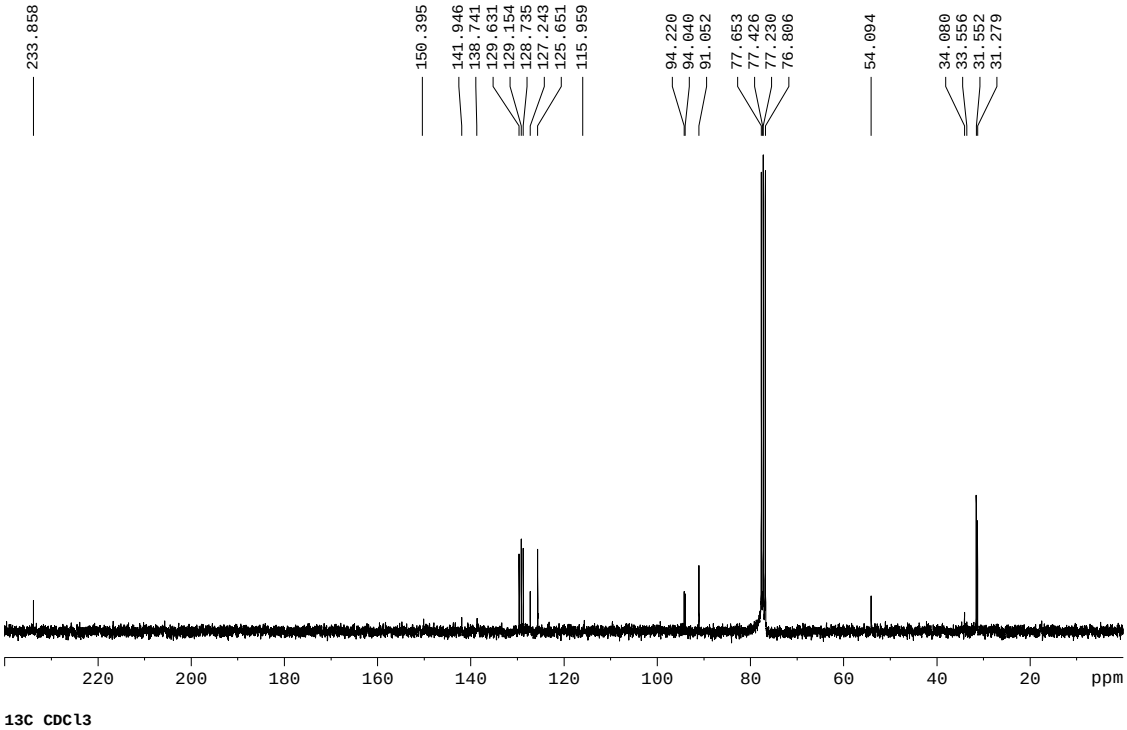

Figure I-18: $^{1}H$, $^{13}C\{^{1}H\}$ NMR spectra of **5q**.

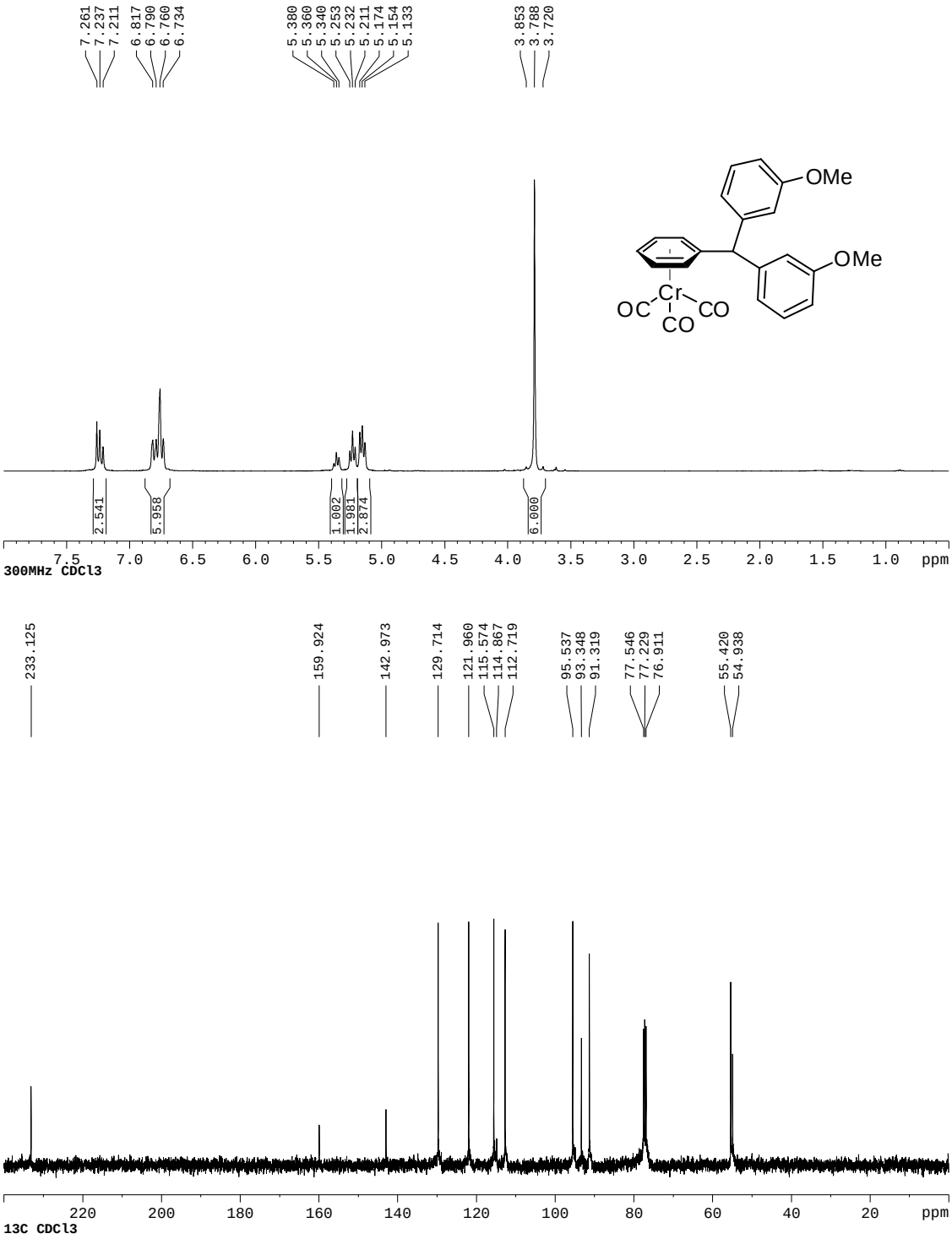

Figure I-19: $^{1}H$, $^{13}C\{^{1}H\}$ NMR spectra of **5r**.

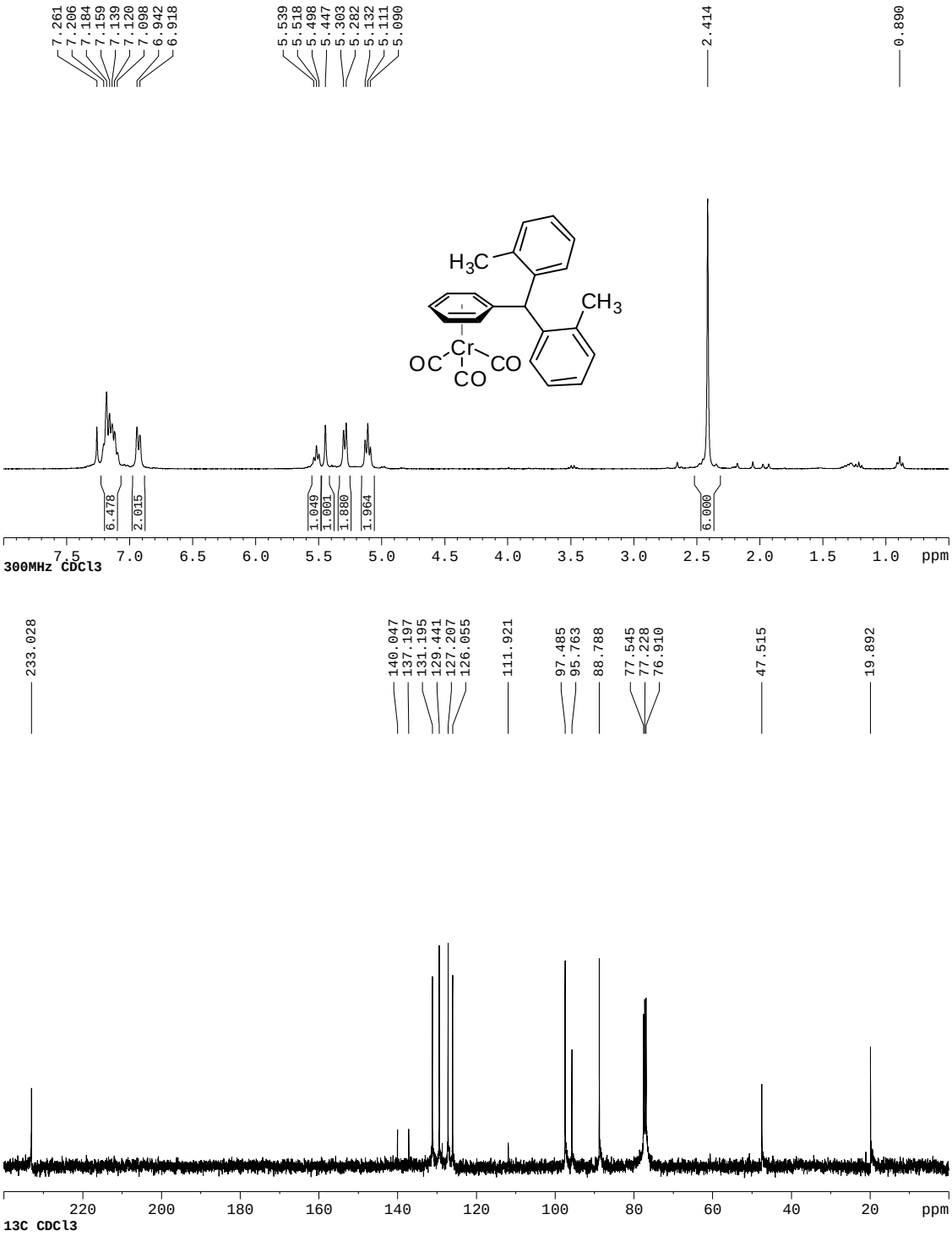

Figure I-20: $^{1}H$, $^{13}C\{^{1}H\}$ NMR spectra of **4b**.

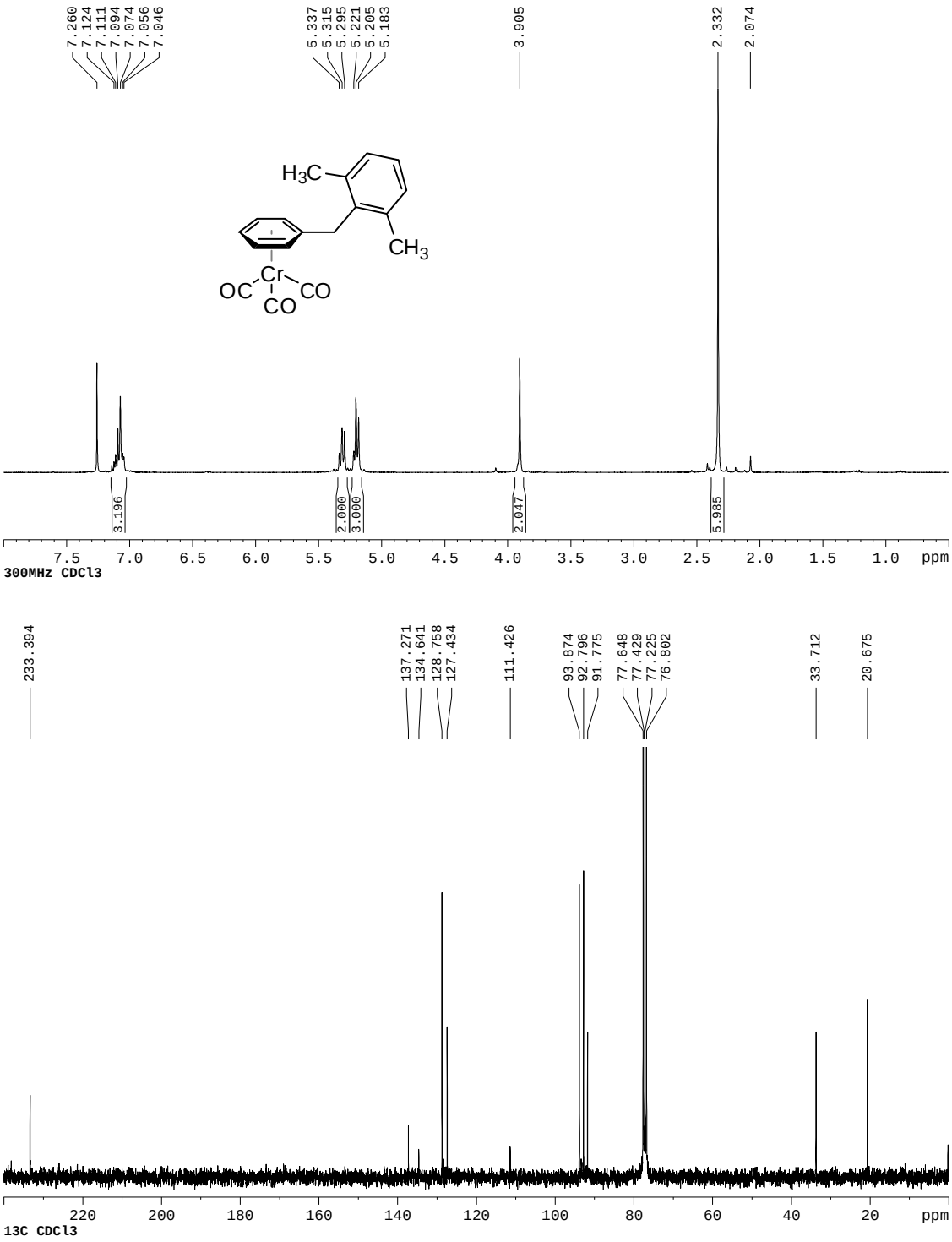

Figure I-21: $^{1}H$, $^{13}C\{^{1}H\}$ NMR spectra of **4c**.

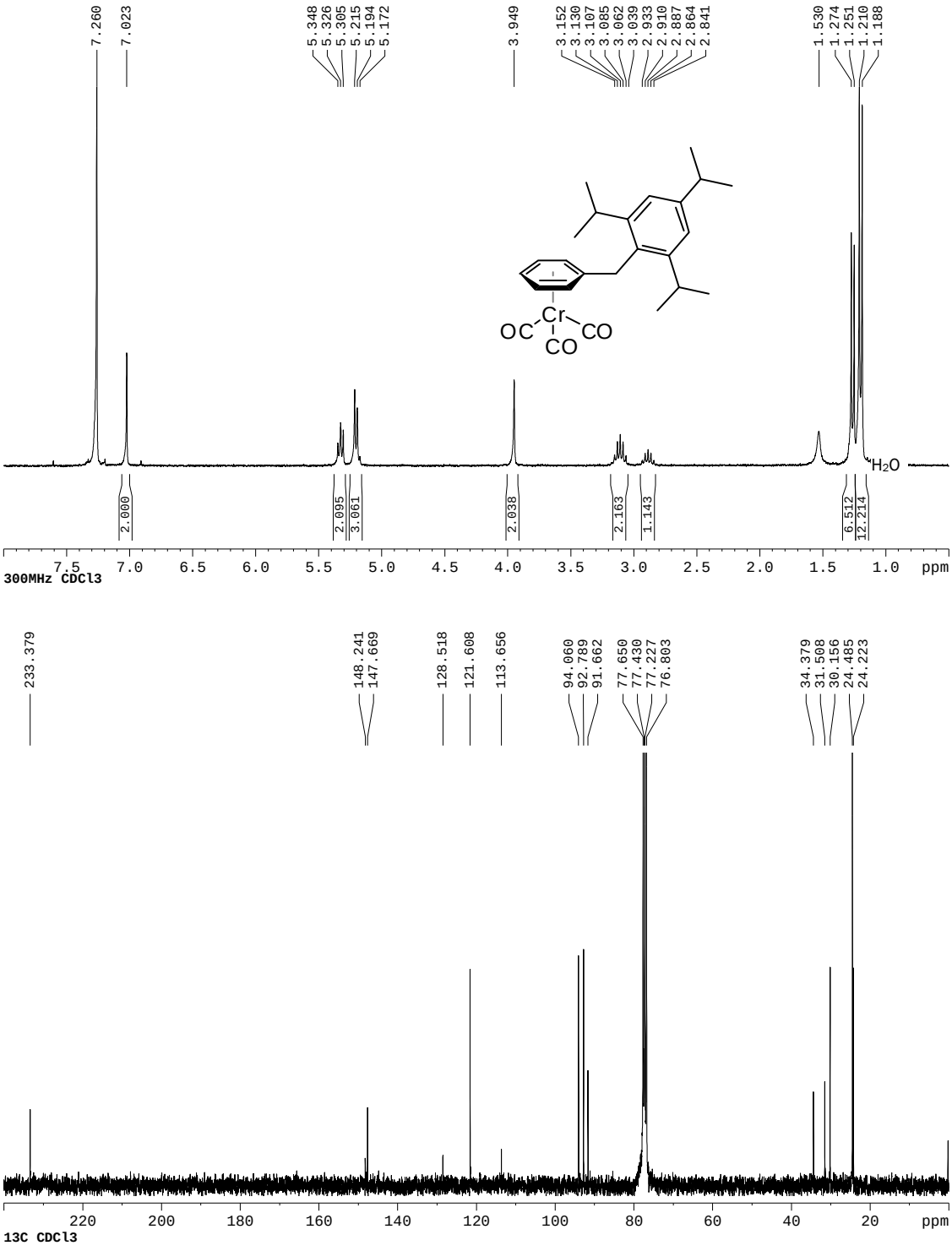

Figure I-22: $^{1}H$, $^{13}C\{^{1}H\}$ NMR spectra of **7**.

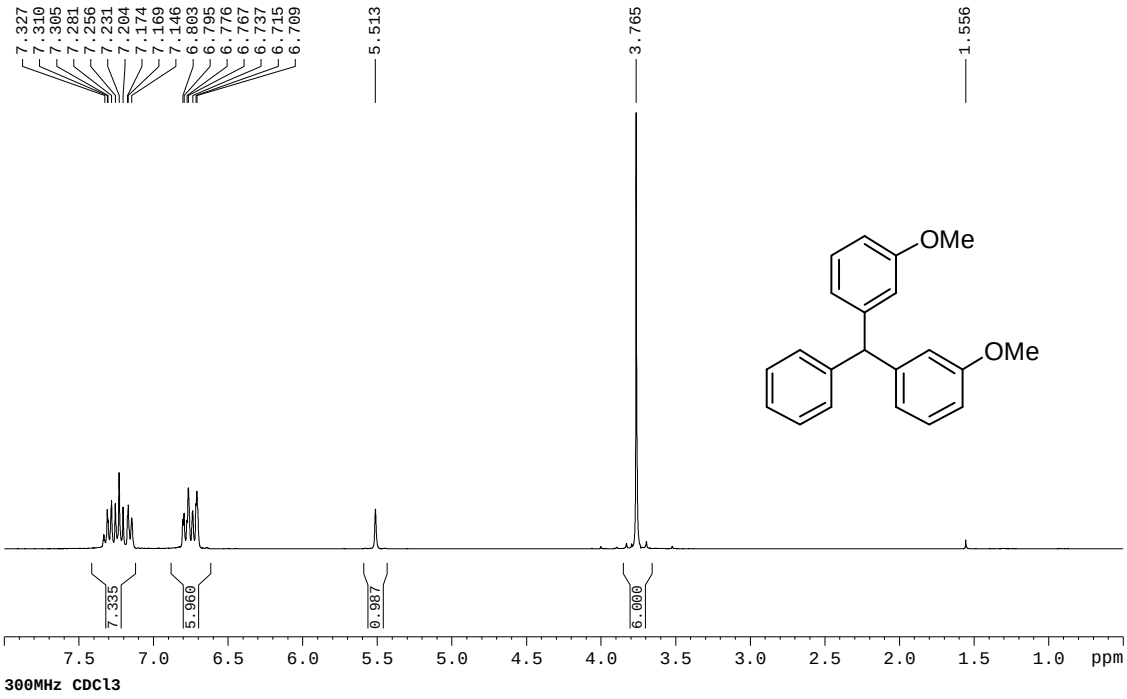


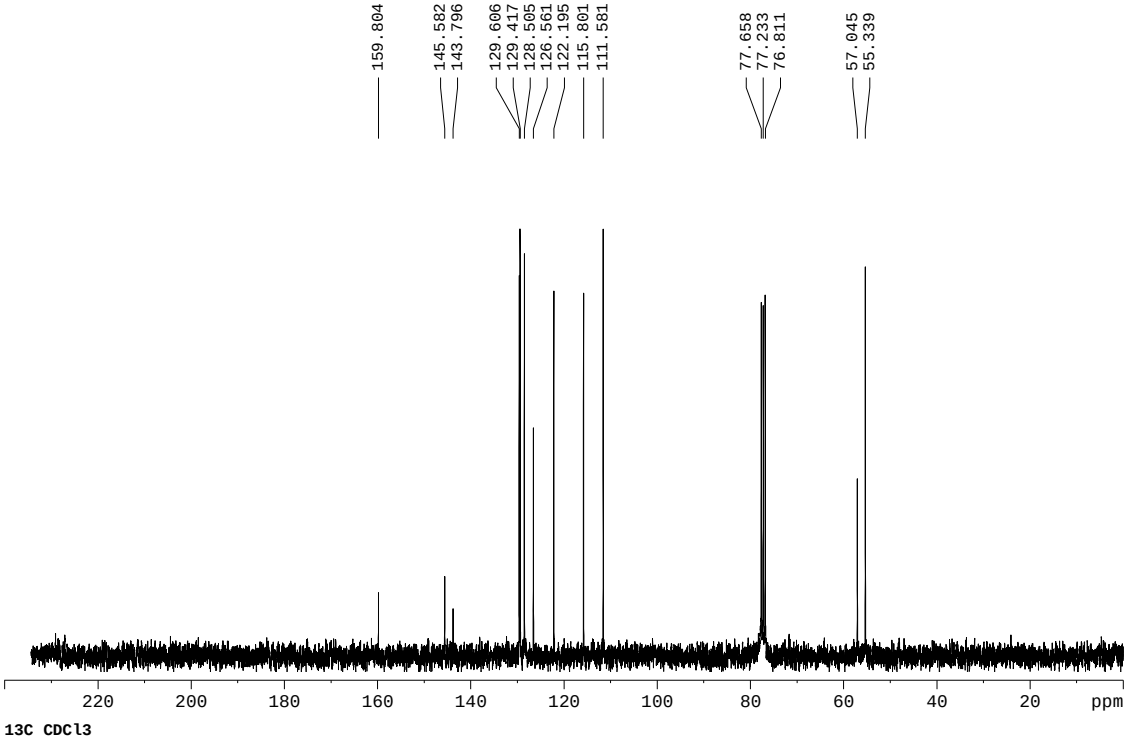

Figure I-23: $^{1}H$, $^{13}C\{^{1}H\}$ NMR spectra of **11**.

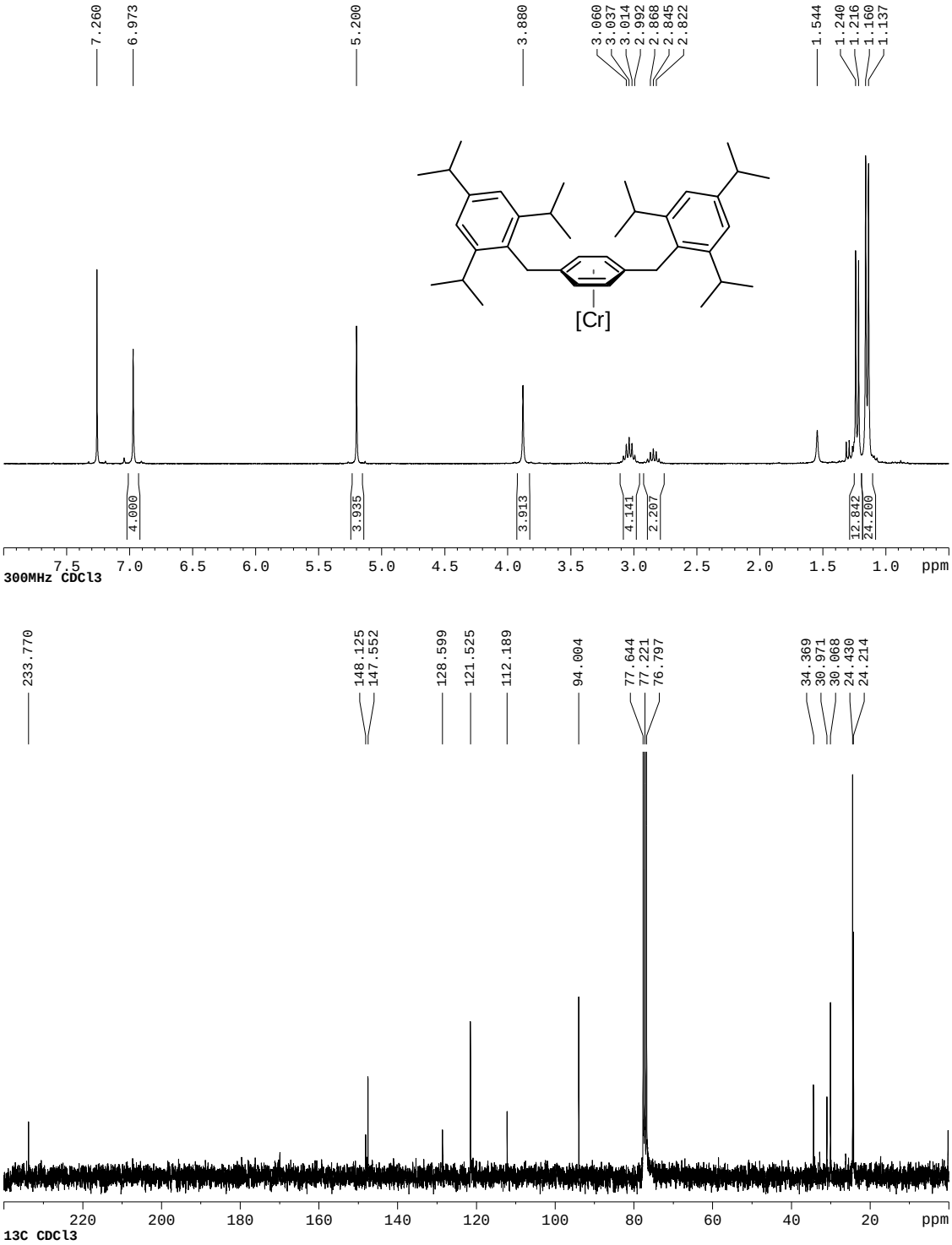

Figure I-24: $^{1}H$, $^{13}C\{^{1}H\}$, $^{19}F\{^{1}H\}$ NMR spectra of **12**.

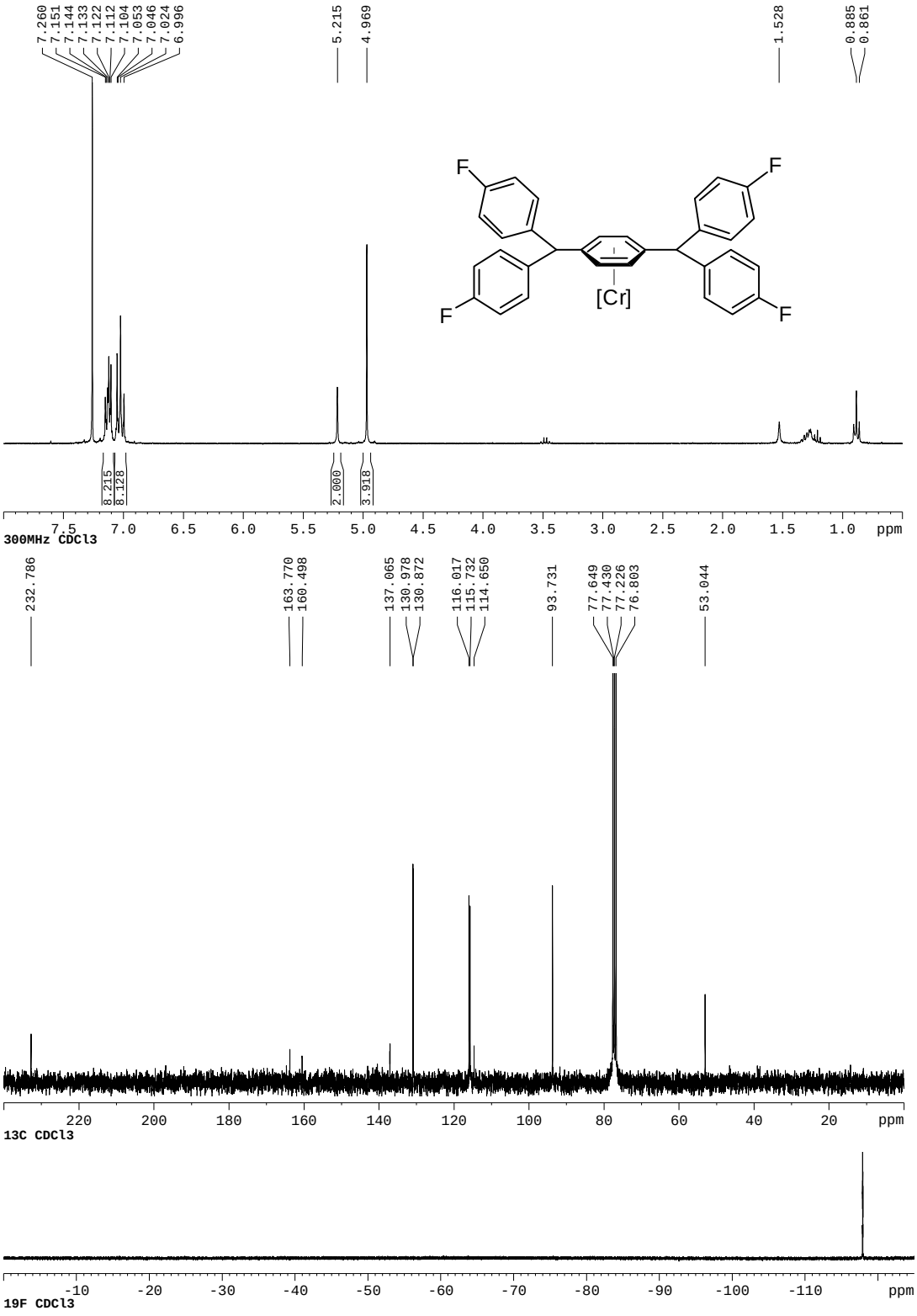

Figure I-25: $^{1}H$, $^{13}C\{^{1}H\}$ NMR spectra of **17**.

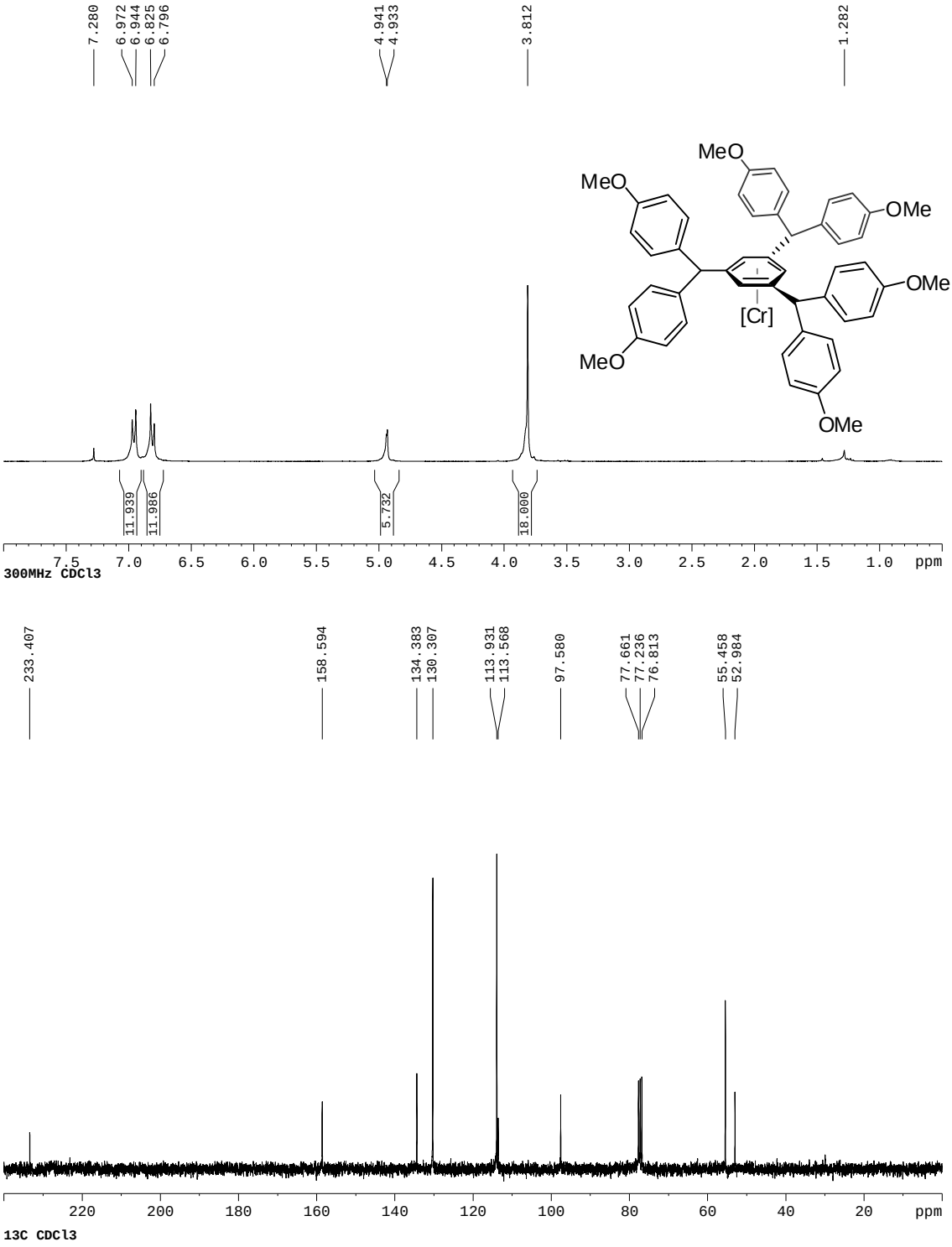

Figure I-26: $^{1}H$, $^{13}C\{^{1}H\}$ NMR spectra of **19**.

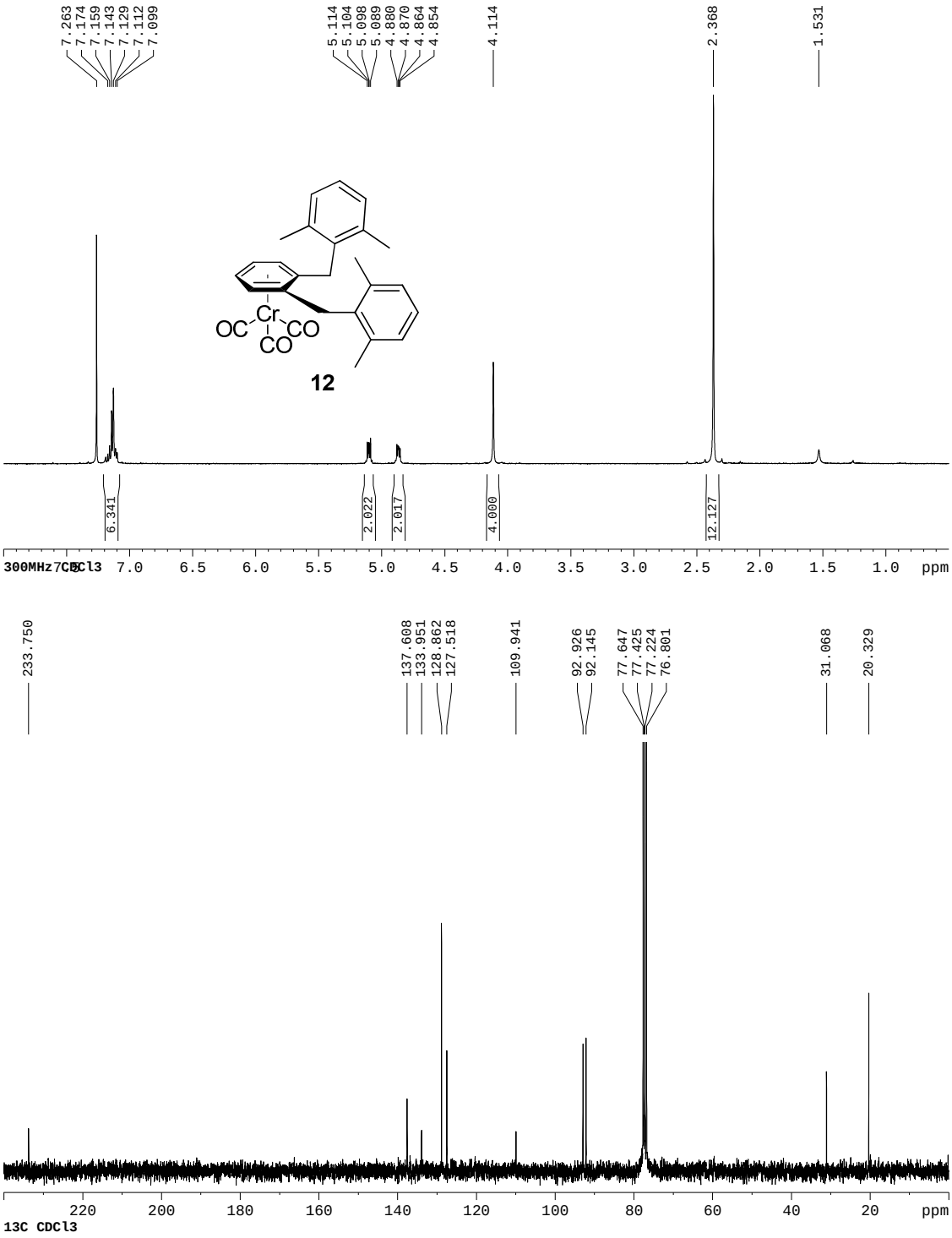

Figure I-27: $^{1}H$, $^{13}C\{^{1}H\}$ NMR spectra of **20**.

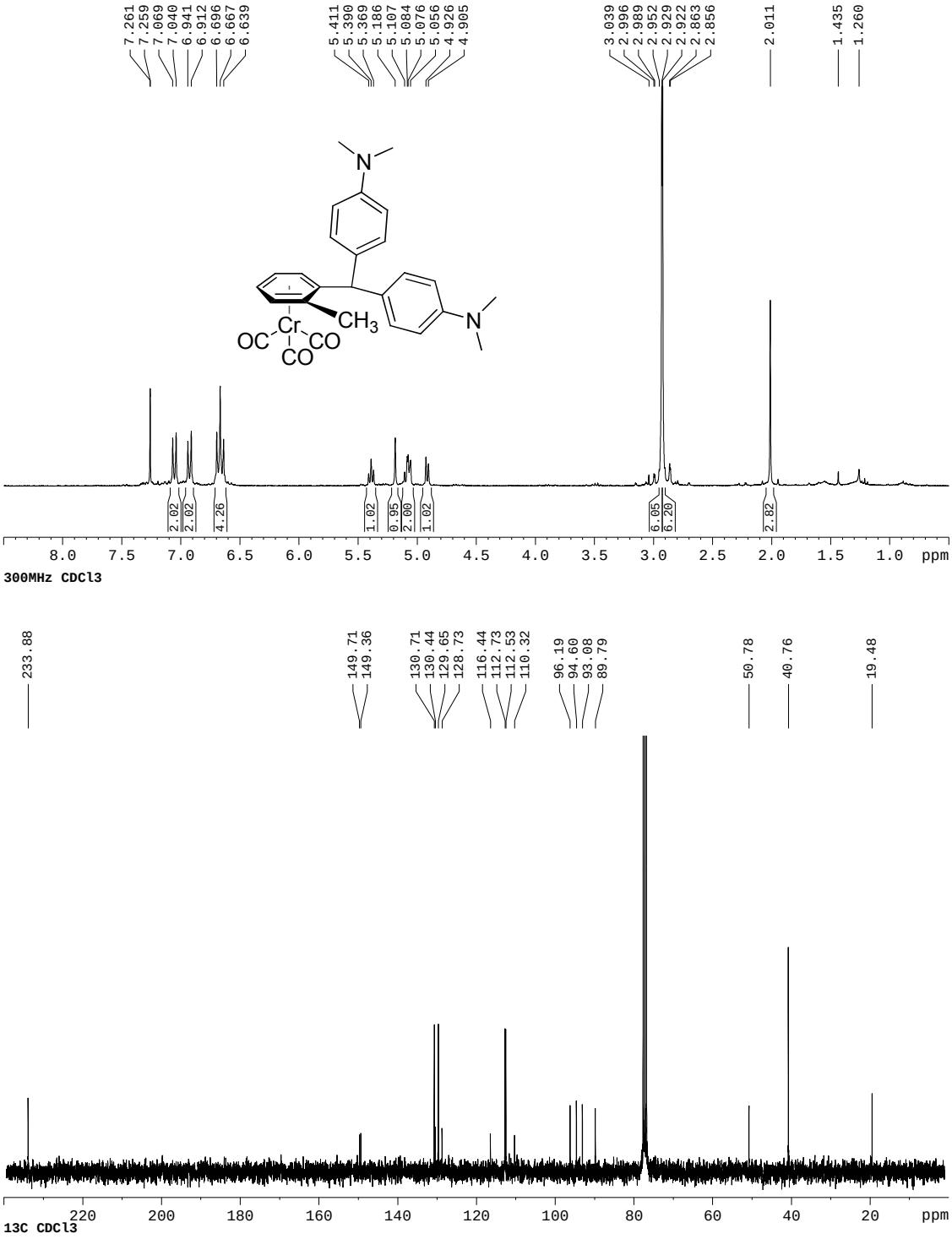

Figure I-28: $^{1}H$, $^{13}C\{^{1}H\}$ NMR spectra of **21**.

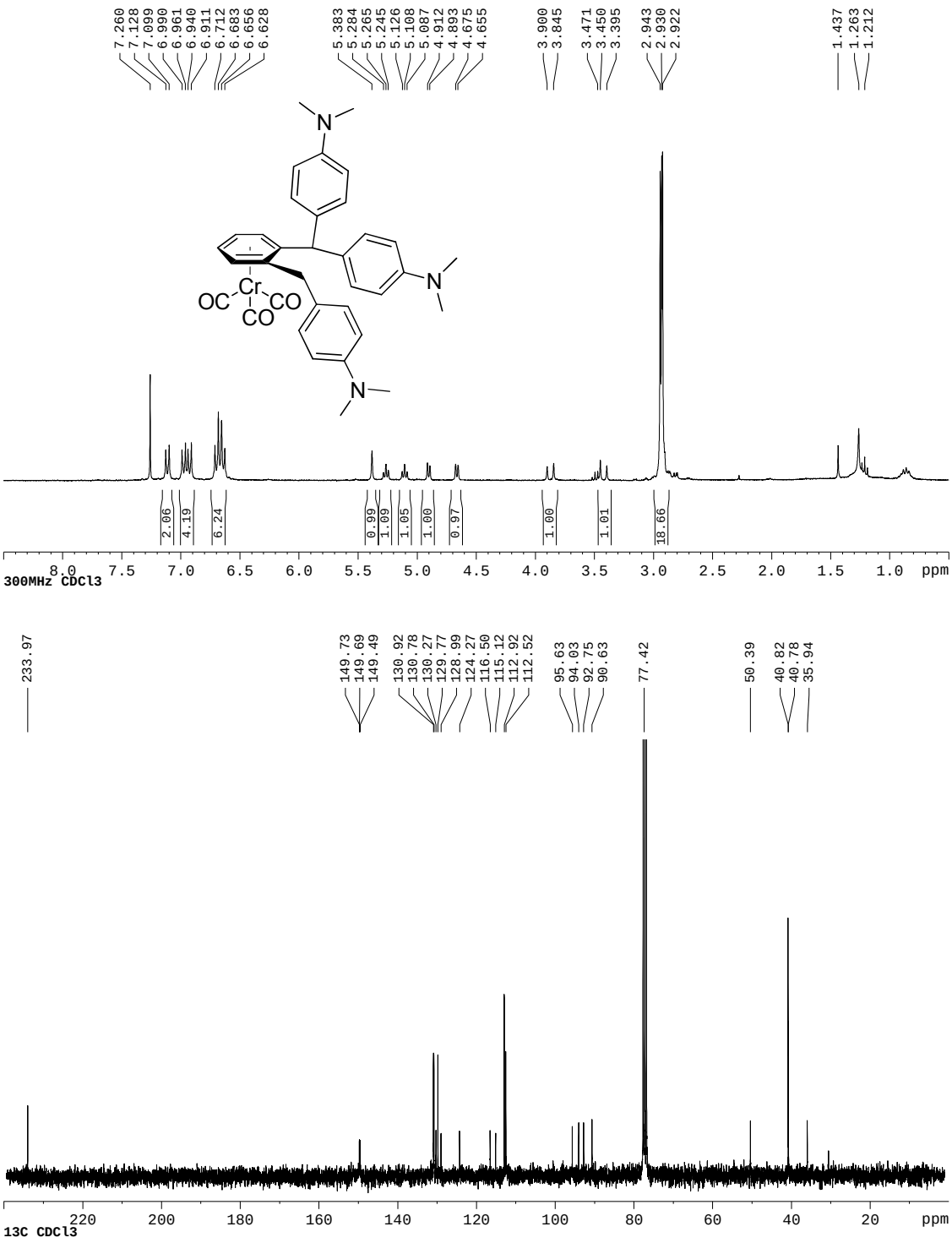

*Diarylmethyl ethers from CrBnOPr (**23**).*

Figure I-29: $^{1}H$, $^{13}C\{^{1}H\}$ NMR spectra of **24a**.

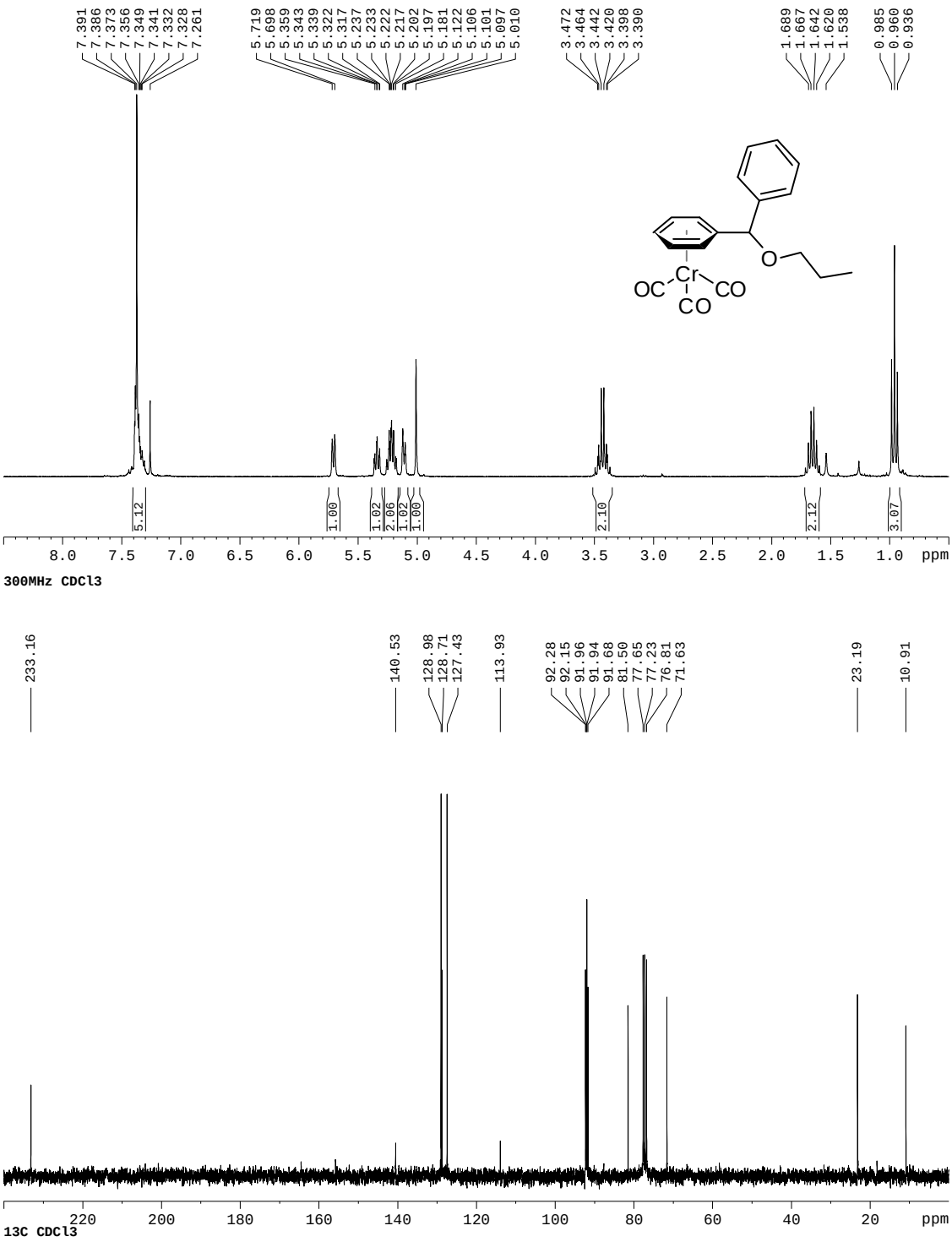

Figure I-30: $^{1}H$, $^{13}C\{^{1}H\}$ $^{19}F\{^{1}H\}$ NMR spectra of **24b**.

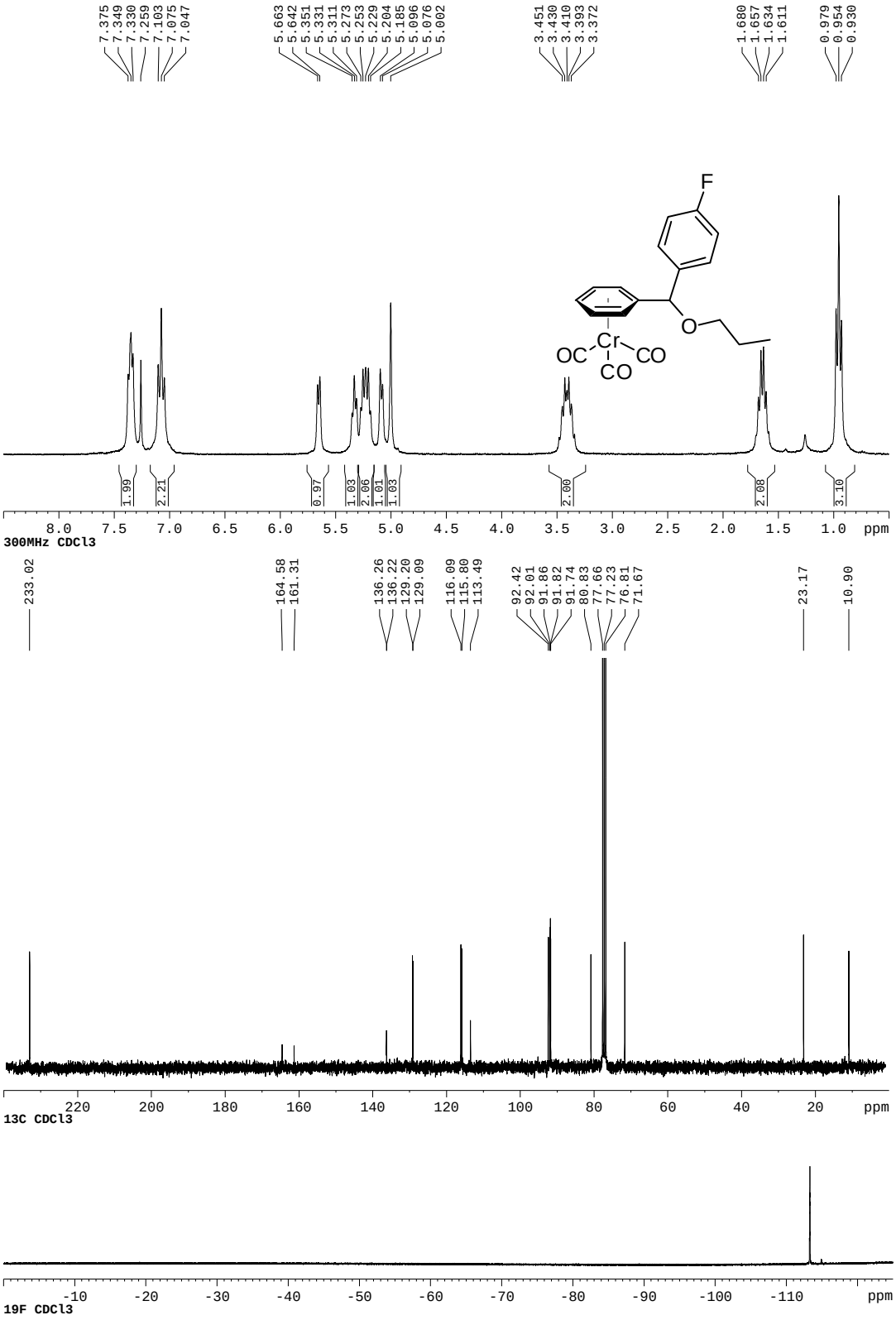

Figure I-31: $^{1}H$, $^{13}C\{^{1}H\}$ NMR spectra of **24c**.

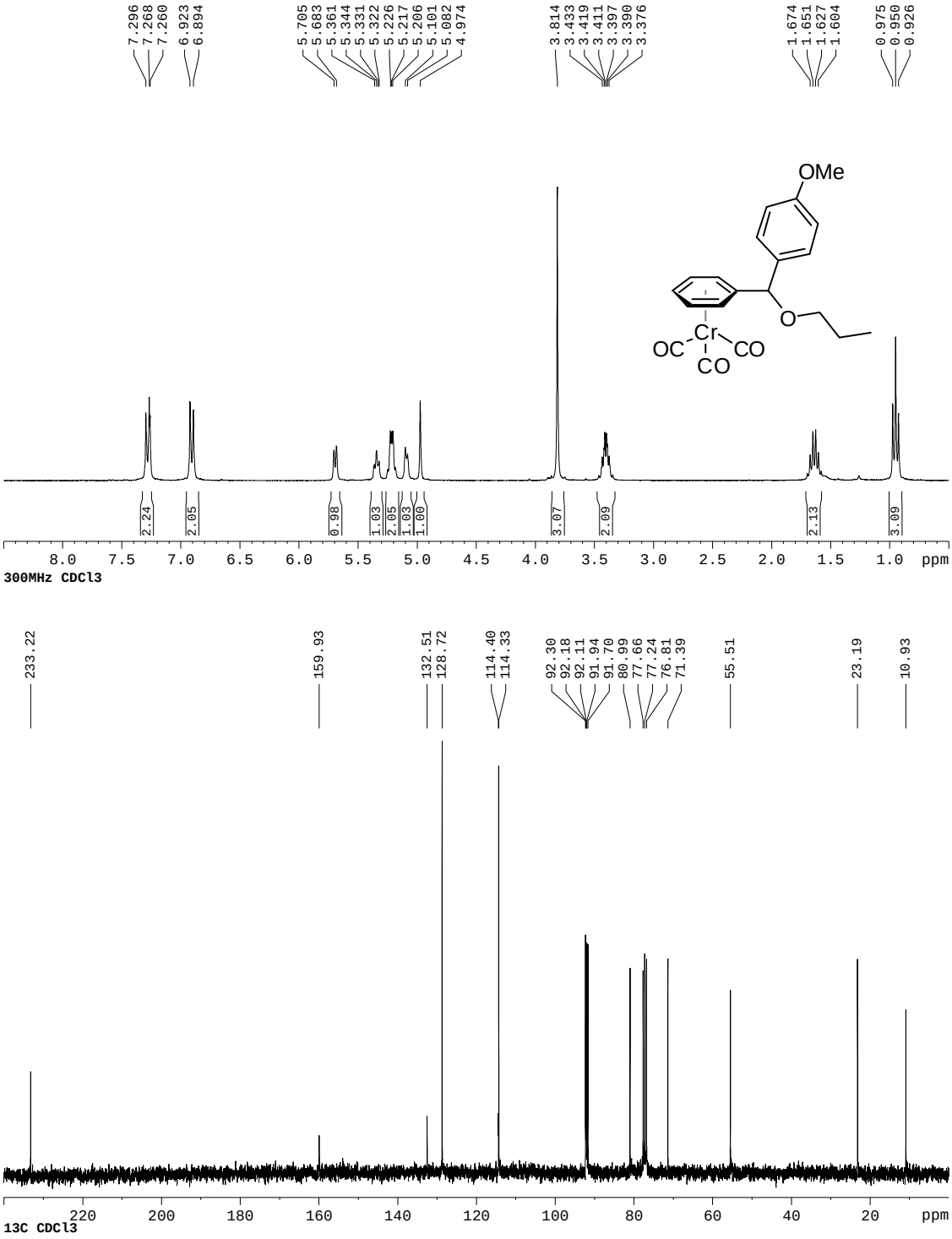

Figure I-32: $^{1}H$, $^{13}C\{^{1}H\}$ NMR spectra of **24d**.

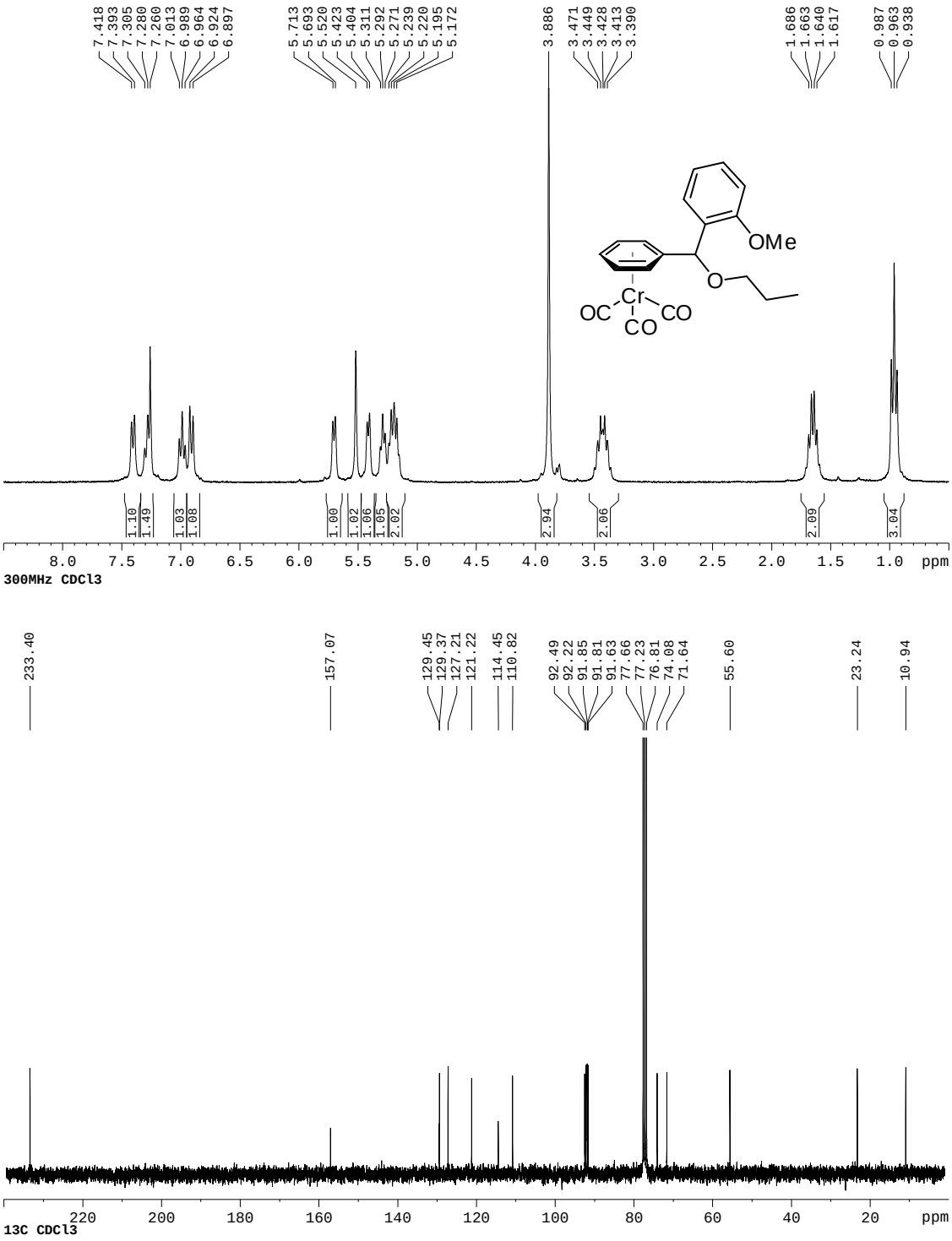

Figure I-33: $^{1}H$, $^{13}C\{^{1}H\}$ NMR spectra of **24e**.

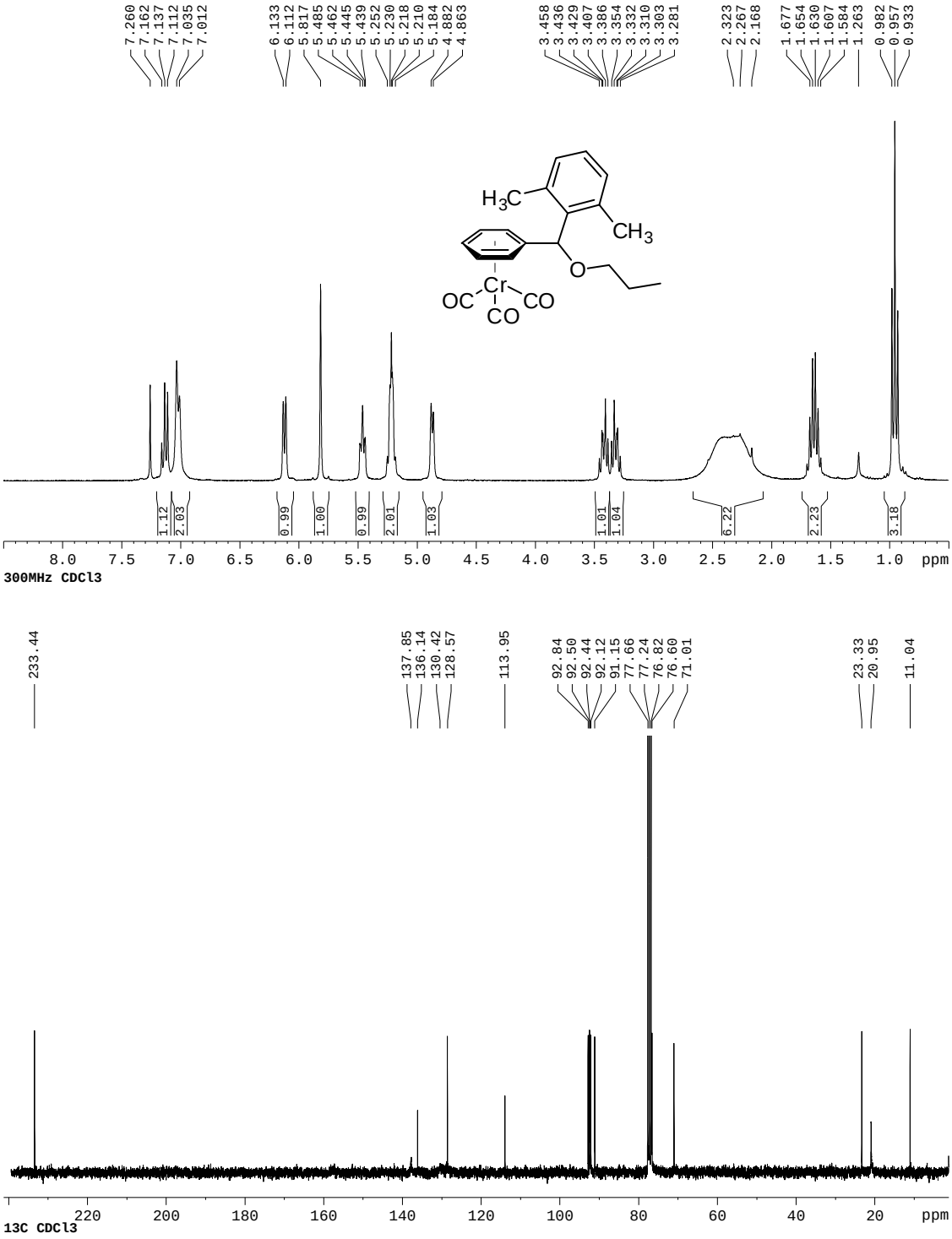

*Triarylmethyl ethers from CrBnOPr (**23**).*

Figure I-34: $^{1}H$, $^{13}C\{^{1}H\}$ NMR spectra of **26a**.

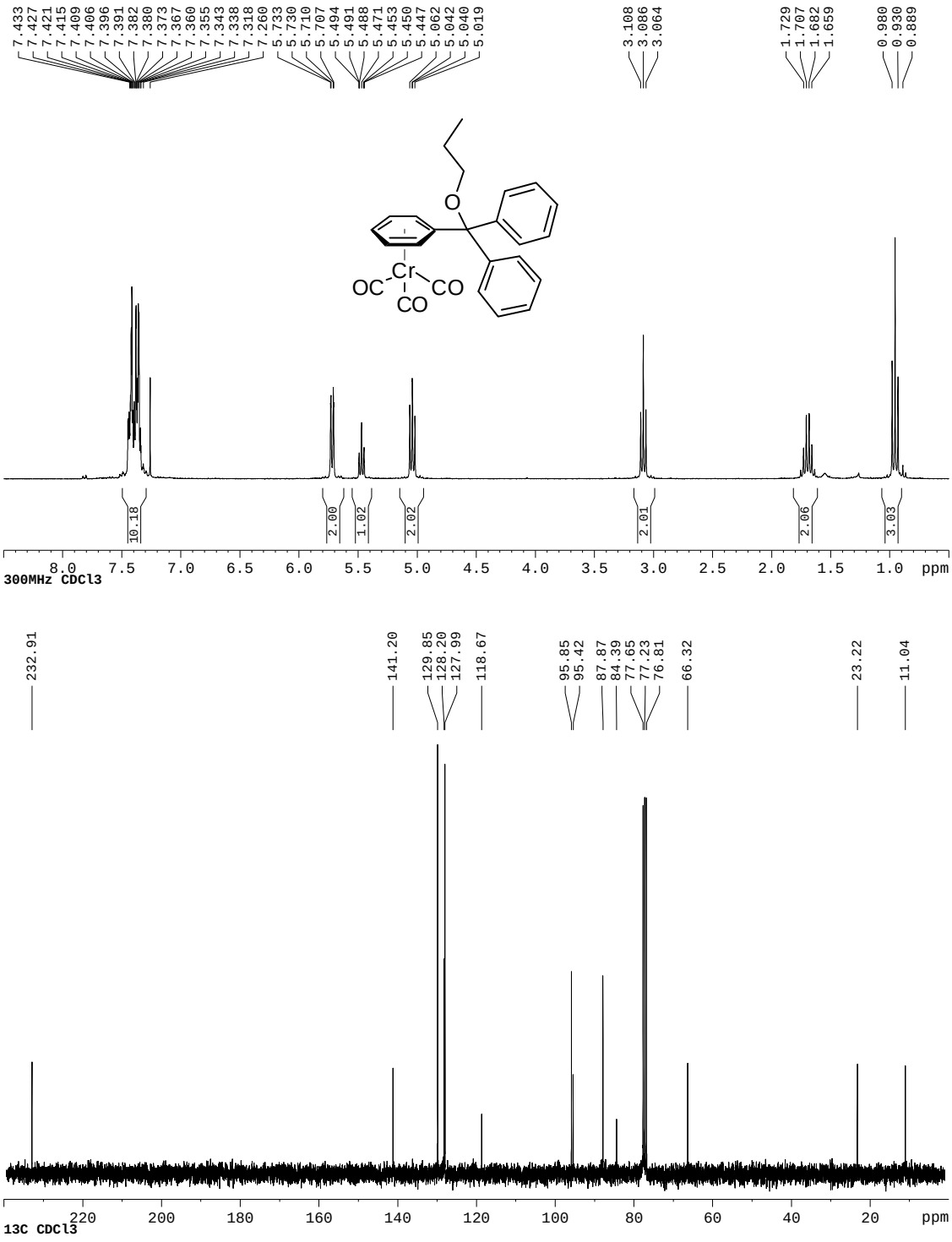

Figure I-35: $^{1}H$, $^{13}C\{^{1}H\}$, $^{19}F\{^{1}H\}$ NMR spectra of **26b**.

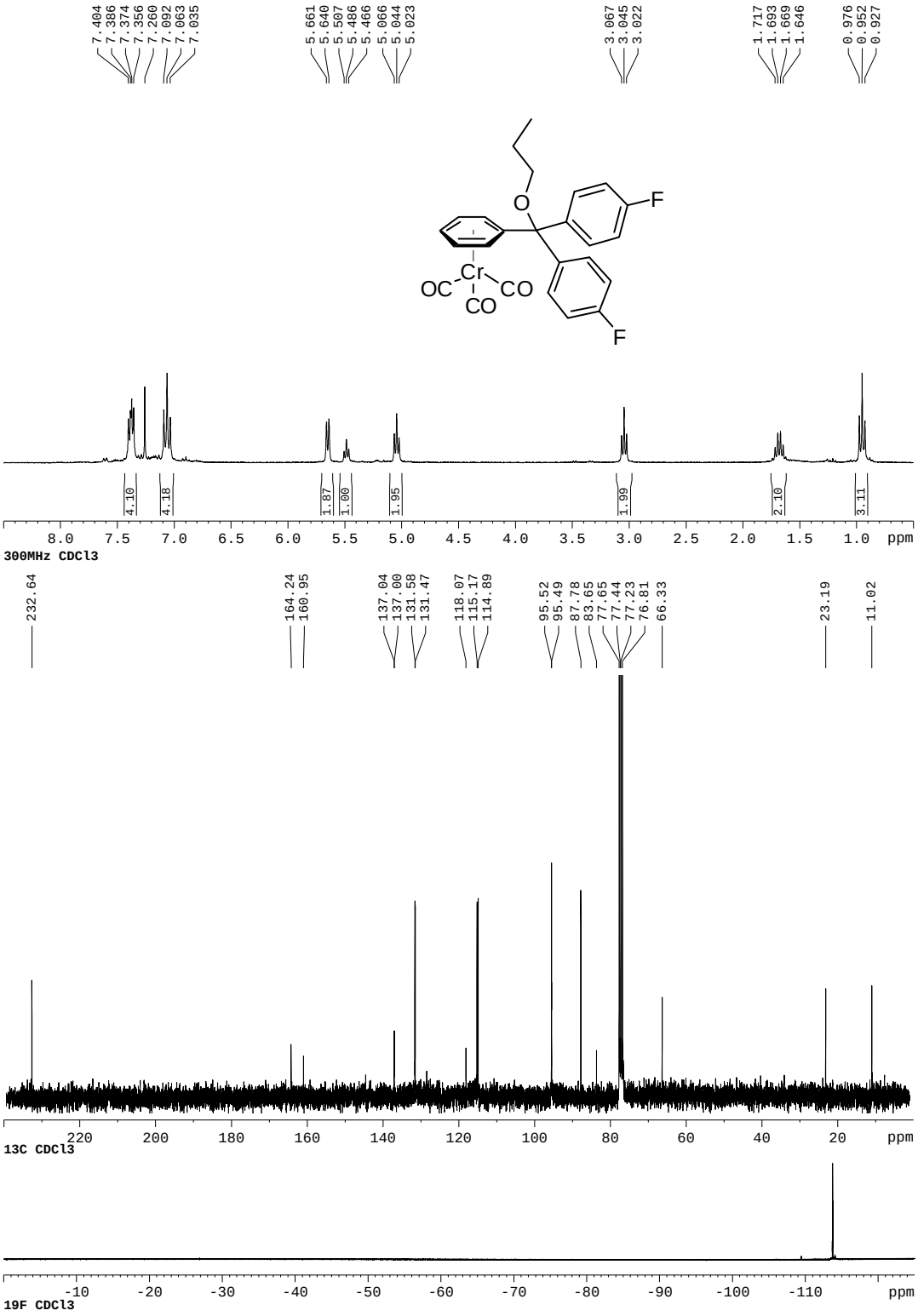

Figure I-36: $^{1}H$, $^{13}C\{^{1}H\}$, $^{19}F\{^{1}H\}$ NMR spectra of **26d**.

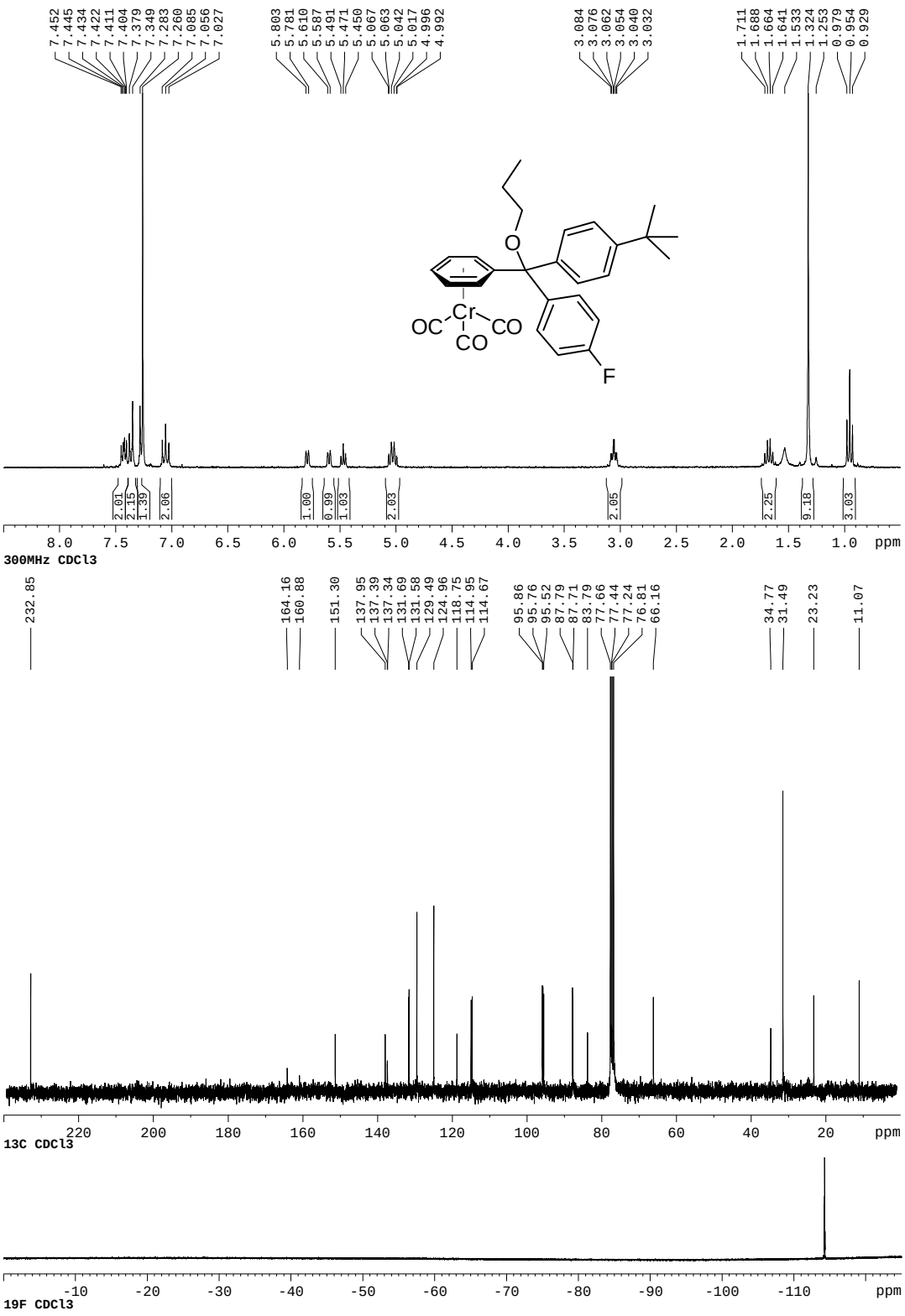

Figure I-37: $^{1}H$, $^{13}C\{^{1}H\}$, $^{19}F\{^{1}H\}$ NMR spectra of **26e**.

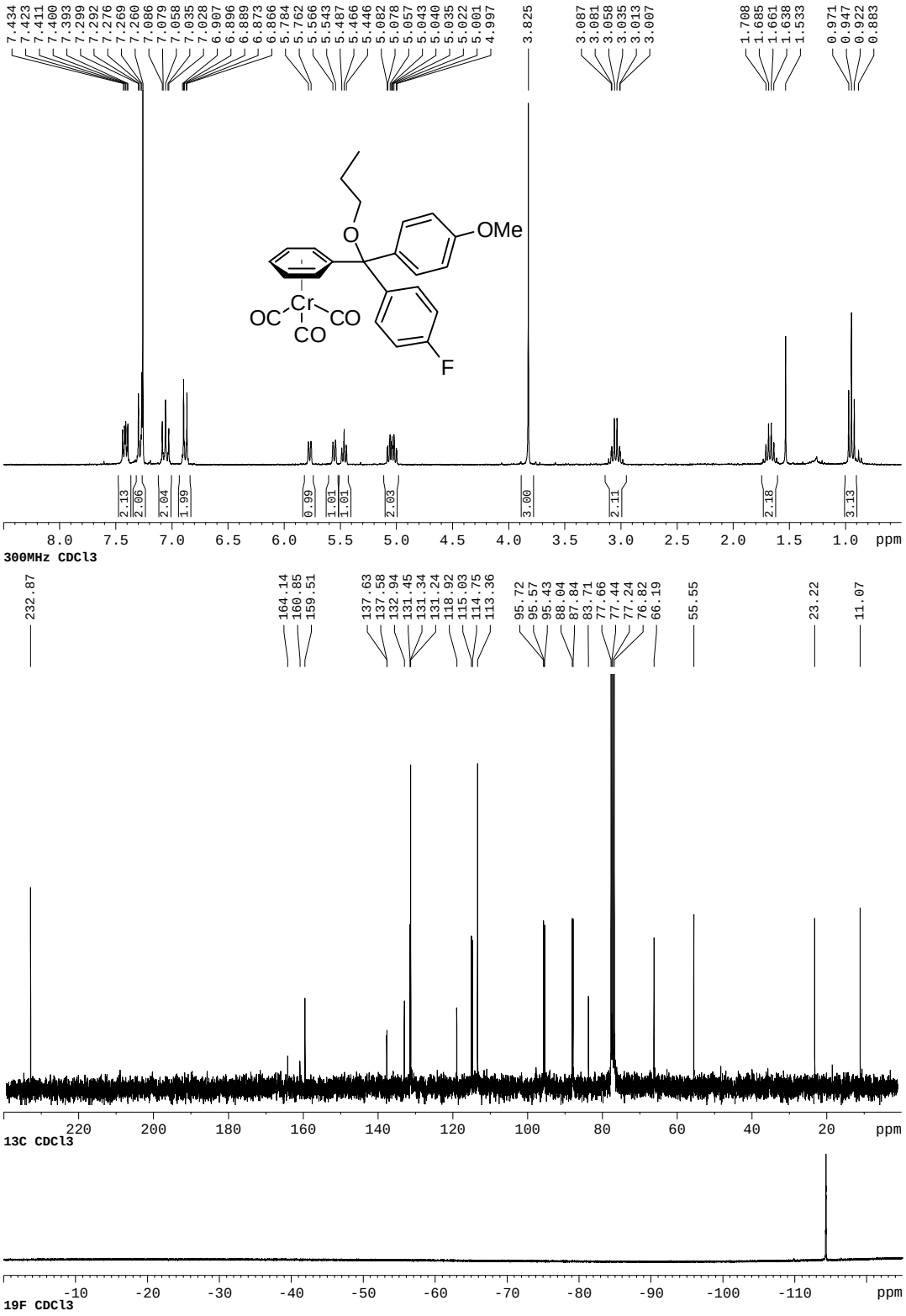

Figure I-38: $^{1}H$, $^{13}C\{^{1}H\}$ NMR spectra of **26f**.

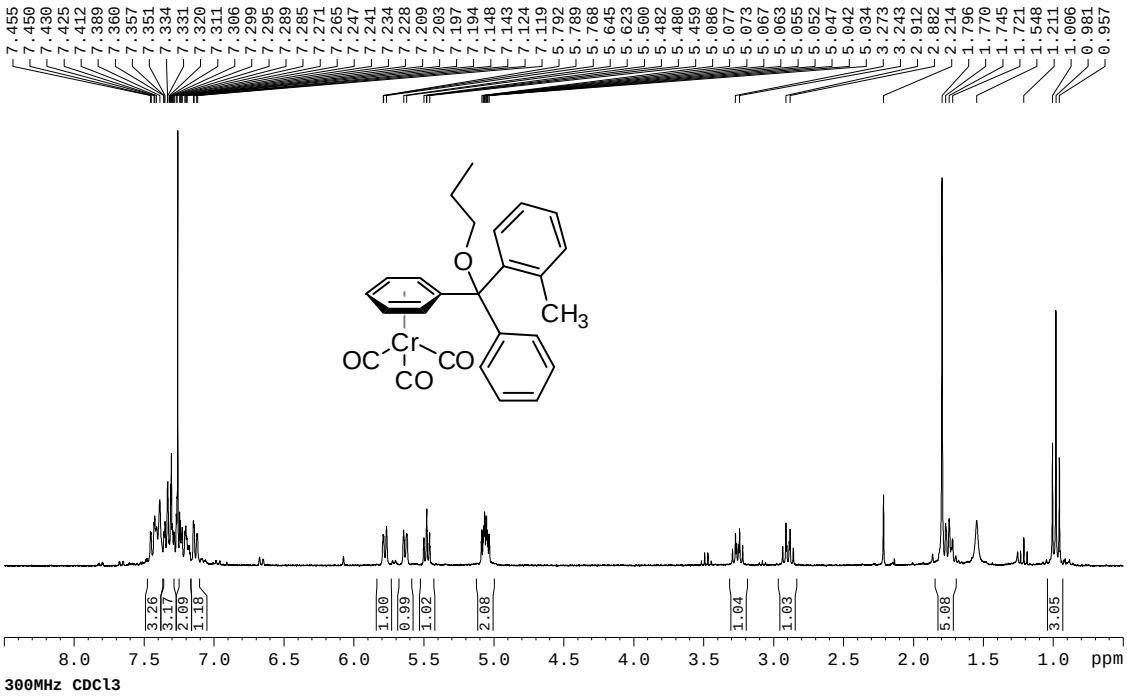


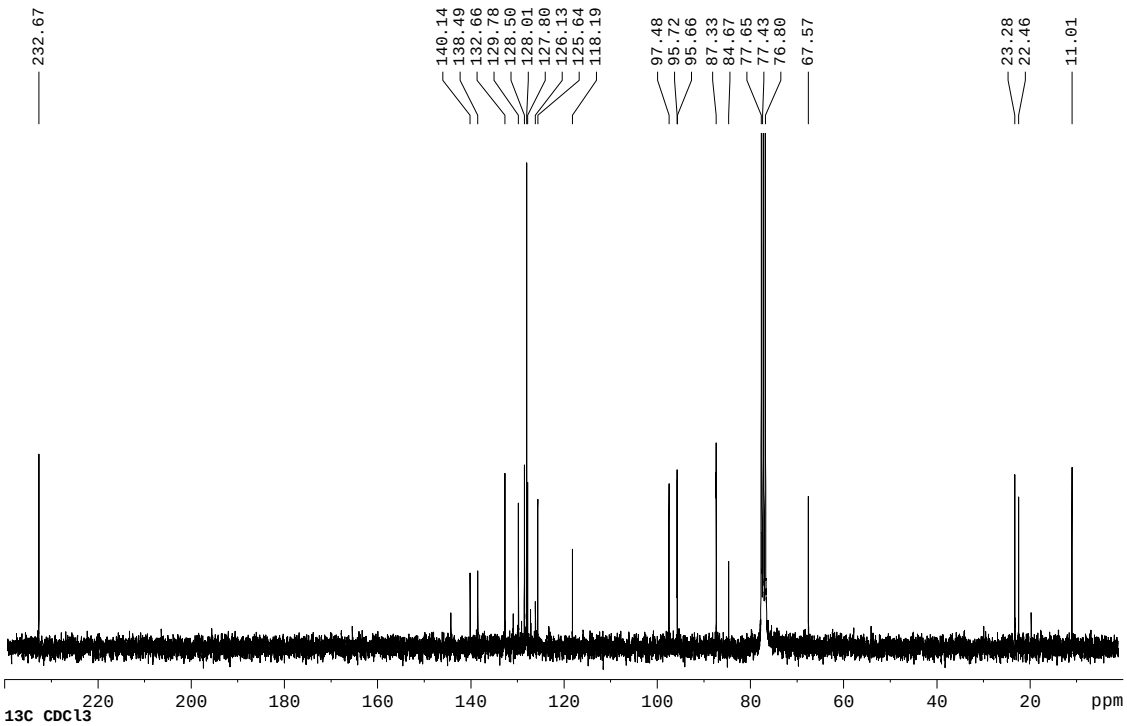

Figure I-39: $^{1}H$, $^{13}C\{^{1}H\}$ NMR spectra of **26g**.

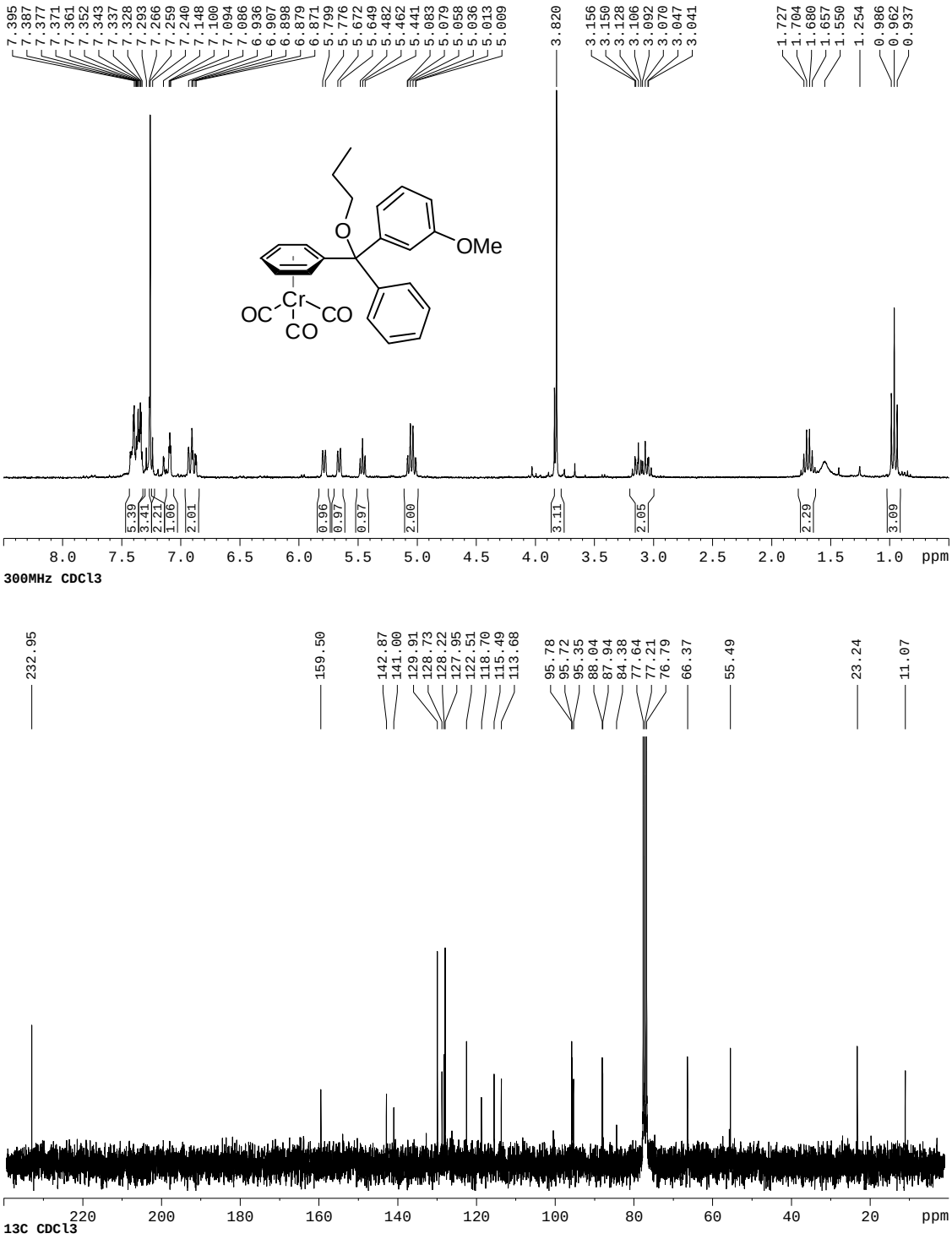

*Diarylmethylamines from dimethyl benzyl amine (**27**).*

Figure I-40: $^{1}H$, $^{13}C\{^{1}H\}$ NMR spectra of **28a**.

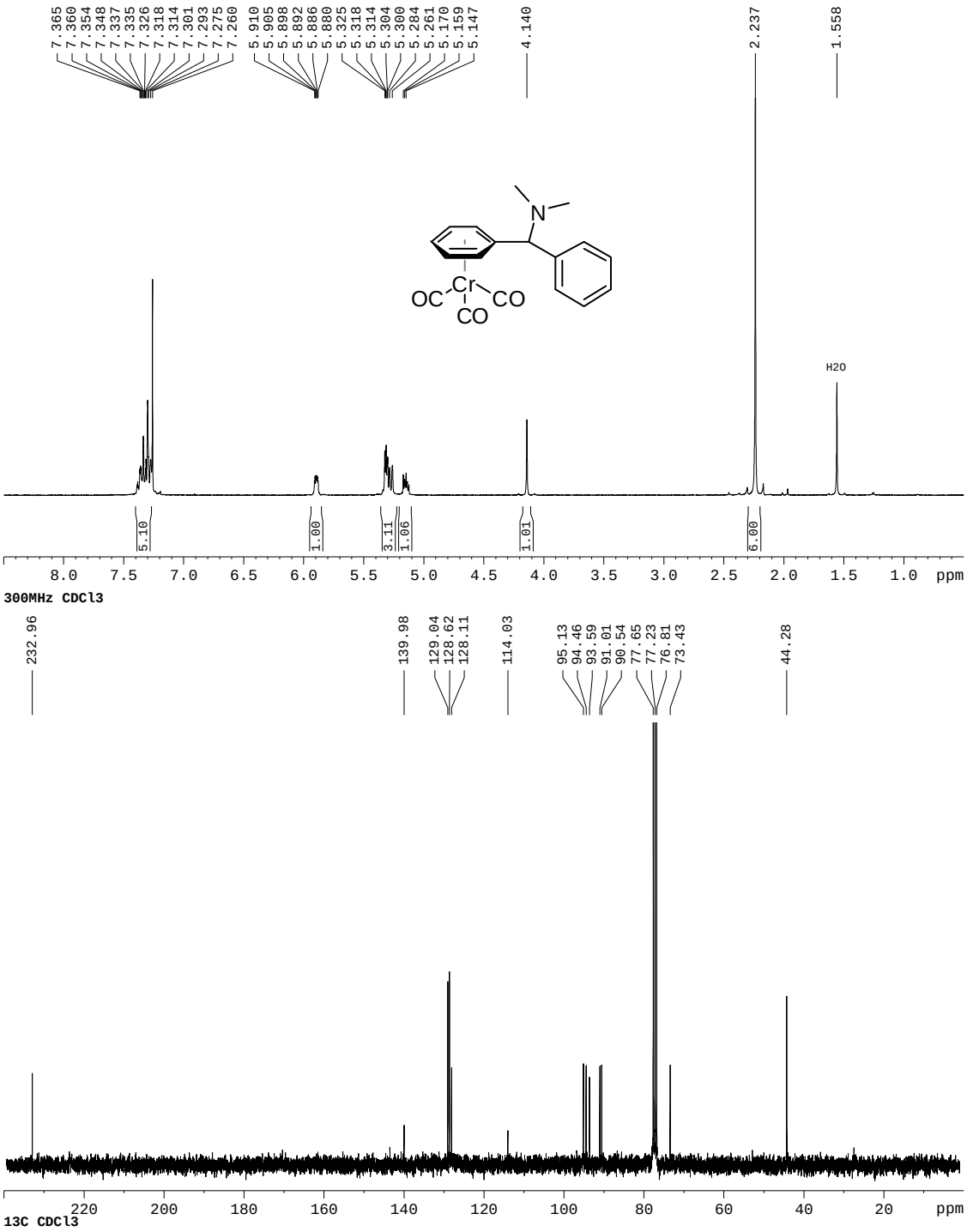

Figure I-41: $^{1}H$, $^{13}C\{^{1}H\}$, $^{19}F$ NMR spectra of **28b**.

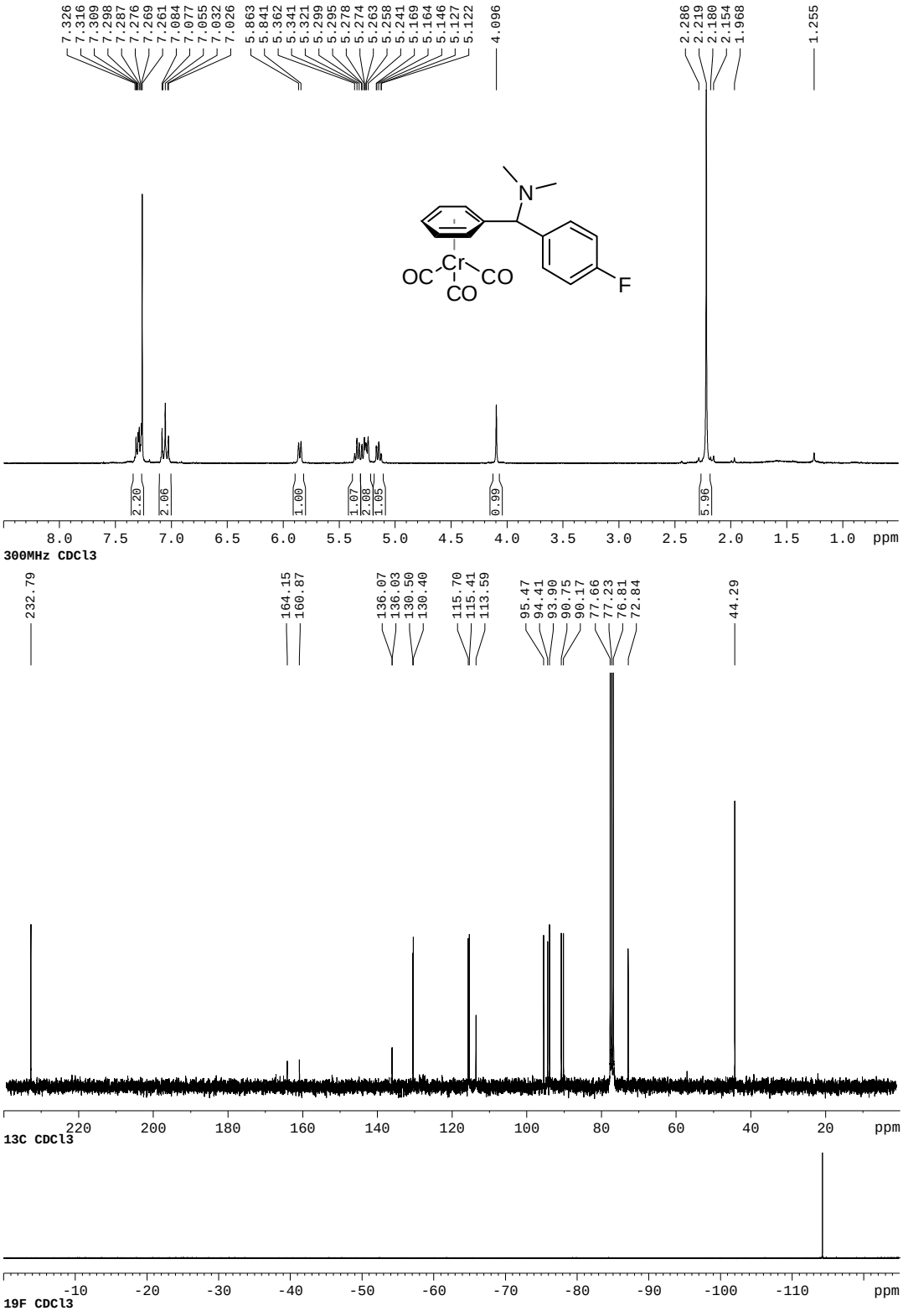

Figure I-42: $^{1}H$, $^{13}C\{^{1}H\}$ NMR spectra of **28c**.

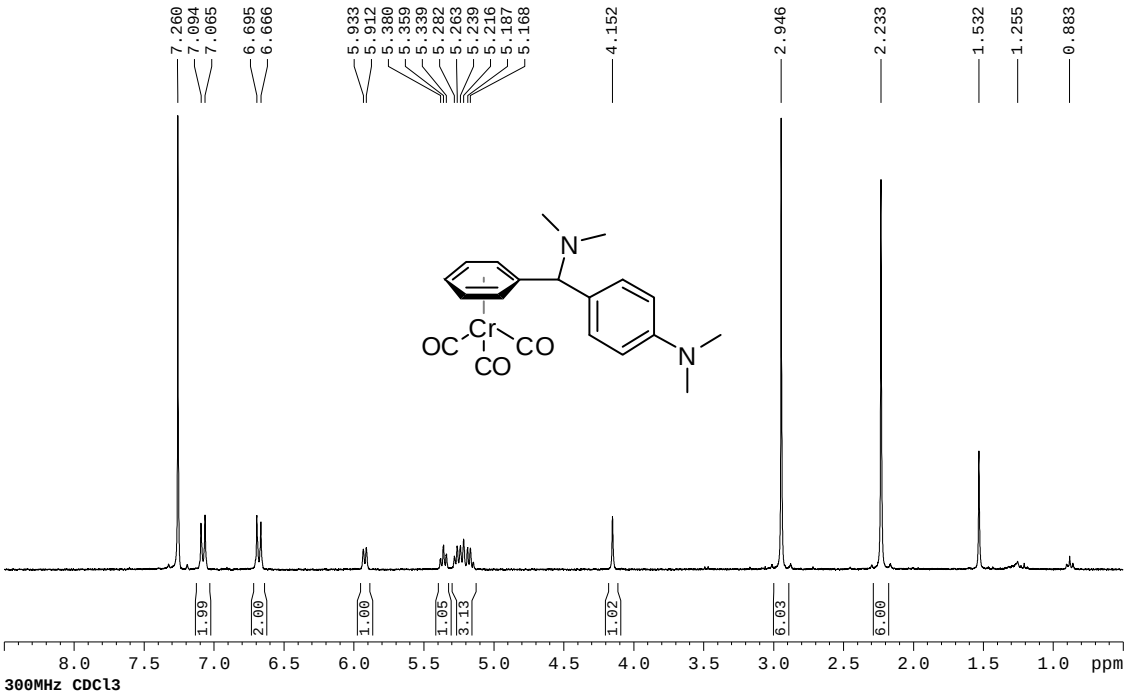


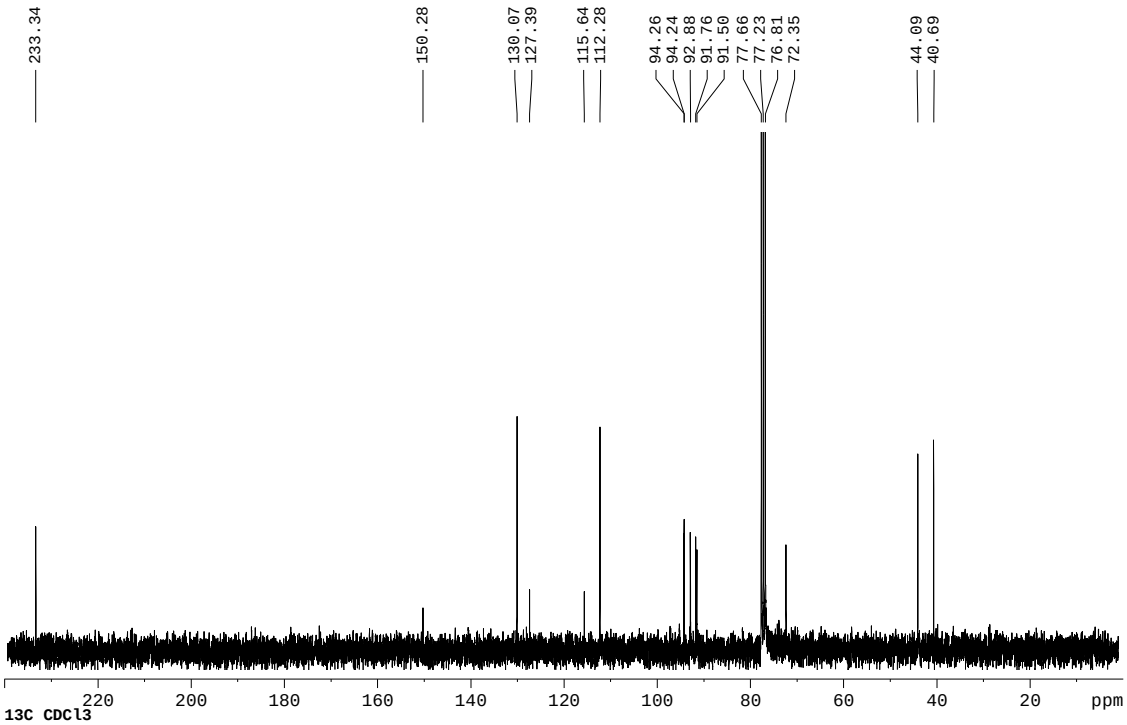

Figure I-43: $^{1}H$, $^{13}C\{^{1}H\}$ NMR spectra of **28d**.

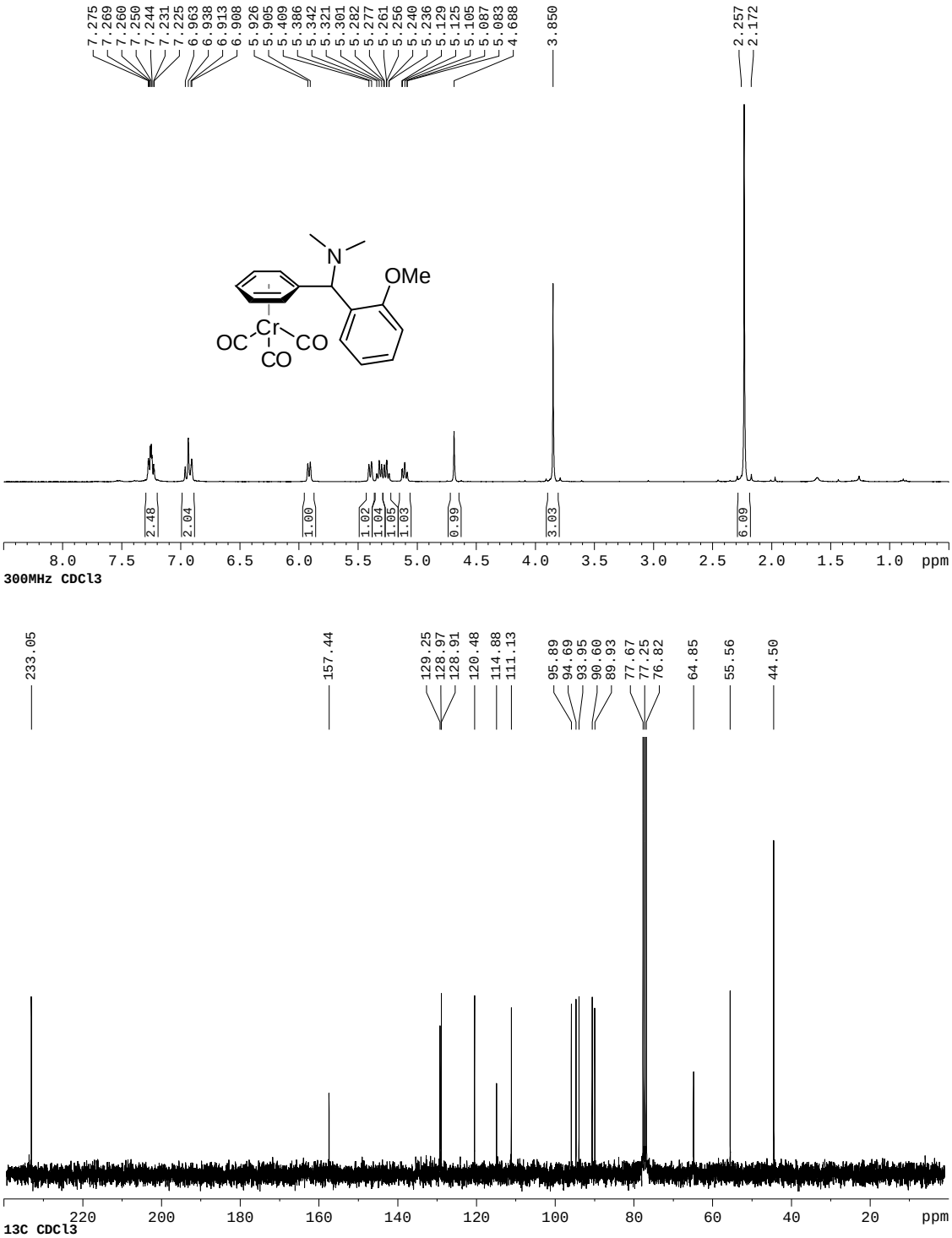

*Products from tricarbonylchomium ethylbenzene derivatives.*

Figure I-44: $^{1}H$, $^{13}C\{^{1}H\}$ NMR spectra of **31b**.

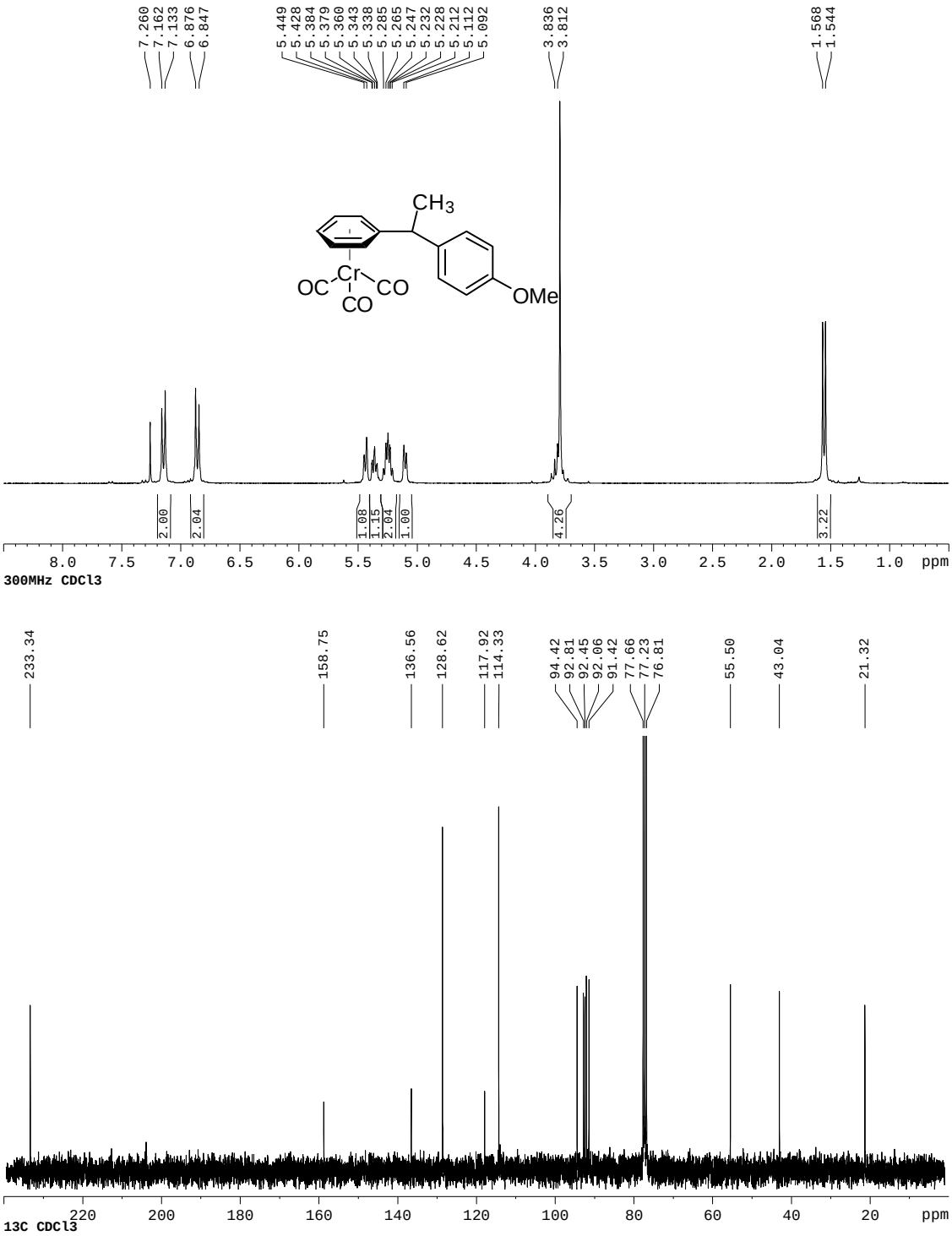

Figure I-45: $^{1}H$ NMR spectrum of quaternary side-product **35**.

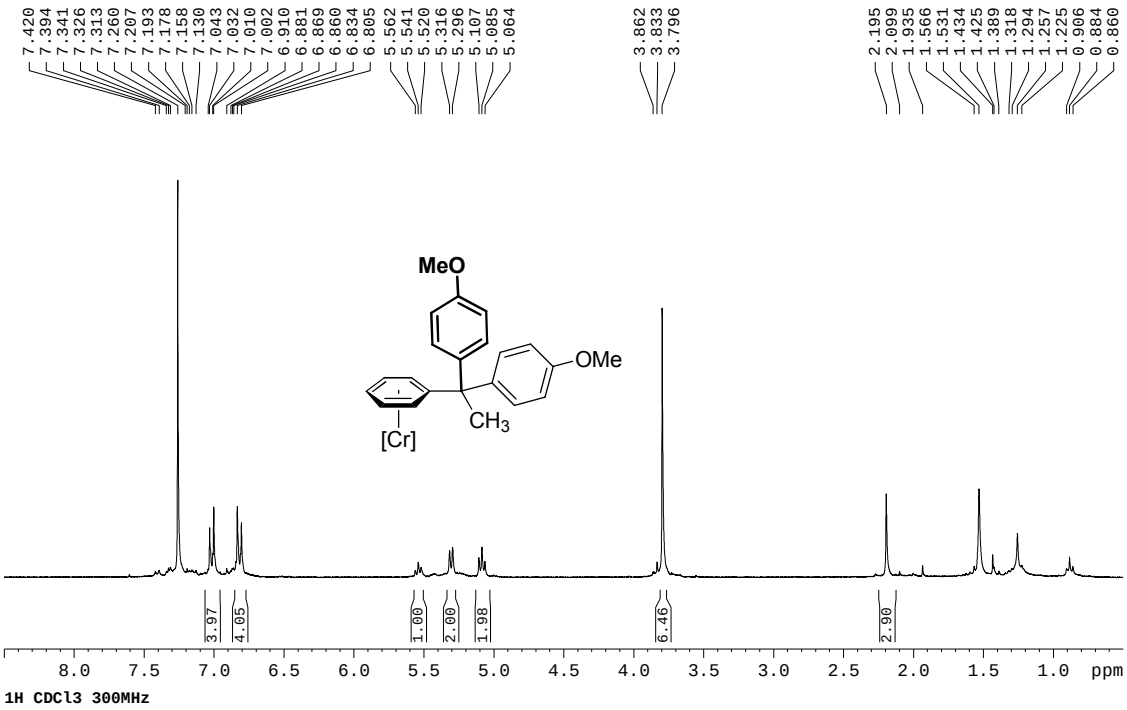

Figure I-46: $^{1}H$, $^{13}C\{^{1}H\}$ NMR spectra of **37**.

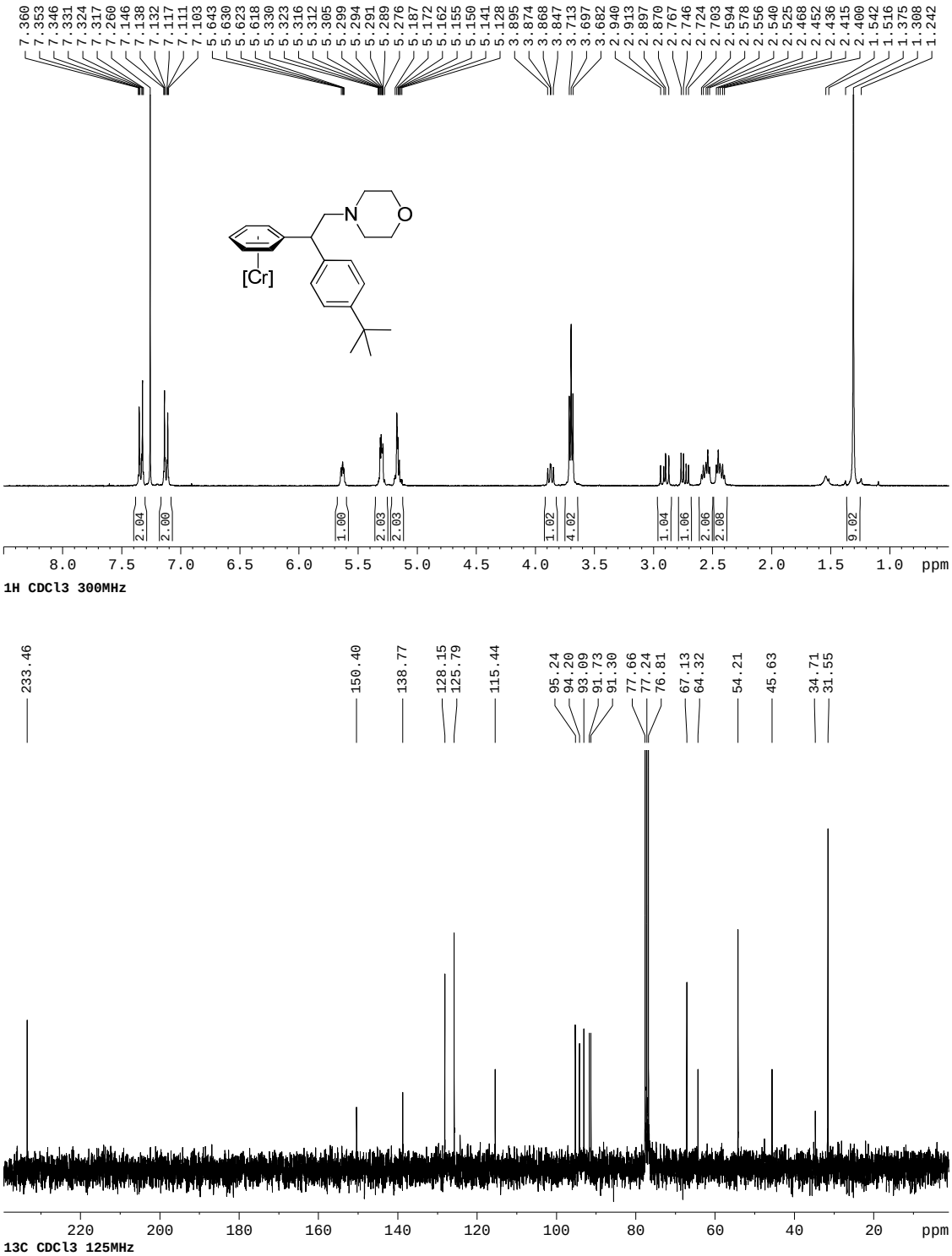

Figure I-47: $^{1}H$, $^{13}C\{^{1}H\}$ NMR spectra of **41a**.

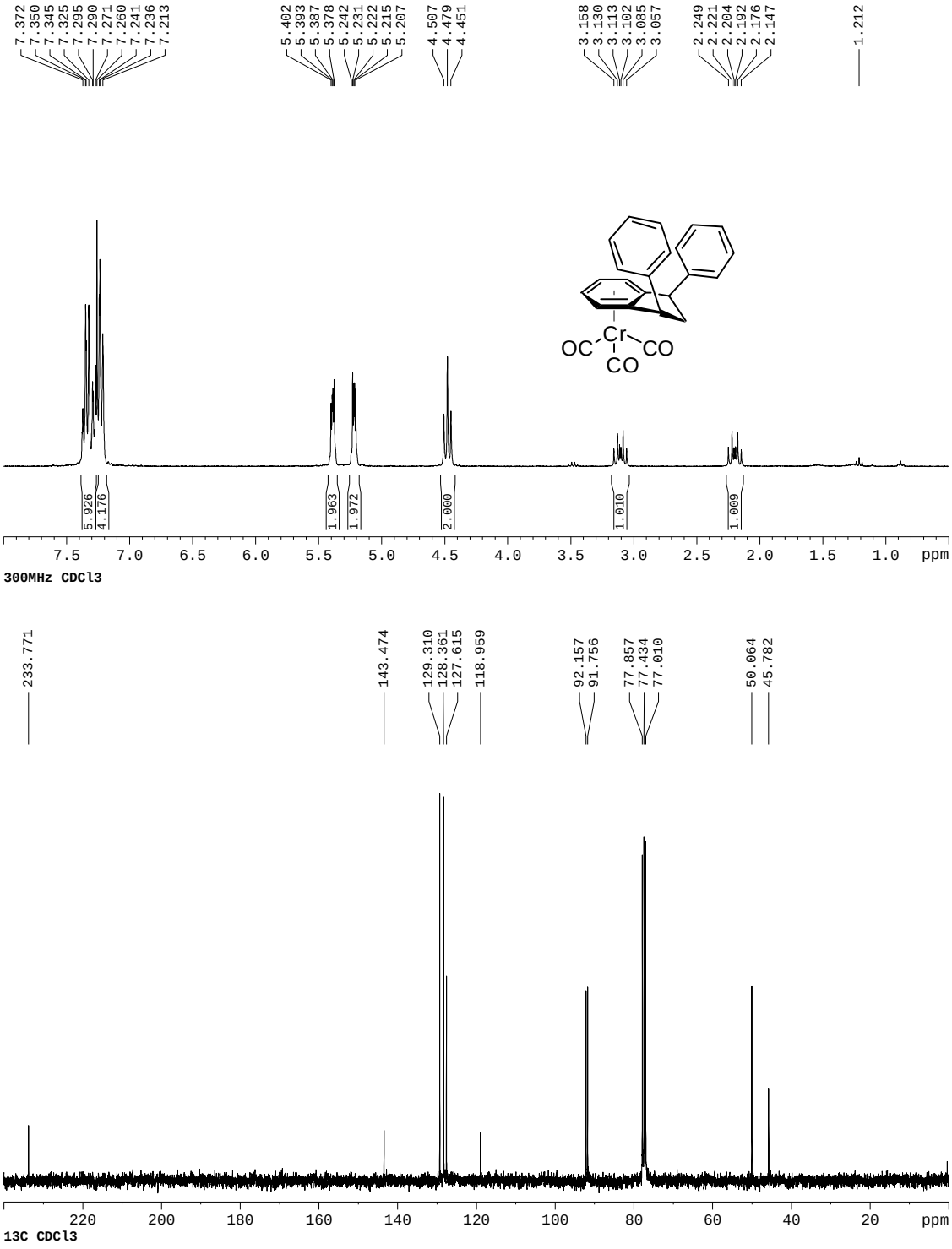

Figure I-48: $^{1}H$, $^{13}C\{^{1}H\}$, $^{19}F\{^{1}H\}$ NMR spectra of **41b**.

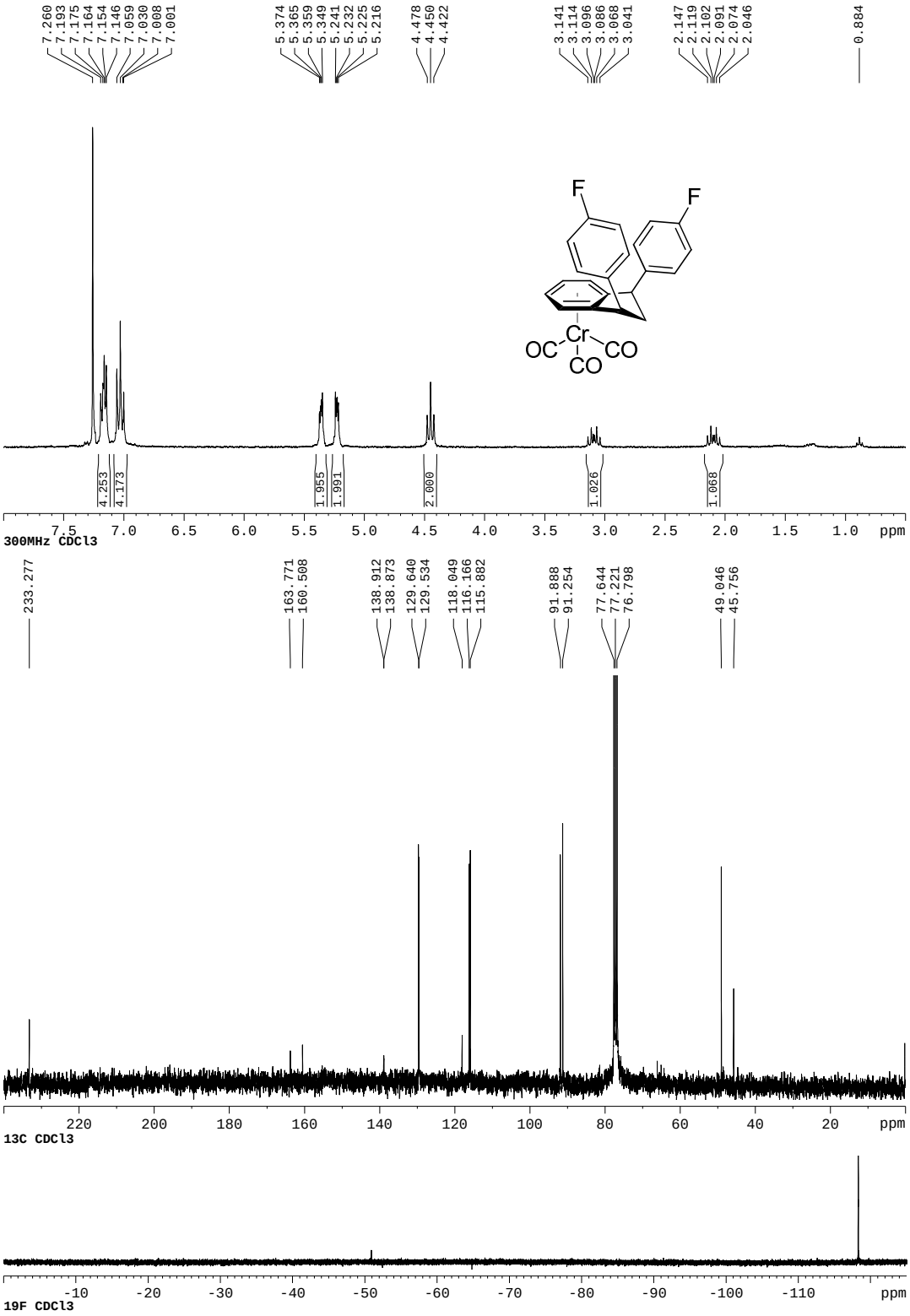

Figure I-49: $^{1}H$, $^{13}C\{^{1}H\}$ NMR spectra of **41c**.

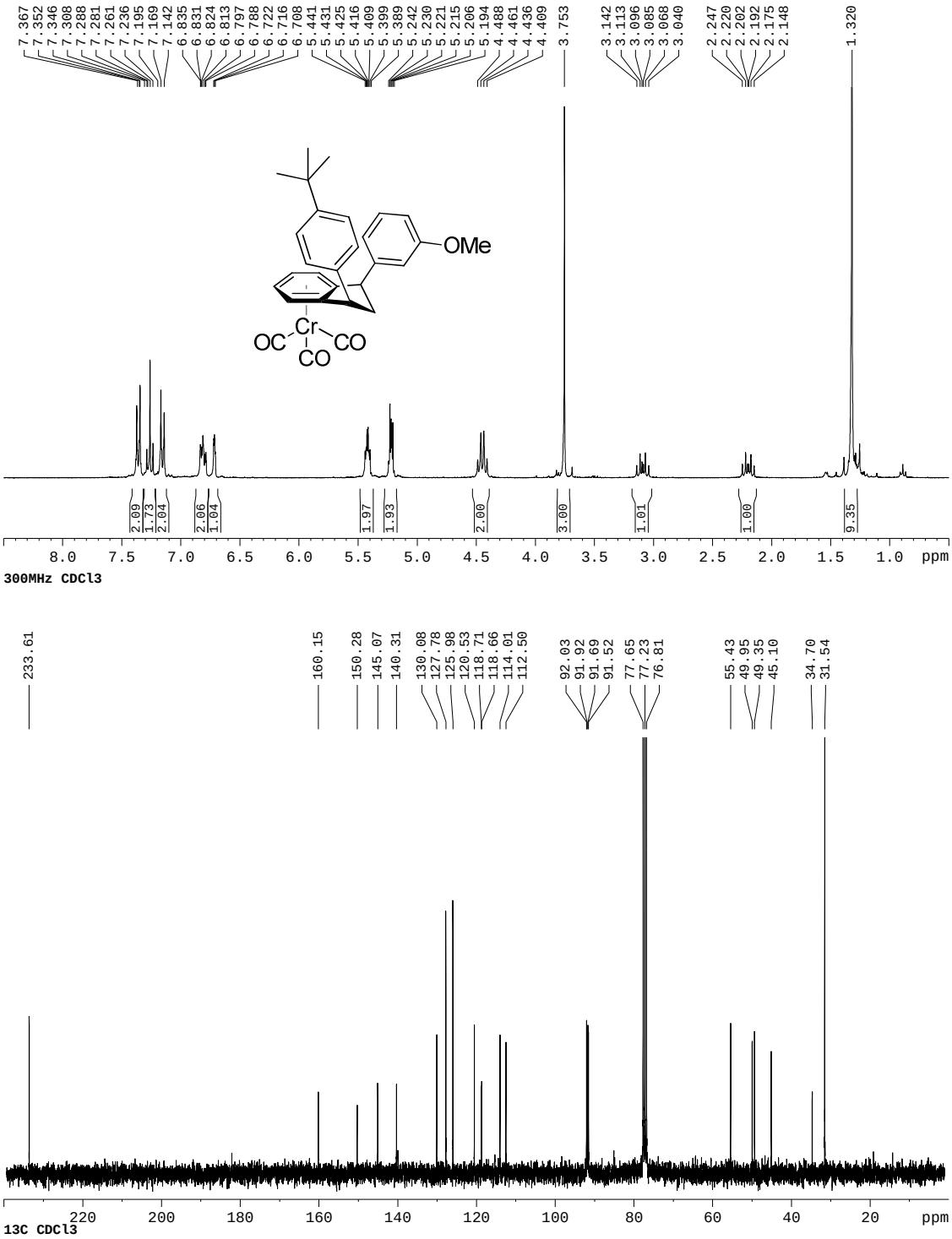

Figure I-50: $^{1}H$, $^{13}C\{^{1}H\}$ NMR spectra of **42a**.

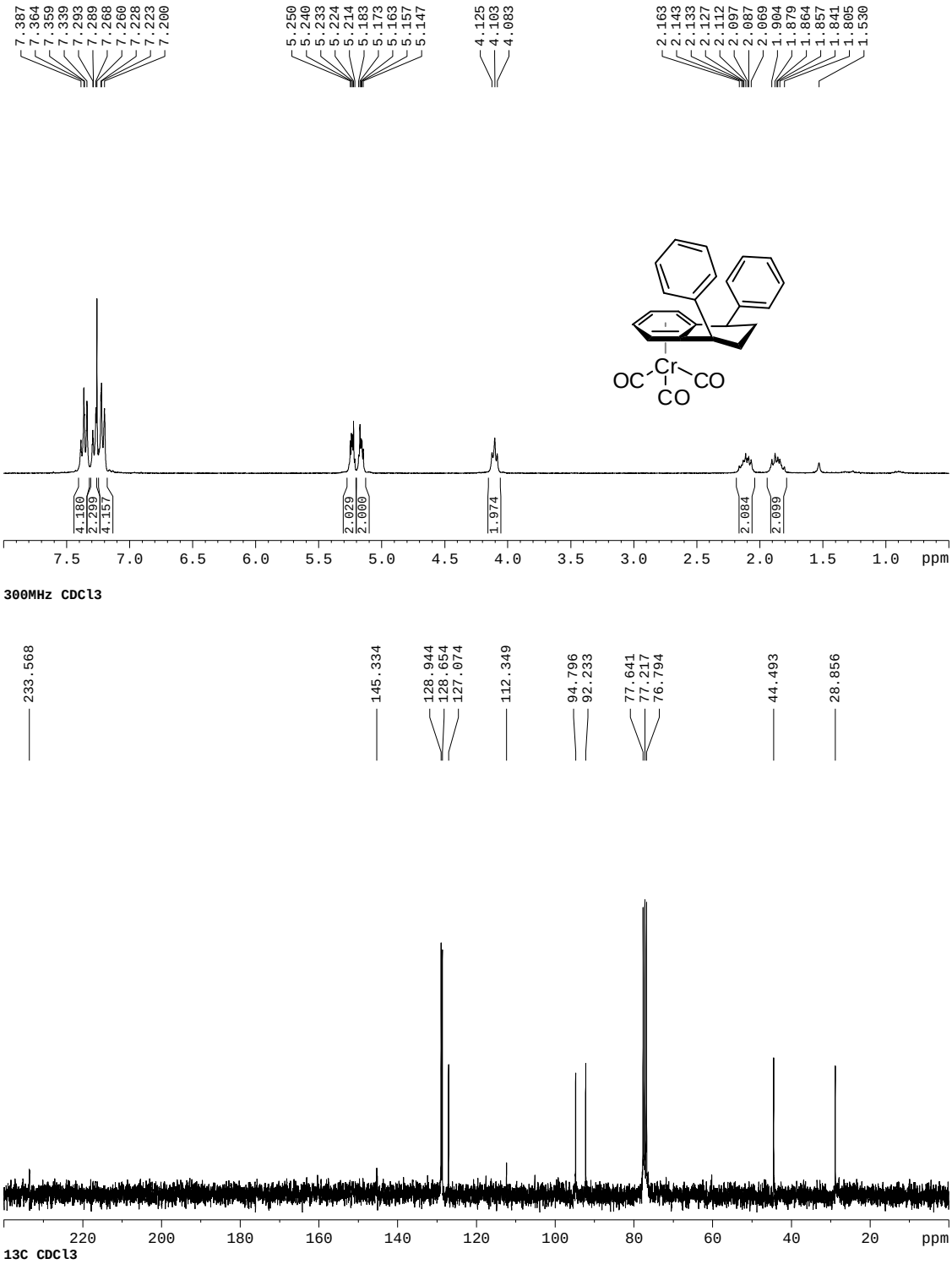

Figure I-51: $^{1}H$, $^{13}C\{^{1}H\}$, $^{19}F\{^{1}H\}$ NMR spectra of **42b**.

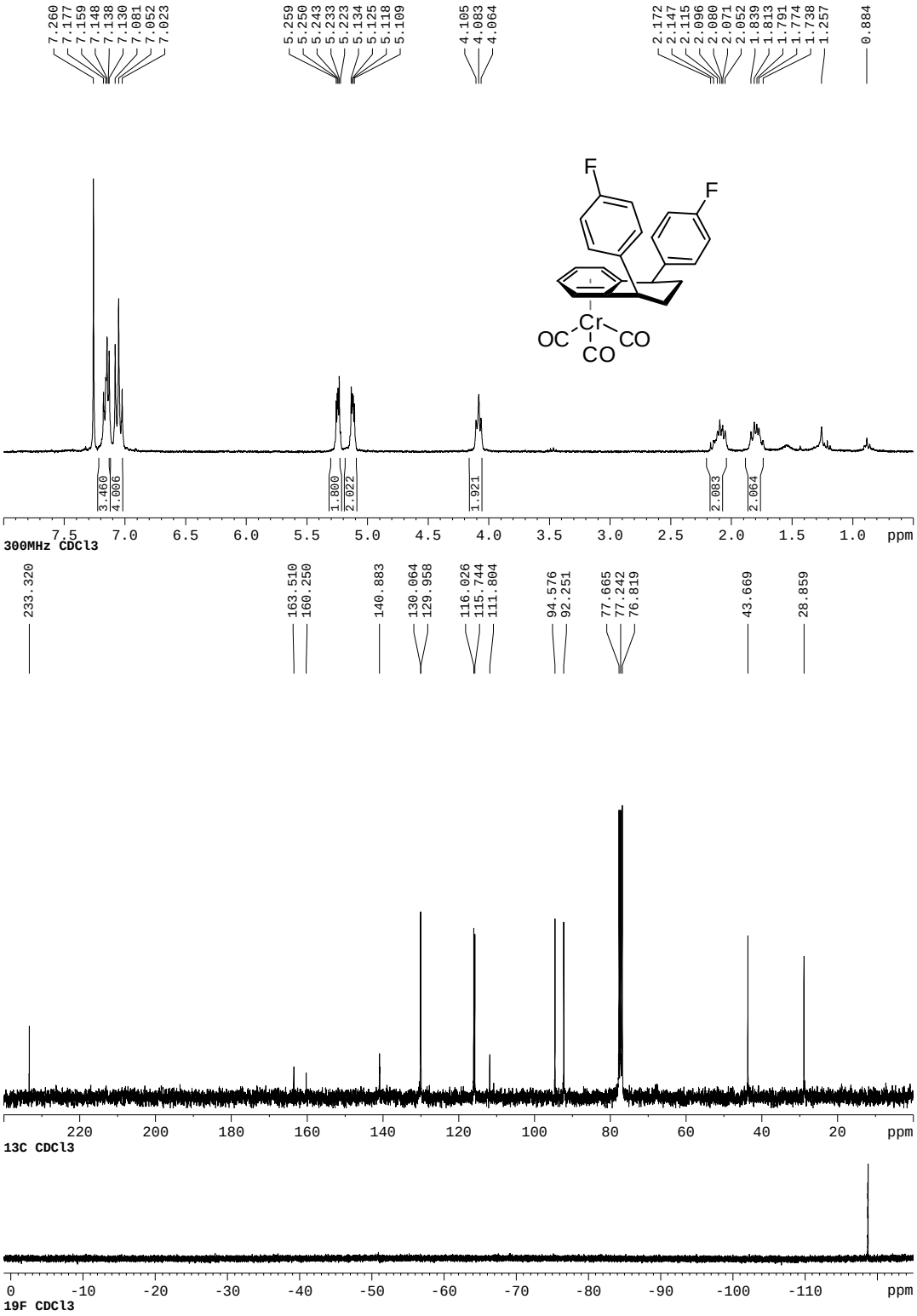

Figure I-52: $^{1}H$, $^{13}C\{^{1}H\}$ NMR spectra of **42c**.

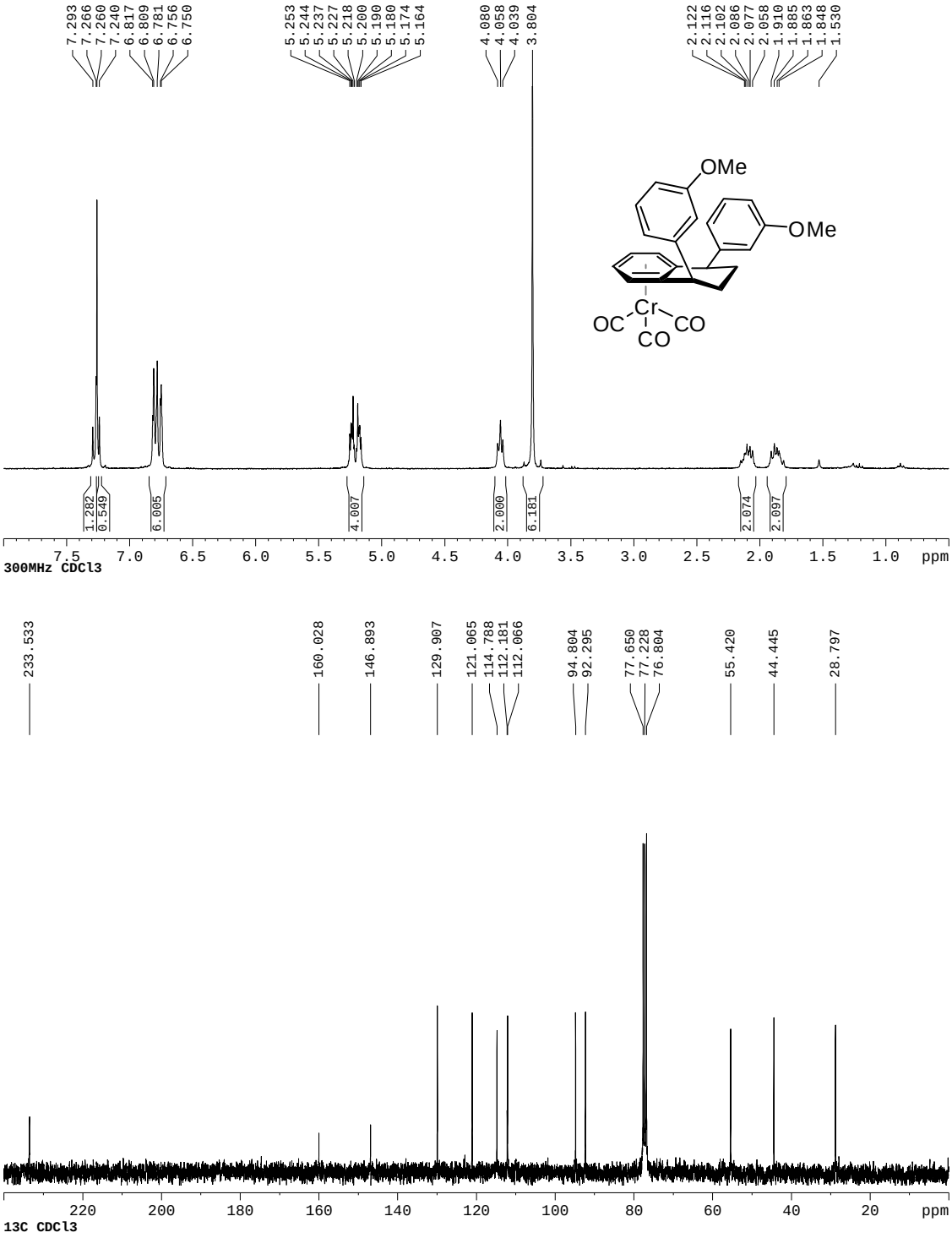

Figure I-53: $^{1}H$, $^{13}C\{^{1}H\}$ NMR spectra of **43a**.

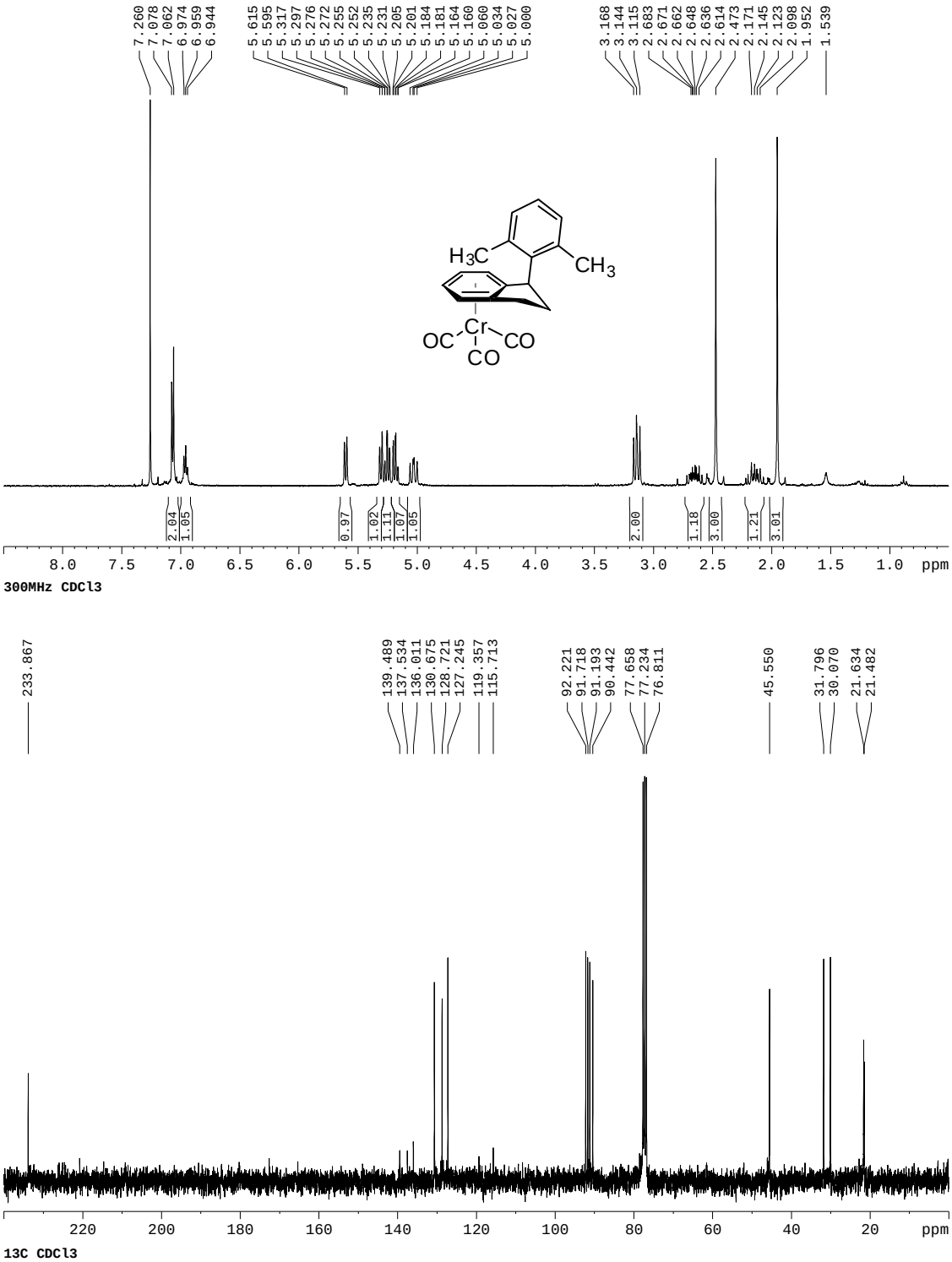

Figure I-54: $^{1}H$, $^{13}C\{^{1}H\}$ NMR spectra of **43b**.

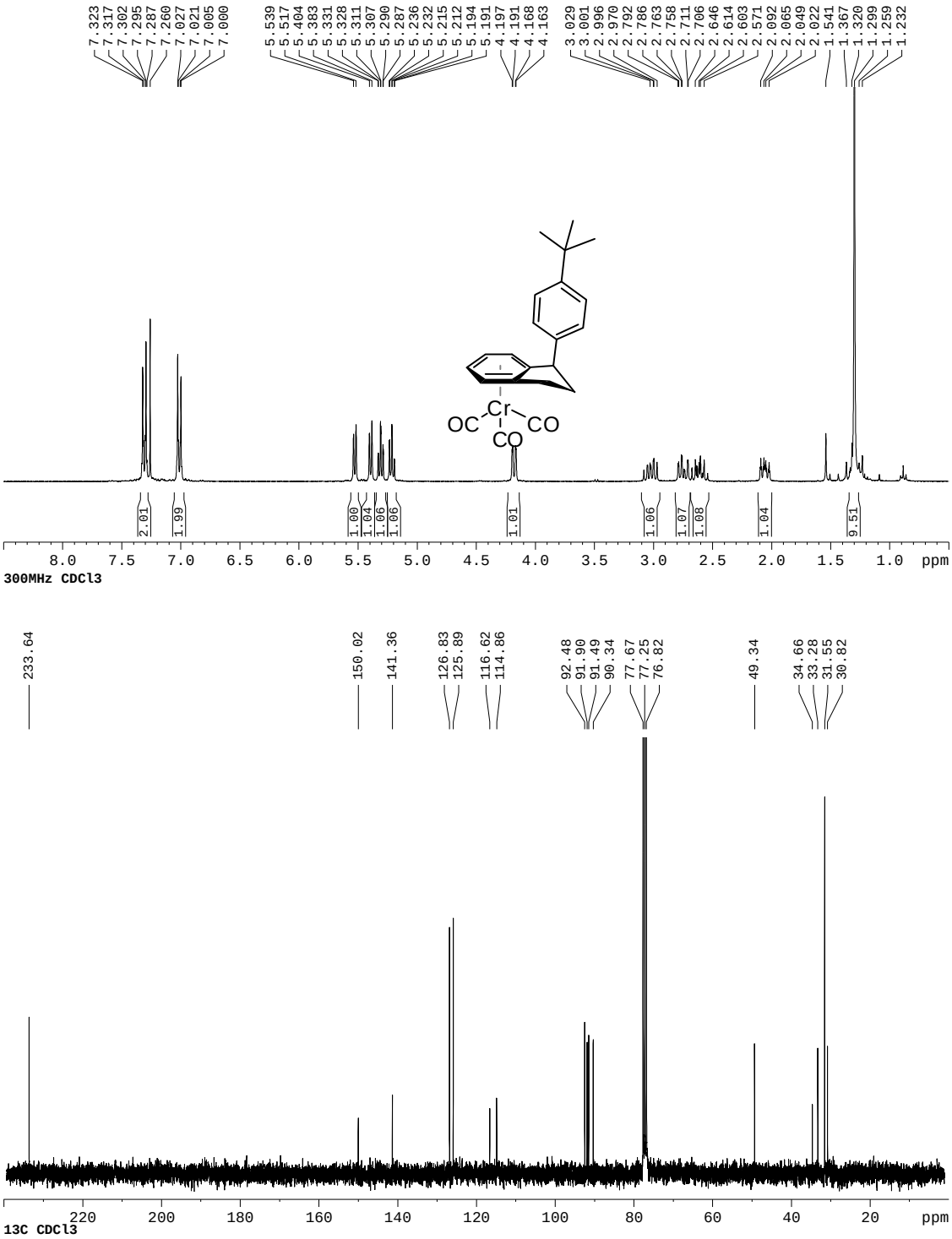

Figure I-55: $^{1}H$, $^{13}C\{^{1}H\}$ NMR spectra of **43c**.

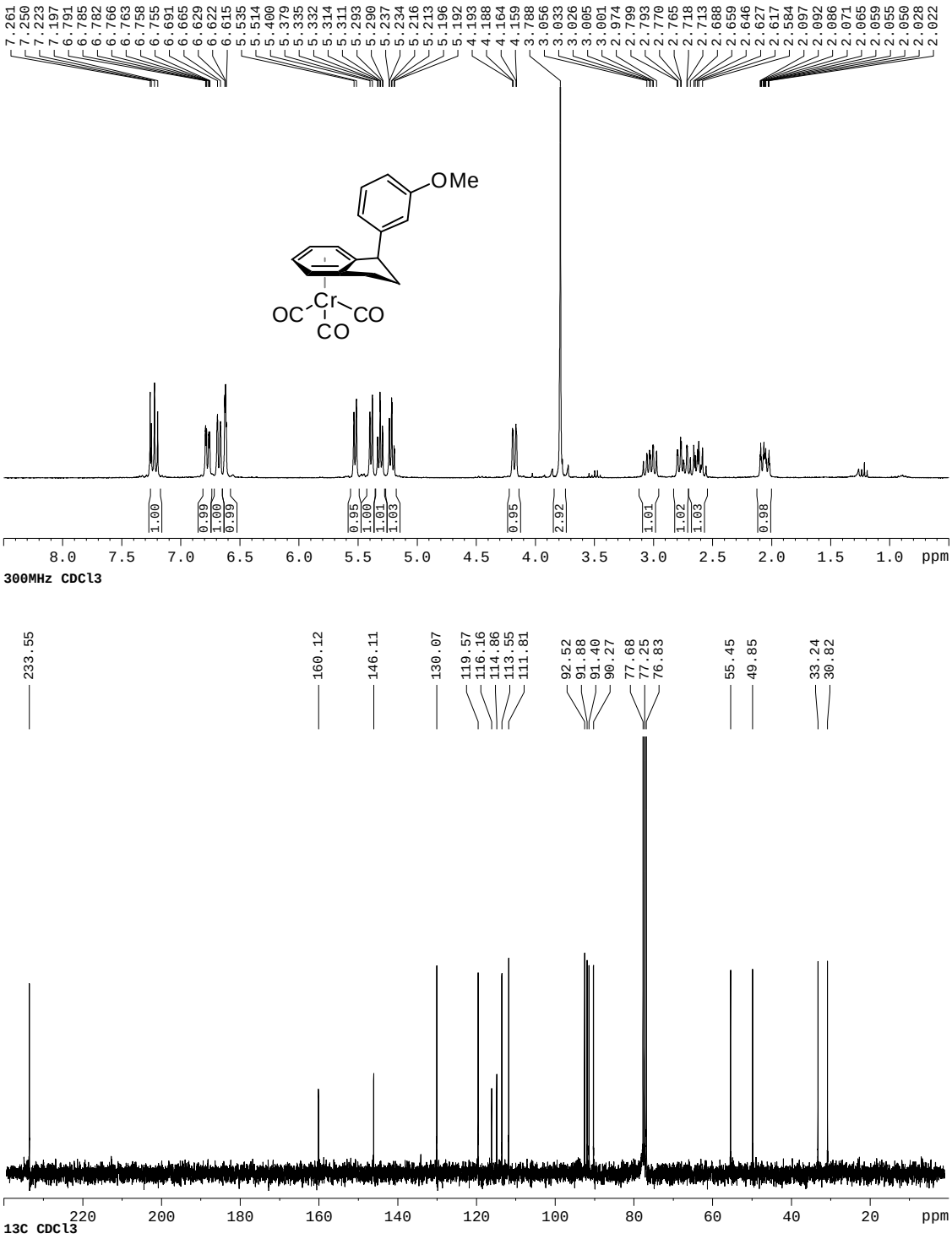

Figure I-56: $^{1}H$, $^{13}C\{^{1}H\}$NMR spectra of **44b**.

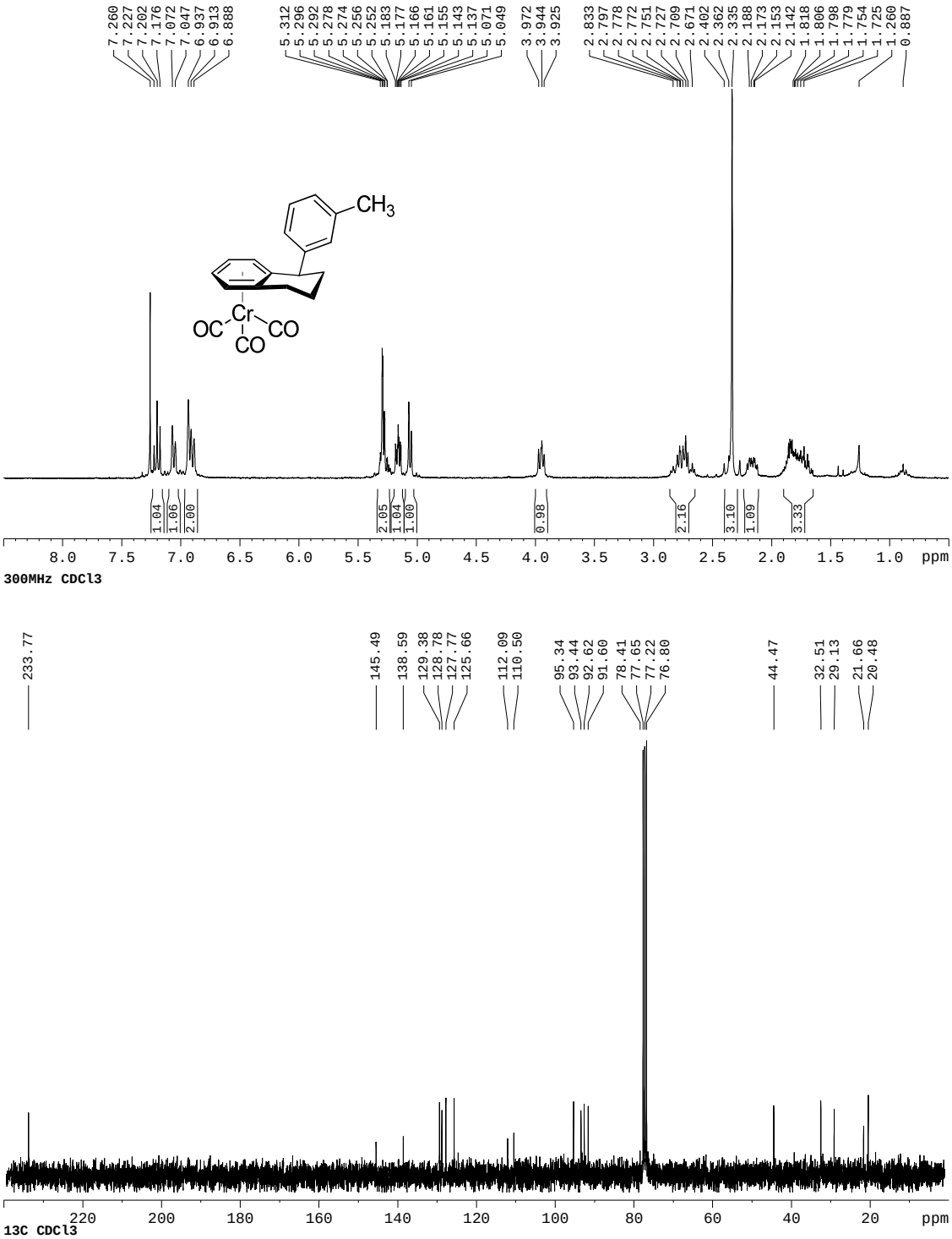

Figure I-57: $^{1}H$, $^{13}C\{^{1}H\}$ NMR spectra of **44c**.

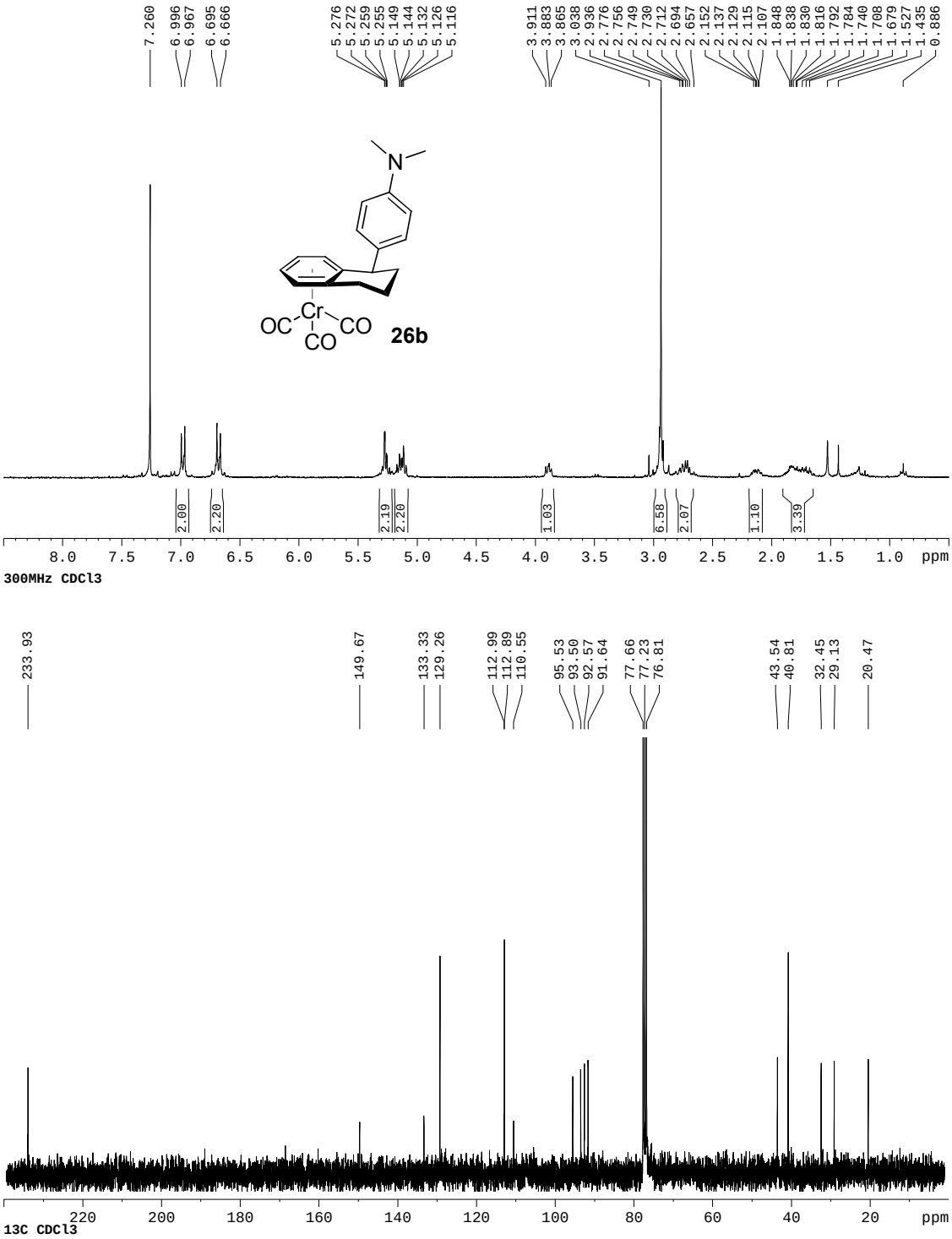

Figure I-58: $^{1}H$, $^{13}C\{^{1}H\}$NMR spectra of **45**.

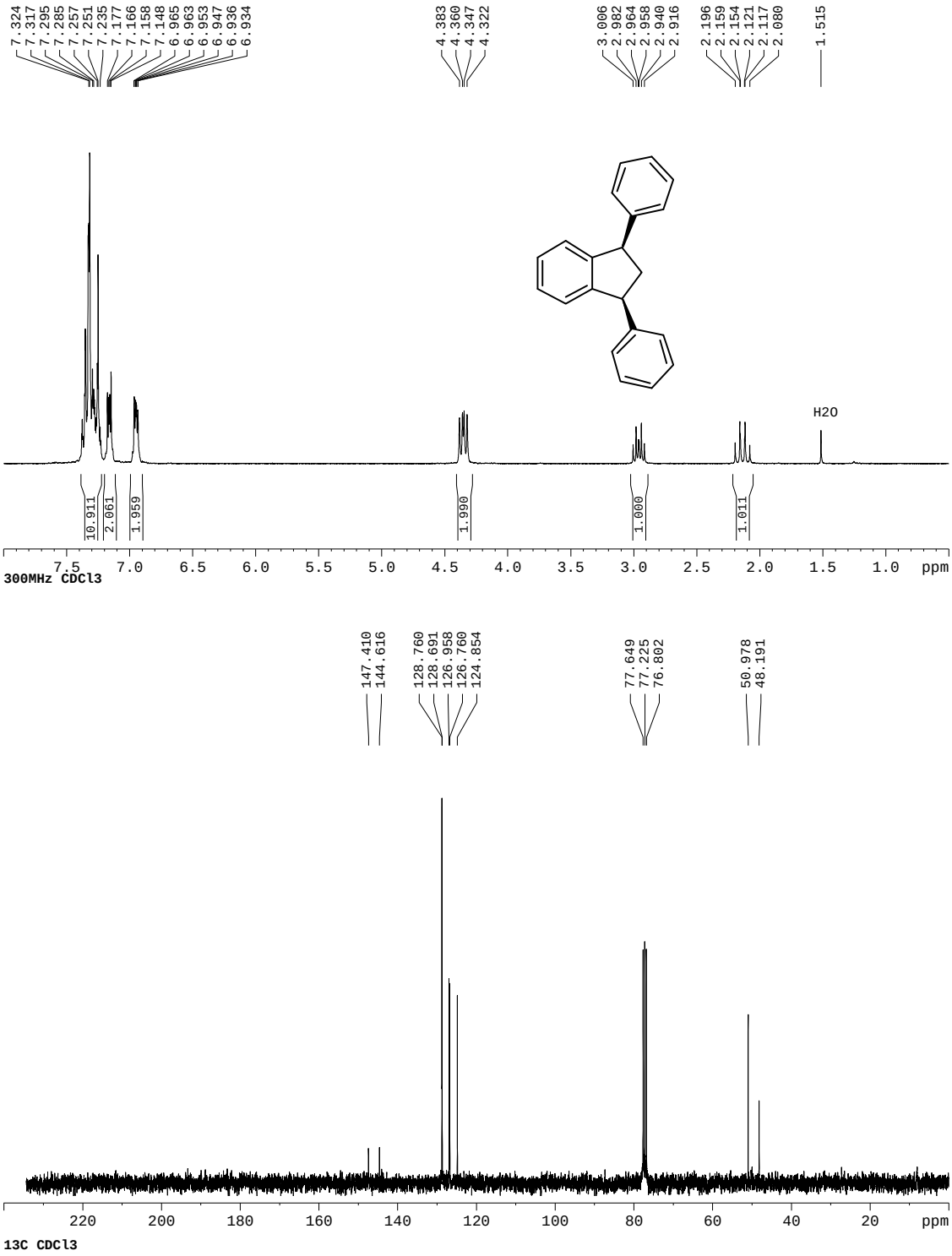

Figure I-59: $^{1}H$, $^{13}C\{^{1}H\}$ NMR spectra of **47a**.

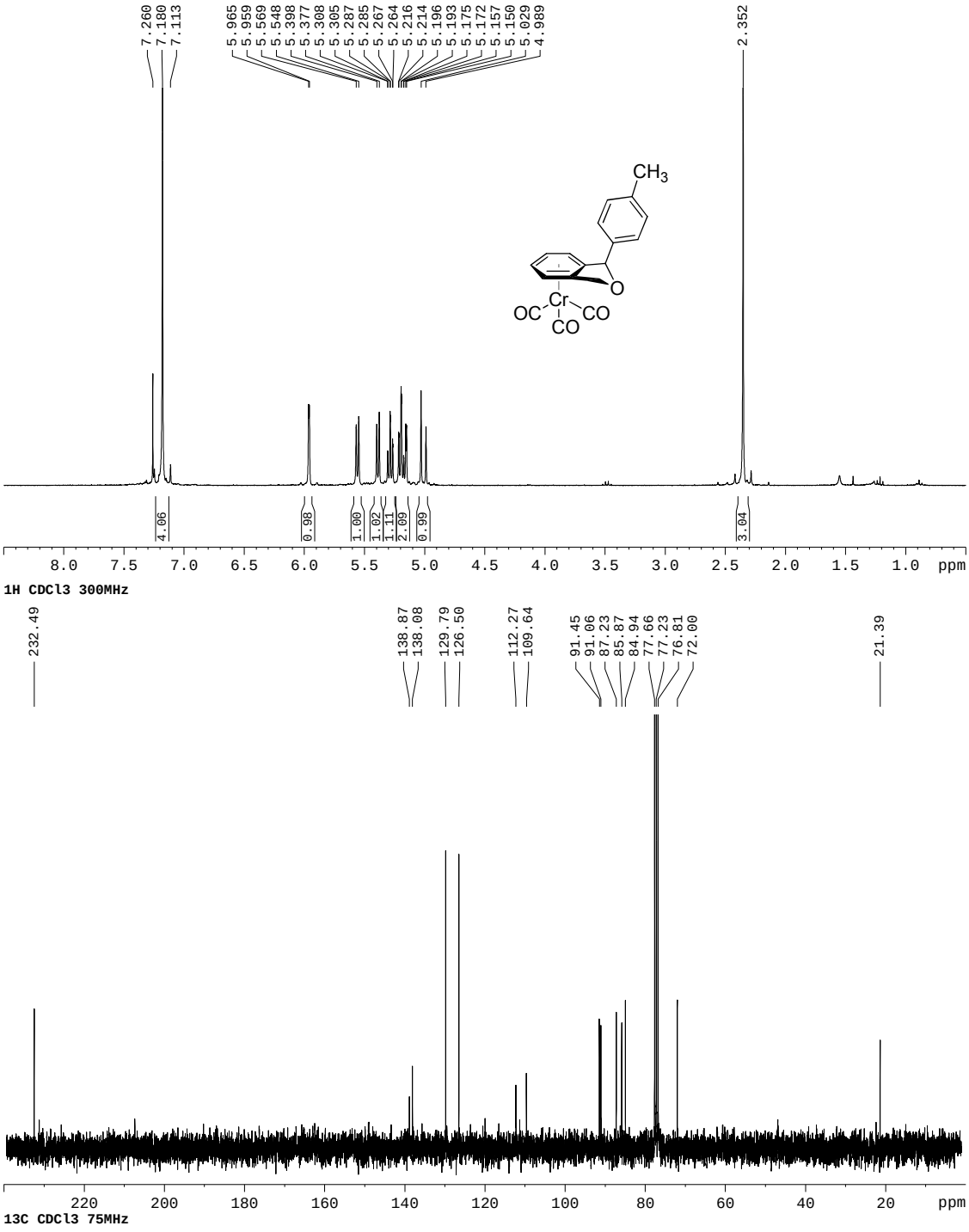

Figure I-60: $^{1}H$, $^{13}C\{^{1}H\}$ NMR spectra of **47b**.

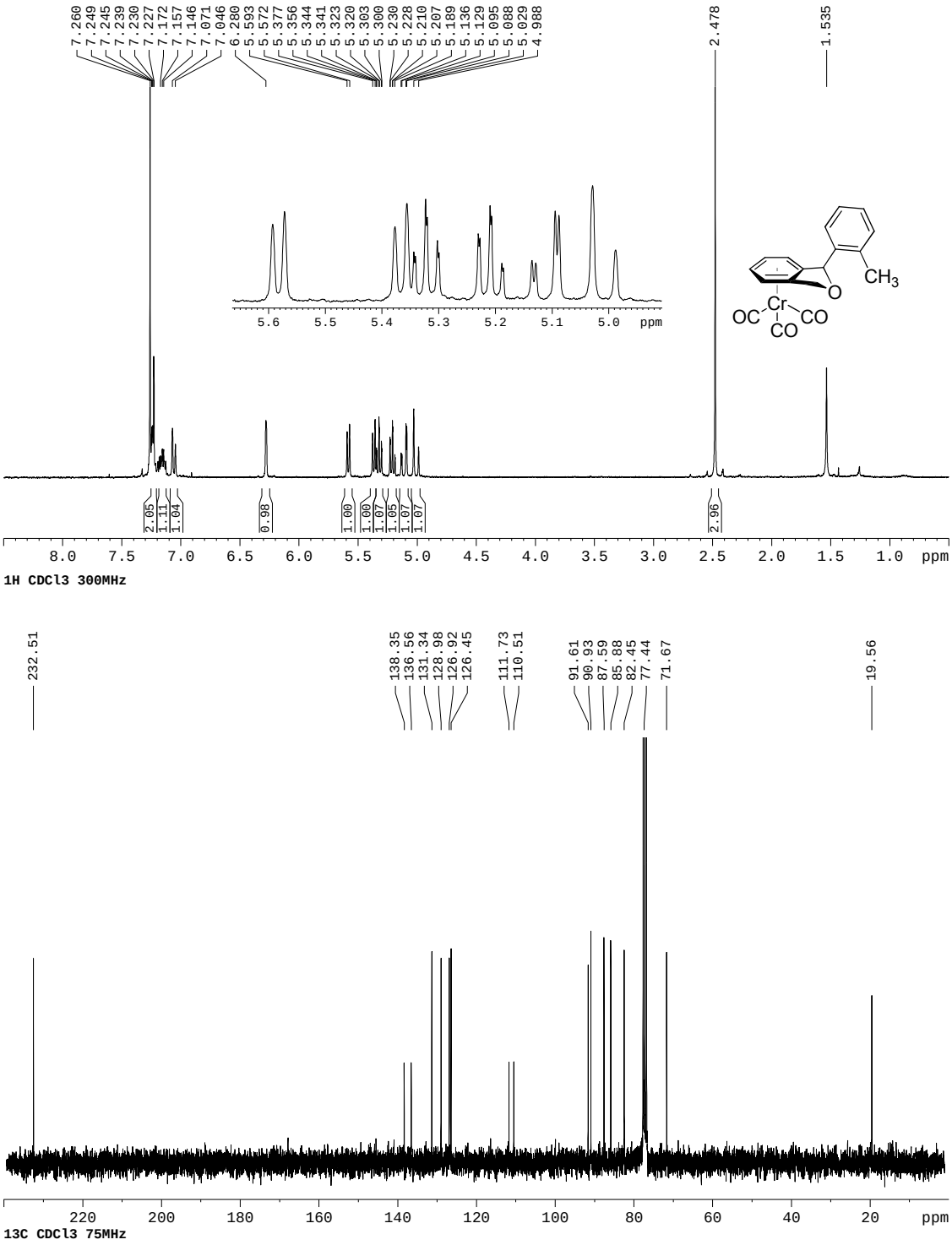

Figure I-61: $^{1}H$, $^{13}C\{^{1}H\}$ NMR spectra of **49**.

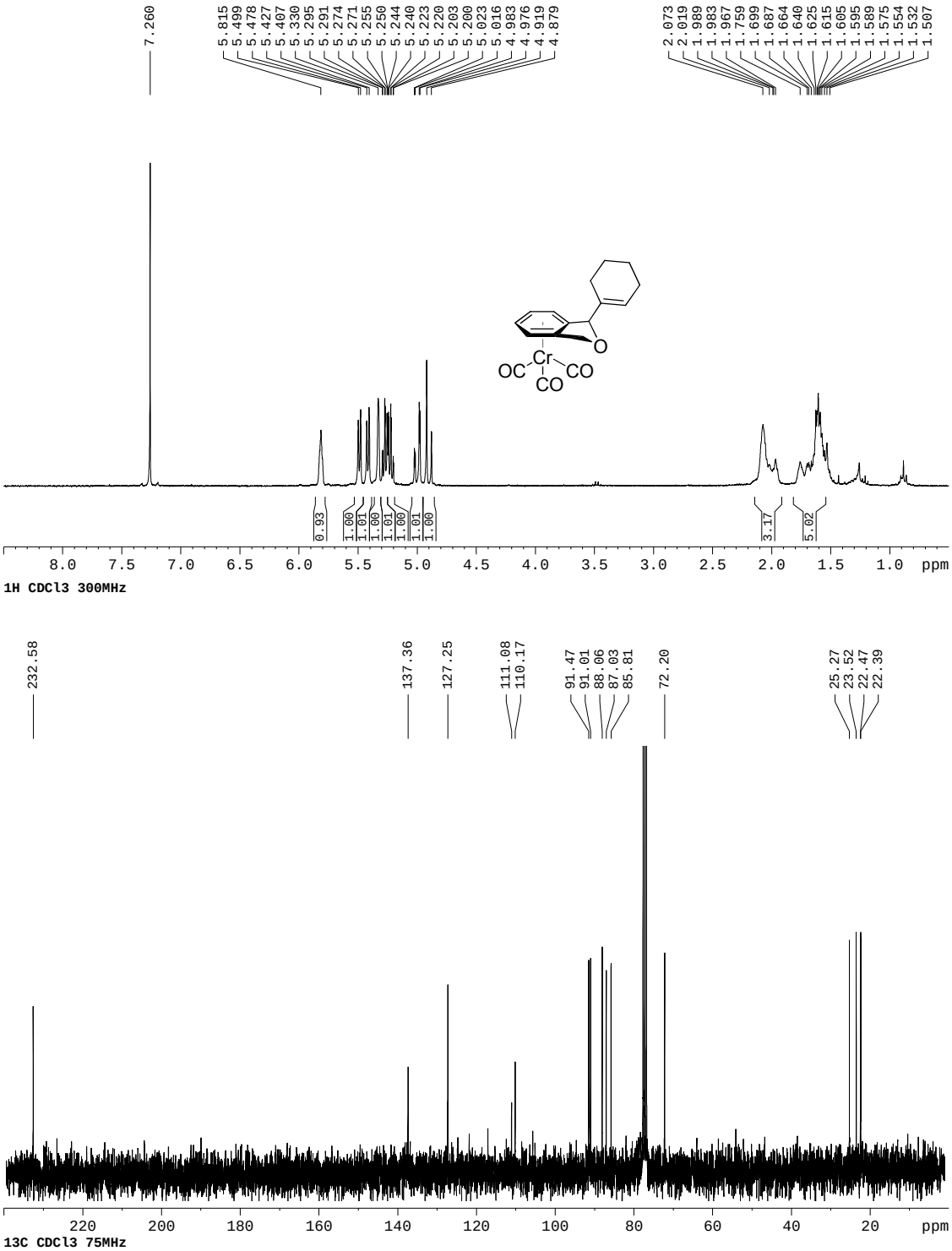

*Walking Product*

Figure I-62: $^{1}H$, $^{13}C\{^{1}H\}$ NMR spectra of **50**.

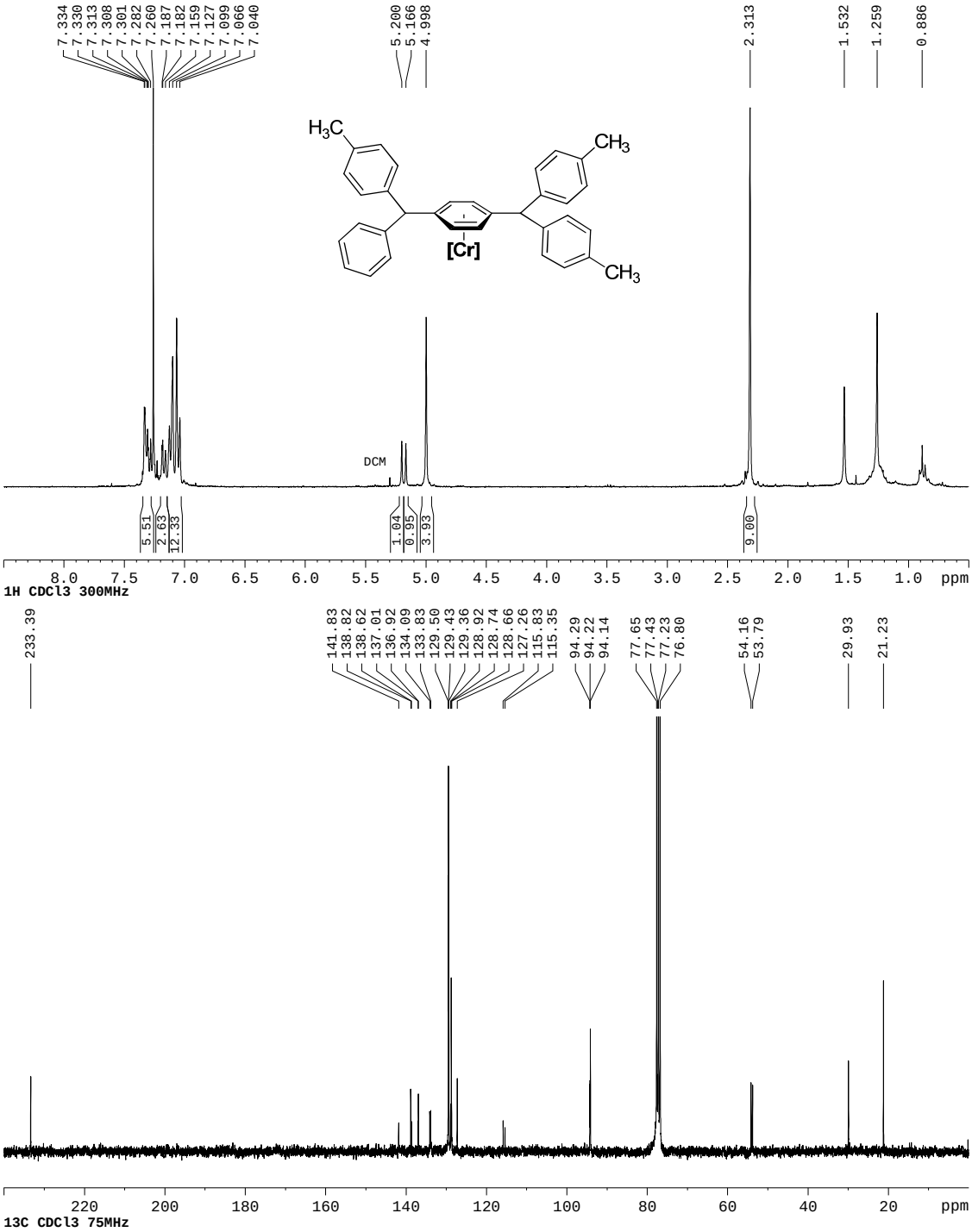

Figure I-63: $^{1}H$, $^{13}C\{^{1}H\}$ NMR spectra of **53**.

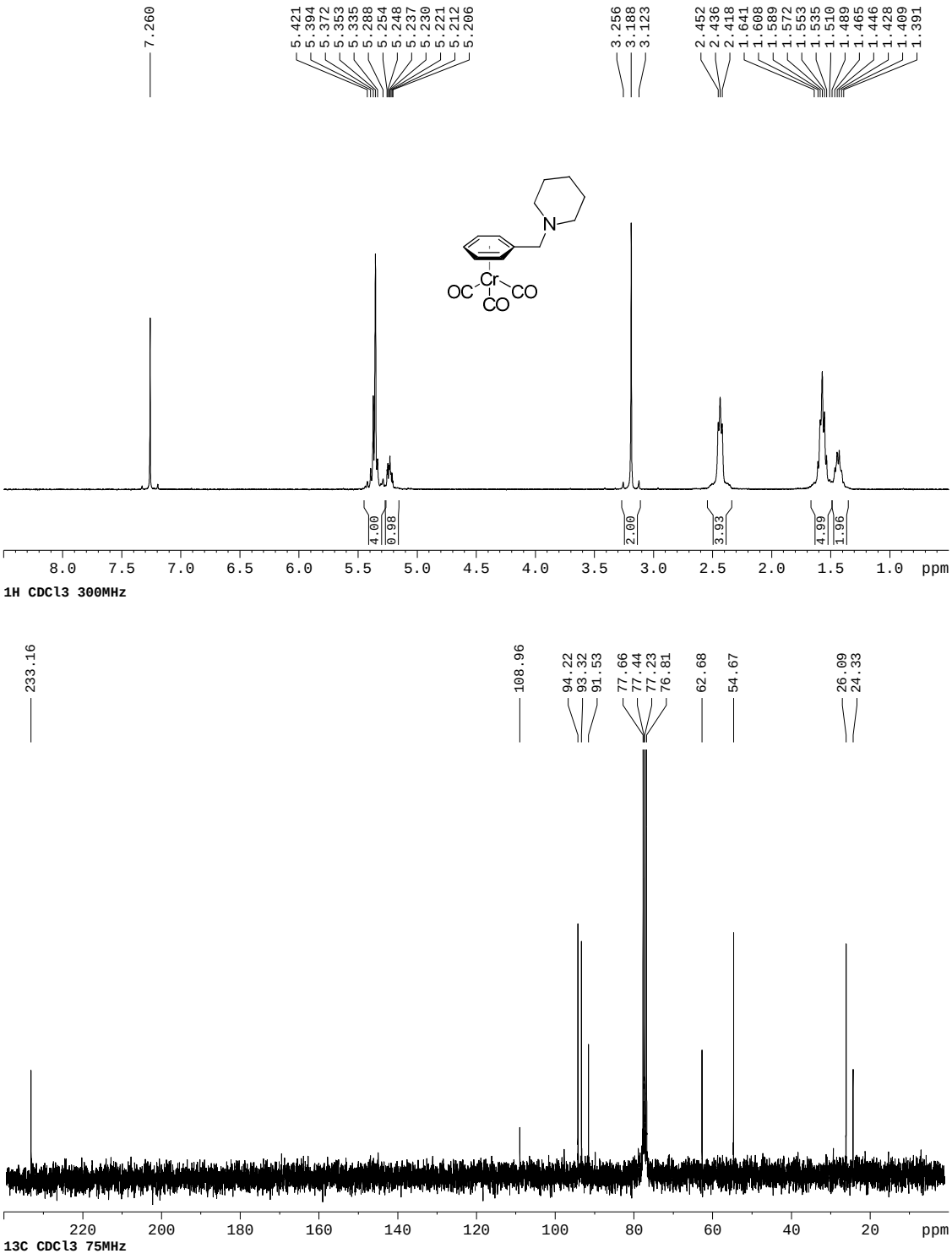

Figure I-64: $^{1}H$, $^{13}C\{^{1}H\}$ NMR spectra of **54**.

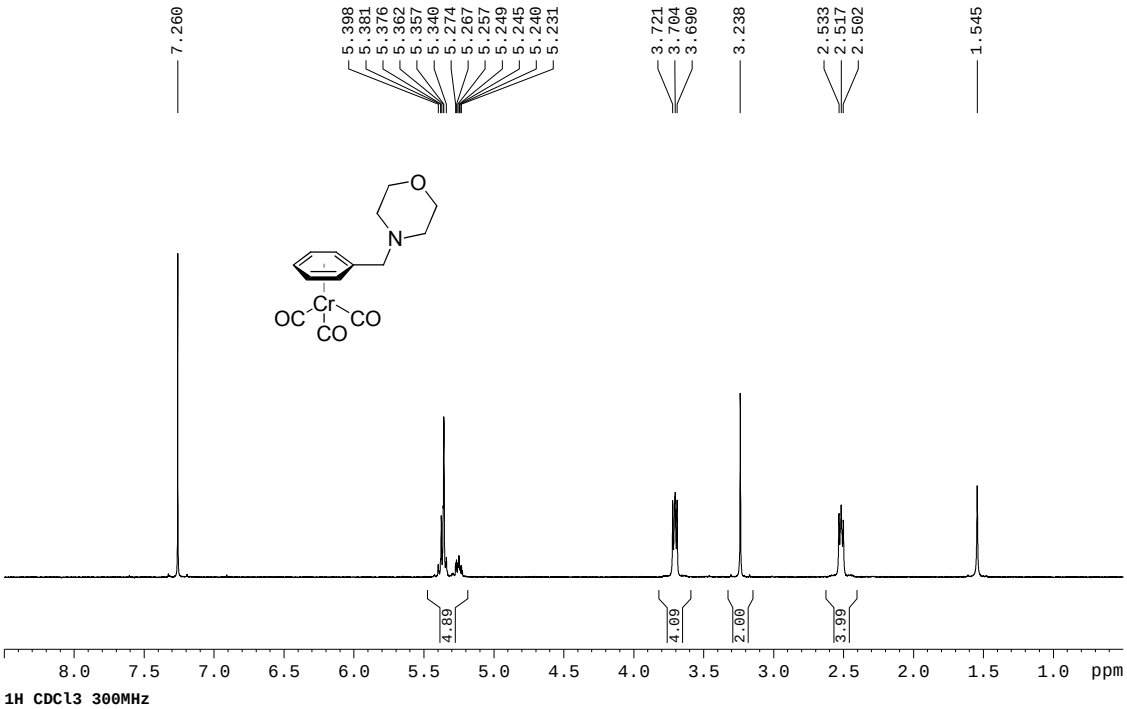


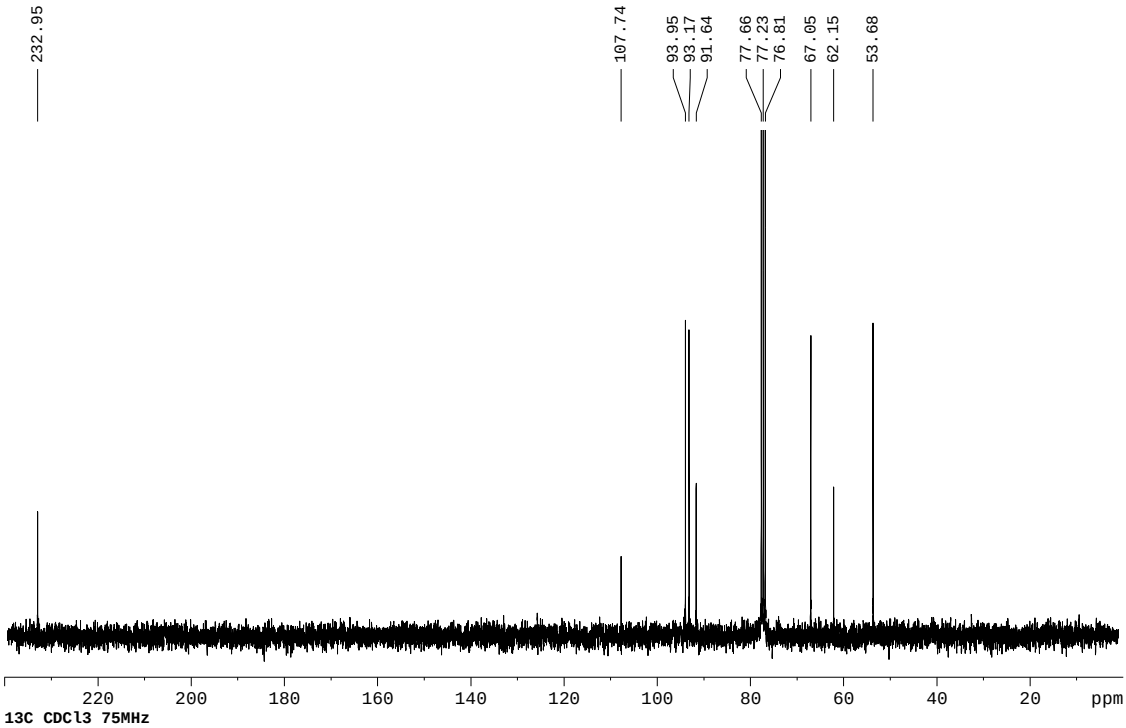

Figure I-65: $^{1}H$, $^{13}C\{^{1}H\}$ NMR spectra of **56**.

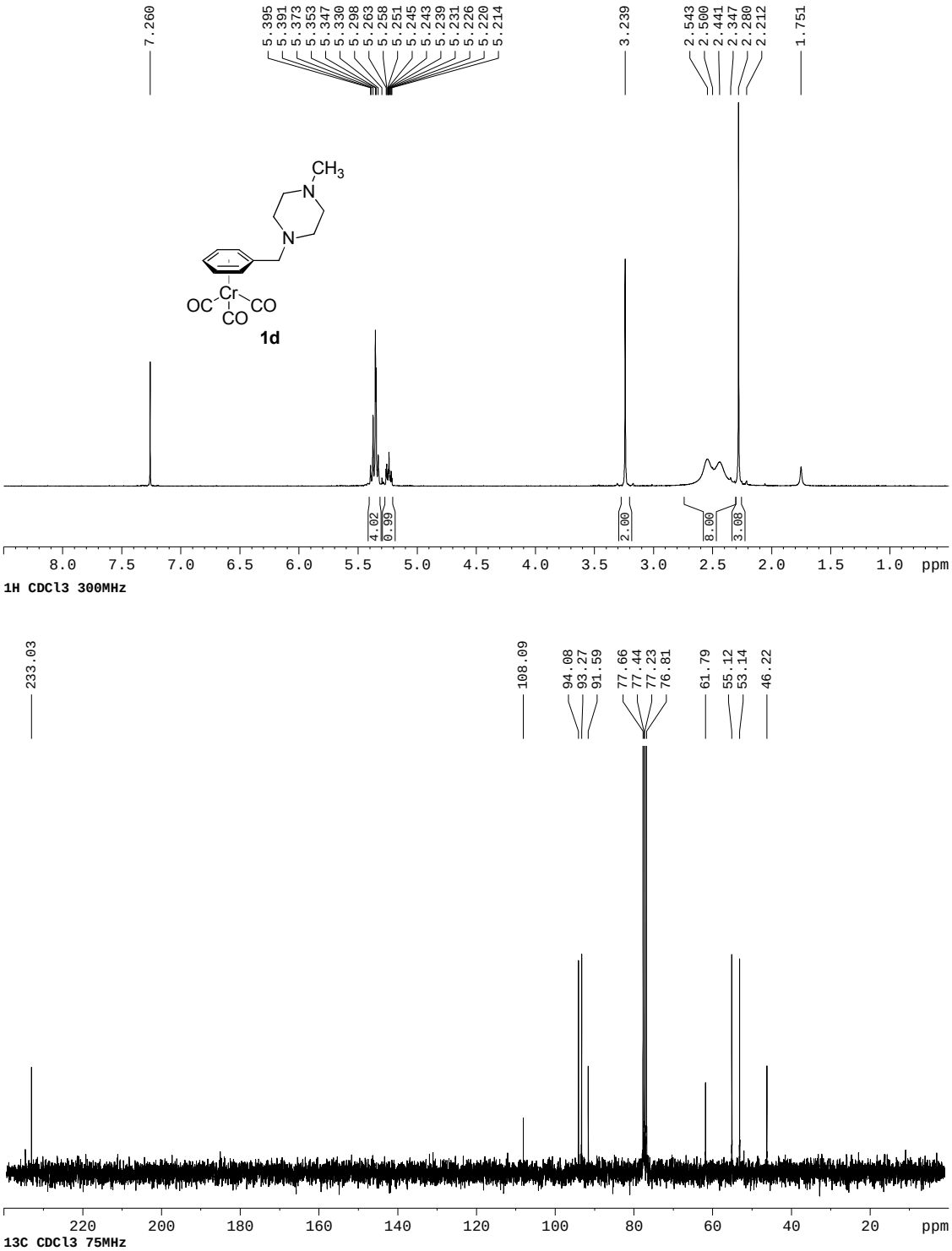

Figure I-66: $^{1}H$, $^{13}C\{^{1}H\}$ NMR spectra of **28f**.

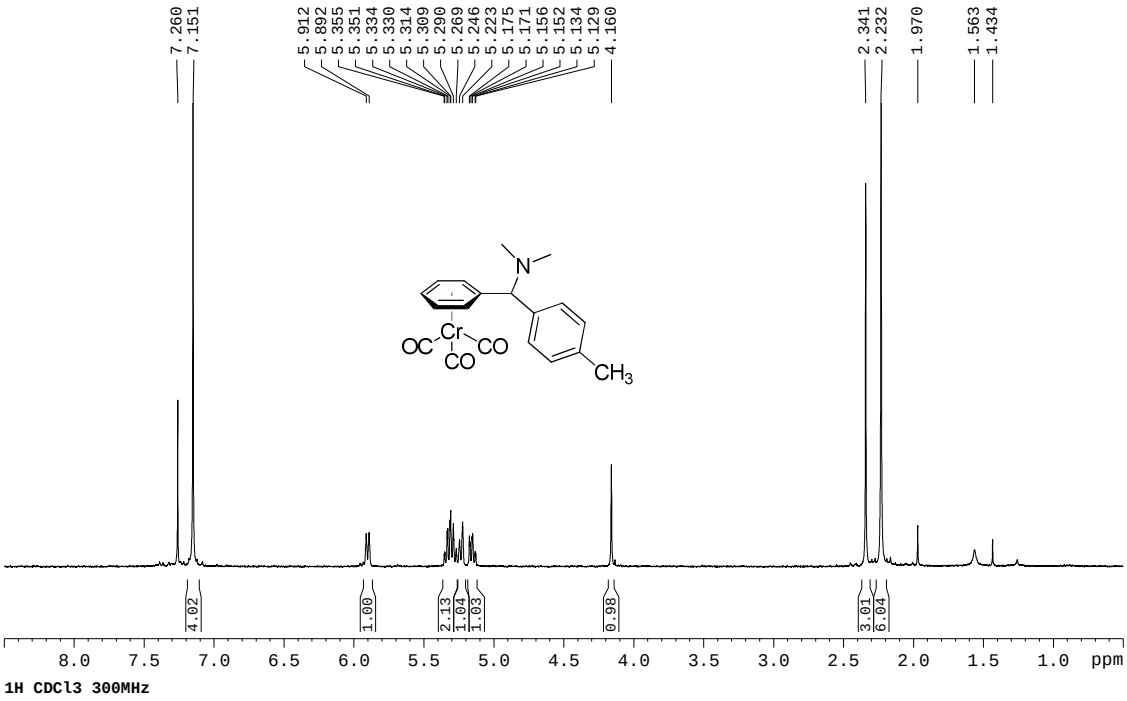


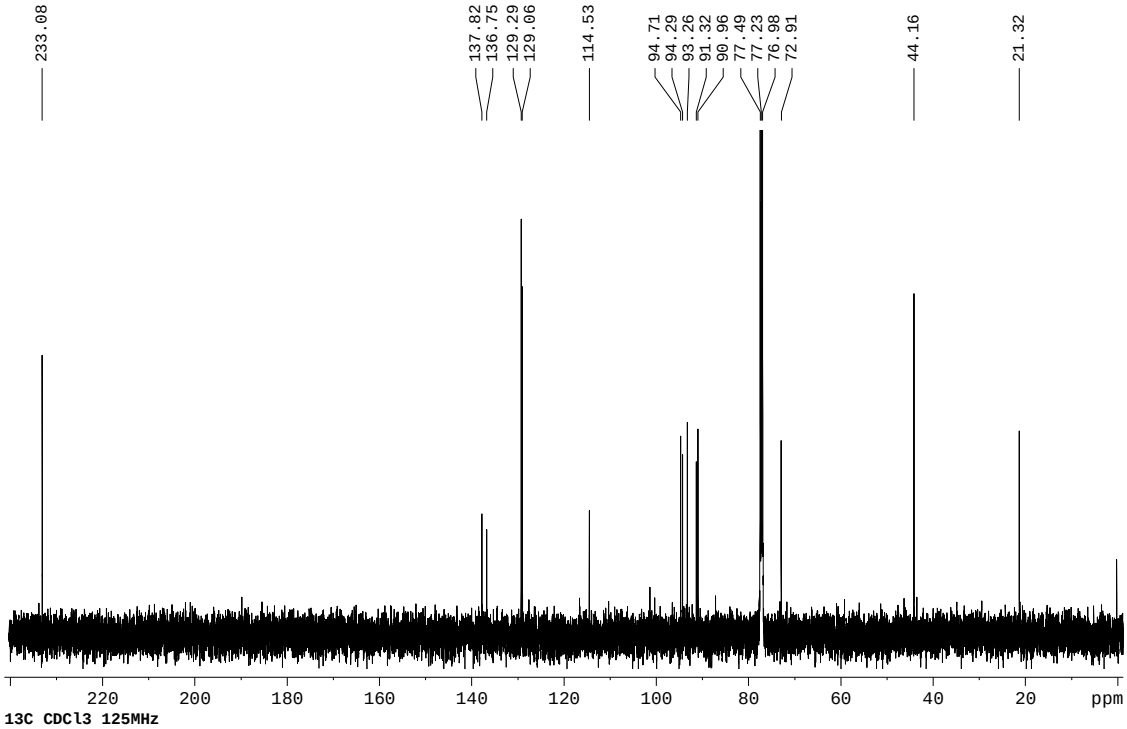

Figure I-67: $^{1}H$, $^{13}C\{^{1}H\}$ NMR spectra of **55a**.

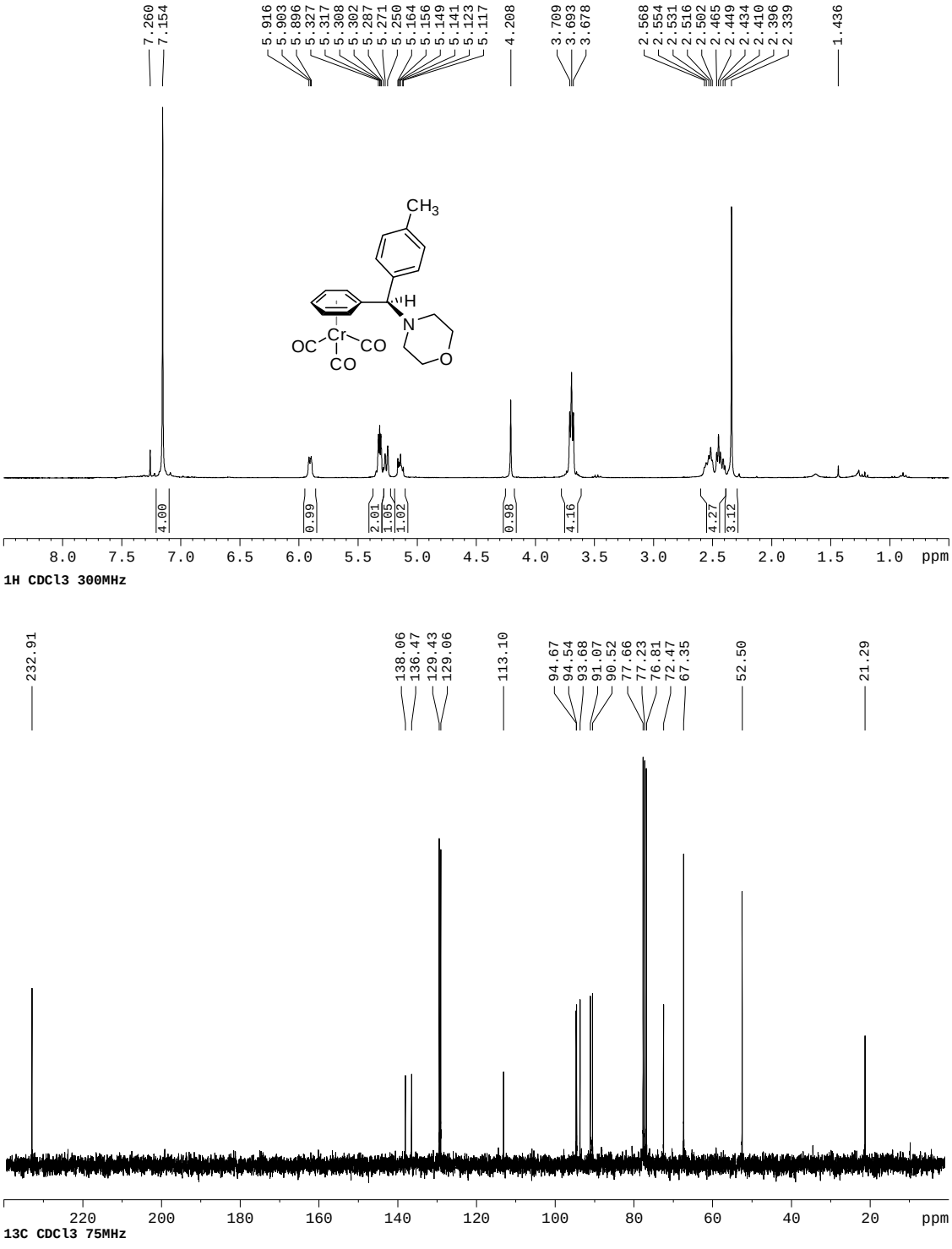

Figure I-68: $^{1}H$, $^{13}C\{^{1}H\}$ NMR spectra of **55b**.

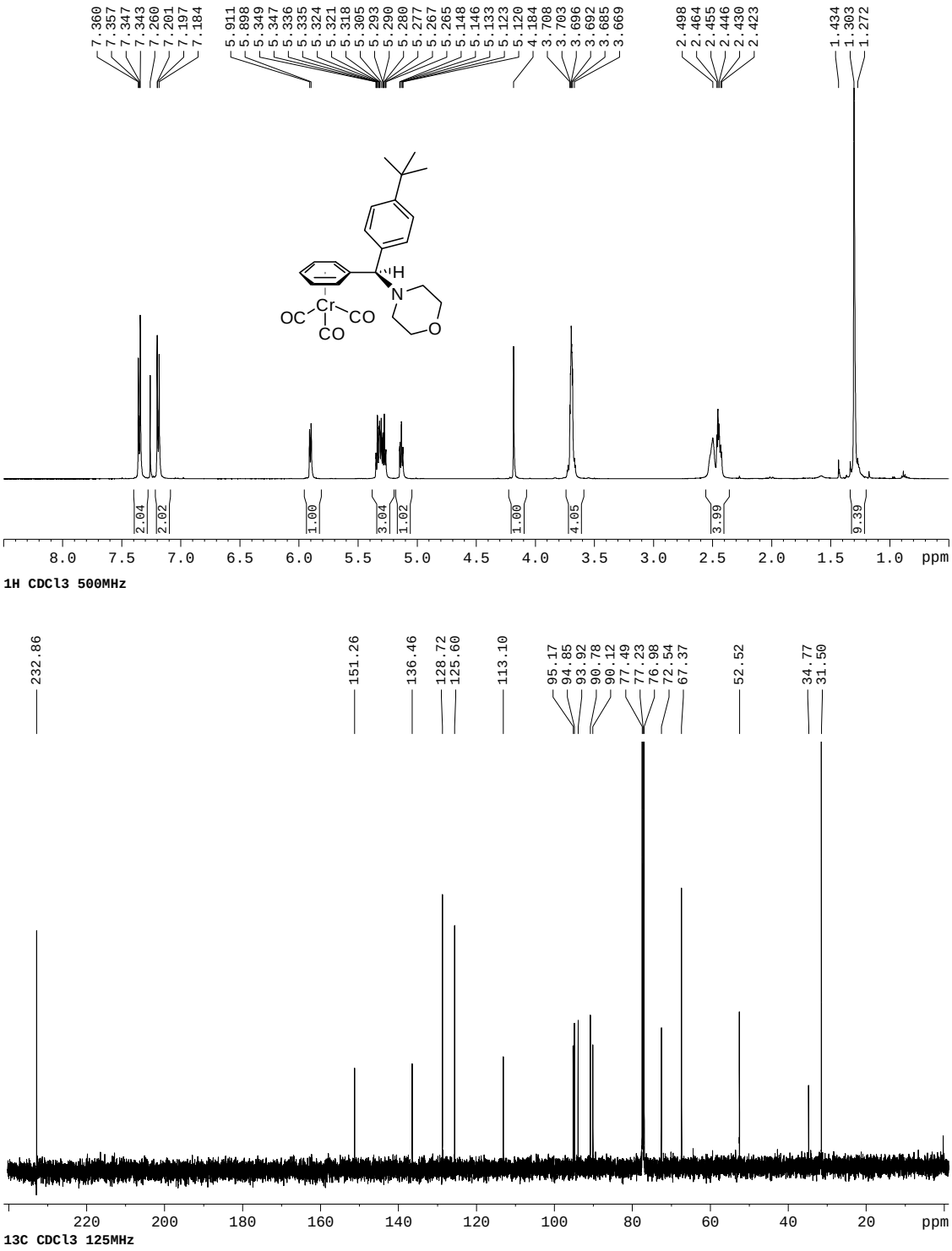

Figure I-69: $^{1}H$, $^{13}C\{^{1}H\}$ NMR spectra of **55c**.

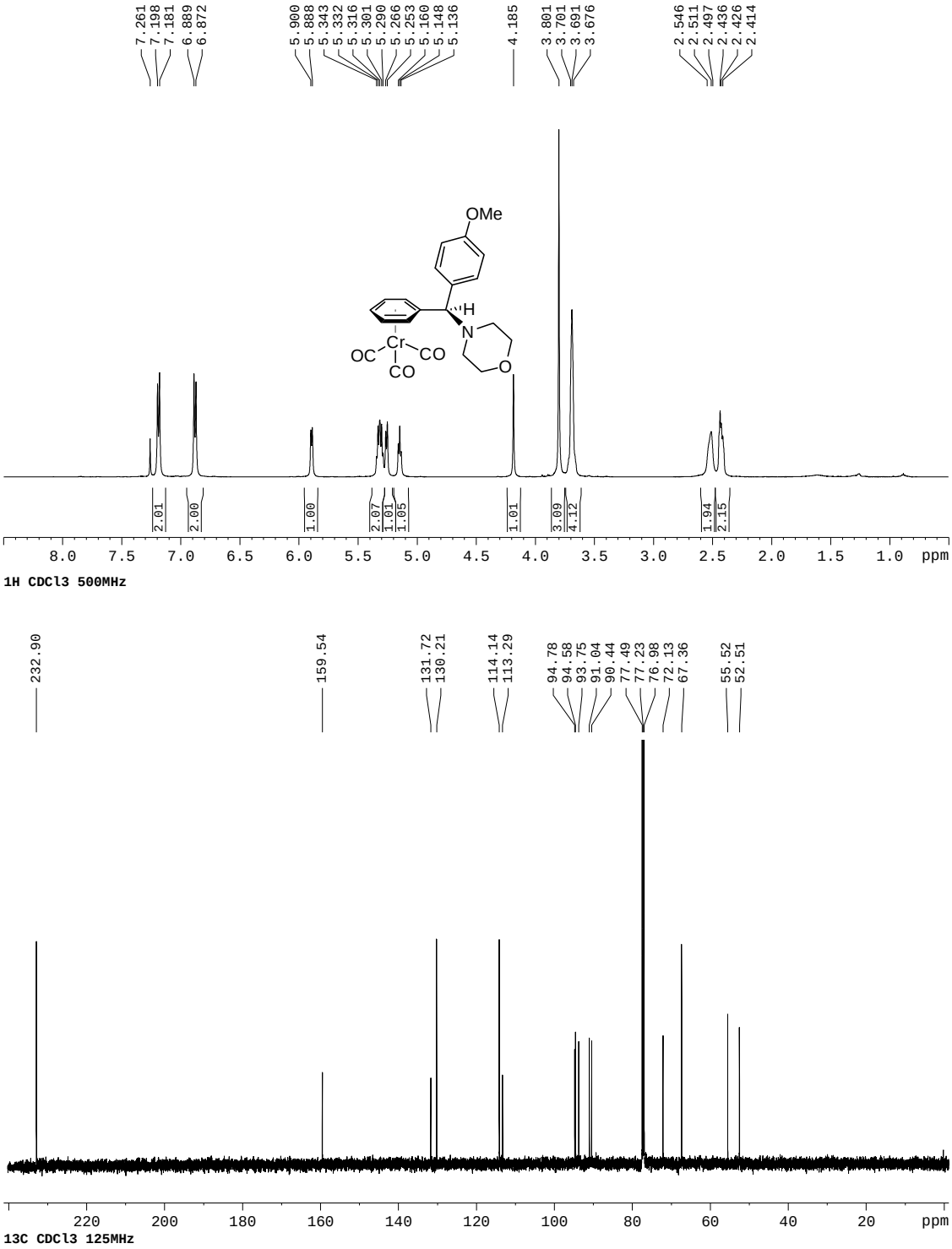

Figure I-70: $^{1}H$, $^{13}C\{^{1}H\}$ NMR spectra of **55d**.

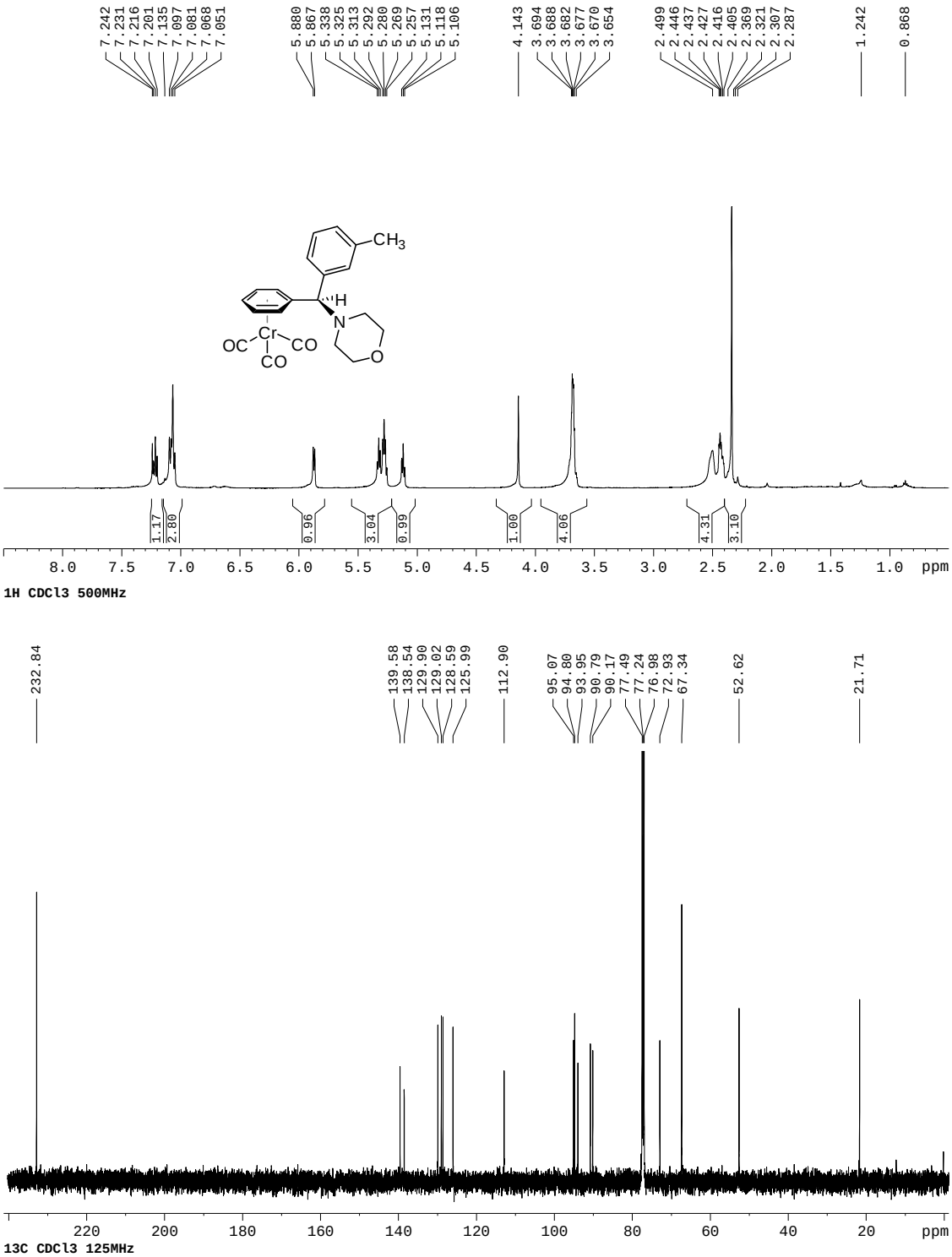

Figure I-71: $^{1}H$, $^{13}C\{^{1}H\}$ NMR spectra of **55e**.

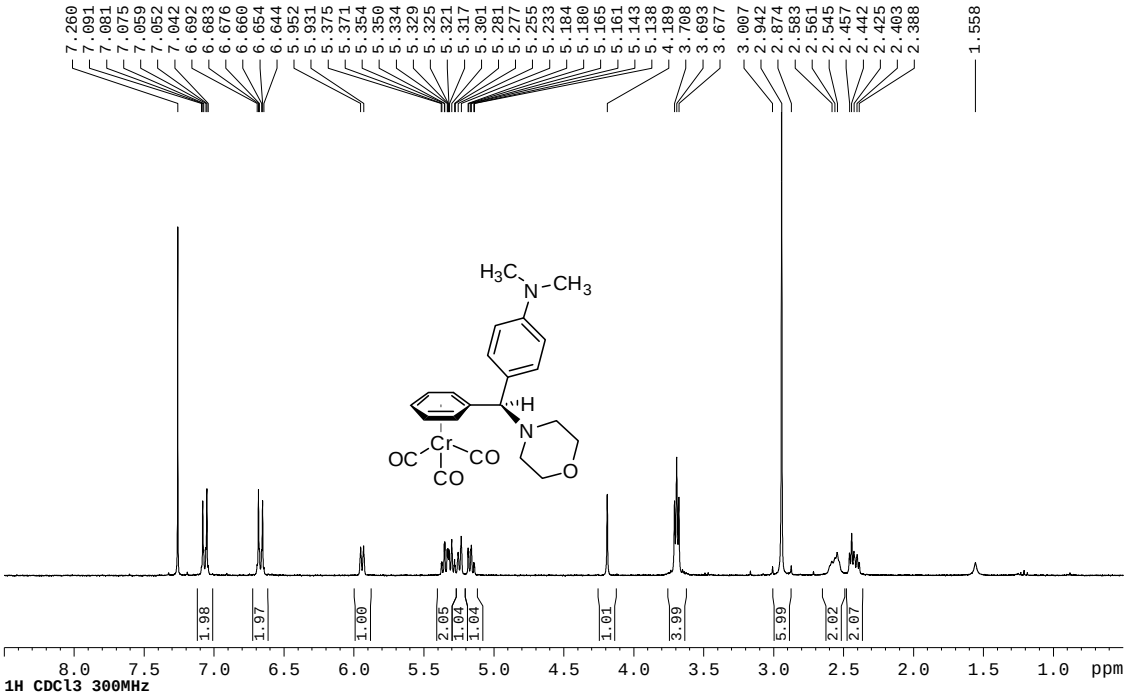


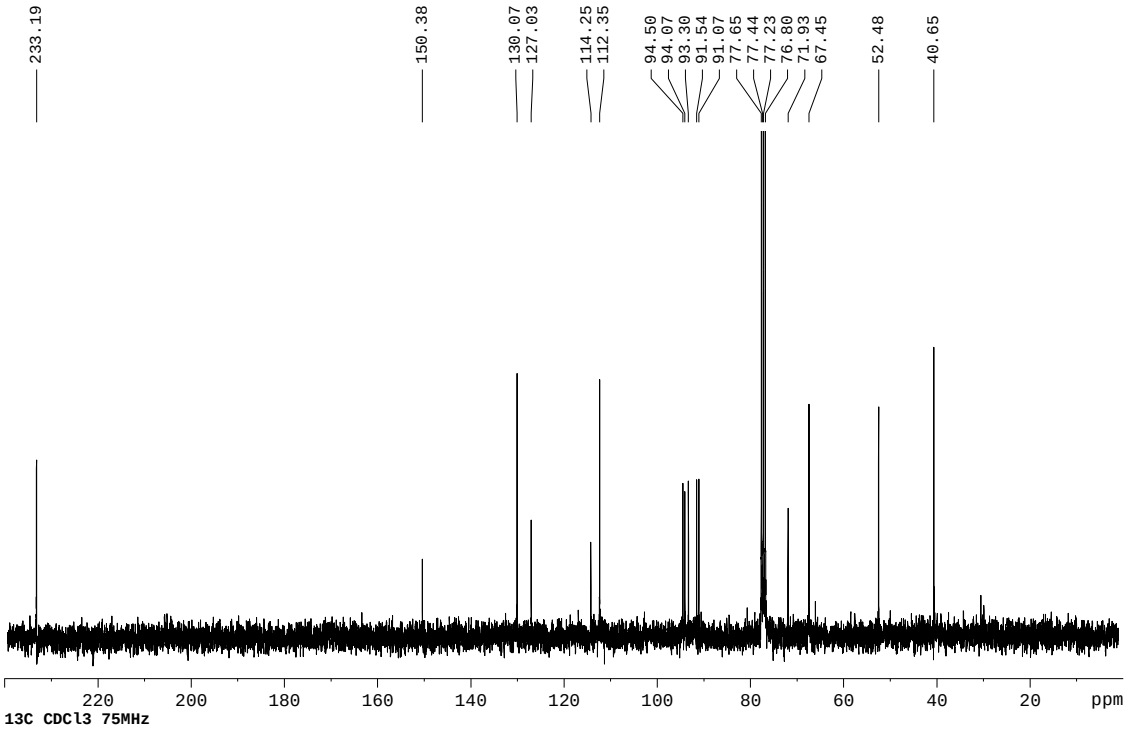

Figure I-72: $^{1}H$, $^{13}C\{^{1}H\}$ NMR spectra of **55f**.

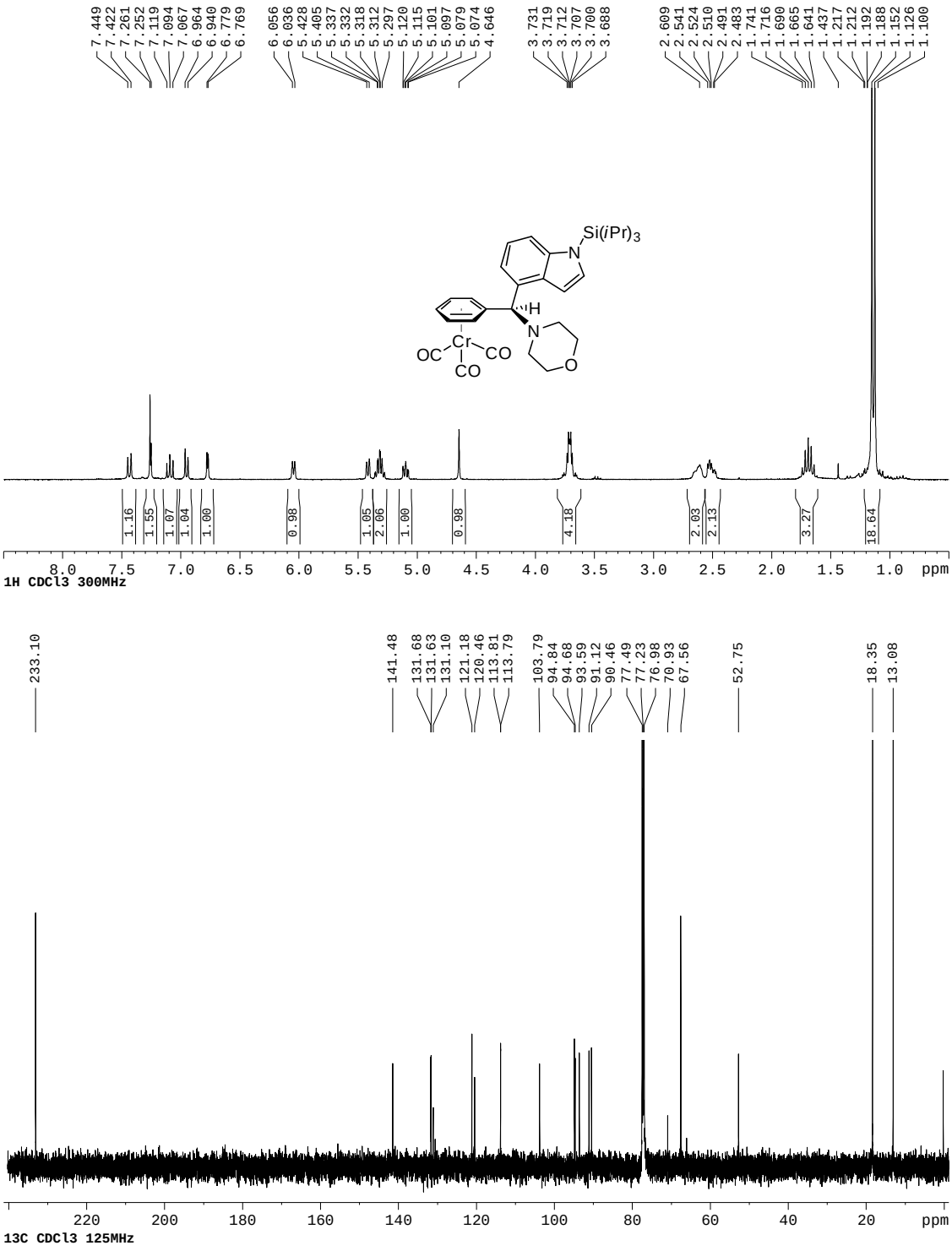

Figure I-73: $^{1}H$, $^{13}C\{^{1}H\}$ NMR spectra of **55g**.

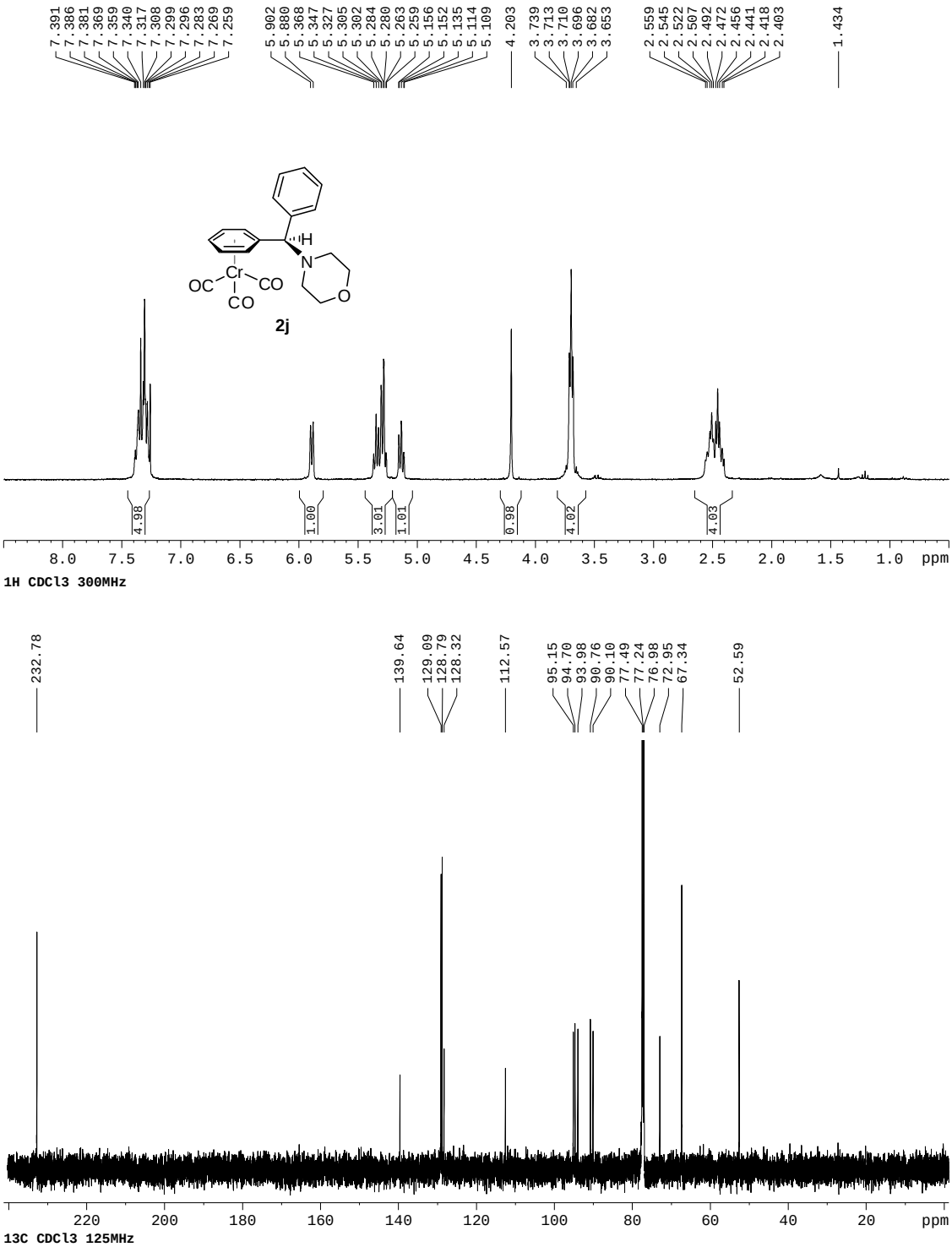

Figure I-74: $^{1}H$, $^{13}C\{^{1}H\}$ NMR spectra of **57**.

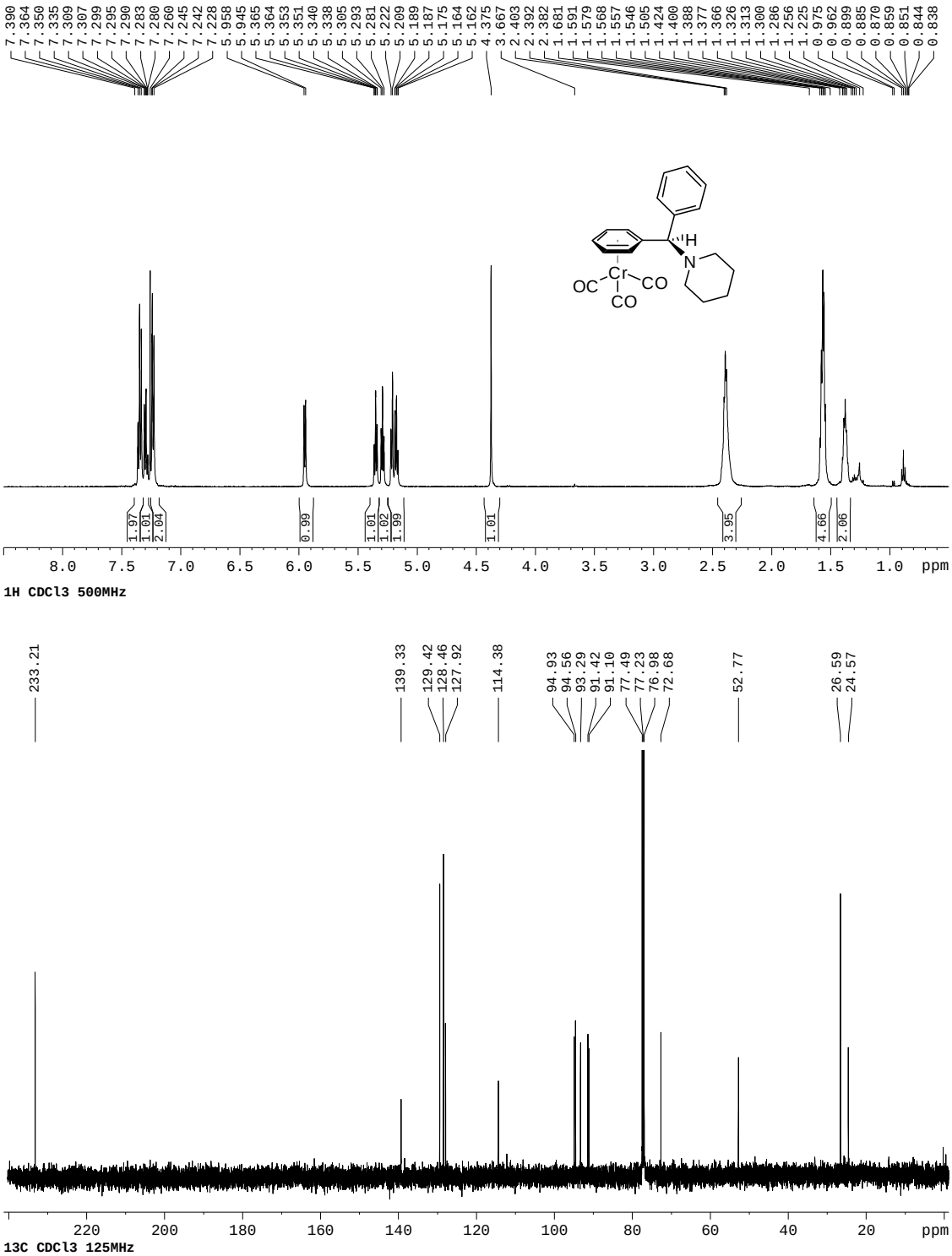

Figure I-75: $^{1}H$, $^{13}C\{^{1}H\}$ NMR spectra of **58**.

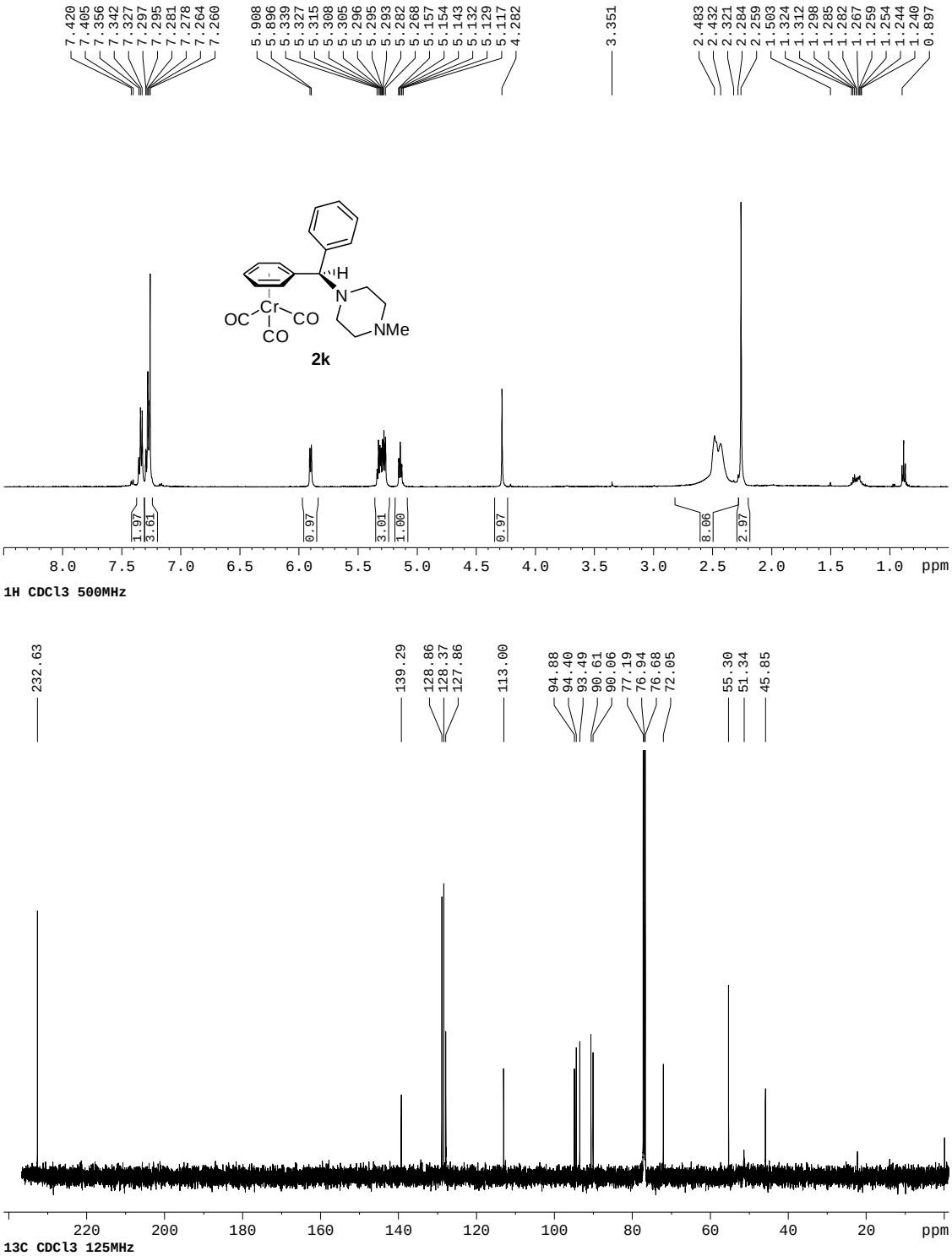

Figure I-76: $^{1}H$, $^{13}C\{^{1}H\}$ NMR spectra of **59**.

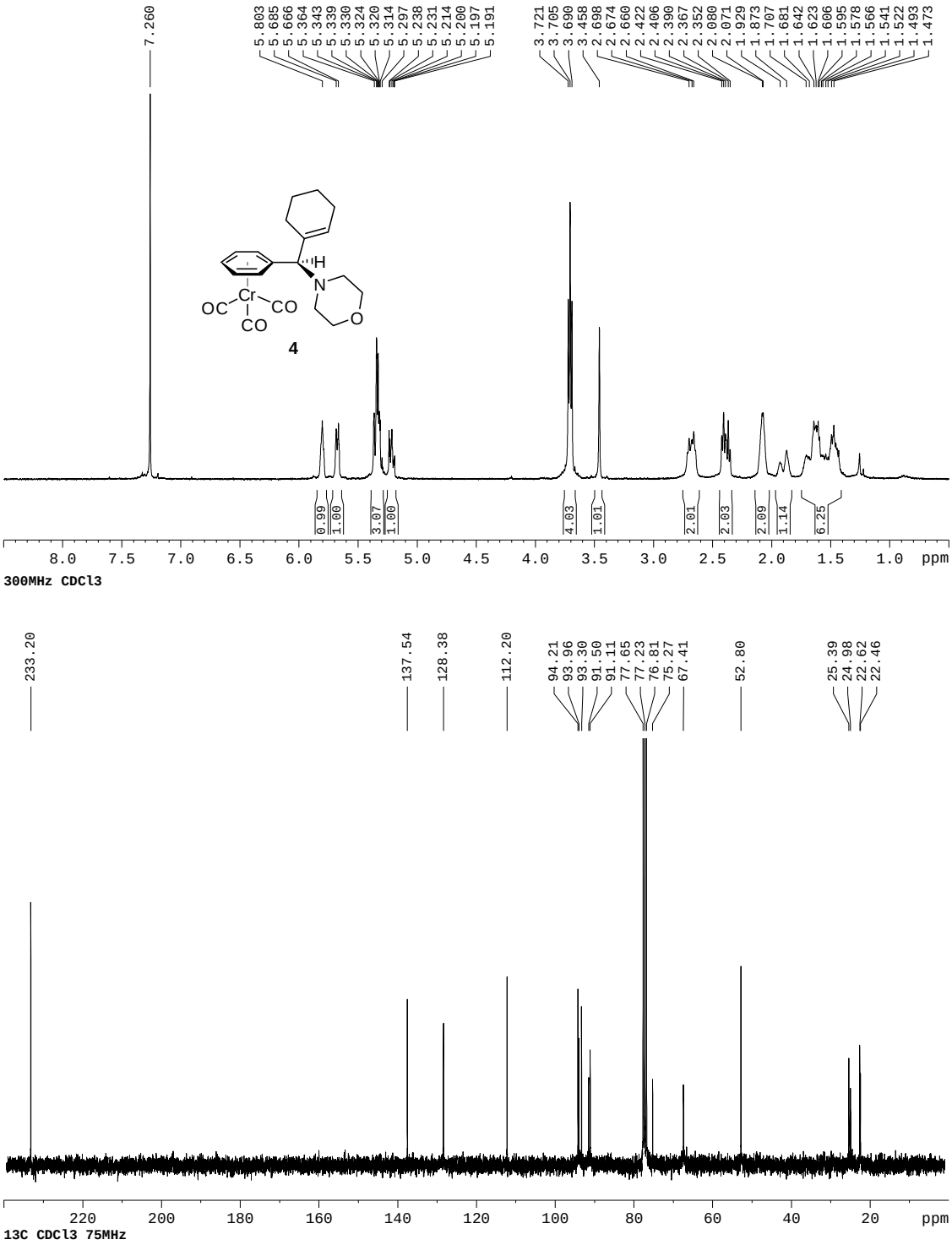

*Deuterium-quenched ortho-lithiated benzylamine*

Figure I-77: $^{1}$H NMR spectra of **28a-D** (60% D) *vs* reference spectrum (Table 3-1, entry 14).

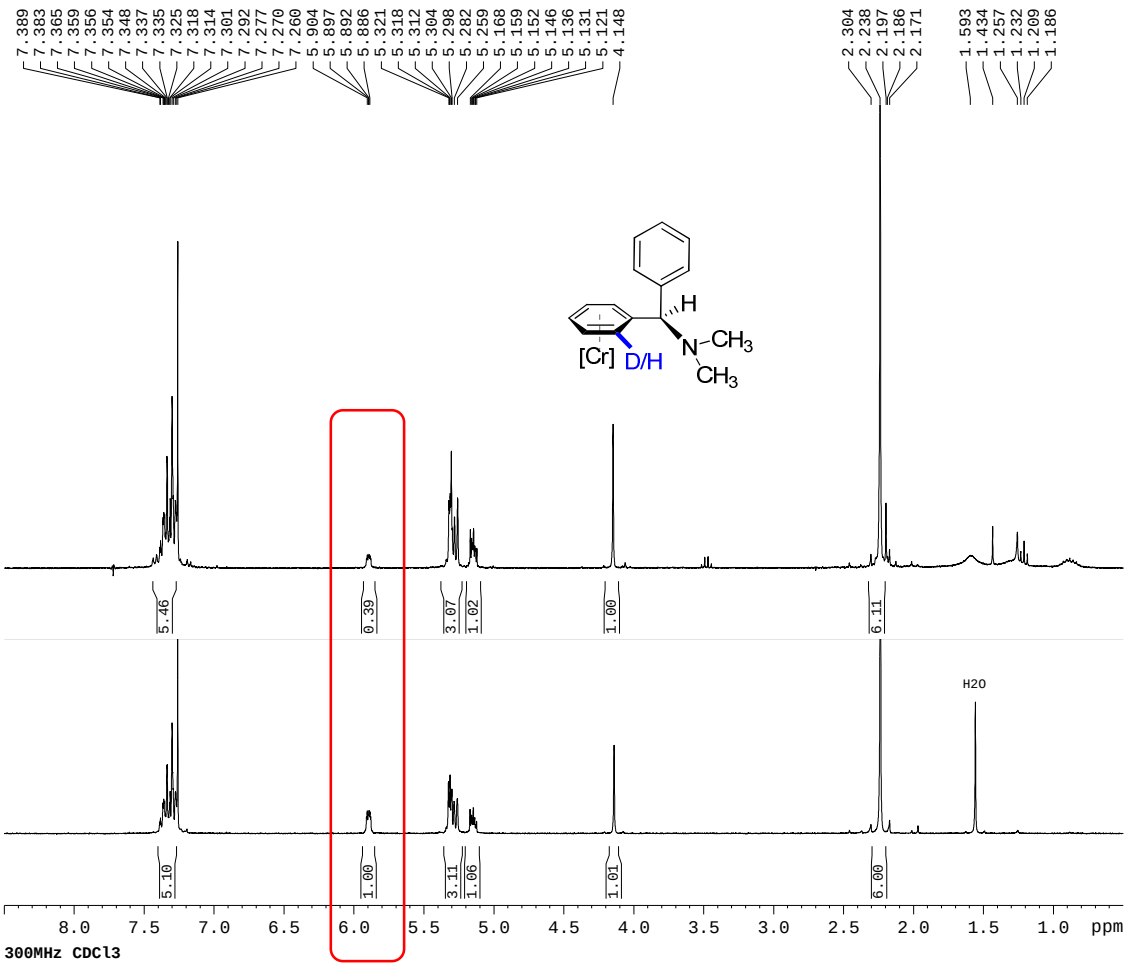

Figure I-78: $^{1}H$, $^{13}C\{^{1}H\}$, $^{31}P\{^{1}H\}$ NMR spectra of **62**.

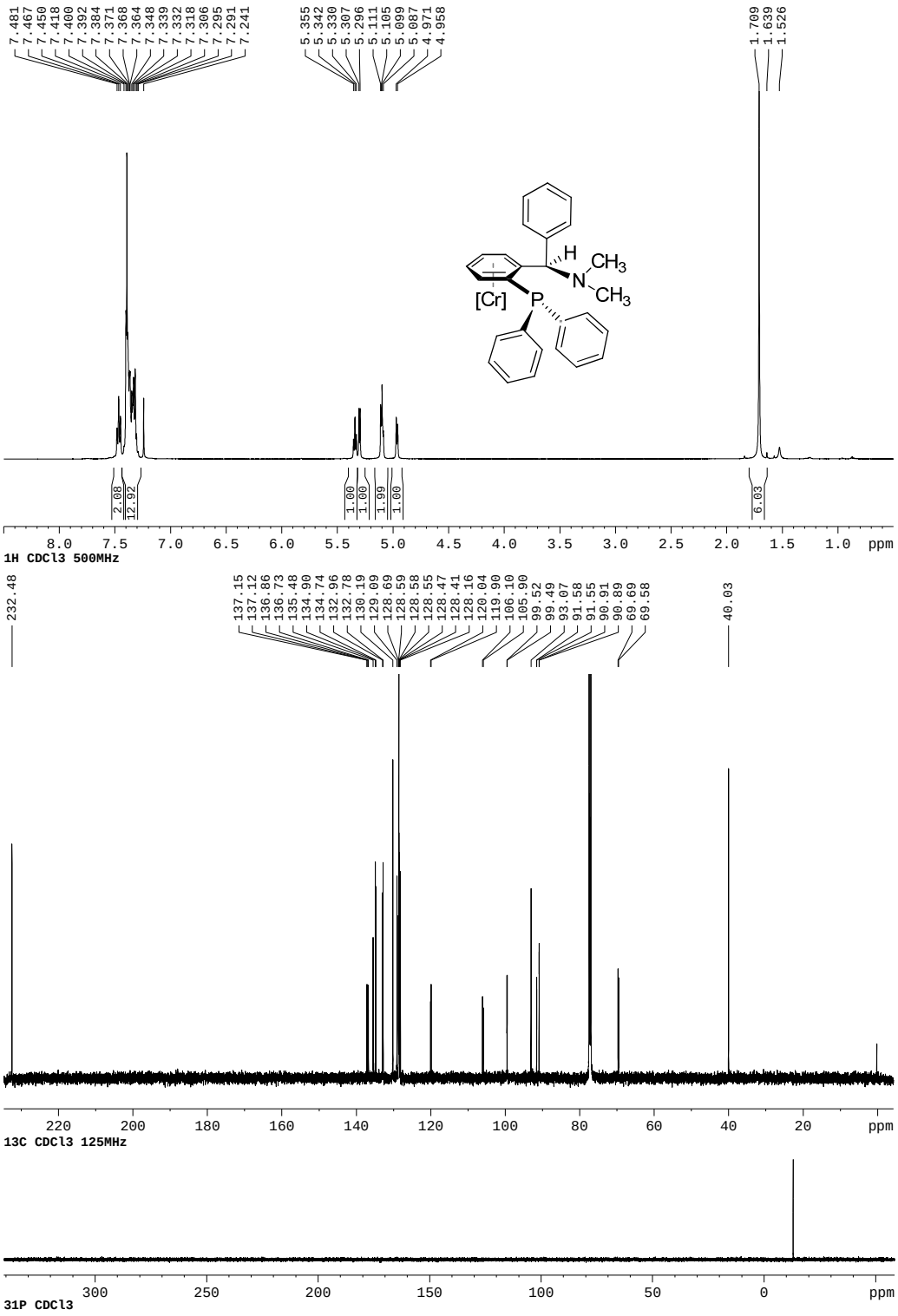

Figure I-79: $^{1}H$, $^{13}C\{^{1}H\}$, $^{31}P$ NMR spectra of **64**.

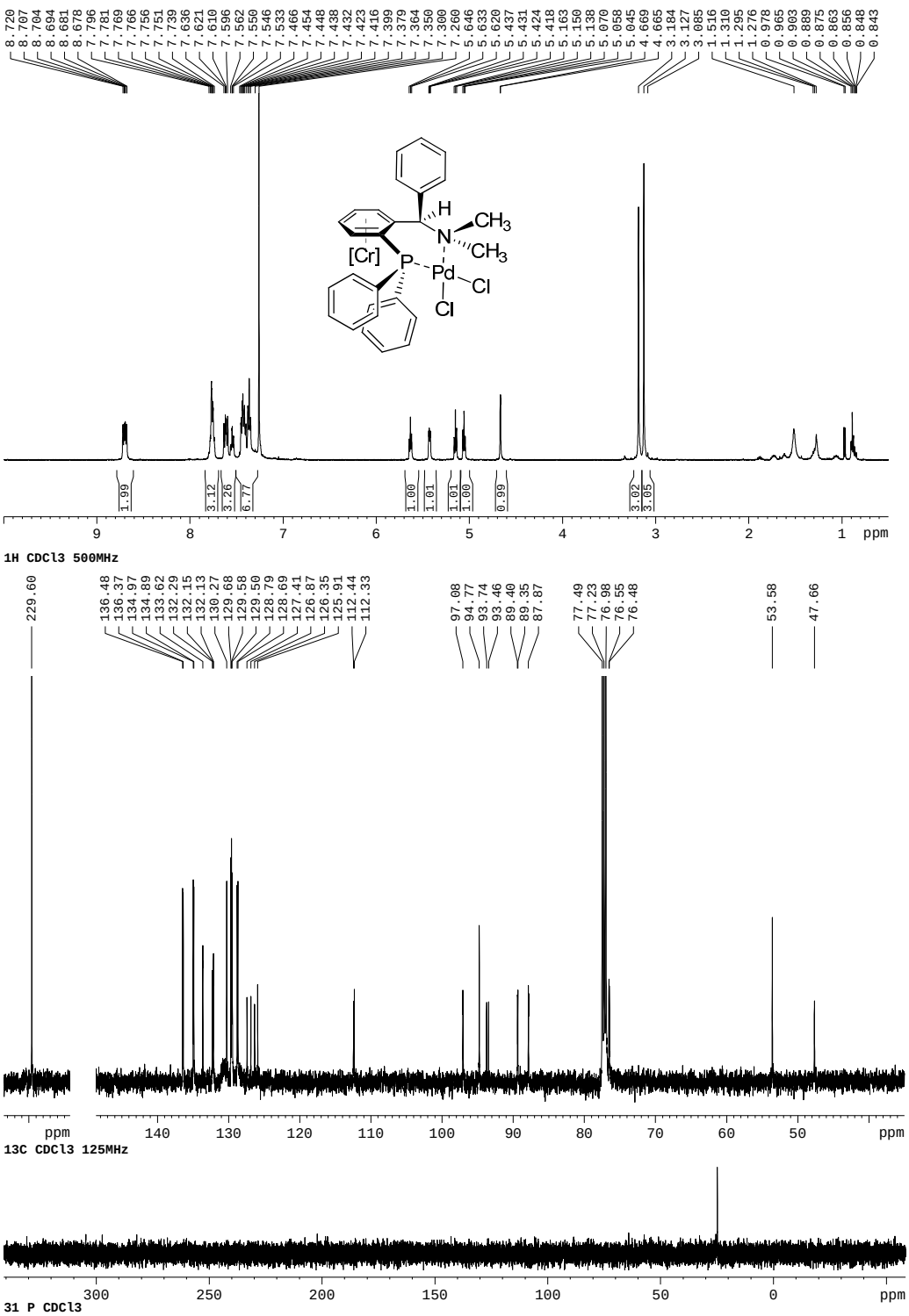

*Product from asymmetric allylation using **64** (cat).*

Figure I-80: $^{1}H$, $^{13}C\{^{1}H\}$ NMR spectra of **68**.

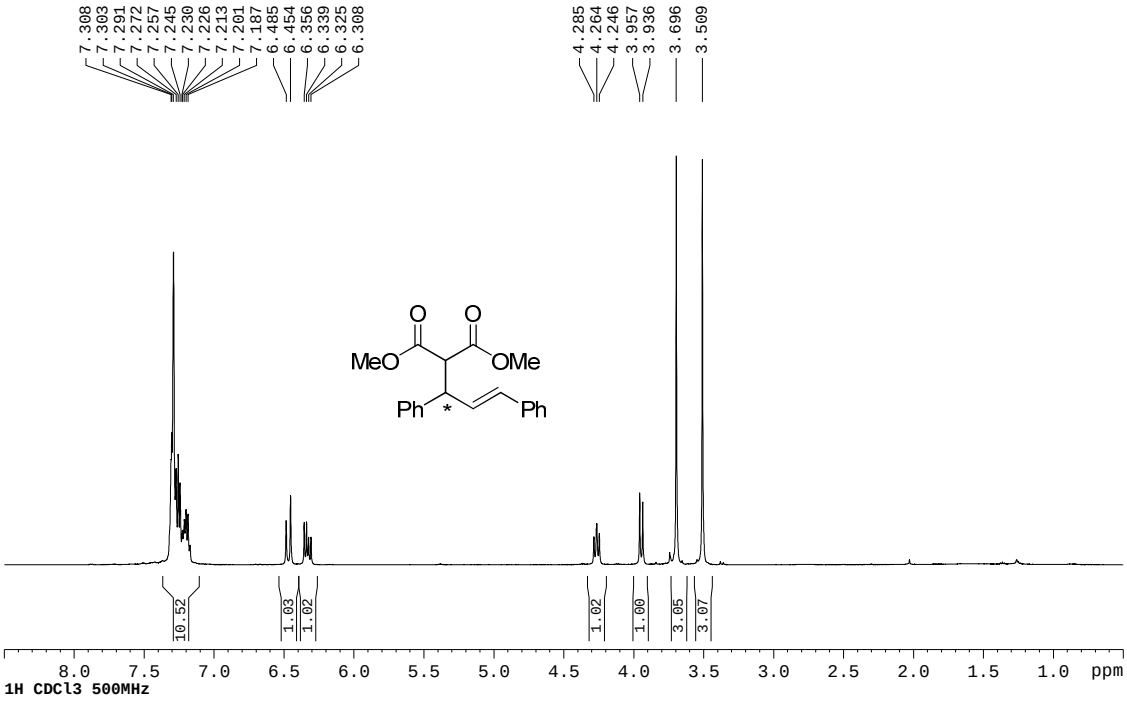


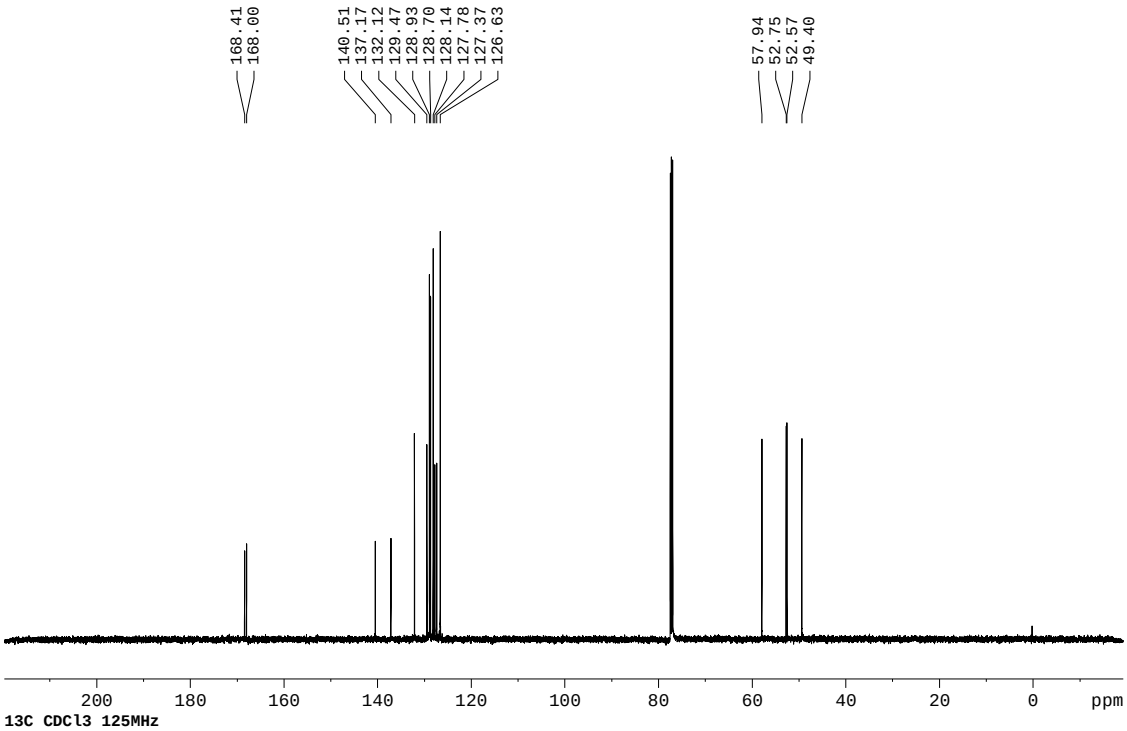

## Appendix II

## IR spectra

The following spectra are representative of tricarbonylchromium-coordinated arene complexes. CO ligands typically shift a few wavenumbers upon coordination to electron-richer or –poorer arene rings.

Figure II-1: IR spectrum of unsymmetrical triarylmethane complex **5i**.

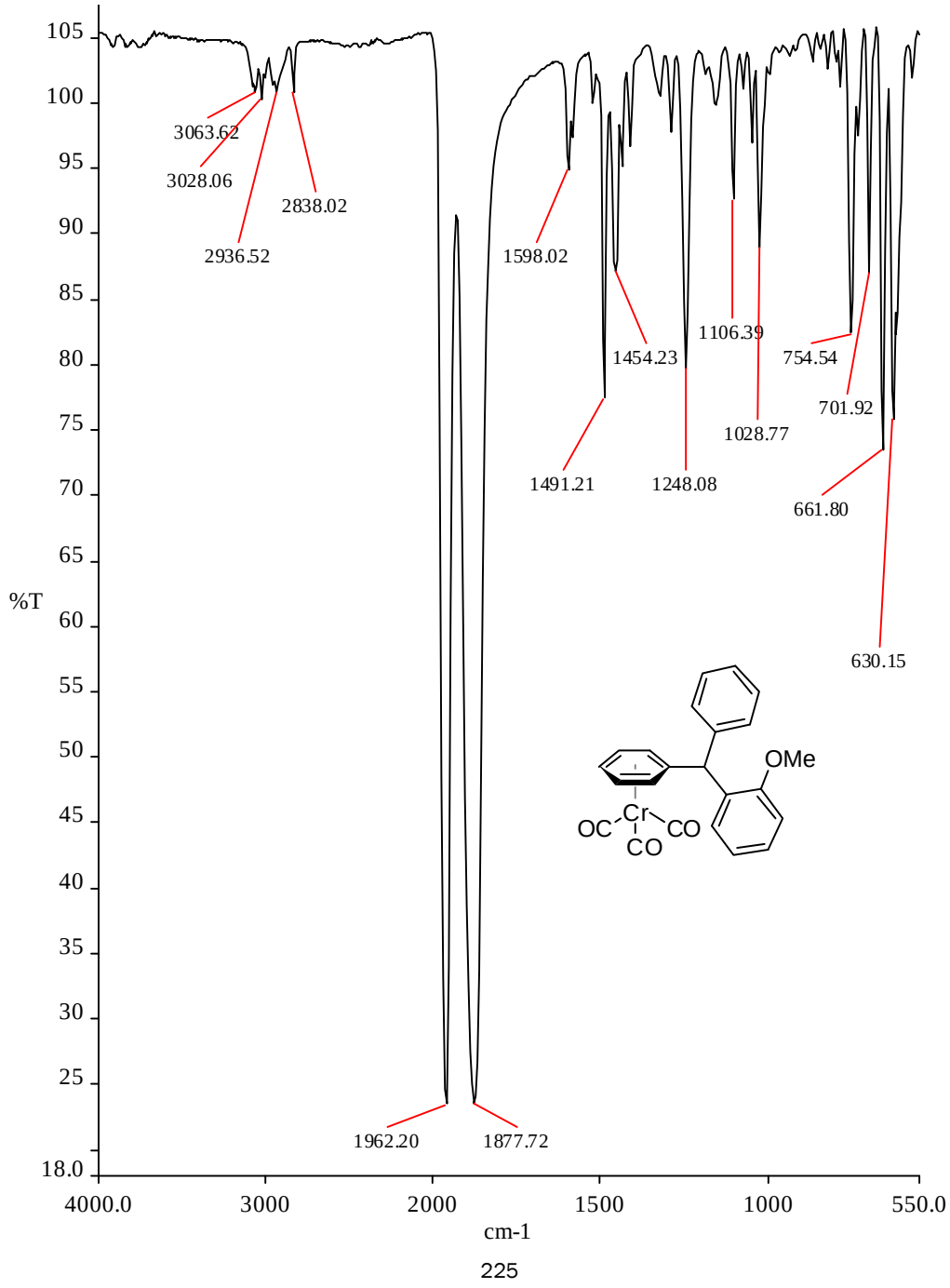

Figure II-2: IR Spectrum of unsymmetrical triarylmethane complex **5k**.

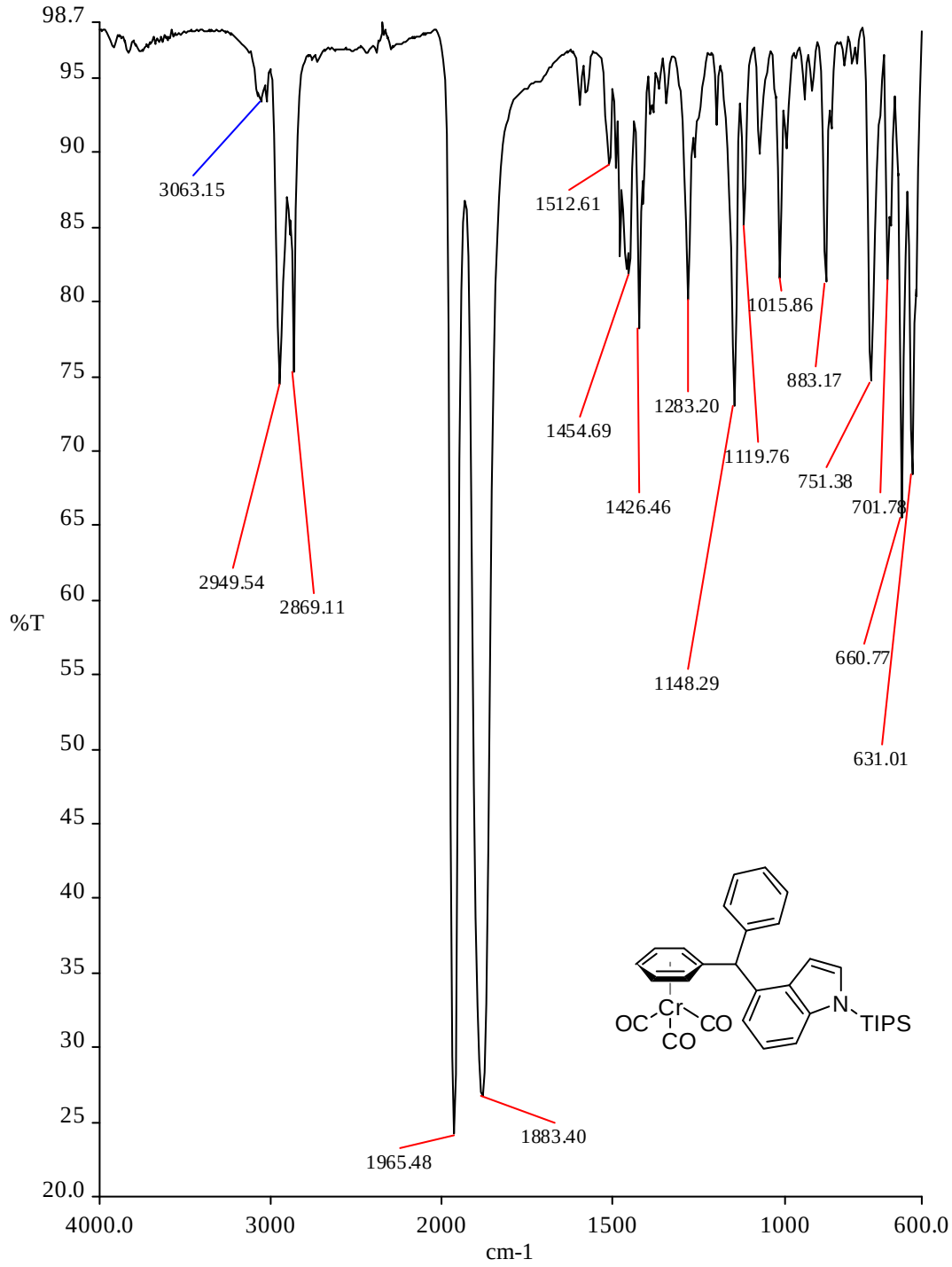

Figure II-3: IR spectrum of symmetrical triarylmethane complex **5m**.

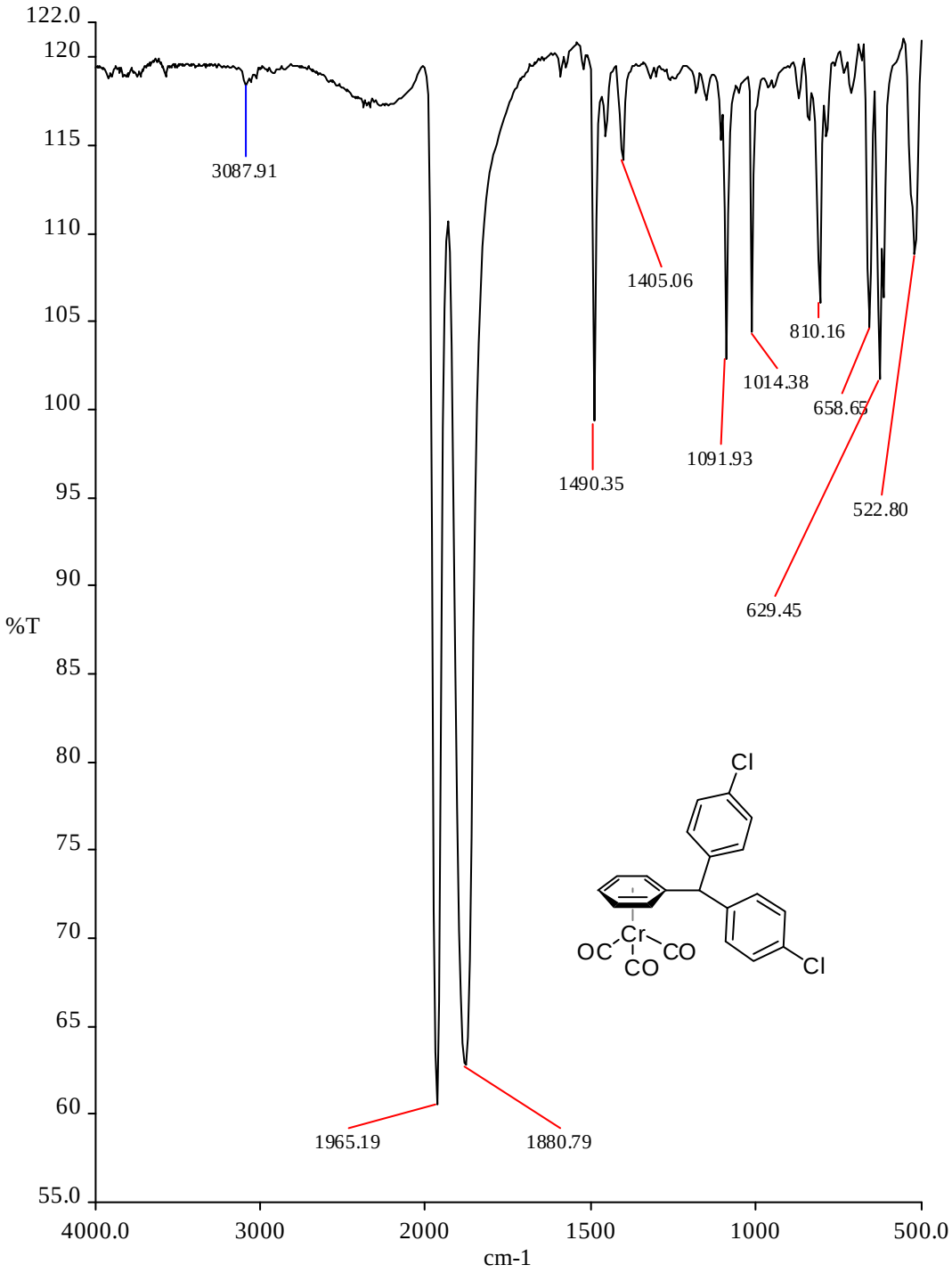

Figure II-4: IR spectrum of polyarylmethane complex **11**.

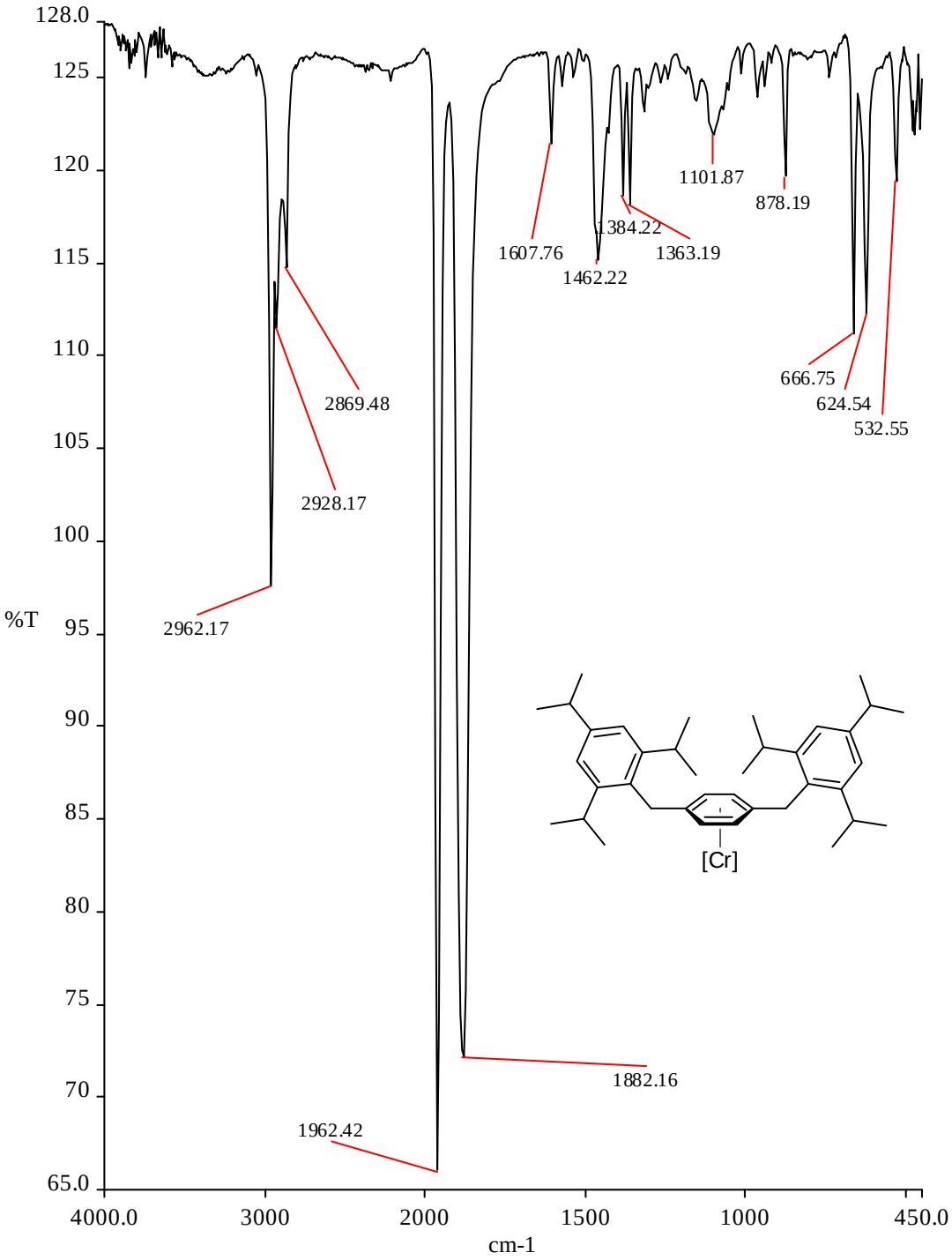

Figure II-5: IR spectrum of polyarylmethane complex **19**.

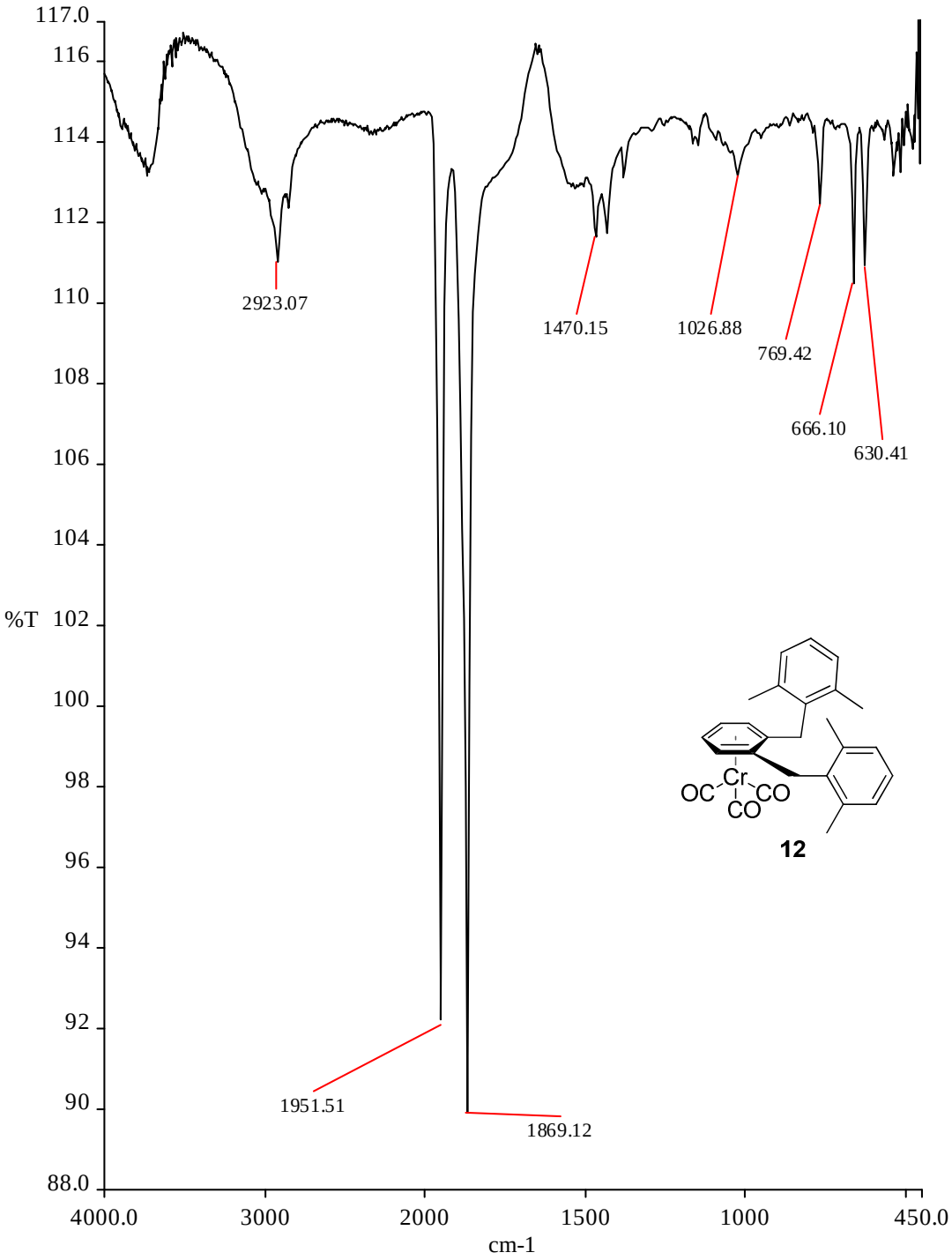

Figure II-6: IR spectrum of polyarylmethane complex **21**.

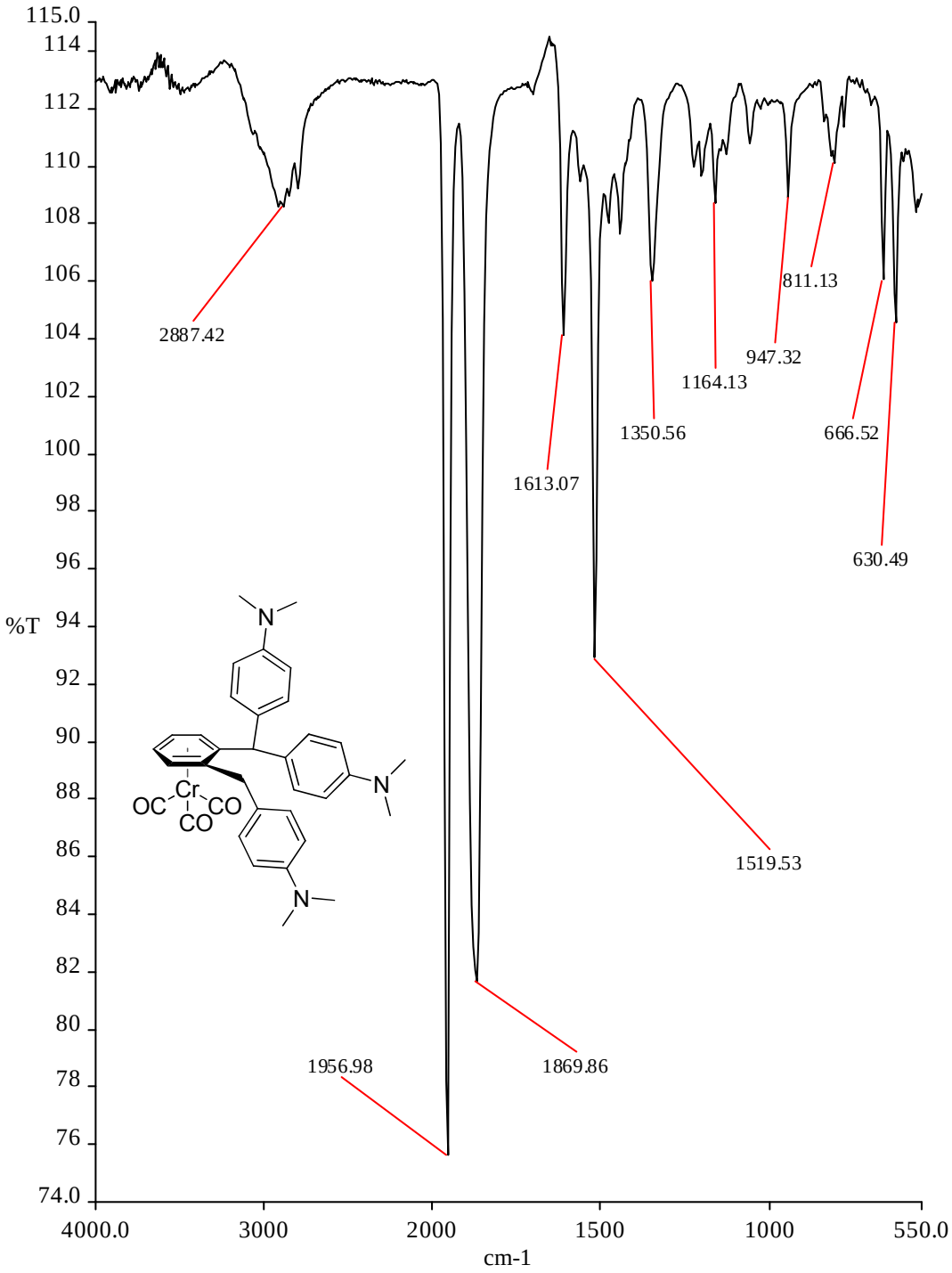

Figure II-7: IR spectrum of diarylmethyl ether complex **24a**.

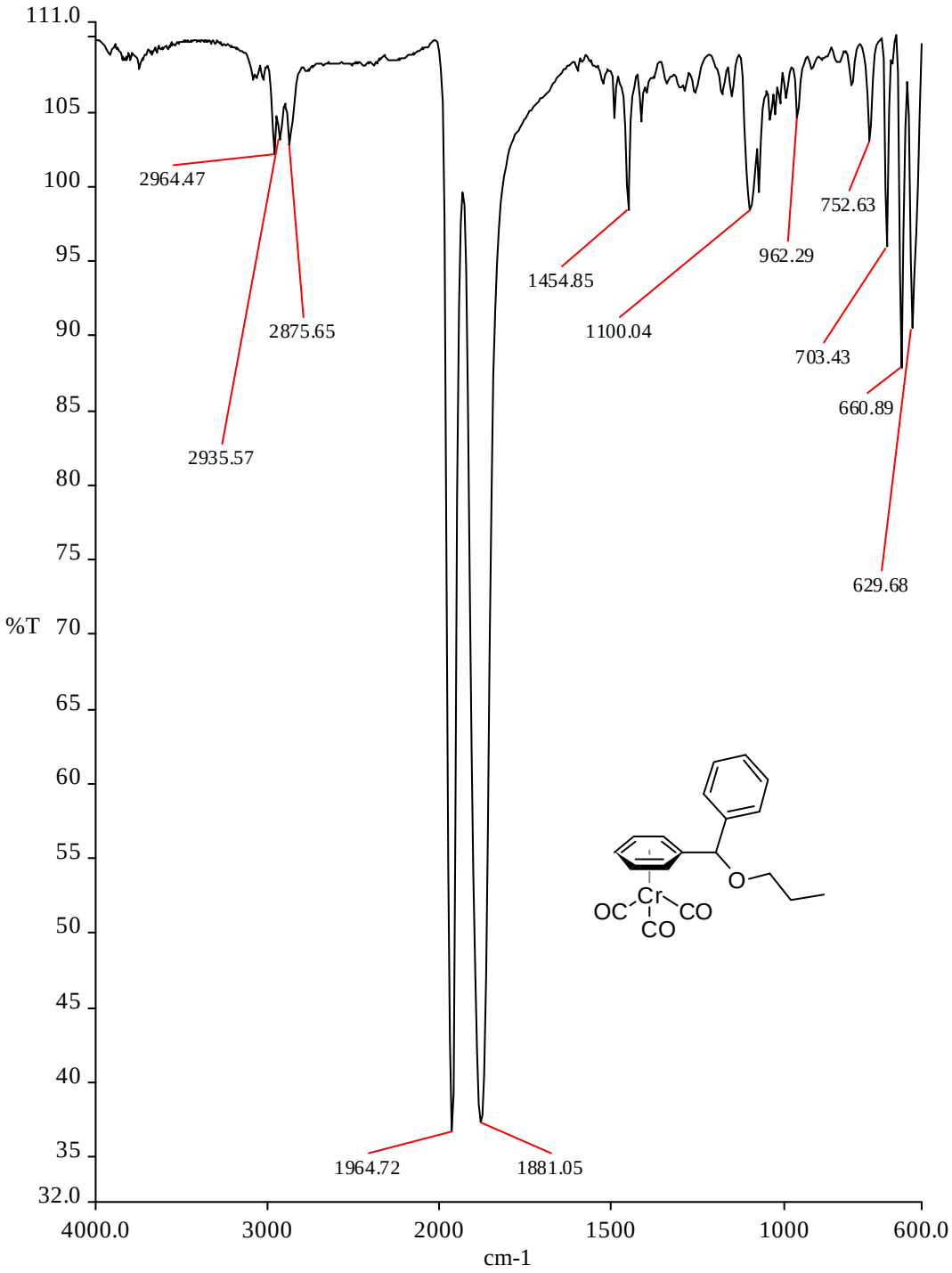

Figure II-8: IR spectrum of triarylmethyl ether complex **26b**.

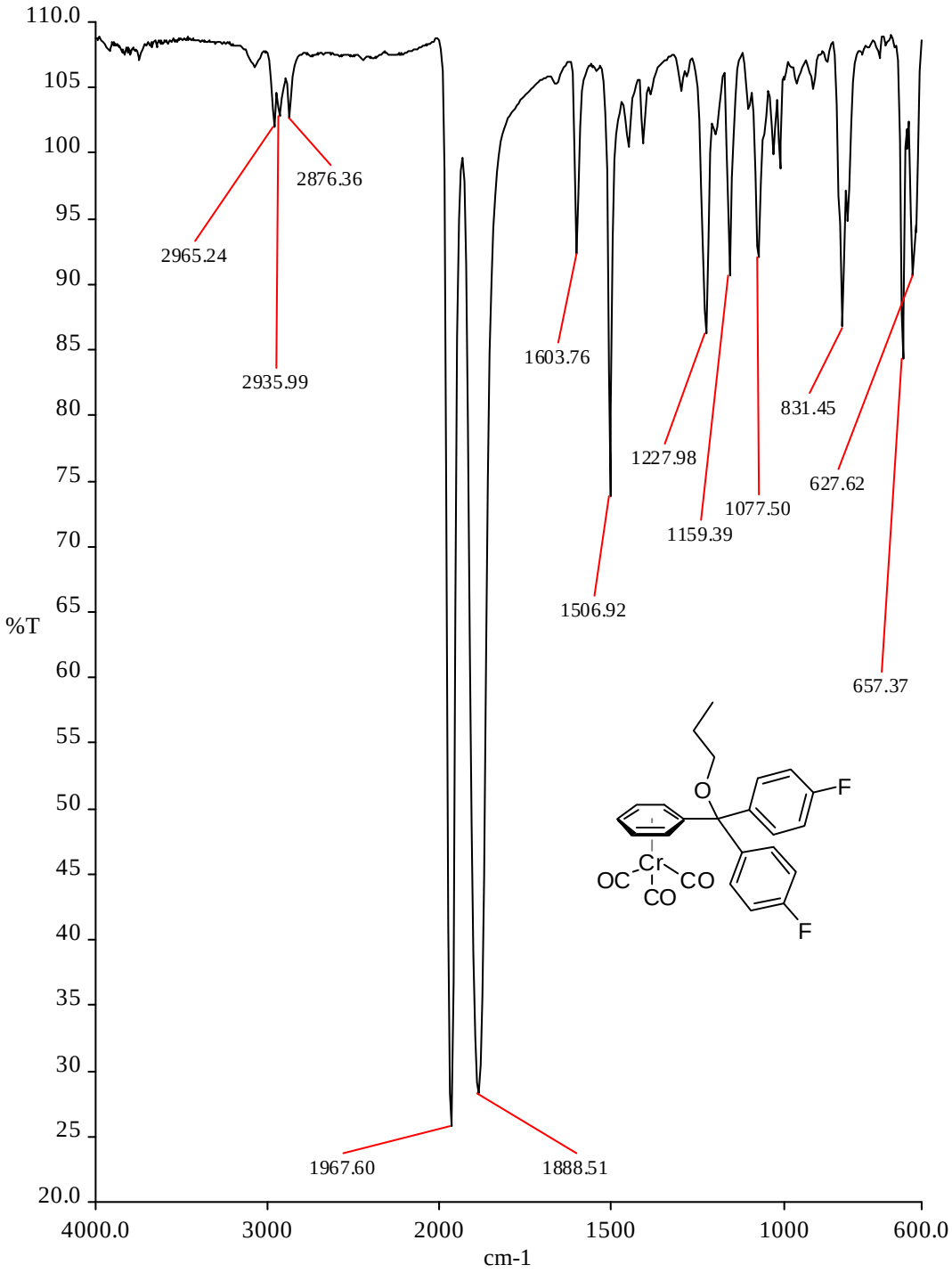

Figure II-9: IR spectrum of tertiary diarylethane complex **31b**.

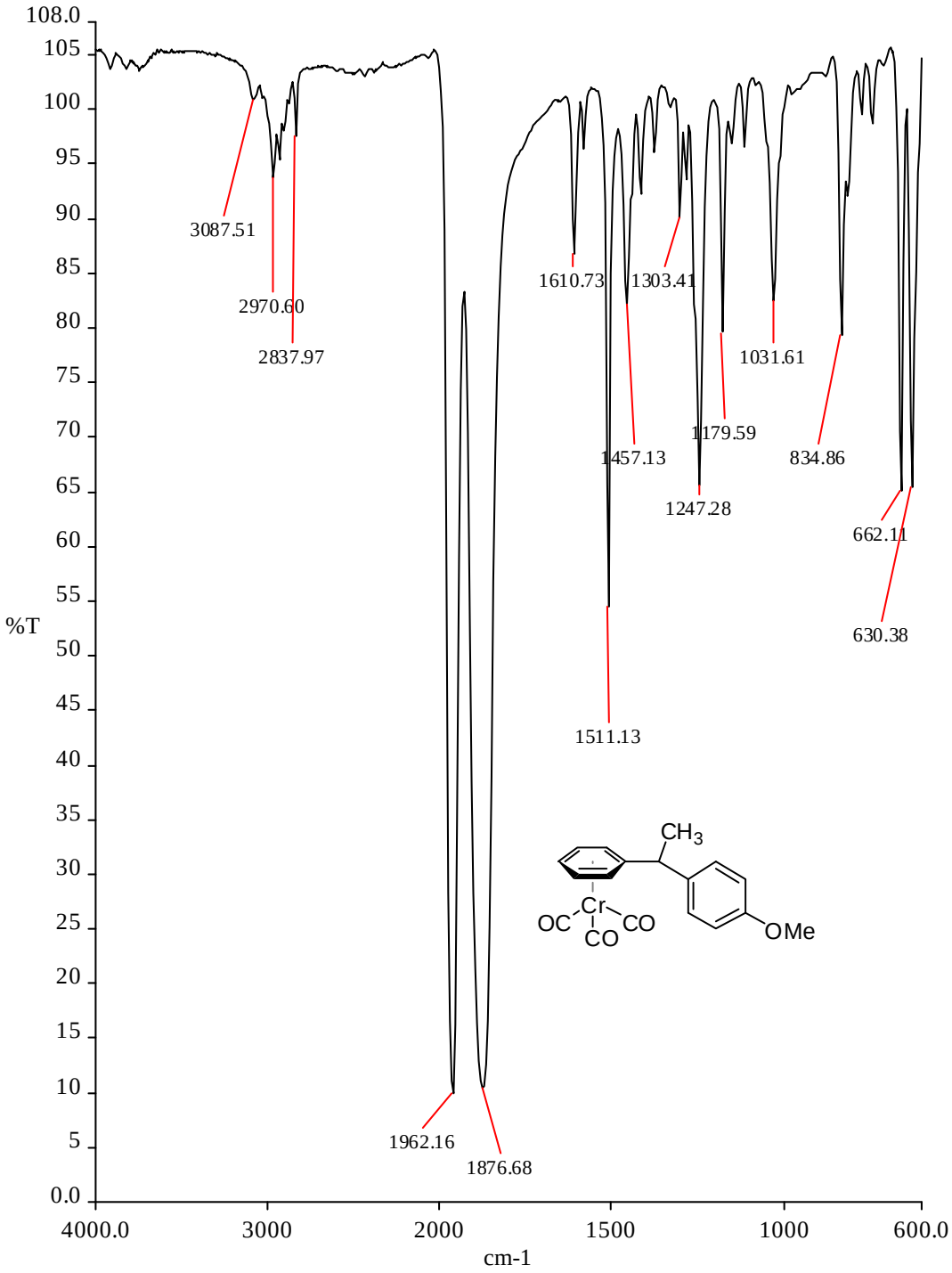

Figure II-10: IR spectrum of *cis*-diaryl indane complex **41b**.

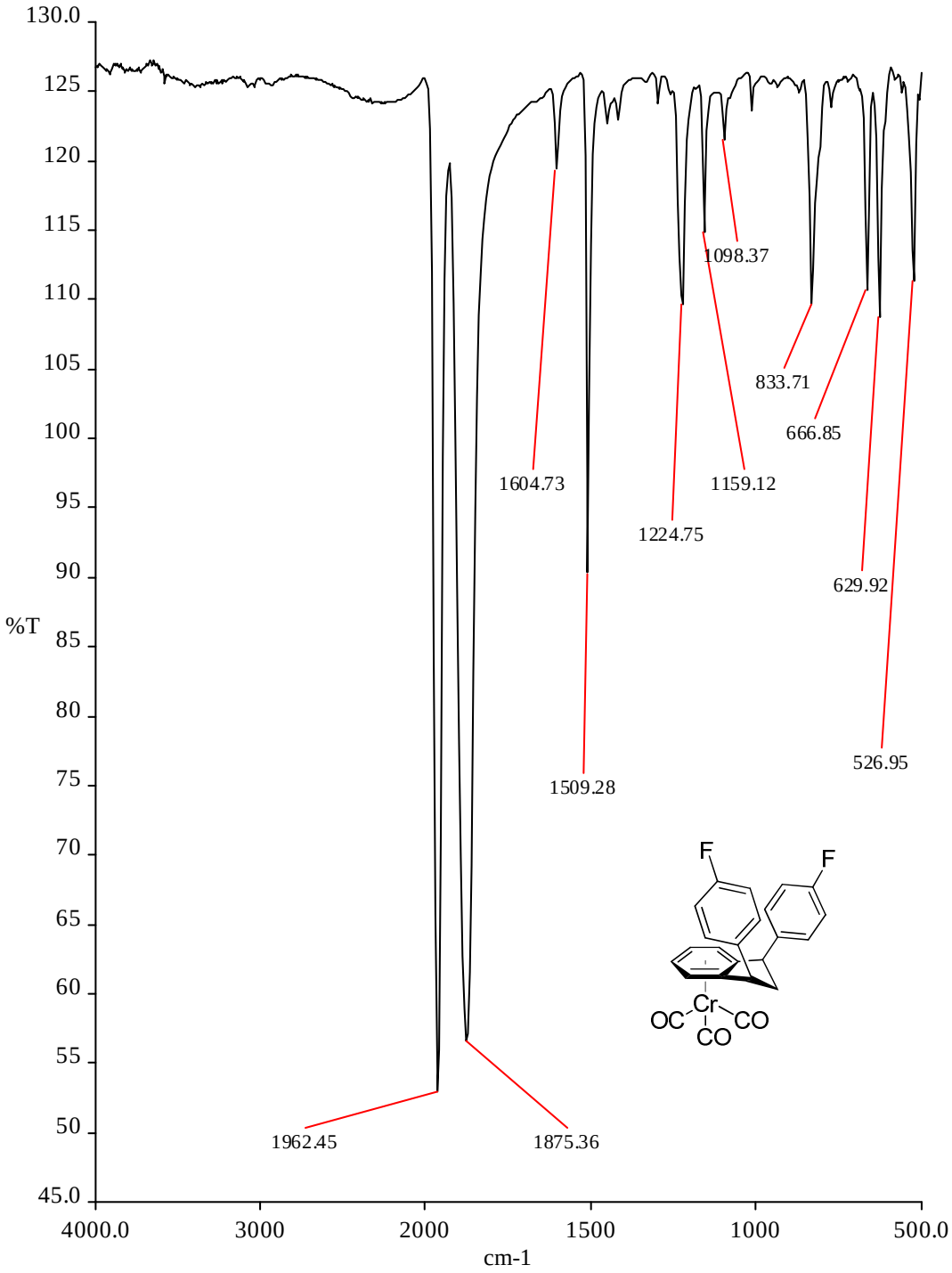

Figure II-11: IR spectrum of *cis*-diaryl tetrahydronaphthalene complex **42c**.

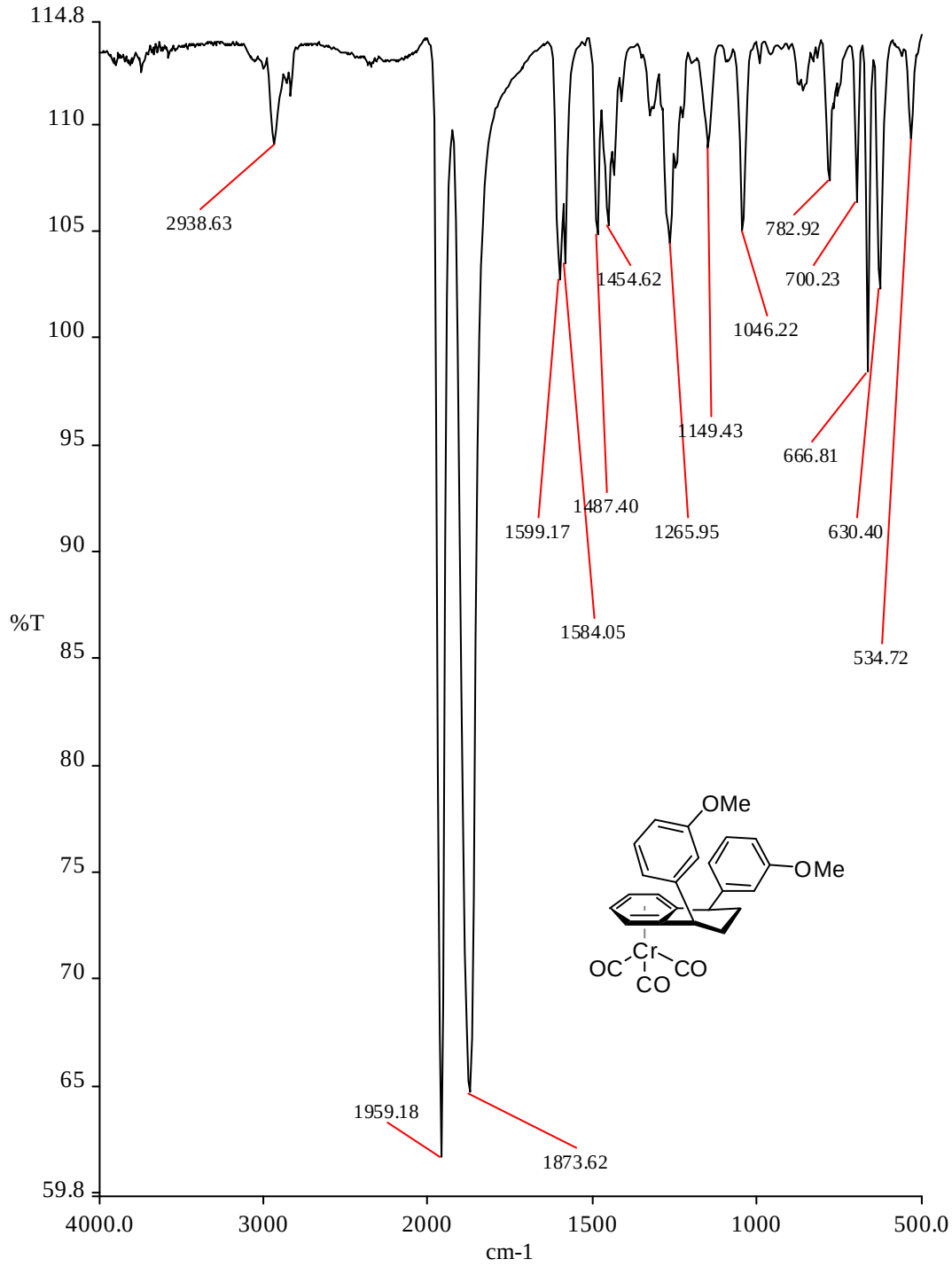

Figure II-12: IR spectrum of 1-aryl indane complex **43c**.

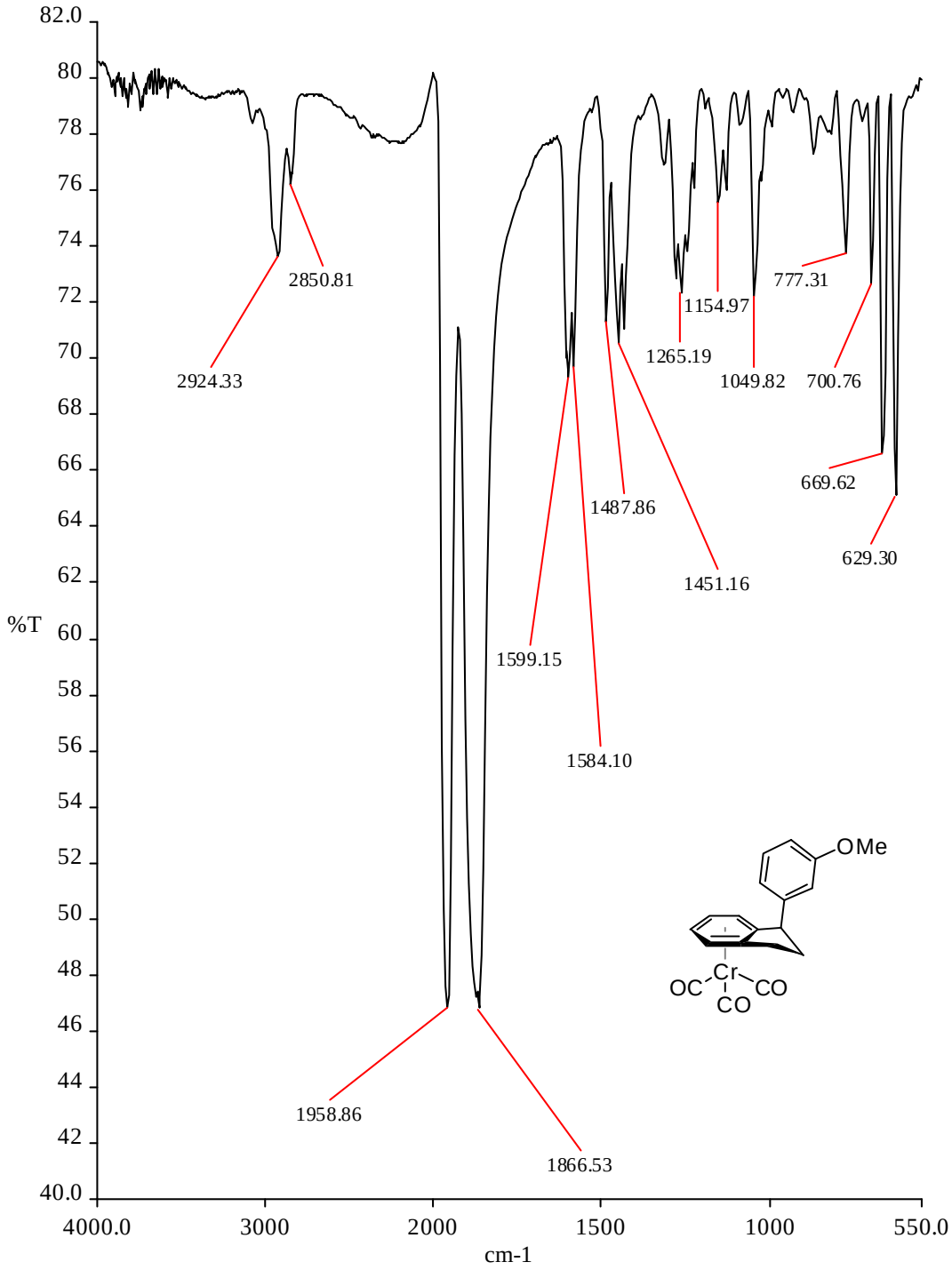

Figure II-13: IR spectrum of 1-aryl tetrahydronaphthalene complex **44b**.

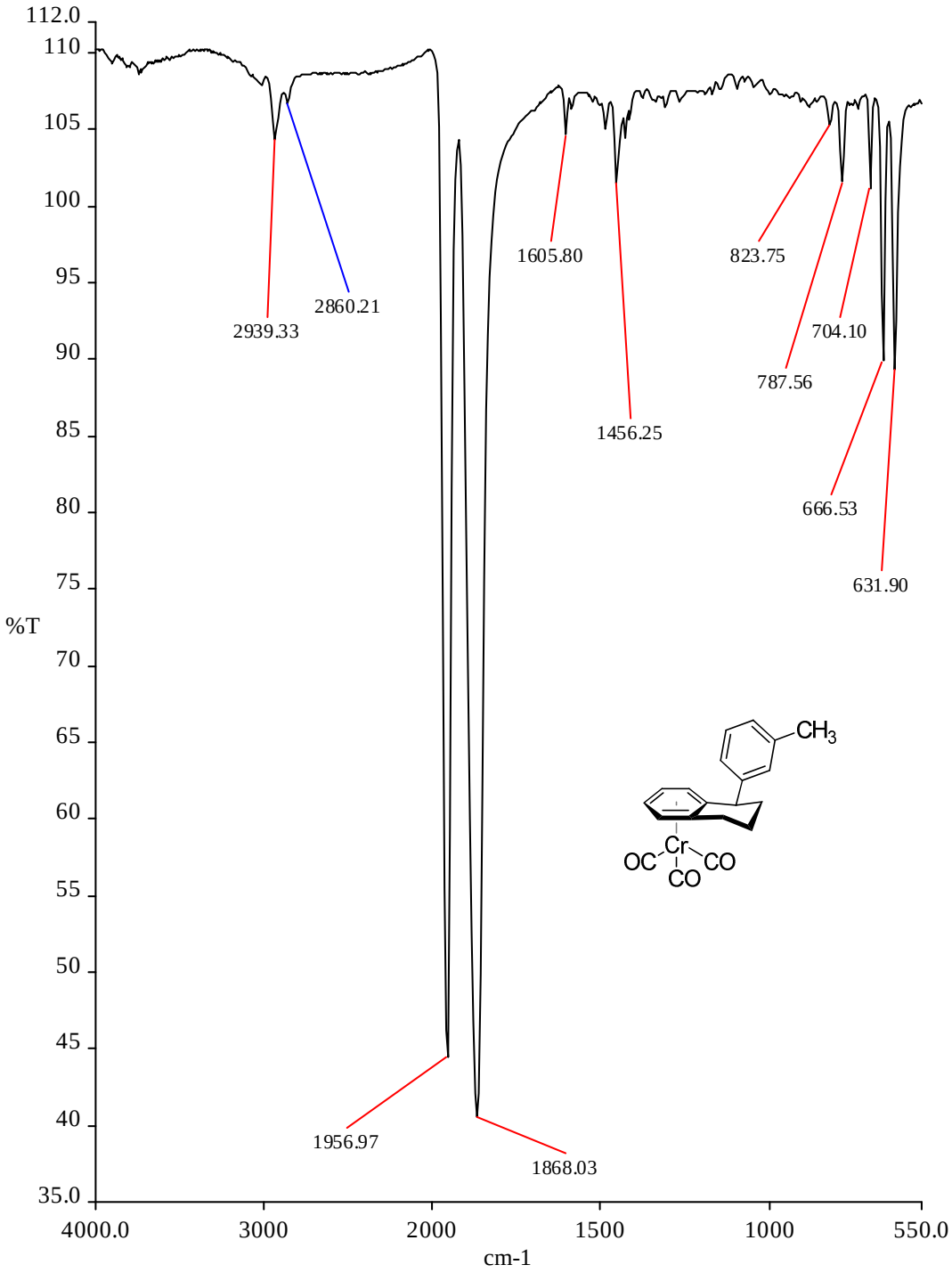

Figure II-14: IR spectrum of arylated phthalan complex **47a**.

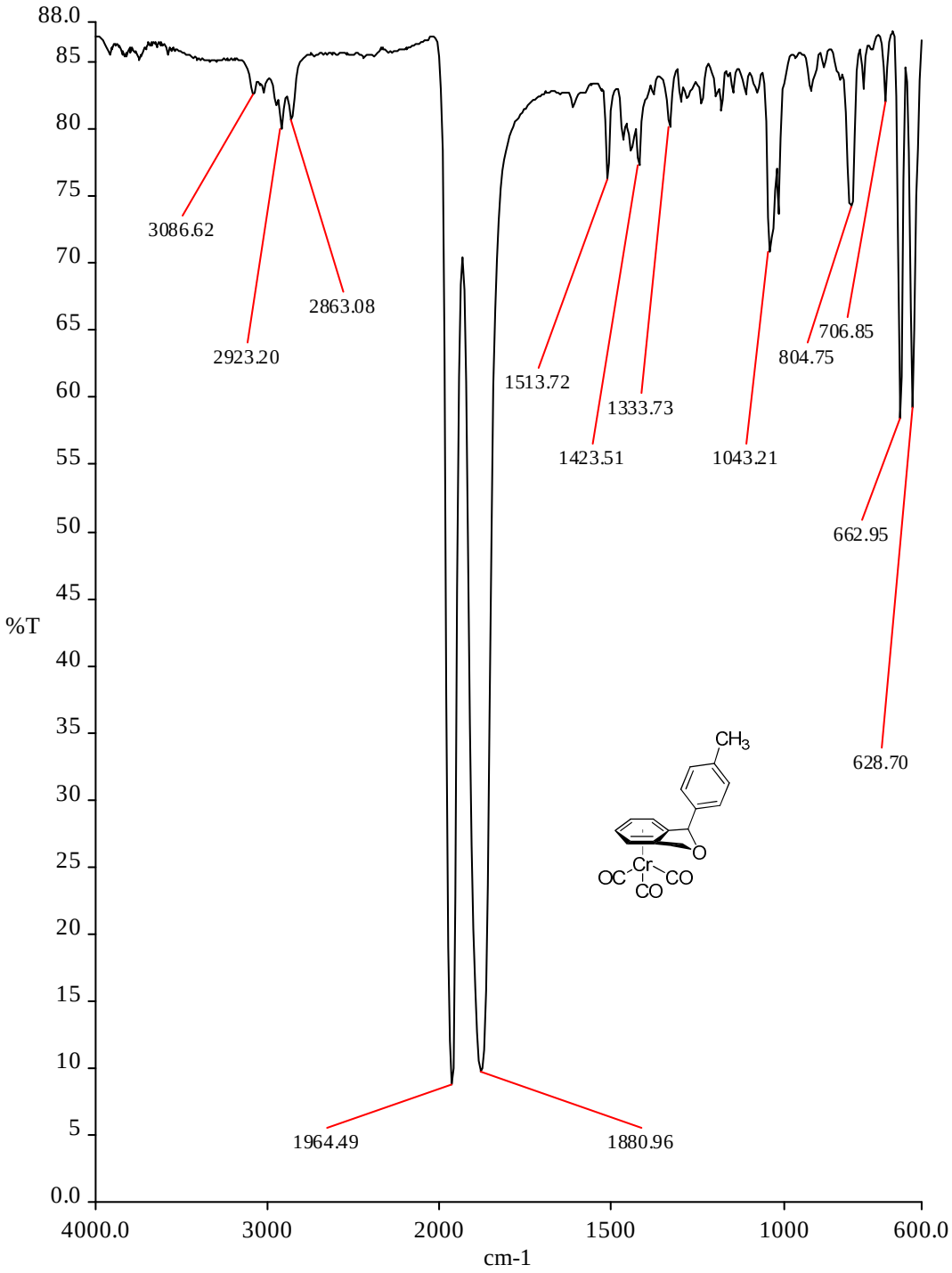

Figure II-15: IR spectrum of benzylpiperidine complex **53**.

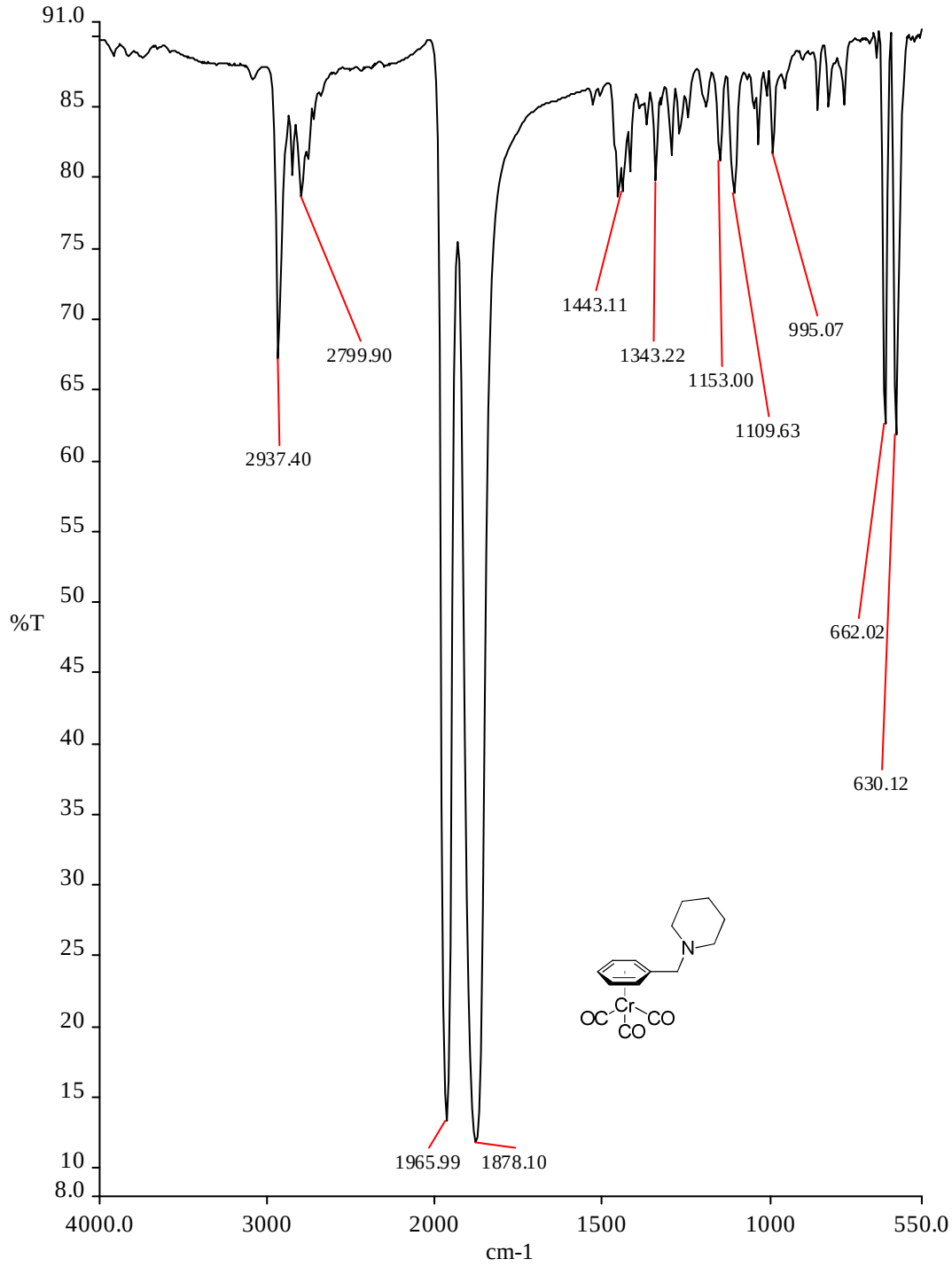

Figure II-16: IR spectrum of benzyl piperazine complex **56**.

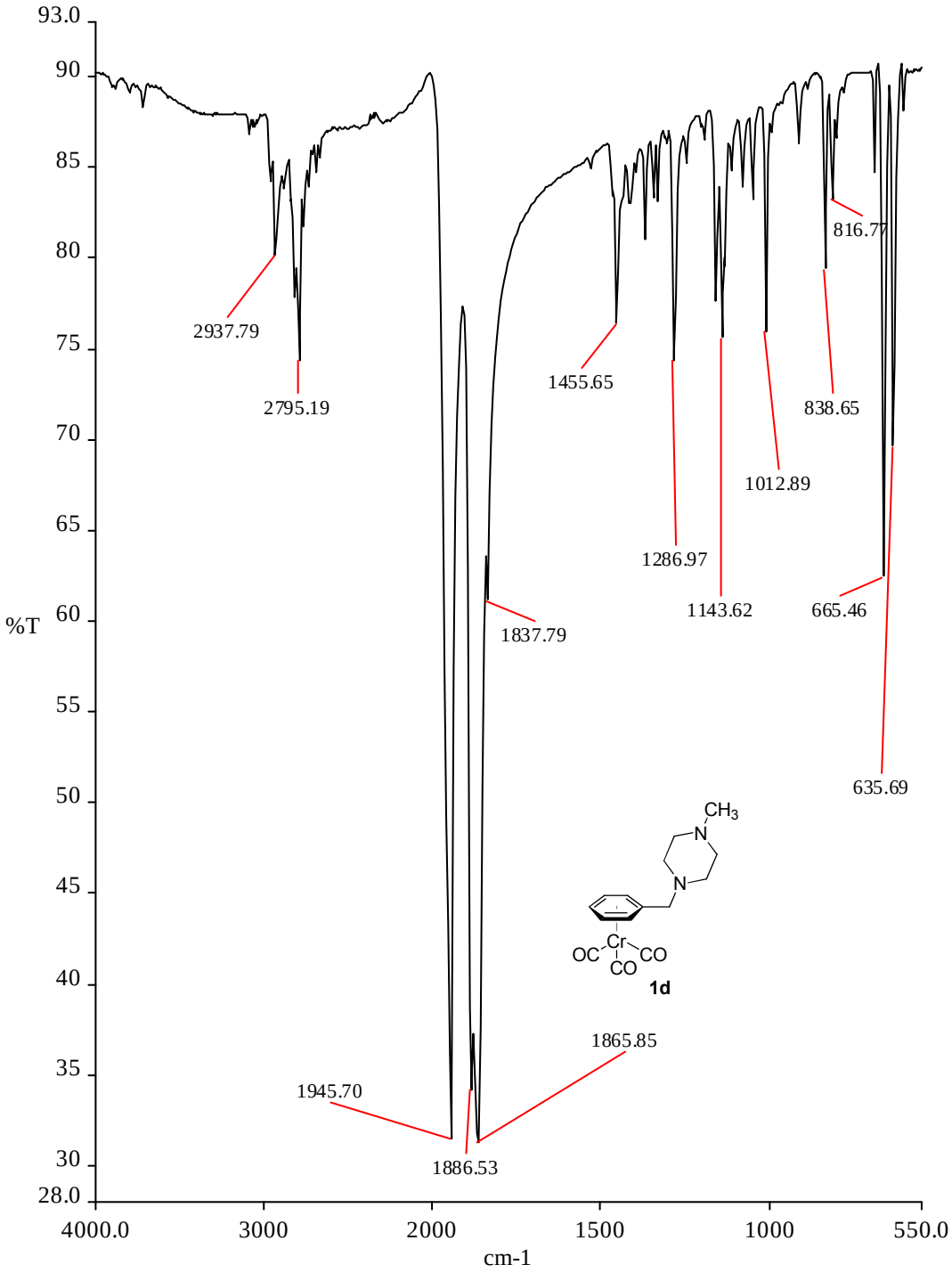

Figure II-17: IR spectrum of diarylmethylamine complex **28a**.

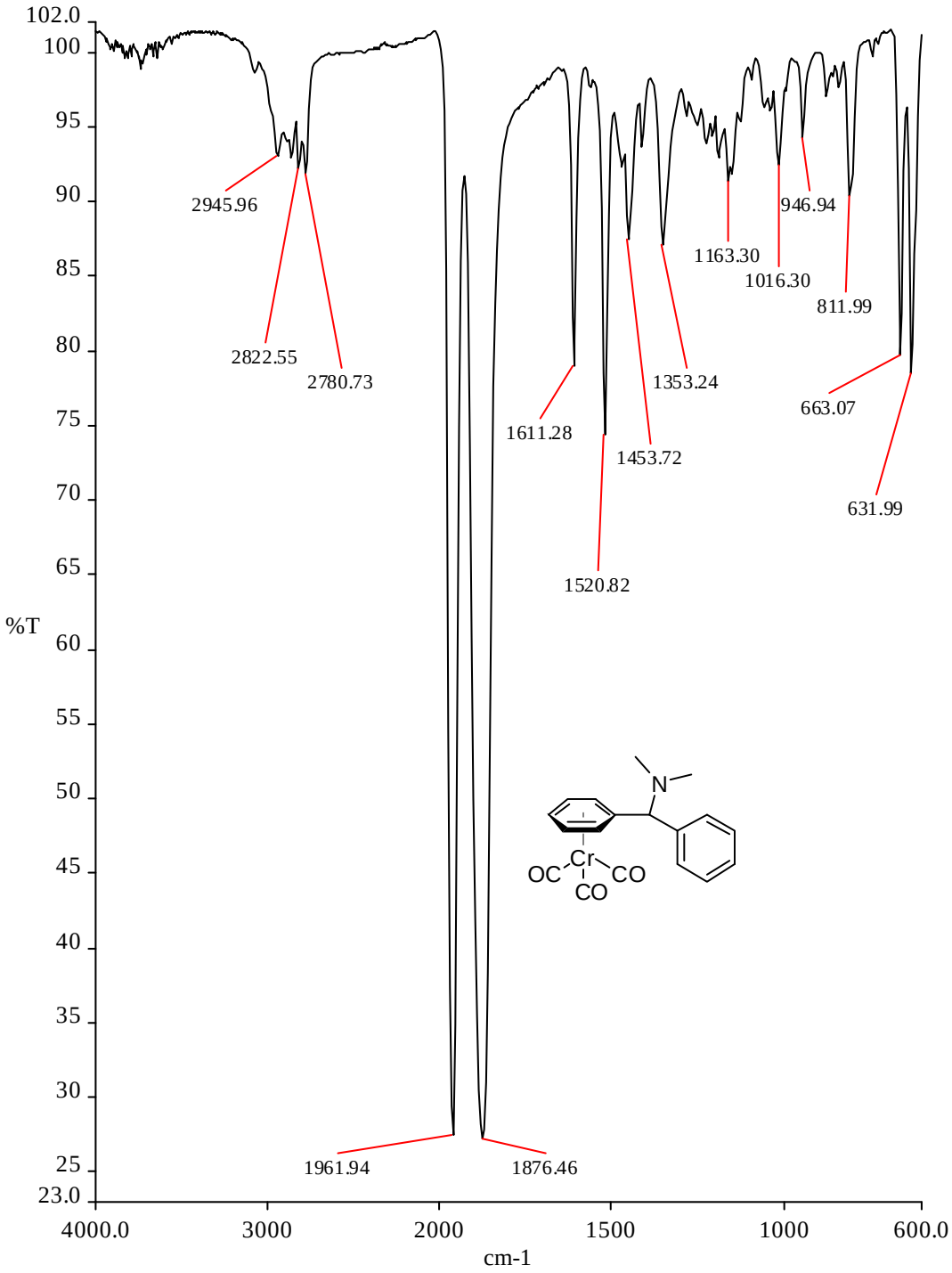

Figure II-18: IR spectrum of diarylmethylamine complex **55b**.

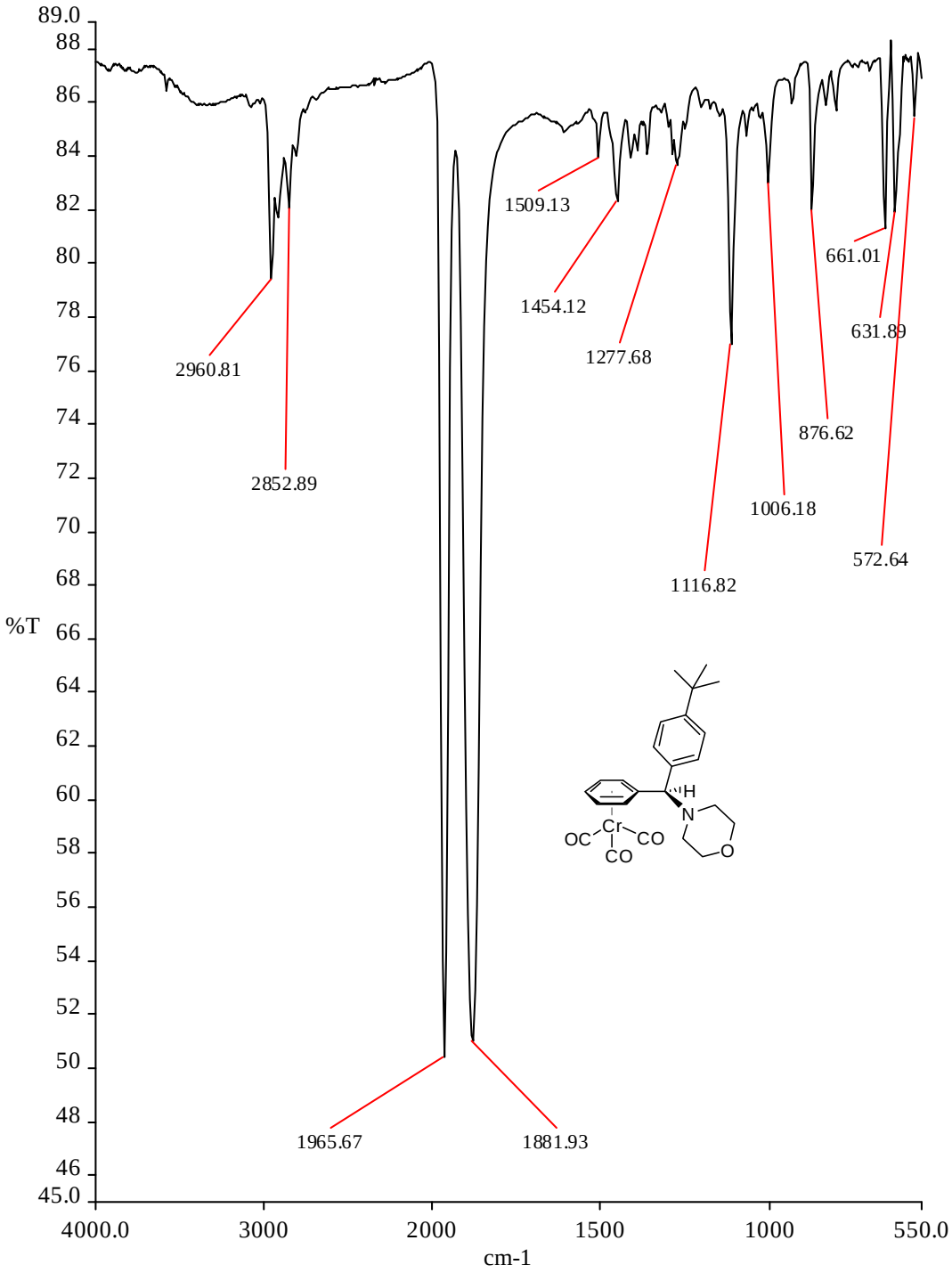

Figure II-19: IR spectrum of diarylmethylamine complex **57**.

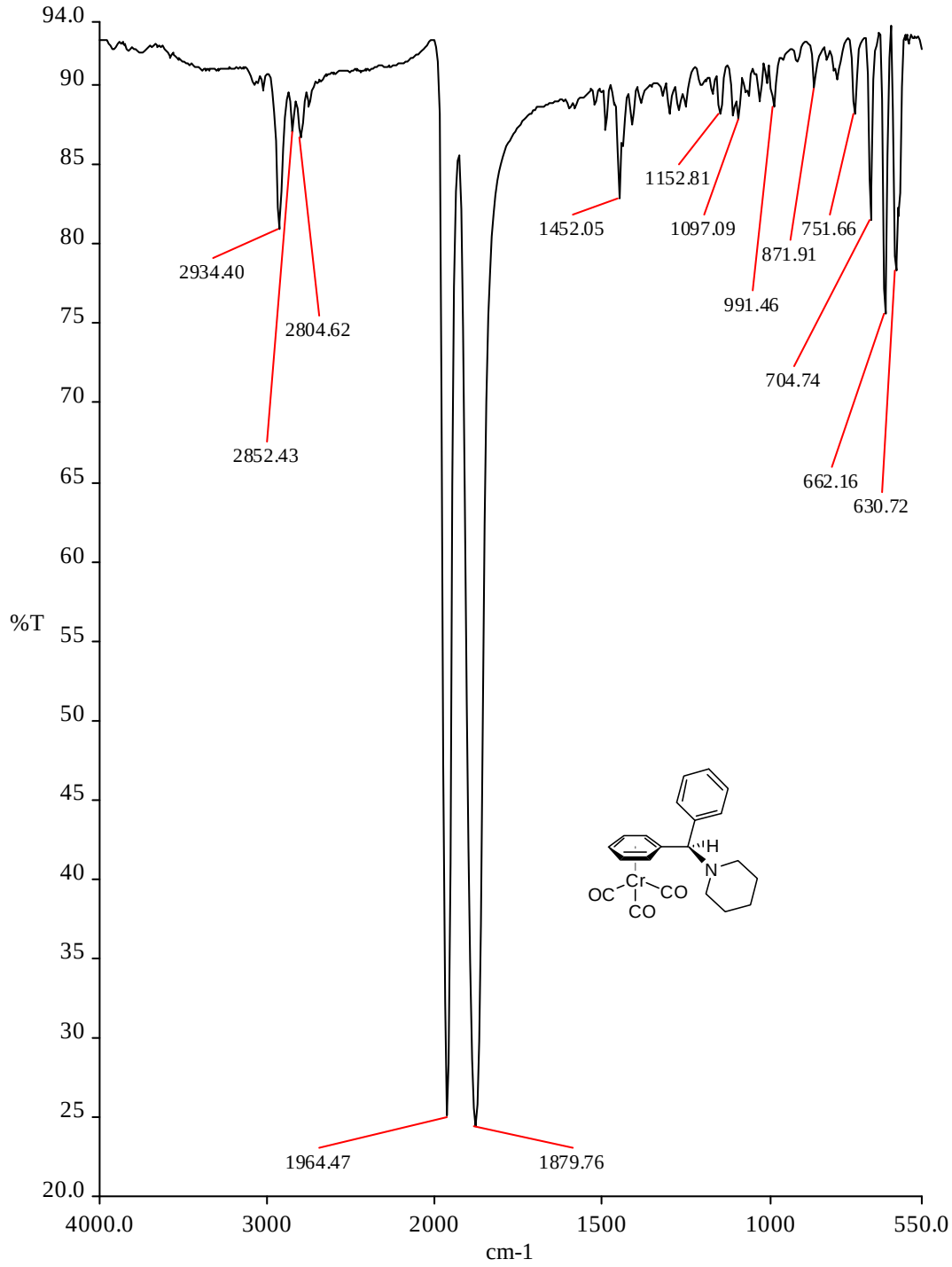

Figure II-20: IR spectrum of diarylmethylamine complex **58**.

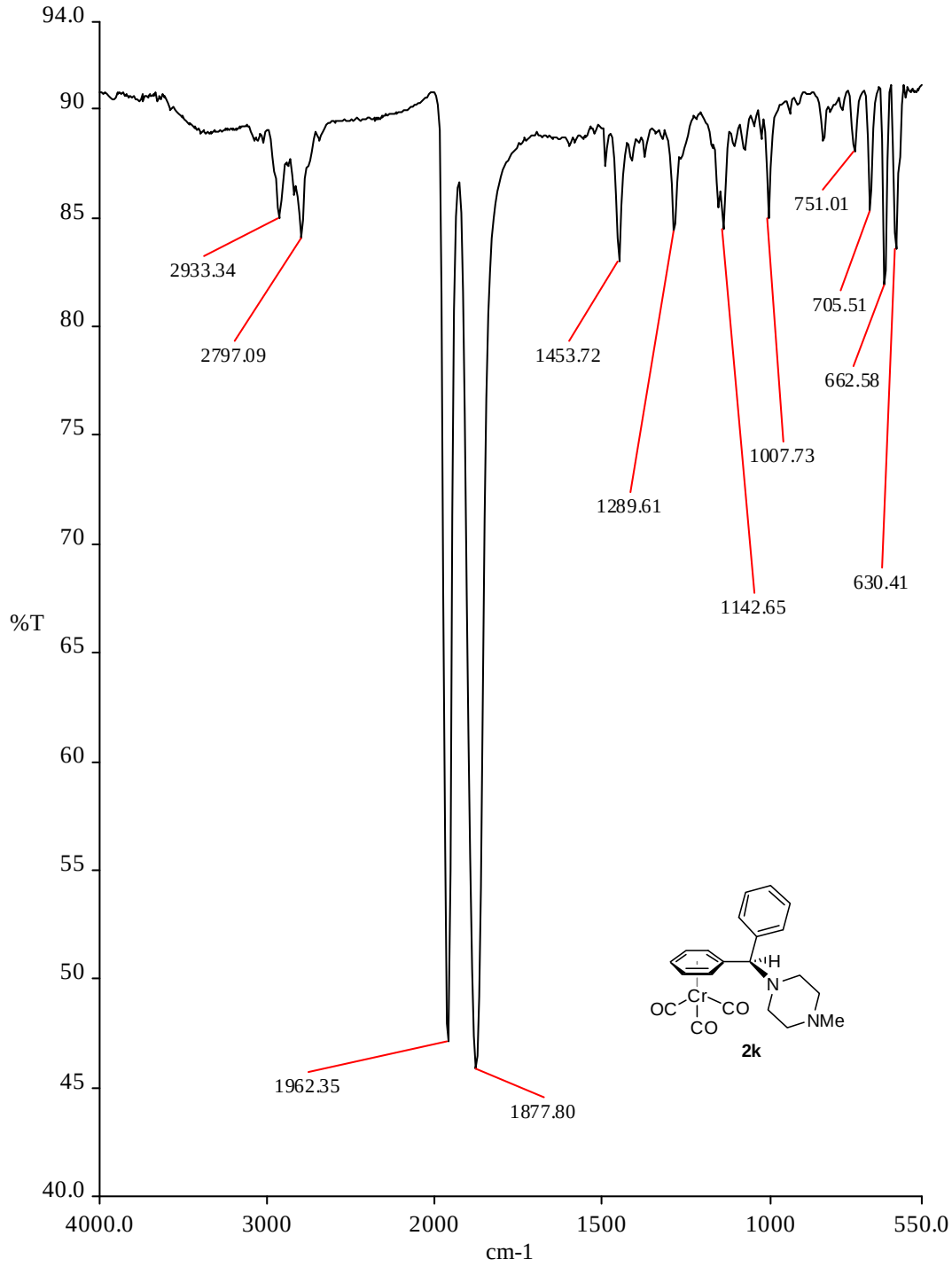

Figure II-21: IR spectrum of α–substituted benzylamine complex **59**.

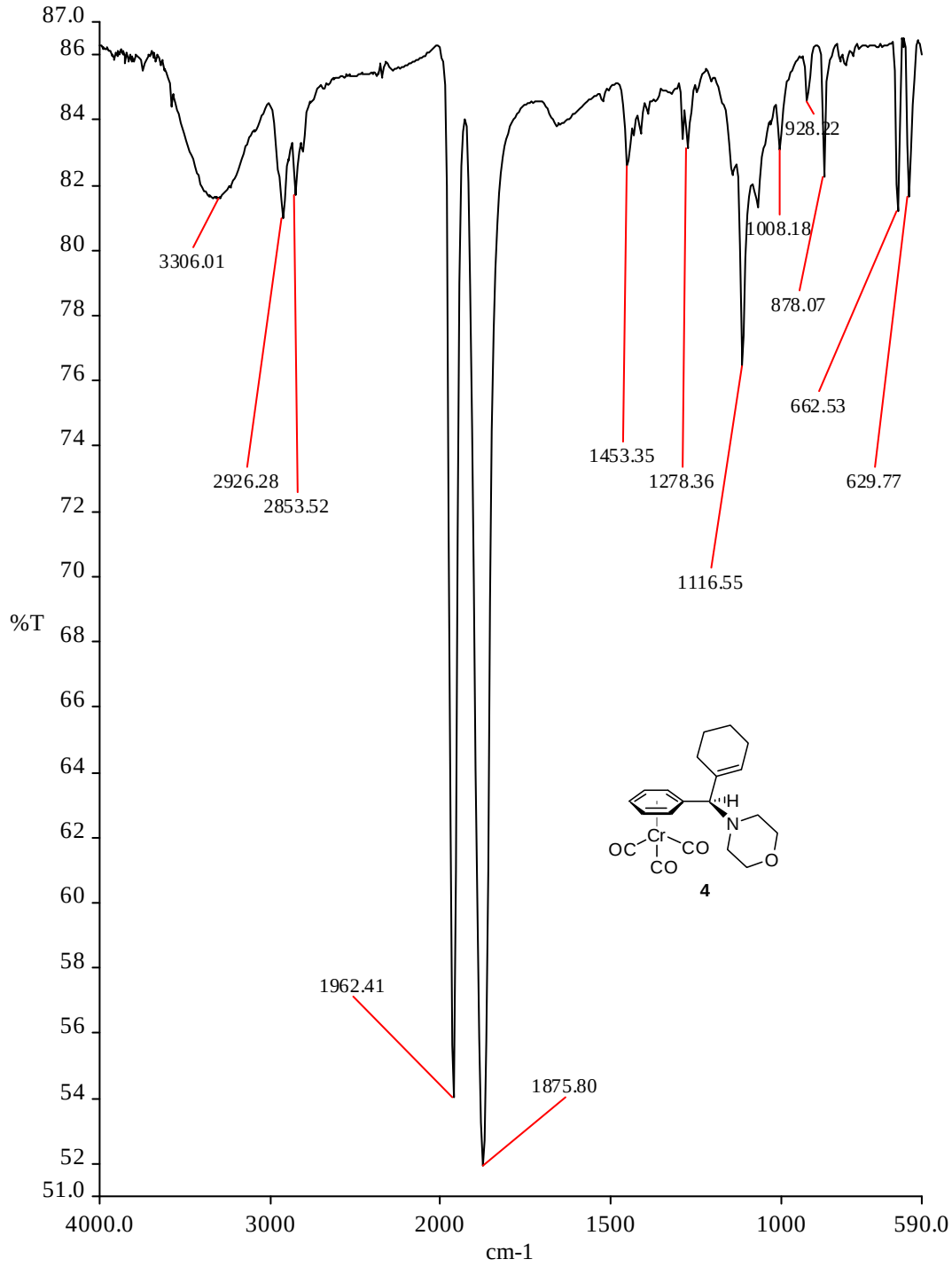

Figure II-22: IR spectrum of PN ligand **62**.

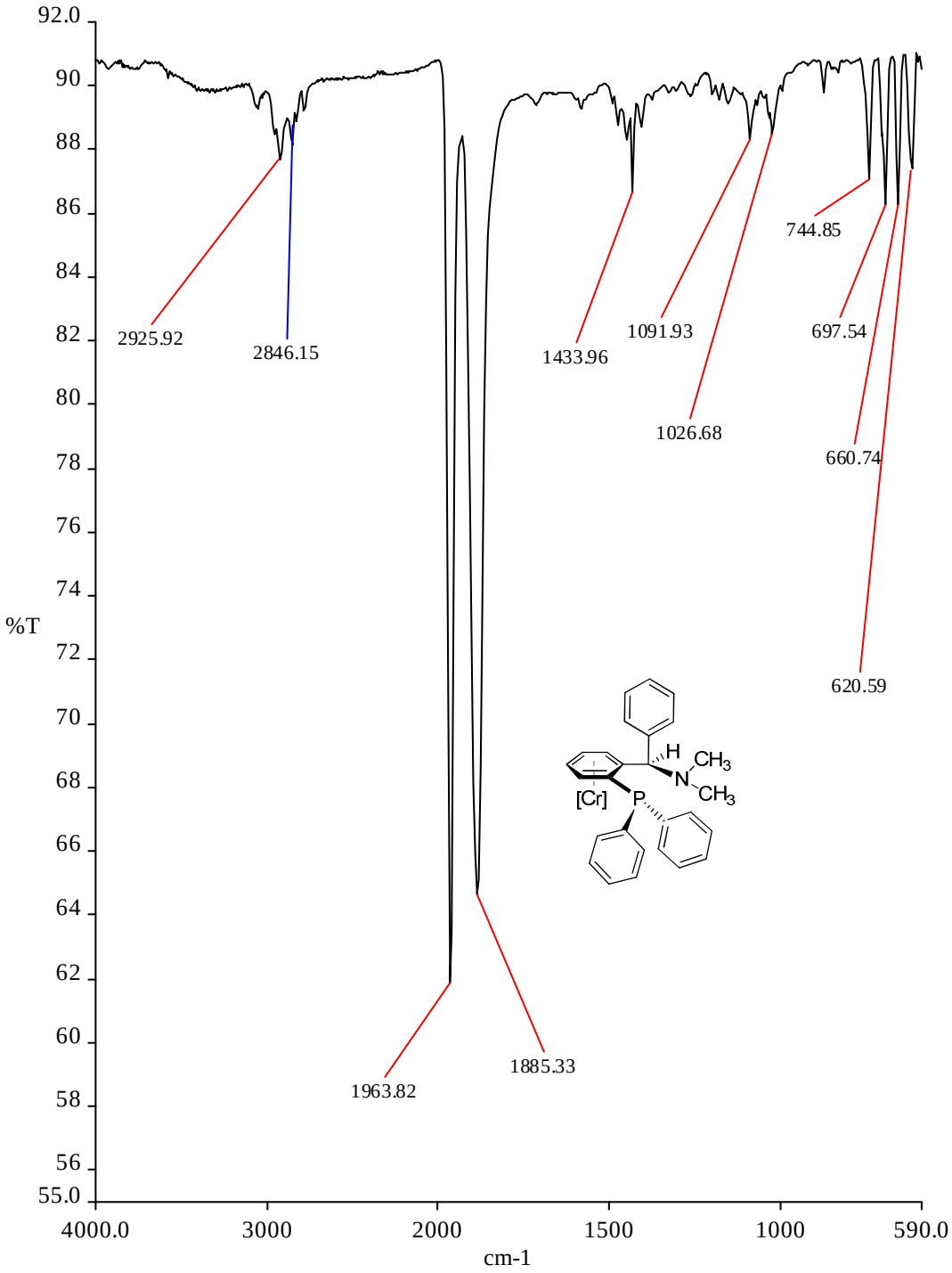

## Appendix III

## Conditions for Chromatographic Resolution of Chiral Compounds

### Conditions for Determination of Enantiomeric Excess on Merck & Co instruments:

The enantiomeric excess for **28f** was determined by chiral SFC using a Chirapak OJ-H column with 25 mM isobutylamine in methanol in supercritical cabon dioxide on an Agilent SFC using Agilent ChemStation software for instrument operation and spectrum analysis. Conditions for the resolution of the racemate are as follows:

**28f**– $Me_2NCH(4\text{-}CH_3\text{-}C_6H_4)(\eta^6\text{-}C_6H_5)Cr(CO)_3$: $t_1$ = 3.1 min, $t_2$ = 3.5 min (OJ-H column, methanol containing 25 mM isobutylamine/$CO_2$ 10/90, 3 mL/min)

### Conditions for Determination of Enantiomeric Excess on Walsh Lab instruments:

The enantiomeric excess for the following compounds were determined by chiral SFC using a Chiralcel IA, AS-H, or OJ-H column with either methanol in supercritical cabon dioxide or 0.5% isopropylamine in methanol in supercritical carbondioxide on a JASCO SFC using JASCO ChomNAV software for instrument operation and spectrum analysis. Conditions for the resolution of the racemates are as follows:

**28a** – $(C_6H_5)$-*N*-$(NMe_2)CH(\eta^6\text{-}C_6H_5)Cr(CO)_3$: $t_1$ = 2.6 min, $t_2$ = 3.4 min (OJ-H column, methanol/$CO_2$ 10/90, 4 mL/min)

**55a** – $(4\text{-}C_6H_4\text{-}CH_3)$-*N*-$(C_4H_8NO)CH(\eta^6\text{-}C_6H_5)Cr(CO)_3$: $t_1$ = 3.4 min, $t_2$ = 3.6 min (IA column, methanol/$CO_2$ 10/90, 4 mL/min)

**55b** – $(4\text{-}C_6H_4\text{-}t\text{Bu})$-*N*-$(C_4H_8NO)CH(\eta^6\text{-}C_6H_5)Cr(CO)_3$: $t_1$ = 4.6 min, $t_2$ = 4.9 min (IA column, methanol/$CO_2$ 7/93, 4 mL/min)

**55c** – $(4\text{-}C_6H_4\text{-}OCH_3)$-*N*-$(C_4H_8NO)CH(\eta^6\text{-}C_6H_5)Cr(CO)_3$: $t_1$ = 2.9 min, $t_2$ = 3.2 min (IA column, methanol/$CO_2$ 15/85, 4 mL/min)

**55d** – $(3\text{-}C_6H_4\text{-}CH_3)$-*N*-$(C_4H_8NO)CH(\eta^6\text{-}C_6H_5)Cr(CO)_3$: $t_1$ = 5.4 min, $t_2$ = 6.0 min (OJ-H column, methanol/$CO_2$ 7/93, 4 mL/min)

**55e** – $(C_6H_5)$-*N*-$(C_4H_8NO)CH(\eta^6\text{-}C_6H_5)Cr(CO)_3$: $t_1$ = 3.5 min, $t_2$ = 4.1 min (OJ-H column, methanol/$CO_2$ 15/85, 4 mL/min)

**55f** – (4-$C_6H_4$-$NMe_2$)-*N*-($C_4H_8NO$)CH($\eta^6$-$C_6H_5$)$Cr(CO)_3$: $t_1$ = 2.2 min, $t_2$ = 2.5 min (IA column, methanol/$CO_2$ 25/75, 4 mL/min)

**55g** – [1-(triisopropylsilyl)-1*H*-indol-4-yl]-*N*-($C_4H_8NO$)CH($\eta^6$-$C_6H_5$)$Cr(CO)_3$: $t_1$ = 2.7 min, $t_2$ = 3.1 min (IA column, methanol/$CO_2$ 20/80, 4 mL/min)

**57** – ($C_6H_5$)-*N*-($C_5H_{10}N$)CH($\eta^6$-$C_6H_5$)$Cr(CO)_3$: $t_1$ = 6.0 min, $t_2$ = 6.7 min (OJ-H column, methanol/$CO_2$ 7/93, 4 mL/min)

**59** – (1-$C_6H_9$)-*N*-($C_5H_8NO$)CH($\eta^6$-$C_6H_5$)$Cr(CO)_3$: $t_1$ = 2.1 min, $t_2$ = 2.4 min (AS-H column, methanol/$CO_2$ 10/90, 4 mL/min)

**61** – (4-$C_6H_4$-OMe)PhCH-*N*-($C_4H_8NO$): $t_1$ = 2.1 min, $t_2$ = 2.5 min (OJ-H column, methanol containing 0.5% isopropylamine/$CO_2$ 20/80, 4 mL/min

**62** – ($C_6H_5$)-*N*-($NMe_2$)CH($\eta^6$-*o*-$C_6H_4$-$PPh_2$)$Cr(CO)_3$: $t_1$ = 9.3 min, $t_2$ = 10.1 min (OJ-H column, methanol containing 0.5% isopropylamine/$CO_2$ 6/94, 4 mL/min)

**68** – (*E*)-dimethyl-2-(1,3-diphenylallyl)malonate: $t_1$ = 13.2 min, $t_2$ = 14.3 min (IA column, methanol/$CO_2$ 2/98, 2mL/min)

## Appendix IV

## X-ray Structure Reports

**Note**: CIF files for **17** (CCDC 775771) and **41b** (CCDC 765716) can be obtained from the Cambridge Crystallographic Data Centre free of charge at www.ccdc.cam.ac.uk/data_request/cif.)

### *X-ray Structure Determination of **5i** – Compound 6150*

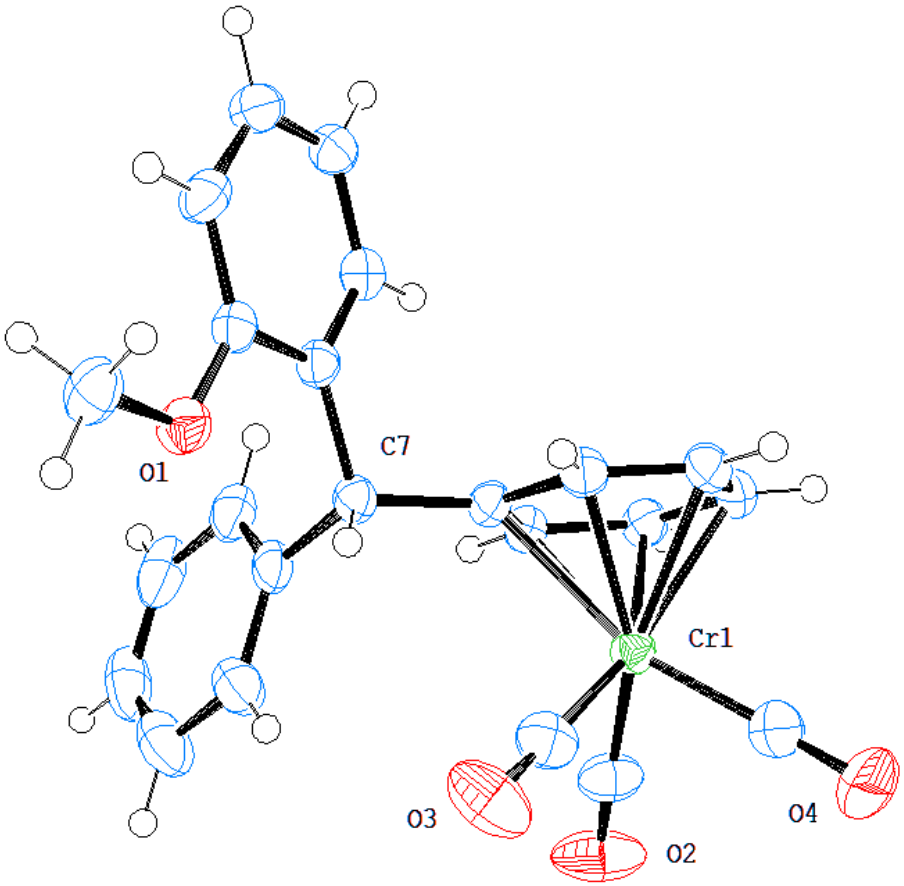


Figure IV-1: ORTEP of **5i**, Compound 6150. Thermal Ellipsoids are at 50% probability.

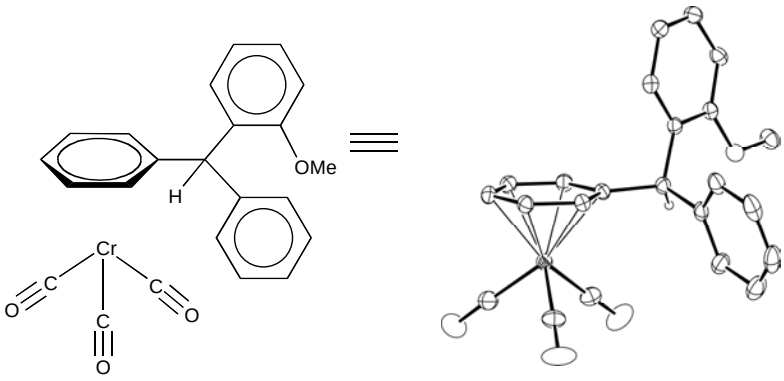


Figure IV-2: ORTEP of **5i**. Hydrogens have been omitted for clarity.

Compound **5i**, $C_{23}H_{18}O_4Cr$, crystallizes in the triclinic space group $P\bar{1}$ with a=7.7736(7)Å, b=10.4752(7)Å, c=12.5974(11)Å, α=74.799(5)°, β=88.249(6)°, γ=79.433(6)°, V=972.96(14)Å$^3$, Z=2, and $d_{calc}$=1.401 g/cm$^3$ . X-ray intensity data were collected on a Rigaku Mercury CCD area detector employing graphite-monochromated Mo-Kα radiation (λ=0.71073 Å) at a temperature of 150(1)K. Preliminary indexing was performed from a series of twelve 0.5° rotation images with exposures of 30 seconds. A total of 460 rotation images were collected with a crystal to detector distance of 35 mm, a 2θ swing angle of -12°, rotation widths of 0.5° and exposures of 20 seconds: scan no. 1 was a φ-scan from 0° to 120° at ω = 10° and χ = 20°; scan no. 2 was a φ-scan from 146.25° to 341.25° at ω = 0° and χ = -30°; scan no. 3 was an ω-scan from -20° to 20° at χ = -90° and φ = 225°; scan no. 4 was an ω-scan from -20° to 20° at χ = -90° and φ = 0°; scan no. 5 was an ω-scan from -20° to 20° at χ = -90° and φ = 45°; scan no. 6 was an ω-scan from -20° to 20° at χ = -90° and φ = 135°; scan no. 7 was an ω-scan from -20° to 20° at χ = -90° and φ = 315°; scan no. 8 was an ω-scan from -20° to 20° at χ = -90° and φ = 90°; scan no. 9 was an ω-scan from -20° to 20° at χ = -90° and φ = 180°; scan no. 10 was an ω-scan from -20° to 20° at χ = -90° and φ = 270°. Rotation images were processed using CrystalClear[1], producing a listing of unaveraged $F^2$ and $\sigma(F^2)$ values which were then passed to the CrystalStructure[2] program package for further processing and structure solution on a Dell Pentium 4 computer. A total of 18198 reflections were measured over the ranges $2.67 \leq \theta \leq 27.45°$, $-9 \leq h \leq 10$, $-13 \leq k \leq 13$, $-16 \leq l \leq 16$ yielding 4369 unique reflections (Rint = 0.0257). The intensity data were corrected for Lorentz and polarization effects and for absorption using REQAB[3] (minimum and maximum transmission 0.8762, 1.0000).

The structure was solved by direct methods (SIR97[4]). Refinement was by full-matrix least squares based on $F^2$ using SHELXL-97.[5] All reflections were used during refinement. The weighting scheme used was $w=1/[\sigma^2(F_o^2)+ 0.0609P^2 + 0.4358P$ $P = (F_o^2 + 2F_c^2)/3$. Non-hydrogen atoms were refined

anisotropically and hydrogen atoms were refined using a riding model. Refinement converged to R1=0.0441 and wR2=0.1095 for 3986 observed reflections for which F > 4σ(F) and R1=0.0486 and wR2=0.1142 and GOF =1.069 for all 4369 unique, non-zero reflections and 255 variables.[a] The maximum Δ/σ in the final cycle of least squares was 0.001 and the two most prominent peaks in the final difference Fourier were +0.575 and -0.462 e/Å$^3$. Table IV-1. lists cell information, data collection parameters, and refinement data. Final positional and equivalent isotropic thermal parameters are given in Table IV-2 and

Table IV-3. Anisotropic thermal parameters are in Table IV-4. Table IV-5 and Table IV-6 list bond distances and bond angles. Figure IV-3 is an ORTEP[6] representation of the molecule with 30% probability thermal ellipsoids displayed.

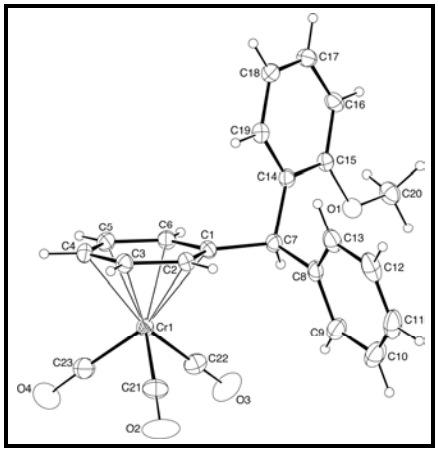


Figure IV-3: ORTEP drawing of the title compound with 30% probability thermal ellipsoids.

Table IV-1. Summary of Structure Determination of **5i**, Compound 6150

| | |
|---|---|
| Empirical formula | $C_{23}H_{18}O_4Cr$ |
| Formula weight | 410.37 |

---

[a] $R1 = \Sigma||F_o| - |F_c|| / \Sigma |F_o|$
$wR2 = [\Sigma w(F_o^2 - F_c^2)^2/\Sigma w(F_o^2)^2]$
$GOF = [\Sigma w(F_o^2 - F_c^2)^2/(n - p)]^{½}$
where n = the number of reflections and p = the number of parameters refined.

| | |
|---|---|
| Temperature | 143(1) K |
| Wavelength | 0.71073 Å |
| Crystal system | triclinic |
| Space group | $P\bar{1}$ |
| Cell constants: | |
| a | 7.7736(7) Å |
| b | 10.4752(7) Å |
| c | 12.5974(11) Å |
| α | 74.799(5)° |
| β | 88.249(6)° |
| γ | 79.433(6)° |
| Volume | 972.96(14) $Å^3$ |
| Z | 2 |
| Density (calculated) | 1.401 $Mg/m^3$ |
| Absorption coefficient | 0.614 $mm^{-1}$ |
| F(000) | 424 |
| Crystal size | 0.28 x o.25 x 0.04 $mm^3$ |
| Theta range for data collection | 2.67 to 27.45° |
| Index ranges | $-9 \le h \le 10$, $-13 \le k \le 13$, $-16 \le l \le 16$ |
| Reflections collected | 18198 |
| Independent reflections | 4369 [R(int) = 0.0257] |
| Completeness to theta = 27.45° | 98.4 % |
| Absorption correction | Semi-empirical from equivalents |
| Max. and min. transmission | 1.0000 and 0.8762 |
| Refinement method | Full-matrix least-squares on $F^2$ |
| Data / restraints / parameters | 4369 / 0 / 255 |
| Goodness-of-fit on $F^2$ | 1.069 |
| Final R indices [I>2sigma(I)] | R1 = 0.0441, wR2 = 0.1095 |
| R indices (all data) | R1 = 0.0486, wR2 = 0.1142 |
| Largest diff. peak and hole | 0.575 and -0.462 e.$Å^{-3}$ |

Table IV-2. Refined Positional Parameters for **5i**, Compound 6150

| Atom | x | y | z | $U_{eq}$,$Å^2$ |
|---|---|---|---|---|
| Cr1 | 0.72320(4) | 0.23582(3) | 0.55370(2) | 0.02729(12) |
| C1 | 0.8567(2) | 0.31375(18) | 0.39595(14) | 0.0268(4) |
| C2 | 0.9589(2) | 0.19246(19) | 0.45528(15) | 0.0274(4) |
| C3 | 1.0135(2) | 0.1757(2) | 0.56539(15) | 0.0298(4) |

| | | | | |
|---|---|---|---|---|
| C4 | 0.9649(2) | 0.2799(2) | 0.61622(15) | 0.0319(4) |
| C5 | 0.8595(3) | 0.4017(2) | 0.55814(16) | 0.0325(4) |
| C6 | 0.8067(2) | 0.41849(19) | 0.44961(15) | 0.0300(4) |
| C7 | 0.8036(2) | 0.34255(18) | 0.27514(14) | 0.0273(4) |
| C8 | 0.8139(3) | 0.2169(2) | 0.23336(15) | 0.0321(4) |
| C9 | 0.6628(3) | 0.1631(2) | 0.23238(18) | 0.0428(5) |
| C10 | 0.6684(4) | 0.0494(3) | 0.1929(2) | 0.0561(7) |
| C11 | 0.8223(4) | -0.0091(2) | 0.1546(2) | 0.0566(7) |
| C12 | 0.9735(4) | 0.0412(2) | 0.15716(18) | 0.0526(6) |
| C13 | 0.9688(3) | 0.1549(2) | 0.19695(17) | 0.0403(5) |
| C14 | 0.9080(2) | 0.44435(18) | 0.20675(14) | 0.0265(4) |
| C15 | 0.8263(2) | 0.54821(19) | 0.11867(15) | 0.0278(4) |
| C16 | 0.9169(3) | 0.6464(2) | 0.06058(16) | 0.0330(4) |
| C17 | 1.0908(3) | 0.6403(2) | 0.08697(17) | 0.0364(4) |
| C18 | 1.1753(3) | 0.5360(2) | 0.17067(17) | 0.0351(4) |
| C19 | 1.0823(2) | 0.4399(2) | 0.23034(16) | 0.0316(4) |
| C20 | 0.5682(3) | 0.6521(2) | 0.00938(17) | 0.0394(5) |
| C21 | 0.6895(3) | 0.0603(2) | 0.5903(2) | 0.0412(5) |
| C22 | 0.5123(3) | 0.2826(2) | 0.47977(19) | 0.0393(5) |
| C23 | 0.6040(3) | 0.2535(3) | 0.6785(2) | 0.0492(6) |
| O1 | 0.65677(17) | 0.54504(14) | 0.09581(11) | 0.0344(3) |
| O2 | 0.6648(2) | -0.04924(17) | 0.6147(2) | 0.0689(6) |
| O3 | 0.3799(2) | 0.31342(19) | 0.43270(18) | 0.0626(5) |
| O4 | 0.5249(3) | 0.2635(3) | 0.75601(19) | 0.0891(8) |

$U_{eq}=1/3[U_{11}(aa^*)^2+U_{22}(bb^*)^2+U_{33}(cc^*)^2+2U_{12}aa^*bb^*\cos\gamma+2U_{13}aa^*cc^*\cos\beta+2U_{23}bb^*cc^*\cos\alpha]$

Table IV-3. Positional Parameters for Hydrogens in **5i**, Compound 6150

| Atom | x | y | z | $U_{iso}$,Å$^2$ |
|---|---|---|---|---|
| H2 | 0.9912 | 0.1223 | 0.4221 | 0.036 |
| H3 | 1.0819 | 0.0951 | 0.6037 | 0.040 |
| H4 | 1.0016 | 0.2692 | 0.6881 | 0.042 |
| H5 | 0.8253 | 0.4707 | 0.5923 | 0.043 |
| H6 | 0.7379 | 0.4991 | 0.4119 | 0.040 |
| H7 | 0.6806 | 0.3871 | 0.2684 | 0.036 |
| H9 | 0.5584 | 0.2028 | 0.2579 | 0.057 |
| H10 | 0.5677 | 0.0134 | 0.1926 | 0.075 |
| H11 | 0.8243 | -0.0833 | 0.1267 | 0.075 |
| H12 | 1.0779 | 0.0000 | 0.1327 | 0.070 |
| H13 | 1.0707 | 0.1890 | 0.1989 | 0.054 |
| H16 | 0.8609 | 0.7165 | 0.0039 | 0.044 |

| | | | | |
|---|---|---|---|---|
| H17 | 1.1508 | 0.7066 | 0.0482 | 0.048 |
| H18 | 1.2929 | 0.5301 | 0.1869 | 0.047 |
| H19 | 1.1387 | 0.3709 | 0.2876 | 0.042 |
| H20a | 0.5581 | 0.7356 | 0.0292 | 0.059 |
| H20b | 0.4535 | 0.6358 | -0.0021 | 0.059 |
| H20c | 0.6334 | 0.6569 | -0.0571 | 0.059 |

Table IV-4. Refined Thermal Parameters (U's) for **5i**, Compound 6150

| Atom | $U_{11}$ | $U_{22}$ | $U_{33}$ | $U_{23}$ | $U_{13}$ | $U_{12}$ |
|---|---|---|---|---|---|---|
| Cr1 | 0.03064(18) | 0.02582(18) | 0.02590(18) | -0.00742(13) | 0.00110(12) | -0.00550(12) |
| C1 | 0.0314(8) | 0.0265(9) | 0.0224(8) | -0.0048(7) | 0.0012(7) | -0.0071(7) |
| C2 | 0.0293(8) | 0.0268(9) | 0.0249(9) | -0.0064(7) | 0.0005(7) | -0.0032(7) |
| C3 | 0.0285(8) | 0.0314(10) | 0.0265(9) | -0.0035(7) | -0.0032(7) | -0.0030(7) |
| C4 | 0.0372(9) | 0.0359(10) | 0.0243(9) | -0.0074(8) | -0.0040(7) | -0.0112(8) |
| C5 | 0.0414(10) | 0.0285(10) | 0.0314(10) | -0.0112(8) | 0.0011(8) | -0.0114(8) |
| C6 | 0.0392(10) | 0.0223(9) | 0.0278(9) | -0.0043(7) | -0.0007(7) | -0.0070(7) |
| C7 | 0.0315(9) | 0.0258(9) | 0.0237(9) | -0.0044(7) | -0.0026(7) | -0.0058(7) |
| C8 | 0.0470(11) | 0.0280(10) | 0.0205(8) | -0.0032(7) | -0.0051(7) | -0.0084(8) |
| C9 | 0.0557(13) | 0.0367(11) | 0.0377(11) | -0.0067(9) | -0.0101(9) | -0.0155(9) |
| C10 | 0.0813(18) | 0.0417(14) | 0.0508(15) | -0.0115(11) | -0.0181(13) | -0.0226(13) |
| C11 | 0.105(2) | 0.0334(12) | 0.0356(12) | -0.0128(10) | -0.0128(13) | -0.0144(13) |
| C12 | 0.0885(19) | 0.0347(12) | 0.0293(11) | -0.0063(9) | 0.0054(11) | -0.0011(12) |
| C13 | 0.0600(13) | 0.0330(11) | 0.0266(10) | -0.0055(8) | 0.0028(9) | -0.0089(9) |
| C14 | 0.0321(9) | 0.0250(9) | 0.0230(8) | -0.0072(7) | 0.0005(7) | -0.0052(7) |
| C15 | 0.0314(9) | 0.0279(9) | 0.0242(8) | -0.0083(7) | 0.0006(7) | -0.0038(7) |
| C16 | 0.0410(10) | 0.0281(10) | 0.0275(9) | -0.0030(8) | 0.0037(8) | -0.0066(8) |
| C17 | 0.0414(10) | 0.0365(11) | 0.0350(10) | -0.0107(9) | 0.0086(8) | -0.0154(8) |
| C18 | 0.0329(9) | 0.0437(12) | 0.0331(10) | -0.0141(9) | 0.0026(8) | -0.0127(8) |
| C19 | 0.0338(9) | 0.0342(10) | 0.0266(9) | -0.0085(8) | -0.0018(7) | -0.0050(7) |
| C20 | 0.0364(10) | 0.0430(12) | 0.0311(10) | -0.0007(9) | -0.0034(8) | 0.0004(8) |
| C21 | 0.0308(10) | 0.0360(11) | 0.0552(14) | -0.0104(10) | 0.0082(9) | -0.0055(8) |
| C22 | 0.0383(10) | 0.0325(11) | 0.0485(12) | -0.0137(9) | 0.0010(9) | -0.0054(8) |
| C23 | 0.0550(13) | 0.0577(15) | 0.0469(13) | -0.0259(12) | 0.0137(11) | -0.0244(11) |
| O1 | 0.0326(7) | 0.0360(8) | 0.0298(7) | -0.0007(6) | -0.0043(5) | -0.0049(5) |
| O2 | 0.0515(10) | 0.0323(9) | 0.1203(19) | -0.0125(10) | 0.0195(11) | -0.0149(7) |
| O3 | 0.0413(9) | 0.0558(11) | 0.0908(15) | -0.0240(10) | -0.0255(9) | 0.0019(8) |
| O4 | 0.1044(17) | 0.126(2) | 0.0716(15) | -0.0647(15) | 0.0553(13) | -0.0615(16) |

The form of the anisotropic displacement parameter is:
$\exp[-2\pi^2(a^{*2}U_{11}h^2+b^{*2}U_{22}k^2+c^{*2}U_{33}l^2+2b^*c^*U_{23}kl+2a^*c^*U_{13}hl+2a^*b^*U_{12}hk)]$

Table IV-5. Bond Distances in **5i**, Compound 6150, Å

| | | | | | |
|---|---|---|---|---|---|
| Cr1-C22 | 1.832(2) | Cr1-C23 | 1.835(2) | Cr1-C21 | 1.840(2) |
| Cr1-C5 | 2.2076(19) | Cr1-C6 | 2.2111(19) | Cr1-C2 | 2.2254(18) |
| Cr1-C4 | 2.2275(18) | Cr1-C3 | 2.2276(18) | Cr1-C1 | 2.2420(18) |
| C1-C2 | 1.404(2) | C1-C6 | 1.424(3) | C1-C7 | 1.526(2) |
| C2-C3 | 1.420(2) | C3-C4 | 1.394(3) | C4-C5 | 1.414(3) |
| C5-C6 | 1.397(3) | C7-C14 | 1.526(2) | C7-C8 | 1.529(3) |
| C8-C13 | 1.385(3) | C8-C9 | 1.394(3) | C9-C10 | 1.399(3) |
| C10-C11 | 1.375(4) | C11-C12 | 1.379(4) | C12-C13 | 1.403(3) |
| C14-C19 | 1.386(3) | C14-C15 | 1.405(2) | C15-O1 | 1.365(2) |
| C15-C16 | 1.389(3) | C16-C17 | 1.388(3) | C17-C18 | 1.383(3) |
| C18-C19 | 1.392(3) | C20-O1 | 1.428(2) | C21-O2 | 1.158(3) |
| C22-O3 | 1.153(3) | C23-O4 | 1.156(3) | | |

Table IV-6. Bond Angles in **5i**, Compound 6150, °

| | | | | | |
|---|---|---|---|---|---|
| C22-Cr1-C23 | 88.10(11) | C22-Cr1-C21 | 87.94(10) | C23-Cr1-C21 | 87.12(11) |
| C22-Cr1-C5 | 116.66(9) | C23-Cr1-C5 | 90.90(9) | C21-Cr1-C5 | 155.26(9) |
| C22-Cr1-C6 | 90.14(9) | C23-Cr1-C6 | 116.64(10) | C21-Cr1-C6 | 156.09(9) |
| C5-Cr1-C6 | 36.85(7) | C22-Cr1-C2 | 116.36(9) | C23-Cr1-C2 | 155.54(10) |
| C21-Cr1-C2 | 93.28(8) | C5-Cr1-C2 | 78.61(7) | C6-Cr1-C2 | 66.39(7) |
| C22-Cr1-C4 | 153.83(9) | C23-Cr1-C4 | 91.90(9) | C21-Cr1-C4 | 118.21(9) |
| C5-Cr1-C4 | 37.17(7) | C6-Cr1-C4 | 66.56(7) | C2-Cr1-C4 | 66.40(7) |
| C22-Cr1-C3 | 153.55(9) | C23-Cr1-C3 | 118.35(10) | C21-Cr1-C3 | 92.99(8) |
| C5-Cr1-C3 | 66.40(7) | C6-Cr1-C3 | 78.45(7) | C2-Cr1-C3 | 37.19(6) |
| C4-Cr1-C3 | 36.46(7) | C22-Cr1-C1 | 89.83(8) | C23-Cr1-C1 | 153.86(10) |
| C21-Cr1-C1 | 118.84(9) | C5-Cr1-C1 | 66.92(7) | C6-Cr1-C1 | 37.29(7) |
| C2-Cr1-C1 | 36.64(6) | C4-Cr1-C1 | 78.81(7) | C3-Cr1-C1 | 66.63(7) |
| C2-C1-C6 | 118.35(16) | C2-C1-C7 | 123.69(16) | C6-C1-C7 | 117.88(16) |
| C2-C1-Cr1 | 71.04(10) | C6-C1-Cr1 | 70.18(10) | C7-C1-Cr1 | 132.96(12) |
| C1-C2-C3 | 120.74(17) | C1-C2-Cr1 | 72.32(10) | C3-C2-Cr1 | 71.49(10) |
| C4-C3-C2 | 120.12(17) | C4-C3-Cr1 | 71.76(11) | C2-C3-Cr1 | 71.32(10) |
| C3-C4-C5 | 119.76(17) | C3-C4-Cr1 | 71.77(10) | C5-C4-Cr1 | 70.65(11) |
| C6-C5-C4 | 120.14(18) | C6-C5-Cr1 | 71.71(11) | C4-C5-Cr1 | 72.18(11) |
| C5-C6-C1 | 120.87(17) | C5-C6-Cr1 | 71.44(11) | C1-C6-Cr1 | 72.53(10) |
| C1-C7-C14 | 108.57(14) | C1-C7-C8 | 114.33(15) | C14-C7-C8 | 113.50(15) |
| C13-C8-C9 | 119.2(2) | C13-C8-C7 | 121.91(18) | C9-C8-C7 | 118.90(19) |
| C8-C9-C10 | 119.9(2) | C11-C10-C9 | 120.2(2) | C10-C11-C12 | 120.5(2) |
| C11-C12-C13 | 119.5(2) | C8-C13-C12 | 120.6(2) | C19-C14-C15 | 118.13(17) |

| | | | | | |
|---|---|---|---|---|---|
| C19-C14-C7 | 121.87(16) | C15-C14-C7 | 119.98(16) | O1-C15-C16 | 123.71(17) |
| O1-C15-C14 | 115.93(16) | C16-C15-C14 | 120.36(17) | C17-C16-C15 | 120.16(18) |
| C18-C17-C16 | 120.25(18) | C17-C18-C19 | 119.22(18) | C14-C19-C18 | 121.80(18) |
| O2-C21-Cr1 | 178.4(2) | O3-C22-Cr1 | 179.3(2) | O4-C23-Cr1 | 178.1(2) |
| C15-O1-C20 | 117.20(15) | | | | |

*X-ray Structure Determination of **5n** – Compound 6140*

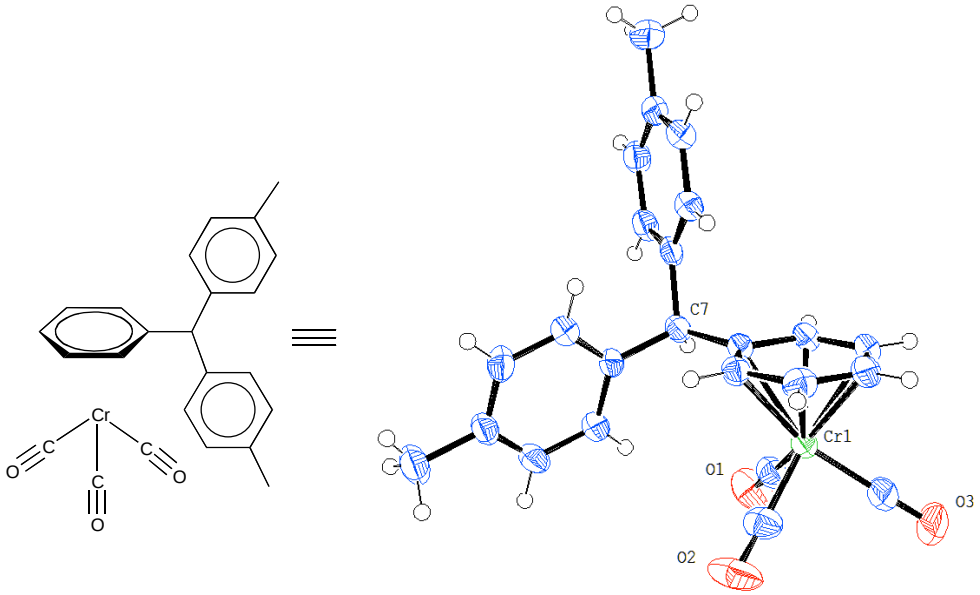


Figure IV-4: ORTEP of **5n**, compound 6140. Thermal Ellipsoids are at 50% probability.

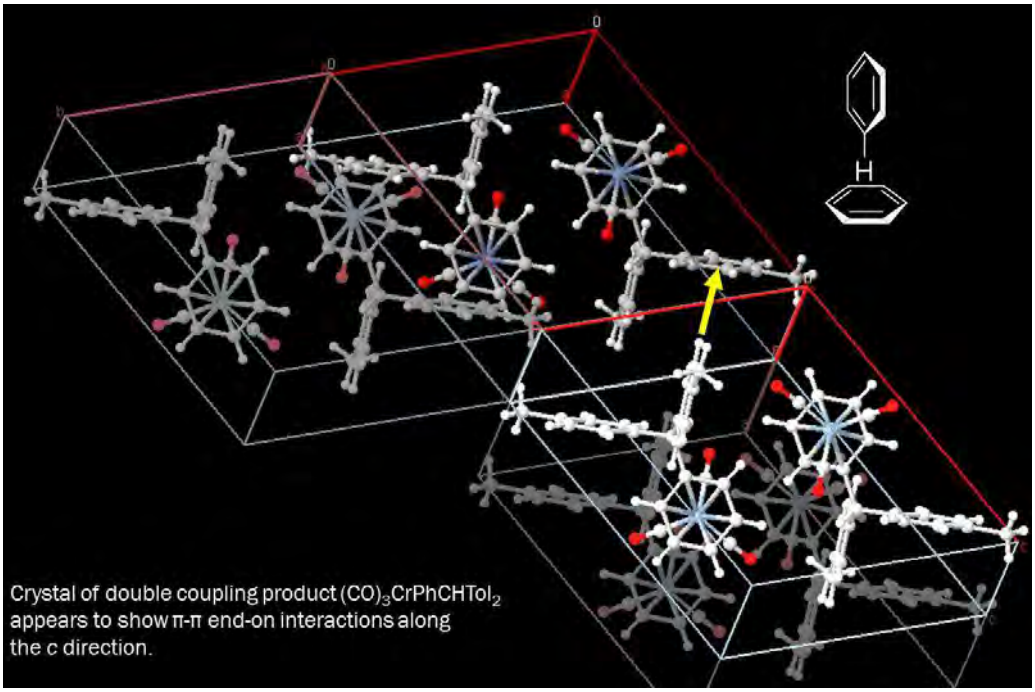


Figure IV-5: Observation of arene end-on π interactions within the crystal structure of **5n**.

Compound 6140 (**5n**), $C_{24}H_{20}O_3Cr$, crystallizes in the triclinic space group $P\bar{1}$ with a=7.674(2)Å, b=10.772(3)Å, c=13.579(4)Å, $\alpha$=102.847(5)°, $\beta$=105.255(7)°, $\gamma$=101.177(3)°, V=1017.2(5)Å$^3$, Z=2 and $d_{calc}$=1.333 g/cm$^3$. X-ray intensity data were collected on a Rigaku Mercury CCD area detector employing graphite-monochromated Mo-$K_\alpha$ radiation ($\lambda$=0.71073 Å) at a temperature of 143K. Preliminary indexing was performed from a series of twelve 0.5° rotation images with exposures of 30 seconds. A total of 742 rotation images were collected with a crystal to detector distance of 35 mm, a 2$\theta$ swing angle of -14°, rotation widths of 0.5° and exposures of 60 seconds: scan no. 1 was a $\phi$-scan from 150° to 300° at $\omega$ = 10° and $\chi$ = 20°; scan no. 2 was a $\phi$-scan from 240° to 360° at $\omega$ = 0° and $\chi$ = -30°; scan no. 3 was an $\omega$-scan from -20° to 4° at $\chi$ = -90° and $\phi$ = 315°; scan no. 4 was an $\omega$-scan from -20° to 17° at $\chi$ = -90° and $\phi$ = 135°; scan no. 5 was an $\omega$-scan from -20° to 20° at $\chi$ = -90° and $\phi$ = 45°. Rotation images were processed using CrystalClear[1], producing a listing of unaveraged $F^2$ and $\sigma(F^2)$ values which were then passed to the CrystalStructure[2] program package for further processing and structure solution on a Dell Pentium III computer. A total of 10895 reflections were measured over the ranges $5.6 \leq 2\theta \leq 54.94$ °, $-7 \leq h \leq 9$, $-13 \leq k \leq 12$, $-17 \leq l \leq 17$ yielding 4553 unique reflections ($R_{int}$ = 0.0307). The intensity data were corrected for Lorentz and polarization effects and for absorption using REQAB[3] (minimum and maximum transmission 0.693, 1.000).

The structure was solved by direct methods (SIR97[4]). Refinement was by full-matrix least squares based on $F^2$ using SHELXL-97[5]. All reflections were used during refinement ($F^2$'s that were experimentally negative were replaced by $F^2$ = 0). The weighting scheme used was $w=1/[\sigma^2(F_o^2)+ 0.0839P^2 + 0.3721P]$ where $P = (F_o^2 + 2F_c^2)/3$ . Non-hydrogen atoms were refined anisotropically and hydrogen atoms were refined using a "riding" model. Refinement converged to $R_1$=0.0542 and $wR_2$=0.1410 for 3578 reflections for which $F > 4\sigma(F)$ and $R_1$=0.0698, $wR_2$=0.1572 and GOF = 1.066 for all 4553 unique, non-zero reflections and 256 variables[a]. The maximum $\Delta/\sigma$ in the final cycle of least squares was 0.016 and the two most prominent peaks in the final difference Fourier were +0.610 and -0.664 e/Å$^3$.

---

[a] $R_1 = \sum ||F_o| - |F_c|| / \sum |F_o|$

$wR_2 = \{ \sum w (F_o^2 - F_c^2)^2 / \sum w(F_o^2)^2\}^{1/2}$

$GOF = \{ \sum w (F_o^2 - F_c^2)^2 / (n - p)\}^{1/2}$

where n = the number of reflections and p = the number of parameters refined.

Table 1. lists cell information, data collection parameters, and refinement data. Final positional and equivalent isotropic thermal parameters are given in Table 2. Anisotropic thermal parameters are in Table 3. Tables 4. and 5. list bond distances and bond angles. Figure IV-3 is an ORTEP[6] representation of the molecule with 30% probability thermal ellipsoids displayed.

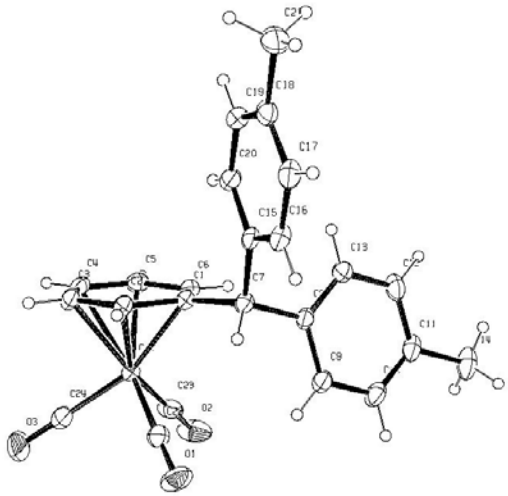


Figure IV-6: ORTEP drawing of the title compound **5n** with 30% probability thermal ellipsoids.

Table IV-7: Summary of Structure Determination of **5n**, Compound 6140

| | |
|---|---|
| Formula: | $C_{24}H_{20}O_3Cr$ |
| Formula weight: | 408.40 |
| Crystal class: | triclinic |
| Space group: | $P\bar{1}$ (#2) |
| Z | 2 |
| Cell constants: | |
| a | 7.674(2)Å |
| b | 10.772(3)Å |
| c | 13.579(4)Å |
| α | 102.847(5)° |
| β | 105.255(7)° |
| γ | 101.177(3)° |
| V | 1017.2(5)Å$^3$ |
| μ | 5.83 cm$^{-1}$ |
| crystal size, mm | 0.40 x 0.10 x 0.02 |
| $D_{calc}$ | 1.333 g/cm$^3$ |

| | |
|---|---|
| F(000) | 424 |
| Radiation: | Mo-$K_\alpha$ ($\lambda$=0.71073Å) |
| 2θ range | 5.6 – 54.94 ° |
| hkl collected: | -7≤ h ≤9; -13≤ k ≤12; -17≤ l ≤17 |
| No. reflections measured: | 10895 |
| No. unique reflections: | 4553 ($R_{int}$=0.0307) |
| No. observed reflections | 3578 (F>4σ) |
| No. reflections used in refinement | 4553 |
| No. parameters | 256 |
| R indices (F>4σ) | $R_1$=0.0542, $wR_2$=0.1410 |
| R indices (all data) | $R_1$=0.0698, $wR_2$=0.1572 |
| GOF: | 1.066 |
| Final Difference Peaks, e/Å$^3$ | +0.610, -0.664 |

Table IV-8. Refined Positional Parameters for **5n**, Compound 6140

| Atom | x | y | z | $U_{eq}$, Å$^2$ |
|---|---|---|---|---|
| Cr1 | 0.75239(6) | 0.76079(4) | 0.55069(3) | 0.0318(2) |
| C1 | 0.8015(4) | 0.6804(3) | 0.3961(2) | 0.0302(5) |
| C2 | 0.7814(4) | 0.5803(3) | 0.4491(2) | 0.0338(6) |
| H2 | 0.6919 | 0.4998 | 0.4137 | 0.045 |
| C3 | 0.8953(4) | 0.6024(3) | 0.5537(2) | 0.0377(6) |
| H3 | 0.8819 | 0.5365 | 0.5874 | 0.050 |
| C4 | 1.0303(4) | 0.7244(3) | 0.6082(2) | 0.0396(6) |
| H4 | 1.1067 | 0.7386 | 0.6775 | 0.053 |
| C5 | 1.0497(4) | 0.8236(3) | 0.5584(2) | 0.0383(6) |
| H5 | 1.1380 | 0.9044 | 0.5947 | 0.051 |
| C6 | 0.9343(4) | 0.8015(3) | 0.4521(2) | 0.0324(5) |
| H6 | 0.9473 | 0.8683 | 0.4193 | 0.043 |
| C7 | 0.6831(4) | 0.6472(2) | 0.2790(2) | 0.0303(5) |
| H7 | 0.5566 | 0.5980 | 0.2719 | 0.040 |
| C8 | 0.6644(4) | 0.7695(3) | 0.2419(2) | 0.0325(5) |
| C9 | 0.5197(4) | 0.8257(3) | 0.2538(2) | 0.0392(6) |
| H9 | 0.4364 | 0.7896 | 0.2853 | 0.052 |
| C10 | 0.4993(5) | 0.9355(3) | 0.2187(2) | 0.0468(7) |
| H10 | 0.4018 | 0.9718 | 0.2273 | 0.062 |
| C11 | 0.6194(5) | 0.9917(3) | 0.1717(2) | 0.0434(7) |
| C12 | 0.7659(5) | 0.9376(3) | 0.1619(2) | 0.0466(7) |
| H12 | 0.8504 | 0.9750 | 0.1316 | 0.062 |

| | | | | |
|---|---|---|---|---|
| C13 | 0.7882(4) | 0.8272(3) | 0.1970(2) | 0.0409(6) |
| H13 | 0.8877 | 0.7924 | 0.1901 | 0.054 |
| C14 | 0.5932(6) | 1.1099(3) | 0.1321(3) | 0.0598(10) |
| H14a | 0.6963 | 1.1410 | 0.1083 | 0.090 |
| H14b | 0.5885 | 1.1791 | 0.1889 | 0.090 |
| H14c | 0.4781 | 1.0845 | 0.0739 | 0.090 |
| C15 | 0.7605(4) | 0.5548(3) | 0.2092(2) | 0.0315(5) |
| C16 | 0.6398(4) | 0.4630(3) | 0.1152(2) | 0.0375(6) |
| H16 | 0.5119 | 0.4559 | 0.0963 | 0.050 |
| C17 | 0.7083(5) | 0.3811(3) | 0.0486(2) | 0.0432(7) |
| H17 | 0.6255 | 0.3213 | -0.0146 | 0.057 |
| C18 | 0.8979(5) | 0.3874(3) | 0.0751(2) | 0.0418(7) |
| C19 | 1.0180(4) | 0.4796(3) | 0.1689(2) | 0.0426(7) |
| H19 | 1.1456 | 0.4857 | 0.1881 | 0.057 |
| C20 | 0.9511(4) | 0.5635(3) | 0.2351(2) | 0.0370(6) |
| H20 | 1.0347 | 0.6257 | 0.2969 | 0.049 |
| C21 | 0.9721(6) | 0.2961(4) | 0.0044(3) | 0.0584(9) |
| H21a | 1.0393 | 0.2480 | 0.0452 | 0.088 |
| H21b | 1.0548 | 0.3474 | -0.0227 | 0.088 |
| H21c | 0.8692 | 0.2351 | -0.0539 | 0.088 |
| C22 | 0.4993(4) | 0.7120(3) | 0.4854(2) | 0.0411(6) |
| C23 | 0.7368(4) | 0.9326(3) | 0.5836(3) | 0.0470(7) |
| C24 | 0.7079(5) | 0.7440(4) | 0.6741(3) | 0.0584(9) |
| O1 | 0.3385(3) | 0.6809(3) | 0.4442(2) | 0.0651(7) |
| O2 | 0.7252(4) | 1.0398(2) | 0.6023(3) | 0.0737(8) |
| O3 | 0.6771(6) | 0.7290(4) | 0.7499(2) | 0.108(2) |

Ueq=1/3[U11(aa*)2+U22(bb*)2+U33(cc*)2+2U12aa*bb*cos□+2U13aa*cc*cos□+2U23bb*cc*cos□]

Table IV-9. Refined Thermal Parameters (U's) for **5n**, Compound 6140

| Atom | $U_{11}$ | $U_{22}$ | $U_{33}$ | $U_{23}$ | $U_{13}$ | $U_{12}$ |
|---|---|---|---|---|---|---|
| Cr1 | 0.0328(3) | 0.0344(3) | 0.0344(3) | 0.0149(2) | 0.0127(2) | 0.0145(2) |
| C1 | 0.0309(12) | 0.0329(13) | 0.0315(12) | 0.0132(10) | 0.0110(10) | 0.0135(10) |
| C2 | 0.0373(14) | 0.0309(13) | 0.0383(14) | 0.0143(10) | 0.0123(11) | 0.0155(11) |
| C3 | 0.046(2) | 0.041(2) | 0.0377(14) | 0.0196(11) | 0.0153(12) | 0.0253(13) |
| C4 | 0.0354(14) | 0.051(2) | 0.0337(14) | 0.0131(12) | 0.0046(11) | 0.0211(13) |
| C5 | 0.0298(13) | 0.043(2) | 0.0390(14) | 0.0076(11) | 0.0091(11) | 0.0092(11) |
| C6 | 0.0302(13) | 0.0351(14) | 0.0364(13) | 0.0144(10) | 0.0131(11) | 0.0112(11) |
| C7 | 0.0325(13) | 0.0285(12) | 0.0316(13) | 0.0105(10) | 0.0089(10) | 0.0118(10) |
| C8 | 0.0376(13) | 0.0360(14) | 0.0262(12) | 0.0117(10) | 0.0072(10) | 0.0162(11) |
| C9 | 0.044(2) | 0.045(2) | 0.0360(14) | 0.0163(12) | 0.0123(12) | 0.0228(13) |
| C10 | 0.058(2) | 0.049(2) | 0.041(2) | 0.0153(13) | 0.0121(14) | 0.034(2) |

| | | | | | | |
|---|---|---|---|---|---|---|
| C11 | 0.065(2) | 0.037(2) | 0.0298(13) | 0.0110(11) | 0.0073(13) | 0.0250(14) |
| C12 | 0.067(2) | 0.042(2) | 0.041(2) | 0.0218(12) | 0.021(2) | 0.018(2) |
| C13 | 0.051(2) | 0.044(2) | 0.041(2) | 0.0203(12) | 0.0203(13) | 0.0250(13) |
| C14 | 0.095(3) | 0.044(2) | 0.042(2) | 0.0190(14) | 0.011(2) | 0.030(2) |
| C15 | 0.0375(13) | 0.0293(13) | 0.0317(12) | 0.0155(10) | 0.0086(10) | 0.0138(10) |
| C16 | 0.043(2) | 0.0331(14) | 0.0332(13) | 0.0110(10) | 0.0030(11) | 0.0132(12) |
| C17 | 0.059(2) | 0.037(2) | 0.0328(14) | 0.0103(11) | 0.0091(13) | 0.0176(14) |
| C18 | 0.062(2) | 0.037(2) | 0.039(2) | 0.0189(12) | 0.0230(14) | 0.0238(14) |
| C19 | 0.046(2) | 0.052(2) | 0.043(2) | 0.0224(13) | 0.0193(13) | 0.0268(14) |
| C20 | 0.0389(14) | 0.040(2) | 0.0360(14) | 0.0136(11) | 0.0106(11) | 0.0175(12) |
| C21 | 0.085(3) | 0.055(2) | 0.054(2) | 0.019(2) | 0.037(2) | 0.038(2) |
| C22 | 0.042(2) | 0.038(2) | 0.050(2) | 0.0201(12) | 0.0180(13) | 0.0146(12) |
| C23 | 0.044(2) | 0.043(2) | 0.064(2) | 0.0170(14) | 0.031(2) | 0.0127(13) |
| C24 | 0.068(2) | 0.083(3) | 0.055(2) | 0.038(2) | 0.032(2) | 0.052(2) |
| O1 | 0.0294(12) | 0.067(2) | 0.097(2) | 0.0310(14) | 0.0126(12) | 0.0119(11) |
| O2 | 0.078(2) | 0.0347(13) | 0.132(2) | 0.0223(13) | 0.068(2) | 0.0223(12) |
| O3 | 0.156(3) | 0.179(4) | 0.082(2) | 0.092(2) | 0.085(2) | 0.123(3) |

The form of the anisotropic displacement parameter is:
$\exp[-2\pi^2(a^{*2}U_{11}h^2+b^{*2}U_{22}k^2+c^{*2}U_{33}l^2+ 2b^*c^*U_{23}kl+2a^*c^*U_{13}hl+2a^*b^*U_{12}hk)]$.

Table IV-10. Bond Distances in **5n**, Compound 6140, Å

| | | | | | |
|---|---|---|---|---|---|
| Cr1-C22 | 1.824(3) | Cr1-C24 | 1.835(3) | Cr1-C23 | 1.840(3) |
| Cr1-C3 | 2.202(3) | Cr1-C2 | 2.207(3) | Cr1-C4 | 2.213(3) |
| Cr1-C5 | 2.217(3) | Cr1-C6 | 2.223(3) | Cr1-C1 | 2.243(2) |
| C1-C6 | 1.398(4) | C1-C2 | 1.430(4) | C1-C7 | 1.530(3) |
| C2-C3 | 1.398(4) | C3-C4 | 1.409(4) | C4-C5 | 1.390(4) |
| C5-C6 | 1.420(4) | C7-C8 | 1.531(4) | C7-C15 | 1.533(3) |
| C8-C13 | 1.379(4) | C8-C9 | 1.392(4) | C9-C10 | 1.390(4) |
| C10-C11 | 1.375(5) | C11-C12 | 1.386(4) | C11-C14 | 1.516(4) |
| C12-C13 | 1.399(4) | C15-C16 | 1.389(4) | C15-C20 | 1.391(4) |
| C16-C17 | 1.395(4) | C17-C18 | 1.388(4) | C18-C19 | 1.386(4) |
| C18-C21 | 1.516(4) | C19-C20 | 1.396(4) | C22-O1 | 1.158(4) |
| C23-O2 | 1.151(4) | C24-O3 | 1.153(4) | | |

Table IV-11. Bond Angles in **5n**, Compound 6140, °

| | | | | | |
|---|---|---|---|---|---|
| C22-Cr1-C24 | 88.2(2) | C22-Cr1-C23 | 87.17(14) | C24-Cr1-C23 | 90.1(2) |
| C22-Cr1-C3 | 117.53(12) | C24-Cr1-C3 | 88.79(12) | C23-Cr1-C3 | 155.22(14) |
| C22-Cr1-C2 | 91.36(12) | C24-Cr1-C2 | 114.97(14) | C23-Cr1-C2 | 154.86(12) |
| C3-Cr1-C2 | 36.96(10) | C22-Cr1-C4 | 154.73(13) | C24-Cr1-C4 | 89.91(13) |

| | | | | | |
|---|---|---|---|---|---|
| C23-Cr1-C4 | 118.04(13) | C3-Cr1-C4 | 37.22(11) | C2-Cr1-C4 | 66.75(10) |
| C22-Cr1-C5 | 154.86(12) | C24-Cr1-C5 | 116.95(14) | C23-Cr1-C5 | 92.12(12) |
| C3-Cr1-C5 | 66.57(11) | C2-Cr1-C5 | 78.77(10) | C4-Cr1-C5 | 36.57(11) |
| C22-Cr1-C6 | 117.57(12) | C24-Cr1-C6 | 154.23(14) | C23-Cr1-C6 | 92.02(12) |
| C3-Cr1-C6 | 78.72(10) | C2-Cr1-C6 | 66.52(10) | C4-Cr1-C6 | 66.53(10) |
| C5-Cr1-C6 | 37.31(10) | C22-Cr1-C1 | 91.46(11) | C24-Cr1-C1 | 152.43(14) |
| C23-Cr1-C1 | 117.44(12) | C3-Cr1-C1 | 67.03(9) | C2-Cr1-C1 | 37.46(9) |
| C4-Cr1-C1 | 78.85(10) | C5-Cr1-C1 | 66.64(10) | C6-Cr1-C1 | 36.47(9) |
| C6-C1-C2 | 118.5(2) | C6-C1-C7 | 123.2(2) | C2-C1-C7 | 118.3(2) |
| C6-C1-Cr1 | 70.96(14) | C2-C1-Cr1 | 69.89(14) | C7-C1-Cr1 | 133.4(2) |
| C3-C2-C1 | 120.5(3) | C3-C2-Cr1 | 71.3(2) | C1-C2-Cr1 | 72.6(2) |
| C2-C3-C4 | 120.1(3) | C2-C3-Cr1 | 71.7(2) | C4-C3-Cr1 | 71.8(2) |
| C5-C4-C3 | 120.1(2) | C5-C4-Cr1 | 71.9(2) | C3-C4-Cr1 | 71.0(2) |
| C4-C5-C6 | 119.9(3) | C4-C5-Cr1 | 71.5(2) | C6-C5-Cr1 | 71.5(2) |
| C1-C6-C5 | 120.8(2) | C1-C6-Cr1 | 72.6(2) | C5-C6-Cr1 | 71.2(2) |
| C1-C7-C8 | 113.4(2) | C1-C7-C15 | 109.5(2) | C8-C7-C15 | 112.3(2) |
| C13-C8-C9 | 118.4(3) | C13-C8-C7 | 121.9(2) | C9-C8-C7 | 119.7(2) |
| C10-C9-C8 | 120.2(3) | C11-C10-C9 | 121.7(3) | C10-C11-C12 | 118.1(3) |
| C10-C11-C14 | 121.1(3) | C12-C11-C14 | 120.8(3) | C11-C12-C13 | 120.8(3) |
| C8-C13-C12 | 120.7(3) | C16-C15-C20 | 118.4(2) | C16-C15-C7 | 119.8(2) |
| C20-C15-C7 | 121.8(2) | C15-C16-C17 | 120.7(3) | C18-C17-C16 | 121.2(3) |
| C19-C18-C17 | 117.9(3) | C19-C18-C21 | 120.8(3) | C17-C18-C21 | 121.3(3) |
| C18-C19-C20 | 121.3(3) | C15-C20-C19 | 120.5(3) | O1-C22-Cr1 | 179.8(3) |
| O2-C23-Cr1 | 178.8(3) | O3-C24-Cr1 | 177.7(4) | | |

*X-ray Structure Determination of **17** – Compound 6147*

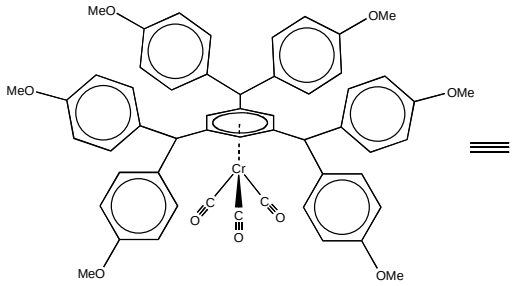


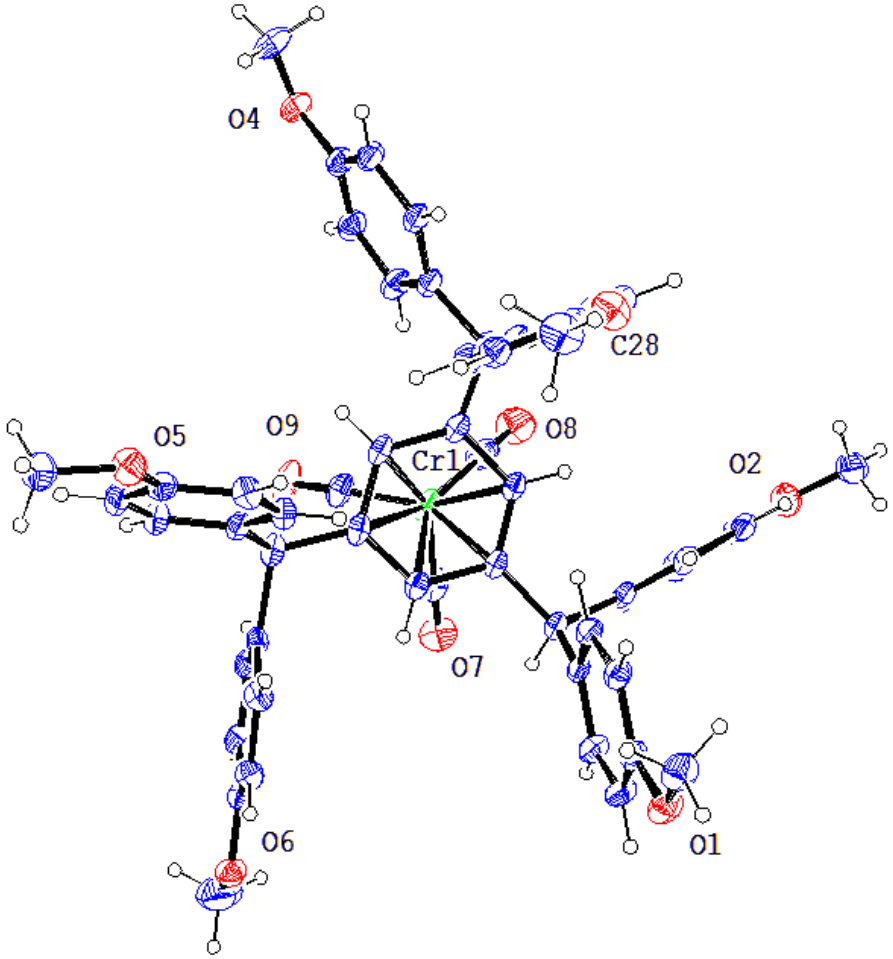


Figure IV-7: ORTEP of **17**, compound 6147. Thermal ellipsoids are at 30% probability.

Compound 6147 (**17**), $C_{54}H_{48}O_9Cr$, crystallizes in the triclinic space group $P\bar{1}$ with a=11.3010(5)Å, b=11.7896(4)Å, c=19.8964(14)Å, α=72.920(6)°, β=82.244(7)°, γ=63.018(5)°, V=2258.1(2)Å$^3$,

Z=2, and dcalc=1.313 g/cm$^3$. X-ray intensity data were collected on a Rigaku Mercury CCD area detector employing graphite-monochromated Mo-Kα radiation (λ=0.71073 Å) at a temperature of 143(1)K. Preliminary indexing was performed from a series of twelve 0.5° rotation images with exposures of 30 seconds. A total of 1120 rotation images were collected with a crystal to detector distance of 35 mm, a 2θ swing angle of -12°, rotation widths of 0.5° and exposures of 30 seconds: scan no. 1 was a ϕ-scan from 0° to 240° at ω = 10° and χ = 20°; scan no. 2 was an ω-scan from -20° to 20° at χ = -90° and ϕ = 0°; scan no. 3 was an ω-scan from -20° to 20° at χ = -90° and ϕ = 45°; scan no. 4 was an ω-scan from -20° to 20° at χ = -90° and ϕ = 90°; scan no. 5 was an ω-scan from -20° to 20° at χ = -90° and ϕ = 135°; scan no. 6 was an ω-scan from -20° to 20° at χ = -90° and ϕ = 180°; scan no. 7 was an ω-scan from -20° to 20° at χ = -90° and ϕ = 225°; scan no. 8 was an ω-scan from -20° to 20° at χ = -90° and ϕ = 270°; scan no. 9 was an ω-scan from -20° to 20° at χ = -90° and ϕ = 315°. Rotation images were processed using CrystalClear[1], producing a listing of unaveraged F$^2$ and σ(F$^2$) values which were then passed to the CrystalStructure[2] program package for further processing and structure solution on a Dell Pentium 4 computer. A total of 32470 reflections were measured over the ranges 2.51 ≤ θ ≤ 25.01°, -13 ≤ h ≤ 13, -14 ≤ k ≤ 14, -23 ≤ l ≤ 23 yielding 7932 unique reflections (Rint = 0.0284). The intensity data were corrected for Lorentz and polarization effects and for absorption using REQAB[3] (minimum and maximum transmission 0.8578, 1.0000).

The structure was solved by direct methods (SIR97[4]). The C45-C46-C47-C48-C49-C50-O5-C51 moiety is disordered by an opening of the C38-C37-C45 bond angle from 109.0(2)° to 123.4(4)° as shown in Figure IV-8:

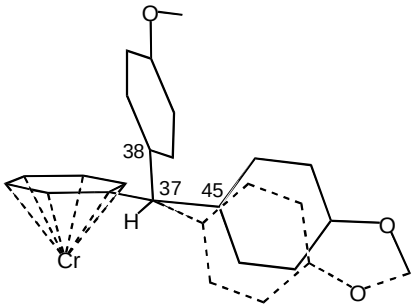


Figure IV-8: The disordered anisole group in **17** is pictured.

The occupancy factors were 0.70:0.30. In addition, the carbonyl ligand C54-O9 was disordered through two positions also with occupancy factors of 0.70:0.30. The minor disorder contribution increases the C52-Cr1-C54 angle from 82.9(2)° to 96.0(5)° and decreases the C53-Cr1-C54 angle

from 93.4(2)° to 77.9(5)°. These two different disordered moieties are, perhaps, related. Below are two space-filling models (Figure IV-9):

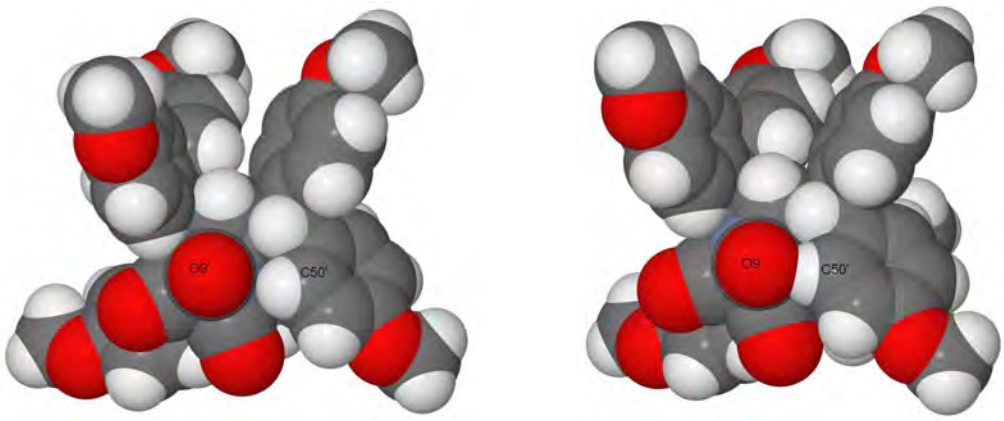


Figure IV-9: The disordered anisole and carbonyl, pictured in space-filling models.

The model on the left displays both minor disorder contributions (primed atoms). The one on the right displays the major disorder contribution for the carbonyl C54-O9 plus the minor contribution for the C45'-C46'-C47'-C48'-C49'-C50'-O6-C51' system. The space-filling model on the right shows a short contact between O9 and the H on C50' (2.1Å) while the H50'-O9' distance in the left molecule is a more reasonable 3.0 Å.

Refinement was by full-matrix least squares based on $F^2$ using SHELXL-97.[5] All reflections were used during refinement. The weighting scheme used was $w=1/[\sigma^2(F_o^2)+ 0.0808P^2 + 1.2532 P = (F_o^2 + 2F_c^2)/3$. Non-hydrogen atoms were refined anisotropically and hydrogen atoms were refined using a riding model. Refinement converged to R1=0.0532 and wR2=0.1427 for 6816 observed reflections for which $F > 4\sigma(F)$ and R1=0.0617 and wR2=0.1517 and GOF =1.048 for all 7932 unique, non-zero reflections and 640 variables.[a] The maximum $\Delta/\sigma$ in the final cycle of least squares was 0.012 and the two most prominent peaks in the final difference Fourier were +0.281 and -0.888 e/Å$^3$.

---

[a] $R1 = \Sigma||F_o| - |F_c|| / \Sigma |F_o|$

$wR2 = [\Sigma w(F_o^2 - F_c^2)^2/\Sigma w(F_o^2)^2]^{½}$

$GOF = [\Sigma w(F_o^2 - F_c^2)^2/(n - p)]^{½}$

where n = the number of reflections and p = the number of parameters refined.

Table IV-12 lists cell information, data collection parameters, and refinement data. Final positional and equivalent isotropic thermal parameters are given in Table IV-13 and Table IV-14. Anisotropic thermal parameters are in Table IV-15

Table IV-15. Table IV-16 and Table IV-17 list bond distances and bond angles. Figure IV-10 is an ORTEP[6] representation of the molecule with 30% probability thermal ellipsoids displayed.

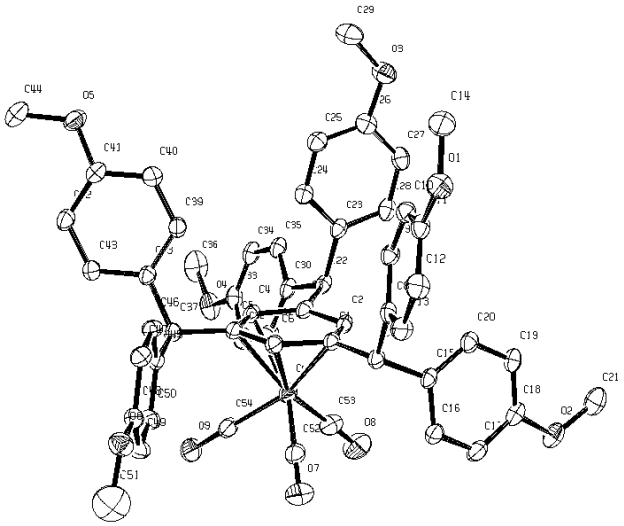


Figure IV-10: ORTEP drawing of the title compound **17** with 30% probability thermal ellipsoids.

Table IV-12: Summary of Structure Determination of **17**, Compound 6147

| | |
|---|---|
| Empirical formula | $C_{54}H_{48}O_9Cr$ |
| Formula weight | 892.92 |
| Temperature | 143(1) K |
| Wavelength | 0.71073 Å |
| Crystal system | triclinic |
| Space group | $P\bar{1}$ |
| Cell constants: | |
| a | 11.3010(5) Å |
| b | 11.7896(4) Å |
| c | 19.8964(14) Å |
| α | 72.920(6)° |
| β | 82.244(7)° |
| γ | 63.018(5)° |
| Volume | 2258.1(2) $Å^3$ |

| | |
|---|---|
| Z | 2 |
| Density (calculated) | 1.313 $Mg/m^3$ |
| Absorption coefficient | 0.312 $mm^{-1}$ |
| F(000) | 936 |
| Crystal size | 0.38 x 0.25 x 0.06 $mm^3$ |
| Theta range for data collection | 2.51 to 25.01° |
| Index ranges | $-13 \le h \le 13$, $-14 \le k \le 14$, $-23 \le l \le 23$ |
| Reflections collected | 32470 |
| Independent reflections | 7932 [R(int) = 0.0284] |
| Completeness to theta = 25.01° | 99.6 % |
| Absorption correction | Semi-empirical from equivalents |
| Max. and min. transmission | 1.0000 and 0.8578 |
| Refinement method | Full-matrix least-squares on $F^2$ |
| Data / restraints / parameters | 7932 / 90 / 640 |
| Goodness-of-fit on $F^2$ | 1.048 |
| Final R indices [I>2sigma(I)] | R1 = 0.0532, wR2 = 0.1427 |
| R indices (all data) | R1 = 0.0617, wR2 = 0.1517 |
| Largest diff. peak and hole | 0.281 and -0.888 $e/Å^{-3}$ |

Table IV-13: Refined Positional Parameters for **17**, Compound 6147

| Atom | x | y | z | $U_{eq}$,$Å^2$ |
|---|---|---|---|---|
| Cr1 | 0.22008(4) | 0.47296(4) | 0.28570(2) | 0.04252(15) |
| C1 | 0.3067(2) | 0.2646(2) | 0.28048(12) | 0.0339(5) |
| C2 | 0.3336(2) | 0.3394(2) | 0.21734(13) | 0.0345(5) |
| C3 | 0.4006(2) | 0.4180(2) | 0.21489(13) | 0.0360(5) |
| C4 | 0.4348(2) | 0.4238(2) | 0.27784(13) | 0.0376(5) |
| C5 | 0.4107(2) | 0.3478(2) | 0.34388(13) | 0.0369(5) |
| C6 | 0.3471(2) | 0.2696(2) | 0.34424(13) | 0.0362(5) |
| C7 | 0.2350(2) | 0.1804(2) | 0.28352(12) | 0.0347(5) |
| C8 | 0.3303(2) | 0.0337(2) | 0.29649(12) | 0.0337(5) |
| C9 | 0.4543(2) | -0.0125(2) | 0.26522(12) | 0.0371(5) |
| C10 | 0.5336(2) | -0.1476(2) | 0.27444(13) | 0.0393(5) |
| C11 | 0.4888(2) | -0.2363(2) | 0.31597(13) | 0.0409(6) |
| C12 | 0.3670(3) | -0.1921(3) | 0.34894(15) | 0.0481(6) |
| C13 | 0.2885(2) | -0.0583(2) | 0.33908(14) | 0.0439(6) |
| O1 | 0.55685(18) | -0.37192(16) | 0.32781(10) | 0.0525(5) |
| C14 | 0.6841(3) | -0.4232(3) | 0.29643(17) | 0.0570(7) |
| C15 | 0.1466(2) | 0.2327(2) | 0.21924(12) | 0.0351(5) |

| | | | | |
|---|---|---|---|---|
| C16 | 0.0150(2) | 0.3254(3) | 0.22107(14) | 0.0435(6) |
| C17 | -0.0650(2) | 0.3838(3) | 0.16226(15) | 0.0496(6) |
| C18 | -0.0155(2) | 0.3494(3) | 0.09979(14) | 0.0458(6) |
| C19 | 0.1136(2) | 0.2546(2) | 0.09716(14) | 0.0440(6) |
| C20 | 0.1936(2) | 0.1971(2) | 0.15719(13) | 0.0394(5) |
| O2 | -0.10289(19) | 0.4150(2) | 0.04456(10) | 0.0590(5) |
| C21 | -0.0611(3) | 0.3759(3) | -0.01909(16) | 0.0657(8) |
| C22 | 0.4449(2) | 0.4763(2) | 0.14303(13) | 0.0385(5) |
| C23 | 0.5663(2) | 0.3636(2) | 0.12206(13) | 0.0375(5) |
| C24 | 0.6762(2) | 0.2863(2) | 0.16597(13) | 0.0422(6) |
| C25 | 0.7873(2) | 0.1847(2) | 0.14726(14) | 0.0440(6) |
| C26 | 0.7908(3) | 0.1601(2) | 0.08313(14) | 0.0446(6) |
| C27 | 0.6820(3) | 0.2366(3) | 0.03844(14) | 0.0469(6) |
| C28 | 0.5713(3) | 0.3358(2) | 0.05831(13) | 0.0438(6) |
| O3 | 0.8950(2) | 0.06334(19) | 0.05864(11) | 0.0596(5) |
| C29 | 1.0084(3) | -0.0196(3) | 0.10333(17) | 0.0657(8) |
| C30 | 0.4665(2) | 0.5980(2) | 0.13572(13) | 0.0394(5) |
| C31 | 0.3676(3) | 0.7079(2) | 0.15639(15) | 0.0471(6) |
| C32 | 0.3816(3) | 0.8223(3) | 0.14432(15) | 0.0491(6) |
| C33 | 0.4938(3) | 0.8318(3) | 0.11104(14) | 0.0489(6) |
| C34 | 0.5929(3) | 0.7255(3) | 0.09056(14) | 0.0485(6) |
| C35 | 0.5787(2) | 0.6090(2) | 0.10318(13) | 0.0417(6) |
| O4 | 0.4963(2) | 0.95084(19) | 0.10084(11) | 0.0643(6) |
| C36 | 0.6173(4) | 0.9583(4) | 0.0757(2) | 0.0890(12) |
| C37 | 0.4561(2) | 0.3551(3) | 0.41088(14) | 0.0423(6) |
| C38 | 0.6070(2) | 0.2981(2) | 0.41344(12) | 0.0354(5) |
| C39 | 0.6917(2) | 0.2111(2) | 0.37475(13) | 0.0400(5) |
| C40 | 0.8281(2) | 0.1592(3) | 0.38072(13) | 0.0442(6) |
| C41 | 0.8833(2) | 0.1909(2) | 0.42644(13) | 0.0407(6) |
| C42 | 0.8009(2) | 0.2777(3) | 0.46492(14) | 0.0448(6) |
| C43 | 0.6642(2) | 0.3308(3) | 0.45767(14) | 0.0432(6) |
| O5 | 1.01942(16) | 0.1314(2) | 0.42968(10) | 0.0541(5) |
| C44 | 1.0794(3) | 0.1456(3) | 0.48296(16) | 0.0604(8) |
| C45 | 0.4046(3) | 0.2791(2) | 0.48139(14) | 0.0316(11) |
| C46 | 0.4775(2) | 0.1450(2) | 0.51281(16) | 0.0381(10) |
| C47 | 0.4259(2) | 0.0811(2) | 0.57084(13) | 0.0396(8) |
| C48 | 0.3014(2) | 0.1514(3) | 0.59744(12) | 0.0373(7) |
| C49 | 0.2284(2) | 0.2855(3) | 0.56601(15) | 0.0440(13) |
| C50 | 0.2800(2) | 0.3493(2) | 0.50798(15) | 0.0407(8) |
| O6 | 0.2609(3) | 0.0792(3) | 0.65550(14) | 0.0484(6) |
| C45' | 0.3826(6) | 0.3302(7) | 0.4657(3) | 0.035(2) |
| C46' | 0.4359(5) | 0.2021(6) | 0.5095(3) | 0.032(2) |

| | | | | |
|---|---|---|---|---|
| C47' | 0.3631(7) | 0.1659(7) | 0.5670(3) | 0.053(2) |
| C48' | 0.2370(7) | 0.2578(9) | 0.5807(3) | 0.050(3) |
| C49' | 0.1836(5) | 0.3858(8) | 0.5368(4) | 0.066(3) |
| C50' | 0.2564(7) | 0.4220(6) | 0.4793(4) | 0.053(2) |
| O6' | 0.1531(8) | 0.2426(8) | 0.6347(4) | 0.078(2) |
| C51 | 0.1482(5) | 0.1391(5) | 0.6849(3) | 0.1000(13) |
| C52 | 0.0789(3) | 0.4580(3) | 0.33658(15) | 0.0486(6) |
| O7 | -0.0103(2) | 0.4474(2) | 0.37004(12) | 0.0668(6) |
| C53 | 0.1023(3) | 0.5918(3) | 0.21510(17) | 0.0529(7) |
| O8 | 0.0239(2) | 0.6669(2) | 0.17237(13) | 0.0764(7) |
| C54 | 0.1857(6) | 0.5979(6) | 0.3335(3) | 0.0478(14) |
| O9 | 0.1626(4) | 0.6755(4) | 0.3645(3) | 0.0716(11) |
| C54' | 0.1881(17) | 0.6297(16) | 0.2999(8) | 0.054(4) |
| O9' | 0.1651(10) | 0.7265(9) | 0.3144(7) | 0.086(3) |

$U_{eq}=1/3[U_{11}(aa^*)^2+U_{22}(bb^*)^2+U_{33}(cc^*)^2+2U_{12}aa^*bb^*\cos\gamma+2U_{13}aa^*cc^*\cos\beta+2U_{23}bb^*cc^*\cos\alpha]$

Table IV-14: Positional Parameters for Hydrogens in **17**, Compound 6147

| Atom | x | y | z | $U_{iso}$,Å$^2$ |
|---|---|---|---|---|
| H2 | 0.3071 | 0.3381 | 0.1754 | 0.046 |
| H4 | 0.4742 | 0.4784 | 0.2770 | 0.050 |
| H6 | 0.3306 | 0.2198 | 0.3870 | 0.048 |
| H7 | 0.1756 | 0.1893 | 0.3244 | 0.046 |
| H9 | 0.4852 | 0.0473 | 0.2377 | 0.049 |
| H10 | 0.6162 | -0.1774 | 0.2527 | 0.052 |
| H12 | 0.3377 | -0.2523 | 0.3778 | 0.064 |
| H13 | 0.2064 | -0.0292 | 0.3613 | 0.058 |
| H14a | 0.6761 | -0.3891 | 0.2463 | 0.086 |
| H14b | 0.7210 | -0.5177 | 0.3085 | 0.086 |
| H14c | 0.7415 | -0.3974 | 0.3133 | 0.086 |
| H16 | -0.0197 | 0.3485 | 0.2628 | 0.058 |
| H17 | -0.1522 | 0.4463 | 0.1645 | 0.066 |
| H19 | 0.1470 | 0.2292 | 0.0559 | 0.058 |
| H20 | 0.2803 | 0.1335 | 0.1552 | 0.052 |
| H21a | 0.0165 | 0.3889 | -0.0367 | 0.099 |
| H21b | -0.1309 | 0.4281 | -0.0532 | 0.099 |
| H21c | -0.0406 | 0.2844 | -0.0103 | 0.099 |
| H22 | 0.3740 | 0.5034 | 0.1101 | 0.051 |
| H24 | 0.6751 | 0.3033 | 0.2089 | 0.056 |
| H25 | 0.8591 | 0.1332 | 0.1778 | 0.059 |
| H27 | 0.6840 | 0.2208 | -0.0049 | 0.062 |
| H28 | 0.4985 | 0.3852 | 0.0284 | 0.058 |

| | | | | |
|---|---|---|---|---|
| H29a | 1.0426 | 0.0337 | 0.1146 | 0.099 |
| H29b | 1.0756 | -0.0803 | 0.0795 | 0.099 |
| H29c | 0.9831 | -0.0679 | 0.1458 | 0.099 |
| H31 | 0.2914 | 0.7033 | 0.1786 | 0.063 |
| H32 | 0.3151 | 0.8939 | 0.1586 | 0.065 |
| H34 | 0.6688 | 0.7310 | 0.0685 | 0.065 |
| H35 | 0.6462 | 0.5373 | 0.0894 | 0.055 |
| H36a | 0.6886 | 0.8908 | 0.1065 | 0.134 |
| H36b | 0.6098 | 1.0433 | 0.0745 | 0.134 |
| H36c | 0.6352 | 0.9458 | 0.0292 | 0.134 |
| H37 | 0.4189 | 0.4482 | 0.4106 | 0.056 |
| H37' | 0.4283 | 0.4498 | 0.4025 | 0.056 |
| H39 | 0.6563 | 0.1875 | 0.3445 | 0.053 |
| H40 | 0.8832 | 0.1025 | 0.3538 | 0.059 |
| H42 | 0.8366 | 0.3004 | 0.4955 | 0.060 |
| H43 | 0.6094 | 0.3902 | 0.4833 | 0.057 |
| H44a | 1.0661 | 0.2353 | 0.4728 | 0.091 |
| H44b | 1.1728 | 0.0882 | 0.4846 | 0.091 |
| H44c | 1.0399 | 0.1227 | 0.5276 | 0.091 |
| H46 | 0.5606 | 0.0981 | 0.4951 | 0.051 |
| H47 | 0.4746 | -0.0083 | 0.5918 | 0.053 |
| H49 | 0.1454 | 0.3323 | 0.5837 | 0.058 |
| H50 | 0.2314 | 0.4387 | 0.4870 | 0.054 |
| H46' | 0.5200 | 0.1409 | 0.5004 | 0.043 |
| H47' | 0.3987 | 0.0806 | 0.5963 | 0.071 |
| H49' | 0.0995 | 0.4470 | 0.5459 | 0.088 |
| H50' | 0.2208 | 0.5074 | 0.4501 | 0.071 |
| H51a | 0.1334 | 0.0769 | 0.7245 | 0.150 |
| H51b | 0.0778 | 0.1766 | 0.6515 | 0.150 |
| H51c | 0.1503 | 0.2079 | 0.7005 | 0.150 |
| H51a' | 0.0713 | 0.1698 | 0.7139 | 0.150 |
| H51b' | 0.2267 | 0.0951 | 0.7134 | 0.150 |
| H51c' | 0.1432 | 0.0787 | 0.6632 | 0.150 |

Table IV-15: Refined Thermal Parameters (U's) for **17**, Compound 6147

| Atom | $U_{11}$ | $U_{22}$ | $U_{33}$ | $U_{23}$ | $U_{13}$ | $U_{12}$ |
|---|---|---|---|---|---|---|
| Cr1 | 0.0338(2) | 0.0332(2) | 0.0653(3) | -0.01982(19) | -0.00877(18) | -0.01221(17) |
| C1 | 0.0295(10) | 0.0285(11) | 0.0458(13) | -0.0135(10) | -0.0066(9) | -0.0104(9) |
| C2 | 0.0318(11) | 0.0294(11) | 0.0450(13) | -0.0107(10) | -0.0097(9) | -0.0125(9) |
| C3 | 0.0310(11) | 0.0268(11) | 0.0510(14) | -0.0095(10) | -0.0101(9) | -0.0110(9) |

| | | | | | | |
|---|---|---|---|---|---|---|
| C4 | 0.0322(11) | 0.0308(11) | 0.0560(15) | -0.0166(11) | -0.0089(10) | -0.0134(9) |
| C5 | 0.0294(11) | 0.0357(12) | 0.0491(14) | -0.0191(10) | -0.0055(9) | -0.0110(9) |
| C6 | 0.0328(11) | 0.0329(11) | 0.0443(13) | -0.0142(10) | -0.0041(9) | -0.0120(9) |
| C7 | 0.0351(11) | 0.0323(11) | 0.0423(13) | -0.0127(10) | -0.0037(9) | -0.0166(9) |
| C8 | 0.0392(12) | 0.0307(11) | 0.0374(12) | -0.0103(9) | -0.0064(9) | -0.0180(10) |
| C9 | 0.0383(12) | 0.0331(12) | 0.0412(13) | -0.0070(10) | -0.0058(9) | -0.0171(10) |
| C10 | 0.0386(12) | 0.0349(12) | 0.0450(13) | -0.0119(10) | -0.0051(10) | -0.0142(10) |
| C11 | 0.0494(14) | 0.0294(11) | 0.0458(14) | -0.0081(10) | -0.0131(10) | -0.0167(10) |
| C12 | 0.0576(15) | 0.0381(13) | 0.0555(16) | -0.0090(12) | 0.0001(12) | -0.0289(12) |
| C13 | 0.0458(13) | 0.0394(13) | 0.0524(15) | -0.0137(11) | 0.0027(11) | -0.0234(11) |
| O1 | 0.0579(11) | 0.0291(9) | 0.0671(12) | -0.0091(8) | -0.0066(9) | -0.0165(8) |
| C14 | 0.0559(16) | 0.0345(13) | 0.0717(19) | -0.0124(13) | -0.0107(14) | -0.0103(12) |
| C15 | 0.0364(11) | 0.0318(11) | 0.0445(13) | -0.0092(10) | -0.0065(9) | -0.0200(10) |
| C16 | 0.0370(12) | 0.0470(14) | 0.0538(15) | -0.0179(12) | -0.0035(10) | -0.0208(11) |
| C17 | 0.0342(12) | 0.0518(15) | 0.0635(17) | -0.0142(13) | -0.0100(11) | -0.0172(11) |
| C18 | 0.0431(13) | 0.0472(14) | 0.0523(15) | -0.0039(12) | -0.0143(11) | -0.0259(12) |
| C19 | 0.0518(14) | 0.0441(14) | 0.0466(14) | -0.0103(11) | -0.0071(11) | -0.0290(12) |
| C20 | 0.0406(12) | 0.0339(12) | 0.0484(14) | -0.0103(10) | -0.0076(10) | -0.0186(10) |
| O2 | 0.0521(11) | 0.0691(13) | 0.0545(12) | -0.0036(10) | -0.0210(9) | -0.0275(10) |
| C21 | 0.0713(19) | 0.078(2) | 0.0526(18) | -0.0013(15) | -0.0188(14) | -0.0418(17) |
| C22 | 0.0373(12) | 0.0328(12) | 0.0487(14) | -0.0057(10) | -0.0132(10) | -0.0177(10) |
| C23 | 0.0396(12) | 0.0307(11) | 0.0464(14) | -0.0059(10) | -0.0090(10) | -0.0191(10) |
| C24 | 0.0443(13) | 0.0400(13) | 0.0436(14) | -0.0092(11) | -0.0064(10) | -0.0191(11) |
| C25 | 0.0428(13) | 0.0380(13) | 0.0480(15) | -0.0059(11) | -0.0060(10) | -0.0165(11) |
| C26 | 0.0516(14) | 0.0332(12) | 0.0503(15) | -0.0087(11) | 0.0032(11) | -0.0219(11) |
| C27 | 0.0627(16) | 0.0409(13) | 0.0444(14) | -0.0118(11) | -0.0027(12) | -0.0277(12) |
| C28 | 0.0547(14) | 0.0356(12) | 0.0452(14) | -0.0025(10) | -0.0138(11) | -0.0243(11) |
| O3 | 0.0613(12) | 0.0501(11) | 0.0567(12) | -0.0185(9) | 0.0040(9) | -0.0137(9) |
| C29 | 0.0608(18) | 0.0498(16) | 0.068(2) | -0.0168(15) | 0.0058(15) | -0.0097(14) |
| C30 | 0.0444(13) | 0.0307(11) | 0.0466(14) | -0.0030(10) | -0.0165(10) | -0.0192(10) |
| C31 | 0.0459(14) | 0.0362(13) | 0.0605(16) | -0.0098(12) | -0.0091(11) | -0.0184(11) |
| C32 | 0.0600(16) | 0.0349(13) | 0.0557(16) | -0.0090(11) | -0.0088(12) | -0.0227(12) |
| C33 | 0.0723(18) | 0.0373(13) | 0.0467(15) | -0.0043(11) | -0.0147(12) | -0.0323(13) |
| C34 | 0.0580(15) | 0.0492(15) | 0.0487(15) | -0.0039(12) | -0.0123(12) | -0.0344(13) |
| C35 | 0.0454(13) | 0.0357(12) | 0.0482(14) | -0.0058(10) | -0.0127(10) | -0.0210(11) |
| O4 | 0.1042(16) | 0.0481(11) | 0.0628(13) | -0.0112(9) | -0.0015(11) | -0.0537(12) |
| C36 | 0.135(3) | 0.082(3) | 0.093(3) | -0.015(2) | 0.003(2) | -0.089(3) |
| C37 | 0.0346(12) | 0.0460(14) | 0.0545(15) | -0.0270(12) | -0.0026(10) | -0.0157(11) |
| C38 | 0.0363(12) | 0.0350(12) | 0.0396(12) | -0.0106(10) | -0.0043(9) | -0.0180(10) |
| C39 | 0.0418(13) | 0.0394(13) | 0.0413(13) | -0.0145(10) | -0.0068(10) | -0.0156(10) |
| C40 | 0.0404(13) | 0.0442(14) | 0.0437(14) | -0.0133(11) | -0.0021(10) | -0.0133(11) |
| C41 | 0.0351(12) | 0.0429(13) | 0.0427(13) | -0.0033(11) | -0.0061(10) | -0.0191(10) |

| | | | | | | |
|---|---|---|---|---|---|---|
| C42 | 0.0430(13) | 0.0516(15) | 0.0499(15) | -0.0157(12) | -0.0079(11) | -0.0256(12) |
| C43 | 0.0406(13) | 0.0452(13) | 0.0501(14) | -0.0220(11) | -0.0031(10) | -0.0177(11) |
| O5 | 0.0344(9) | 0.0664(12) | 0.0574(11) | -0.0137(9) | -0.0060(8) | -0.0186(9) |
| C44 | 0.0457(15) | 0.072(2) | 0.0624(18) | -0.0053(15) | -0.0155(13) | -0.0280(14) |
| C45 | 0.0296(19) | 0.032(3) | 0.032(2) | -0.010(2) | -0.0090(18) | -0.009(2) |
| C46 | 0.028(2) | 0.037(2) | 0.041(2) | -0.0112(19) | -0.0018(16) | -0.0062(18) |
| C47 | 0.0343(18) | 0.0391(19) | 0.0406(19) | -0.0088(16) | -0.0043(14) | -0.0118(15) |
| C48 | 0.0370(18) | 0.0399(19) | 0.041(2) | -0.0173(16) | 0.0016(15) | -0.0183(16) |
| C49 | 0.038(2) | 0.037(2) | 0.056(3) | -0.023(2) | 0.0065(19) | -0.0113(19) |
| C50 | 0.041(2) | 0.037(2) | 0.048(2) | -0.0199(17) | 0.0038(17) | -0.0151(17) |
| O6 | 0.0519(15) | 0.0502(15) | 0.0486(15) | -0.0168(12) | 0.0099(11) | -0.0273(12) |
| C45' | 0.042(5) | 0.035(6) | 0.030(5) | -0.011(4) | -0.016(4) | -0.012(4) |
| C46' | 0.026(5) | 0.041(6) | 0.026(5) | -0.014(4) | 0.000(4) | -0.010(5) |
| C47' | 0.060(5) | 0.072(6) | 0.039(5) | -0.009(5) | -0.007(4) | -0.040(5) |
| C48' | 0.054(6) | 0.083(8) | 0.033(5) | -0.024(5) | 0.015(4) | -0.046(6) |
| C49' | 0.068(6) | 0.071(6) | 0.060(6) | -0.035(5) | 0.015(5) | -0.025(5) |
| C50' | 0.056(5) | 0.046(5) | 0.049(5) | -0.015(4) | 0.000(4) | -0.014(4) |
| O6' | 0.081(5) | 0.079(5) | 0.066(5) | -0.017(4) | 0.021(4) | -0.036(4) |
| C51 | 0.111(3) | 0.100(3) | 0.100(3) | -0.013(3) | 0.016(3) | -0.067(3) |
| C52 | 0.0392(14) | 0.0416(14) | 0.0625(17) | -0.0198(12) | -0.0100(12) | -0.0092(11) |
| O7 | 0.0482(11) | 0.0631(13) | 0.0796(15) | -0.0163(11) | 0.0047(10) | -0.0192(10) |
| C53 | 0.0444(14) | 0.0384(14) | 0.0743(19) | -0.0117(13) | -0.0029(13) | -0.0180(12) |
| O8 | 0.0653(13) | 0.0530(12) | 0.0862(16) | 0.0051(12) | -0.0241(12) | -0.0128(11) |
| C54 | 0.036(2) | 0.042(3) | 0.069(4) | -0.021(3) | -0.010(3) | -0.013(2) |
| O9 | 0.0586(19) | 0.064(2) | 0.114(3) | -0.059(3) | -0.004(2) | -0.0223(18) |
| C54' | 0.055(6) | 0.048(9) | 0.063(9) | -0.022(7) | -0.010(8) | -0.020(6) |
| O9' | 0.083(6) | 0.054(6) | 0.131(9) | -0.052(6) | -0.002(7) | -0.021(5) |

The form of the anisotropic displacement parameter is:
$\exp[-2\pi^2(a^{*2}U_{11}h^2+b^{*2}U_{22}k^2+c^{*2}U_{33}l^2+2b^*c^*U_{23}kl+2a^*c^*U_{13}hl+2a^*b^*U_{12}hk)]$

Table IV-16: Bond Distances in **17**, Compound 6147, Å

| | | | | | |
|---|---|---|---|---|---|
| Cr1-C54' | 1.816(18) | Cr1-C52 | 1.821(3) | Cr1-C53 | 1.834(3) |
| Cr1-C54 | 1.851(7) | Cr1-C6 | 2.203(2) | Cr1-C4 | 2.218(2) |
| Cr1-C2 | 2.220(2) | Cr1-C5 | 2.224(2) | Cr1-C1 | 2.224(2) |
| Cr1-C3 | 2.265(2) | C1-C2 | 1.392(3) | C1-C6 | 1.430(3) |
| C1-C7 | 1.525(3) | C2-C3 | 1.426(3) | C3-C4 | 1.388(3) |
| C3-C22 | 1.519(3) | C4-C5 | 1.427(4) | C5-C6 | 1.401(3) |
| C5-C37 | 1.529(3) | C7-C15 | 1.529(3) | C7-C8 | 1.531(3) |
| C8-C9 | 1.385(3) | C8-C13 | 1.390(3) | C9-C10 | 1.397(3) |
| C10-C11 | 1.376(4) | C11-C12 | 1.380(4) | C11-O1 | 1.384(3) |
| C12-C13 | 1.382(4) | O1-C14 | 1.419(3) | C15-C20 | 1.381(3) |

| | | | | | |
|---|---|---|---|---|---|
| C15-C16 | 1.393(3) | C16-C17 | 1.381(4) | C17-C18 | 1.387(4) |
| C18-02 | 1.372(3) | C18-C19 | 1.383(4) | C19-C20 | 1.401(3) |
| 02-C21 | 1.422(4) | C22-C30 | 1.524(3) | C22-C23 | 1.530(3) |
| C23-C28 | 1.388(4) | C23-C24 | 1.391(3) | C24-C25 | 1.386(3) |
| C25-C26 | 1.381(4) | C26-03 | 1.370(3) | C26-C27 | 1.390(4) |
| C27-C28 | 1.378(4) | 03-C29 | 1.432(4) | C30-C35 | 1.387(4) |
| C30-C31 | 1.404(4) | C31-C32 | 1.377(4) | C32-C33 | 1.385(4) |
| C33-04 | 1.371(3) | C33-C34 | 1.376(4) | C34-C35 | 1.401(4) |
| 04-C36 | 1.424(4) | C37-C45' | 1.324(5) | C37-C38 | 1.525(3) |
| C37-C45 | 1.620(3) | C38-C43 | 1.386(3) | C38-C39 | 1.391(3) |
| C39-C40 | 1.383(3) | C40-C41 | 1.386(4) | C41-05 | 1.373(3) |
| C41-C42 | 1.380(4) | C42-C43 | 1.388(3) | 05-C44 | 1.419(3) |
| C45-C46 | 1.3950 | C45-C50 | 1.3950 | C46-C47 | 1.3950 |
| C47-C48 | 1.3950 | C48-06 | 1.378(3) | C48-C49 | 1.3950 |
| C49-C50 | 1.3950 | 06-C51 | 1.299(5) | C45'-C50' | 1.3950 |
| C45'-C46' | 1.3950 | C46'-C47' | 1.3949 | C47'-C48' | 1.3950 |
| C48'-06' | 1.361(9) | C48'-C49' | 1.3950 | C49'-C50' | 1.3950 |
| 06'-C51 | 1.348(9) | C52-07 | 1.166(3) | C53-08 | 1.158(3) |
| C54-09 | 1.166(7) | C54'-09' | 1.165(18) | | |

Table IV-17: Bond Angles in **17**, Compound 6147, °

| | | | | | |
|---|---|---|---|---|---|
| C54'-Cr1-C52 | 96.0(5) | C54'-Cr1-C53 | 77.9(5) | C52-Cr1-C53 | 87.32(12) |
| C54'-Cr1-C54 | 20.9(4) | C52-Cr1-C54 | 82.9(2) | C53-Cr1-C54 | 93.4(2) |
| C54'-Cr1-C6 | 130.4(5) | C52-Cr1-C6 | 88.49(10) | C53-Cr1-C6 | 151.72(11) |
| C54-Cr1-C6 | 113.75(19) | C54'-Cr1-C4 | 88.5(5) | C52-Cr1-C4 | 150.05(11) |
| C53-Cr1-C4 | 122.50(11) | C54-Cr1-C4 | 91.8(2) | C6-Cr1-C4 | 66.66(9) |
| C54'-Cr1-C2 | 142.0(5) | C52-Cr1-C2 | 120.28(10) | C53-Cr1-C2 | 92.06(11) |
| C54-Cr1-C2 | 156.4(2) | C6-Cr1-C2 | 66.26(8) | C4-Cr1-C2 | 66.05(8) |
| C54'-Cr1-C5 | 98.5(5) | C52-Cr1-C5 | 112.70(11) | C53-Cr1-C5 | 159.98(11) |
| C54-Cr1-C5 | 88.70(19) | C6-Cr1-C5 | 36.90(9) | C4-Cr1-C5 | 37.48(9) |
| C2-Cr1-C5 | 78.61(8) | C54'-Cr1-C1 | 165.9(5) | C52-Cr1-C1 | 91.44(10) |
| C53-Cr1-C1 | 114.47(11) | C54-Cr1-C1 | 151.28(19) | C6-Cr1-C1 | 37.70(8) |
| C4-Cr1-C1 | 79.14(8) | C2-Cr1-C1 | 36.52(9) | C5-Cr1-C1 | 67.52(8) |
| C54'-Cr1-C3 | 106.8(5) | C52-Cr1-C3 | 157.11(10) | C53-Cr1-C3 | 95.56(11) |
| C54-Cr1-C3 | 119.5(2) | C6-Cr1-C3 | 78.23(8) | C4-Cr1-C3 | 36.05(8) |
| C2-Cr1-C3 | 37.07(8) | C5-Cr1-C3 | 66.33(8) | C1-Cr1-C3 | 66.66(8) |
| C2-C1-C6 | 117.8(2) | C2-C1-C7 | 122.4(2) | C6-C1-C7 | 119.8(2) |
| C2-C1-Cr1 | 71.61(13) | C6-C1-Cr1 | 70.36(12) | C7-C1-Cr1 | 128.40(14) |
| C1-C2-C3 | 122.1(2) | C1-C2-Cr1 | 71.88(13) | C3-C2-Cr1 | 73.16(13) |
| C4-C3-C2 | 118.5(2) | C4-C3-C22 | 124.0(2) | C2-C3-C22 | 117.0(2) |

| | | | | | |
|---|---|---|---|---|---|
| C4-C3-Cr1 | 70.15(13) | C2-C3-Cr1 | 69.77(13) | C22-C3-Cr1 | 138.49(15) |
| C3-C4-C5 | 121.5(2) | C3-C4-Cr1 | 73.79(13) | C5-C4-Cr1 | 71.46(13) |
| C6-C5-C4 | 118.4(2) | C6-C5-C37 | 123.1(2) | C4-C5-C37 | 118.5(2) |
| C6-C5-Cr1 | 70.74(13) | C4-C5-Cr1 | 71.06(12) | C37-C5-Cr1 | 129.87(15) |
| C5-C6-C1 | 121.6(2) | C5-C6-Cr1 | 72.36(13) | C1-C6-Cr1 | 71.94(13) |
| C1-C7-C15 | 111.64(19) | C1-C7-C8 | 112.27(17) | C15-C7-C8 | 112.90(18) |
| C9-C8-C13 | 118.2(2) | C9-C8-C7 | 123.1(2) | C13-C8-C7 | 118.6(2) |
| C8-C9-C10 | 121.0(2) | C11-C10-C9 | 119.6(2) | C10-C11-C12 | 120.2(2) |
| C10-C11-O1 | 124.9(2) | C12-C11-O1 | 114.9(2) | C11-C12-C13 | 119.9(2) |
| C12-C13-C8 | 121.1(2) | C11-O1-C14 | 117.4(2) | C20-C15-C16 | 117.8(2) |
| C20-C15-C7 | 122.6(2) | C16-C15-C7 | 119.5(2) | C17-C16-C15 | 121.4(2) |
| C16-C17-C18 | 120.1(2) | O2-C18-C19 | 125.3(3) | O2-C18-C17 | 115.2(2) |
| C19-C18-C17 | 119.6(2) | C18-C19-C20 | 119.5(2) | C15-C20-C19 | 121.5(2) |
| C18-O2-C21 | 117.5(2) | C3-C22-C30 | 116.4(2) | C3-C22-C23 | 106.90(18) |
| C30-C22-C23 | 113.4(2) | C28-C23-C24 | 117.7(2) | C28-C23-C22 | 121.2(2) |
| C24-C23-C22 | 121.0(2) | C25-C24-C23 | 121.6(2) | C26-C25-C24 | 119.7(2) |
| O3-C26-C25 | 125.1(2) | O3-C26-C27 | 115.4(2) | C25-C26-C27 | 119.5(2) |
| C28-C27-C26 | 120.1(2) | C27-C28-C23 | 121.4(2) | C26-O3-C29 | 117.5(2) |
| C35-C30-C31 | 117.5(2) | C35-C30-C22 | 121.5(2) | C31-C30-C22 | 120.8(2) |
| C32-C31-C30 | 121.1(3) | C31-C32-C33 | 120.5(3) | O4-C33-C34 | 124.7(3) |
| O4-C33-C32 | 115.6(3) | C34-C33-C32 | 119.8(2) | C33-C34-C35 | 119.6(3) |
| C30-C35-C34 | 121.5(2) | C33-O4-C36 | 117.0(3) | C45'-C37-C38 | 123.4(4) |
| C45'-C37-C5 | 111.4(4) | C38-C37-C5 | 111.18(19) | C45'-C37-C45 | 18.0(3) |
| C38-C37-C45 | 109.0(2) | C5-C37-C45 | 112.3(2) | C43-C38-C39 | 117.6(2) |
| C43-C38-C37 | 119.1(2) | C39-C38-C37 | 123.3(2) | C40-C39-C38 | 120.9(2) |
| C39-C40-C41 | 120.6(2) | O5-C41-C42 | 124.7(2) | O5-C41-C40 | 115.9(2) |
| C42-C41-C40 | 119.4(2) | C41-C42-C43 | 119.5(2) | C38-C43-C42 | 122.1(2) |
| C41-O5-C44 | 117.7(2) | C46-C45-C50 | 120.0 | C46-C45-C37 | 121.70(16) |
| C50-C45-C37 | 118.17(16) | C45-C46-C47 | 120.0 | C48-C47-C46 | 120.0 |
| O6-C48-C47 | 115.2(2) | O6-C48-C49 | 124.8(2) | C47-C48-C49 | 120.0 |
| C50-C49-C48 | 120.0 | C45-C50-C49 | 120.0 | C51-O6-C48 | 118.8(3) |
| C37-C45'-C50' | 123.8(4) | C37-C45'-C46' | 116.2(4) | C50'-C45'-C46' | 120.0 |
| C47'-C46'-C45' | 120.0 | C46'-C47'-C48' | 120.0 | O6'-C48'-C47' | 128.6(7) |
| O6'-C48'-C49' | 111.3(7) | C47'-C48'-C49' | 120.0 | C50'-C49'-C48' | 120.0 |
| C49'-C50'-C45' | 120.0 | C51-O6'-C48' | 135.1(8) | O6-C51-O6' | 80.1(4) |
| O7-C52-Cr1 | 179.0(3) | O8-C53-Cr1 | 177.3(3) | O9-C54-Cr1 | 178.6(6) |
| O9'-C54'-Cr1 | 174.7(15) | | | | |

*X-ray Structure Determination of* ***28c*** *– Compound 6172*

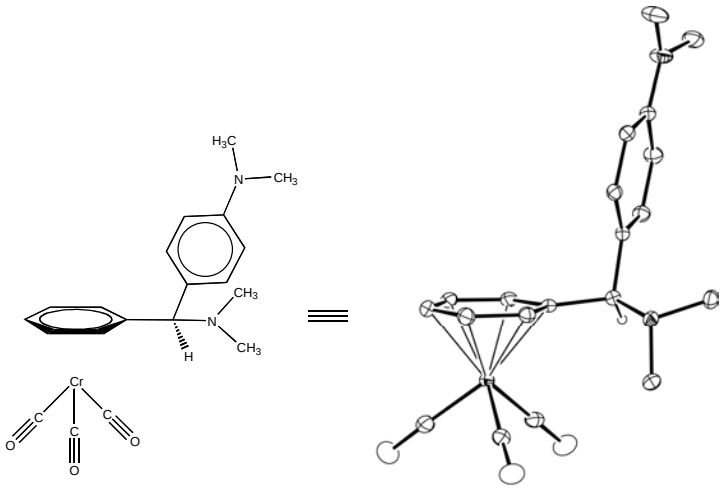

Figure IV-11: ORTEP of **28c** (Compound 6172). Non-benzylic hydrogens omitted for clarity.

Compound 6172, **28c**, $C_{20}H_{22}N_2O_3Cr$, crystallizes in the triclinic space group $P\bar{1}$ with a=7.4340(3)Å, b=11.2179(5)Å, c=11.9275(5)Å, α=69.553(2)°, β=85.657(2)°, γ=84.310(2)°, V=926.52(7)Å$^3$, Z=2, and $d_{calc}$=1.399 g/cm$^3$ . X-ray intensity data were collected on a Bruker APEXII CCD area detector employing graphite-monochromated Mo-Kα radiation (λ=0.71073 Å) at a temperature of 143(1)K. Preliminary indexing was performed from a series of thirty-six 0.5° rotation frames with exposures of 10 seconds. A total of 3272 frames were collected with a crystal to detector distance of 37.602 mm, rotation widths of 0.5° and exposures of 10 seconds (Table IV-18):

Table IV-18: Compound 6172 (**28c**) data collection details.

| scan type | 2θ | ω | ϕ | χ | frames |
|---|---|---|---|---|---|
| ϕ | 24.50 | 7.41 | -347.52 | 28.88 | 739 |
| ϕ | -23.00 | -25.79 | -313-20 | 73.66 | 701 |
| ϕ | 19.50 | 59.55 | -1.00 | -26.26 | 692 |
| ϕ | 015.50 | 258.48 | -351.72 | 19.46 | 739 |
| ω | 17.00 | -36.93 | -41.64 | 83.36 | 109 |
| ϕ | 9.50 | 3.52 | 69.52 | 96.28 | 292 |

Rotation frames were integrated using SAINT[7], producing a listing of unaveraged $F^2$ and $\sigma(F^2)$ values which were then passed to the SHELXTL[8] program package for further processing and structure

solution. A total of 30767 reflections were measured over the ranges $1.82 \leq \theta \leq 27.61°$, $-9 \leq h \leq 9$, $-14 \leq k \leq 14$, $-15 \leq l \leq 15$ yielding 4246 unique reflections (Rint = 0.0202). The intensity data were corrected for Lorentz and polarization effects and for absorption using SADABS[9] (minimum and maximum transmission 0.6805, 0.7456).

The structure was solved by direct methods (SHELXS-97[10]). Refinement was by full-matrix least squares based on $F^2$ using SHELXL-97.[10] All reflections were used during refinement. The weighting scheme used was $w=1/[\sigma^2(F_o^2)+ (0.0364P)^2 + 0.4191P]$ where $P = (F_o^2 + 2F_c^2)/3$. Non-hydrogen atoms were refined anisotropically and hydrogen atoms were refined using a riding model. Refinement converged to R1=0.0258 and wR2=0.0739 for 4079 observed reflections for which $F > 4\sigma(F)$ and R1=0.0269 and wR2=0.0750 and GOF =1.071 for all 4246 unique, non-zero reflections and 240 variables.[a] The maximum $\Delta/\sigma$ in the final cycle of least squares was 0.001 and the two most prominent peaks in the final difference Fourier were +0.362 and -0.261 e/Å$^3$.

Table IV-19 lists cell information, data collection parameters, and refinement data. Final positional and equivalent isotropic thermal parameters are given in Table IV-20 and Table IV-21. Anisotropic thermal parameters are in Table IV-22. Table IV-23 and Table IV-24 list bond distances and bond angles. Figure IV-12 is an ORTEP[6] representation of the molecule with 30% probability thermal ellipsoids displayed.

---

[a] $R1 = \Sigma||F_o| - |F_c|| / \Sigma |F_o|$

$wR2 = [\Sigma w(F_o^2 - F_c^2)^2/\Sigma w(F_o^2)^2]^{½}$

$GOF = [\Sigma w(F_o^2 - F_c^2)^2/(n - p)]^{½}$

where n = the number of reflections and p = the number of parameters refined.

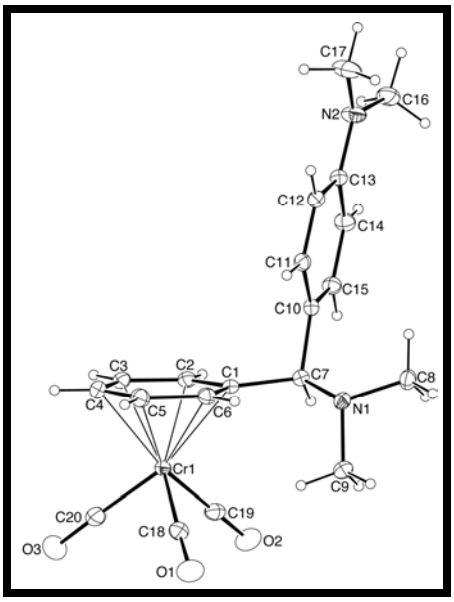


Figure IV-12: ORTEP drawing of the title compound **28c** with 30% probability thermal ellipsoids.

Table IV-19: Summary of Structure Determination of **28c**, Compound 6172

| | |
|---|---|
| Empirical formula | $C_{20}H_{22}N_2O_3Cr$ |
| Formula weight | 390.40 |
| Temperature | 143(1) K |
| Wavelength | 0.71073 Å |
| Crystal system | triclinic |
| Space group | $P\bar{1}$ |
| Cell constants: | |
| a | 7.4340(3) Å |
| b | 11.2179(5) Å |
| c | 11.9275(5) Å |
| α | 69.553(2)° |
| β | 85.657(2)° |
| γ | 84.310(2)° |
| Volume | 926.52(7) $Å^3$ |
| Z | 2 |
| Density (calculated) | 1.399 $Mg/m^3$ |
| Absorption coefficient | 0.639 $mm^{-1}$ |
| F(000) | 408 |

| | |
|---|---|
| Crystal size | 0.30 x 0.25 x 0.10 $mm^3$ |
| Theta range for data collection | 1.82 to 27.61° |
| Index ranges | $-9 \le h \le 9$, $-14 \le k \le 14$, $-15 \le l \le 15$ |
| Reflections collected | 30767 |
| Independent reflections | 4246 [R(int) = 0.0202] |
| Completeness to theta = 27.61° | 98.7 % |
| Absorption correction | Semi-empirical from equivalents |
| Max. and min. transmission | 0.7456 and 0.6805 |
| Refinement method | Full-matrix least-squares on $F^2$ |
| Data / restraints / parameters | 4246 / 0 / 240 |
| Goodness-of-fit on $F^2$ | 1.071 |
| Final R indices [I>2sigma(I)] | R1 = 0.0258, wR2 = 0.0739 |
| R indices (all data) | R1 = 0.0269, wR2 = 0.0750 |
| Largest diff. peak and hole | 0.362 and -0.261 e.$Å^{-3}$ |

Table IV-20: Refined Positional Parameters for **28c**, Compound 6172

| Atom | x | y | z | $U_{eq}$, $Å^2$ |
|---|---|---|---|---|
| Cr1 | 0.49378(2) | 0.214571(19) | 0.073169(17) | 0.02191(7) |
| C1 | 0.43441(15) | 0.21945(12) | 0.25942(10) | 0.0210(2) |
| C2 | 0.32561(17) | 0.31712(13) | 0.17606(11) | 0.0253(2) |
| C3 | 0.21343(17) | 0.28844(14) | 0.10160(12) | 0.0300(3) |
| C4 | 0.21017(18) | 0.16095(15) | 0.10664(13) | 0.0326(3) |
| C5 | 0.31934(19) | 0.06456(14) | 0.18574(12) | 0.0308(3) |
| C6 | 0.43141(17) | 0.09386(12) | 0.26280(11) | 0.0249(2) |
| C7 | 0.53710(16) | 0.25756(11) | 0.34612(11) | 0.0208(2) |
| C8 | 0.74574(18) | 0.18126(13) | 0.50930(12) | 0.0285(3) |
| C9 | 0.83305(18) | 0.15298(14) | 0.32468(13) | 0.0300(3) |
| C10 | 0.39727(16) | 0.28511(11) | 0.43567(11) | 0.0210(2) |
| C11 | 0.29701(17) | 0.18915(12) | 0.51434(11) | 0.0232(2) |
| C12 | 0.17910(17) | 0.21175(12) | 0.60189(11) | 0.0240(2) |
| C13 | 0.15438(17) | 0.33369(12) | 0.61240(11) | 0.0244(2) |
| C14 | 0.25025(18) | 0.43059(12) | 0.52963(12) | 0.0281(3) |
| C15 | 0.36994(17) | 0.40592(12) | 0.44383(12) | 0.0253(2) |
| C16 | 0.0453(2) | 0.47492(15) | 0.72360(15) | 0.0372(3) |
| C17 | -0.0568(3) | 0.25719(18) | 0.78383(16) | 0.0477(4) |
| C18 | 0.67705(19) | 0.09700(14) | 0.05987(13) | 0.0303(3) |
| C19 | 0.66607(18) | 0.32872(13) | 0.04491(12) | 0.0281(3) |
| C20 | 0.4704(2) | 0.26357(19) | -0.08993(14) | 0.0444(4) |
| N1 | 0.67782(14) | 0.15859(10) | 0.40677(10) | 0.0237(2) |

| | | | | |
|---|---|---|---|---|
| N2 | 0.04007(17) | 0.35707(12) | 0.70029(12) | 0.0353(3) |
| O1 | 0.79650(16) | 0.02648(12) | 0.05139(12) | 0.0484(3) |
| O2 | 0.77713(15) | 0.39915(11) | 0.02784(11) | 0.0427(3) |
| O3 | 0.4601(2) | 0.2934(2) | -0.19190(12) | 0.0808(6) |

$U_{eq}=1/3[U_{11}(aa^*)^2+U_{22}(bb^*)^2+U_{33}(cc^*)^2+2U_{12}aa^*bb^*\cos\gamma+2U_{13}aa^*cc^*\cos\beta+2U_{23}bb^*cc^*\cos\alpha]$

Table IV-21: Positional Parameters for Hydrogens in **28c**, Compound 6172

| Atom | x | y | z | $U_{iso}$, Å$^2$ |
|---|---|---|---|---|
| H2 | 0.3293 | 0.4014 | 0.1711 | 0.034 |
| H3 | 0.1412 | 0.3531 | 0.0489 | 0.040 |
| H4 | 0.1355 | 0.1413 | 0.0574 | 0.043 |
| H5 | 0.3189 | -0.0192 | 0.1881 | 0.041 |
| H6 | 0.5031 | 0.0290 | 0.3157 | 0.033 |
| H7 | 0.5949 | 0.3362 | 0.3012 | 0.028 |
| H8a | 0.8316 | 0.1123 | 0.5489 | 0.043 |
| H8b | 0.6466 | 0.1864 | 0.5643 | 0.043 |
| H8c | 0.8034 | 0.2599 | 0.4818 | 0.043 |
| H9a | 0.8846 | 0.2340 | 0.2952 | 0.045 |
| H9b | 0.7938 | 0.1334 | 0.2587 | 0.045 |
| H9c | 0.9223 | 0.0879 | 0.3665 | 0.045 |
| H11 | 0.3094 | 0.1084 | 0.5080 | 0.031 |
| H12 | 0.1156 | 0.1456 | 0.6543 | 0.032 |
| H14 | 0.2334 | 0.5129 | 0.5322 | 0.037 |
| H15 | 0.4331 | 0.4718 | 0.3907 | 0.034 |
| H16a | 0.1681 | 0.4875 | 0.7336 | 0.056 |
| H16b | -0.0261 | 0.4705 | 0.7953 | 0.056 |
| H16c | -0.0028 | 0.5449 | 0.6574 | 0.056 |
| H17a | -0.1291 | 0.2223 | 0.7413 | 0.072 |
| H17b | -0.1338 | 0.2908 | 0.8359 | 0.072 |
| H17c | 0.0274 | 0.1913 | 0.8305 | 0.072 |

Table IV-22: Refined Thermal Parameters (U's) for **28c**, Compound 6172

| Atom | $U_{11}$ | $U_{22}$ | $U_{33}$ | $U_{23}$ | $U_{13}$ | $U_{12}$ |
|---|---|---|---|---|---|---|
| Cr1 | 0.01851(11) | 0.02856(12) | 0.01900(11) | -0.00940(8) | -0.00008(7) | 0.00048(7) |
| C1 | 0.0173(5) | 0.0270(6) | 0.0192(5) | -0.0092(4) | 0.0023(4) | -0.0016(4) |
| C2 | 0.0206(5) | 0.0304(6) | 0.0249(6) | -0.0114(5) | 0.0005(5) | 0.0033(5) |
| C3 | 0.0187(6) | 0.0444(8) | 0.0264(6) | -0.0130(6) | -0.0021(5) | 0.0045(5) |
| C4 | 0.0218(6) | 0.0527(9) | 0.0296(7) | -0.0209(6) | 0.0005(5) | -0.0084(6) |
| C5 | 0.0320(7) | 0.0346(7) | 0.0302(7) | -0.0154(6) | 0.0034(5) | -0.0115(5) |

| | | | | | | |
|---|---|---|---|---|---|---|
| C6 | 0.0253(6) | 0.0263(6) | 0.0224(6) | -0.0075(5) | 0.0015(5) | -0.0043(5) |
| C7 | 0.0195(5) | 0.0212(5) | 0.0214(5) | -0.0073(4) | -0.0002(4) | -0.0015(4) |
| C8 | 0.0252(6) | 0.0326(7) | 0.0276(6) | -0.0093(5) | -0.0068(5) | -0.0015(5) |
| C9 | 0.0211(6) | 0.0363(7) | 0.0330(7) | -0.0141(6) | -0.0017(5) | 0.0040(5) |
| C10 | 0.0189(5) | 0.0254(6) | 0.0201(5) | -0.0097(4) | -0.0019(4) | -0.0008(4) |
| C11 | 0.0238(6) | 0.0231(5) | 0.0254(6) | -0.0114(5) | -0.0017(5) | -0.0023(4) |
| C12 | 0.0222(6) | 0.0262(6) | 0.0245(6) | -0.0092(5) | 0.0002(5) | -0.0049(4) |
| C13 | 0.0206(5) | 0.0296(6) | 0.0252(6) | -0.0128(5) | 0.0001(5) | -0.0003(5) |
| C14 | 0.0304(6) | 0.0237(6) | 0.0321(7) | -0.0132(5) | 0.0027(5) | -0.0012(5) |
| C15 | 0.0257(6) | 0.0237(6) | 0.0264(6) | -0.0085(5) | 0.0018(5) | -0.0041(5) |
| C16 | 0.0352(7) | 0.0417(8) | 0.0415(8) | -0.0254(7) | 0.0067(6) | 0.0007(6) |
| C17 | 0.0538(10) | 0.0508(10) | 0.0413(9) | -0.0218(7) | 0.0245(8) | -0.0148(8) |
| C18 | 0.0289(6) | 0.0352(7) | 0.0308(7) | -0.0170(6) | 0.0011(5) | -0.0022(5) |
| C19 | 0.0252(6) | 0.0290(6) | 0.0261(6) | -0.0065(5) | 0.0027(5) | 0.0026(5) |
| C20 | 0.0247(7) | 0.0760(12) | 0.0294(7) | -0.0154(7) | -0.0019(6) | 0.0015(7) |
| N1 | 0.0202(5) | 0.0259(5) | 0.0252(5) | -0.0092(4) | -0.0032(4) | 0.0005(4) |
| N2 | 0.0352(6) | 0.0357(6) | 0.0383(7) | -0.0195(5) | 0.0138(5) | -0.0046(5) |
| O1 | 0.0395(6) | 0.0477(7) | 0.0647(8) | -0.0323(6) | 0.0035(6) | 0.0097(5) |
| O2 | 0.0350(6) | 0.0373(6) | 0.0501(7) | -0.0075(5) | 0.0052(5) | -0.0106(5) |
| O3 | 0.0491(8) | 0.1584(18) | 0.0246(6) | -0.0199(8) | -0.0075(6) | 0.0006(9) |

The form of the anisotropic displacement parameter is:
$\exp[-2\pi^2(a^{*2}U_{11}h^2+b^{*2}U_{22}k^2+c^{*2}U_{33}l^2+2b^*c^*U_{23}kl+2a^*c^*U_{13}hl+2a^*b^*U_{12}hk)]$

Table IV-23: Bond Distances in **28c**, Compound 6172, Å

| | | | | | |
|---|---|---|---|---|---|
| Cr1-C19 | 1.8309(14) | Cr1-C18 | 1.8380(14) | Cr1-C20 | 1.8444(16) |
| Cr1-C2 | 2.2048(12) | Cr1-C3 | 2.2118(13) | Cr1-C5 | 2.2151(14) |
| Cr1-C4 | 2.2187(13) | Cr1-C6 | 2.2339(12) | Cr1-C1 | 2.2505(12) |
| C1-C6 | 1.3977(17) | C1-C2 | 1.4241(17) | C1-C7 | 1.5258(16) |
| C2-C3 | 1.3973(19) | C3-C4 | 1.413(2) | C4-C5 | 1.395(2) |
| C5-C6 | 1.4242(18) | C7-N1 | 1.4743(15) | C7-C10 | 1.5217(16) |
| C8-N1 | 1.4668(16) | C9-N1 | 1.4669(16) | C10-C15 | 1.3864(17) |
| C10-C11 | 1.3936(17) | C11-C12 | 1.3876(17) | C12-C13 | 1.4096(17) |
| C13-N2 | 1.3794(16) | C13-C14 | 1.4005(18) | C14-C15 | 1.3881(18) |
| C16-N2 | 1.4476(19) | C17-N2 | 1.428(2) | C18-O1 | 1.1522(18) |
| C19-O2 | 1.1570(18) | C20-O3 | 1.150(2) | | |

Table IV-24: Bond Angles in **28c**, Compound 6172, °

| | | | | | |
|---|---|---|---|---|---|
| C19-Cr1-C18 | 87.46(6) | C19-Cr1-C20 | 88.89(7) | C18-Cr1-C20 | 88.12(7) |
| C19-Cr1-C2 | 89.86(5) | C18-Cr1-C2 | 152.18(6) | C20-Cr1-C2 | 119.53(6) |

| | | | | | |
|---|---|---|---|---|---|
| C19-Cr1-C3 | 115.47(6) | C18-Cr1-C3 | 157.07(6) | C20-Cr1-C3 | 92.33(6) |
| C2-Cr1-C3 | 36.89(5) | C19-Cr1-C5 | 155.30(6) | C18-Cr1-C5 | 92.67(6) |
| C20-Cr1-C5 | 115.81(7) | C2-Cr1-C5 | 78.61(5) | C3-Cr1-C5 | 66.56(5) |
| C19-Cr1-C4 | 152.63(6) | C18-Cr1-C4 | 119.89(6) | C20-Cr1-C4 | 90.77(6) |
| C2-Cr1-C4 | 66.68(5) | C3-Cr1-C4 | 37.19(6) | C5-Cr1-C4 | 36.69(6) |
| C19-Cr1-C6 | 117.98(5) | C18-Cr1-C6 | 90.77(6) | C20-Cr1-C6 | 153.05(7) |
| C2-Cr1-C6 | 66.25(5) | C3-Cr1-C6 | 78.58(5) | C5-Cr1-C6 | 37.34(5) |
| C4-Cr1-C6 | 66.62(5) | C19-Cr1-C1 | 91.10(5) | C18-Cr1-C1 | 115.08(5) |
| C20-Cr1-C1 | 156.79(6) | C2-Cr1-C1 | 37.26(4) | C3-Cr1-C1 | 66.83(5) |
| C5-Cr1-C1 | 66.52(5) | C4-Cr1-C1 | 78.77(5) | C6-Cr1-C1 | 36.32(4) |
| C6-C1-C2 | 118.55(11) | C6-C1-C7 | 123.84(11) | C2-C1-C7 | 117.46(11) |
| C6-C1-Cr1 | 71.20(7) | C2-C1-Cr1 | 69.63(7) | C7-C1-Cr1 | 134.68(8) |
| C3-C2-C1 | 121.15(12) | C3-C2-Cr1 | 71.83(7) | C1-C2-Cr1 | 73.11(7) |
| C2-C3-C4 | 119.78(12) | C2-C3-Cr1 | 71.28(7) | C4-C3-Cr1 | 71.67(8) |
| C5-C4-C3 | 119.77(12) | C5-C4-Cr1 | 71.52(8) | C3-C4-Cr1 | 71.14(8) |
| C4-C5-C6 | 120.29(13) | C4-C5-Cr1 | 71.80(8) | C6-C5-Cr1 | 72.05(7) |
| C1-C6-C5 | 120.44(12) | C1-C6-Cr1 | 72.49(7) | C5-C6-Cr1 | 70.62(7) |
| N1-C7-C10 | 111.44(10) | N1-C7-C1 | 112.56(10) | C10-C7-C1 | 106.87(9) |
| C15-C10-C11 | 117.99(11) | C15-C10-C7 | 120.80(11) | C11-C10-C7 | 121.18(11) |
| C12-C11-C10 | 121.29(11) | C11-C12-C13 | 120.83(11) | N2-C13-C14 | 121.20(12) |
| N2-C13-C12 | 121.50(12) | C14-C13-C12 | 117.30(11) | C15-C14-C13 | 121.13(12) |
| C10-C15-C14 | 121.38(12) | O1-C18-Cr1 | 177.45(13) | O2-C19-Cr1 | 178.84(13) |
| O3-C20-Cr1 | 178.40(15) | C8-N1-C9 | 107.56(10) | C8-N1-C7 | 112.16(10) |
| C9-N1-C7 | 111.28(10) | C13-N2-C17 | 120.45(12) | C13-N2-C16 | 119.72(12) |
| C17-N2-C16 | 118.67(12) | | | | |

*X-ray Structure Determination of **41b** – Compound 6146*

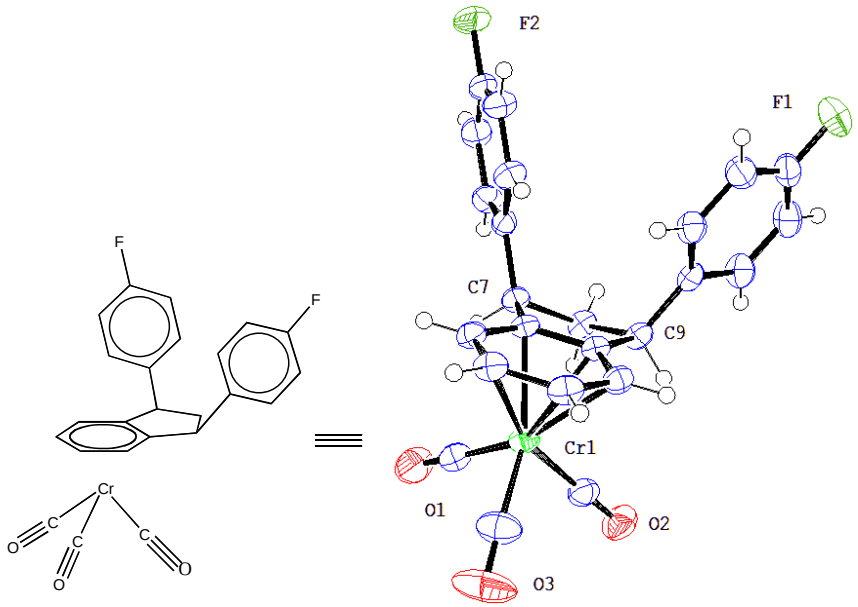


Figure IV-13: ORTEP of 6146. Thermal ellipsoids are at 50% probability.

Compound 6146, **41b**, $C_{24}H_{16}O_3F_2Cr$, crystallizes in the monoclinic space group C 2/c (systematic absences hkl: h+k=odd, and h0l: l=odd) with a=24.939(2)Å, b=7.0155(6)Å, c=22.123(2)Å, β=96.174(2)°, V=3848.2(6)Å$^3$, Z=8, and dcalc=1.527 g/cm$^3$. X-ray intensity data were collected on a Rigaku Mercury CCD area detector employing graphite-monochromated Mo-Kα radiation (λ=0.71073 Å) at a temperature of 143(1)K. Preliminary indexing was performed from a series of twelve 0.5° rotation images with exposures of 30 seconds. A total of 860 rotation images were collected with a crystal to detector distance of 35 mm, a 2θ swing angle of -12°, rotation widths of 0.5° and exposures of 20 seconds: scan no. 1 was a ϕ-scan from 0° to 270° at ω = 10° and χ = 20°; scan no. 2 was an ω-scan from -20° to 20° at χ = -90° and ϕ = 0°; scan no. 3 was an ω-scan from -20° to 20° at χ = -90° and ϕ = 45°; scan no. 4 was an ω-scan from -20° to 20° at χ = -90° and ϕ = 135°; scan no. 5 was an ω-scan from -20° to 20° at χ = -90° and ϕ = 225°. Rotation images were processed using CrystalClear[1], producing a listing of unaveraged $F^2$ and $\sigma(F^2)$ values which were then passed to the CrystalStructure[2] program package for further processing and structure solution on a Dell Pentium 4 computer. A total of 25535 reflections were measured over the ranges $2.60 \leq \theta \leq 27.48°$, $-31 \leq h \leq 32$, $-8 \leq k \leq 9$, $-28 \leq l \leq 28$ yielding 4388 unique reflections (Rint = 0.0245). The intensity data were corrected for Lorentz and polarization effects and for absorption using REQAB[3] (minimum and maximum transmission 0.8845, 1.0000).

The structure was solved by direct methods (SIR97[4]). Refinement was by full-matrix least squares based on $F^2$ using SHELXL-97.[2] All reflections were used during refinement. The weighting scheme used was $w=1/[\sigma^2(F_o^2)+ 0.0527P^2 + 3.9864 P = (F_o^2 + 2F_c^2)/3$. Non-hydrogen atoms were refined anisotropically and hydrogen atoms were refined using a riding model. Refinement converged to R1=0.0399 and wR2=0.1019 for 3935 observed reflections for which $F > 4\sigma(F)$ and R1=0.0453 and wR2=0.1062 and GOF =1.081 for all 4388 unique, non-zero reflections and 272 variables.[a] The maximum $\Delta/\sigma$ in the final cycle of least squares was 0.001 and the two most prominent peaks in the final difference Fourier were +0.358 and -0.456 e/Å$^3$.

Table IV-25 lists cell information, data collection parameters, and refinement data. Final positional and equivalent isotropic thermal parameters are given in Table IV-26 and Table IV-273. Anisotropic thermal parameters are in Table IV-28. Table IV-29 and Table IV-30 list bond distances and bond angles. Figure IV-14 is an ORTEP[6] representation of the molecule with 30% probability thermal ellipsoids displayed.

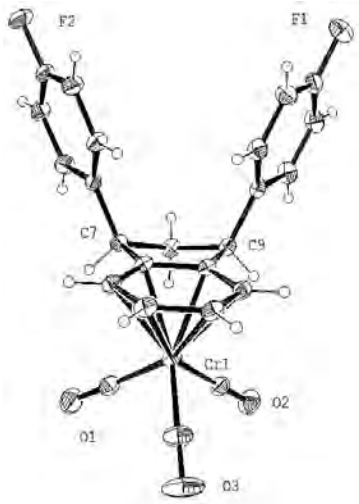


Figure IV-14. ORTEP drawing of the title compound **41b** with 30% probability thermal ellipsoids.

---

[a] $R1 = \Sigma||F_o| - |F_c|| / \Sigma |F_o|$
$wR2 = [\Sigma w(F_o^2 - F_c^2)^2/\Sigma w(F_o^2)^2]^{1/2}$
$GOF = [\Sigma w(F_o^2 - F_c^2)^2/(n - p)]^{1/2}$
where n = the number of reflections and p = the number of parameters refined.

Table IV-25. Summary of Structure Determination of **41b**, Compound 6146

| | |
|---|---|
| Empirical formula | $C_{24}H_{16}O_3F_2Cr$ |
| Formula weight | 442.37 |
| Temperature | 143(1) K |
| Wavelength | 0.71073 Å |
| Crystal system | monoclinic |
| Space group | C 2/c |
| Cell constants: | |
| a | 24.939(2) Å |
| b | 7.0155(6) Å |
| c | 22.123(2) Å |
| β | 96.174(2)° |
| Volume | 3848.2(6) $Å^3$ |
| Z | 8 |
| Density (calculated) | 1.527 $Mg/m^3$ |
| Absorption coefficient | 0.637 $mm^{-1}$ |
| F(000) | 1808 |
| Crystal size | 0.32 x 0.22 x 0.20 $mm^3$ |
| Theta range for data collection | 2.60 to 27.48°. |
| Index ranges | $-31 \le h \le 32$, $-8 \le k \le 9$, $-28 \le l \le 28$ |
| Reflections collected | 25535 |
| Independent reflections | 4388 [R(int) = 0.0245] |
| Completeness to theta = 27.48° | 99.6 % |
| Absorption correction | Semi-empirical from equivalents |
| Max. and min. transmission | 1.0000 and 0.8845 |
| Refinement method | Full-matrix least-squares on $F^2$ |
| Data / restraints / parameters | 4388 / 0 / 272 |
| Goodness-of-fit on $F^2$ | 1.081 |
| Final R indices [I>2sigma(I)] | R1 = 0.0399, wR2 = 0.1019 |
| R indices (all data) | R1 = 0.0453, wR2 = 0.1062 |
| Largest diff. peak and hole | 0.358 and -0.456 $e.Å^{-3}$ |

Table IV-26. Refined Positional Parameters for **41b**, Compound 6146

| Atom | x | y | z | $U_{eq}$,$Å^2$ |
|---|---|---|---|---|
| Cr1 | 0.363037(11) | 0.61187(4) | 0.496441(12) | 0.02815(11) |
| C1 | 0.40850(7) | 0.7832(2) | 0.43538(7) | 0.0263(3) |
| C2 | 0.42260(8) | 0.8477(3) | 0.49575(8) | 0.0304(4) |
| C3 | 0.38170(8) | 0.9042(3) | 0.53048(8) | 0.0330(4) |

| | | | | |
|---|---|---|---|---|
| C4 | 0.32692(8) | 0.8990(3) | 0.50581(8) | 0.0323(4) |
| C5 | 0.31281(7) | 0.8347(3) | 0.44616(8) | 0.0291(4) |
| C6 | 0.35401(7) | 0.7773(2) | 0.41063(7) | 0.0256(3) |
| C7 | 0.34841(7) | 0.6965(3) | 0.34683(7) | 0.0264(3) |
| C8 | 0.40516(7) | 0.6078(3) | 0.34256(8) | 0.0298(4) |
| C9 | 0.44553(7) | 0.7113(3) | 0.39047(8) | 0.0284(4) |
| C10 | 0.47860(7) | 0.8686(3) | 0.36465(8) | 0.0283(4) |
| C11 | 0.46822(8) | 1.0603(3) | 0.37159(9) | 0.0348(4) |
| C12 | 0.49903(8) | 1.1997(3) | 0.34719(10) | 0.0399(5) |
| C13 | 0.54066(8) | 1.1426(3) | 0.31529(9) | 0.0366(4) |
| C14 | 0.55301(8) | 0.9553(3) | 0.30756(10) | 0.0415(5) |
| C15 | 0.52206(8) | 0.8185(3) | 0.33283(9) | 0.0370(4) |
| C16 | 0.33158(7) | 0.8413(3) | 0.29718(8) | 0.0271(4) |
| C17 | 0.32854(8) | 1.0351(3) | 0.30719(9) | 0.0345(4) |
| C18 | 0.31347(8) | 1.1610(3) | 0.25983(10) | 0.0412(5) |
| C19 | 0.30100(8) | 1.0866(3) | 0.20245(9) | 0.0393(5) |
| C20 | 0.30270(8) | 0.8966(3) | 0.19048(9) | 0.0396(5) |
| C21 | 0.31840(8) | 0.7738(3) | 0.23809(8) | 0.0343(4) |
| C22 | 0.31621(8) | 0.4297(3) | 0.46254(10) | 0.0374(4) |
| C23 | 0.41655(8) | 0.4322(3) | 0.49842(9) | 0.0346(4) |
| C24 | 0.35055(10) | 0.5254(3) | 0.57254(10) | 0.0483(5) |
| F1 | 0.57046(5) | 1.2803(2) | 0.29085(6) | 0.0543(3) |
| F2 | 0.28576(5) | 1.2088(2) | 0.15585(6) | 0.0567(4) |
| O1 | 0.28722(7) | 0.3159(2) | 0.43932(9) | 0.0568(4) |
| O2 | 0.45045(6) | 0.3197(2) | 0.49826(8) | 0.0483(4) |
| O3 | 0.34419(11) | 0.4625(3) | 0.61938(8) | 0.0806(7) |

$U_{eq}=1/3[U_{11}(aa^*)^2+U_{22}(bb^*)^2+U_{33}(cc^*)^2+2U_{12}aa^*bb^*\cos\gamma+2U_{13}aa^*cc^*\cos\beta+2U_{23}bb^*cc^*\cos\alpha]$

Table IV-27. Positional Parameters for Hydrogens in **41b**, Compound 6146

| Atom | x | y | z | $U_{iso}$,Å$^2$ |
|---|---|---|---|---|
| H2 | 0.4585 | 0.8523 | 0.5120 | 0.040 |
| H3 | 0.3906 | 0.9458 | 0.5702 | 0.044 |
| H4 | 0.3002 | 0.9383 | 0.5292 | 0.043 |
| H5 | 0.2768 | 0.8298 | 0.4301 | 0.039 |
| H7 | 0.3217 | 0.5936 | 0.3445 | 0.035 |
| H8A | 0.4158 | 0.6257 | 0.3021 | 0.040 |
| H8B | 0.4046 | 0.4723 | 0.3511 | 0.040 |
| H9 | 0.4702 | 0.6167 | 0.4107 | 0.038 |
| H11 | 0.4399 | 1.0969 | 0.3931 | 0.046 |
| H12 | 0.4917 | 1.3284 | 0.3523 | 0.053 |
| H14 | 0.5814 | 0.9203 | 0.2859 | 0.055 |

| | | | | |
|---|---|---|---|---|
| H15 | 0.5304 | 0.6903 | 0.3285 | 0.049 |
| H17 | 0.3367 | 1.0823 | 0.3464 | 0.046 |
| H18 | 0.3119 | 1.2915 | 0.2667 | 0.055 |
| H20 | 0.2935 | 0.8504 | 0.1513 | 0.053 |
| H21 | 0.3202 | 0.6436 | 0.2305 | 0.046 |

Table IV-28. Refined Thermal Parameters (U's) for **41b**, Compound 6146

| Atom | $U_{11}$ | $U_{22}$ | $U_{33}$ | $U_{23}$ | $U_{13}$ | $U_{12}$ |
|---|---|---|---|---|---|---|
| Cr1 | 0.03367(18) | 0.02876(18) | 0.02193(16) | 0.00161(10) | 0.00262(12) | 0.00441(11) |
| C1 | 0.0298(8) | 0.0250(9) | 0.0239(8) | 0.0018(6) | 0.0016(6) | 0.0026(7) |
| C2 | 0.0338(9) | 0.0311(9) | 0.0252(8) | -0.0007(7) | -0.0017(7) | 0.0008(7) |
| C3 | 0.0456(11) | 0.0307(10) | 0.0222(8) | -0.0037(7) | 0.0014(8) | 0.0025(8) |
| C4 | 0.0408(10) | 0.0301(10) | 0.0271(9) | -0.0008(7) | 0.0086(8) | 0.0083(8) |
| C5 | 0.0307(8) | 0.0290(9) | 0.0277(8) | 0.0022(7) | 0.0029(7) | 0.0062(7) |
| C6 | 0.0309(8) | 0.0249(8) | 0.0206(7) | 0.0019(6) | 0.0007(6) | 0.0040(7) |
| C7 | 0.0301(8) | 0.0266(9) | 0.0220(8) | -0.0009(6) | 0.0011(6) | 0.0019(7) |
| C8 | 0.0323(9) | 0.0298(10) | 0.0270(9) | -0.0034(7) | 0.0017(7) | 0.0051(7) |
| C9 | 0.0296(8) | 0.0304(9) | 0.0247(8) | -0.0019(7) | 0.0006(7) | 0.0057(7) |
| C10 | 0.0253(8) | 0.0350(10) | 0.0238(8) | -0.0022(7) | -0.0006(6) | 0.0049(7) |
| C11 | 0.0300(9) | 0.0376(10) | 0.0380(10) | -0.0016(8) | 0.0090(8) | 0.0062(8) |
| C12 | 0.0364(10) | 0.0345(11) | 0.0494(12) | 0.0013(9) | 0.0082(9) | 0.0017(8) |
| C13 | 0.0292(9) | 0.0464(12) | 0.0341(10) | -0.0013(8) | 0.0030(7) | -0.0065(8) |
| C14 | 0.0322(10) | 0.0533(13) | 0.0405(11) | -0.0103(10) | 0.0107(8) | -0.0009(9) |
| C15 | 0.0331(9) | 0.0385(11) | 0.0405(10) | -0.0088(8) | 0.0085(8) | 0.0037(8) |
| C16 | 0.0239(8) | 0.0332(9) | 0.0242(8) | 0.0017(7) | 0.0025(6) | 0.0012(7) |
| C17 | 0.0392(10) | 0.0337(10) | 0.0298(9) | -0.0005(8) | -0.0009(8) | 0.0046(8) |
| C18 | 0.0434(11) | 0.0353(11) | 0.0445(11) | 0.0095(9) | 0.0032(9) | 0.0061(9) |
| C19 | 0.0298(9) | 0.0533(13) | 0.0346(10) | 0.0200(9) | 0.0020(8) | 0.0042(8) |
| C20 | 0.0396(10) | 0.0548(14) | 0.0235(9) | 0.0040(8) | -0.0006(8) | -0.0039(9) |
| C21 | 0.0389(10) | 0.0375(10) | 0.0260(8) | -0.0008(8) | 0.0011(7) | -0.0029(8) |
| C22 | 0.0380(10) | 0.0332(10) | 0.0404(10) | 0.0064(8) | 0.0006(8) | 0.0067(8) |
| C23 | 0.0367(9) | 0.0360(10) | 0.0301(9) | 0.0024(8) | -0.0014(7) | 0.0005(8) |
| C24 | 0.0712(15) | 0.0381(12) | 0.0380(11) | 0.0022(9) | 0.0165(10) | 0.0069(11) |
| F1 | 0.0470(7) | 0.0568(9) | 0.0619(8) | 0.0016(7) | 0.0177(6) | -0.0146(6) |
| F2 | 0.0538(8) | 0.0679(10) | 0.0474(7) | 0.0322(7) | 0.0007(6) | 0.0082(7) |
| O1 | 0.0559(9) | 0.0398(9) | 0.0700(11) | 0.0025(8) | -0.0147(8) | -0.0060(8) |
| O2 | 0.0438(8) | 0.0417(9) | 0.0583(10) | 0.0022(7) | 0.0003(7) | 0.0133(7) |
| O3 | 0.144(2) | 0.0624(12) | 0.0417(10) | 0.0168(9) | 0.0402(12) | 0.0117(13) |

The form of the anisotropic displacement parameter is:
$\exp[-2\pi^2(a^{*2}U_{11}h^2+b^{*2}U_{22}k^2+c^{*2}U_{33}l^2+2b^*c^*U_{23}kl+2a^*c^*U_{13}hl+2a^*b^*U_{12}hk)]$

Table IV-29 Bond Distances in **41b**, Compound 6146, Å

| | | | | | |
|---|---|---|---|---|---|
| Cr1-C23 | 1.833(2) | Cr1-C22 | 1.836(2) | Cr1-C24 | 1.847(2) |
| Cr1-C1 | 2.2102(17) | Cr1-C6 | 2.2157(16) | Cr1-C3 | 2.2171(19) |
| Cr1-C2 | 2.2246(19) | Cr1-C5 | 2.2249(18) | Cr1-C4 | 2.2252(18) |
| C1-C6 | 1.410(2) | C1-C2 | 1.418(2) | C1-C9 | 1.514(2) |
| C2-C3 | 1.399(3) | C3-C4 | 1.416(3) | C4-C5 | 1.403(3) |
| C5-C6 | 1.418(2) | C6-C7 | 1.513(2) | C7-C16 | 1.522(2) |
| C7-C8 | 1.558(2) | C8-C9 | 1.560(2) | C9-C10 | 1.525(3) |
| C10-C11 | 1.381(3) | C10-C15 | 1.399(2) | C11-C12 | 1.388(3) |
| C12-C13 | 1.376(3) | C13-C14 | 1.365(3) | C13-F1 | 1.365(2) |
| C14-C15 | 1.386(3) | C16-C17 | 1.381(3) | C16-C21 | 1.396(2) |
| C17-C18 | 1.391(3) | C18-C19 | 1.377(3) | C19-C20 | 1.360(3) |
| C19-F2 | 1.363(2) | C20-C21 | 1.384(3) | C22-O1 | 1.159(3) |
| C23-O2 | 1.157(2) | C24-O3 | 1.153(3) | | |

Table IV-30. Bond Angles in **41b**, Compound 6146, °

| | | | | | |
|---|---|---|---|---|---|
| C23-Cr1-C22 | 87.73(9) | C23-Cr1-C24 | 86.91(10) | C22-Cr1-C24 | 88.95(10) |
| C23-Cr1-C1 | 88.20(8) | C22-Cr1-C1 | 118.32(8) | C24-Cr1-C1 | 152.07(9) |
| C23-Cr1-C6 | 112.78(8) | C22-Cr1-C6 | 90.74(8) | C24-Cr1-C6 | 160.28(9) |
| C1-Cr1-C6 | 37.15(6) | C23-Cr1-C3 | 120.17(8) | C22-Cr1-C3 | 152.10(8) |
| C24-Cr1-C3 | 92.52(9) | C1-Cr1-C3 | 66.53(7) | C6-Cr1-C3 | 78.75(7) |
| C23-Cr1-C2 | 91.53(8) | C22-Cr1-C2 | 155.60(8) | C24-Cr1-C2 | 115.38(9) |
| C1-Cr1-C2 | 37.30(6) | C6-Cr1-C2 | 67.11(6) | C3-Cr1-C2 | 36.71(7) |
| C23-Cr1-C5 | 149.82(8) | C22-Cr1-C5 | 89.18(8) | C24-Cr1-C5 | 123.05(9) |
| C1-Cr1-C5 | 67.07(6) | C6-Cr1-C5 | 37.23(6) | C3-Cr1-C5 | 66.80(7) |
| C2-Cr1-C5 | 79.31(7) | C23-Cr1-C4 | 157.12(9) | C22-Cr1-C4 | 114.97(8) |
| C24-Cr1-C4 | 95.90(8) | C1-Cr1-C4 | 78.69(7) | C6-Cr1-C4 | 66.48(6) |
| C3-Cr1-C4 | 37.18(7) | C2-Cr1-C4 | 66.71(7) | C5-Cr1-C4 | 36.75(7) |
| C6-C1-C2 | 120.41(15) | C6-C1-C9 | 111.45(14) | C2-C1-C9 | 128.12(15) |
| C6-C1-Cr1 | 71.63(10) | C2-C1-Cr1 | 71.90(10) | C9-C1-Cr1 | 127.52(12) |
| C3-C2-C1 | 119.09(17) | C3-C2-Cr1 | 71.35(11) | C1-C2-Cr1 | 70.80(10) |
| C2-C3-C4 | 120.73(16) | C2-C3-Cr1 | 71.93(11) | C4-C3-Cr1 | 71.72(11) |
| C5-C4-C3 | 120.32(16) | C5-C4-Cr1 | 71.61(10) | C3-C4-Cr1 | 71.10(11) |
| C4-C5-C6 | 119.31(16) | C4-C5-Cr1 | 71.64(10) | C6-C5-Cr1 | 71.03(10) |
| C1-C6-C5 | 120.13(15) | C1-C6-C7 | 111.21(14) | C5-C6-C7 | 128.60(16) |
| C1-C6-Cr1 | 71.21(9) | C5-C6-Cr1 | 71.73(10) | C7-C6-Cr1 | 126.41(12) |
| C6-C7-C16 | 114.44(15) | C6-C7-C8 | 102.28(13) | C16-C7-C8 | 113.86(14) |
| C7-C8-C9 | 107.29(14) | C1-C9-C10 | 113.41(15) | C1-C9-C8 | 101.90(14) |
| C10-C9-C8 | 114.68(14) | C11-C10-C15 | 117.71(18) | C11-C10-C9 | 123.20(16) |

| | | | | | |
|---|---|---|---|---|---|
| C15-C10-C9 | 119.08(17) | C10-C11-C12 | 121.64(17) | C13-C12-C11 | 118.30(19) |
| C14-C13-F1 | 119.47(18) | C14-C13-C12 | 122.49(19) | F1-C13-C12 | 118.04(19) |
| C13-C14-C15 | 118.25(18) | C14-C15-C10 | 121.59(19) | C17-C16-C21 | 118.20(17) |
| C17-C16-C7 | 123.87(16) | C21-C16-C7 | 117.93(17) | C16-C17-C18 | 121.32(19) |
| C19-C18-C17 | 118.0(2) | C20-C19-F2 | 118.8(2) | C20-C19-C18 | 122.84(19) |
| F2-C19-C18 | 118.4(2) | C19-C20-C21 | 118.29(19) | C20-C21-C16 | 121.35(19) |
| O1-C22-Cr1 | 177.8(2) | O2-C23-Cr1 | 178.41(18) | O3-C24-Cr1 | 176.3(2) |

*X-ray Structure Determination of **(R)-(−)-55a** – Compound 6164*

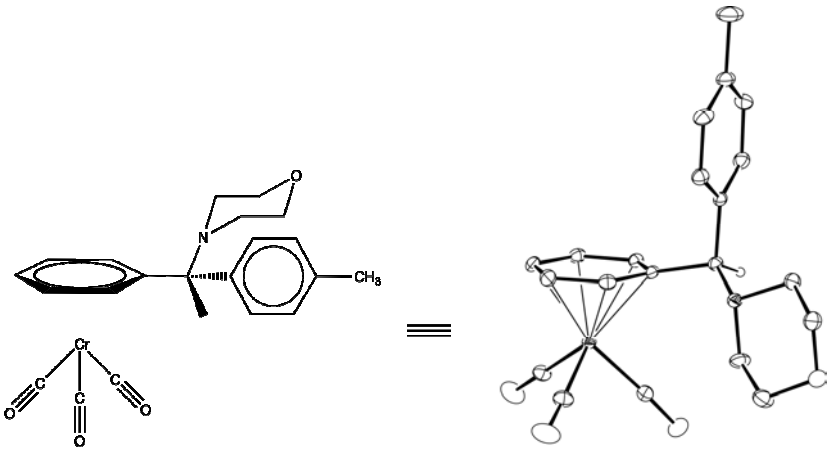


Figure IV-15: ORTEP of (R)-(−)-**55a** (Compound 6164). Non-benzylic Hydrogens are omitted for clarity.

Compound 6164, $C_{21}H_{21}NO_4Cr$, crystallizes in the monoclinic space group C2 (systematic absences hkl: h+k=odd) with a=13.0670(18)Å, b=11.7445(16)Å, c=13.2607(19)Å, β=112.443(6)°, V=1880.9(5)Å$^3$, Z=4, and $d_{calc}$=1.424 g/cm$^3$ . X-ray intensity data were collected on a Bruker APEXII CCD area detector employing graphite-monochromated Mo-Kα radiation (λ=0.71073 Å) at a temperature of 143(1)K. Preliminary indexing was performed from a series of thirty-six 0.5° rotation frames with exposures of 5 seconds. A total of 2582 frames were collected with a crystal to detector distance of 37.600 mm, rotation widths of 0.5° and exposures of 5 seconds (Table IV-31):

Table IV-31: Compound **(*R*)-(−)-55a** (6164) data collection details.

| scan type | 2θ | ω | ϕ | χ | frames |
|---|---|---|---|---|---|
| ϕ | -23.000 | 315.83 | -347.52 | 28.88 | 739 |
| ω | -25.50 | -29.49 | 47.91 | -56.95 | 173 |
| ω | 17.00 | -38.50 | -175.56 | 82.07 | 116 |
| ω | 17.00 | -33.20 | -41.64 | 83.36 | 76 |
| ϕ | -23.00 | -25.79 | -321.05 | 73.66 | 739 |
| ϕ | 19.50 | 59.55 | -11.29 | -26.26 | 739 |

Rotation frames were integrated using SAINT[7], producing a listing of unaveraged $F^2$ and $\sigma(F^2)$ values which were then passed to the SHELXTL[8] program package for further processing and structure solution on a Dell Pentium 4 computer. A total of 22873 reflections were measured over the ranges

$1.66 \leq \theta \leq 27.59°$, $-16 \leq h \leq 16$, $-15 \leq k \leq 15$, $-17 \leq l \leq 17$ yielding 4252 unique reflections (Rint = 0.0256). The intensity data were corrected for Lorentz and polarization effects and for absorption using SADABS[9] (minimum and maximum transmission 0.6459, 0.7456).

The structure was solved by direct methods (SHELXS-97[10]). Refinement was by full-matrix least squares based on $F^2$ using SHELXL-97.[10] All reflections were used during refinement. The weighting scheme used was $w=1/[\sigma^2(F_o^2)+ (0.0907P)^2 + 0.3133P]$ where $P = (F_o^2 + 2F_c^2)/3$. Non-hydrogen atoms were refined anisotropically and hydrogen atoms were refined using a riding model. Refinement converged to R1=0.0212 and wR2=0.0611 for 4167 observed reflections for which $F > 4\sigma(F)$ and R1=0.0228 and wR2=0.0690 and GOF =1.159 for all 4252 unique, non-zero reflections and 246 variables.[a] The maximum $\Delta/\sigma$ in the final cycle of least squares was 0.011 and the two most prominent peaks in the final difference Fourier were +0.374 and -0.397 e/Å$^3$.

Table IV-32 lists cell information, data collection parameters, and refinement data. Final positional and equivalent isotropic thermal parameters are given in Table IV-33 and Table IV-34. Anisotropic thermal parameters are in Table IV-35. Table IV-36 and Table IV-37 list bond distances and bond angles. Figure IV-16 is an ORTEP[6] representation of the molecule with 30% probability thermal ellipsoids displayed.

---

[a] $R1 = \Sigma||F_o| - |F_c|| / \Sigma |F_o|$
$wR2 = [\Sigma w(F_o^2 - F_c^2)^2/\Sigma w(F_o^2)^2]^{½}$
$GOF = [\Sigma w(F_o^2 - F_c^2)^2/(n - p)]^{½}$
where n = the number of reflections and p = the number of parameters refined.

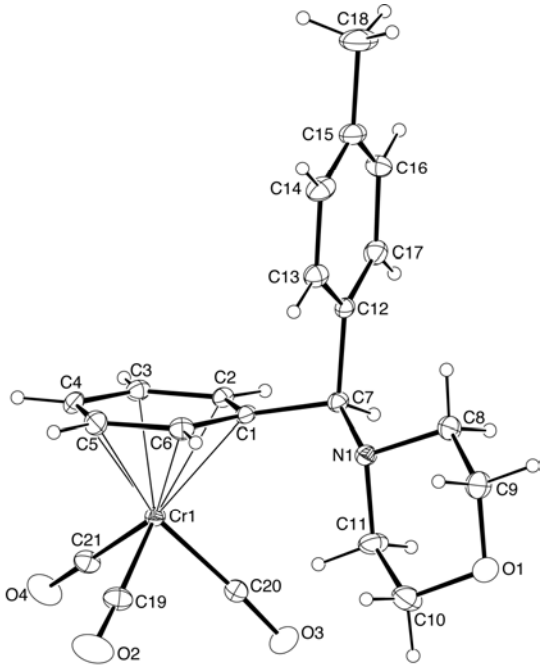


Figure IV-16: ORTEP drawing of the title compound **(*R*)-(−)-55a** with 30% probability thermal ellipsoids.

Table IV-32: Summary of Structure Determination of **(*R*)-(−)-55a**, Compound 6164

| | |
|---|---|
| Empirical formula | $C_{21}H_{21}NO_4Cr$ |
| Formula weight | 403.39 |
| Temperature | 143(1) K |
| Wavelength | 0.71073 Å |
| Crystal system | monoclinic |
| Space group | C2 |
| Cell constants: | |
| a | 13.0670(18) Å |
| b | 11.7445(16) Å |
| c | 13.2607(19) Å |
| β | 112.443(6)° |
| Volume | 1880.9(5) $Å^3$ |
| Z | 4 |
| Density (calculated) | 1.424 $Mg/m^3$ |
| Absorption coefficient | 0.635 $mm^{-1}$ |
| F(000) | 840 |
| Crystal size | 0.30 x 0.18 x 0.12 $mm^3$ |

| | |
|---|---|
| Theta range for data collection | 1.66 to 27.59° |
| Index ranges | -16 ≤ h ≤ 16, -15 ≤ k ≤ 15, -17 ≤ l ≤ 17 |
| Reflections collected | 22873 |
| Independent reflections | 4252 [R(int) = 0.0256] |
| Completeness to theta = 27.59° | 98.9 % |
| Absorption correction | Semi-empirical from equivalents |
| Max. and min. transmission | 0.7456 and 0.6459 |
| Refinement method | Full-matrix least-squares on $F^2$ |
| Data / restraints / parameters | 4252 / 1 / 246 |
| Goodness-of-fit on $F^2$ | 1.159 |
| Final R indices [I>2sigma(I)] | R1 = 0.0212, wR2 = 0.0611 |
| R indices (all data) | R1 = 0.0228, wR2 = 0.0690 |
| Absolute structure parameter | 0.030(12) |
| Largest diff. peak and hole | 0.374 and -0.397 e.$Å^{-3}$ |

Table IV-33: Refined Positional Parameters for **(*R*)-(−)-55a**, Compound 6164

| Atom | x | y | z | Ueq, Å2 |
|---|---|---|---|---|
| Cr1 | 0.216130(15) | 0.59473(2) | 0.844746(15) | 0.01760(7) |
| C1 | 0.35432(11) | 0.57262(12) | 0.77968(11) | 0.0183(3) |
| C2 | 0.35622(12) | 0.68460(14) | 0.82039(12) | 0.0199(3) |
| C3 | 0.36387(13) | 0.70279(14) | 0.92752(13) | 0.0223(3) |
| C4 | 0.36675(11) | 0.60925(16) | 0.99530(11) | 0.0248(3) |
| C5 | 0.36072(14) | 0.49890(16) | 0.95434(14) | 0.0260(4) |
| C6 | 0.35431(13) | 0.48056(14) | 0.84646(14) | 0.0225(3) |
| C7 | 0.37143(11) | 0.55924(12) | 0.67238(12) | 0.0190(3) |
| C8 | 0.35744(14) | 0.43843(15) | 0.51976(13) | 0.0282(4) |
| C9 | 0.30065(15) | 0.33590(16) | 0.45398(15) | 0.0321(4) |
| C10 | 0.14376(17) | 0.3691(2) | 0.49099(17) | 0.0430(5) |
| C11 | 0.19862(13) | 0.47059(19) | 0.56152(15) | 0.0340(4) |
| C12 | 0.49774(12) | 0.55857(13) | 0.70689(11) | 0.0197(3) |
| C13 | 0.55980(13) | 0.46133(14) | 0.75156(13) | 0.0249(3) |
| C14 | 0.67480(13) | 0.46374(16) | 0.78495(14) | 0.0308(4) |
| C15 | 0.72954(14) | 0.56261(16) | 0.77617(14) | 0.0328(4) |
| C16 | 0.66750(14) | 0.65851(17) | 0.73453(15) | 0.0317(4) |
| C17 | 0.55190(13) | 0.65719(14) | 0.69919(13) | 0.0259(3) |
| C18 | 0.85466(15) | 0.5622(2) | 0.8113(2) | 0.0518(6) |
| C19 | 0.13046(13) | 0.47004(15) | 0.84658(15) | 0.0286(3) |
| C20 | 0.10648(13) | 0.63857(16) | 0.71478(13) | 0.0275(3) |
| C21 | 0.14124(13) | 0.67826(14) | 0.91096(14) | 0.0259(3) |

| | | | | |
|---|---|---|---|---|
| N1 | 0.31994(10) | 0.45683(11) | 0.60992(10) | 0.0212(2) |
| O1 | 0.18416(10) | 0.34909(12) | 0.40756(10) | 0.0325(3) |
| O2 | 0.07897(12) | 0.39205(12) | 0.85048(15) | 0.0484(4) |
| O3 | 0.03417(11) | 0.66639(16) | 0.63594(11) | 0.0445(4) |
| O4 | 0.09438(12) | 0.73255(13) | 0.95255(13) | 0.0422(3) |

$U_{eq}=1/3[U_{11}(aa^*)^2+U_{22}(bb^*)^2+U_{33}(cc^*)^2+2U_{12}aa^*bb^*\cos\gamma+2U_{13}aa^*cc^*\cos\beta+2U_{23}bb^*cc^*\cos\alpha]$

Table IV-34: Positional Parameters for Hydrogens in **(*R*)-(−)-55a**, Compound 6164

| Atom | x | y | z | $U_{iso}$, Å$^2$ |
|---|---|---|---|---|
| H2 | 0.3524 | 0.7467 | 0.7755 | 0.027 |
| H3 | 0.3670 | 0.7766 | 0.9539 | 0.030 |
| H4 | 0.3726 | 0.6210 | 1.0667 | 0.033 |
| H5 | 0.3609 | 0.4370 | 0.9981 | 0.035 |
| H6 | 0.3501 | 0.4067 | 0.8199 | 0.030 |
| H7 | 0.3412 | 0.6264 | 0.6269 | 0.025 |
| H8a | 0.4370 | 0.4270 | 0.5489 | 0.038 |
| H8b | 0.3408 | 0.5052 | 0.4732 | 0.038 |
| H9a | 0.3278 | 0.3236 | 0.3962 | 0.043 |
| H9b | 0.3190 | 0.2692 | 0.5007 | 0.043 |
| H10a | 0.1564 | 0.3019 | 0.5366 | 0.057 |
| H10b | 0.0645 | 0.3821 | 0.4581 | 0.057 |
| H11a | 0.1801 | 0.5393 | 0.5176 | 0.045 |
| H11b | 0.1707 | 0.4787 | 0.6193 | 0.045 |
| H13 | 0.5246 | 0.3950 | 0.7591 | 0.033 |
| H14 | 0.7155 | 0.3982 | 0.8135 | 0.041 |
| H16 | 0.7030 | 0.7257 | 0.7297 | 0.042 |
| H17 | 0.5115 | 0.7229 | 0.6705 | 0.034 |
| H18a | 0.8756 | 0.5046 | 0.7715 | 0.078 |
| H18b | 0.8886 | 0.5463 | 0.8880 | 0.078 |
| H18c | 0.8788 | 0.6353 | 0.7967 | 0.078 |

Table IV-35: Refined Thermal Parameters (U's) for **(*R*)-(−)-55a**, Compound 6164

| Atom | $U_{11}$ | $U_{22}$ | $U_{33}$ | $U_{23}$ | $U_{13}$ | $U_{12}$ |
|---|---|---|---|---|---|---|
| Cr1 | 0.01573(10) | 0.01960(11) | 0.01721(10) | -0.00149(9) | 0.00601(7) | 0.00030(9) |
| C1 | 0.0133(5) | 0.0229(9) | 0.0166(6) | -0.0023(5) | 0.0032(5) | 0.0012(5) |
| C2 | 0.0167(7) | 0.0222(8) | 0.0193(7) | 0.0014(6) | 0.0050(5) | 0.0006(5) |
| C3 | 0.0189(7) | 0.0232(8) | 0.0229(8) | -0.0054(6) | 0.0059(6) | -0.0012(6) |
| C4 | 0.0193(6) | 0.0369(10) | 0.0155(6) | -0.0023(7) | 0.0036(5) | 0.0009(6) |
| C5 | 0.0225(7) | 0.0302(9) | 0.0245(8) | 0.0083(7) | 0.0080(6) | 0.0058(6) |

| | | | | | | |
|---|---|---|---|---|---|---|
| C6 | 0.0191(7) | 0.0207(8) | 0.0269(8) | 0.0000(6) | 0.0081(6) | 0.0036(5) |
| C7 | 0.0168(6) | 0.0203(6) | 0.0183(6) | 0.0006(5) | 0.0051(5) | 0.0017(5) |
| C8 | 0.0263(8) | 0.0370(9) | 0.0234(8) | -0.0104(7) | 0.0116(6) | -0.0067(6) |
| C9 | 0.0331(9) | 0.0366(10) | 0.0282(8) | -0.0114(7) | 0.0138(7) | -0.0024(7) |
| C10 | 0.0347(10) | 0.0609(13) | 0.0401(10) | -0.0281(10) | 0.0218(9) | -0.0225(10) |
| C11 | 0.0203(7) | 0.0470(11) | 0.0338(9) | -0.0204(8) | 0.0092(7) | -0.0055(7) |
| C12 | 0.0167(6) | 0.0264(7) | 0.0155(6) | -0.0036(5) | 0.0055(5) | 0.0010(5) |
| C13 | 0.0235(7) | 0.0246(7) | 0.0254(7) | -0.0029(6) | 0.0080(6) | 0.0003(6) |
| C14 | 0.0221(7) | 0.0340(9) | 0.0320(8) | -0.0049(7) | 0.0054(6) | 0.0107(7) |
| C15 | 0.0186(7) | 0.0510(11) | 0.0283(8) | -0.0132(7) | 0.0082(6) | -0.0019(6) |
| C16 | 0.0251(8) | 0.0395(10) | 0.0310(8) | -0.0034(7) | 0.0114(7) | -0.0104(7) |
| C17 | 0.0252(8) | 0.0266(8) | 0.0233(7) | 0.0031(6) | 0.0064(6) | 0.0004(6) |
| C18 | 0.0197(8) | 0.0750(18) | 0.0585(13) | -0.0204(11) | 0.0124(8) | -0.0036(8) |
| C19 | 0.0224(7) | 0.0263(8) | 0.0376(9) | -0.0023(7) | 0.0119(7) | 0.0017(6) |
| C20 | 0.0209(7) | 0.0382(8) | 0.0247(7) | -0.0006(6) | 0.0101(6) | 0.0009(6) |
| C21 | 0.0239(7) | 0.0239(7) | 0.0310(8) | -0.0024(6) | 0.0117(6) | -0.0028(6) |
| N1 | 0.0190(6) | 0.0253(6) | 0.0192(6) | -0.0051(5) | 0.0072(5) | -0.0032(5) |
| O1 | 0.0299(6) | 0.0406(7) | 0.0260(6) | -0.0146(5) | 0.0097(5) | -0.0088(5) |
| O2 | 0.0405(8) | 0.0289(7) | 0.0797(11) | -0.0010(7) | 0.0272(8) | -0.0079(6) |
| O3 | 0.0269(6) | 0.0685(10) | 0.0301(7) | 0.0093(7) | 0.0020(5) | 0.0094(7) |
| O4 | 0.0431(8) | 0.0363(7) | 0.0594(9) | -0.0140(6) | 0.0335(7) | -0.0005(6) |

The form of the anisotropic displacement parameter is:
$\exp[-2\pi^2(a^{*2}U_{11}h^2+b^{*2}U_{22}k^2+c^{*2}U_{33}l^2+2b^*c^*U_{23}kl+2a^*c^*U_{13}hl+2a^*b^*U_{12}hk)]$

Table IV-36: Bond Distances in **(*R*)-(−)-55a**, Compound 6164, Å

| | | | | | |
|---|---|---|---|---|---|
| Cr1-C21 | 1.8295(16) | Cr1-C20 | 1.8447(16) | Cr1-C19 | 1.8491(17) |
| Cr1-C5 | 2.2027(17) | Cr1-C4 | 2.2110(14) | Cr1-C3 | 2.2191(16) |
| Cr1-C2 | 2.2407(16) | Cr1-C6 | 2.2422(16) | Cr1-C1 | 2.2939(14) |
| C1-C6 | 1.398(2) | C1-C2 | 1.418(2) | C1-C7 | 1.5304(19) |
| C2-C3 | 1.402(2) | C3-C4 | 1.411(2) | C4-C5 | 1.396(3) |
| C5-C6 | 1.417(2) | C7-N1 | 1.4697(19) | C7-C12 | 1.5353(19) |
| C8-N1 | 1.4709(19) | C8-C9 | 1.506(2) | C9-O1 | 1.416(2) |
| C10-O1 | 1.416(2) | C10-C11 | 1.515(3) | C11-N1 | 1.475(2) |
| C12-C17 | 1.381(2) | C12-C13 | 1.395(2) | C13-C14 | 1.395(2) |
| C14-C15 | 1.392(3) | C15-C16 | 1.374(3) | C15-C18 | 1.519(2) |
| C16-C17 | 1.400(2) | C19-O2 | 1.149(2) | C20-O3 | 1.157(2) |
| C21-O4 | 1.159(2) | | | | |

Table IV-37: Bond Angles in **(*R*)-(−)-55a**, Compound 6164, °

| | | | | | |
|---|---|---|---|---|---|
| C21-Cr1-C20 | 86.09(7) | C21-Cr1-C19 | 88.91(7) | C20-Cr1-C19 | 88.58(8) |
| C21-Cr1-C5 | 116.01(7) | C20-Cr1-C5 | 157.47(7) | C19-Cr1-C5 | 87.58(7) |
| C21-Cr1-C4 | 88.86(7) | C20-Cr1-C4 | 158.16(7) | C19-Cr1-C4 | 112.58(7) |
| C5-Cr1-C4 | 36.87(7) | C21-Cr1-C3 | 88.83(7) | C20-Cr1-C3 | 121.42(7) |
| C19-Cr1-C3 | 149.67(7) | C5-Cr1-C3 | 66.47(6) | C4-Cr1-C3 | 37.14(6) |
| C21-Cr1-C2 | 115.64(7) | C20-Cr1-C2 | 96.88(7) | C19-Cr1-C2 | 155.09(7) |
| C5-Cr1-C2 | 78.09(6) | C4-Cr1-C2 | 66.37(6) | C3-Cr1-C2 | 36.64(6) |
| C21-Cr1-C6 | 153.13(7) | C20-Cr1-C6 | 120.77(7) | C19-Cr1-C6 | 90.89(6) |
| C5-Cr1-C6 | 37.17(6) | C4-Cr1-C6 | 66.49(6) | C3-Cr1-C6 | 77.99(6) |
| C2-Cr1-C6 | 65.43(6) | C21-Cr1-C1 | 152.04(6) | C20-Cr1-C1 | 97.03(6) |
| C19-Cr1-C1 | 118.87(6) | C5-Cr1-C1 | 65.81(6) | C4-Cr1-C1 | 77.95(5) |
| C3-Cr1-C1 | 65.78(5) | C2-Cr1-C1 | 36.43(5) | C6-Cr1-C1 | 35.87(5) |
| C6-C1-C2 | 118.71(13) | C6-C1-C7 | 123.03(13) | C2-C1-C7 | 117.49(13) |
| C6-C1-Cr1 | 70.05(8) | C2-C1-Cr1 | 69.74(8) | C7-C1-Cr1 | 140.96(9) |
| C3-C2-C1 | 120.74(15) | C3-C2-Cr1 | 70.84(9) | C1-C2-Cr1 | 73.83(9) |
| C2-C3-C4 | 120.08(15) | C2-C3-Cr1 | 72.52(9) | C4-C3-Cr1 | 71.12(9) |
| C5-C4-C3 | 119.43(13) | C5-C4-Cr1 | 71.24(9) | C3-C4-Cr1 | 71.74(9) |
| C4-C5-C6 | 120.45(15) | C4-C5-Cr1 | 71.89(9) | C6-C5-Cr1 | 72.93(9) |
| C1-C6-C5 | 120.52(15) | C1-C6-Cr1 | 74.08(8) | C5-C6-Cr1 | 69.90(9) |
| N1-C7-C1 | 114.21(12) | N1-C7-C12 | 111.87(12) | C1-C7-C12 | 104.21(11) |
| N1-C8-C9 | 110.17(13) | O1-C9-C8 | 112.01(14) | O1-C10-C11 | 112.55(15) |
| N1-C11-C10 | 111.04(15) | C17-C12-C13 | 119.12(14) | C17-C12-C7 | 119.77(13) |
| C13-C12-C7 | 121.02(14) | C12-C13-C14 | 119.95(16) | C15-C14-C13 | 121.06(16) |
| C16-C15-C14 | 118.31(15) | C16-C15-C18 | 121.77(18) | C14-C15-C18 | 119.92(18) |
| C15-C16-C17 | 121.38(16) | C12-C17-C16 | 120.14(16) | O2-C19-Cr1 | 178.23(18) |
| O3-C20-Cr1 | 176.62(14) | O4-C21-Cr1 | 179.05(16) | C7-N1-C8 | 110.82(12) |
| C7-N1-C11 | 109.90(13) | C8-N1-C11 | 107.38(12) | C10-O1-C9 | 109.77(14) |

*X-ray Structure Determination of* **62** *– Compound 6168 / 6170*

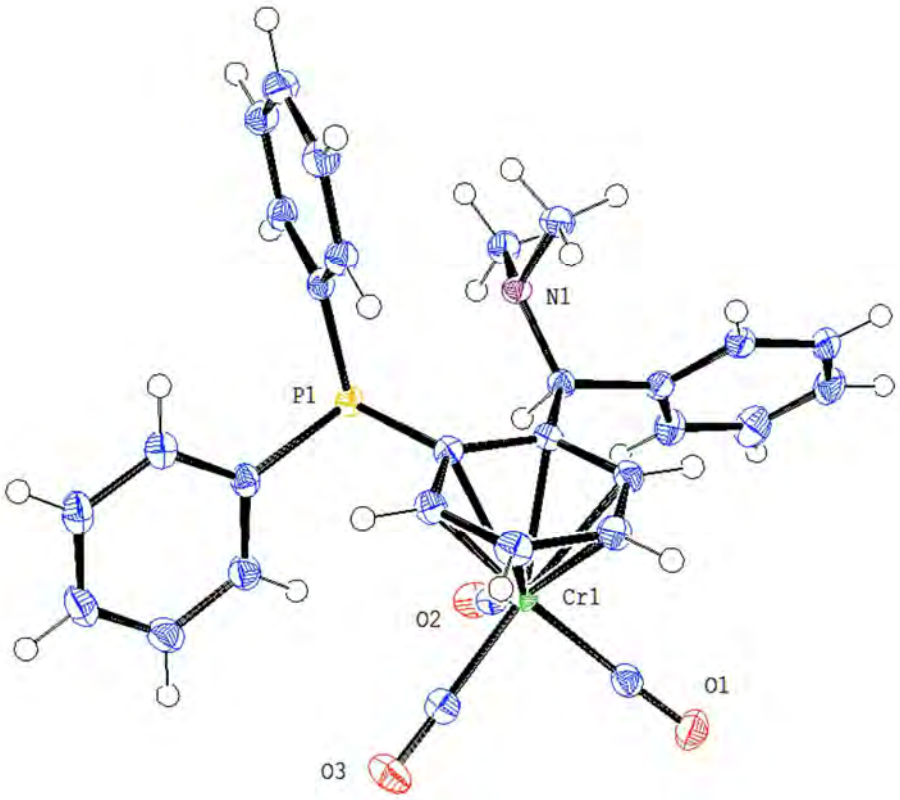


Figure IV-17: ORTEP of **62** (Compound 6168). Thermal elipsoids are at 50% probability.

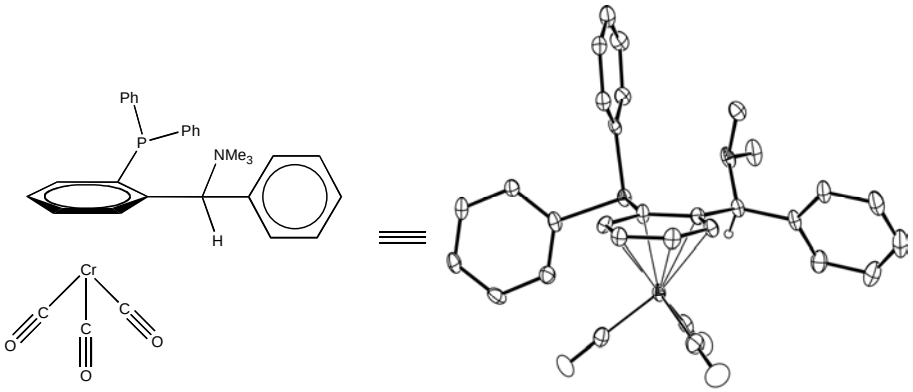


Figure IV-18: Structure of **62**, compound 6170. Non-benzylic hydrogens are omitted for clarity.

Compound 6170, $C_{30}H_{26}PNO_3Cr$, crystallizes in the monoclinic space group $P2_1/c$ (systematic absences 0k0: k=odd and h0l: l=odd) with a=12.6326(12)Å, b=22.959(2)Å, c=17.7411(17)Å, β=90.424(5)°, V=5145.3(8)Å$^3$, Z=8, and $d_{calc}$=1.372 g/cm$^3$ . X-ray intensity data were collected on a Bruker APEXII CCD area detector employing graphite-monochromated Mo-Kα radiation (λ=0.71073 Å) at a temperature of 100(1)K. Preliminary indexing was performed from a series of thirty-six 0.5° rotation frames with exposures of 30 seconds. A total of 1153 frames were collected with a crystal to detector distance of 37.6008 mm, rotation widths of 0.5° and exposures of 30 seconds (Table IV-38):

Table IV-38: Compound 6170 (**62**) data collection details.

| scan type | 2θ | ω | ϕ | χ | frames |
|---|---|---|---|---|---|
| ϕ | 19.50 | 59.55 | -11.29 | -26.26 | 739 |
| ω | 17.00 | -37.62 | -175.56 | 82.07 | 114 |
| ϕ | -23.00 | -25.79 | -321.05 | 73.66 | 300 |

Rotation frames were integrated using SAINT[7], producing a listing of unaveraged $F^2$ and $\sigma(F^2)$ values which were then passed to the SHELXTL[8] program package for further processing and structure solution. A total of 54860 reflections were measured over the ranges $1.77 \leq \theta \leq 27.61°$, $-15 \leq h \leq 16$, $-29 \leq k \leq 29$, $-21 \leq l \leq 22$ yielding 11677 unique reflections (Rint = 0.0604). The intensity data were corrected for Lorentz and polarization effects and for absorption using SADABS (minimum and maximum transmission 0.5874, 0.7456).

The structure was solved by direct methods (SHELXS-97[10]). Refinement was by full-matrix least squares based on $F^2$ using SHELXL-97. [10] All reflections were used during refinement. The weighting scheme used was $w=1/[\sigma^2(F_o^2)+ (0.0548P)^2 + 14.3472P]$ where $P = (F_o^2 + 2F_c^2)/3$. Non-hydrogen atoms were refined anisotropically and hydrogen atoms were refined using a riding model. Refinement converged to R1=0.0676 and wR2=0.1583 for 8873 observed reflections for which $F > 4\sigma(F)$ and R1=0.0930 and wR2=0.1720 and GOF =1.078 for all 11677 unique, non-zero reflections

and 655 variables.[a] The maximum $\Delta/\sigma$ in the final cycle of least squares was 0.001 and the two most prominent peaks in the final difference Fourier were +0.464 and -1.076 e/Å$^3$.

Table IV-39 lists cell information, data collection parameters, and refinement data. Final positional and equivalent isotropic thermal parameters are given in Table IV-40 and Table IV-41. Anisotropic thermal parameters are in Table IV-42. Table IV-43 and Table IV-44 list bond distances and bond angles. Figure IV-19 and Figure IV-20 are ORTEP[6] representations of the molecule with 30% probability thermal ellipsoids displayed.

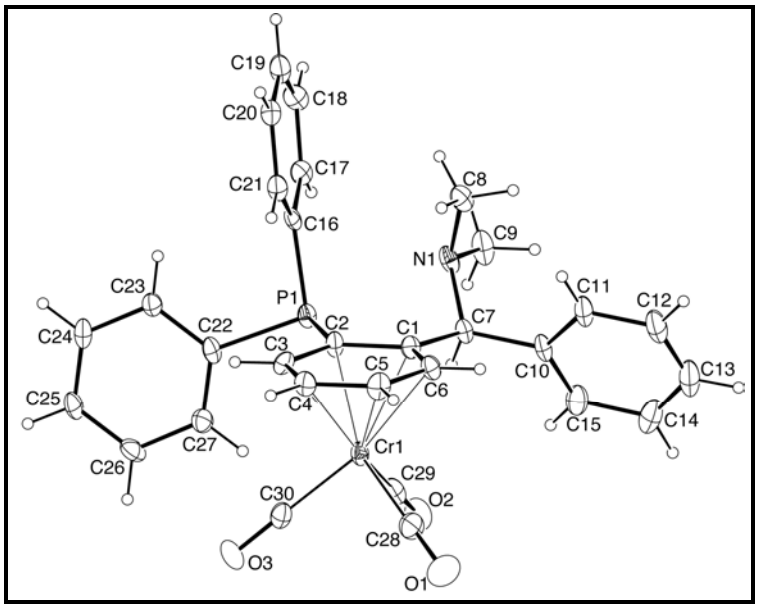


Figure IV-19: ORTEP drawing of molecule no. 1 of the asymmetric unit with 30% probability thermal ellipsoids.

[a] $R1 = \Sigma||F_o| - |F_c|| / \Sigma |F_o|$
$wR2 = [\Sigma w(F_o^2 - F_c^2)^2/\Sigma w(F_o^2)^2]^{½}$
$GOF = [\Sigma w(F_o^2 - F_c^2)^2/(n - p)]^{½}$
where n = the number of reflections and p = the number of parameters refined.

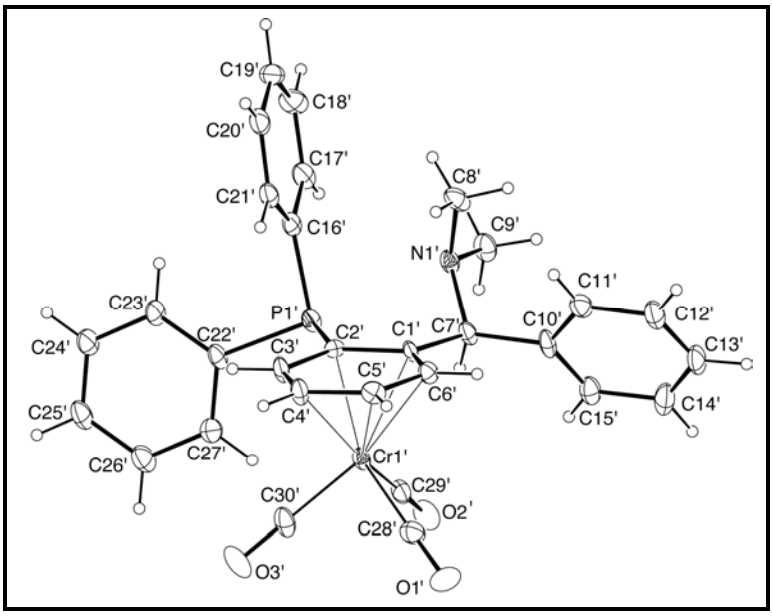


Figure IV-20: ORTEP drawing of molecule no. 2 of the asymmetric unit with 30% probability thermal ellipsoids.

Table IV-39 Summary of Structure Determination of **62**, Compound 6170

| | |
|---|---|
| Empirical formula | $C_{30}H_{26}PNO_3Cr$ |
| Formula weight | 531.49 |
| Temperature | 100(1) K |
| Wavelength | 0.71073 Å |
| Crystal system | monoclinic |
| Space group | $P2_1/c$ |
| Cell constants: | |
| a | 12.6326(12) Å |
| b | 22.959(2) Å |
| c | 17.7411(17) Å |
| β | 90.424(5)° |
| Volume | 5145.3(8) $Å^3$ |
| Z | 8 |
| Density (calculated) | 1.372 $Mg/m^3$ |
| Absorption coefficient | 0.539 $mm^{-1}$ |
| F(000) | 2208 |
| Crystal size | 0.32 x 0.25 x 0.05 $mm^3$ |
| Theta range for data collection | 1.77 to 27.61° |

| | |
|---|---|
| Index ranges | -15 ≤ h ≤ 16, -29 ≤ k ≤ 29, -21 ≤ l ≤ 22 |
| Reflections collected | 54860 |
| Independent reflections | 11677 [R(int) = 0.0604] |
| Completeness to theta = 27.61° | 97.7 % |
| Absorption correction | Semi-empirical from equivalents |
| Max. and min. transmission | 0.7456 and 0.5874 |
| Refinement method | Full-matrix least-squares on $F^2$ |
| Data / restraints / parameters | 11677 / 0 / 655 |
| Goodness-of-fit on $F^2$ | 1.078 |
| Final R indices [I>2sigma(I)] | R1 = 0.0676, wR2 = 0.1583 |
| R indices (all data) | R1 = 0.0930, wR2 = 0.1720 |
| Largest diff. peak and hole | 0.464 and -1.076 e.Å$^{-3}$ |

Table IV-40: Refined Positional Parameters for **62**, Compound 6170

| Atom | x | y | z | $U_{eq}$, Å$^2$ |
|---|---|---|---|---|
| Cr1 | 0.74037(9) | 0.65890(3) | 0.47911(4) | 0.0260(2) |
| C1 | 0.8433(5) | 0.6667(2) | 0.5820(3) | 0.0248(12) |
| C2 | 0.8417(6) | 0.6064(2) | 0.5581(3) | 0.0274(14) |
| C3 | 0.8674(5) | 0.5934(2) | 0.4836(3) | 0.0255(13) |
| C4 | 0.8965(6) | 0.6376(2) | 0.4320(3) | 0.0289(14) |
| C5 | 0.8983(6) | 0.6955(2) | 0.4558(3) | 0.0321(15) |
| C6 | 0.8724(5) | 0.7098(2) | 0.5306(3) | 0.0288(13) |
| C7 | 0.8078(5) | 0.6793(2) | 0.6621(3) | 0.0256(12) |
| C8 | 0.9839(6) | 0.6613(2) | 0.7203(4) | 0.0336(14) |
| C9 | 0.8266(7) | 0.6416(3) | 0.7895(3) | 0.0431(19) |
| C10 | 0.7917(5) | 0.7436(2) | 0.6809(3) | 0.0287(13) |
| C11 | 0.8735(7) | 0.7846(2) | 0.6837(3) | 0.0389(16) |
| C12 | 0.8533(8) | 0.8410(3) | 0.7062(4) | 0.049(2) |
| C13 | 0.7527(9) | 0.8578(3) | 0.7247(4) | 0.055(2) |
| C14 | 0.6701(7) | 0.8191(3) | 0.7203(4) | 0.050(2) |
| C15 | 0.6906(6) | 0.7612(3) | 0.6989(3) | 0.0385(16) |
| C16 | 0.9368(5) | 0.5275(2) | 0.6614(3) | 0.0251(13) |
| C17 | 0.9443(5) | 0.5043(2) | 0.7333(3) | 0.0290(13) |
| C18 | 1.0419(6) | 0.4901(3) | 0.7660(4) | 0.0370(16) |
| C19 | 1.1317(7) | 0.4983(3) | 0.7258(4) | 0.0390(16) |
| C20 | 1.1274(6) | 0.5207(2) | 0.6545(3) | 0.0306(13) |
| C21 | 1.0290(6) | 0.5354(2) | 0.6226(3) | 0.0318(14) |
| C22 | 0.7710(6) | 0.4866(2) | 0.5624(3) | 0.0278(14) |
| C23 | 0.8367(6) | 0.4384(2) | 0.5541(3) | 0.0286(13) |

| | | | | |
|---|---|---|---|---|
| C24 | 0.7985(6) | 0.3901(2) | 0.5133(3) | 0.0346(15) |
| C25 | 0.6980(6) | 0.3902(2) | 0.4808(3) | 0.0329(14) |
| C26 | 0.6344(6) | 0.4381(3) | 0.4886(4) | 0.0364(15) |
| C27 | 0.6721(6) | 0.4862(2) | 0.5305(3) | 0.0331(14) |
| C28 | 0.6844(7) | 0.7244(3) | 0.4322(4) | 0.0418(17) |
| C29 | 0.6228(6) | 0.6594(3) | 0.5382(4) | 0.0361(16) |
| C30 | 0.6674(6) | 0.6110(2) | 0.4124(3) | 0.0326(15) |
| N1 | 0.8735(5) | 0.6461(2) | 0.7143(2) | 0.0302(12) |
| O1 | 0.6497(6) | 0.7649(2) | 0.4035(3) | 0.0688(18) |
| O2 | 0.5493(5) | 0.6602(2) | 0.5756(3) | 0.0522(14) |
| O3 | 0.6194(4) | 0.58078(19) | 0.3717(3) | 0.0436(12) |
| P1 | 0.80551(14) | 0.54892(5) | 0.62589(8) | 0.0251(3) |
| Cr1' | 0.76283(9) | 0.33838(3) | -0.02722(4) | 0.0252(2) |
| C1' | 0.6618(5) | 0.3264(2) | 0.0726(3) | 0.0238(13) |
| C2' | 0.6612(5) | 0.3876(2) | 0.0522(3) | 0.0194(11) |
| C3' | 0.6341(6) | 0.4032(2) | -0.0221(3) | 0.0298(14) |
| C4' | 0.6063(6) | 0.3616(2) | -0.0768(3) | 0.0313(15) |
| C5' | 0.6043(5) | 0.3022(2) | -0.0568(3) | 0.0289(13) |
| C6' | 0.6331(5) | 0.2853(2) | 0.0180(3) | 0.0253(12) |
| C7' | 0.6986(6) | 0.3098(2) | 0.1523(3) | 0.0269(13) |
| C8' | 0.5218(6) | 0.3282(3) | 0.2075(4) | 0.0375(16) |
| C9' | 0.6807(7) | 0.3456(3) | 0.2806(3) | 0.0369(15) |
| C10' | 0.7081(6) | 0.2446(2) | 0.1686(3) | 0.0311(14) |
| C11' | 0.6236(6) | 0.2058(2) | 0.1653(3) | 0.0331(14) |
| C12' | 0.6379(7) | 0.1484(3) | 0.1864(3) | 0.0393(16) |
| C13' | 0.7335(7) | 0.1282(2) | 0.2117(4) | 0.0431(17) |
| C14' | 0.8190(7) | 0.1657(3) | 0.2141(4) | 0.0455(18) |
| C15' | 0.8062(6) | 0.2239(2) | 0.1933(3) | 0.0345(14) |
| C16' | 0.5690(6) | 0.4627(2) | 0.1583(3) | 0.0278(13) |
| C17' | 0.5611(6) | 0.4817(2) | 0.2327(3) | 0.0357(16) |
| C18' | 0.4636(6) | 0.4951(3) | 0.2612(4) | 0.0433(18) |
| C19' | 0.3728(6) | 0.4892(3) | 0.2175(4) | 0.0382(16) |
| C20' | 0.3795(6) | 0.4705(2) | 0.1439(4) | 0.0371(16) |
| C21' | 0.4754(5) | 0.4577(2) | 0.1144(3) | 0.0296(13) |
| C22' | 0.7333(6) | 0.5063(2) | 0.0674(3) | 0.0282(14) |
| C23' | 0.6721(6) | 0.5569(2) | 0.0644(3) | 0.0334(15) |
| C24' | 0.7084(6) | 0.6065(2) | 0.0279(4) | 0.0391(17) |
| C25' | 0.8053(6) | 0.6063(3) | -0.0052(3) | 0.0390(16) |
| C26' | 0.8673(7) | 0.5562(3) | -0.0023(4) | 0.0407(17) |
| C27' | 0.8325(6) | 0.5066(3) | 0.0343(3) | 0.0327(14) |
| C28' | 0.8232(6) | 0.2765(3) | -0.0761(3) | 0.0358(15) |
| C29' | 0.8798(6) | 0.3378(2) | 0.0359(3) | 0.0314(14) |

| | | | | |
|---|---|---|---|---|
| C30' | 0.8345(7) | 0.3887(3) | -0.0892(3) | 0.0373(18) |
| N1' | 0.6338(5) | 0.34307(18) | 0.2054(2) | 0.0270(11) |
| O1' | 0.8623(4) | 0.2375(2) | -0.1055(3) | 0.0509(14) |
| O2' | 0.9561(5) | 0.3365(2) | 0.0741(3) | 0.0475(13) |
| O3' | 0.8792(5) | 0.4196(2) | -0.1274(3) | 0.0525(14) |
| P1' | 0.70019(14) | 0.44188(5) | 0.12531(8) | 0.0257(3) |

$U_{eq}=1/3[U_{11}(aa^*)^2+U_{22}(bb^*)^2+U_{33}(cc^*)^2+2U_{12}aa^*bb^*\cos\gamma+2U_{13}aa^*cc^*\cos\beta+2U_{23}bb^*cc^*\cos\alpha]$

Table IV-41: Positional Parameters for Hydrogens in **62**, Compound 6170

| Atom | x | y | z | $U_{iso}$, Å$^2$ |
|---|---|---|---|---|
| H3 | 0.8654 | 0.5549 | 0.4675 | 0.034 |
| H4 | 0.9142 | 0.6281 | 0.3827 | 0.038 |
| H5 | 0.9167 | 0.7248 | 0.4222 | 0.043 |
| H6 | 0.8747 | 0.7485 | 0.5460 | 0.038 |
| H7 | 0.7373 | 0.6619 | 0.6657 | 0.034 |
| H8A | 1.0128 | 0.6657 | 0.6707 | 0.050 |
| H8B | 1.0213 | 0.6310 | 0.7466 | 0.050 |
| H8C | 0.9911 | 0.6972 | 0.7475 | 0.050 |
| H9A | 0.8219 | 0.6797 | 0.8116 | 0.065 |
| H9B | 0.8703 | 0.6172 | 0.8208 | 0.065 |
| H9C | 0.7571 | 0.6250 | 0.7854 | 0.065 |
| H11 | 0.9418 | 0.7737 | 0.6705 | 0.052 |
| H12 | 0.9083 | 0.8679 | 0.7089 | 0.065 |
| H13 | 0.7402 | 0.8958 | 0.7404 | 0.073 |
| H14 | 0.6015 | 0.8309 | 0.7312 | 0.067 |
| H15 | 0.6354 | 0.7345 | 0.6970 | 0.051 |
| H17 | 0.8827 | 0.4980 | 0.7606 | 0.039 |
| H18 | 1.0452 | 0.4753 | 0.8148 | 0.049 |
| H19 | 1.1968 | 0.4885 | 0.7470 | 0.052 |
| H20 | 1.1892 | 0.5261 | 0.6273 | 0.041 |
| H21 | 1.0264 | 0.5509 | 0.5741 | 0.042 |
| H22 | 0.7942 | 0.5189 | 0.5895 | 0.037 |
| H23 | 0.9045 | 0.4382 | 0.5751 | 0.038 |
| H24 | 0.8413 | 0.3574 | 0.5080 | 0.046 |
| H25 | 0.6742 | 0.3579 | 0.4538 | 0.044 |
| H26 | 0.5673 | 0.4389 | 0.4667 | 0.048 |
| H27 | 0.6286 | 0.5185 | 0.5366 | 0.044 |
| H3' | 0.6347 | 0.4424 | -0.0354 | 0.040 |
| H4' | 0.5894 | 0.3731 | -0.1257 | 0.042 |
| H5' | 0.5843 | 0.2742 | -0.0921 | 0.038 |
| H6' | 0.6327 | 0.2460 | 0.0308 | 0.034 |

| | | | | |
|---|---|---|---|---|
| H7' | 0.7705 | 0.3254 | 0.1575 | 0.036 |
| H8'1 | 0.5129 | 0.2919 | 0.2337 | 0.056 |
| H8'2 | 0.4949 | 0.3246 | 0.1570 | 0.056 |
| H8'3 | 0.4838 | 0.3583 | 0.2334 | 0.056 |
| H9'1 | 0.6444 | 0.3743 | 0.3100 | 0.055 |
| H9'2 | 0.7541 | 0.3560 | 0.2769 | 0.055 |
| H9'3 | 0.6745 | 0.3083 | 0.3044 | 0.055 |
| H11' | 0.5575 | 0.2185 | 0.1489 | 0.044 |
| H12' | 0.5809 | 0.1228 | 0.1833 | 0.052 |
| H13' | 0.7410 | 0.0897 | 0.2271 | 0.057 |
| H14' | 0.8851 | 0.1522 | 0.2296 | 0.061 |
| H15' | 0.8636 | 0.2492 | 0.1960 | 0.046 |
| H17' | 0.6215 | 0.4854 | 0.2626 | 0.048 |
| H18' | 0.4582 | 0.5083 | 0.3106 | 0.058 |
| H19' | 0.3071 | 0.4980 | 0.2379 | 0.051 |
| H20' | 0.3186 | 0.4667 | 0.1146 | 0.049 |
| H21' | 0.4798 | 0.4455 | 0.0646 | 0.039 |
| H22' | 0.7081 | 0.4730 | 0.0912 | 0.038 |
| H23' | 0.6060 | 0.5575 | 0.0872 | 0.044 |
| H24' | 0.6666 | 0.6398 | 0.0260 | 0.052 |
| H25' | 0.8300 | 0.6394 | -0.0296 | 0.052 |
| H26' | 0.9332 | 0.5560 | -0.0253 | 0.054 |
| H27' | 0.8753 | 0.4737 | 0.0367 | 0.043 |

Table IV-42: Refined Thermal Parameters (U's) for **62**, Compound 6170

| Atom | $U_{11}$ | $U_{22}$ | $U_{33}$ | $U_{23}$ | $U_{13}$ | $U_{12}$ |
|---|---|---|---|---|---|---|
| Cr1 | 0.0409(6) | 0.0173(4) | 0.0197(4) | 0.0001(3) | -0.0003(5) | -0.0009(4) |
| C1 | 0.027(3) | 0.021(2) | 0.026(3) | 0.000(2) | 0.004(2) | -0.005(2) |
| C2 | 0.050(4) | 0.017(2) | 0.016(2) | 0.0018(19) | 0.002(3) | 0.000(2) |
| C3 | 0.035(4) | 0.018(2) | 0.024(3) | 0.009(2) | 0.005(3) | 0.004(2) |
| C4 | 0.043(4) | 0.029(3) | 0.014(2) | 0.003(2) | 0.005(3) | 0.001(3) |
| C5 | 0.050(4) | 0.023(3) | 0.023(3) | 0.011(2) | 0.007(3) | -0.002(3) |
| C6 | 0.036(4) | 0.023(2) | 0.027(3) | -0.002(2) | 0.000(3) | -0.007(2) |
| C7 | 0.034(3) | 0.022(2) | 0.020(2) | -0.0041(18) | 0.003(2) | -0.005(2) |
| C8 | 0.044(4) | 0.026(3) | 0.031(3) | 0.004(2) | -0.002(3) | -0.011(3) |
| C9 | 0.078(6) | 0.027(3) | 0.024(3) | 0.002(2) | 0.010(3) | -0.011(3) |
| C10 | 0.046(4) | 0.019(2) | 0.021(2) | -0.0038(19) | 0.003(2) | -0.009(2) |
| C11 | 0.063(5) | 0.023(3) | 0.031(3) | -0.006(2) | 0.002(3) | -0.004(3) |
| C12 | 0.085(6) | 0.026(3) | 0.035(3) | -0.005(3) | -0.008(4) | -0.009(3) |
| C13 | 0.094(7) | 0.029(3) | 0.040(3) | -0.010(3) | 0.005(4) | 0.001(4) |

| | | | | | | |
|---|---|---|---|---|---|---|
| C14 | 0.069(5) | 0.037(4) | 0.046(4) | -0.003(3) | 0.015(4) | 0.014(4) |
| C15 | 0.053(4) | 0.031(3) | 0.032(3) | -0.002(2) | 0.012(3) | -0.001(3) |
| C16 | 0.038(4) | 0.015(2) | 0.022(3) | -0.0008(19) | -0.005(2) | -0.007(2) |
| C17 | 0.035(4) | 0.020(3) | 0.032(3) | 0.005(2) | 0.001(3) | -0.008(2) |
| C18 | 0.052(5) | 0.029(3) | 0.030(3) | 0.008(2) | -0.007(3) | -0.007(3) |
| C19 | 0.054(5) | 0.030(3) | 0.033(3) | -0.007(2) | 0.001(3) | -0.001(3) |
| C20 | 0.035(4) | 0.027(3) | 0.031(3) | -0.005(2) | 0.003(3) | -0.001(2) |
| C21 | 0.047(4) | 0.024(3) | 0.024(3) | -0.001(2) | 0.002(3) | -0.002(3) |
| C22 | 0.046(4) | 0.018(2) | 0.019(2) | 0.0017(19) | 0.002(3) | -0.009(2) |
| C23 | 0.034(3) | 0.024(3) | 0.028(3) | -0.002(2) | 0.000(3) | -0.002(2) |
| C24 | 0.054(4) | 0.020(2) | 0.029(3) | -0.005(2) | 0.008(3) | -0.001(3) |
| C25 | 0.053(4) | 0.018(2) | 0.028(3) | -0.001(2) | -0.002(3) | -0.010(3) |
| C26 | 0.034(4) | 0.035(3) | 0.039(3) | 0.000(3) | -0.011(3) | -0.011(3) |
| C27 | 0.039(4) | 0.024(3) | 0.036(3) | 0.000(2) | -0.005(3) | -0.001(2) |
| C28 | 0.054(5) | 0.026(3) | 0.045(4) | 0.005(3) | -0.009(4) | -0.001(3) |
| C29 | 0.042(4) | 0.033(3) | 0.033(3) | -0.010(2) | -0.006(3) | -0.007(3) |
| C30 | 0.043(4) | 0.028(3) | 0.027(3) | 0.000(2) | 0.005(3) | 0.005(3) |
| N1 | 0.050(3) | 0.024(2) | 0.016(2) | 0.0000(17) | 0.002(2) | -0.012(2) |
| O1 | 0.089(5) | 0.040(3) | 0.077(4) | 0.018(3) | -0.020(4) | 0.012(3) |
| O2 | 0.039(3) | 0.064(3) | 0.054(3) | -0.021(3) | 0.012(3) | -0.008(3) |
| O3 | 0.055(3) | 0.037(2) | 0.039(2) | -0.010(2) | -0.007(3) | -0.013(2) |
| P1 | 0.0377(9) | 0.0177(6) | 0.0198(6) | 0.0021(5) | 0.0023(7) | -0.0042(6) |
| Cr1' | 0.0421(6) | 0.0178(4) | 0.0158(4) | -0.0003(3) | 0.0041(4) | -0.0010(4) |
| C1' | 0.040(4) | 0.015(2) | 0.017(2) | 0.0042(18) | 0.009(2) | -0.001(2) |
| C2' | 0.018(3) | 0.019(2) | 0.021(2) | -0.0044(18) | 0.000(2) | -0.0017(19) |
| C3' | 0.049(4) | 0.017(2) | 0.023(3) | 0.006(2) | 0.003(3) | -0.001(2) |
| C4' | 0.056(5) | 0.019(3) | 0.019(3) | 0.002(2) | 0.003(3) | 0.001(3) |
| C5' | 0.032(4) | 0.030(3) | 0.025(3) | -0.006(2) | 0.001(3) | -0.004(2) |
| C6' | 0.031(3) | 0.021(2) | 0.025(3) | -0.001(2) | 0.001(3) | -0.004(2) |
| C7' | 0.043(4) | 0.018(2) | 0.020(2) | 0.0001(18) | 0.006(2) | -0.005(2) |
| C8' | 0.049(4) | 0.028(3) | 0.036(3) | -0.007(2) | 0.017(3) | -0.013(3) |
| C9' | 0.056(4) | 0.034(3) | 0.020(3) | 0.001(2) | -0.001(3) | 0.000(3) |
| C10' | 0.059(4) | 0.019(2) | 0.015(2) | 0.0028(18) | 0.000(3) | -0.004(3) |
| C11' | 0.038(4) | 0.027(3) | 0.034(3) | 0.000(2) | 0.007(3) | -0.004(2) |
| C12' | 0.061(5) | 0.024(3) | 0.033(3) | 0.004(2) | 0.006(3) | -0.004(3) |
| C13' | 0.069(5) | 0.018(2) | 0.043(3) | 0.006(2) | 0.011(4) | 0.002(3) |
| C14' | 0.069(5) | 0.031(3) | 0.036(3) | 0.008(3) | -0.003(4) | 0.012(3) |
| C15' | 0.052(4) | 0.025(3) | 0.027(3) | 0.000(2) | -0.002(3) | -0.003(3) |
| C16' | 0.043(4) | 0.015(2) | 0.026(3) | -0.0025(19) | 0.006(3) | -0.004(2) |
| C17' | 0.056(4) | 0.021(3) | 0.030(3) | -0.006(2) | 0.010(3) | -0.007(3) |
| C18' | 0.056(5) | 0.038(3) | 0.036(4) | -0.012(3) | 0.016(3) | -0.004(3) |
| C19' | 0.038(4) | 0.028(3) | 0.049(4) | -0.002(3) | 0.018(3) | -0.001(3) |

| | | | | | | |
|---|---|---|---|---|---|---|
| C20' | 0.050(4) | 0.024(3) | 0.038(3) | 0.005(2) | 0.007(3) | -0.002(3) |
| C21' | 0.045(4) | 0.020(2) | 0.024(3) | 0.001(2) | 0.005(3) | -0.003(2) |
| C22' | 0.046(4) | 0.016(2) | 0.023(2) | -0.0016(19) | 0.005(3) | -0.009(2) |
| C23' | 0.055(5) | 0.014(2) | 0.032(3) | -0.004(2) | 0.009(3) | -0.002(2) |
| C24' | 0.061(5) | 0.018(2) | 0.038(3) | -0.003(2) | 0.015(4) | -0.002(3) |
| C25' | 0.059(5) | 0.025(3) | 0.033(3) | 0.003(2) | 0.006(3) | -0.012(3) |
| C26' | 0.050(5) | 0.032(3) | 0.041(3) | 0.003(3) | 0.007(3) | -0.010(3) |
| C27' | 0.035(4) | 0.028(3) | 0.035(3) | 0.001(2) | 0.001(3) | -0.002(2) |
| C28' | 0.041(4) | 0.036(3) | 0.031(3) | -0.002(2) | 0.010(3) | 0.000(3) |
| C29' | 0.040(4) | 0.028(3) | 0.026(3) | 0.007(2) | 0.006(3) | 0.001(3) |
| C30' | 0.068(6) | 0.027(3) | 0.017(3) | 0.000(2) | 0.003(3) | -0.002(3) |
| N1' | 0.042(3) | 0.020(2) | 0.019(2) | -0.0002(16) | 0.003(2) | -0.002(2) |
| O1' | 0.056(3) | 0.034(2) | 0.064(3) | -0.018(2) | 0.021(3) | 0.008(2) |
| O2' | 0.051(4) | 0.054(3) | 0.037(3) | 0.013(2) | 0.000(3) | -0.005(3) |
| O3' | 0.071(4) | 0.053(3) | 0.034(3) | 0.014(2) | 0.010(3) | -0.017(3) |
| P1' | 0.0401(9) | 0.0172(6) | 0.0200(6) | -0.0037(5) | 0.0047(7) | -0.0052(6) |

The form of the anisotropic displacement parameter is:
$\exp[-2\pi^2(a^{*2}U_{11}h^2+b^{*2}U_{22}k^2+c^{*2}U_{33}l^2+2b^*c^*U_{23}kl+2a^*c^*U_{13}hl+2a^*b^*U_{12}hk)]$

Table IV-43: Bond Distances in **62**, Compound 6170, Å

| | | | | | |
|---|---|---|---|---|---|
| Cr1-C29 | 1.824(8) | Cr1-C30 | 1.856(7) | Cr1-C28 | 1.857(7) |
| Cr1-C3 | 2.200(6) | Cr1-C4 | 2.203(7) | Cr1-C5 | 2.206(7) |
| Cr1-C6 | 2.226(6) | Cr1-C1 | 2.241(6) | Cr1-C2 | 2.241(6) |
| C1-C6 | 1.396(7) | C1-C2 | 1.447(7) | C1-C7 | 1.520(7) |
| C2-C3 | 1.396(7) | C2-P1 | 1.846(5) | C3-C4 | 1.417(7) |
| C4-C5 | 1.395(8) | C5-C6 | 1.408(8) | C7-N1 | 1.456(8) |
| C7-C10 | 1.526(7) | C8-N1 | 1.440(9) | C9-N1 | 1.467(8) |
| C10-C15 | 1.379(9) | C10-C11 | 1.398(9) | C11-C12 | 1.381(9) |
| C12-C13 | 1.370(13) | C13-C14 | 1.373(12) | C14-C15 | 1.406(9) |
| C16-C21 | 1.371(9) | C16-C17 | 1.385(8) | C16-P1 | 1.836(7) |
| C17-C18 | 1.397(9) | C18-C19 | 1.358(10) | C19-C20 | 1.367(9) |
| C20-C21 | 1.403(9) | C22-C27 | 1.367(9) | C22-C23 | 1.391(8) |
| C22-P1 | 1.871(5) | C23-C24 | 1.409(8) | C24-C25 | 1.390(10) |
| C25-C26 | 1.370(9) | C26-C27 | 1.413(8) | C28-O1 | 1.145(8) |
| C29-O2 | 1.145(9) | C30-O3 | 1.168(8) | Cr1'-C28' | 1.834(6) |
| Cr1'-C30' | 1.837(6) | Cr1'-C29' | 1.848(8) | Cr1'-C6' | 2.199(6) |
| Cr1'-C3' | 2.206(7) | Cr1'-C1' | 2.208(5) | Cr1'-C2' | 2.223(5) |
| Cr1'-C4' | 2.223(7) | Cr1'-C5' | 2.228(7) | C1'-C6' | 1.397(7) |
| C1'-C2' | 1.451(7) | C1'-C7' | 1.533(8) | C2'-C3' | 1.406(8) |
| C2'-P1' | 1.863(5) | C3'-C4' | 1.406(8) | C4'-C5' | 1.409(8) |
| C5'-C6' | 1.428(8) | C7'-N1' | 1.467(7) | C7'-C10' | 1.528(7) |

| | | | | | |
|---|---|---|---|---|---|
| C8'-N1' | 1.457(9) | C9'-N1' | 1.457(8) | C10'-C11' | 1.392(9) |
| C10'-C15' | 1.395(10) | C11'-C12' | 1.382(8) | C12'-C13' | 1.366(11) |
| C13'-C14' | 1.381(11) | C14'-C15' | 1.396(8) | C16'-C17' | 1.394(8) |
| C16'-C21' | 1.416(9) | C16'-P1' | 1.825(7) | C17'-C18' | 1.370(10) |
| C18'-C19' | 1.386(11) | C19'-C20' | 1.378(9) | C20'-C21' | 1.355(10) |
| C22'-C27' | 1.388(9) | C22'-C23' | 1.397(8) | C22'-P1' | 1.851(5) |
| C23'-C24' | 1.389(8) | C24'-C25' | 1.362(10) | C25'-C26' | 1.392(10) |
| C26'-C27' | 1.383(8) | C28'-O1' | 1.148(7) | C29'-O2' | 1.174(8) |
| C30'-O3' | 1.136(8) | | | | |

Table IV-44: Bond Angles in **62**, Compound 6170, °

| | | | | | |
|---|---|---|---|---|---|
| C29-Cr1-C30 | 88.1(3) | C29-Cr1-C28 | 86.8(3) | C30-Cr1-C28 | 90.5(3) |
| C29-Cr1-C3 | 125.4(3) | C30-Cr1-C3 | 88.7(3) | C28-Cr1-C3 | 147.7(3) |
| C29-Cr1-C4 | 162.6(3) | C30-Cr1-C4 | 93.9(3) | C28-Cr1-C4 | 110.4(3) |
| C3-Cr1-C4 | 37.5(2) | C29-Cr1-C5 | 147.8(2) | C30-Cr1-C5 | 123.5(3) |
| C28-Cr1-C5 | 87.1(3) | C3-Cr1-C5 | 66.8(2) | C4-Cr1-C5 | 36.9(2) |
| C29-Cr1-C6 | 111.8(3) | C30-Cr1-C6 | 160.0(3) | C28-Cr1-C6 | 92.4(3) |
| C3-Cr1-C6 | 78.5(2) | C4-Cr1-C6 | 66.6(2) | C5-Cr1-C6 | 37.0(2) |
| C29-Cr1-C1 | 90.1(3) | C30-Cr1-C1 | 148.1(2) | C28-Cr1-C1 | 121.2(3) |
| C3-Cr1-C1 | 66.8(2) | C4-Cr1-C1 | 79.1(2) | C5-Cr1-C1 | 66.6(2) |
| C6-Cr1-C1 | 36.43(19) | C29-Cr1-C2 | 96.2(3) | C30-Cr1-C2 | 111.0(2) |
| C28-Cr1-C2 | 158.4(3) | C3-Cr1-C2 | 36.6(2) | C4-Cr1-C2 | 67.0(2) |
| C5-Cr1-C2 | 79.0(2) | C6-Cr1-C2 | 66.6(2) | C1-Cr1-C2 | 37.67(19) |
| C6-C1-C2 | 119.2(5) | C6-C1-C7 | 123.8(5) | C2-C1-C7 | 117.0(5) |
| C6-C1-Cr1 | 71.2(4) | C2-C1-Cr1 | 71.2(3) | C7-C1-Cr1 | 127.1(4) |
| C3-C2-C1 | 118.7(5) | C3-C2-P1 | 121.6(4) | C1-C2-P1 | 119.7(4) |
| C3-C2-Cr1 | 70.1(3) | C1-C2-Cr1 | 71.2(3) | P1-C2-Cr1 | 130.5(4) |
| C2-C3-C4 | 121.4(5) | C2-C3-Cr1 | 73.3(4) | C4-C3-Cr1 | 71.3(3) |
| C5-C4-C3 | 119.3(5) | C5-C4-Cr1 | 71.7(4) | C3-C4-Cr1 | 71.1(4) |
| C4-C5-C6 | 120.3(5) | C4-C5-Cr1 | 71.4(4) | C6-C5-Cr1 | 72.3(4) |
| C1-C6-C5 | 121.0(5) | C1-C6-Cr1 | 72.3(4) | C5-C6-Cr1 | 70.7(4) |
| N1-C7-C1 | 108.9(5) | N1-C7-C10 | 116.3(5) | C1-C7-C10 | 115.4(4) |
| C15-C10-C11 | 118.6(5) | C15-C10-C7 | 117.4(5) | C11-C10-C7 | 124.0(6) |
| C12-C11-C10 | 120.3(8) | C13-C12-C11 | 120.4(7) | C12-C13-C14 | 120.7(6) |
| C13-C14-C15 | 119.0(8) | C10-C15-C14 | 120.9(7) | C21-C16-C17 | 117.5(6) |
| C21-C16-P1 | 124.1(4) | C17-C16-P1 | 118.4(5) | C16-C17-C18 | 121.8(6) |
| C19-C18-C17 | 119.2(6) | C18-C19-C20 | 120.8(7) | C19-C20-C21 | 119.5(7) |
| C16-C21-C20 | 121.3(5) | C27-C22-C23 | 119.8(5) | C27-C22-P1 | 117.5(5) |
| C23-C22-P1 | 122.3(5) | C22-C23-C24 | 118.5(6) | C25-C24-C23 | 121.4(6) |
| C26-C25-C24 | 119.6(5) | C25-C26-C27 | 119.0(6) | C22-C27-C26 | 121.7(6) |

| | | | | | |
|---|---|---|---|---|---|
| O1-C28-Cr1 | 179.7(8) | O2-C29-Cr1 | 179.3(6) | O3-C30-Cr1 | 178.3(6) |
| C8-N1-C7 | 117.8(5) | C8-N1-C9 | 110.3(5) | C7-N1-C9 | 112.6(5) |
| C16-P1-C2 | 100.8(3) | C16-P1-C22 | 102.0(3) | C2-P1-C22 | 102.3(2) |
| C28'-Cr1'-C30' | 89.7(3) | C28'-Cr1'-C29' | 87.0(3) | C30'-Cr1'-C29' | 88.4(3) |
| C28'-Cr1'-C6' | 93.3(3) | C30'-Cr1'-C6' | 159.8(3) | C29'-Cr1'-C6' | 111.7(2) |
| C28'-Cr1'-C3' | 148.4(3) | C30'-Cr1'-C3' | 88.2(3) | C29'-Cr1'-C3' | 124.5(3) |
| C6'-Cr1'-C3' | 78.9(2) | C28'-Cr1'-C1' | 121.8(2) | C30'-Cr1'-C1' | 148.1(2) |
| C29'-Cr1'-C1' | 88.7(3) | C6'-Cr1'-C1' | 37.0(2) | C3'-Cr1'-C1' | 67.7(2) |
| C28'-Cr1'-C2' | 159.7(2) | C30'-Cr1'-C2' | 110.5(2) | C29'-Cr1'-C2' | 94.7(2) |
| C6'-Cr1'-C2' | 67.30(19) | C3'-Cr1'-C2' | 37.0(2) | C1'-Cr1'-C2' | 38.23(18) |
| C28'-Cr1'-C4' | 111.7(3) | C30'-Cr1'-C4' | 93.1(3) | C29'-Cr1'-C4' | 161.2(2) |
| C6'-Cr1'-C4' | 67.3(2) | C3'-Cr1'-C4' | 37.0(2) | C1'-Cr1'-C4' | 80.2(2) |
| C2'-Cr1'-C4' | 67.2(2) | C28'-Cr1'-C5' | 88.6(3) | C30'-Cr1'-C5' | 122.7(3) |
| C29'-Cr1'-C5' | 148.6(2) | C6'-Cr1'-C5' | 37.6(2) | C3'-Cr1'-C5' | 66.4(2) |
| C1'-Cr1'-C5' | 67.6(2) | C2'-Cr1'-C5' | 79.4(2) | C4'-Cr1'-C5' | 36.9(2) |
| C6'-C1'-C2' | 118.7(5) | C6'-C1'-C7' | 123.1(4) | C2'-C1'-C7' | 118.1(5) |
| C6'-C1'-Cr1' | 71.2(3) | C2'-C1'-Cr1' | 71.4(3) | C7'-C1'-Cr1' | 126.7(5) |
| C3'-C2'-C1' | 118.8(5) | C3'-C2'-P1' | 122.9(4) | C1'-C2'-P1' | 118.3(4) |
| C3'-C2'-Cr1' | 70.9(3) | C1'-C2'-Cr1' | 70.3(3) | P1'-C2'-Cr1' | 129.1(3) |
| C4'-C3'-C2' | 122.2(5) | C4'-C3'-Cr1' | 72.1(4) | C2'-C3'-Cr1' | 72.1(3) |
| C3'-C4'-C5' | 119.3(5) | C3'-C4'-Cr1' | 70.9(4) | C5'-C4'-Cr1' | 71.7(4) |
| C4'-C5'-C6' | 119.4(5) | C4'-C5'-Cr1' | 71.4(4) | C6'-C5'-Cr1' | 70.1(4) |
| C1'-C6'-C5' | 121.6(5) | C1'-C6'-Cr1' | 71.9(3) | C5'-C6'-Cr1' | 72.3(4) |
| N1'-C7'-C10' | 115.5(4) | N1'-C7'-C1' | 107.2(5) | C10'-C7'-C1' | 116.2(4) |
| C11'-C10'-C15' | 118.3(5) | C11'-C10'-C7' | 124.1(6) | C15'-C10'-C7' | 117.5(6) |
| C12'-C11'-C10' | 120.1(7) | C13'-C12'-C11' | 121.6(7) | C12'-C13'-C14' | 119.3(6) |
| C13'-C14'-C15' | 119.9(8) | C10'-C15'-C14' | 120.7(7) | C17'-C16'-C21' | 118.7(6) |
| C17'-C16'-P1' | 117.2(6) | C21'-C16'-P1' | 124.0(4) | C18'-C17'-C16' | 119.4(7) |
| C17'-C18'-C19' | 120.9(6) | C20'-C19'-C18' | 120.3(7) | C21'-C20'-C19' | 119.6(7) |
| C20'-C21'-C16' | 121.1(6) | C27'-C22'-C23' | 118.8(5) | C27'-C22'-P1' | 116.6(5) |
| C23'-C22'-P1' | 124.0(5) | C24'-C23'-C22' | 120.9(7) | C25'-C24'-C23' | 119.9(6) |
| C24'-C25'-C26' | 119.6(6) | C27'-C26'-C25' | 121.1(7) | C26'-C27'-C22' | 119.6(6) |
| O1'-C28'-Cr1' | 178.7(7) | O2'-C29'-Cr1' | 177.6(6) | O3'-C30'-Cr1' | 179.7(8) |
| C8'-N1'-C9' | 111.9(5) | C8'-N1'-C7' | 116.2(5) | C9'-N1'-C7' | 112.6(5) |
| C16'-P1'-C22' | 100.3(3) | C16'-P1'-C2' | 99.3(3) | C22'-P1'-C2' | 102.0(2) |

*X-ray Structure Determination of* ***63*** *– Compound 6176*

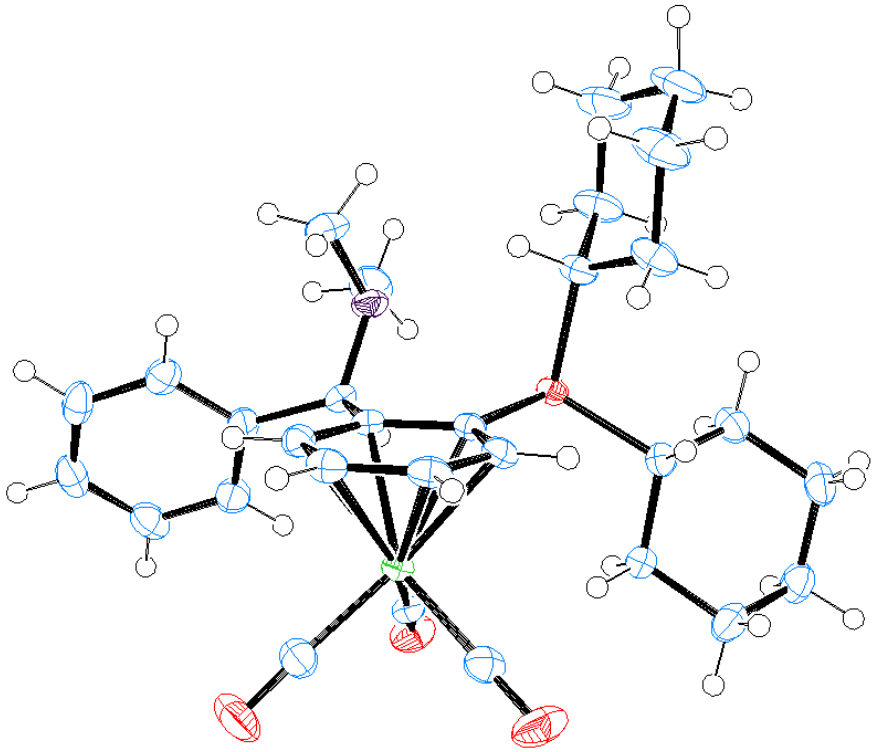

Figure IV-21: Ortep of **63**, (6176), ellipsoids at 50% probability.

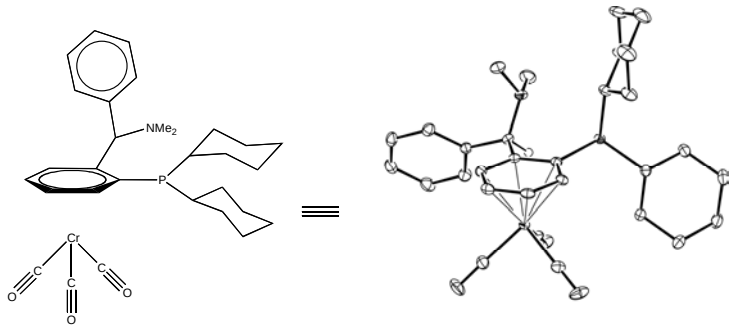


Figure IV-22: Ortep of **63**, compound 6176. Hydrogens have been omitted for clarity.

Compound 6176, $C_{30}H_{38}PNO_3Cr$, crystallizes in the triclinic space group $P\bar{1}$ with a=7.9887(5)Å, b=12.8657(8)Å, c=14.8683(8)Å, α=82.084(3)°, β=76.229(3)°, γ=72.184(3)°, V=1409.58(15)Å$^3$, Z=2, and $d_{calc}$=1.281 g/cm$^3$ . X-ray intensity data were collected on a Bruker APEXII CCD area detector

employing graphite-monochromated Mo-Kα radiation (λ=0.71073 Å) at a temperature of 143(1)K. Preliminary indexing was performed from a series of thirty-six 0.5° rotation frames with exposures of 10 seconds. A total of 6459 frames were collected with a crystal to detector distance of 60.000 mm, rotation widths of 0.5° and exposures of 10 seconds (Table IV-45):

Table IV-45: Compound 6176 (**63**) data collection details.

| scan type | 2θ | ω | ϕ | χ | frames |
|---|---|---|---|---|---|
| ϕ | 32.00 | 44.52 | -7.34 | -24.38 | 732 |
| ω | -30.50 | -48.67 | -113.49 | -76.00 | 110 |
| ω | 17.00 | 118.95 | -9.70 | -74.54 | 83 |
| ω | 37.00 | 19.02 | -158.86 | -31.86 | 270 |
| ω | -25.50 | -143.45 | -50.02 | 28.88 | 302 |
| ϕ | -20.50 | 38.83 | -243.10 | -48.25 | 460 |
| ϕ | -25.50 | 14.38 | -291.60 | 25.13 | 485 |
| ϕ | -38.00 | 203.97 | -294.06 | 59.32 | 554 |
| ϕ | -28.00 | -11.47 | -25.82 | -55.24 | 716 |
| ϕ | -35.50 | -32.13 | -192.47 | 85.83 | 399 |
| ω | -30.50 | -203.72 | 39.52 | 96.28 | 100 |
| ω | 19.50 | 121.66 | -82.44 | -97.28 | 150 |
| ω | -38.00 | -55.58 | 63.99 | -90.90 | 135 |
| ω | 39.50 | 145.10 | -135.73 | -99.82 | 139 |
| ϕ | -33.00 | 126.21 | 24.24 | -92.80 | 353 |
| ω | 24.50 | 122.57 | -139.95 | -99.10 | 173 |
| ϕ | -30.50 | 197.97 | -200.70 | 96.28 | 559 |
| ϕ | 39.50 | 188.53 | -72.44 | -97.28 | 739 |

During preliminary investigation of the crystals under the microscope, an unusual polarization pattern was noticed. The crystal grew as a non-merohedral twin; the program CELL_NOW[11] was used to index the diffraction images and to determine the twinning mechanism. The crystal was twinned by a rotation of 180° about the 100 direct axis. Rotation frames were integrated using SAINT[7], producing a listing of unaveraged F2 and σ(F2) values which were then passed to the SHELXTL[8] program package for further processing and structure solution. A total of 49113 reflections were measured over the ranges $1.67 \leq \theta \leq 27.52°$, $-9 \leq h \leq 10$, $-16 \leq k \leq 16$, $0 \leq l \leq 19$ yielding 6558 unique reflections (Rint = 0.0507). The intensity data were corrected for Lorentz and polarization effects and for absorption using TWINABS[12] (minimum and maximum transmission 0.6510, 0.7456).

The structure was solved by direct methods (SHELXS-97[10]). Refinement was by full-matrix least squares based on $F^2$ using SHELXL-97.[10] All reflections were used during refinement. The weighting scheme used was $w=1/[\sigma^2(F_o^2)+ (0.0561P)^2 + 0.0496P]$ where $P = (F_o^2 + 2F_c^2)/3$. Non-hydrogen atoms were refined anisotropically and hydrogen atoms were refined using a riding model. Refinement converged to R1=0.0317 and wR2=0.0820 for 6076 observed reflections for which $F > 4\sigma(F)$ and R1=0.0363 and wR2=0.0841 and GOF =1.073 for all 6558 unique, non-zero reflections and 329 variables.[a] The maximum $\Delta/\sigma$ in the final cycle of least squares was 0.001 and the two most prominent peaks in the final difference Fourier were +0.465 and -0.357 e/Å$^3$. The twinning parameter refined to a value of 0.3897(8).

Table IV-46 lists cell information, data collection parameters, and refinement data. Final positional and equivalent isotropic thermal parameters are given in Table IV-47 and Table IV-48. Anisotropic thermal parameters are in Table IV-49. Table IV-50 and Table IV-51 list bond distances and bond angles. Figure IV-23 is an ORTEP[6] representation of the molecule with 30% probability thermal ellipsoids displayed.

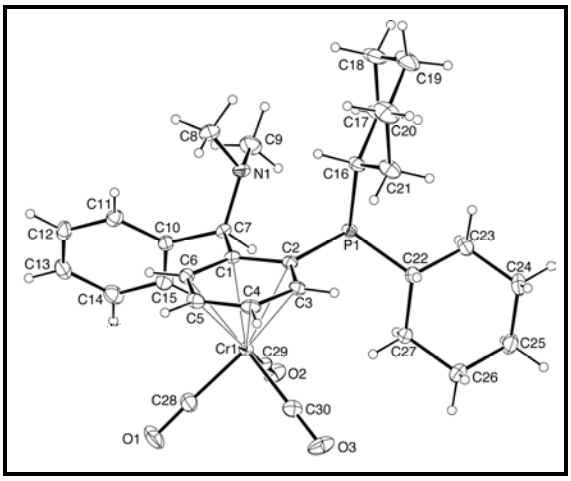


Figure IV-23: ORTEP drawing of the title compound **63** with 30% probability thermal ellipsoids.

---

[a] $R1 = \Sigma||F_o| - |F_c|| / \Sigma |F_o|$
$wR2 = [\Sigma w(F_o^2 - F_c^2)^2/\Sigma w(F_o^2)^2]^{½}$
$GOF = [\Sigma w(F_o^2 - F_c^2)^2/(n - p)]^{½}$
where n = the number of reflections and p = the number of parameters refined.

Table IV-46: Summary of Structure Determination of **63**, Compound 6176

| | |
|---|---|
| Empirical formula | $C_{30}H_{38}PNO_3Cr$ |
| Formula weight | 543.58 |
| Temperature | 143(1) K |
| Wavelength | 0.71073 Å |
| Crystal system | triclinic |
| Space group | $P\bar{1}$ |
| Cell constants: | |
| a | 7.9887(5) Å |
| b | 12.8657(8) Å |
| c | 14.8683(8) Å |
| α | 82.084(3)° |
| β | 76.229(3)° |
| γ | 72.184(3)° |
| Volume | 1409.58(15) $Å^3$ |
| Z | 2 |
| Density (calculated) | 1.281 $Mg/m^3$ |
| Absorption coefficient | 0.493 $mm^{-1}$ |
| F(000) | 576 |
| Crystal size | 0.40 x 0.18 x 0.08 $mm^3$ |
| Theta range for data collection | 1.67 to 27.52° |
| Index ranges | $-9 \le h \le 10, -16 \le k \le 16, 0 \le l \le 19$ |
| Reflections collected | 49113 |
| Independent reflections | 6558 [R(int) = 0.0507] |
| Completeness to theta = 27.52° | 99.8 % |
| Absorption correction | Semi-empirical from equivalents |
| Max. and min. transmission | 0.7456 and 0.6510 |
| Refinement method | Full-matrix least-squares on $F^2$ |
| Data / restraints / parameters | 6558 / 0 / 329 |
| Goodness-of-fit on $F^2$ | 1.073 |
| Final R indices [I>2sigma(I)] | R1 = 0.0317, wR2 = 0.0820 |
| R indices (all data) | R1 = 0.0363, wR2 = 0.0841 |
| Largest diff. peak and hole | 0.465 and -0.357 $e.Å^{-3}$ |

Table IV-47: Refined Positional Parameters for **63**, Compound 6176

| Atom | x | y | z | $U_{eq}$, Å$^2$ |
|---|---|---|---|---|
| Cr1 | 0.63070(4) | 0.47432(2) | 0.772530(17) | 0.01871(8) |
| C1 | 0.6377(3) | 0.30693(13) | 0.83712(11) | 0.0192(3) |
| C2 | 0.6078(2) | 0.31214(14) | 0.74393(12) | 0.0192(3) |
| C3 | 0.4657(3) | 0.39719(15) | 0.71833(13) | 0.0221(4) |
| C4 | 0.3489(3) | 0.47509(16) | 0.78127(14) | 0.0251(4) |
| C5 | 0.3764(3) | 0.46831(15) | 0.87059(13) | 0.0249(4) |
| C6 | 0.5213(3) | 0.38467(15) | 0.89874(12) | 0.0228(4) |
| C7 | 0.7930(3) | 0.21644(14) | 0.86563(11) | 0.0206(4) |
| C8 | 0.6003(4) | 0.0923(2) | 0.93161(16) | 0.0458(6) |
| C9 | 0.9149(4) | 0.01871(17) | 0.86514(17) | 0.0425(6) |
| C10 | 0.8527(3) | 0.23580(14) | 0.95062(12) | 0.0225(4) |
| C11 | 0.7546(3) | 0.22848(16) | 1.04197(12) | 0.0275(4) |
| C12 | 0.8171(3) | 0.24617(16) | 1.11600(13) | 0.0328(5) |
| C13 | 0.9779(3) | 0.27207(16) | 1.10143(14) | 0.0334(5) |
| C14 | 1.0761(3) | 0.27962(16) | 1.01167(14) | 0.0349(4) |
| C15 | 1.0144(3) | 0.26071(17) | 0.93732(13) | 0.0294(4) |
| C16 | 0.5748(3) | 0.12468(15) | 0.68514(14) | 0.0252(4) |
| C17 | 0.6633(3) | 0.00116(17) | 0.67647(17) | 0.0370(5) |
| C18 | 0.5224(4) | -0.06197(19) | 0.7068(2) | 0.0473(6) |
| C19 | 0.3738(4) | -0.0189(2) | 0.6518(2) | 0.0516(7) |
| C20 | 0.2879(3) | 0.1041(2) | 0.6592(2) | 0.0489(6) |
| C21 | 0.4266(3) | 0.16798(19) | 0.62931(16) | 0.0350(5) |
| C22 | 0.7573(3) | 0.26583(15) | 0.54783(11) | 0.0226(4) |
| C23 | 0.8500(3) | 0.17576(16) | 0.47936(12) | 0.0279(4) |
| C24 | 0.8816(3) | 0.22440(19) | 0.37858(13) | 0.0328(5) |
| C25 | 0.9906(3) | 0.30455(19) | 0.36586(13) | 0.0349(5) |
| C26 | 0.8996(4) | 0.39555(18) | 0.43239(13) | 0.0360(5) |
| C27 | 0.8680(3) | 0.34725(16) | 0.53260(11) | 0.0280(4) |
| C28 | 0.6563(3) | 0.57844(18) | 0.83716(13) | 0.0311(4) |
| C29 | 0.8782(3) | 0.42901(15) | 0.73983(13) | 0.0235(4) |
| C30 | 0.6210(3) | 0.57622(15) | 0.67155(13) | 0.0280(4) |
| N1 | 0.7554(3) | 0.11162(11) | 0.86551(10) | 0.0261(3) |
| O1 | 0.6762(3) | 0.64421(16) | 0.87564(12) | 0.0507(5) |
| O2 | 1.0329(2) | 0.39981(13) | 0.72137(10) | 0.0342(3) |
| O3 | 0.6140(3) | 0.63969(13) | 0.60928(11) | 0.0461(4) |
| P1 | 0.74858(6) | 0.19985(4) | 0.66797(3) | 0.01897(10) |

$U_{eq}=1/3[U_{11}(aa^*)^2+U_{22}(bb^*)^2+U_{33}(cc^*)^2+2U_{12}aa^*bb^*\cos\gamma+2U_{13}aa^*cc^*\cos\beta+2U_{23}bb^*cc^*\cos\alpha]$

Table IV-48 Positional Parameters for Hydrogens in **63**, Compound 6176

| Atom | x | y | z | $U_{iso}$, Å$^2$ |
|---|---|---|---|---|
| H3 | 0.4471 | 0.4029 | 0.6582 | 0.029 |
| H4 | 0.2547 | 0.5302 | 0.7626 | 0.033 |
| H5 | 0.2999 | 0.5186 | 0.9123 | 0.033 |
| H6 | 0.5396 | 0.3812 | 0.9587 | 0.030 |
| H7 | 0.8958 | 0.2157 | 0.8140 | 0.027 |
| H8a | 0.6316 | 0.0674 | 0.9909 | 0.069 |
| H8b | 0.5626 | 0.0377 | 0.9103 | 0.069 |
| H8c | 0.5040 | 0.1591 | 0.9373 | 0.069 |
| H9a | 0.8859 | -0.0473 | 0.8609 | 0.064 |
| H9b | 0.9567 | 0.0138 | 0.9214 | 0.064 |
| H9c | 1.0074 | 0.0284 | 0.8129 | 0.064 |
| H11 | 0.6461 | 0.2115 | 1.0529 | 0.037 |
| H12 | 0.7506 | 0.2406 | 1.1761 | 0.044 |
| H13 | 1.0194 | 0.2842 | 1.1513 | 0.044 |
| H14 | 1.1838 | 0.2974 | 1.0011 | 0.046 |
| H15 | 1.0829 | 0.2648 | 0.8775 | 0.039 |
| H16 | 0.5126 | 0.1318 | 0.7503 | 0.033 |
| H17a | 0.7240 | -0.0120 | 0.6126 | 0.049 |
| H17b | 0.7525 | -0.0248 | 0.7149 | 0.049 |
| H18a | 0.5797 | -0.1390 | 0.6975 | 0.063 |
| H18b | 0.4706 | -0.0549 | 0.7725 | 0.063 |
| H19a | 0.2825 | -0.0568 | 0.6751 | 0.069 |
| H19b | 0.4234 | -0.0337 | 0.5871 | 0.069 |
| H20a | 0.1992 | 0.1297 | 0.6205 | 0.065 |
| H20b | 0.2263 | 0.1178 | 0.7229 | 0.065 |
| H21a | 0.3683 | 0.2449 | 0.6389 | 0.047 |
| H21b | 0.4789 | 0.1612 | 0.5637 | 0.047 |
| H22 | 0.6354 | 0.3035 | 0.5384 | 0.030 |
| H23a | 0.9644 | 0.1333 | 0.4944 | 0.037 |
| H23b | 0.7759 | 0.1268 | 0.4858 | 0.037 |
| H24a | 0.9442 | 0.1658 | 0.3376 | 0.044 |
| H24b | 0.7666 | 0.2613 | 0.3618 | 0.044 |
| H25a | 1.0039 | 0.3362 | 0.3024 | 0.046 |
| H25b | 1.1096 | 0.2664 | 0.3772 | 0.046 |
| H26a | 0.9748 | 0.4439 | 0.4256 | 0.048 |
| H26b | 0.7856 | 0.4383 | 0.4171 | 0.048 |
| H27a | 0.8060 | 0.4062 | 0.5733 | 0.037 |
| H27b | 0.9832 | 0.3106 | 0.5492 | 0.037 |

Table IV-49: Refined Thermal Parameters (U's) for **63**, Compound 6176

| Atom | $U_{11}$ | $U_{22}$ | $U_{33}$ | $U_{23}$ | $U_{13}$ | $U_{12}$ |
|---|---|---|---|---|---|---|
| Cr1 | 0.01881(16) | 0.01728(13) | 0.02139(13) | -0.00128(9) | -0.00471(12) | -0.00672(13) |
| C1 | 0.0179(8) | 0.0174(7) | 0.0228(7) | 0.0009(6) | -0.0029(7) | -0.0076(7) |
| C2 | 0.0169(8) | 0.0192(8) | 0.0226(8) | -0.0017(6) | -0.0027(7) | -0.0078(7) |
| C3 | 0.0210(9) | 0.0204(9) | 0.0281(9) | -0.0019(7) | -0.0086(7) | -0.0080(8) |
| C4 | 0.0178(9) | 0.0192(8) | 0.0381(10) | 0.0000(7) | -0.0053(8) | -0.0062(8) |
| C5 | 0.0194(9) | 0.0193(8) | 0.0330(9) | -0.0056(7) | 0.0002(8) | -0.0037(8) |
| C6 | 0.0233(9) | 0.0224(9) | 0.0221(8) | -0.0017(6) | -0.0016(7) | -0.0078(8) |
| C7 | 0.0203(9) | 0.0209(8) | 0.0196(7) | 0.0021(6) | -0.0023(7) | -0.0076(7) |
| C8 | 0.0601(17) | 0.0476(14) | 0.0365(11) | -0.0002(10) | 0.0052(11) | -0.0381(14) |
| C9 | 0.0589(16) | 0.0207(10) | 0.0481(12) | 0.0021(8) | -0.0235(12) | -0.0038(11) |
| C10 | 0.0256(10) | 0.0180(8) | 0.0224(8) | 0.0009(6) | -0.0078(7) | -0.0031(8) |
| C11 | 0.0286(10) | 0.0242(9) | 0.0267(9) | 0.0023(7) | -0.0070(8) | -0.0042(8) |
| C12 | 0.0442(13) | 0.0244(10) | 0.0214(8) | -0.0028(7) | -0.0062(9) | 0.0022(10) |
| C13 | 0.0451(13) | 0.0245(10) | 0.0319(10) | -0.0068(7) | -0.0182(9) | -0.0016(9) |
| C14 | 0.0370(12) | 0.0335(10) | 0.0413(10) | -0.0042(8) | -0.0171(10) | -0.0129(10) |
| C15 | 0.0288(11) | 0.0320(10) | 0.0279(9) | -0.0015(7) | -0.0060(8) | -0.0093(9) |
| C16 | 0.0222(9) | 0.0231(9) | 0.0320(9) | -0.0076(7) | -0.0009(8) | -0.0104(8) |
| C17 | 0.0351(12) | 0.0211(10) | 0.0569(14) | -0.0101(9) | -0.0043(10) | -0.0117(9) |
| C18 | 0.0528(16) | 0.0292(11) | 0.0647(15) | -0.0119(10) | 0.0000(13) | -0.0240(12) |
| C19 | 0.0473(15) | 0.0536(15) | 0.0669(16) | -0.0243(12) | 0.0023(13) | -0.0352(14) |
| C20 | 0.0295(12) | 0.0543(15) | 0.0723(17) | -0.0162(12) | -0.0075(12) | -0.0225(12) |
| C21 | 0.0244(10) | 0.0357(11) | 0.0507(12) | -0.0095(9) | -0.0101(10) | -0.0123(9) |
| C22 | 0.0223(9) | 0.0247(9) | 0.0214(8) | -0.0021(6) | -0.0061(7) | -0.0062(8) |
| C23 | 0.0261(10) | 0.0312(10) | 0.0283(9) | -0.0086(7) | -0.0028(8) | -0.0101(8) |
| C24 | 0.0303(11) | 0.0467(12) | 0.0239(9) | -0.0110(8) | -0.0039(8) | -0.0122(10) |
| C25 | 0.0380(12) | 0.0447(12) | 0.0217(8) | -0.0023(8) | -0.0008(9) | -0.0152(11) |
| C26 | 0.0477(14) | 0.0344(10) | 0.0240(9) | 0.0033(7) | -0.0046(9) | -0.0137(11) |
| C27 | 0.0381(12) | 0.0302(9) | 0.0199(8) | -0.0006(7) | -0.0048(8) | -0.0173(9) |
| C28 | 0.0285(11) | 0.0387(11) | 0.0284(9) | -0.0094(8) | 0.0018(8) | -0.0157(10) |
| C29 | 0.0307(11) | 0.0206(9) | 0.0218(8) | 0.0033(7) | -0.0066(8) | -0.0122(8) |
| C30 | 0.0245(10) | 0.0269(8) | 0.0357(9) | 0.0009(7) | -0.0120(9) | -0.0087(9) |
| N1 | 0.0320(9) | 0.0182(7) | 0.0280(7) | 0.0025(5) | -0.0046(7) | -0.0100(7) |
| O1 | 0.0518(11) | 0.0618(11) | 0.0513(10) | -0.0312(9) | 0.0052(9) | -0.0348(10) |
| O2 | 0.0207(8) | 0.0401(8) | 0.0402(8) | 0.0059(6) | -0.0045(6) | -0.0114(7) |
| O3 | 0.0456(11) | 0.0417(8) | 0.0528(9) | 0.0247(7) | -0.0210(9) | -0.0188(9) |
| P1 | 0.0166(2) | 0.0190(2) | 0.0220(2) | -0.00243(15) | -0.00335(18) | -0.00619(18) |

The form of the anisotropic displacement parameter is:
$\exp[-2\pi^2(a^{*2}U_{11}h^2+b^{*2}U_{22}k^2+c^{*2}U_{33}l^2+2b^*c^*U_{23}kl+2a^*c^*U_{13}hl+2a^*b^*U_{12}hk)]$

Table IV-50: Bond Distances in **63**, Compound 6176, Å

| | | | | | |
|---|---|---|---|---|---|
| Cr1-C28 | 1.837(2) | Cr1-C29 | 1.844(2) | Cr1-C30 | 1.8519(18) |
| Cr1-C6 | 2.2035(18) | Cr1-C3 | 2.2134(19) | Cr1-C5 | 2.217(2) |
| Cr1-C4 | 2.2209(19) | Cr1-C1 | 2.2238(16) | Cr1-C2 | 2.2545(17) |
| C1-C6 | 1.408(2) | C1-C2 | 1.450(2) | C1-C7 | 1.518(2) |
| C2-C3 | 1.401(3) | C2-P1 | 1.8649(17) | C3-C4 | 1.422(3) |
| C4-C5 | 1.384(3) | C5-C6 | 1.421(3) | C7-N1 | 1.469(2) |
| C7-C10 | 1.527(3) | C8-N1 | 1.451(3) | C9-N1 | 1.456(3) |
| C10-C15 | 1.387(3) | C10-C11 | 1.404(3) | C11-C12 | 1.383(3) |
| C12-C13 | 1.384(4) | C13-C14 | 1.385(3) | C14-C15 | 1.389(3) |
| C16-C21 | 1.529(3) | C16-C17 | 1.539(3) | C16-P1 | 1.874(2) |
| C17-C18 | 1.532(3) | C18-C19 | 1.523(4) | C19-C20 | 1.528(4) |
| C20-C21 | 1.525(3) | C22-C27 | 1.529(3) | C22-C23 | 1.539(2) |
| C22-P1 | 1.8643(17) | C23-C24 | 1.536(3) | C24-C25 | 1.508(3) |
| C25-C26 | 1.528(3) | C26-C27 | 1.527(2) | C28-O1 | 1.152(3) |
| C29-O2 | 1.152(3) | C30-O3 | 1.147(2) | | |

Table IV-51: Bond Angles in **63**, Compound 6176, °

| | | | | | |
|---|---|---|---|---|---|
| C28-Cr1-C29 | 86.74(9) | C28-Cr1-C30 | 87.42(9) | C29-Cr1-C30 | 90.77(9) |
| C28-Cr1-C6 | 93.77(8) | C29-Cr1-C6 | 113.16(8) | C30-Cr1-C6 | 156.07(9) |
| C28-Cr1-C3 | 152.19(9) | C29-Cr1-C3 | 120.92(8) | C30-Cr1-C3 | 89.28(8) |
| C6-Cr1-C3 | 78.59(7) | C28-Cr1-C5 | 91.28(8) | C29-Cr1-C5 | 150.43(8) |
| C30-Cr1-C5 | 118.64(9) | C6-Cr1-C5 | 37.49(7) | C3-Cr1-C5 | 66.33(7) |
| C28-Cr1-C4 | 115.06(9) | C29-Cr1-C4 | 158.18(8) | C30-Cr1-C4 | 91.21(9) |
| C6-Cr1-C4 | 66.64(7) | C3-Cr1-C4 | 37.40(7) | C5-Cr1-C4 | 36.34(7) |
| C28-Cr1-C1 | 121.10(8) | C29-Cr1-C1 | 88.61(8) | C30-Cr1-C1 | 151.37(8) |
| C6-Cr1-C1 | 37.08(6) | C3-Cr1-C1 | 66.84(7) | C5-Cr1-C1 | 67.30(7) |
| C4-Cr1-C1 | 79.38(7) | C28-Cr1-C2 | 158.87(8) | C29-Cr1-C2 | 92.38(7) |
| C30-Cr1-C2 | 113.71(7) | C6-Cr1-C2 | 67.19(6) | C3-Cr1-C2 | 36.54(7) |
| C5-Cr1-C2 | 79.14(6) | C4-Cr1-C2 | 67.00(7) | C1-Cr1-C2 | 37.79(6) |
| C6-C1-C2 | 119.33(16) | C6-C1-C7 | 121.94(15) | C2-C1-C7 | 118.73(14) |
| C6-C1-Cr1 | 70.67(10) | C2-C1-Cr1 | 72.25(9) | C7-C1-Cr1 | 129.69(12) |
| C3-C2-C1 | 117.96(15) | C3-C2-P1 | 123.46(13) | C1-C2-P1 | 118.41(13) |
| C3-C2-Cr1 | 70.14(10) | C1-C2-Cr1 | 69.96(9) | P1-C2-Cr1 | 135.46(9) |
| C2-C3-C4 | 122.13(17) | C2-C3-Cr1 | 73.33(10) | C4-C3-Cr1 | 71.59(11) |
| C5-C4-C3 | 119.51(18) | C5-C4-Cr1 | 71.66(11) | C3-C4-Cr1 | 71.02(11) |
| C4-C5-C6 | 120.14(17) | C4-C5-Cr1 | 72.00(11) | C6-C5-Cr1 | 70.75(11) |
| C1-C6-C5 | 120.91(17) | C1-C6-Cr1 | 72.24(10) | C5-C6-Cr1 | 71.76(10) |
| N1-C7-C1 | 107.81(15) | N1-C7-C10 | 117.23(14) | C1-C7-C10 | 115.42(14) |

| | | | | | |
|---|---|---|---|---|---|
| C15-C10-C11 | 117.80(18) | C15-C10-C7 | 118.36(16) | C11-C10-C7 | 123.83(18) |
| C12-C11-C10 | 120.9(2) | C11-C12-C13 | 120.56(19) | C12-C13-C14 | 119.2(2) |
| C13-C14-C15 | 120.4(2) | C10-C15-C14 | 121.21(19) | C21-C16-C17 | 111.20(18) |
| C21-C16-P1 | 117.86(14) | C17-C16-P1 | 111.03(15) | C18-C17-C16 | 110.72(19) |
| C19-C18-C17 | 111.1(2) | C18-C19-C20 | 111.3(2) | C21-C20-C19 | 112.0(2) |
| C20-C21-C16 | 110.48(19) | C27-C22-C23 | 109.09(16) | C27-C22-P1 | 109.33(12) |
| C23-C22-P1 | 108.03(13) | C24-C23-C22 | 111.48(16) | C25-C24-C23 | 111.36(16) |
| C24-C25-C26 | 110.77(18) | C27-C26-C25 | 110.48(17) | C26-C27-C22 | 112.66(16) |
| O1-C28-Cr1 | 178.07(19) | O2-C29-Cr1 | 178.51(18) | O3-C30-Cr1 | 179.6(2) |
| C8-N1-C9 | 112.06(18) | C8-N1-C7 | 117.61(15) | C9-N1-C7 | 112.38(18) |
| C22-P1-C2 | 104.27(8) | C22-P1-C16 | 104.80(9) | C2-P1-C16 | 96.08(8) |

*X-ray Structure Determination of* ***64*** *– Compound 6177*

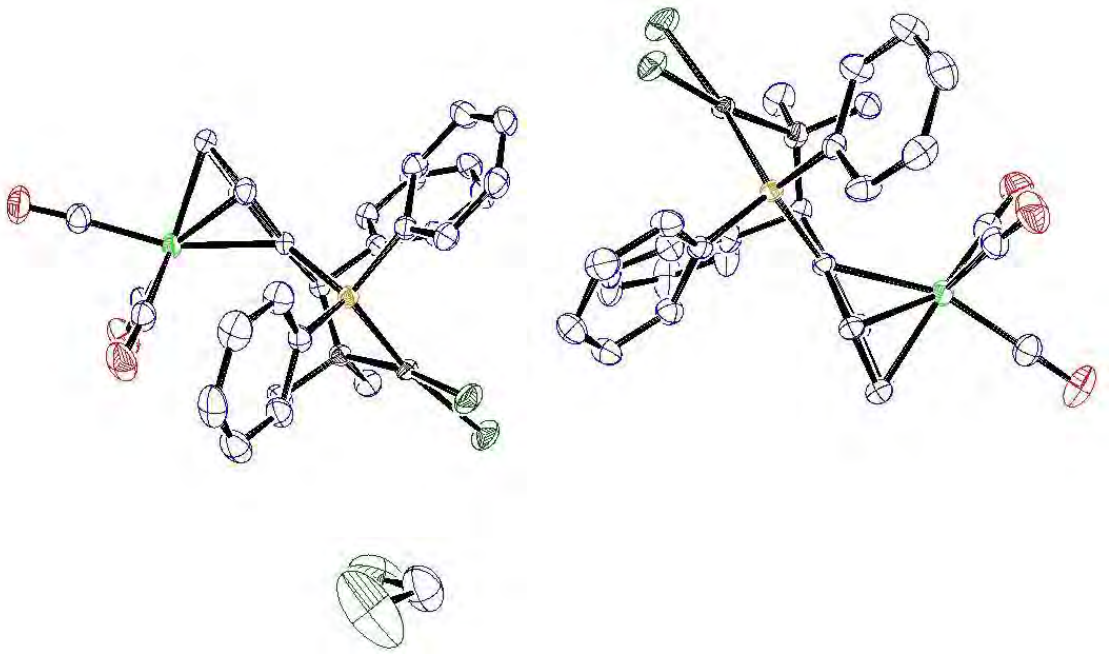

Figure IV-24: Crystal structure of **64**, Compound 6177, including co-crystallized methylene chloride in the asymmetric unit. Hydrogens are omitted for clarity. Thermal ellipsoids are at 50% probability.

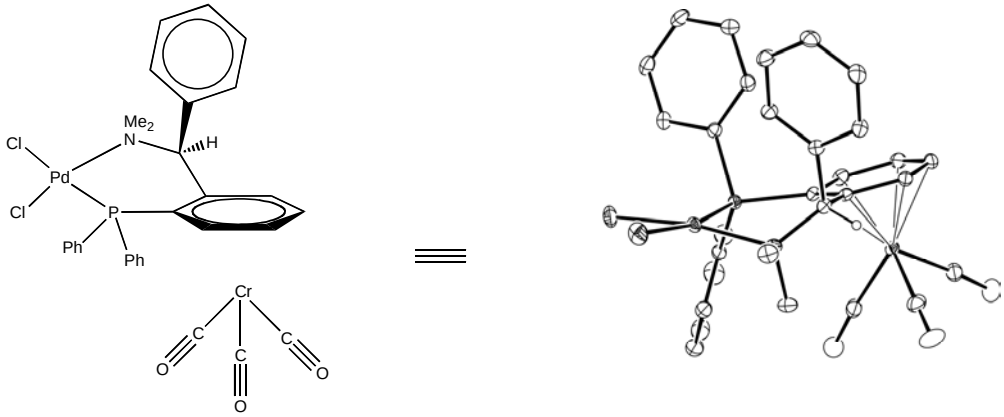


Figure IV-25: One molecule in **64** (6177), thermal ellipsoids at 30% probability. Hydrogens and methylene chloride are omitted for clarity.

Compound 6177 (**64**) $C_{30}H_{26}Cl_2CrNO_3PPd \bullet \frac{1}{2}CH_2Cl_2$, crystallizes in the monoclinic space group $P2_1/n$ (systematic absences 0k0: k=odd and h0l: h+l=odd) with a=9.7931(7)Å, b=36.732(3)Å, c=17.2211(12)Å, β=103.145(4)°, V=6032.5(8)Å$^3$, Z=8, and $d_{calc}$=1.654 g/cm$^3$ . X-ray intensity data

were collected on a Bruker APEXII CCD area detector employing graphite-monochromated Mo-Kα radiation (λ=0.71073 Å) at a temperature of 143(1)K. Preliminary indexing was performed from a series of thirty-six 0.5° rotation frames with exposures of 10 seconds. A total of 3490 frames were collected with a crystal to detector distance of 46.000 mm, rotation widths of 0.5° and exposures of 10 seconds:

Table IV-52: Compound 6177 (**64**) data collection details.

| scan type | 2θ | ω | ϕ | χ | frames |
|---|---|---|---|---|---|
| ϕ | -25.50 | -38.99 | -345.79 | 32.61 | 739 |
| ϕ | 17.00 | -21.84 | -22.08 | 69.08 | 69 |
| ω | -23.00 | -36.18 | 66.68 | -41.06 | 98 |
| ω | -20.50 | 10.56 | -199.91 | -39.24 | 147 |
| ω | 32.00 | -37.54 | 32.82 | 78.00 | 149 |
| ϕ | 32.00 | 38.60 | -71.53 | 75.13 | 242 |
| ω | -28.00 | -146.26 | -242.50 | 57.63 | 254 |
| ϕ | 27.00 | 38.57 | 21.50 | 47.18 | 288 |
| ϕ | -28.00 | -32.64 | -138.81 | 30.75 | 323 |
| ϕ | 32.00 | 128.69 | -15.62 | -35.57 | 739 |
| ϕ | 32.00 | -38.01 | -227.10 | 88.14 | 242 |
| ω | -20.50 | -50.08 | -38.09 | 98.49 | 75 |
| ω | 12.00 | -42.83 | 61.66 | 91.29 | 125 |

Rotation frames were integrated using SAINT[7], producing a listing of unaveraged $F^2$ and $\sigma(F^2)$ values which were then passed to the SHELXTL[8] program package for further processing and structure solution. A total of 160579 reflections were measured over the ranges $1.64 \leq \theta \leq 27.63°$, $-12 \leq h \leq 12$, $-47 \leq k \leq 47$, $-22 \leq l \leq 22$ yielding 13999 unique reflections (Rint = 0.0307). The intensity data were corrected for Lorentz and polarization effects and for absorption using SADABS[9] (minimum and maximum transmission 0.6517, 0.7456).

The structure was solved by direct methods (SHELXS-97[10]). Refinement was by full-matrix least squares based on $F^2$ using SHELXL-97.[10] All reflections were used during refinement. The weighting scheme used was $w=1/[\sigma^2(F_o^2)+ (0.0408P)^2 + 29.7477P]$ where $P = (F_o^2 + 2F_c^2)/3$. Non-hydrogen atoms were refined anisotropically and hydrogen atoms were refined using a riding model. Refinement converged to R1=0.0497 and wR2=0.1252 for 13161 observed reflections for which $F > 4\sigma(F)$ and R1=0.0527 and wR2=0.1269 and GOF =1.192 for all 13999 unique, non-zero reflections

and 735 variables.[a] The maximum $\Delta/\sigma$ in the final cycle of least squares was 0.003 and the two most prominent peaks in the final difference Fourier were +3.756 and -1.669 e/Å$^3$.

Table IV-53 lists cell information, data collection parameters, and refinement data. Final positional and equivalent isotropic thermal parameters are given in Table IV-54 and Table IV-55. Anisotropic thermal parameters are in Table IV-56. Table IV-57 and Table IV-58 list bond distances and bond angles. Figure IV-26 and Figure IV-27 are ORTEP[6] representations of the molecule with 30% probability thermal ellipsoids displayed.

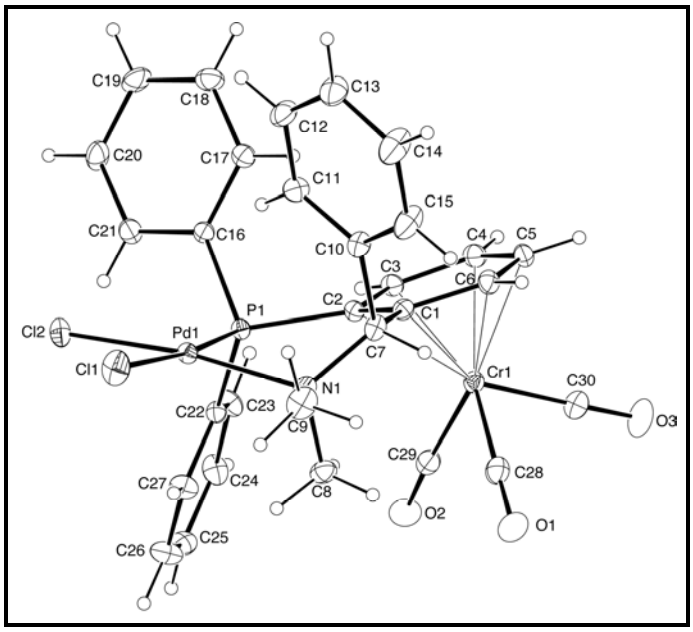


Figure IV-26: ORTEP drawing of molecule no. 1 of the asymmetric unit with 30% probability thermal ellipsoids.

[a] $R1 = \Sigma||F_o| - |F_c|| / \Sigma |F_o|$
$wR2 = [\Sigma w(F_o^2 - F_c^2)^2/\Sigma w(F_o^2)^2]^{½}$
$GOF = [\Sigma w(F_o^2 - F_c^2)^2/(n - p)]^{½}$
where n = the number of reflections and p = the number of parameters refined.

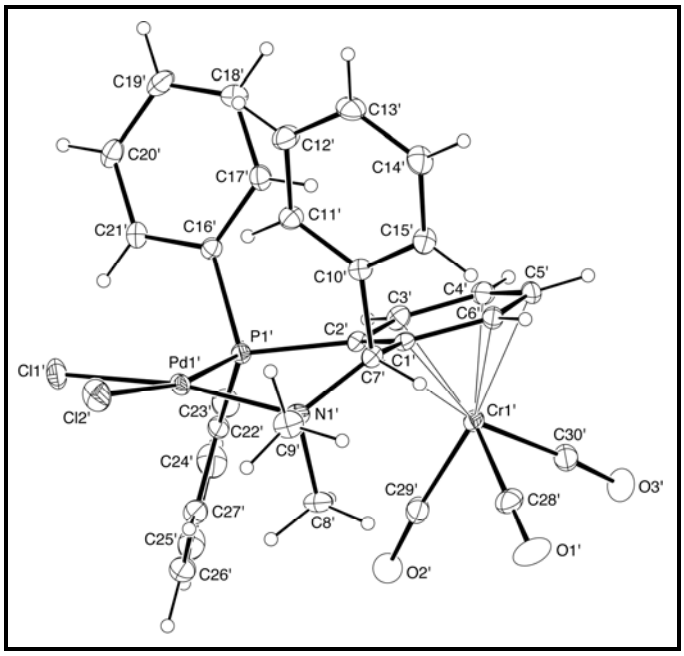


Figure IV-27: ORTEP drawing of molecule no. 2 of the asymmetric unit with 30% probability thermal ellipsoids.

Table IV-53: Summary of Structure Determination of **64**, Compound 6177

| | |
|---|---|
| Empirical formula | $C_{61}H_{54}Cl_6Cr_2N_2O_6P_2Pd_2$ |
| Formula weight | 1502.50 |
| Temperature | 143(1) K |
| Wavelength | 0.71073 Å |
| Crystal system | monoclinic |
| Space group | $P2_1/n$ |
| Cell constants: | |
| a | 9.7931(7) Å |
| b | 36.732(3) Å |
| c | 17.2211(12) Å |
| β | 103.145(4)° |
| Volume | 6032.5(8) $Å^3$ |
| Z | 4 |
| Density (calculated) | 1.654 $Mg/m^3$ |
| Absorption coefficient | 1.309 $mm^{-1}$ |
| F(000) | 3016 |
| Crystal size | 0.32 x 0.20 x 0.12 $mm^3$ |
| Theta range for data collection | 1.64 to 27.63° |

| | |
|---|---|
| Index ranges | $-12 \leq h \leq 12, -47 \leq k \leq 47, -22 \leq l \leq 22$ |
| Reflections collected | 160579 |
| Independent reflections | 13999 [R(int) = 0.0307] |
| Completeness to theta = 27.63° | 99.7 % |
| Absorption correction | Semi-empirical from equivalents |
| Max. and min. transmission | 0.7456 and 0.6517 |
| Refinement method | Full-matrix least-squares on $F^2$ |
| Data / restraints / parameters | 13999 / 0 / 735 |
| Goodness-of-fit on $F^2$ | 1.192 |
| Final R indices [I>2sigma(I)] | R1 = 0.0497, wR2 = 0.1252 |
| R indices (all data) | R1 = 0.0527, wR2 = 0.1269 |
| Largest diff. peak and hole | 3.756 and -1.669 e.Å$^{-3}$ |

Table IV-54: Refined Positional Parameters for **64**, Compound 6177

| Atom | x | y | z | $U_{eq}$, Å$^2$ |
|---|---|---|---|---|
| Pd1 | 0.56114(3) | 0.158899(8) | 0.670998(18) | 0.01752(8) |
| Cl1 | 0.80145(11) | 0.16557(4) | 0.67748(8) | 0.0388(3) |
| Cl2 | 0.53142(11) | 0.21712(3) | 0.62333(7) | 0.0267(2) |
| Cr1 | 0.17618(7) | 0.077934(18) | 0.74675(4) | 0.02058(14) |
| P1 | 0.32745(10) | 0.15850(3) | 0.65251(6) | 0.01605(18) |
| N1 | 0.5844(4) | 0.10813(10) | 0.7300(2) | 0.0223(7) |
| C1 | 0.3361(4) | 0.08107(11) | 0.6707(2) | 0.0190(7) |
| C2 | 0.2536(4) | 0.11309(10) | 0.6583(2) | 0.0174(7) |
| C3 | 0.1038(4) | 0.10962(11) | 0.6380(2) | 0.0209(8) |
| C4 | 0.0379(4) | 0.07568(12) | 0.6267(3) | 0.0249(8) |
| C5 | 0.1214(5) | 0.04377(12) | 0.6401(3) | 0.0260(9) |
| C6 | 0.2677(5) | 0.04646(11) | 0.6621(3) | 0.0237(8) |
| C7 | 0.4958(4) | 0.07776(11) | 0.6868(3) | 0.0220(8) |
| C8 | 0.5524(5) | 0.11534(13) | 0.8094(3) | 0.0278(9) |
| C9 | 0.7322(5) | 0.09438(15) | 0.7482(3) | 0.0359(11) |
| C10 | 0.5379(4) | 0.06846(12) | 0.6087(3) | 0.0234(8) |
| C11 | 0.5126(5) | 0.09218(12) | 0.5441(3) | 0.0267(9) |
| C12 | 0.5484(6) | 0.08286(14) | 0.4735(3) | 0.0337(10) |
| C13 | 0.6100(6) | 0.04974(14) | 0.4661(3) | 0.0381(11) |
| C14 | 0.6397(7) | 0.02658(15) | 0.5309(4) | 0.0496(16) |
| C15 | 0.6025(6) | 0.03556(14) | 0.6015(3) | 0.0414(13) |
| C16 | 0.2360(4) | 0.17207(11) | 0.5528(2) | 0.0192(7) |
| C17 | 0.2075(4) | 0.14662(12) | 0.4912(3) | 0.0239(8) |
| C18 | 0.1527(5) | 0.15744(14) | 0.4125(3) | 0.0314(10) |

| | | | | |
|---|---|---|---|---|
| C19 | 0.1257(5) | 0.19390(15) | 0.3958(3) | 0.0362(11) |
| C20 | 0.1506(5) | 0.21934(13) | 0.4568(3) | 0.0341(11) |
| C21 | 0.2054(5) | 0.20874(12) | 0.5347(3) | 0.0261(9) |
| C22 | 0.2672(4) | 0.18847(10) | 0.7213(2) | 0.0191(7) |
| C23 | 0.1259(4) | 0.19730(12) | 0.7110(3) | 0.0265(9) |
| C24 | 0.0822(5) | 0.21866(12) | 0.7671(3) | 0.0305(10) |
| C25 | 0.1790(5) | 0.23275(13) | 0.8309(3) | 0.0309(10) |
| C26 | 0.3196(5) | 0.22504(14) | 0.8408(3) | 0.0339(10) |
| C27 | 0.3642(4) | 0.20257(12) | 0.7861(3) | 0.0269(9) |
| C28 | 0.3078(5) | 0.06467(13) | 0.8376(3) | 0.0303(9) |
| C29 | 0.1275(5) | 0.11576(13) | 0.8085(3) | 0.0293(9) |
| C30 | 0.0526(5) | 0.04921(13) | 0.7859(3) | 0.0296(9) |
| O1 | 0.3856(4) | 0.05668(11) | 0.8957(2) | 0.0433(9) |
| O2 | 0.0964(5) | 0.13702(10) | 0.8485(2) | 0.0446(9) |
| O3 | -0.0233(4) | 0.03081(11) | 0.8093(3) | 0.0449(9) |
| Pd1' | 0.53953(3) | 0.082469(8) | 0.217642(18) | 0.01978(8) |
| Cl1' | 0.34817(11) | 0.10238(3) | 0.26056(7) | 0.0327(2) |
| Cl2' | 0.47738(13) | 0.02239(3) | 0.24554(8) | 0.0371(3) |
| Cr1' | 0.83350(7) | 0.165431(18) | 0.07867(4) | 0.02058(14) |
| P1' | 0.58848(10) | 0.14133(3) | 0.21461(6) | 0.01730(19) |
| N1' | 0.6980(4) | 0.06693(9) | 0.1582(2) | 0.0207(7) |
| C1' | 0.8540(4) | 0.12502(11) | 0.1789(2) | 0.0182(7) |
| C2' | 0.7547(4) | 0.15165(11) | 0.1879(2) | 0.0181(7) |
| C3' | 0.7933(5) | 0.18941(11) | 0.1883(2) | 0.0235(8) |
| C4' | 0.9263(5) | 0.20010(12) | 0.1822(2) | 0.0256(9) |
| C5' | 1.0264(4) | 0.17360(13) | 0.1737(2) | 0.0265(9) |
| C6' | 0.9895(4) | 0.13698(12) | 0.1706(2) | 0.0226(8) |
| C7' | 0.8406(4) | 0.08376(11) | 0.1838(2) | 0.0192(7) |
| C8' | 0.6360(5) | 0.07596(13) | 0.0726(2) | 0.0278(9) |
| C9' | 0.7215(5) | 0.02677(12) | 0.1606(3) | 0.0299(9) |
| C10' | 0.9188(4) | 0.07133(10) | 0.2672(2) | 0.0197(7) |
| C11' | 0.8636(4) | 0.07492(12) | 0.3340(2) | 0.0238(8) |
| C12' | 0.9420(5) | 0.06508(13) | 0.4088(3) | 0.0302(9) |
| C13' | 1.0774(5) | 0.05215(13) | 0.4172(3) | 0.0318(10) |
| C14' | 1.1332(5) | 0.04841(13) | 0.3513(3) | 0.0311(10) |
| C15' | 1.0539(5) | 0.05763(12) | 0.2764(3) | 0.0255(8) |
| C16' | 0.6209(4) | 0.16148(11) | 0.3129(2) | 0.0200(7) |
| C17' | 0.7578(4) | 0.16162(12) | 0.3611(3) | 0.0247(8) |
| C18' | 0.7820(5) | 0.17393(14) | 0.4390(3) | 0.0308(10) |
| C19' | 0.6728(5) | 0.18680(13) | 0.4697(3) | 0.0306(10) |
| C20' | 0.5372(5) | 0.18736(12) | 0.4224(3) | 0.0289(9) |
| C21' | 0.5110(4) | 0.17453(12) | 0.3449(3) | 0.0251(8) |

| | | | | |
|---|---|---|---|---|
| C22' | 0.4556(4) | 0.16850(12) | 0.1500(2) | 0.0223(8) |
| C23' | 0.4460(5) | 0.20589(13) | 0.1618(3) | 0.0315(10) |
| C24' | 0.3483(5) | 0.22681(15) | 0.1103(3) | 0.0393(12) |
| C25' | 0.2602(5) | 0.21057(16) | 0.0461(3) | 0.0402(12) |
| C26' | 0.2653(5) | 0.17385(17) | 0.0337(3) | 0.0393(12) |
| C27' | 0.3629(5) | 0.15199(14) | 0.0854(3) | 0.0295(9) |
| C28' | 0.8499(5) | 0.13058(14) | 0.0042(3) | 0.0318(10) |
| C29' | 0.6576(5) | 0.17539(14) | 0.0147(3) | 0.0299(9) |
| C30' | 0.8949(5) | 0.19781(14) | 0.0116(3) | 0.0303(10) |
| O1' | 0.8590(5) | 0.10958(12) | -0.0437(2) | 0.0479(10) |
| O2' | 0.5541(4) | 0.18095(13) | -0.0290(2) | 0.0494(11) |
| O3' | 0.9262(4) | 0.21750(12) | -0.0334(2) | 0.0451(10) |
| C31 | 0.1944(8) | 0.0213(3) | 0.0880(5) | 0.077(2) |
| Cl3 | 0.3140(3) | 0.00227(8) | 0.04210(15) | 0.1011(9) |
| Cl4 | 0.1067(5) | 0.05833(10) | 0.03509(18) | 0.1470(16) |

$U_{eq}=1/3[U_{11}(aa^*)^2+U_{22}(bb^*)^2+U_{33}(cc^*)^2+2U_{12}aa^*bb^*\cos\gamma+2U_{13}aa^*cc^*\cos\beta+2U_{23}bb^*cc^*\cos\alpha]$

Table IV-55: Positional Parameters for Hydrogens in **64**, Compound 6177

| Atom | x | y | z | $U_{iso}$, Å$^2$ |
|---|---|---|---|---|
| H3 | 0.0490 | 0.1306 | 0.6321 | 0.028 |
| H4 | -0.0592 | 0.0740 | 0.6107 | 0.033 |
| H5 | 0.0788 | 0.0210 | 0.6342 | 0.035 |
| H6 | 0.3213 | 0.0253 | 0.6713 | 0.032 |
| H7 | 0.5199 | 0.0563 | 0.7208 | 0.029 |
| H8a | 0.4550 | 0.1215 | 0.8023 | 0.042 |
| H8b | 0.6090 | 0.1352 | 0.8349 | 0.042 |
| H8c | 0.5725 | 0.0940 | 0.8421 | 0.042 |
| H9a | 0.7376 | 0.0721 | 0.7778 | 0.054 |
| H9b | 0.7929 | 0.1122 | 0.7793 | 0.054 |
| H9c | 0.7609 | 0.0901 | 0.6993 | 0.054 |
| H11 | 0.4710 | 0.1146 | 0.5485 | 0.036 |
| H12 | 0.5308 | 0.0990 | 0.4308 | 0.045 |
| H13 | 0.6313 | 0.0431 | 0.4181 | 0.051 |
| H14 | 0.6854 | 0.0047 | 0.5272 | 0.066 |
| H15 | 0.6211 | 0.0194 | 0.6442 | 0.055 |
| H17 | 0.2252 | 0.1221 | 0.5026 | 0.032 |
| H18 | 0.1346 | 0.1403 | 0.3717 | 0.042 |
| H19 | 0.0906 | 0.2014 | 0.3435 | 0.048 |
| H20 | 0.1303 | 0.2437 | 0.4453 | 0.045 |
| H21 | 0.2221 | 0.2260 | 0.5751 | 0.035 |
| H23 | 0.0610 | 0.1889 | 0.6666 | 0.035 |

| | | | | |
|---|---|---|---|---|
| H24 | -0.0127 | 0.2235 | 0.7618 | 0.041 |
| H25 | 0.1492 | 0.2476 | 0.8675 | 0.041 |
| H26 | 0.3845 | 0.2348 | 0.8838 | 0.045 |
| H27 | 0.4589 | 0.1970 | 0.7930 | 0.036 |
| H3' | 0.7275 | 0.2071 | 0.1927 | 0.031 |
| H4' | 0.9495 | 0.2247 | 0.1837 | 0.034 |
| H5' | 1.1161 | 0.1806 | 0.1701 | 0.035 |
| H6' | 1.0547 | 0.1197 | 0.1630 | 0.030 |
| H7' | 0.8948 | 0.0740 | 0.1473 | 0.025 |
| H8'1 | 0.6972 | 0.0674 | 0.0402 | 0.042 |
| H8'2 | 0.6249 | 0.1019 | 0.0667 | 0.042 |
| H8'3 | 0.5462 | 0.0644 | 0.0560 | 0.042 |
| H9'1 | 0.7905 | 0.0208 | 0.1310 | 0.045 |
| H9'2 | 0.6351 | 0.0146 | 0.1375 | 0.045 |
| H9'3 | 0.7540 | 0.0191 | 0.2150 | 0.045 |
| H11' | 0.7733 | 0.0840 | 0.3287 | 0.032 |
| H12' | 0.9035 | 0.0672 | 0.4532 | 0.040 |
| H13' | 1.1305 | 0.0460 | 0.4675 | 0.042 |
| H14' | 1.2241 | 0.0397 | 0.3569 | 0.041 |
| H15' | 1.0916 | 0.0546 | 0.2318 | 0.034 |
| H17' | 0.8322 | 0.1534 | 0.3405 | 0.033 |
| H18' | 0.8725 | 0.1735 | 0.4708 | 0.041 |
| H19' | 0.6898 | 0.1951 | 0.5221 | 0.041 |
| H20' | 0.4640 | 0.1964 | 0.4429 | 0.038 |
| H21' | 0.4199 | 0.1746 | 0.3139 | 0.033 |
| H23' | 0.5063 | 0.2169 | 0.2049 | 0.042 |
| H24' | 0.3421 | 0.2517 | 0.1190 | 0.052 |
| H25' | 0.1961 | 0.2248 | 0.0105 | 0.054 |
| H26' | 0.2034 | 0.1633 | -0.0095 | 0.052 |
| H27' | 0.3661 | 0.1270 | 0.0771 | 0.039 |
| H31a | 0.2419 | 0.0293 | 0.1409 | 0.102 |
| H31b | 0.1262 | 0.0029 | 0.0939 | 0.102 |

Table IV-56: Refined Thermal Parameters (U's) for **64**, Compound 6177

| Atom | $U_{11}$ | $U_{22}$ | $U_{33}$ | $U_{23}$ | $U_{13}$ | $U_{12}$ |
|---|---|---|---|---|---|---|
| Pd1 | 0.01246(13) | 0.02048(15) | 0.01989(14) | -0.00123(11) | 0.00421(10) | -0.00117(10) |
| Cl1 | 0.0140(5) | 0.0473(7) | 0.0544(7) | 0.0103(6) | 0.0065(5) | -0.0032(4) |
| Cl2 | 0.0265(5) | 0.0192(4) | 0.0376(6) | -0.0010(4) | 0.0144(4) | -0.0022(4) |
| Cr1 | 0.0215(3) | 0.0198(3) | 0.0218(3) | 0.0002(2) | 0.0078(2) | -0.0013(2) |
| P1 | 0.0132(4) | 0.0162(4) | 0.0185(4) | 0.0002(3) | 0.0030(3) | 0.0000(3) |

| | | | | | | |
|---|---|---|---|---|---|---|
| N1 | 0.0161(15) | 0.0265(18) | 0.0241(17) | 0.0050(14) | 0.0039(13) | 0.0024(13) |
| C1 | 0.0189(18) | 0.0206(18) | 0.0187(18) | 0.0005(14) | 0.0065(14) | 0.0011(14) |
| C2 | 0.0147(17) | 0.0188(18) | 0.0186(17) | -0.0006(14) | 0.0035(14) | -0.0007(14) |
| C3 | 0.0154(17) | 0.026(2) | 0.0212(19) | -0.0009(15) | 0.0033(14) | -0.0021(15) |
| C4 | 0.0205(19) | 0.030(2) | 0.025(2) | -0.0018(17) | 0.0056(16) | -0.0053(16) |
| C5 | 0.033(2) | 0.022(2) | 0.025(2) | -0.0042(16) | 0.0110(17) | -0.0091(17) |
| C6 | 0.029(2) | 0.0185(19) | 0.027(2) | -0.0016(16) | 0.0122(17) | 0.0005(16) |
| C7 | 0.0204(19) | 0.0206(19) | 0.027(2) | 0.0043(16) | 0.0095(16) | 0.0044(15) |
| C8 | 0.025(2) | 0.036(2) | 0.022(2) | 0.0027(17) | 0.0021(16) | -0.0012(18) |
| C9 | 0.018(2) | 0.044(3) | 0.044(3) | 0.011(2) | 0.0034(19) | 0.0093(19) |
| C10 | 0.0200(19) | 0.024(2) | 0.029(2) | 0.0023(16) | 0.0108(16) | 0.0033(15) |
| C11 | 0.028(2) | 0.026(2) | 0.027(2) | -0.0004(17) | 0.0068(17) | 0.0066(17) |
| C12 | 0.043(3) | 0.035(2) | 0.028(2) | 0.0038(19) | 0.017(2) | 0.001(2) |
| C13 | 0.051(3) | 0.034(3) | 0.037(3) | -0.001(2) | 0.025(2) | 0.004(2) |
| C14 | 0.077(4) | 0.031(3) | 0.054(3) | 0.010(2) | 0.041(3) | 0.025(3) |
| C15 | 0.059(3) | 0.029(2) | 0.045(3) | 0.012(2) | 0.031(3) | 0.019(2) |
| C16 | 0.0154(17) | 0.0214(19) | 0.0195(18) | 0.0011(15) | 0.0012(14) | -0.0017(14) |
| C17 | 0.0222(19) | 0.025(2) | 0.025(2) | -0.0016(16) | 0.0052(16) | -0.0004(16) |
| C18 | 0.028(2) | 0.041(3) | 0.022(2) | -0.0028(19) | 0.0005(17) | -0.0048(19) |
| C19 | 0.032(2) | 0.049(3) | 0.021(2) | 0.012(2) | -0.0068(18) | -0.005(2) |
| C20 | 0.034(2) | 0.028(2) | 0.035(3) | 0.0124(19) | -0.004(2) | -0.0030(19) |
| C21 | 0.025(2) | 0.022(2) | 0.028(2) | 0.0020(16) | -0.0017(17) | 0.0004(16) |
| C22 | 0.0196(18) | 0.0175(18) | 0.0216(18) | 0.0001(14) | 0.0073(15) | 0.0002(14) |
| C23 | 0.0180(19) | 0.025(2) | 0.035(2) | -0.0060(18) | 0.0028(17) | -0.0002(16) |
| C24 | 0.026(2) | 0.024(2) | 0.045(3) | -0.0044(19) | 0.015(2) | 0.0033(17) |
| C25 | 0.041(3) | 0.029(2) | 0.026(2) | -0.0025(18) | 0.0129(19) | 0.0101(19) |
| C26 | 0.035(2) | 0.037(3) | 0.026(2) | -0.0089(19) | -0.0008(19) | 0.006(2) |
| C27 | 0.0193(19) | 0.032(2) | 0.028(2) | -0.0038(18) | 0.0006(16) | 0.0052(17) |
| C28 | 0.030(2) | 0.030(2) | 0.033(2) | 0.0025(19) | 0.0110(19) | -0.0034(18) |
| C29 | 0.036(2) | 0.027(2) | 0.026(2) | 0.0024(18) | 0.0098(19) | -0.0007(18) |
| C30 | 0.028(2) | 0.029(2) | 0.033(2) | 0.0056(18) | 0.0094(18) | 0.0024(18) |
| O1 | 0.045(2) | 0.047(2) | 0.0330(19) | 0.0122(16) | -0.0020(16) | -0.0022(17) |
| O2 | 0.066(3) | 0.037(2) | 0.0350(19) | -0.0069(16) | 0.0212(19) | 0.0053(18) |
| O3 | 0.039(2) | 0.042(2) | 0.061(3) | 0.0155(19) | 0.0256(19) | -0.0033(16) |
| Pd1' | 0.01847(14) | 0.01954(15) | 0.02056(15) | 0.00285(11) | 0.00283(11) | -0.00395(11) |
| Cl1' | 0.0216(5) | 0.0396(6) | 0.0394(6) | 0.0040(5) | 0.0125(4) | -0.0043(4) |
| Cl2' | 0.0405(6) | 0.0257(5) | 0.0447(7) | 0.0112(5) | 0.0087(5) | -0.0084(5) |
| Cr1' | 0.0197(3) | 0.0242(3) | 0.0179(3) | 0.0053(2) | 0.0044(2) | 0.0000(2) |
| P1' | 0.0161(4) | 0.0184(5) | 0.0174(4) | 0.0010(4) | 0.0039(4) | -0.0001(4) |
| N1' | 0.0249(17) | 0.0167(16) | 0.0196(16) | -0.0008(12) | 0.0033(13) | -0.0012(13) |
| C1' | 0.0200(18) | 0.0214(18) | 0.0128(16) | 0.0019(14) | 0.0029(14) | 0.0005(15) |
| C2' | 0.0192(18) | 0.0201(18) | 0.0155(17) | 0.0015(14) | 0.0052(14) | -0.0015(14) |

| | | | | | | |
|---|---|---|---|---|---|---|
| C3' | 0.030(2) | 0.0190(19) | 0.0226(19) | 0.0025(15) | 0.0084(16) | 0.0000(16) |
| C4' | 0.029(2) | 0.026(2) | 0.0213(19) | 0.0033(16) | 0.0044(16) | -0.0086(17) |
| C5' | 0.0192(19) | 0.039(2) | 0.0202(19) | 0.0066(17) | 0.0027(15) | -0.0081(17) |
| C6' | 0.0179(18) | 0.030(2) | 0.0196(18) | 0.0054(16) | 0.0036(15) | 0.0014(16) |
| C7' | 0.0202(18) | 0.0191(18) | 0.0187(18) | 0.0017(14) | 0.0056(14) | 0.0039(14) |
| C8' | 0.033(2) | 0.028(2) | 0.0188(19) | -0.0007(16) | -0.0007(17) | -0.0014(18) |
| C9' | 0.039(2) | 0.018(2) | 0.033(2) | -0.0015(17) | 0.0070(19) | 0.0010(18) |
| C10' | 0.0239(19) | 0.0142(17) | 0.0201(18) | 0.0011(14) | 0.0036(15) | 0.0007(14) |
| C11' | 0.0226(19) | 0.026(2) | 0.0219(19) | 0.0031(16) | 0.0035(16) | 0.0059(16) |
| C12' | 0.032(2) | 0.037(2) | 0.022(2) | 0.0026(18) | 0.0051(18) | 0.0043(19) |
| C13' | 0.030(2) | 0.035(2) | 0.026(2) | 0.0073(18) | -0.0034(18) | 0.0023(19) |
| C14' | 0.023(2) | 0.034(2) | 0.035(2) | 0.0100(19) | 0.0042(18) | 0.0078(18) |
| C15' | 0.025(2) | 0.025(2) | 0.028(2) | 0.0046(17) | 0.0084(17) | 0.0038(16) |
| C16' | 0.0218(19) | 0.0194(18) | 0.0193(18) | 0.0002(14) | 0.0059(15) | -0.0008(15) |
| C17' | 0.0210(19) | 0.026(2) | 0.028(2) | -0.0011(17) | 0.0083(16) | -0.0002(16) |
| C18' | 0.029(2) | 0.039(3) | 0.022(2) | -0.0008(18) | 0.0018(17) | -0.0013(19) |
| C19' | 0.046(3) | 0.029(2) | 0.021(2) | -0.0036(17) | 0.0139(19) | -0.006(2) |
| C20' | 0.035(2) | 0.028(2) | 0.029(2) | -0.0031(18) | 0.0176(19) | -0.0017(18) |
| C21' | 0.0216(19) | 0.027(2) | 0.028(2) | 0.0009(17) | 0.0097(16) | -0.0005(16) |
| C22' | 0.0158(17) | 0.030(2) | 0.0201(19) | 0.0056(16) | 0.0029(15) | 0.0043(15) |
| C23' | 0.029(2) | 0.031(2) | 0.034(2) | 0.0050(19) | 0.0061(19) | 0.0064(18) |
| C24' | 0.032(2) | 0.038(3) | 0.047(3) | 0.015(2) | 0.008(2) | 0.013(2) |
| C25' | 0.027(2) | 0.057(3) | 0.037(3) | 0.023(2) | 0.008(2) | 0.016(2) |
| C26' | 0.023(2) | 0.068(4) | 0.026(2) | 0.004(2) | 0.0025(18) | 0.003(2) |
| C27' | 0.025(2) | 0.041(3) | 0.023(2) | 0.0013(18) | 0.0060(17) | 0.0016(19) |
| C28' | 0.033(2) | 0.040(3) | 0.022(2) | 0.0062(19) | 0.0053(18) | 0.006(2) |
| C29' | 0.026(2) | 0.038(3) | 0.027(2) | 0.0068(19) | 0.0092(18) | 0.0011(18) |
| C30' | 0.024(2) | 0.038(2) | 0.029(2) | 0.0100(19) | 0.0046(17) | 0.0005(18) |
| O1' | 0.063(3) | 0.054(2) | 0.0262(18) | -0.0057(17) | 0.0109(17) | 0.013(2) |
| O2' | 0.0283(18) | 0.084(3) | 0.0330(19) | 0.021(2) | 0.0006(15) | 0.0083(19) |
| O3' | 0.040(2) | 0.057(2) | 0.039(2) | 0.0250(18) | 0.0097(16) | -0.0046(18) |
| C31 | 0.056(4) | 0.117(7) | 0.057(4) | 0.010(5) | 0.012(3) | 0.021(4) |
| Cl3 | 0.0944(17) | 0.130(2) | 0.0785(15) | -0.0494(15) | 0.0186(12) | 0.0190(15) |
| Cl4 | 0.203(4) | 0.146(3) | 0.0797(17) | -0.0071(17) | 0.007(2) | 0.113(3) |

The form of the anisotropic displacement parameter is:
$\exp[-2\pi^2(a^{*2}U_{11}h^2+b^{*2}U_{22}k^2+c^{*2}U_{33}l^2+2b^*c^*U_{23}kl+2a^*c^*U_{13}hl+2a^*b^*U_{12}hk)]$

Table IV-57: Bond Distances in **64**, Compound 6177, Å

| | | | | | |
|---|---|---|---|---|---|
| Pd1-N1 | 2.111(4) | Pd1-P1 | 2.2378(10) | Pd1-Cl2 | 2.2854(11) |
| Pd1-Cl1 | 2.3434(11) | Cr1-C30 | 1.845(5) | Cr1-C28 | 1.851(5) |

| | | | | | |
|---|---|---|---|---|---|
| Cr1-C29 | 1.876(5) | Cr1-C3 | 2.183(4) | Cr1-C5 | 2.189(4) |
| Cr1-C4 | 2.201(4) | Cr1-C6 | 2.204(4) | Cr1-C2 | 2.256(4) |
| Cr1-C1 | 2.262(4) | P1-C22 | 1.812(4) | P1-C16 | 1.816(4) |
| P1-C2 | 1.830(4) | N1-C8 | 1.496(6) | N1-C9 | 1.498(5) |
| N1-C7 | 1.502(6) | C1-C2 | 1.416(5) | C1-C6 | 1.429(6) |
| C1-C7 | 1.530(5) | C2-C3 | 1.435(5) | C3-C4 | 1.397(6) |
| C4-C5 | 1.418(6) | C5-C6 | 1.400(6) | C7-C10 | 1.532(6) |
| C10-C15 | 1.382(6) | C10-C11 | 1.390(6) | C11-C12 | 1.383(6) |
| C12-C13 | 1.377(7) | C13-C14 | 1.381(8) | C14-C15 | 1.385(7) |
| C16-C17 | 1.394(6) | C16-C21 | 1.400(6) | C17-C18 | 1.397(6) |
| C18-C19 | 1.382(7) | C19-C20 | 1.385(7) | C20-C21 | 1.382(6) |
| C22-C27 | 1.390(6) | C22-C23 | 1.393(6) | C23-C24 | 1.386(6) |
| C24-C25 | 1.378(7) | C25-C26 | 1.378(7) | C26-C27 | 1.395(6) |
| C28-O1 | 1.149(6) | C29-O2 | 1.128(6) | C30-O3 | 1.144(6) |
| Pd1'-N1' | 2.122(4) | Pd1'-P1' | 2.2180(10) | Pd1'-Cl1' | 2.2853(11) |
| Pd1'-Cl2' | 2.3672(11) | Cr1'-C28' | 1.844(5) | Cr1'-C30' | 1.851(5) |
| Cr1'-C29' | 1.858(5) | Cr1'-C3' | 2.198(4) | Cr1'-C6' | 2.199(4) |
| Cr1'-C4' | 2.211(4) | Cr1'-C5' | 2.220(4) | Cr1'-C2' | 2.247(4) |
| Cr1'-C1' | 2.250(4) | P1'-C22' | 1.808(4) | P1'-C16' | 1.808(4) |
| P1'-C2' | 1.829(4) | N1'-C9' | 1.492(5) | N1'-C8' | 1.499(5) |
| N1'-C7' | 1.499(5) | C1'-C2' | 1.412(5) | C1'-C6' | 1.436(5) |
| C1'-C7' | 1.525(5) | C2'-C3' | 1.437(5) | C3'-C4' | 1.387(6) |
| C4'-C5' | 1.413(7) | C5'-C6' | 1.391(6) | C7'-C10' | 1.534(5) |
| C10'-C11' | 1.385(6) | C10'-C15' | 1.390(6) | C11'-C12' | 1.389(6) |
| C12'-C13' | 1.385(7) | C13'-C14' | 1.374(7) | C14'-C15' | 1.389(6) |
| C16'-C21' | 1.401(6) | C16'-C17' | 1.407(6) | C17'-C18' | 1.384(6) |
| C18'-C19' | 1.381(7) | C19'-C20' | 1.391(7) | C20'-C21' | 1.383(6) |
| C22'-C23' | 1.394(6) | C22'-C27' | 1.404(6) | C23'-C24' | 1.381(6) |
| C24'-C25' | 1.374(8) | C25'-C26' | 1.368(8) | C26'-C27' | 1.402(7) |
| C28'-O1' | 1.148(6) | C29'-O2' | 1.135(6) | C30'-O3' | 1.152(6) |
| C31-Cl3 | 1.704(8) | C31-Cl4 | 1.751(9) | | |

Table IV-58: Bond Angles in **64**, Compound 6177, °

| | | | | | |
|---|---|---|---|---|---|
| N1-Pd1-P1 | 93.30(10) | N1-Pd1-Cl2 | 172.08(10) | P1-Pd1-Cl2 | 84.98(4) |
| N1-Pd1-Cl1 | 94.14(10) | P1-Pd1-Cl1 | 172.29(4) | Cl2-Pd1-Cl1 | 87.92(4) |
| C30-Cr1-C28 | 86.0(2) | C30-Cr1-C29 | 86.8(2) | C28-Cr1-C29 | 86.2(2) |
| C30-Cr1-C3 | 120.43(18) | C28-Cr1-C3 | 153.30(18) | C29-Cr1-C3 | 90.96(18) |
| C30-Cr1-C5 | 85.58(19) | C28-Cr1-C5 | 123.3(2) | C29-Cr1-C5 | 148.8(2) |
| C3-Cr1-C5 | 67.37(16) | C30-Cr1-C4 | 90.41(19) | C28-Cr1-C4 | 160.95(19) |
| C29-Cr1-C4 | 112.27(19) | C3-Cr1-C4 | 37.16(15) | C5-Cr1-C4 | 37.68(17) |

| | | | | | |
|---|---|---|---|---|---|
| C30-Cr1-C6 | 109.92(19) | C28-Cr1-C6 | 96.37(19) | C29-Cr1-C6 | 163.20(18) |
| C3-Cr1-C6 | 79.25(16) | C5-Cr1-C6 | 37.15(16) | C4-Cr1-C6 | 67.34(16) |
| C30-Cr1-C2 | 157.42(18) | C28-Cr1-C2 | 116.40(17) | C29-Cr1-C2 | 97.27(17) |
| C3-Cr1-C2 | 37.68(13) | C5-Cr1-C2 | 79.47(15) | C4-Cr1-C2 | 67.46(15) |
| C6-Cr1-C2 | 66.68(15) | C30-Cr1-C1 | 147.04(18) | C28-Cr1-C1 | 93.53(18) |
| C29-Cr1-C1 | 126.11(18) | C3-Cr1-C1 | 66.95(14) | C5-Cr1-C1 | 67.23(15) |
| C4-Cr1-C1 | 79.46(15) | C6-Cr1-C1 | 37.30(14) | C2-Cr1-C1 | 36.52(14) |
| C22-P1-C16 | 106.71(19) | C22-P1-C2 | 109.08(18) | C16-P1-C2 | 100.71(18) |
| C22-P1-Pd1 | 112.17(13) | C16-P1-Pd1 | 113.66(13) | C2-P1-Pd1 | 113.71(13) |
| C8-N1-C9 | 105.2(3) | C8-N1-C7 | 111.5(3) | C9-N1-C7 | 106.0(3) |
| C8-N1-Pd1 | 105.2(3) | C9-N1-Pd1 | 113.1(3) | C7-N1-Pd1 | 115.5(2) |
| C2-C1-C6 | 119.0(4) | C2-C1-C7 | 128.2(4) | C6-C1-C7 | 112.6(3) |
| C2-C1-Cr1 | 71.5(2) | C6-C1-Cr1 | 69.2(2) | C7-C1-Cr1 | 134.9(3) |
| C1-C2-C3 | 118.7(4) | C1-C2-P1 | 123.1(3) | C3-C2-P1 | 117.5(3) |
| C1-C2-Cr1 | 72.0(2) | C3-C2-Cr1 | 68.4(2) | P1-C2-Cr1 | 139.2(2) |
| C4-C3-C2 | 121.8(4) | C4-C3-Cr1 | 72.1(2) | C2-C3-Cr1 | 73.9(2) |
| C3-C4-C5 | 119.0(4) | C3-C4-Cr1 | 70.7(2) | C5-C4-Cr1 | 70.7(2) |
| C6-C5-C4 | 120.2(4) | C6-C5-Cr1 | 72.0(2) | C4-C5-Cr1 | 71.6(2) |
| C5-C6-C1 | 121.2(4) | C5-C6-Cr1 | 70.8(2) | C1-C6-Cr1 | 73.5(2) |
| N1-C7-C1 | 118.8(3) | N1-C7-C10 | 111.1(3) | C1-C7-C10 | 109.1(3) |
| C15-C10-C11 | 118.6(4) | C15-C10-C7 | 119.6(4) | C11-C10-C7 | 121.8(4) |
| C12-C11-C10 | 120.9(4) | C13-C12-C11 | 120.3(5) | C12-C13-C14 | 119.1(5) |
| C13-C14-C15 | 120.9(5) | C10-C15-C14 | 120.3(5) | C17-C16-C21 | 118.7(4) |
| C17-C16-P1 | 120.4(3) | C21-C16-P1 | 120.6(3) | C16-C17-C18 | 120.9(4) |
| C19-C18-C17 | 119.3(4) | C18-C19-C20 | 120.2(4) | C21-C20-C19 | 120.6(4) |
| C20-C21-C16 | 120.3(4) | C27-C22-C23 | 119.5(4) | C27-C22-P1 | 119.1(3) |
| C23-C22-P1 | 121.3(3) | C24-C23-C22 | 119.9(4) | C25-C24-C23 | 120.1(4) |
| C26-C25-C24 | 120.6(4) | C25-C26-C27 | 119.7(4) | C22-C27-C26 | 120.0(4) |
| O1-C28-Cr1 | 177.3(5) | O2-C29-Cr1 | 176.0(4) | O3-C30-Cr1 | 178.6(5) |
| N1'-Pd1'-P1' | 93.73(9) | N1'-Pd1'-Cl1' | 170.18(10) | P1'-Pd1'-Cl1' | 83.87(4) |
| N1'-Pd1'-Cl2' | 95.58(10) | P1'-Pd1'-Cl2' | 168.66(4) | Cl1'-Pd1'-Cl2' | 88.00(5) |
| C28'-Cr1'-C30' | 85.4(2) | C28'-Cr1'-C29' | 86.6(2) | C30'-Cr1'-C29' | 83.8(2) |
| C28'-Cr1'-C3' | 159.38(19) | C30'-Cr1'-C3' | 115.17(19) | C29'-Cr1'-C3' | 96.15(19) |
| C28'-Cr1'-C6' | 90.82(18) | C30'-Cr1'-C6' | 118.92(18) | C29'-Cr1'-C6' | 156.85(18) |
| C3'-Cr1'-C6' | 78.65(16) | C28'-Cr1'-C4' | 151.09(19) | C30'-Cr1'-C4' | 90.04(19) |
| C29'-Cr1'-C4' | 121.4(2) | C3'-Cr1'-C4' | 36.67(16) | C6'-Cr1'-C4' | 66.57(16) |
| C28'-Cr1'-C5' | 114.3(2) | C30'-Cr1'-C5' | 91.72(18) | C29'-Cr1'-C5' | 158.3(2) |
| C3'-Cr1'-C5' | 66.55(17) | C6'-Cr1'-C5' | 36.68(16) | C4'-Cr1'-C5' | 37.20(17) |
| C28'-Cr1'-C2' | 121.74(18) | C30'-Cr1'-C2' | 152.77(19) | C29'-Cr1'-C2' | 95.28(17) |
| C3'-Cr1'-C2' | 37.71(14) | C6'-Cr1'-C2' | 66.73(15) | C4'-Cr1'-C2' | 67.13(15) |
| C5'-Cr1'-C2' | 79.08(15) | C28'-Cr1'-C1' | 93.93(18) | C30'-Cr1'-C1' | 156.56(17) |
| C29'-Cr1'-C1' | 119.56(17) | C3'-Cr1'-C1' | 66.91(15) | C6'-Cr1'-C1' | 37.64(14) |

| | | | | | |
|---|---|---|---|---|---|
| C4'-Cr1'-C1' | 79.22(15) | C5'-Cr1'-C1' | 67.15(15) | C2'-Cr1'-C1' | 36.59(14) |
| C22'-P1'-C16' | 107.39(19) | C22'-P1'-C2' | 106.74(18) | C16'-P1'-C2' | 100.02(18) |
| C22'-P1'-Pd1' | 115.05(15) | C16'-P1'-Pd1' | 111.70(13) | C2'-P1'-Pd1' | 114.66(13) |
| C9'-N1'-C8' | 105.7(3) | C9'-N1'-C7' | 105.8(3) | C8'-N1'-C7' | 109.9(3) |
| C9'-N1'-Pd1' | 112.2(3) | C8'-N1'-Pd1' | 103.8(3) | C7'-N1'-Pd1' | 118.8(2) |
| C2'-C1'-C6' | 118.3(4) | C2'-C1'-C7' | 127.8(4) | C6'-C1'-C7' | 113.7(3) |
| C2'-C1'-Cr1' | 71.6(2) | C6'-C1'-Cr1' | 69.2(2) | C7'-C1'-Cr1' | 134.8(3) |
| C1'-C2'-C3' | 118.8(4) | C1'-C2'-P1' | 123.9(3) | C3'-C2'-P1' | 116.5(3) |
| C1'-C2'-Cr1' | 71.8(2) | C3'-C2'-Cr1' | 69.3(2) | P1'-C2'-Cr1' | 138.8(2) |
| C4'-C3'-C2' | 121.5(4) | C4'-C3'-Cr1' | 72.2(3) | C2'-C3'-Cr1' | 73.0(2) |
| C3'-C4'-C5' | 119.9(4) | C3'-C4'-Cr1' | 71.2(2) | C5'-C4'-Cr1' | 71.8(3) |
| C6'-C5'-C4' | 119.3(4) | C6'-C5'-Cr1' | 70.8(2) | C4'-C5'-Cr1' | 71.0(2) |
| C5'-C6'-C1' | 122.0(4) | C5'-C6'-Cr1' | 72.5(2) | C1'-C6'-Cr1' | 73.1(2) |
| N1'-C7'-C1' | 118.6(3) | N1'-C7'-C10' | 112.7(3) | C1'-C7'-C10' | 108.5(3) |
| C11'-C10'-C15' | 118.8(4) | C11'-C10'-C7' | 122.9(4) | C15'-C10'-C7' | 118.3(4) |
| C10'-C11'-C12' | 120.5(4) | C13'-C12'-C11' | 120.1(4) | C14'-C13'-C12' | 119.9(4) |
| C13'-C14'-C15' | 120.0(4) | C14'-C15'-C10' | 120.7(4) | C21'-C16'-C17' | 118.8(4) |
| C21'-C16'-P1' | 121.4(3) | C17'-C16'-P1' | 119.6(3) | C18'-C17'-C16' | 120.2(4) |
| C19'-C18'-C17' | 120.5(4) | C18'-C19'-C20' | 120.0(4) | C21'-C20'-C19' | 120.2(4) |
| C20'-C21'-C16' | 120.4(4) | C23'-C22'-C27' | 119.2(4) | C23'-C22'-P1' | 121.1(3) |
| C27'-C22'-P1' | 119.6(3) | C24'-C23'-C22' | 121.0(5) | C25'-C24'-C23' | 119.4(5) |
| C26'-C25'-C24' | 121.0(5) | C25'-C26'-C27' | 120.6(5) | C26'-C27'-C22' | 118.8(5) |
| O1'-C28'-Cr1' | 178.1(4) | O2'-C29'-Cr1' | 175.1(4) | O3'-C30'-Cr1' | 176.1(4) |
| Cl3-C31-Cl4 | 112.6(5) | | | | |

# 9References


[1] CrystalClear: Rigaku Corporation, 1999.

[2] CrystalStructure: Crystal Structure Analysis Package, Rigaku Corp. Rigaku/MSC (2002).

[3] REQAB4: R.A. Jacobsen, (1994). Private Communication.

[4] SIR97: Altomare, A., M. Burla, M. Camalli, G. Cascarano, C. Giacovazzo, A. Guagliardi, A. Moliterni, G. Polidori & R. Spagna (1999). *J. Appl. Cryst.*, **32**, 115-119.

[5] SHELXL-97: Program for the Refinement of Crystal Structures, Sheldrick, G.M. (1997), University of Göttingen, Germany.

[6] "ORTEP-II: A Fortran Thermal Ellipsoid Plot Program for Crystal Structure Illustrations". C.K. Johnson (1976) ORNL-5138.

[7] Bruker (2009) SAINT. Bruker AXS Inc., Madison, Wisconsin, USA.

[8] Bruker (2009) SHELXTL. Bruker AXS Inc., Madison, Wisconsin, USA.

[9] Sheldrick, G.M. (2007) SADABS. University of Gottingen, Germany.

[10] Sheldrick, G.M. (2008) Acta Cryst. A64,112-122.

[11] Sheldrick, G.M. (2008) CELL_NOW. University of Gottingen, Germany.

[12] Sheldrick, G.M. (2007) TWINABS. University of Gottingen, Germany.

## Appendix V

## HTE chiral predosed catalysts

The following is a list of chiral catalysts predosed into wells and screened for converstion with low-barrier high-throughput experimentation (HTE) conditions:

Table V-1: SDD Plate 1

| | |
|---|---|
| A 1 | (R)-Solphos A001-1 |
| A 2 | (S)-xylyl-binap |
| A 3 | (S)-Cl,MeO-Biphep |
| A 4 | (R,R)-Me-DuPhos |
| A 5 | EtBPE |
| A 6 | SL-J002-1 : (R,S)-Ph2P-Fc-P(tBu)2 |
| A 7 | SL-J007-1 |
| A 8 | SL-J009-1 |
| A 9 | SL-J012-1 |
| A 10 | (R)-CTH-JAFAPHOS |
| A 11 | (R,R)-Et-FerroTANE |
| A 12 | (R,R,S,S)-Tangphos |
| B 1 | (R)-(S)-Me-BoPhoz |
| B 2 | SL-W001-1 |
| B 3 | SL-W006-1 |
| B 4 | SL-W005-1 |
| B 5 | CTH-(R)-3,5-xylyl-PHANEPHOS |
| B 6 | (S,S)-SL-M002-1 |
| B 7 | (S,S)-SL-M001-1 |
| B 8 | (S,S)-SL-T001-1 |
| B 9 | (S)-(+)-(2,6-Dimethyl-3,5-dioxa-4-phospha-cyclohepta[2,1-a;3,4-a']dinaphthalen-4-yl)dimethylamine |
| B 10 | (R)-MONOPHOS |
| B 11 | catASium D(R) |
| B 12 | catASium I |
| C 1 | (2S,4S)-tBu-(-)-4-(Diphenylphosphino)-2-(diphenylphosphinomethyl)pyrrolidine carboxylate |

C 2 (3S,4S)-(-)-1-Benzyl-3,4-bis(diphenylphosphino)pyrrolidine

C 3 (1R,1R',2R,2R')-(-)-2,2'-DIPHENYLPHOSPHINO-1,1'-BICYCLOPENTYL

C 4 SL-T021-2: Ph2P-Fc-CH(OH)Ph-PPh2

C 5 (R,R)-SL-M004-1

C 6 Walphos 9-1

C 7 (R,R) SL-W018-1

C 8 (R,R)-SL-W019-1

C 9 (R,R) SL-W020-1

C 10 (R,R)-SL-W021-1

C 11 SL-T025-2: xyl2P-Fc-CH(OH)Ph-Pxyl2

C 12 (4S,5S)-(+)-4,5-Bis(diphenylphosphinomethyl)-2,2-dimethyl-1,3-dioxolane

D 1 (S,S)-SL-M001-1

D 2 (S,S)-SL-M002-1

D 3 (S,S)-SL-M003-1

D 4 (3S,3'S,4S,4'S,11bS,11'bS)-(+)-4,4'-Di-t-butyl-4,4',5,5'-tetrahydro-3,3'-bi-3H-dinaphtho[2,1-c:1',2'-e]phosphepin

D 5 (S,S)-SL-T001-1

D 6 (R,S)-SL-T002-1

D 7 SL-T026-2: Ph2P-Fc-CH(OH)Ph-P(3,5-Me-4-MeO)2

D 8 (S)-(-)-2,2'-Bis(N-diphenylphosphinoamino)-5,5',6,6',7,7',8,8'-octahydro-1,1'-binaphthyl

D 9 R,S-(o-tolyl)2P-F-C-P(o-tolyl)2

D 10 (R)-(S)-Et2P-F-C-PtBu2

D 11 s-f-binaphane

D 12 SL-T027-2: xyl2P-Fc-CH(OH)Ph-P(3,5-CF3-Ph)2

E 1 (S)-CTH-JAFAPHOS

E 2 (R,R)-Me-DuPhos

E 3 (+)-1,2-Bis((2R,5R)-2,5-di-i-propylphospholano)benzene

E 4 (R,R) Et-DuPhos

E 5 (R)-(+)-BIS-(1,2-DIPHENYLPHOSPHINO)PROPANE

E 6 SL-W023-1: (3,5-Me-4-MeO)2PPh-Fc-CHMe-P(Nor)2

E 7 SL-W-A1: Ph2PPh-Fc-CHMe-PtBu2

E 8 SL-J215-2: (S)-(R)-Fur2P-Fc-Pcy2

E 9 SL-J302-1: (R)-(S)-Et2P-Fc-PCy2

E 10 SL-J011-1: (R)-(S)-(4-CF3-Ph)2-PFc-PtBu2

E 11 SL-J304-1: (R)-(S)-Ph,Me-PFc-PCy2

E 12 SL-J408-1: (R)-(S)-xyl2P-Fc-Pxyl2

F 1 SL-J411-2: (S)-(R)-Fur2P-Fc-P(3,5-Me2-4-OMe-Ph)2

F 2 SL-J412-1: (R)-(S)-xyl2P-Fc-P(3,5-(CF3)2-Ph)2

F 3 SL-W022-1

F 4 SL-F011-2 (Twinphos, analog of Me-BoPhoz)

F 5 SL-F013-2 (Twinphos, analog of P(cyco)-BoPhoz)

F 6 SL-J851-2

F 7 SL-J852-2

F 8 SL-J853-2

F 9 (S,S)-Ph-BPE

F 10 SL-W016-1

F 11 [(1R,2R,3S)-(+)-1,2-Dimethyl-2,3-bis(diphenylphosphinomethyl)cyclopentyl]methanol

F 12 SL-W017-1

G 1 (R)-(-)-1-[(S)-2-(DIPHENYLPHOSPHINO)FERROCENYL]ETHYLDICYLCOHEXYLPHOSPHINE

G 2 (R)-(-)-1-[(S)-2-(DIPHENYLPHOSPHINO)FERROCENYL]ETHYLDI-T-BUTYLPHOSPHINE

G 3 (R)-(-)-1-[(S)-2-(DICYCLOHEXYLPHOSPHINO)FERROCENYL]ETHYLDIPHENYLPHOSPHINE

G 4 (R)-(S)-(3,5-(CF3)2Ph)2PF-Pcy2

G 5 (R)-(S)-(3,5-(CF3)2Ph)2PF-Pxyl2

G 6 (R)-(S)-(4-CF3-Ph)2-PFc-PCy2

G 7 (R)-(S)-(3,5-Me2-4-MeOPh)2PF-PtBu2

G 8 (R)-(S)-Fur2PF-PtBu2

G 9 (R)-(S)-oTol2PF-Pxyl2

G 10 (R)-(S)-(3,5-Me2-4-MeOPh)2PF-PoTol2

G 11 (2-Furyl)2P-Fc-P(o-Tolyl)2

G 12 SL-J503-1: (R)-(S)-Et2P-Fc-P(o-Tolyl)2

H 1 (R)-(S)-xyl2P-Fc-PtBu2

H 2 (R)-(-)-1-[(S)-2-(DICYCLOHEXYLPHOSPHINO)FERROCENYL]ETHYLDICYCLOHEXYLPHOSPHINE

H 3 (R)-(S)-Ph2P-Fc-P(4-CF3-Ph)2

H 4 (R)-(S)-(4-MeO-3,5-Me2Ph)2PF-Pcy2

| | |
|---|---|
| H 5 | (R)-(S)-cy2PF-PtBu2 |
| H 6 | (R)-(S)-(p-Tol)2PF-PtBu2 |
| H 7 | (S)-(R)-Fur2P-Fc-Pxyl2 |
| H 8 | (R)-(S)-(3,5-Me2-4-MeOPh)2PF-Pxyl2 |
| H 9 | (R)-(S)-cy2PF-Po-Tol2 |
| H 10 | (R)-(R)-(S)-PhMePF-Pcy2 |
| H 11 | SL-J507-1: (R)-(S)-Et2P-Fc-P(xylyl)2 |
| H 12 | SL-J034-1: (R)-(R)-Ph2P-(2-TMS-Fc)-P(cHex)2 |

Table V-2: SDD Plate 2

| | |
|---|---|
| A 1 | Catasium MN An(R) |
| A 2 | Catasium MNN (R) |
| A 3 | Catasium MN MesF (R) |
| A 4 | Catasium MN Mes (R) |
| A 5 | (S,S)-Me-UCAP-DTBM |
| A 6 | (R,R)-QuinoxP* |
| A 7 | SL-P051-1: (R,R,R)-Me-KEPHOS |
| A 8 | SL-P053-2: (S,S,R)-Me-KEPHOS |
| A 9 | SL-J005-1: Ph2P-Fc-Pxyl2 |
| A 10 | SL-J014-1: (R)-(S)-(4-F-Ph)2P-Fc-PtBu2 |
| A 11 | SL-J031-1: PPh2-Fc-P(cyclopentyl)2 |
| A 12 | SL-J211-1: (o-Tol)2P-Fc-PtBu2 |
| B 1 | SL-J213-1: (3,5-CF3-Ph)2P-Fc-P(cyclopentyl)2 |
| B 2 | SL-J216-1: (1-naphthyl)2P-Fc-PtBu2 |
| B 3 | SL-J219-1: (2-MeO-Ph)2P-Fc-PtBu2 |
| B 4 | SL-J220-1: (3,5-Me-4-MeO-Ph)2P-Fc-P(cyclopentyl)2 |
| B 5 | SL-J221-1: (3,5-Me-4-MeO-Ph)2P-Fc-P(2,4,4-Me-pentyl)2 |
| B 6 | SL-J222-1: (3,5-Me-4-MeO-Ph)2P-Fc-P(neopentyl)2 |
| B 7 | SL-J305-1: Cy2P-Fc-P(norbornyl)2 |
| B 8 | SL-J404-1: (R)-(S)-(1-napthyl)2P-Fc-Pxyl2 |
| B 9 | SL-J409-1: (R)-(S)-(1-Naphthyl)2PF-PPh2 |
| B 10 | SL-J502-1: tBu2P-Fc-PPh2 |
| B 11 | SL-J505-1: tBu2P-Fc-P(o-Tol)2 |

B 12 SL-J506-1: tBu2P-Fc-P(4-CF3-Ph)2

C 1 (-)-TMBTP

C 2 (R)-(+)-2,2'-BIS(DI-P-TOLYLPHOSPHINO)-1,1'-BINAPHTHYL (note structure incorrect)

C 3 (R)-Hexaphemp

C 4 (S)-(-)-6,6'-Bis(diphenylphosphino)-1,1'-biphenyl-2,2'-diylbis(acetate),

C 5 (R)-(+)-5,5'-DICHLORO-6,6'-DIMETHOXY-2,2'-BIS(DIPHENYLPHOSPHINO)-1,1'-BIPHENYL

C 6 (R)-segphos

C 7 SL-A109-2

C 8 (R)-(+)-2,2',6,6'-Tetramethoxy-4,4'-bis(diphenylphosphino)-3,3'-bipyridine

C 9 (R)-DTBM-SEGPHOS

C 10 s-c1-tunaphos

C 11 s-c3-tunaphos

C 12 s-c5-tunaphos

D 1 (S)-(+)-2,2'-BIS(DIPHENYLPHOSPHINO)-1,1'-BINAPHTHYL

D 2 (R)-(+)-2,2'-BIS[DI(3,5-XYLYL)PHOSPHINO]-1,1'-BINAPHTHYL

D 3 (1R)-(+)-[Di(3,5-dimethylphenyl)phosphino]-2-(4-diphenylphosphino-2,5-dimethylthien-3-yl)-1,7,7-trimethylbicyclo[2.2.1]hept-2-ene [catASium T2]

D 4 (R)-DM-SEGPHOS

D 5 (R)-(-)-5,5'-Bis(diphenylphosphino)-2,2,2',2'-tetrafluoro-4,4'-bi-1,3-benzodioxole

D 6 SL-A120-2

D 7 (R)-H8-BINAP

D 8 (S)-(-)-2,2',6,6'-Tetramethoxy-4,4'-bis(di(3,5-xylyl)phosphino)-3,3'-bipyridine

D 9 (S)-(-)-6,6'-Bis(diphenylphosphino)-1,1'-biphenyl-2,2'-diylbis(cyclohexylcarboxylate),

D 10 c2-tunaphos

D 11 s-C4-tunaphos

D 12 s-c6-tunaphos

E 1 (R)-MP2-SEGPHOS

E 2 (R)-P3-SEGPHOS

E 3 (+)-Cy-SEGPHOS

E 4 SL-A102-1

E 5 SL-A107-1

E 6 SL-A104-1

E 7 SL-A121-1

E 8 SL-A108-1

E 9 SL-A116-1

E 10 SL-A118-1

E 11 (1R,2R)-(+)-1,2-Diaminocyclohexane-N,N'-bis(2'-diphenylphosphinobenzoyl)

E 12 (1R,2R)-(+)-1,2-Diaminocyclohexane-N,N'-bis(2-diphenylphosphino-1-naphthoyl)

F 1 (4R)-(+)-4,5-DIHYDRO-2-[2'-(DIPHENYLPHOSPHINO)PHENYL]-4-ISOPROPYLOXAZOLE

F 2 (R)-(-)-2-[2-(Diphenylphosphino)phenyl]-4-phenyl-2-oxazoline

F 3 SL-N003-2 ((S)-4-Isopropyl-2-[(S)-2-(diphenylphosphino)ferrocen-1-yl]oxazoline)

F 4 SL-N008-2 ((S)-4-Isopropyl-2-[(S)-2-(bis(3,5.dimethyl-4-methoxyphenyl)phosphino)ferrocen-1-yl]oxazoline)

F 5 SL-N011-2 ((S)-4-Isopropyl-2-[(S)-2-(bis(1-naphtyl)phosphino)ferrocen-1-yl]oxazoline)

F 6 SL-N012-2 ((S)-4-Isopropyl-2-[(S)-2-(bis(2-methoxyphenyl)phosphino)ferrocen-1-yl]oxazoline)

F 7 SL-N004-2

F 8 SL-N007-2

F 9 SL-N013-1

F 10 (S)-Xyl-SDP

F 11 (S)-Tol-SDP

F 12 (S)-SDP

G 1 (R)-MonoPhos

G 2 (S)-N-Me-N-Bn-MonoPhos

G 3 (S)-PipPhos

G 4 (S)-2,6-Me-MonoPhos

G 5 (S,R)-(a-MeBn)-MonoPhos

G 6 (S,R,R)-(a-MeBn)2-MonoPhos

G 7 (S,S,S)-(a-MeBn)2-MonoPhos

G 8 (S)-H8-MonoPhos

G 9 (S)-H8-PipPhos

G 10 (R)-BINOL-P-OiPr

G 11 (R)-BINOL-P-OiBu

| | |
|---|---|
| G 12 | (R,R)-TADDOL-P-NMe2 |
| H 1 | (R)-SIPHOS |
| H 2 | (R)-SIPHOS-PE |
| H 3 | (R)-ShiP |
| H 4 | (S,S)-Mikami Ligand |
| H 5 | (S,S)-tBu-Mikami Ligand |
| H 6 | (R)-Quinap |
| H 7 | (R)-N-PINAP |
| H 8 | (R)-MOP |
| H 9 | (R,R)-Me-DuPhos Monoxide |
| H 10 | (S,S)-Me-RajPhos |
| H 11 | (S,S)-Et-RajPhos |
| H 12 | (S,S,S)-DiazaPhos-PPE |

Table V-3: Upenn Chiral Phosphines Plate

| | |
|---|---|
| A 1 | (S)-Binap |
| A 2 | (R)-segphos |
| A 3 | (S)-SDP |
| A 4 | (R)-3,5-xylyl-PHANEPHOS |
| A 5 | (R)-Cl,MeO-BIPHEP |
| A 6 | (R,R)-Trost Ligand |
| B 1 | (R)-BINAPHANE |
| B 2 | (R)-CTH-JAFAPHOS |
| B 3 | SL-M001-1 |
| B 4 | SL-J005-1: Ph2P-Fc-Pxyl2 |
| B 5 | (R,R)-SL-W002-1 |
| B 6 | (S,S)-SL-T001-1 |
| C 1 | (+)-Cy-SEGPHOS |
| C 2 | SL-J008-1 |
| C 3 | SL-M002-2 |
| C 4 | SL-J002-1 |
| C 5 | SL-W003-1 |
| C 6 | SL-T002-1 |

| | |
|---|---|
| D 1 | (S,S)-Ph-BPE |
| D 2 | (1S,1'S,2R,2'R)-DuanPhos |
| D 3 | (R,R)-QuinoxP* |
| D 4 | (R,R)-Me-DuPhos |
| D 5 | (R)-Pfaltz (Ph |
| D 6 | (S)-PipPhos |

Table V-4: Mandyphos and Taniaphos Plate

| | |
|---|---|
| A 1 | SL-M001 (Ph mandyphos) |
| A 2 | SL-M002 (Cy Mandyphos) |
| A 3 | SL-M003 (CF3 Mandyphos) |
| A 4 | SL-M004 (Me MeO mandyphos) |
| A 5 | SL-M009 (xyl mandyphos) |
| A 6 | SL-M012 (otol mandyphos) |
| B 1 | SL-T001 (ph taniaphos) |
| B 2 | SL-T002 (cy taniaphos) |
| B 3 | SL-T021 |
| B 4 | SL-T025 |
| B 5 | SL-T026 |
| B 6 | SL-T027 |
| C 1 | SL-M001 (Ph mandyphos) |
| C 2 | SL-M002 (Cy Mandyphos) |
| C 3 | SL-M003 (CF3 Mandyphos) |
| C 4 | SL-M004 (Me MeO mandyphos) |
| C 5 | SL-M009 (xyl mandyphos) |
| C 6 | SL-M012 (otol mandyphos) |
| D 1 | SL-T001 (ph taniaphos) |
| D 2 | SL-T002 (cy taniaphos) |
| D 3 | SL-T021 |
| D 4 | SL-T025 |
| D 5 | SL-T026 |
| D 6 | SL-T027 |

## Appendix VI

## Terms and Acronyms

The following are terms, abbreviations, and acronyms used within this thesis, as well as informally within my lab notebooks and excel sheet list of reactions.

| | |
|---|---|
| $\eta$ | Hapticity (contiguous donor atoms of ligand) |
| $\kappa$ | Hapticity (non-contiguous donor atoms of ligand) |
| ArOTf | Aryl Triflate, Aryl Trifluoromethanesulfonate, $ArOSO_2CF_3$ |
| Bn | Benzyl ($PhCH_2$- or $C_6H_5CH_2$) |
| COD | 1,5-Cyclooctadiene ligand |
| CrBnA | $\eta^6$-Tricarbonylchromium *N*,*N*-dimethylbenzylamine (**27**) |
| CrBnMorph | $\eta^6$-Tricarbonylchromium *N*-benzylmorpholine (**54**) |
| CrBOM | $\eta^6$-Tricarbonylchromium benzylmethyl ether |
| CrBOP | $\eta^6$-Tricarbonylchromium benzylpropyl ether (**23**) |
| CrDHI | $\eta^6$-Tricarbonylchromium dihidroindane, $\eta^6$-Tricarbonylchromium Indan (**39**) |
| CrDPM | $\eta^6$-Tricarbonylchromium diphenylmethane (**4a**) |
| CrEtPh | $\eta^6$-Tricarbonylchromium ethylbenzene (**30**) |
| CrMes | $\eta^6$-Tricarbonylchromium mesitylene (**9**) |
| CrOxyl | $\eta^6$-Tricarbonylchromium *o*-xylene (**18**) |
| CrBnPip | $\eta^6$-Tricarbonylchromium *N*-benzylpiperidine (**53**) |
| CrBnPpz | $\eta^6$-Tricarbonylchromium *N*,*N*′-benzylmethylpiperazine (**56**) |
| CrPth | $\eta^6$-Tricarbonylchromium phthalan (**46**) |
| CrPxyl | $\eta^6$-Tricarbonylchromium *p*-xylene (**8**) |
| CrTAM | $\eta^6$-Tricarbonylchromium triarylmethane family (**5a**, etc) |
| CrTHN | $\eta^6$-Tricarbonylchromium tetrahydronaphthalene (**40**) |
| CrTol | $\eta^6$-Tricarbonylchromium toluene (**3**) |
| Cy | Cyclohexyl group, $C_6H_{11}$ |
| CyH | 1-Cyclohexenyl, $C_6H_9$ |
| D–A | Diels-Alder |
| DCM | Dichloromethane, Methylene chloride |
| Diox | 1,4-dioxane |
| DMSO | Dimethyl sulfoxide |
| DOM | Directed *ortho* metalation, selective metalation (of arenes) using a directing group. |

| | |
|---|---|
| EAS | Electrophilic Aromatic Substitution |
| ee | = 100 × (major enantiomer−minor), (sum of enantiomers) enantiomeric excess |
| F–C | Friedel-Crafts |
| H–B | Hüenig's Base, diisopropylethylamine |
| Hex | Hexanes |
| HMDS-H | $HN(SiMe_3)_2$, Hexamethyldisilazane. |
| HRMS | High-resolution mass spectrometry |
| HTE | Low-barrier high-throughput experimentation, a parallel microscale reaction screening method for the rapid identification of reagents and reaction conditions. |
| KHMDS | $KN(Si(CH_3)_3)_2$, Potassium hexamethylsilazide |
| LDA | Lithium Diisopropylamide, $LiN(i\text{-}Pr)_2$ |
| LiCKOR | Schlosser's base; superbase made of equimolar amounts of Butyllithium and KOtBu |
| LiHMDS | or LHMDS: $LiN(Si(CH_3)_3)_2$, Lithium hexamethyldisilazide |
| Mandy | Mandyphos, usually cyclohexyl Mandyphos |
| NaHMDS | $NaN(Si(CH_3)_3)_2$, Sodium hexamethylsilazide |
| Norb | Norbornadiene |
| OTf | Triflate, trifluoromethanesulfonate, $-OSO_2CF_3$ group |
| Pent | *n*-Pentane |
| PMDETA | or PMDTA, PMETA: *N*,*N*′,*N*″,*N*‴-Pentamethyldiethylenetriamine |
| PTFE | teflon [poly(tetrafluoroethylene)] |
| *s&n* base | superbase made of equimolar amounts of *sec*-butyllithium and *n*-butyllihtium |
| Tania | Taniaphos, usually cyclohexyl Taniaphos |
| TEA | Triethylamine, $NEt_3$ |
| TEEDA | *N*,*N*,*N*′,*N*′-Tetraethylethylenediamine |
| THF | Tetrahydrofuran |
| TLC | Thin-Layer Chromatography |
| TMEDA | *N*,*N*,*N*′,*N*′-Tetramethylethylenediamine |
| Tol | Toluene; 4-Tolyl- group |
| X | Halide (F, Br, Cl, I) or other anionic ligand (OTf) |
| Z | Shorthand for any covalently bonded group on the benzylic position of $\eta^6$-tricarbonylchromium-coordinated starting materials. |

## Bibliography

The following is the list of full references cited in this dissertation.

### Books


1) Blaser, H. U.; Federsel, H.; Federsel, H. J. In *Asymmetric Catalysis on Industrial Scale: Challenges, Approaches and Solutions*; John Wiley & Sons: 2010; pp 580.

2) Börner, A. In *Phosphorus Ligands in Asymmetric Catalysis: Synthesis and Applications*; John Wiley & Sons: 2008.

3) Collman, J. P.; Hegedus, L. S.; Norton, J. R.; Finke, R. G. In *Synthetic Applications of Arene Transition-Metal Complexes; Principles and Applications of Organotransition Metal Chemistry*; University Science Books: Mill Valley, CA 94941, 1987; pp 921-19.

4) Dai, L. X.; Hou, X. L. In *Chiral Ferrocenes in Asymmetric Catalysis: Synthesis and Applications*; Wiley-VCH: 2009.

5) Hartwig, J. In *Organotransition Metal Chemistry: From Bonding to Catalysis*; University Science Books: 2010.

6) Herndon, J. W.; Laurent, S. E. "($\eta^6$-Benzene)tricarbonylchromium," in *Encyclopedia of Reagents for Organic Synthesis*, John Wiley & Sons, Chichester, 2008.

7) Kauffman, M. C.; Walsh, P. J.: Arylation and Alkenylation of Carbonyl and Imino Groups. In *Stereoselective Synthesis 2*; Molander, G. A., Ed.; Thieme: Stuttgart, **2011**; Vol. 2; pp 449-495.

8) Kündig, E. P. In *Topics in Organometallic Chemistry Vol. 7*, Berline; New York: 2004.

9) Li, J. J. In *Contemporary drug synthesis*; Wiley-Interscience: 2004; pp 221.

10) *Mosby's Medical Dictionary*; Elsevier: 2008; pp 2056.

11) Rappoport, Z.; Marek, I. In *The Chemistry of Organolithium Compounds*, John Wiley & Sons: 2004.

12) Sheldon, R. A.; Arends, I. W. C. E.; Hanefeld, U. In *Introduction: Green Chemistry and Catalysis;* Green Chemistry and Catalysis; Wiley-VCH Verlag GmbH & Co. KGaA: 2007; pp 1-47.

13) Sundberg, R. J. In *Indoles*; Academic Press: 1996; pp 175.

14) Uemura, M. In *Org. React., Vol. 67,* John Wiley, NJ: 2006, pp. 217.

15) Walsh, P. J.; Kozlowski, M. C. In *Fundamentals of asymmetric catalysis*; University Science Books: 2008.

16) Woolins, J. D., Ed. In *Inorganic Experiments*; VCH: Weinheim, 1994; 194-195.

## Journal Articles


1) Abdelrahim, M.; Newman, K.; Vanderlaag, K.; Samudio, I.; Safe, S. 3,3′-Diindolylmethane (DIM) and its derivatives induce apoptosis in pancreatic cancer cells through endoplasmic reticulum stress-dependent upregulation of DR5. *Carcinogenesis* **2006**, *27*, 717-728.

2) Ackermann, L.; Born, R.; Spatz, J. H.; Meyer, D. Efficient Aryl/(Hetero)Aryl Coupling by Activation of C–Cl and C–F Bonds Using Nickel Complexes of Air-Stable Phosphine Oxides. *Angew. Chem. , Int. Ed.* **2005**, *44*, 7216-7219.

3) Ahlbrecht, H.; Dollinger, H. α-Metallierte amine durch deprotonierung aliphatischer N-methylamine. *Tetrahedron Lett.* **1984**, *25*, 1353-1356.

4) Ahlrichs, R.; Bar, M.; Haser, M.; Horn, H.; Kolmel, C. Electronic-structure calculations on workstation computers – the program system Turbomole. *Chem. Phys. Lett.* **1989**, *162*, 165-169.

5) Albicker, M. R.; Cramer, N. Enantioselective Palladium-Catalyzed Direct Arylations at Ambient Temperature: Access to Indanes with Quaternary Stereocenters. *Angew. Chem. Int. Edit.* **2009**, *48*, 1939-1942.

6) Andersson, P. G.; Schink, H. E.; Osterlund, K. Asymmetric Total Synthesis of (+)-Tolterodine, a New Muscarinic Receptor Antagonist, via Copper-Assisted Asymmetric Conjugate Addition of Aryl Grignard Reagents to 3-Phenyl-prop-2-enoyl-oxazolidinones. *J. Org. Chem.* **1998**, *63*, 8067-8070.

7) Antonini, S.; Calderazzo, F.; Englert, U.; Grigiotti, E.; Pampaloni, G.; Zanello, P. Synthesis, electrochemistry, and crystal and molecular structures of some molybdenum(0) arene derivatives with fluorinated and phenyl-substituted arene ligands. *J. Organomet. Chem.* **2004**, *689*, 2158-2168.

8) Antonova, M. V.; Moiseev, S. K.; Kalinin, V. N.; Shapiro, I. O. Kinetic CH-acidity of benzenetricarbonylchromium and its derivatives. *Russ. Chem. Bull*. **1989**, *38*, 2256-2259.

9) Ashraf, M.; Jackson, W. R. The stereochemistry of organometallic compounds. Part XII. The acid strengths of some tricarbonyl(alkylbenzoic acid)chromium compounds, their nuclear magnetic resonance spectra, and the spectra of some related compounds. *J.Chem.Soc., Perkin Trans.2* **1972**, 103-106

10) Barceloux, D. G.; Barceloux, D. Chromium. *Clin. Toxicol.* **1999**, *37*, 173-194.

11) Baudoin, O. Transition metal-catalyzed arylation of unactivated C($sp^3$)–H bonds. *Chem. Soc. Rev.* **2011**, *40*, 4902-4911.

12) Becke, A.D. Density-functional thermochemistry. 3. The role of exact exchange. *J. Chem. Phys*. **1993**, *98*, 5648-5652.

13) Berger, A.; Djukic, J.; Michon, C. Metalated ($\eta^6$-arene)tricarbonylchromium complexes in organometallic chemistry. *Coord. Chem. Rev.*, **2002**, *225*, 215-238.

14) Bishop, M. J.; McNutt, R. W. An efficient synthesis of the benzhydrylpiperazine delta opioid agonist (+)-BW373U86. *Bioorg. Med. Chem. Lett.* **1995**, *5*, 1311-1314.

15) Boaz, N. W. Enzymatic esterification of 1-ferrocenylethanol: An alternate approach to chiral ferrocenyl bis-phosphines. *Tetrahedron Lett.* **1989**, *30*, 2061-2064.

16) Bolm, C.; Muniz, K. Planar chiral arene chromium(0) complexes: potential ligands for asymmetric catalysis. *Chem. Soc. Rev.* **1999**, *28*, 51-59.

17) Bordwell, F. G. Equilibrium acidities in dimethyl sulfoxide solution. *Acc. Chem. Res.* **1988**, *21*, 456-463.

18) Bordwell, F. G.; Algrim, D.; Vanier, N. R. Acidities of anilines and toluenes. *J. Org. Chem.* **1977**, *42*, 1817-1819.

19) Bordwell, F. G.; Matthews, W. S.; Vanier, N. R. Acidities of carbon acids. IV. Kinetic vs. equilibrium acidities as measures of carbanion stabilities. Relative effects of phenylthio, diphenylphosphino, and phenyl groups. *J. Am. Chem. Soc.* **1975**, *97*, 442-443.

20) Braun, W.; Calmuschi, B.; Drexler, H.; Englert, U.; Heller, D.; Salzer, A., (*R*,*R*)-Tricarbonyl{$\eta^6$-1-(diphenylphosphino)-2-[1-(diphenylphosphino)ethyl]benzene}chromium(0), (R,R)-tricarbonyl-1$\kappa^3$C-{$\mu$-1($\eta^6$):2$\kappa^2$*P*,*P*'-1-(diphenylphosphino)-2-[1-(diphenylphosphino)ethyl]benzene}[2($\eta^4$)-norbornadiene]chromium(0)rhodium(I) tetrafluoroborate methanol 0.75-solvate and (*R*,*R*)-tricarbonyl-1$\kappa^3$C-{$\mu$-1($\eta^6$):2$\kappa^2$*P*,*P*'-1-(diphenylphosphino)-2-[1-(diphenylphosphino)ethyl]benzene}[2($\eta^4$)-(*Z*,*Z*)-cycloocta-1,5-diene]chromium(0)rhodium(I) tetrafluoroborate methanol 1.5-solvate. *Acta Crystallogr. , Sect. C: Cryst. Struct. Commun.* **2004,** *60*, m532-m536.

21) Brewer, A. R. E.; Drake, A. F.; Gibson, S. E.; Rendell, J. T. Interplay between Core and Peripheral Chirality in Polyethers. *Org. Lett.* **2007**, *9*, 3487-3490.

22) Broom, D. C.; Jutkiewicz, E. M.; Rice, K. C.; Traynor, J. R.; Woods, J. H. Behavioral Effects of δ-Opioid Receptor Agonists: Potential Antidepressants? *The Japanese Journal of Pharmacology* **2002**, *90*, 1-6.

23) Calderon, S. N.; Rice, K. C.; Rothman, R. B.; Porreca, F.; Flippen-Anderson, J.; Xu, H.; Becketts, K.; Smith, L. E.; Bilsky, E. J.; Davis, P.; Horvath, R. Probes for Narcotic Receptor Mediated Phenomena. 23.1 Synthesis, Opioid Receptor Binding, and Bioassay of the Highly Selective δ Agonist (+)-4-[(αR)-α-((2S,5R)-4-Allyl-2,5-dimethyl-1-piperazinyl)-3-methoxybenzyl]- N,N-diethylbenzamide (SNC 80) and Related Novel Nonpeptide δ Opioid Receptor Ligands. *J. Med. Chem*. **1997**, *40*, 695-704

24) Cambie, Richard C. *et al* Chemistry of the podocarpaceae. LXXI. Preparation, structure, and reactions of some (arene)tricarbonylchromium(0) complexes. Crystal structure of α-tricarbonyl[(8,9,11,12,13,14-η)-methylpodocarpa-8,11,13-trien-19-oate]chromium(0). *J. Organomet. Chem*. **1988**, *342*, 315-337.

25) Catino, A. J.; Nichols, J. M.; Nettles, B. J.; Doyle, M. P. The Oxidative Mannich Reaction Catalyzed by Dirhodium Caprolactamate. *J. Am. Chem. Soc.* **2006**, *128*, 5648-5649.

26) Caubere, P. Unimetal super bases. *Chem. Rev.* **1993**, *93*, 2317-2334.

27) Ceccon, A.; Gambaro, A.; Santi, S.; Valle, G.; Venzo, A. Synthesis and characterization of $\eta^6$-$Cr(CO)_3$-indenyl-$\eta^3$-rhodium-$\eta^4$-$C_8H_{12}$: an $\eta^3$:$\eta^6$ co-ordination for the indenyl ligand. *J. Chem. Soc. , Chem. Commun.* **1989**, 51-53.

28) Childers, S. R.; Fleming, L. M.; Selley, D. E.; McNutt, R. W.; Chang, K. J. BW373U86: a nonpeptidic delta-opioid agonist with novel receptor-G protein-mediated actions in rat brain membranes and neuroblastoma cells. *Molecular Pharmacology* **1993**, *44*, 827-834.

29) Clarke, M. L.; Heydt, M. *Organometallics* **2005**, *24*, 6475-6478.

30) Cohen, M. D.; Kargacin, B.; Klein, C. B.; Costa, M. Mechanisms of Chromium Carcinogenicity and Toxicity. *Crit. Rev. Toxicol*. **1993**, *23*, 255-281.

31) Costa, M. R.; Curto, M. J.; Davies, S. G.; Sanders, J.; Teixeira, F. C. Synthesis of (R)-{η$^6$-[O-methyl-N-(α-methylbenzyl)hydroxyamino]benzene} chromium tricarbonyl via nucleophilic aromatic substitution of (η$^6$-fluorobenzene) chromium tricarbonyl. *J. Chem. Soc., Perkin Trans 1* **2001**, 2850-2855.

32) Crabtree, S.; Ellis, P.; Catalyst Preparation for the 21st Century. *Platinum Metals Rev*. **2010**, *54*, 162.

33) Cram, D. J.; Wilkinson, D. I. Macro Rings. XXIII. Carbonylchromium Complexes of Paracyclophanes and Model Compounds. *J. Am. Chem. Soc.* **1960**, *82*, 5721-5723.

34) Dai, L.; Tu, T.; You, S.; Deng, W.; Hou, X. Asymmetric Catalysis with Chiral Ferrocene Ligands. *Acc. Chem. Res*. **2003**, *36*, 659-667.

35) Djukic, J.; Maisse, A.; Pfeffer, M.; de Cian, A.; Fischer, J. Synthesis and Reactivity of New Cyclomanganated (η6-Arene)tricarbonylchromium Complexes. *Organometallics* **1997**, *16*, 657–667.

36) Dreher, S. D.; Dormer, P. G.; Sandrock, D. L.; Molander, G. A. Efficient Cross-Coupling of Secondary Alkyltrifluoroborates with Aryl Chlorides - Reaction Discovery Using Parallel Microscale Experimentation. *J. Am. Chem. Soc.* **2008**, *130*, 9257-9259.

37) Dunina, V.; Golovan, E.; Gulyukina, N.; Grishin, Y.; Beletskaya, I. Configurationally stable asymmetric nitrogen atom in the palladium(II) aminophosphine complex. *Russ. Chem. Bull.* **1997**, *46*, 1331-1334.

38) Duxbury, D. F. The Photochemistry and Photophysics of Triphenylmethane Dyes in Solid Liquid Media. *Chem. Rev.* **1993**, *93*, 381-433.

39) Elliott, J. D.; Lago, M. A.; Cousins, R. D.; Gao, A.; Leber, J. D.; Erhard, K. F.; Nambi, P.; Elshourbagy, N. A.; Kumar, C. *J. Med. Chem.* **1994**, *37*, 1553-1557.

40) Esquivias, J.; Arrayás, R. G.; Carretero. J. C.; *Angew. Chem., Int. Ed.* **2006**, *45*, 629.

41) Farnia, G.; Sandona, G.; Marcuzzi, F.; Melloni, G. Electrochemical reduction of activated carbon–carbon double bonds. Part 2. Mechanism and stereochemistry of the reduction of self-protonating indenes. *J. Chem. Soc. , Perkin Trans. 2,* **1988**, 247-254.

42) Fischer, E. O.; Öfele, K. Über Aromatenkomplexe von Metallen, XIII Benzol-Chrom-Tricarbonyl. *Chem. Ber.* **1957**, *90*, 2532-2535.

43) Frisch, A. C.; Beller, M. *Angew. Chem., Int. Ed*. **2005**, *44*, 674-688.

44) Furness, M. S.; Zhang, X.; Coop, A.; Jacobson, A. E.; Rothman, R. B.; Dersch, C. M.; Xu, H.; Porreca, F.; Rice, K. C. Probes for Narcotic Receptor-Mediated Phenomena. 27.1 Synthesis and Pharmacological Evaluation of Selective δ-Opioid Receptor Agonists from 4-[(αR)-α-(2S,5R)-4-Substituted-2,5-dimethyl-1-piperazinyl-3-methoxybenzyl]- N,N-diethylbenzamides and Their Enantiomers. *J. Med. Chem*. **2000**, *43*, 3193-3196.

45) Gibson, S. E.; Saladin, S. A.; Sur, S. Unusual trisubstitutions on ($\eta^6$-arene)tricarbonylchromium(0) complexes and evidence for the formation of a trianion. *Chem. Commun.* **2000**, 2011-2012.

46) Haag, B.; Mosrin, M.; Ila, H.; Malakhov, V.; Knochel, P. Regio- and Chemoselective Metalation of Arenes and Heteroarenes Using Hindered Metal Amide Bases. Angew. Chem. Int. Ed. **2011**, *asap*.

47) Hamann, B. C.; Hartwig, J. F. Palladium-Catalyzed Direct α-Arylation of Ketones. Rate Acceleration by Sterically Hindered Chelating Ligands and Reductive Elimination from a Transition Metal Enolate Complex. *J. Am. Chem. Soc.* **1997**, 11I9, 12382-12383.

48) Hayashi, T.; Ishigedani, M. Rhodium-Catalyzed Asymmetric Arylation of Imines with Organostannanes. Asymmetric Synthesis of Diarylmethylamines. *J. Am. Chem. Soc.* **2000**, *122*, 976-977.

49) Hayashi, Y.; Sakai, H.; Kaneta, N.; Uemura, M. New chiral chelating phosphine complexes containing tricarbonyl($\eta^6$-arene) chromium for highly enantioselective allylic alkylation. *Journal of Organometallic Chemistry* **1995**, *503*, 143-148.

50) Hermanns, N.; Dahmen, S.; Bolm, C.; Bräse, S. Asymmetric, Catalytic Phenyl Transfer to Imines: Highly Enantioselective Synthesis of Diarylmethylamines. *Angew. Chem. Int. Ed.* **2002**, *41*, 3692-3694.

51) Hevia, E.; Mulvey, R. E. Split Personality of Lithium Chloride: Recent Salt Effects in Organometallic Recipes. *Angew. Chem. Int. Ed.* **2011**, *50*, 6448-6450.

52) Hoff, C. D., Thermochemistry of molybdenum tricarbonyl complexes of arenes and cyclic polyolefins. *J. Organomet. Chem.* **1985**, *282*, 201-214.

53) Hou, X.; Dong, D. X.; Yuan, K. Synthesis of new chiral benzylically substituted P,N-ligands and their applications in the asymmetric Heck reaction. *Tetrahedron: Asymmetry* **2004**, *15*, 2189-2191.

54) Imao, D.; Glasspoole, B. W.; Laberge, V. S.; Crudden, C. M. Cross Coupling Reactions of Chiral Secondary Organoboronic Esters With Retention of Configuration. *J. Am. Chem. Soc.* **2009**, *131*, 5024.

55) Indig, G. L.; Anderson, G. S.; Nichols, M. G.; Bartlett, J. A.; Mellon, W. S.; Sieber, F. Effect of molecular structure on the performance of triarylmethane dyes as therapeutic agents for photochemical purging of autologous bone marrow grafts from residual tumor cells. *J. Pharm. Sci.* **2000**, *1,* 88-99.

56) Ireland, T.; Tappe, K.; Grossheimann, G.; Knochel, P. Synthesis of a New Class of Chiral 1,5-Diphosphanylferrocene Ligands and Their Use in Enantioselective Hydrogenation. *Chem. -Eur. J.* **2002**, *8*, 843-852.

57) Jahra, H. C.; Niegerb, M.; Dötz, K. H. Controlled haptotropic rearrangements – towards a stereospecific molecular switch based on chiral arene chromium complexes. *Chem. Commun.* **2003**, 2866-2867.

58) Jaouen, G.; Top, S.; McGlinchey, M. J. A Carbon-13 NMR Spectroscopic Study of a $Cr(CO)_3$-Stabilised Benzyl Anion. *J. Organomet. Chem.* **1980**, *195*, C9-C12.

59) Jurd, L. New anti-tumor agents. 1. Heterocyclic benzodioxole lactones. *J. Heterocycl. Chem.* **1996**, *33*, 1227-1232.

60) Kalinin, V. N.; Cherepanov, I. A.; Moiseev, S. K. Benzylic functionalization of ($\eta^6$-alkylarene)chromium tricarbonyl complexes. *J. Organomet. Chem.* **1997**, *536-537*, 437-455.

61) Kaganovich, V. S.; Rybinskaya, M. I. Cr, Co, and Mn arene π-complexes based on diphenyl- and triphenylmethane. *Russ. Chem. Bull.* **1993**, *42*, 1734-1737.

62) Kamikawa, K.; Sugimoto, S.; Uemura, M. Palladium-Catalyzed Amination of Aryl Bromides Utilizing Arene−Chromium Complexes as Ligands. *J. Org. Chem*. **1998**, *63*, 8407-8410.

63) Katritzky, A. R.; Gupta, V.; Garot, C.; Stevens, C. V.; Gordeev, M. F.; *Heterocycles* **1994**, *38*, 345.

64) Katritzky, A. R.; Qi, M. The generation and reactions of non-stabilized α-aminocarbanions. *Tetrahedron* **1998**, *54*, 2647-2668.

65) Katritzky, A. R.; Yao, J.; Bao, W.; Qi, M.; Steel, P. J. 2-Benzotriazolylaziridines and Their Reactions with Diethyl Acetylenedicarboxylate. *J. Org. Chem*. **1999**, *64*, 346-350.

66) Kauffman, M. C.; Walsh, P. J. In *Arylation and Alkenylation of Carbonyl and Imino Groups*; Molander, G. A., Ed.; Stereoselective Synthesis 2; Thieme: Stuttgart, **2011**; Vol. 2, pp 449-495.

67) Kazmierski, I.; Gosmini, C.; Paris, J.; Périchon, J. 2,2′-Bipyridine: An Efficient Ligand in the Cobalt-Catalyzed Synthesis of Organozinc Reagents from Aryl Chlorides and Sulfonates. *Synlett* **2006**, *2006*, 881,884.

68) Kessar, S. V.; Singh, P. Lewis Acid Complexation of Tertiary Amines and Related Compounds: A Strategy for α-Deprotonation and Stereocontrol. *Chem. Rev.* **1997**, *97*, 721-738.

69) Klamt, A.; Schüürmann, G. COSMO: A new approach to dielectric screening in solvents with explicit expressions for the screening energy and its gradient. *J. Chem. Soc., Perkin Trans. 2* **1993**, *5*, 799-805.

70) Kofink, C. C.; Knochel, P. Synthesis of Functionalized Diarylmethanes via a Copper-Catalyzed Cross-Coupling of Arylmagnesium Reagents with Benzylic Phosphates. *Org. Lett.* **2006**, *8*, 4121-4124.

71) Krasovskiy, A.; Krasovskaya, V.; Knochel, P. Mixed Mg/Li Amides of the Type $R_2NMgCl \bullet LiCl$ as Highly Efficient Bases for the Regioselective Generation of Functionalized Aryl and Heteroaryl Magnesium Compounds. *Angew. Chem. Int. Ed.* **2006**, *45*, 2958-2961.

72) Kündig, E. P.; Fabritius, C.; Grossheimann, G.; Romanens, P.; Butenschön, H.; Wey, H. G. Synthesis of Substituted Arene Molybdenum Complexes by Arene Exchange. *Organometallics* **2004**, *23*, 3741-3744.

73) Kuwano, R.; Yokogi, M. Suzuki−Miyaura Cross-Coupling of Benzylic Carbonates with Arylboronic Acids. *Org. Lett*. **2005**, *7,* 945-947.

74) Lantaño, B.; Aguirre, J. M.; Finkielsztein, L.; Alesso, E. N.; Brunet, E.; Moltrasio, G. Y. A Formal [3 + 2] Alkene Addition to Benzhydrol Cations. A Practical and Mild Methodology for the Synthesis of Substituted 1-Arylindanes and Related Compounds. *Synth. Commum*. **2004**, *34*, 625-641.

75) Le Borgne, M.; Marchand, P.; Delevoye-Seiller, B.; Robert, J.; Le Baut, G.; Hartmann, R. W.; Palzer, M. New selective nonsteroidal aromatase inhibitors: Synthesis and inhibitory activity of 2,3 or 5-(α-azolylbenzyl)-1H-indoles. *Bioorg. Med. Chem. Lett*. **1999**, *9*, 333-336.

76) Le Gall, E.; Haurena, C.; Sengmany, S.; Martens, T.; Troupel, M. Three-Component Synthesis of α-Branched Amines under Barbier-like Conditions. *J. Org. Chem*. **2009**, *74*, 7970-7973.

77) Lézé, M.; Palusczak, A.; Hartmann, R. W.; Le Borgne, M. Synthesis of 6- or 4-functionalized indoles via a reductive cyclization approach and evaluation as aromatase inhibitors. *Bioorg. Med. Chem. Lett.* **2008**, *18*, 4713-4715.

78) Li, Y.; Li, B.; Lu, X.; Lin, S.; Shi, Z. Cross Dehydrogenative Arylation (CDA) of a Benzylic C—H Bond with Arenes by Iron Catalysis. *Angew. Chem. Int. Edit. Engl*. **2009**, *48*, 3817-3820.

79) Liégault, B.; Renaud, J.-L.; Bruneau, C.; *Chem. Soc. Rev.* **2008**, *37*, 290.

80) Lotz, M.; Ireland, T.; Almena Perea, J. J.; Knochel, P. Stereoselective substitution of α-aminoalkylferrocenes with diorganozincs. A fast synthesis of new chiral FERRIPHOS ligands for asymmetric catalysis. *Tetrahedron: Asymmetry* **1999**, *10*, 1839-1842.

81) Ma, Y.; Hoepker, A. C.; Gupta, L.; Faggin, M. F.; Collum, D. B. 1,4-Addition of Lithium Diisopropylamide to Unsaturated Esters: Role of Rate-Limiting Deaggregation, Autocatalysis, Lithium Chloride Catalysis, and Other Mixed Aggregation Effects. *J. Am. Chem. Soc.* **2010**, *132*, 15610-15623.

82) Mahaffy, C. A. L.; Pauson, P. L. ($\eta^6$-Arene)tricarbonylchromium complexes. *Inorg. Synth.* **1990**, *28*, 136-140.

83) Marquarding, D.; Klusacek, H.; Gokel, G.; Hoffmann, P.; Ugi, I. Stereoselective syntheses. VI. Correlation of central and planar chirality in ferrocene derivatives. *J. Am. Chem. Soc.* **1970**, *92*, 5389-5393.

84) McGrew, G. I.; Temaismithi, J.; Carroll, P. J.; Walsh, P. J. Synthesis of Polyarylated Methanes through Cross-Coupling of Tricarbonylchromium-Activated Benzyllithiums. *Angew. Chem. Int. Ed.* **2010**, *49*, 5541-5544.

85) McLaughlin, M. Suzuki-Miyaura Cross-Coupling of Benzylic Phosphates with Arylboronic Acids. **Org. Lett. 2005**, *7*, 4875-4878.

86) Merlic, C. A.; Walsh, J. C.; Tantillo, D. J.; Houk, K. N. Chemical Hermaphroditism: The Potential of the $Cr(CO)_3$ Moiety To Stabilize Transition States and Intermediates with Anionic, Cationic, or Radical Character at the Benzylic Position. *J. Am. Chem. Soc.* **1999**, *121*, 3596-3606.

87) Molander, G. A.; Elia, M. D. Suzuki−Miyaura Cross-Coupling Reactions of Benzyl Halides with Potassium Aryltrifluoroborates. *J. Org. Chem*. **2006**, *71*, 9198-9202.

88) Molander, G. A.; Ellis, N. Organotrifluoroborates: Protected Boronic Acids That Expand the Versatility of the Suzuki Coupling Reaction. *Acc. Chem. Res.* **2007**, *40*, 275.

89) Monovich, L. G.; Le Huérou, Y.; Rönn, M.; Molander, G. A. Total Synthesis of (−)-Steganone Utilizing a Samarium(II) Iodide Promoted 8-Endo Ketyl−Olefin Cyclization. *J. Am. Chem. Soc.* **2000**, *122*, 52-57.

90) Müller, T. J. J.; Netz, A.; Ansorge, M.; Schmälzlin, E.; Bräuchle, C.; Meerholz, K. Syntheses and NLO Properties of Chromium Carbonyl Arene Complexes with Conjugated Side Chains: The Amphoteric Nature of Chromium Carbonyl Complexation in Push−Pull Chromophores. *Organometallics* **1999**, *18*, 5066-5074.

91) Murahashi, S. Palladium-catalyzed cross-coupling reaction of organic halides with Grignard reagents, organolithium compounds and heteroatom nucleophiles. *J. Organomet. Chem.* **2002**, *653*, 27-33.

92) Murai, T.; Asai, F. Three-Component Coupling Reactions of Thioformamides with Organolithium and Grignard Reagents Leading to Formation of Tertiary Amines and a Thiolating Agent. *J. Am. Chem. Soc.* **2007**, *129*, 780-781.

93) Muthyala, R.; Katritzky, A. R.; Lan, X. A synthetic study on the preparation of triarylmethanes. *Dyes and Pigments* **1994**, *25*, 303-324.

94) Nair, V.; Abhilash, K. G.; Vidya, N.; Practical Synthesis of Triaryl- and Triheteroarylmethanes by Reaction of Aldehydes and Activated Arenes Promoted by Gold(III) Chloride. *Org. Lett.* **2005**, *7*, 5857.

95) Nair, V.; Thomas, S.; Mathew, S. C.; Abhilash, K. G. Recent advances in the chemistry of triaryl- and triheteroarylmethanes. *Tetrahedron* **2006**, *62*, 6731-6747.

96) Netherton, M. R.; Fu, G. C. *Adv. Syn. & Catal*. **2004**, *346*, 1525-1532.

97) Ohlsson and Bengt *et al* Indanetricarbonylchromium: the effects of 1-syn- and 1-anti substituents on the regioselectivity of nucleophilic addition. Crystal structures of 1-syn- and 1-anti-methoxyindanetricarbonylchromium. *J. Organomet. Chem.* **1989**, *365*, 243-267.

98) Ohlstein, E. H.; Nambi, P.; Douglas, S. A.; Edwards, R. M.; Gellai, M.; Lago, A.; Leber, J. K.; Cousins, R. D.; Gao, A. M.; Frazee, J. S.; Peishoff, C. E.; Bean, J. W.; Eggleston, D. S.; Elshourbagy, N. A.; Kumar, C.; Lee, J. A.; Yue, T. L.; Louden, C.; Brooks, D. P.; Weinstock, J.; Feuerstein, G.; Poste, G.; Ruffolo, R. R.; Gleason, J. G.; Elliott, J. D. SB 209670, a rationally designed potent nonpeptide endothelin receptor antagonist. *Proc. Natl. Acad. Sci. U. S. A.* **1994**, *91*, 8052-8056.

99) Opalka, C. J.; DAmbra, T. E.; Faccone, J. J.; Bodson, G.; Cossement, E. A Novel Synthesis of the Enantiomers of an Antihistamine Drug by Piperazine Formation from a Primary Amine. *Synthesis* **1995**, *1995*, 766-768.

100) Palchaudhuri, R.; Nesterenko, V.; Hergenrother, P. J. The Complex Role of the Triphenylmethyl Motif in Anticancer Compounds. *J. Am. Chem. Soc*. **2008**, *130*, 10274-10281.

101) Palucki, M.; Buchwald, S. L. Palladium-Catalyzed α-Arylation of Ketones. *J. Am. Chem. Soc.* **1997**, *119*, 11108-11109.

102) Parai, M. K.; Panda, G.; Chaturvedi, V.; Manju, Y. K.; Sinha, S. Thiophene containing triarylmethanes as antitubercular agents. *Bioorg. Med. Chem. Lett.* **2008**, *1,* 289-292.

103) Peascoe, W.; Applequist, D. E. Influence of aggregate composition on relative reactivities of alkyllithiums. *J. Org. Chem.* **1973**, *38*, 1510-1512.

104) Pfaltz, A.; Drury, W. J. Design of chiral ligands for asymmetric catalysis: From C2-symmetric P,P- and N,N-ligands to sterically and electronically nonsymmetrical P,N-ligands. *Proceedings of the National Academy of Sciences of the United States of America* **2004**, *101*, 5723-5726.

105) Pfletschinger, A.; Dargel, T. K.; Bats, J. W.; Schmalz, H.-G.; Koch, W. Structural and Energetical Characterization of Reactive Intermediates Derived from Toluene–$Cr(CO)_3$. *Chem. Eur. J.* **1999**, *5*, 537.

106) Pflum, D. A.; Krishnamurthy, D.; Han, Z.; Wald, S. A.; Senanayake, C. H. Asymmetric synthesis of cetirizine dihydrochloride. *Tetrahedron Lett.* **2002**, *43*, 923-926.

107) Pflum, D. A.; Wilkinson, H. S.; Tanoury, G. J.; Kessler, D. W.; Kraus, H. B.; Senanayake, C. H.; Wald, S. A. A Large-Scale Synthesis of Enantiomerically Pure Cetirizine Dihydrochloride Using Preparative Chiral HPLC. *Organic Process Research & Development* **2001**, *5*, 110-115.

108) Ramesh, C.; Barerjee, J.; Pal, R.;Das, B.; *Adv. Syn. & Catal.* **2003**, *345*, 557.

109) Ratni, H.; Kundig, E. P. Synthesis of (-)-Lasubine(I) via a Planar Chiral [($\eta^6$-arene)$Cr(CO)_3$] Complex. *Org. Lett.* **1999**, *1*, 1997-1999.

110) Ritter, K. Synthetic Transformations of Vinyl and Aryl Triflates. *Synthesis* **2002**, *1993*, 735,762.

111) Rosillo, M.; Dominguez, G.; Perez-Castells, J. Chromium arene complexes in organic synthesis. *Chem. Soc. Rev.* **2007**, *36*, 1589-1604.

112) Schäfer, G.; Bode, J. W. Friedel-Crafts Benzylation of Activated and Deactivated Arenes. *Angew. Chem. Int. Ed.* **2011**, *asap*.

113) Schiemann, K.; Showalter, H. D. H. Development of Polymer-Supported Benzotriazole as a Novel Traceless Linker for Solid-Phase Organic Synthesis. *J. Org. Chem.* **1999**, *64*, 4972-4975.

114) Schlosser, M. Superbases for organic synthesis. *Pure Appl. Chem.* **1988**, *60*, 1627-1634.

115) Semmelhack, M. F.; Chlenov, A.; Ho, D. M. Accelerated Arene Ligand Exchange in the (Arene)$Cr(CO)_2$L Series. *J. Am. Chem. Soc.* **2005**, *127*, 7759-7773.

116) Semmelhack, M. F.; Hall, H. T. Intermediates in the reaction of carbanions with .pi.-(chlorobenzene)chromium tricarbonyl. *J. Am. Chem. Soc.* **1974**, *96*, 7092-7094.

117) Shi, B.; Maugel, N.; Zhang, Y.; Yu, J. *Angew. Chem. Int. Edit.* **2008**, *47*, 4882-4886.

118) Shintani, R.; Soh, Y.; Hayashi, T. Rhodium-Catalyzed Asymmetric Arylation of Azomethine Imines. *Org. Lett.* **2010**, *12*, 4106-4109.

119) Spindler, F.; Malan, C.; Lotz, M.; Kesselgruber, M.; Pittelkow, U.; Rivas-Nass, A.; Briel, O.; Blaser, H. Modular chiral ligands: the profiling of the Mandyphos and Taniaphos ligand families. *Tetrahedron: Asymmetry* **2004**, *15*, 2299-2306.

120) Sun, F.; Zheng, X.; Gu, Q.; He, Q.; You, S. *Eur. J.Org. Chem.* **2010**, *2010*, 47-50.

121) Togni, A. Planar-Chiral Ferrocenes: Synthetic Methods and Applications. *Angew. Chem. Int. Ed.* **1996**, *35*, 1475-1477.

122) Torregrossa, M. M.; Isgor, C.; Folk, J. E.; Rice, K. C.; Watson, S. J.; Woods, J. H. The [delta]-Opioid Receptor Agonist (+)BW373U86 Regulates BDNF mRNA Expression in Rats. *Neuropsychopharmacology* **2003**, *29*, 649-659.

123) Traylor, T. G.; Stewart, K. J. Mechanisms of arene exchange in (arene)tricarbonylchromium compounds: intermolecular and intramolecular exchanges in complexes of propenylbenzene, stilbenes, and 1,1-diphenylethylene. *J. Am. Chem. Soc.* **1986**, *108*, 6977-6985.

124) Truong, T.; Alvarado, J.; Tran, L. D.; Daugulis, O. Nickel, Manganese, Cobalt, and Iron-Catalyzed Deprotonative Arene Dimerization. *Org. Lett.* **2010**, *12*, 1200-1203.

125) Tsai, A. S.; Tauchert, M. E.; Bergman, R. G.; Ellman, J. A. Rhodium(III)-Catalyzed Arylation of Boc-Imines via C−H Bond Functionalization. *J. Am. Chem. Soc.* **2011**, *133*, 1248-1250.

126) Uemura, M.; Daimon, A.; Hayashi, Y. An asymmetric synthesis of an axially chiral biaryl via an (arene)chromium complex: formal synthesis of (-)-steganone. *J. Chem. Soc., Chem. Commun*. **1995**, 1943-1944.

127) Uemura, M.; Miyake, R.; Nishimura, H.; Matsumoto, Y.; Hayashi, T. New chiral phosphine ligands containing (η6-arene)chromium and catalytic asymmetric cross-coupling reactions. *Tetrahedron: Asymmetry* **1992**, *3*, 213-216.

128) Vasen, D.; Salzer, A.; Gerhards, F.; Gais, H.; Sturmer, R.; Bieler, N. H.; Togni, A. Optically Active Transition-Metal Complexes. 10.1 Bifunctional Arene−Chromium−Tricarbonyl Complexes Derived from (R)-Phenylethanamine: Easily Accessible Planar-Chiral Diphosphines and Their Application in Enantioselective Hydrogenation, Hydroamination, and Allylic Sulfonation. *Organometallics* **2000**, *19*, 539-546.

129) Watson, I. D. G.; Yudin, A. K. *J. Am. Chem. Soc.* **2005**, *127*, 17516.

130) Weigend, F.; Ahlrichs, R. Balanced basis sets of split valence, triple zeta valence and quadruple zeta valence quality for H to Rn: Design and assessment of accuracy. *Phys. Chem. Chem. Phys.* **2005**, *7*, 3297-3305.

131) Welch, W. M.; Kraska, A. R.; Sarges, R.; Koe, B. K. Nontricyclic antidepressant agents derived from cis- and trans-1-amino-4-aryltetralins. *J. Med. Chem.* **1984**, *27*, 1508-1515

132) Welsch, M. E.; Snyder, S. A.; Stockwell, B. R. Privileged scaffolds for library design and drug discovery. *Curr. Opin. Chem. Biol.* **2010**, *14*, 347-361.

133) Yadav, J. S.; Reddy, B. V. S.; Sunitha, S.; *Adv. Syn. & Catal.* **2003**, *345*, 349.

134) Yoon, T. P.; Jacobsen, E. N. Privileged Chiral Catalysts. *Science* **2003**, *299*, 1691-1693.

135) Yu, J. -.; Kuwano, R. Suzuki-Miyaura Coupling of Diarylmethyl Carbonates with Arylboronic Acids: A New Access to Triarylmethane. *Org. Lett.* **2008**, *10*, 973-976.